

Progress in Drug Research 75

Series Editor: K. D. Rainsford

W. Richard Chegwidden

Nicholas D. Carter *Editors*

The Carbonic Anhydrases: Current and Emerging Therapeutic Targets

 Springer

Progress in Drug Research

Volume 75

Series Editor

K.D. Rainsford, Sheffield Hallam University, Sheffield, UK

Progress in Drug Research is a prestigious book series which provides extensive expert-written reviews on highly topical areas in current pharmaceutical and pharmacological research.

Founded in 1959 by Ernst Jucker, the series moved from its initial focus on medicinal chemistry to a much wider scope. Today it encompasses all fields concerned with the development of new therapeutic drugs and the elucidation of their mechanisms of action, reflecting the increasingly complex nature of modern drug research. Invited authors present their biological, chemical, biochemical, physiological, immunological, pharmaceutical, toxicological, pharmacological and clinical expertise in carefully written reviews and provide the newcomer and the specialist alike with an up-to-date list of prime references.

Starting with volume 61, Progress in Drug Research is continued as a series of monographs and contributed volumes.

More information about this series at <http://www.springer.com/series/4857>

W. Richard Chegwidden · Nicholas D. Carter
Editors

The Carbonic Anhydrases: Current and Emerging Therapeutic Targets

 Springer

Editors

W. Richard Chegwidden
LECOM
Erie, PA, USA

Nicholas D. Carter
St. George's, University of London
London, UK

ISSN 0071-786X

Progress in Drug Research

ISBN 978-3-030-79510-8

<https://doi.org/10.1007/978-3-030-79511-5>

ISSN 2297-4555 (electronic)

ISBN 978-3-030-79511-5 (eBook)

© Springer Nature Switzerland AG 2021

This work is subject to copyright. All rights are reserved by the Publisher, whether the whole or part of the material is concerned, specifically the rights of translation, reprinting, reuse of illustrations, recitation, broadcasting, reproduction on microfilms or in any other physical way, and transmission or information storage and retrieval, electronic adaptation, computer software, or by similar or dissimilar methodology now known or hereafter developed.

The use of general descriptive names, registered names, trademarks, service marks, etc. in this publication does not imply, even in the absence of a specific statement, that such names are exempt from the relevant protective laws and regulations and therefore free for general use.

The publisher, the authors and the editors are safe to assume that the advice and information in this book are believed to be true and accurate at the date of publication. Neither the publisher nor the authors or the editors give a warranty, expressed or implied, with respect to the material contained herein or for any errors or omissions that may have been made. The publisher remains neutral with regard to jurisdictional claims in published maps and institutional affiliations.

This Springer imprint is published by the registered company Springer Nature Switzerland AG
The registered company address is: Gewerbestrasse 11, 6330 Cham, Switzerland

My co-editor, Professor Nick Carter, died on 27th March, 2021, before the publication of this volume. A splendid friend for more than 30 years, and a great scientist, he will be much missed by many.

W. Richard Chegwidden

Dedication to Richard Tashian



Richard E. Tashian

1922–2020

Richard Tashian made an immense contribution to our knowledge and understanding of the carbonic anhydrases across a broad front, from his earlier work on the protein structures and activities of carbonic anhydrase isozymes to his later studies on the structure, organization, expression and evolution of the genes encoding them. Over the years, his laboratory touched on most facets of carbonic anhydrase research in a long series of distinguished endeavours.

From his earliest schooldays in Rhode Island, Richard Tashian's declared ambition was to become a scientist, and his tolerant parents soon found their basement taken over as a chemistry laboratory and a museum of biological specimens.

Richard Tashian graduated from the University of Rhode Island in 1947 and received his Ph.D. in Zoology from Purdue University in 1951. His undergraduate education was interrupted during World War II, when he enlisted in the Air Force. Posted in England as a meteorologist, he learned that, by definition, a shower lasted no longer than twenty minutes, a cameo of meteorological trivia that served him well for more than 70 years! Clearly anyone who would attempt to forecast the weather in England would be game for anything, and after Purdue, the young Tashian entered his "intrepid explorer" phase, undertaking ecological studies in tropical rain forests of Central America and the Caribbean. In his later years, much to his delight, his work of that period was often still cited in books on tropical birds.

In the late fifties, Tashian entered the field of biochemical genetics, first at Columbia University, New York, and later at the University of Michigan in Ann Arbor, where he remained for the remainder of his career.

In 1960, his study of esterase isozymes from human hemolysates led him into the world of carbonic anhydrase. Indeed, it was he who first discovered the esterase activity of this enzyme. Other firsts achieved in his laboratory include the first characterization of an enzyme variant due to a point mutation (CA I Guam, 1966), the histochemical localization of specific carbonic anhydrase isozymes in mammalian tissue (with S. Spicer, 1979), the first complete structural analysis of a carbonic anhydrase gene (mouse Car 2, with K. Wiebauer, 1985), the tissue localization of an acatalytic carbonic anhydrase-related protein by *in situ* hybridization (CA-RP VIII, 1997), and the intriguing discovery (with E. Nevo) that the red cells of certain animals which operate under low oxygen tension are notably deficient in the high activity isozyme, CA II (1998/99).

The identification of human deficiencies of the two major CA isozymes of the red blood cell were also notable achievements (CA I deficiency with A. Kendall, 1977, and CA II deficiency with W. Sly, 1983). The complete amino acid sequences of many different carbonic anhydrase isozymes were determined in his laboratory, initially from isolated proteins and later from cDNAs. These and other data led to the construction of comprehensive phylogenetic trees for the carbonic anhydrase gene families (with D. Hewett-Emmett).

As a Professor Emeritus, long after he ceased to play an active role at the laboratory bench, he remained for many years a pre-eminent elder statesman of the carbonic anhydrase field, continuing his editorial work and actively participating in research conferences into his last decade.

A gentleman in the best sense, a truly committed, lifelong academic, and something of a polymath, Richard Tashian possessed a sense of humour that was legendary among his close acquaintances. His warmth, wit and ability to relate to others on an individual level attracted many to his stimulating laboratory. He is remembered with loyalty and affection by those who worked with him over the years.

Richard Chegwiddden

Adapted from *The Carbonic Anhydrases: New Horizons* (Chegwiddden WR et al., eds) Birkhauser Verlag, 2000.

Preface

Carbonic anhydrase (CA; EC 4.2.1.1) is seemingly ubiquitous in its expression in various forms throughout nature, since the reaction that it catalyzes—the reversible hydration of CO_2 to bicarbonate and a proton—lies at the heart of a wide range of vital physiological processes. Consequently, the existing and potential therapeutic applications of targeting CA cover a plethora of diseases and disorders, and have generated extensive and increasing interest in recent years.

The primary purpose of this book is to assemble and integrate the wealth of diverse information that is accumulating in this burgeoning field. Its inter-disciplinary approach embraces both the up-to-date application of CA-targeting, and the latest research data that provide a platform for the development of novel applications.

The interested audience comprises scientists and physicians alike. The scientists include not only researchers specifically studying the carbonic anhydrases, but also those in areas of science and medicine to which carbonic anhydrase is relevant. They also include pharmacologists, pharmacists and chemists involved in drug action, design, and production. The physician audience includes all those in the many clinical disciplines in which the targeting of carbonic anhydrase isozymes is, or may become, clinically relevant. Such areas include, among others, nephrology, neurology, oncology, ophthalmology, pulmonology, urology, and vascular medicine.

Chapter 1 integrates text with a tabular format to provide an easily accessible reference guide to the properties and roles of the various human CA isozymes, and the disorders and diseases currently and potentially addressed by their therapeutic targeting. This sets the scene for a series of chapters on more specialist clinically-related topics, written by an expert team of distinguished scientists and physicians who have made signal contributions to the carbonic anhydrase field. Since much attention has been given in recent years to the association of carbonic anhydrase isozymes with cancer, several chapters are focused on various aspects of this topic. Other chapters feature the roles of carbonic anhydrase, and potential of modulating its activity, in an impressively broad range of pathological conditions.

We wish to thank all the authors and co-authors for their excellent contributions to this volume, and the patient staff at Springer Nature for their assistance. We also wish to thank the series editor, Prof. K. D. Rainsford, for his steadfast support.

Erie, USA

W. Richard Chegwidden

Contents

1	The Carbonic Anhydrases in Health and Disease	1
	W. Richard Chegwidden	
2	Carbonic Anhydrase Isozymes as Diagnostic Biomarkers and Therapeutic Targets	13
	Seppo Parkkila	
3	Targeting Carbonic Anhydrases in Cardiovascular and Pulmonary Disease	37
	Erik R. Swenson, Akshay Kumar, Nimisha Kumar, and Bernardo V. Alvarez	
4	Carbonic Anhydrase Inhibitors in Ophthalmology: Glaucoma and Macular Oedema	79
	Marianne Levon Shahsuvaryan	
5	Targeting Carbonic Anhydrase Isozymes in the Treatment of Neurological Disorders	103
	Ashok Aspatwar, Jukka Peltola, and Seppo Parkkila	
6	Potential of Carbonic Anhydrase Inhibitors in the Treatment of Oxidative Stress and Diabetes	121
	Zafer Gurel and Nader Sheibani	
7	An Overview of Carbonic Anhydrase-Related Neoplasms	147
	Martina Takacova and Silvia Pastorekova	
8	Carbonic Anhydrase IX Interactome and the Regulation of Cancer Progression	179
	Mridula Swayampakula, Geetha Venkateswaran, Paul C. McDonald, and Shoukat Dedhar	
9	Carbonic Anhydrase IX: Current and Emerging Therapies	205
	R. I. J. Merckx, P. F. A. Mulders, and E. Oosterwijk	

10 Carbonic Anhydrase Inhibitors: Designing Isozyme-Specific Inhibitors as Therapeutic Agents	221
Claudiu T. Supuran	
11 Carbonic Anhydrase Inhibitors: Identifying Therapeutic Cancer Agents Through Virtual Screening	237
Giulio Poli, Claudiu T. Supuran, and Tiziano Tuccinardi	
12 Targeting Carbonic Anhydrase IX in Tumor Imaging and Theranostic Cancer Therapy	253
Joseph Lau, Kuo-Shyan Lin, and François Bénard	
Index	281

Chapter 1

The Carbonic Anhydrases in Health and Disease



W. Richard Chegwidden

Abstract The zinc metalloenzyme carbonic anhydrase (CA; EC 4.2.1.1) catalyzes the reversible hydration of CO₂ and is expressed in human in 15 different isoforms—12 active isozymes and three catalytically inactive isoforms. Since the enzyme is fundamental to many physiological processes, chiefly involving ion transport, pH regulation, and substrate provision for metabolism, it has been implicated in many diseases and disorders. Consequently, carbonic anhydrase inhibitors, such as the classical sulfonamide inhibitor acetazolamide, have long been employed therapeutically. Initially developed for congestive heart failure, acetazolamide was subsequently employed for many years in the treatment of glaucoma, and other conditions such as acute mountain sickness. Over recent years, however, the number of diseases, with pathologies involving carbonic anhydrase, has expanded enormously providing potential for novel therapies through the modification of carbonic anhydrase activity. These are highlighted in the following chapter. In particular, a wealth of evidence has linked carbonic anhydrase, particularly the carbonic anhydrase IX isozyme (CA IX), with cancer. Alongside this has been a complimentary development of novel methods of drug delivery targeting CA IX.

Keywords Carbonic anhydrase · CA inhibitors · Acetazolamide · Therapeutic target · Therapeutic application · Drug delivery systems

Carbonic anhydrase (CA) catalyzes the reversible hydration of carbon dioxide to bicarbonate ($\text{CO}_2 + \text{H}_2\text{O} \leftrightarrow \text{HCO}_3^- + \text{H}^+$), a reaction of such profound importance that the enzyme is seemingly ubiquitous in nature, being represented by seven distinct gene families— α , β , γ , δ , ζ , η , and θ —of which only the α -family is present in human. The human family comprises 12 active isozyme members that differ in tissue distribution, sub-cellular location, catalytic power and inhibitory characteristics (see Tables 1.1 and 1.2), and three isoforms, designated CA-related proteins (CA-RPs), that are inactive owing to the absence of one or more of the histidine residues that

W. R. Chegwidden (✉)
LECOM, 1858 West Grandview Boulevard, Erie, PA 16509, USA
e-mail: wrchegwidden@lecom.edu; wrc.2417@gmail.com

© Springer Nature Switzerland AG 2021
W. R. Chegwidden and N. D. Carter (eds.), *The Carbonic Anhydrases: Current and Emerging Therapeutic Targets*, Progress in Drug Research 75,
https://doi.org/10.1007/978-3-030-79511-5_1

Table 1.1 Tissue distribution and sub-cellular location of human carbonic anhydrase isozymes

Isozyme	Sub-cellular location	Principal sites of tissue expression
CA I	Cytoplasmic	Red blood cell, intestine, eye
CA II	Cytoplasmic	Ubiquitous (certain cells of virtually all tissues)
CA III	Cytoplasmic	Red muscle, white and brown adipose tissue
CA IV	Membrane-bound (extracellular)	Kidney, lung, pancreas, gut, brain, eye, probably universally present in capillary endothelium
CA VA	Mitochondrial	Liver
CA VB	Mitochondrial	Widespread
CA VI	Secreted	Salivary and mammary glands
CA VII	Cytoplasmic	CNS (lower expression widespread)
CA VIII ^a	Cytoplasmic	Brain, especially Purkinje cells of cerebellum, (lower expression widespread)
CA IX	Transmembrane (extra-cellular domain)	Various tumours, gastric mucosa
CA X ^a	Cytoplasmic	Brain
CA XI ^a	Cytoplasmic	Brain (lower expression widespread)
CA XII	Transmembrane (extra-cellular domain)	Widespread, especially kidney, colon, prostate
CA XIII	Cytoplasmic	Kidney, brain, lung, gut, reproductive organs
CA XIV	Transmembrane (extra-cellular domain)	Widespread, especially kidney and heart

^aCA VIII, CA X and CA XI lack activity because of substitution of one or more of the histidine residues required to bind the catalytically essential zinc ion. Consequently they are commonly designated CA-related proteins (CA-RP VIII, CA-RP X and CA-RP XI). Although no definitive roles have been firmly established for any of these three CA-RP molecules, recent studies suggest a role for CA-RP VIII as an allosteric modulator in pain regulation, through the regulation of neuronal cytosolic calcium levels (Zhuang et al. 2015, 2018)

N.B. CA XV is an additional catalytically active α -CA isozyme that is not expressed in human or chimpanzee (Hilvo et al. 2005)

coordinate the catalytically active zinc ion in the active site (CA-RP VIII, CA-RP X, and CA-RP XI) [for recent reviews see Supuran and Nocentini 2019; Supuran and De Simone 2015]. A thirteenth active α -CA isozyme (CA XV) is not expressed in human or chimpanzee (Hilvo et al. 2005).

The CA reaction is so fundamental that the active isozymes participate in a host of crucial physiological processes, variously involving H⁺, CO₂, ion and water transport, pH regulation, and provision of bicarbonate as substrate for a range of metabolic reactions. Some of the major physiological functions of the carbonic anhydrase isozymes are summarized in Table 1.3.

Table 1.2 CO₂-hydration activity and acetazolamide inhibition of human carbonic anhydrase isozymes

Isozyme	Activity level	k_{cat}/K_M (M ⁻¹ s ⁻¹) ^a	Acetazolamide (Az) inhibition	K_I (Az) (nM) ^b
CA I	Moderate	5.0×10^7	Moderate	250
CA II	High	1.5×10^8	Strong	12
CA III	Low	2.5×10^5	Weak	2×10^5
CA IV	High	5.1×10^7	Strong	74
CA VA	Moderate	2.9×10^7	Strong	63
CA VB	High	9.8×10^7	Strong	54
CA VI	Moderate	4.9×10^7	Strong	11
CA VII	High	8.3×10^7	Strong	2.5
CA IX	High	5.4×10^7	Strong	25
CA XII	Moderate	3.5×10^7	Strong	5.7
CA XIII	Moderate	1.1×10^7	Strong	16
CA XIV	Moderate	3.9×10^7	Strong	41

^a k_{cat}/K_M values are taken from Hilvo, Baranauskiene et al. (2008)

^b K_I (Az) values are taken from Supuran et al. (2015) and Hilvo, Innocenti et al. (2008) (human CA XIII)

The tight evolutionary conservation of the inactive CA isoforms (CA-RPs) strongly suggests that they also possess important physiological functions (Tashian et al. 2000). In recent years, evidence has accumulated that indicates an important role for CA-RP VIII as an allosteric modulator in pain regulation through the regulation of neuronal cytosolic calcium levels (Zhuang et al. 2015, 2018).

Reflecting this wide range of functions, CA isozymes have been implicated in many diseases and disorders (Table 1.4). Consequently, CA inhibitors have, through the years, found therapeutic application in a wide and growing range of clinical conditions including acute mountain sickness (Swenson and Teppems 2007; Swenson 2014a; Lipman et al. 2019), bipolar disorder (Hayes 1994), chronic obstructive pulmonary disease (COPD) (Adamson and Swenson 2017; Van Berkel and Elefritz 2018), glaucoma (Becker 1955; Masini et al. 2013), gastric ulcer (Buzás and Supuran 2016), macular edema (Cox et al. 1988; Wolfensberger 2017), obesity (Scozzafava et al. 2013), epilepsy (Aggerwal et al. 2013; Silberstein et al. 2005), sleep apnea (Eskandari et al. 2014, 2018), and migraine (Brandes et al. 2004; Silberstein et al. 2004; Silberstein 2017). A vasodilatory effect of CA inhibitors has also been demonstrated (Swenson 2014b), raising the possibility of a role for such agents in hypertensive-related diseases. This effect, along with a contribution to the maintenance of blood gas stability may, at least in part, account for the effectiveness of acetazolamide in the treatment of obstructive sleep apnea. In recent years, much attention has been given to the potential of CA inhibitors and CA-targeted drugs to treat cancer, and most recently, evidence has also accumulated suggesting possible roles for CA inhibitors in therapy for hemorrhagic stroke (Li et al. 2016), protection

Table 1.3 Major physiological functions of the human carbonic anhydrase isozymes^{a,b}

Function	CA isozymes principally involved ^c
<i>Respiration and Acid/Base Regulation</i>	
Hydration of CO ₂ to HCO ₃ ⁻ in peripheral tissues	CA II (in red cells)
Dehydration of HCO ₃ ⁻ to CO ₂ at lungs	CA IV (in capillary surfaces and pulmonary microvasculature)
Elimination of H ⁺ in kidney	CA II
Reabsorption of HCO ₃ ⁻ in kidney	CA IV, CA XII
<i>Vision</i>	
Production of aqueous humour (ciliary body)	CA II, CA IV, CA XII
<i>Bone Development and Function</i>	
Differentiation of osteoclasts	CA II
Provision of H ⁺ in osteoclasts for bone resorption	CA II
<i>Metabolic Processes</i>	
Provision of bicarbonate for gluconeogenesis and ureogenesis	CA V
Provision of bicarbonate for pyrimidine synthesis	CA II (possibly also CAV)
Provision of bicarbonate for fatty acid synthesis	CA V (possibly also CAII)
Insulin secretion (production of HCO ₃ ⁻ in pancreatic β cells)	CA V
<i>CSF Production</i>	
Provision of H ⁺ and regulation of pH (choroid plexus)	CA II, CA XII
<i>Gustation and Olfaction</i>	
Maintenance of appropriate CO ₂ levels	CA I, CA II, and/or CA IV
<i>Saliva Production</i>	
Production of HCO ₃ ⁻ (acinar and ductal cells)	CA II
<i>G.L. Tract Protection</i>	
Removal of acid from dental surfaces	CA VI
Removal of acid from gastro-oesophageal mucosa	CA II, VI
<i>Gastric Acid Production</i>	
Production of H ⁺ in stomach (parietal cells)	CA II
<i>Bile Production</i>	
Provision of HCO ₃ ⁻ for bile (liver epithelial duct cells)	CA II
Acidification of bile (gall bladder epithelium)	CA II, CA IV

(continued)

Table 1.3 (continued)

Function	CA isozymes principally involved ^c
<i>Pancreatic Juice Production</i>	
Provision of HCO ₃ ⁻ in pancreas (epithelial duct cells)	CA II
<i>Reproductive System</i>	
Regulation of pH and HCO ₃ ⁻ content of seminal fluid	CA II, CA IV, CA XIII
<i>Muscle Function</i>	
Protection as anti-oxidant against ROS	CA III
Facilitated CO ₂ diffusion	CA II, III, Membrane-bound CA
Buffering in SR (H ⁺ exchanged for Ca ⁺⁺)	Membrane-bound CA (CA IV?)
<i>Oncogenesis</i>	
Regulation of the tumor microenvironment to facilitate tumor growth and metastasis	CA IX and XII

^aEstablished and putative functions

^bThis table is adapted from Chegwidan and Carter (2000)

^cOther CA isozymes may also play a part in several of the processes listed below, in addition to those indicated as being principally involved

against diabetic brain injury (Price et al. 2017), and Alzheimer disease (Fossati et al. 2016).

The CA inhibitor acetazolamide (DIAMOX) first reached the market almost 70 years ago (Maren 1952). Initially developed as a diuretic for the treatment of congestive heart failure (Friedberg et al. 1953), it was adopted soon afterwards for the treatment of glaucoma (Breinin and Görtz 1954; Becker 1954), for which it remained central for several decades. The subsequent development of carbonic anhydrase inhibitors for topical application represented a major advance, since they obviated the undesirable systemic side effects frequently encountered with orally administered carbonic anhydrase inhibitors at the concentrations required to inhibit the enzyme activity in the ciliary processes (Talluto et al. 1997).

In ophthalmology, whilst CA inhibitors have been employed for some time in topically-administered combination therapy for glaucoma (Supuran et al. 2019), in recent years, they have also found use in the treatment of macular edema, secondary to a number of conditions such as retinitis pigmentosa and hereditary retinoschisis, and as a sequela of cataract and vitreoretinal surgery (Strong et al. 2017; Wolfensberger 1999). In addition, the topical CA inhibitors dorzolamide (TRUSOPT) and brinzolamide (AZOPT) have been demonstrated to be effective in the treatment of chronic central serous retinopathy (CSCR) (Liew et al. 2020) and infantile nystagmus syndrome (INS) (Hertle et al. 2015), respectively.

In neurology, CA inhibitors are used for epilepsy (Aggerwal et al. 2013; Silberstein et al. 2005) and for migraine (Silberstein et al. 2005; Silberstein 2017), and to decrease CSF production in pseudotumor cerebri (Thurtell and Wall 2013). There is now a

Table 1.4 Diseases and disorders associated with carbonic anhydrase isozymes

CA isozyme ^a	Associated diseases/disorders
CA I	Bipolar disorder (Hayes 1994; Song et al. 2015), Glaucoma (Maren 1987; Wistrand 2000), Retinal/cerebral edema (Gao et al. 2007),
CA II	Acute mountain sickness (Swenson and Teppems 2007; Swenson 2014a), Alzheimer disease (Jang et al. 2010; Provensi et al. 2019), COPD (Heming et al. 2012), Edema (Supuran 2008), Epilepsy (Aggerwal et al. 2013; Zavala-Tecuapetla et al. 2020), Pulmonary hypertension (Hudalla et al. 2019), Pseudotumor cerebri (Thurtell and Wall 2013), Sleep apnea (Wang et al. 2015)
CA III	Myasthenia gravis (Du et al. 2017), Oxidative stress (Zimmerman et al. 2014; Di Fiore et al. 2018)
CA IV	COPD (Heming et al. 2012), Glaucoma (Matsui et al. 1996), Retinitis pigmentosa (Datta et al. 2009), Stroke (Tang et al. 2006)
CA VA/CA VB	Alzheimer disease (Provensi et al. 2019), Obesity (Spencer et al. 1988; De Simone et al. 2008; De Simone and Supuran 2009)
CA VI	Cariogenesis (Kivelä et al. 1999)
CA VII	Epilepsy (Aggerwal et al. 2013; Zavala-Tecuapetla et al. 2020), Oxidative stress (Di Fiore et al. 2018)
CA IX	Cancer (Závada et al. 1993; Benej et al. 2014)
CA XII	Cancer (Benej et al. 2014; Pastorekova et al. 2006), Glaucoma (Liao et al. 2003)
CA XIV	Epilepsy (Aggerwal et al. 2013; Shah et al. 2005), Retinopathy (Ogilvie et al. 2007)

^aNote Other CA isozymes may also be implicated in several of these diseases/disorders, in addition to those specified above

growing evidence that CA inhibitors may afford a significant neuroprotective effect following both ischemic and hemorrhagic brain injury, inhibiting cerebral edema, reducing cellular levels of ROS, and improving nerve function (Li et al. 2016). Furthermore, mitochondrial carbonic anhydrase, which is considered a major player in glucose-induced production of reactive oxygen species, has been identified as a potential target for the treatment of diabetic injury to the brain and possibly other insulin-insensitive tissues such as eye and kidney (Price et al. 2017; Salameh et al. 2016).

There is also encouraging evidence, obtained through in vitro studies employing human neuronal and glial cell cultures, and in vivo studies employing a rodent AD model, suggesting that CA inhibition may become central to a new therapeutic strategy for Alzheimer disease and related cerebral amyloidosis (Fossati et al. 2016; Solesio et al. 2018).

Possibly, the most significant advances in recent years have been in the association of carbonic anhydrase isozymes with cancer. Whilst both intracellular and extracellular isozymes have been demonstrated to play roles in tumorigenesis, the

emergence of the cell surface isozyme CA IX as an attractive diagnostic and therapeutic biomarker for targeting a wide range of hypoxic, solid malignancies has generated the most interest and activity.

The inhibition of growth of human cancer cells by direct action of specific carbonic anhydrase inhibitors was first observed by Chegwiddden and Spencer (1995, 2003; Chegwiddden et al. 2000) who subsequently reported similar inhibition, by carbonic anhydrase inhibitors, of solid human tumors xenografted into immunodeficient mice (Chegwiddden and Linville 2007). Carbonic anhydrase inhibitors were also shown to inhibit the invasion of renal cancer cells (Parkkila et al. 2000; Chegwiddden et al. 2006) from a range of human cell lines expressing different CA isozymes.

The discovery and characterization of carbonic anhydrase IX, a tumor-associated protein with a central carbonic anhydrase domain, initially designated MN protein, provided significant impetus to the investigation of the then putative role of carbonic anhydrase in cancer (Pastoreková et al. 1992; Pastorek et al. 1994). Whilst many others have made notable contributions, the Pasteroková laboratory, where MN protein was first discovered and characterized, has remained central in this field of endeavor (Benej et al. 2014; Pastoreková and Gillies 2019).

Although the expression of CA IX is almost negligible in normal tissues, where it is restricted to certain tissues of the GI tract and gall bladder epithelia, this isozyme is strongly over-expressed in numerous aggressive malignancies, such as renal, pancreatic, head and neck, ovarian, hepatocellular, lung (NSCLC), and several brain cancers, where, under the regulation of the hypoxia-induced HIF-1 transcription factor, it is a key player in the pH regulation required for cancer cell survival and growth (Pastoreková and Gillies 2019; Thiry et al. 2006; Lau et al. 2017). Thus, this isozyme both provides a therapeutic target in its own right, and also serves as a biomarker for targeting with other cytotoxic agents, thereby avoiding off-target effects.

There are now multiple reports of successful inhibition, by CA inhibitors, of the growth of cultured cells and of xenografts, both derived from a range of human tumors. Several CA inhibitors, both small molecule drug conjugates (SMDCs) and CA IX-selective biological molecules, have entered preclinical or clinical trials for cancer treatment (Lau et al. 2017; Supuran 2017). Among these, the sulfonamide inhibitor SLC-0111 has recently completed phase I clinical trials (Supuran 2017).

Furthermore, there has also been a recent proliferation of activity in the application of novel nanoparticle drug delivery systems directed at CA IX (Kazokaite et al. 2017), ranging from immuno-liposomes (Lin et al. 2017) to “prickly” nanoparticles that destroy targeted cancer cells through physical nano-piercing (Zhang et al. 2017).

References

- Adamson R, Swenson ER (2017) Acetazolamide use in severe chronic obstructive pulmonary disease. Pros and cons. *Ann Am Thorac Soc* 14(7):1086–1093. <https://doi.org/10.1513/AnnalsATS.201701-016FR>

- Aggerwal M, Kondeti B, McKenna R (2013) Anticonvulsant/antiepileptic carbonic anhydrase inhibitors: a patent review. *Expert Opin Ther Patents* 23(6):717–724
- Becker B (1954) Decreases in intraocular pressure in man by a carbonic anhydrase inhibitor, diamox, a preliminary report. *Am J Ophthalmol* 37(1):13–15. [https://doi.org/10.1016/0002-9394\(54\)92027-9](https://doi.org/10.1016/0002-9394(54)92027-9)
- Becker B (1955) Longterm acetazolamide (Diamox) administration in therapy of glaucoma. *Arch Ophthalmol* 54:187–192
- Benej M, Pastorekova S, Pastorek (2014) Carbonic anhydrase IX: regulation and role in cancer. In: Frost SC, McKenna R (eds) Carbonic anhydrase: mechanism, regulation, links to disease, and industrial applications. *J Subcell Biochem* 75:199–219. https://doi.org/10.1007/978-94-007-7359-2_11
- Brandes JL, Saper JR, Diamond M, Couch JR, Lewis DW, Schmitt J, Neto W, Schwabe S, Jacobs D (2004) Topiramate for migraine prevention: a randomized controlled trial. *JAMA* 291(8):965–973. <https://doi.org/10.1001/jama.291.8.965>
- Breinin GM, Görtz H (1954) Carbonic anhydrase inhibitor acetazolamide (diamox): a new approach to the therapy of glaucoma. *AMA Arch Ophthalmol* 52(3):333–348. <https://doi.org/10.1001/archophth.1954.00920050335001>
- Buzás GM, Supuran CT (2016) The history and rationale of using carbonic anhydrase inhibitors in the treatment of peptic ulcers. In memoriam Ioan Pușcaș (1932–2015). *J Enzyme Inhib Med Chem* 31(4):527–533
- Chegwidden WR, Carter ND (2000) Introduction to the carbonic anhydrases. In: Chegwidden WR, Carter ND, Edwards YH (eds) *The carbonic anhydrases: new horizons*. Birkhauser Verlag, Basel, pp 13–28
- Chegwidden WR, Dodgson SJ, Spencer IM (2000) The roles of carbonic anhydrase in biosynthetic processes, cell growth and cancer in animals. In: Chegwidden WR, Carter ND, Edwards YH (eds) *The carbonic anhydrases: new horizons*. Birkhauser Verlag, Basel, pp 343–363
- Chegwidden WR, Linville DG (2007) Growth inhibition of renal cell carcinoma by carbonic anhydrase inhibitors. *J Amer Osteopath Assoc* 107:356–357
- Chegwidden WR, Spencer IM (1995) Sulphonamide inhibitors of carbonic anhydrase inhibit the growth of human lymphoma cells in culture. *Inflammopharmacology* 3:231–239
- Chegwidden WR, Spencer IM (2003) Carbonic anhydrases in cell growth and cancer In: Scharrenberger C, Wittman-Liebold B (eds) *Genes, gene families and isozymes*. Moduzzi Editore SpA, Bologna, pp 189–197
- Chegwidden WR, Gandhi N, Linville DG, Martin A (2006) Inhibition of human renal cancer cell invasion by sulphonamides. *J Amer Osteopath Assoc* 106:503
- Cox SN, Hay E, Bird AC (1988) Treatment of chronic macula edema with acetazolamide. *Arch Ophthalmol* 106(9):1190–1195. <https://doi.org/10.1001/archophth.1988.01060140350030>
- Datta R, Waheed A, Bonapace G, Shah GN, Sly WS (2009) Pathogenesis of retinitis pigmentosa associated with apoptosis-induced mutations in carbonic anhydrase IV. *Proc Natl Acad Sci USA* 106:3437–3442
- De Simone G, Supuran CT (2009) Drug design of antiobesity carbonic anhydrase inhibitors. In: Supuran CT, Winum J-Y (eds) *Drug design of zinc-enzyme inhibitors: functional, structural and disease applications*. Wiley, Hoboken, NJ, pp 241–254
- De Simone G, Fiore A, Supuran CT (2008) Are carbonic anhydrase inhibitors suitable for obtaining antiobesity drugs? *Curr Pharmaceut Des* 14:655–660
- Di Fiore A, Monti DM, Scaloni A, De Simone G and Monti SM (2018) Protective role of carbonic anhydrases III and VII in cellular defense mechanisms upon redox unbalance. *Oxid Med Cell Longev*. Article ID 2018306, 9 p. <https://doi.org/10.1155/2018/2018.306>
- Du A, Huang S, Zhao X, Feng K, Zhang S, Huang J, Miao X, Baggi F, Ostrom RS, Zhang Y, Chen X, Xu C (2017) Suppression of CHRN endocytosis by carbonic anhydrase CAR3 in the pathogenesis of myasthenia gravis. *Autophagy*. <https://doi.org/10.1080/15548627.2017.1375633>

- Eskandari D, Zou D, Karimi M, Grote L, Hedner J (2014) Zonisamide reduces obstructive sleep apnoea: a randomized placebo-controlled study. *Eur Respir J* 44:140–149. <https://doi.org/10.1183/09031936.00158413>
- Eskandari D, Zou D, Grote L, Hoff E, Hedner J (2018) Acetazolamide reduces blood pressure and sleep-disordered breathing in patients with hypertension and obstructive sleep apnea: a randomized controlled trial. *J Clin Sleep Med* 14(3):309–317
- Fossati S, Giannoni P, Solesio ME, Cocklin SL, Cabrera E, Ghiso J, Rostagno A (2016) The carbonic anhydrase inhibitor methazolamide prevents amyloid beta-induced mitochondrial dysfunction and caspase activation protecting neuronal and glial cells *in vitro* and in the mouse brain. *Neurobiol Dis* 86:29–40. <https://doi.org/10.1016/j.nbd.2015.11.006>
- Friedberg CK, Taymoo R, Minor JB, Halpern M (1953) The use of diamox, a carbonic anhydrase inhibitor, as an oral diuretic in patients with congestive heart failure. *N Engl J Med* 248(21):883–889. <https://doi.org/10.1056/NEJM19530521482102>
- Gao BB, Clermont A, Rook S, Fonda SJ, Srinivasav VJ, Wojtkowski M, Fujimoto JG, Avery RL, Arrigg PG, Bursell S-E, Aiello LP, Feener EP (2007) Extracellular carbonic anhydrase mediates hemorrhagic retinal and cerebral vascular permeability through prekallikrein activation. *Nat Med* 13(2):181–188. <https://doi.org/10.1038/nm1534>
- Hayes SG (1994) Acetazolamide in bipolar affective disorders. *Ann Clin Psychiatry* 6(2):91–98. <https://doi.org/10.3109/10401239409148987>
- Heming N, Saïk U, Faisy C (2012) Acetazolamide: a second wind for a respiratory stimulant in the intensive care unit? *Crit Care* 16:318–323
- Hertle RW, Yang D, Adkinson T, Reed M (2015) Topical brinzolamide (Azopt) versus placebo in the treatment of infantile nystagmus syndrome (INS). *Br J Ophthalmol* 99(4):471–476. <https://doi.org/10.1136/bjophthalmol-2014-305915>
- Hilvo M, Baranauskiene L, Salzano AM, Scaloni A, Matuli D, Innocenti A, Scozzafava A, Monti SM, Di Fiore A, De Simone, Lindfors M, Jänis J, Valjakka J, Pastorekova S, Pastorek J, Kulomaa MS, Norlund HR, Supuran C, Parkkila S (2008) Biochemical characterization of CA IX, one of the most active carbonic anhydrase isozymes. *J Biol Chem* 283(41):27799–27809
- Hilvo M, Tolvanen M, Clark A, Shen B, Shah GN, Waheed A, Halmi HM, Hamalainen JM, Vihinen M, Sly WS, Parkkila S (2005) Characterization of CA XV, a new GPI-anchored form of carbonic anhydrase. *Biochem J* 392:83–92
- Hilvo M, Innocenti A, Monti SM, De Simone G, Supuran C, Parkkila S (2008) Recent advances in research on the most novel carbonic anhydrases. *Curr Pharm Des* 14:672–678
- Hudalla H, Michael Z, Christodoulou N, Willis GR, Fernandez-Gonzalez A, Filatava EJ, Dieffenbach P, Fredenburgh LE, Stearman RS, Geraci MW, Kourembanas S, Christou H (2019) Carbonic anhydrase inhibition ameliorates inflammation and experimental pulmonary hypertension. *Am J Respir Cell Mol Biol* 61(4):512–524
- Jang BG, Yun S-M, Ahn K, Song JH, Jo SA, Kim Y-Y, Kim DK, Park MH, Han C, Koh YH (2010) Plasma carbonic anhydrase II protein is elevated in Alzheimer's disease. *J Alzheimers Dis* 21(3):939–945. <https://doi.org/10.3233/JAD-2010-100384>
- Kazokaite J, Aspatwar A, Parkkila S, Matulis D (2017) An update on anticancer drug development and delivery targeting carbonic anhydrase IX. *PeerJ* 5:e4068. <https://doi.org/10.7717/peerj.4068>
- Kivelä J, Parkkila S, Parkkila AK, Rajaniemi H (1999) A low concentration of carbonic anhydrase isoenzyme VI in whole saliva is associated with caries prevalence. *Caries Res* 33:178–184
- Lau J, Lin K-S, Bénard F (2017) Past, present, and future: development of theranostic agents targeting carbonic anhydrase IX. *Theranostics* 7(17):4322–4339. <https://doi.org/10.7150/thno.21848>
- Liao SY, Ivanov S, Ivanova A, Ghosh S, Cote MA, Keefe K, Cova-Prados M, Stanbridge EJ, Lerman MI (2003) Expression of cell surface transmembrane carbonic anhydrase genes *CA9* and *CA12* in the human eye: overexpression of *CA12* (*CAXII*) in glaucoma. *J Med Genet* 40:257–261
- Liew G, Ho I-V, Ong S, Gopinath B, Mitchell P (2020) Efficacy of topical carbonic anhydrase inhibitors in reducing duration of chronic central serous chorioretinopathy. *Trans Vis Sci Tech* 9(13):6–13. <https://doi.org/10.1167/tvst.9.13.6>

- Lin C, Wong BCK, Chen H, Bian Z, Zhang G, Zhang X, Riaz MK, Tyagi D, Lin G, Zhang Y, Wang J, Lu A, Yang Z (2017) Pulmonary delivery of triptolide-loaded liposomes decorated with anti-carbonic anhydrase IX antibody for lung cancer therapy. *Sci Rep* 7(1):1097–1108. <https://doi.org/10.1038/s41598-017-00957-4>
- Lipman GS, Jurkiewicz C, Winstead-Derlega C, Navylt A, Burns P, Walker A, Phillips C, Reilly A, Burnier A, Romero J, Warner K, Hackett P (2019) Day of ascent dosing of acetazolamide for prevention of acute mountain sickness. *High Alt Med Biol* 20(3):271–278. <https://doi.org/10.1089/ham.2019.0007>
- Li M, Wang W, Mai H, Zhang X, Wang J, Gao Y, Wang Y, Deng G, Zhou S, Chen Q, Wang X (2016) Methazolamide improves neurological behavior by inhibition of neuron apoptosis in subarachnoid hemorrhagic mice. *Sci Rep* 6:35055–35067. <https://doi.org/10.1038/srep35055>
- Maren TH (1987) Carbonic anhydrase: general perspectives and advances in glaucoma research. *Drug Dev Res* 10:255–276
- Maren TH (1952) Pharmacological and renal effects of diamox (6063), a new carbonic anhydrase inhibitor. *Trans N Y Acad Sci* 15(2):53. <https://doi.org/10.1111/j.2164-0947.1952.tb01153.x>
- Masini E, Carta F, Scozzafava A, Supuran CT (2013) Antiglaucoma carbonic anhydrase inhibitors: a patent review. *Expert Opin Ther Pat* 23:705–716
- Matsui H, Murakami M, Wynns GC, Conroy CW, Mead A, Maren TH, Sears ML (1996) Membrane carbonic anhydrase (IV) and ciliary epithelium carbonic anhydrase activity is present in the basolateral membranes of the non-pigmented ciliary epithelium of rabbit eyes. *Exp Eye Res* 62:409–417
- Ogilvie JM, Ohlemiller KK, Shah GN, Ulsamov B, Becker TA, Waheed A, Hennig AK, Lukasiewicz PD, Sly WS (2007) Carbonic anhydrase XIV deficiency produces a functional defect in the retinal light response. *Proc Natl Acad Sci USA* 104:8514–8519
- Parkkila S, Rajaniemi H, Parkkila A-K, Kivela J, Waheed A, Pastorekova S, Pastorek J, Sly WS (2000) Carbonic anhydrase inhibitor suppresses invasion of renal cancer cells *in vitro*. *Proc Natl Acad Sci USA* 97:2220–2224
- Pastoreková S, Gillies R (2019) The role of carbonic anhydrase in cancer development: links to hypoxia, acidosis and beyond. *Cancer Metastasis Rev* 38:65–77. <https://doi.org/10.1007/s10555-019-09799-0>
- Pastoreková S, Závadová K, Košťál M, Babuošiková O, Závada J (1992) A novel quasi-viral agent, MaTu is a two-component system. *Virology* 187:620–626
- Pastorekova S, Parkkila S, Závada J (2006) Tumor-associated carbonic anhydrases and their clinical significance. *Adv Clin Chem* 42:167–216
- Pastorek J, Pastoreková S, Callebaur I, Mornon JP, Zelnik V, Opavsky R, Zát'ovicová M, Liao S, Portelle D, Stanbridge EJ, Závada J, Burny A and Kettmann R (1994) Cloning and characterization of MN, a tumor-associated protein with a domain homologous to carbonic anhydrase and a putative helix-loop-helix DNA binding segment *Oncogene* 9:2877–2888
- Price TO, Sheibani N, Shah GN (2017) Regulation of high glucose-induced apoptosis of brain pericytes by mitochondrial CA VA: a specific target for prevention of diabetic cerebrovascular pathology. *Biochem Biophys Acta* 1863(4):929–935. <https://doi.org/10.1016/j.bbdis.2017.01.025>
- Provensi P, Carta F, Nocentini A, Supuran CT, Casamenti F, Passani MB, Fossati S (2019) A new kid on the block? Carbonic anhydrases as possible new targets in Alzheimer's disease. *Int J Mol Sci* 20(19):4724–4740. <https://doi.org/10.3390/ijms20194724>
- Salameh TS, Shah GN, Price TO, Hayden MR, Banks WA (2016) Blood-brain barrier disruption and neurovascular unit dysfunction in diabetic mice: protection with the mitochondrial carbonic anhydrase inhibitor topiramate. *J Pharmacol Exp Ther* 359:452–459. <https://doi.org/10.1124/jpet.116.237057>
- Scozzafava A, Supuran CT, Carta F (2013) Antiobesity carbonic anhydrase inhibitors: a literature and patent review. *Expert Opin Ther Pat* 23(6):725–735. <https://doi.org/10.1517/13543776.2013.790957>

- Shah GN, Ulsamov B, Waheed A, Becker T, Makani S, Svichar N, Chester M, Sly WS (2005) Carbonic anhydrase IV and XIV knockout mice: roles of the respective carbonic anhydrases in buffering the extracellular space in brain. *Proc Natl Acad Sci USA* 102:16771–16776
- Silberstein SB (2017) Topiramate in migraine prevention: a 2016 perspective. *Headache* 57(1):165–178. <https://doi.org/10.1111/head.12997>
- Silberstein SD, Neto W, Schmitt J, Jacobs D (2004) Topiramate in migraine prevention: results of a large controlled trial. *Arch Neurol* 61(4):490–495. <https://doi.org/10.1001/archneur.61.4.490>
- Silberstein SB, Ben-Menachem E, Shank RP, Wiegand F (2005) Topiramate monotherapy in epilepsy and migraine. *Clin Ther* 27(2):154–165. <https://doi.org/10.1016/j.clinthera.2005.02.013>
- Solesio ME, Peixoto PM, Debure L, Madamba SM, de Leon MJ, Wisniewski T, Pavlov EV, Fossati S (2018) Carbonic anhydrase inhibition selectively prevents amyloid β neurovascular mitochondrial toxicity. *Aging Cell* 17:e12787. <https://doi.org/10.1111/accel.12787>
- Song YR, Wu B, Yang YT, Chen J, Zhang LJ, Zhang ZW, Shi HY, Huang CL, Pan JX, Xie P (2015) Specific alterations in plasma proteins during depressed, manic, and euthymic states of bipolar disorder. *Braz J Med Biol Res* 48(11):973–982. <https://doi.org/10.1590/1414-431X20154550>
- Spencer IM, Hargreaves I, Chegwiddden WR (1988) Carbonic anhydrase: a role in the control of fatty acid synthesis? *Isozyme Bull* 21:166
- Strong S, Liew G, Michaelides M (2017) Retinitis pigmentosa-associated cystoid macular oedema: pathogenesis and avenues of intervention. *Br J Ophthalmol* 101:31–37. <https://doi.org/10.1136/brjophthalmol-2016-309376>
- Supuran CT (2008) Diuretics: from classical carbonic anhydrase inhibitors to novel applications of the sulfonamides. *Curr Pharmaceut Des* 14:641–648
- Supuran CT (2017) Carbonic anhydrase inhibition and the management of hypoxic tumors. *Metabolites* 7:48–60. <https://doi.org/10.3390/metabo7030048>
- Supuran CT, De Simone G (eds) (2015) Carbonic anhydrases as biocatalysts. Elsevier B.V.
- Supuran CT, Nocentini A (eds) (2019) Carbonic anhydrases: biochemistry and pharmacology of an evergreen pharmaceutical target. Elsevier Inc.
- Supuran CT, Capasso C, De Simone G (2015b) Carbonic anhydrase II as target for drug design. In: Supuran CT, De Simone G (eds) Carbonic anhydrases as biocatalysts. Elsevier, B.V, pp 51–90
- Supuran CT, Altamimi ASA, Carta F (2019) Carbonic anhydrase inhibition and the management of glaucoma: a literature and patent review 2013–2019. *Expert Opin Ther Pat* 29(10):781–792. <https://doi.org/10.1080/13543776.2109.1679117>
- Swenson ER (2014a) Carbonic anhydrase inhibitors and high altitude illnesses. In: Frost SC, McKenna R (eds) Carbonic anhydrase: mechanism, regulation, links to disease, and industrial applications. *Subcellular Biochem* 75:361–386. https://doi.org/10.1007/978-94-007-7359-2_18
- Swenson ER (2014b) New insights into carbonic anhydrase inhibition, vasodilation, and treatment of hypertensive-related diseases. *Curr Hypertens Rep* 16(9):467. <https://doi.org/10.1007/s11906-014-0467-3>
- Swenson ER, Teppems LJ (2007) Prevention of acute mountain sickness by acetazolamide: as yet an unfinished story. *J Appl Physiol* 102:1305–1307
- Talluto DM, Wyse TB, Krupin T (1997) Topical carbonic anhydrase inhibitors. *Curr Opin Ophthalmol* 8(2):2–6. <https://doi.org/10.1097/00055735-199704000-00002>
- Tang Y, Xu H, Du X, Lit L, Walker W, Lu A, Ran R, Gregg JP, Reilly M, Pancioli A, Khoury JC, et al (2006) Gene expression in blood changes rapidly in neutrophils and monocytes after ischemic stroke in humans: a microarray study. *J Cereb Blood Flow Metab* 26:1089–1102
- Tashian RE, Hewett-Emmett D, Carter N, Bergenheim NCH (2000) Carbonic anhydrase (CA)-related proteins (CA-RPs), and transmembrane proteins with CA or CA-RP domains In: Chegwiddden WR, Carter, ND and Edwards, YH (eds) The carbonic anhydrases: new horizons. Birkhauser Verlag, Basel, pp 105–120
- Thiry A, Dogné J-M, Masareel B, Supuran CT (2006) Targeting tumor-associated carbonic anhydrase IX in cancer therapy. *Trends Pharmacol Sci* 27(11):566–573. <https://doi.org/10.1016/j.tips.2006.09.002>

- Thurtell MJ, Wall M (2013) Idiopathic intracranial hypertension (pseudotumor cerebri): recognition, treatment, and ongoing management. *Curr Treat Options Neurol* 15(1):1–12
- Van Berkel MA, Elefritz JL (2018) Evaluating off-label uses of acetazolamide. *Am J Health Syst Pharm* 75(8):524–531. <https://doi.org/10.2146/ajhp170279>
- Wang T, Eskandari D, Zou D, Grote L, Hedner J (2015) Increased carbonic anhydrase activity is associated with sleep apnea severity and related hypoxemia. *Sleep* 38(7):1067–1073. <https://doi.org/10.5665/sleep.4814>
- Wistrand P (2000) Carbonic anhydrase inhibition in ophthalmology: carbonic anhydrases in cornea, lens, retina and lacrimal gland. In: Chegwiddden WR, Carter, ND and Edwards, YH (eds) *The carbonic anhydrases: new horizons*. Birkhauser Verlag, Basel, pp 413–424
- Wolfensberger TJ (1999) The role of carbonic anhydrase inhibitors in the management of macular edema. *Doc Ophthalmol* 97(3–4):387–397. <https://doi.org/10.1023/a:1002143802926>
- Wolfensberger TJ (2017) Macular edema—rationale for therapy. *Dev Ophthalmol* 58:74–86. <https://doi.org/10.1159/000455275>
- Závada J, Závadová Z, Pastoreková S, Ciampor F, Pastorek J, Zelnick V (1993) Expression of MaTu-MN protein in human cultures and in clinical specimens. *Int J Cancer* 54:268–274
- Zavala-Tecuapetla C, Cuellar-Herrera M, Luna-Munguia H (2020) Insights into potential targets for therapeutic intervention in epilepsy. *Int J Mol Sci* 21:8473–8626. <https://doi.org/10.3390/ijms21228573>
- Zhang H, Liu D, Wang L, Liu Z, Wu R, Janoniene A, Ma M, Pan, G, Baranauskiene L, Zhang L, Cui W, Petrikaite V, Matulis D, Zhao H, Pan J, Santos HA (2017) Microfluidic encapsulation of prickly zinc-doped copper oxide nanoparticles with VD1142 modified spermine acetalated dextran for efficient cancer therapy. *Adv Healthc Mater* 6(11). <https://doi.org/10.1002/adhm.201601406>
- Zhuang GZ, Keeler B, Grant J, Bianchi L, Fu ES, Zhang YP, Erasso DM, Cui J-G, Wiltshire T, Li Q, Hao SKD, Candiotti K, Wishnek SM, Smith SB, Maixner W, Diatchenko L, Martin ER, Levitt RC (2015) Carbonic anhydrase-8 regulates inflammatory pain by inhibiting the ITPR1-cytosolic free calcium pathway. *PLoS One* 10(3):e0118273. <https://doi.org/10.1371/journal.pone.0118273>
- Zhuang GZ, Upadhyay U, Tong X, Kang Y, Erasso DM, Fu ES, Sarantopoulos KD, Martin ER, Wiltshire T, Diatchenko L, Smith SB, Maixner W, Levitt RC (2018) Human carbonic anhydrase-8 AAV8 gene therapy inhibits nerve growth factor signaling producing prolonged analgesia and anti-hyperalgesia in mice. *Gene Ther* 25(4):297–311. <https://doi.org/10.1038/s41434-018-0018-7>
- Zimmerman UJ, Wang P, Zhang X, Bogdanovich S, Forster R (2014) Anti-oxidative response of carbonic anhydrase III in skeletal muscle. *IUBMB Life* 56:343–347

Chapter 2

Carbonic Anhydrase Isozymes as Diagnostic Biomarkers and Therapeutic Targets



Seppo Parkkila

Abstract The early immunohistochemical studies of carbonic anhydrases (CAs) were mainly focused on their normal tissue distribution. Only a few studies included samples from pathologic diseases, particularly cancer. This line of research remained inactive until the discovery of CA IX—the first cancer-associated isozyme. The association of CA IX with hypoxic regions of tumors became obvious, and experimental results confirmed hypoxia regulation. CA IX is now widely considered a biomarker of tumor hypoxia and prognosis. Even though it has several characteristics of a promising biomarker, the implementation of CA IX in clinical pathology has progressed slowly. CA IX research has also produced promising therapeutic molecules, some of which are already in clinical trials. CA XII is another cancer-associated isozyme; however, it is not yet used as a clinical biomarker in routine diagnostics nor is it utilized in therapeutic applications. Surprisingly, the well-known isozyme CA II has turned out to be an attractive candidate as a diagnostic marker, at least in the special case of gastrointestinal stromal tumors. As a conclusion, certain CA isozymes have definite promise as histopathological markers and therapeutic targets. Even though the implementation of new approaches is a slow process in clinical medicine, the first step has been taken to utilize the unique properties of CA isozymes in diagnostics and therapy.

Keywords Biomarker paper · Biomarker · Cancer · Carbonic anhydrase · Diagnostics · Hypoxia · Prognosis

S. Parkkila (✉)

Faculty of Medicine and Health Technology, Tampere University, Arvo Ylpön katu 34, 33520 Tampere, Finland

e-mail: seppo.parkkila@tuni.fi

Fimlab Ltd, Tampere University Hospital, Tampere, Finland

© Springer Nature Switzerland AG 2021

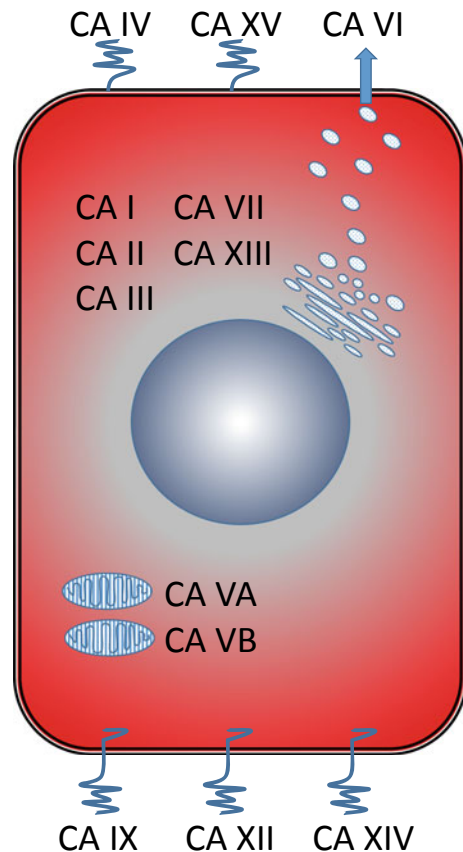
W. R. Chegwidden and N. D. Carter (eds.), *The Carbonic Anhydrases: Current and Emerging Therapeutic Targets*, Progress in Drug Research 75,

https://doi.org/10.1007/978-3-030-79511-5_2

2.1 Short Introduction of Mammalian Carbonic Anhydrases

Among vertebrates, the α -carbonic anhydrases (CAs) are the dominant enzyme forms, and they have distinctive subcellular localizations, tissue distributions, activities, and biological functions. Their key roles include various biological functions, such as the regulation of pH homeostasis, ion transport, gluconeogenesis, ureagenesis, respiration, bone resorption, as well as formation of biological fluids. Thirteen active isozymes have been identified in mammals thus far: five cytoplasmic (CA I, CA II, CA III, CA VII, and CA XIII), five membrane-associated (CA IV, CA IX, CA XII, CA XIV, and CA XV), two mitochondrial (CA VA and CA VB), and one secreted form (CA VI) (Fig. 2.1) (Sly and Hu 1995; Parkkila and Parkkila 1996; Lehtonen et al. 2004; Hilvo et al. 2005). In addition, the CA gene family includes three carbonic anhydrase-related proteins (CARPs) that lack CA catalytic activity due to missing histidine residues in their active sites (Tashian et al. 2000). As with

Fig. 2.1 A typical subcellular localization pattern of the enzymatically active mammalian carbonic anhydrases. CA IV and CA XV are anchored to the plasma membrane through a glycosyl phosphatidylinositol (GPI) linkage. CA XV is not expressed in human tissues (Hilvo et al. 2005). CA IX, XII, and XIV are transmembrane enzymes whose catalytic sites are located to the cell exterior. CA IX and XII are confined to the basolateral plasma membrane, whereas CA XIV has also shown expression at the apical membrane (Kaunisto et al. 2002). CA VA and VB are mitochondrial enzymes, and CA VI is secreted via secretory granules into milk and saliva. The remaining isozymes are expressed in the cytosol



their catalytic activities, all isozymes also differ in their affinity for CA inhibitors. Some of the developed CA inhibitors are clinically used as therapeutic agents in the management of certain diseases, such as glaucoma and epilepsy (Thiry et al. 2007; Mincione et al. 2007; Supuran and Scozzafava 2007). It has become evident that CAs and their inhibitors offer interesting opportunities for both developing novel drugs and as diagnostic tools to improve the health and wellbeing of humans and other species.

2.2 CA II as a Biomarker

CA II, although it is the most active and widely expressed isozyme in human tissues, has attracted much less attention in cancer research compared to the classical tumor-associated isozymes, CA IX and XII. It was first demonstrated by immunohistochemistry that colorectal adenomas and adenocarcinomas do not stain for CA II (Gramlich et al. 1990). Low expression of CA II was later confirmed in a study where CA I, II, and XIII were investigated in parallel tissue sections (Kummola et al. 2005), as well as in a study where the expression of various CA isozymes was analyzed using a microarray technique (Niemela et al. 2007).

CA II is highly expressed in the epithelium of the pancreatic ducts, where it is involved in the production of bicarbonate-rich pancreatic juice (Parkkila and Parkkila 1996; Parkkila et al. 1995a). The expression rate of CA II in the ductal cells, which is sustained after malignant transformation, does not correlate with the malignancy of tumors, suggesting a limited value for CA II reactivity in histopathological diagnostics of pancreatic adenocarcinoma (Parkkila et al. 1995a).

It is well-known that CA II is prominently present in both gastric parietal cells and bicarbonate-producing surface epithelial cells of the stomach, whereas it is only weakly expressed in the esophageal epithelium (Parkkila et al. 1994). Recently, the expression and clinical significance of CA II, IX, and XII were investigated in Barrett's esophagus and esophageal adenocarcinoma (EAC) (Nortunen et al. 2018). Even though CA II was significantly downregulated in metastatic disease, it was concluded that none of the tested isozymes could provide additional value as a biomarker for esophageal adenocarcinoma.

Two recent articles have provided congruent results showing that the reduction of CA II expression in gastric tumors is associated with tumor growth, metastasis, and poor prognosis. The first report demonstrated that the expression of CA II was significantly higher in the normal gastric mucosa than in the intraepithelial neoplasia and gastric carcinoma (Li et al. 2012). The positive signal for CA II was significantly more frequent in gastric carcinoma at early stages compared to more advanced stages. The rate of positive CA II signal was significantly lower in poorly differentiated gastric carcinoma than in moderately or well-differentiated tumors. The patients with CA II-positive tumors showed a better survival rate than those with CA II-negative tumors. The second publication confirmed that CA II expression is significantly decreased in gastric cancer compared with the normal gastric mucosa (Hu et al. 2014).

Low expression was significantly associated with tumor size, depth of invasion, lymph node involvement, distant metastasis, and TNM stage, and it predicted poor survival in gastric cancer patients.

Viikilä et al. recently investigated the expression of CA II, VII, IX, and XII in a series of colorectal carcinoma samples from 593 patients (Viikila et al. 2016). Only CA II and XII showed statistically significant correlations to patient survival in that higher expression indicated poorer prognosis. CA II staining associated with the patient age group, while no other significant correlation was reported between the isozymes and various clinicopathological parameters.

The most promising results for CA II as a potential biomarker were published in 2010, when the enzyme was identified in gastrointestinal stromal tumors (GISTs) (Parkkila et al. 2010). GISTs represent the most common mesenchymal tumor category of the gastrointestinal tract and include tumors with low malignancy and those that behave as highly malignant metastasizing neoplasias. KIT expression is a nearly consistent phenotypic feature of GISTs, and oncogenic activation of KIT or PDGFRA receptor tyrosine kinase signaling is considered pathogenetically important (Miettinen and Lasota 2006). GISTs originate from Cajal cells of the gastrointestinal wall (Kindblom et al. 1998); thus, the tumors can arise in various gastrointestinal locations. The Western blotting experiments first indicated that CA II is highly expressed in GIST cell lines (Parkkila et al. 2010). Subsequently, CA II expression was analyzed in 175 GISTs, of which 95% showed positive immunostaining. The CA II expression in GISTs did not correlate with particular *KIT* or *PDGFRA* mutation types. CA II was absent or expressed at low levels in the other mesenchymal tumor categories that were analyzed in that particular study. High CA II expression was associated with a better disease-specific survival rate than low or no expression. The results indicated that CA II is quite selective to this tumor type among various mesenchymal tumors; therefore, it might be a useful biomarker in diagnostics.

Recently, CA II expression was studied in another type of gastrointestinal tumors, called pseudomyxoma peritonei (Jarvinen et al. 2017). The specimens were collected from 89 patients with this malignancy; the tissue sections were immunostained for CA II, and the expression was analyzed against the survival of the patients. Positive CA II expression was found in 65% of patients. The 5-year overall survival rates for the CA II-positive and -negative cases were 80 and 59%, respectively, reaching a clear statistical significance. It was suggested based on the results that the expression of CA II acts as an independent prognostic biomarker in pseudomyxoma peritonei.

CA II is expressed in at least many, if not in most, cases of hematological malignancies. Leppilampi et al. investigated the presence of CA isozymes in malignant hematopoietic cell lines and malignant blast cells of bone marrow samples (Leppilampi et al. 2002). Three out of six malignant hematopoietic cell lines expressed CA II, whereas no expression was detected for CA I, IX, or XII. The positive reactions were found in 62% of acute myeloid leukemia samples, 73% of acute lymphoblastic leukemias, and 50% of chronic myelomonocytic leukemias. The results indicated that CA II expression is not restricted to one cell lineage but may result from a genetic aberration that occurs in both myeloid and lymphatic lineages or in their progenitor cells.

CA II is expressed in various brain tumors, including astrocytic tumors, oligodendrogliomas, ependymal and choroid plexus tumors, and tumors of nerve sheath cell origin (Parkkila et al. 1995b). In brain tumors, a significant fraction of CA II reactivity is, in fact, located in the capillary endothelium (Haapasalo et al. 2007). A similar pattern of ectopic CA II expression has been demonstrated in the endothelium of neovessels of several other cancers, including melanoma and esophageal, renal, and lung tumors (Yoshiura et al. 2005).

2.3 CA IX as a Biomarker

Among different CA isozymes, CA IX has shown the highest promise as a potential biomarker of certain tumors. In fact, there are already over 1000 publications available on the combined topics of CA IX and cancer, although CA IX is not fully specific for cancer cells only. Among various normal tissues, CA IX is abundantly present in the basolateral plasma membranes of the gastrointestinal epithelia (Pastorekova et al. 1997). The highest levels of the enzyme are present in the epithelial cells of both gastric and gall bladder mucosa. The expression is prominent also in the proximal gut, i.e., in the duodenum and jejunum, and it is moderate in the ileum and colon, while it diminishes towards the rectum (Saarnio et al. 1998a). In contrast to the gastric epithelium, where the enzyme is highly expressed by the surface epithelial cells and parietal cells, the expression in the intestinal epithelium is confined to the deep proliferating areas, the crypts of Lieberkühn. As the cells migrate along the intestinal villus, they differentiate and gradually lose their CA IX expression, suggesting that it may have a role in the proliferation and differentiation of epithelial cells. In addition to the stomach, gallbladder, and intestine, CA IX expression has been detected in the human biliary epithelium, pancreatic ducts, male reproductive organs, and mesothelium (Pastorekova et al. 1997; Saarnio et al. 2001; Kivela et al. 2000a; Karhumaa et al. 2001; Ivanov et al. 2001).

CA IX is a highly active enzyme with catalytic activity in the same range with CA II (Hilvo et al. 2008). The high enzyme activity of CA IX may be of potential significance for tumor growth and invasion. According to the current paradigm, CA IX functionally contributes to the acidification of the extracellular microenvironment surrounding cancer cells by interacting directly with ion transport proteins; accordingly, it may neutralize the intracellular space of tumor cells (Ivanov et al. 1998; Svasstova et al. 2004). The protons produced by CA IX may remain outside and increase the acidity of the tumor microenvironment (Pastorekova et al. 2006). In fact, there are several pieces of evidence that CA IX physically and functionally interacts with bicarbonate transport proteins AE1, AE2, and AE3 and with sodium-dependent electroneutral bicarbonate cotransporter (NBCn1) (Morgan et al. 2007; Svasstova et al. 2012; McDonald et al. 2018). CA IX also associates with proteins involved in amino acid transport, including AA transport heavy chain subunit, CD98hc (SLC3A2), L-type AA transporter, LAT1 (SLC7A5), alanine-serine-cysteine-preferring transporter

2, ASCT2 (SLC1A5), and sodium-coupled neutral amino acid transporter 2, SNAT2 (SLC38A2) (McDonald et al. 2018).

It is well-documented that CA IX is highly expressed in various tumors, including those that arise from the GI tract (Pastorekova et al. 2006, 2004). As the first example, many colorectal tumors overexpress CA IX (Niemela et al. 2007; Saarnio et al. 1998b). CA IX is the only CA isozyme that is overexpressed in hereditary nonpolyposis colorectal cancer (HNPCC) (Niemela et al. 2007). In colorectal tumors, CA IX has shown high expression in premalignant lesions and often a lower signal in poorly differentiated malignancies, suggesting that it might be a useful marker in the early diagnosis of colorectal tumorigenesis. More recent studies have indicated, however, that CA IX is not a prognostic factor in colorectal cancer (Viikila et al. 2016).

Turner et al. were the first to suggest that tumor-associated CA IX may play a role in the proliferation and regeneration of esophageal squamous epithelium, and loss of its expression may be related to cancer progression in Barrett's-associated adenocarcinomas (Turner et al. 1997). Later, it was reported that 44.5% of esophageal carcinomas show strong CA IX expression, and the high expression is an independent prognostic factor for shorter overall and disease-free survival (Birner et al. 2011). In another study, high CA IX expression was associated with tumorigenesis markers BMI1, MCM4, and MCM7, suggesting that CA IX may play a role in early tumorigenesis (Huber et al. 2015). In contrast to the previous results, CA IX was not found to be a significant prognostic marker in patients with esophageal adenocarcinoma. In the most recent study, Nortunen et al. analyzed CA IX expression in a series of esophageal adenocarcinomas and Barrett's esophagus (Nortunen et al. 2018). The normal squamous epithelium of the esophagus was almost completely negative for CA IX. The signal was strong in gastric metaplasia and present in all cell types across the epithelium. The expression levels decreased from gastric metaplasia to intestinal metaplasia, dysplastic lesions, and finally to adenocarcinoma. In intestinal metaplasia, the expression was still strong and showed basal dominance. The CA IX expression in carcinomas showed no significant correlation with clinicopathological variables or survival, although high CA IX expression appeared to associate weakly with nodal spread.

In the liver, CA IX is localized to the biliary epithelial cells (Pastorekova et al. 1997). Analogously, CA IX is expressed by the biliary epithelial tumors (Saarnio et al. 2001). It seems plausible that CA IX expression indicates better prognosis in intrahepatic cholangiocarcinoma (Gu 2015), even though CA IX is typically associated with poor prognosis in many other tumor categories. One of these examples is hepatocellular carcinoma, in which CA IX is expressed only in a minority of cases. In a large cohort of patients, Kang et al. showed that 15.1% of the cases expressed CA IX at low level, and 5.2% belonged to the high CA IX-positive group (Kang et al. 2015). CA IX expression was a prognostic factor for poorer survival after surgery for hepatocellular carcinoma. In addition, the high CA IX-positive group had even a poorer prognosis than the low CA IX-positive group. Recently, it was further confirmed that CA IX is, indeed, a predictive factor for poor prognosis after radical surgery for hepatocellular carcinoma (Hyuga et al. 2017). Finkelmeier et al. recently published an interesting study where they analyzed circulating CA IX enzyme levels in patients

with hepatocellular carcinoma or cirrhosis (Finkelmeier et al. 2018). They included 215 patients with hepatocellular carcinoma in the study. The median serum CA IX concentration in patients with hepatocellular carcinoma was 370 pg/ml, and it was significantly higher than in controls (41 pg/ml). The patients with high serum CA IX concentrations (>400 pg/ml) had an increased mortality risk. Surprisingly, the serum CA IX concentration in cirrhotic patients did not differ significantly from the patients with hepatocellular carcinoma. Higher CA IX levels in cirrhotic patients correlated with portal hypertension and esophageal varices, and the patients with ethanol-induced cirrhosis had the highest CA IX levels.

Ectopic expression through hypoxia regulation is an important hallmark of CA IX; therefore, CA IX is most highly expressed in tumors that originate from CA IX-negative tissues. Because the normal gastric mucosa contains the highest levels of CA IX among normal tissues, it was not surprising that gastric carcinomas showed relatively low expression (Leppilampi et al. 2003). Nakamura et al. have shown that the expression of CA IX in gastric cancer is predominantly regulated by the methylation of a single CpG rather than by hypoxia (Nakamura et al. 2011). A subgroup of gastric cancers retain CA IX expression in cancer cells at the invasion front (Chen et al. 2005). It has been shown that overexpression of CA IX is important for tumor invasion and metastasis; as such, it may serve as a useful prognostic indicator of long-term survival in patients with gastric adenocarcinoma (Senol et al. 2016).

CA IX is not prominently expressed in any normal neural tissues. Interestingly, it is highly expressed in some cases of brain tumors. The first publication on this topic was published by Haapasalo et al., showing a positive signal for CA IX in 78% of astrocytomas (Haapasalo et al. 2006). The staining pattern followed the distribution of hypoxic regions within tumor specimens. The CA IX immunoreactivity showed a strong association with tumor malignancy grades. CA IX showed no association with p53 expression, nor did it correlate with epidermal growth factor receptor-amplification, apoptosis, or cell proliferation. CA IX intensity had significant prognostic value in survival analysis, which was confirmed later by other researchers (Cetin et al. 2018). In oligodendroglial tumors, CA IX was positive in 80% of the cases, and it again correlated with poorer outcome (Jarvela et al. 2008). CA IX expression has also been studied in rare pediatric brain tumors, including primitive neuroectodermal tumors and medulloblastomas (Nordfors et al. 2010). CA IX-positive staining was observed in 23% of the cases, and its expression predicted poor prognosis of patients. Since the presence of hypoxic and necrotic areas represents an important criterion in glioma diagnostics, CA IX has become a useful biomarker for this tumor category. Accordingly, the neuropathologists of Tampere University Hospital already utilize CA IX immunostaining as a routine diagnostic asset for this clinical purpose (Dr. Hannu Haapasalo, personal communication).

CA IX expression has been studied in a variety of lung cancers. Ramsey et al. analyzed CA IX immunohistochemical expression in pulmonary/pleural tumors, including metastatic clear cell renal carcinoma of the lung, mesothelioma, squamous cell carcinoma, small cell carcinoma, and adenocarcinoma (Ramsey et al. 2012). All cases of metastatic clear cell carcinomas and mesotheliomas were positive for CA

IX. Most cases of lung squamous cell carcinoma and small cell carcinoma were positive, while the enzyme was less frequently present in pulmonary adenocarcinoma. The high expression of CA IX in mesotheliomas was later confirmed in a series of 27 malignant pleural mesotheliomas (Kivela et al. 2013). According to the immunohistochemical and follow-up data, CA IX expression predicts a poor survival rate in lung cancer (Kim et al. 2004, 2005). The presence of CA IX has been specifically linked to the expression of proteins that are involved in angiogenesis, apoptosis inhibition, and cell–cell adhesion disruption, which explains the strong association of the enzyme with poor clinical outcomes (Giatromanolaki et al. 2001). However, recent studies have indicated that the inclusion of CA IX as one criterion does not improve the prognostic accuracy of blood biomarkers for the diagnostics of non-small cell lung cancer (Carvalho et al. 2016).

Cervical cancer was one of the first cancer types in which CA IX expression was studied in detail (Liao et al. 1994). Loncaster et al. (2001) showed clinical evidence that CA IX expression in cervical cancer correlates with the levels of tumor hypoxia and associates with a poor prognosis of the disease (Loncaster et al. 2001). The authors suggested that the level of CA IX expression may be used to select patients who would benefit most from hypoxia-modification therapies or bioreductive drugs. Maseide et al. noticed that high CA IX expression predicts a poor prognosis for patients with soft tissue sarcoma (Maseide et al. 2004). Hynninen et al. investigated the expression of CA II, CA IX, and CA XII in a series of gynecological malignancies, including adenocarcinomas and mesenchymal tumors, such as sarcomas and leiomyomas (Hynninen et al. 2012). Positive staining of CA II, CA IX, and CA XII was detected in many cases of sarcomas. The study confirmed the earlier positive results of CA IX expression in leiomyosarcoma (Mayer et al. 2008), and it also added new data on the expression levels of CA IX in stromal sarcomas and mixed Müllerian tumors. In addition to the results for CA IX, the findings showed that CA II and CA XII are often weakly or moderately expressed in these mesenchymal tumors. Among these tumors, all isozymes showed variable staining results, suggesting that they have only limited value in sarcoma diagnostics if used alone. The specimens involved a total of 33 leiomyomas, all of which were negative for CA II and CA XII. Previously, using another series of tumors, Mayer et al. reported that all leiomyomas are negative for CA IX (Mayer et al. 2008). In contrast, Hynninen et al. reported that 33 leiomyoma specimens included five cases that were CA IX-positive. The biological role and mechanism of CA IX induction in leiomyomas remained unresolved, however. There were at least no other visible signs of hypoxia in the tissue sections.

Ovarian tumors is another category of tumors in which CA IX is highly expressed (Hynninen et al. 2006). Most cases of borderline mucinous cystadenomas, mucinous cystadenocarcinomas, and serous cystadenocarcinomas are moderately or strongly positive for CA IX. In malignant tumors, the expression patterns have shown clear correlations to hypoxic regions. The high expression levels of CA IX in mucinous and serous cystadenocarcinomas suggested that these tumors could be considered potential candidates for CA IX-targeted therapy.

The current literature already includes a number of publications on CA IX expression in breast tumors. A study by Bartosová et al. indicated that ectopic activation of

the *CA9* gene may be implicated in breast carcinogenesis, and it also suggested that CA IX could be a breast cancer marker (Bartosova et al. 2002). The main conclusion from several expression studies is that CA IX indicates poor prognosis in breast cancer (Brennan et al. 2006; Hussain et al. 2007; Chia et al. 2001), even though Span et al. demonstrated that CA IX is more predictive than prognostic in this cancer type (Span et al. 2007).

The expression of CA IX has been examined in head and neck squamous cell carcinoma (HNSCC) (Beasley et al. 2001). The enzyme was related to the location of tumor microvessels, angiogenesis, necrosis, and tumor stage, and it was considered a potential target for future therapy in HNSCC. The follow-up studies have included CA IX in the panels of possible predictive markers in HNSCC (Schutter et al. 2005; Le et al. 2007). Although combinations of markers have been associated with treatment outcome, their clinical value as predictive factors must still be established (Hoogsteen et al. 2007).

Both CA IX and CA XII have been investigated in both the normal skin and skin tumors (Syrjanen et al. 2014). In the normal skin, the highest expression of CA IX was detected in hair follicles, sebaceous glands, and basal parts of the epidermis. CA XII was detected in all epithelial components of the skin. Both CA IX and CA XII expression levels were significantly different in epidermal, appendageal, and melanocytic tumor categories. Both CA IX and XII showed the most intense immunostaining in epidermal tumors, whereas virtually all melanocytic tumors were devoid of CA IX and XII immunostaining. In premalignant lesions, CA IX expression significantly increased when the tumors progressed to more severe dysplasia forms.

The story about CA IX in kidney tumors and its role as a prognostic marker is rather complicated because of an alternative mechanism of upregulation of CA IX expression due to von Hippel-Lindau gene mutations in certain tumors. Human renal cancer cell lines and renal cancers have shown high expression of CA IX mRNA and CA IX protein (McKiernan et al. 1997; Parkkila et al. 2000). CA IX is mostly, but not fully, specific to clear cell renal cell carcinoma among various kidney tumors. Notably, the most common tumor of the pediatric kidney, Wilms' tumor, has shown 63% positivity for CA IX, although the median fraction of positive cells was only 5% (Dungwa et al. 2011). Sandlund et al. assessed CA IX expression in different subtypes of renal cell cancer (Sandlund et al. 2007). They found that the expression is higher in conventional clear cell renal cell carcinoma compared to other renal cancer types. They also reported that the patients with clear cell carcinoma have a less favorable prognosis when the CA IX expression is low. In line with those findings, CA IX has also been described as a prognostic marker in metastatic clear cell carcinoma (Bui et al. 2003). Limited CA IX expression in the area of 85% or less has been associated with poorer cancer-specific survival (Pickering and Larkin 2015). This exact criterion seems to be valid in metastatic tumors only, and based on present knowledge, CA IX expression may not represent a reliable prognostic factor in localized clear cell renal cell carcinomas (Pickering and Larkin 2015). The present literature available on CA IX in renal cancer suggests that the enzyme may represent not only a useful prognostic marker for metastatic clear cell renal cell carcinoma but also a promising therapeutic target for novel oncological applications, including

immunotherapy and radioisotopic methods (Pastorekova et al. 2006; Bleumer et al. 2006).

The thyroid cancers express both CA IX and CA XII with different patterns (Takacova et al. 2014). Among various thyroid tumors, the highest expression of CA IX was reported in medullary thyroid carcinoma and anaplastic carcinoma, where positive immunostaining was reported in 91.67 and 100% of cases, respectively. Only limited expression of CA IX was detected in well-differentiated tumors (3.8% of papillary thyroid carcinoma and 12% of follicular thyroid carcinoma). The highest positivity for CA XII was found in papillary carcinoma (91.7%).

Very recent investigations have demonstrated CA IX expression in lymphoma cells (Mehes et al. 2019). More specifically, positive signal was found in Reed-Sternberg cells of Hodgkin's lymphoma in 39/81 samples (48.1%). In contrast, CA XII expression in these cells was present in only 18/77 samples (23.4%). For the CA IX-positive group, 72 month-progression-free survival was significantly lower compared with the CA IX-negative cases, while the overall survival did not differ significantly.

As this chapter indicates, there have been many studies investigating the prognostic value of CA IX expression in patients with solid tumors. In 2016, van Kuijk et al. published the first meta-analysis covering 147 studies on CA IX expression in various tumor categories (excluding renal cancer because of different regulation) (Kuijk et al. 2016). Overall, the results showed that high CA IX expression is an adverse prognostic marker in solid tumors (excluding renal tumors). A strong association between high expression and poor prognosis was reported in the majority of different tumor sites, supporting a pivotal role of CA IX in disease progression and treatment resistance in various cancers.

2.4 CA IX Immunoassay Data

Currently, CA IX immunoassay reagents and methods are available from several commercial sources, even though it is not always possible to define the original manufacturer based on the incomplete datasheet or other public data. Some examples of the commercial assays are shown in Table 2.1. Many articles have been already published where CA IX concentrations were detected from human biological fluids, including serum, plasma, pleural effusion, or urine. In most studies, the data have been collected from patients with renal cancer (Lucarini et al. 2018; Gigante et al. 2012; Li et al. 2008; Zavada et al. 2003; Zhou et al. 2010; Papworth et al. 2010; Pena et al. 2010). Based on immunohistochemical data, it is obvious that CA IX expression is much more common in clear cell renal cell carcinoma than in other neoplasms of the kidney (Genega et al. 2010). Immunoassay results of CA IX have recently shown that the expression levels are very high in the plasma of patients with clear cell renal cell carcinoma (Lucarini et al. 2018). High serum CA IX levels are significantly associated with shorter overall survival (Gigante et al. 2012), suggesting that increased shedding of the enzyme into circulation is a hallmark for poor prognosis.

Table 2.1 Examples of commercially available ELISA immunoassays for CA IX

Manufacturer/distributor	Name of the assay	Detection range (pg/ml)	References
Boster Biological Technology	PicoKine™ ELISA	15.6–1000	
R&D Systems	Human Carbonic Anhydrase IX Quantikine ELISA Kit	15.6–1000	Gigante et al. (2012), Tanaka et al. (2008), Goodison et al. (2012), Shimizu et al. (2016)
R&D Systems	Human Carbonic Anhydrase IX DuoSet ELISA	15.6–1000	Dungwa et al. (2011), Liao and Lee (2012)
Biomatik	Carbonic Anhydrase IX (Human) ELISA Kit	32–2000	
LifeSpan BioSciences	Human CA9/Carbonic Anhydrase IX ELISA Kit (CLIA)	8–500	
LifeSpan BioSciences	Human CA9/Carbonic Anhydrase IX ELISA Kit (Sandwich ELISA)	0.205–20	
LifeSpan BioSciences	Human CA9/Carbonic Anhydrase IX ELISA Kit (Sandwich ELISA)	32–2000	
LifeSpan BioSciences	Human CA9/Carbonic Anhydrase IX ELISA Kit (Sandwich ELISA)	15.6–1000	
Assay Solution	Human Carbonic Anhydrase IX ELISA Kit (Colorimetric)	31.3–2000	
GenWay Biotech	Human Carbonic Anhydrase IX ELISA Kit	32–2000	
Aviva Systems Biology	Carbonic Anhydrase IX ELISA Kit (Human)	32–2000	
Biorbyt	Human Carbonic Anhydrase IX (CA9) ELISA kit	–	
Bioassay Technology Laboratory	Human Carbonic Anhydrase 9 ELISA kit	50–30,000	
Creative Diagnostics	Carbonic Anhydrase IX ELISA Kit	32–2000	
Pacific Biomarkers	CA 9 (Carbonic Anhydrase IX)	–	
Sigma-Aldrich	Human Carbonic Anhydrase IX ELISA Kit	–	

(continued)

Table 2.1 (continued)

Manufacturer/distributor	Name of the assay	Detection range (pg/ml)	References
Cloud-Clone Corp	ELISA Kit for Carbonic Anhydrase IX (CA9)	7.81–500	

Woelber et al. analyzed the CA IX levels in both ovarian (Woelber et al. 2010) and cervical cancer patients (Woelber et al. 2011). They found that the enzyme concentration did not change significantly during the first-line therapy of ovarian cancer and were not prognostically relevant. Similarly, the serum concentrations of CA IX did not correlate with intratumoral expression of the enzyme or other clinicopathological variables in cervical cancer. Ilie et al. analyzed CA IX levels from patients with non-small cell lung cancer and found that the high plasma level of CA IX is an independent biomarker of poor prognosis (Ilie et al. 2010). Ostheimer et al. combined three markers, including osteopontin, vascular endothelial growth factor, and CA IX (Ostheimer et al. 2014). They found that high pretreatment plasma levels of these markers additively correlated with prognosis in M0-stage non-small cell lung cancer. CA IX concentrations have also been studied from pleural effusions of patients with various pathologies (Liao and Lee 2012). It was found that CA IX levels were significantly higher in the effusions collected from the patients with malignant diseases compared to those collected from patients with various benign diseases. Rosenberg et al. investigated CA IX levels by ELISA in patients with head and neck cancer (Rosenberg et al. 2016). They found that high pretreatment CA IX concentration is a negative prognostic factor in locally advanced tumors.

2.5 CA XII in Cancer

CA XII is broadly similar in overall structure to CA IX, excluding the proteoglycan-like domain of CA IX. The expression of CA XII is also induced by hypoxic conditions (Ivanov et al. 1998), but its distribution in tissues does not correlate with hypoxic regions to the same extent as CA IX. It has been demonstrated that the expression of CA XII is under estrogen receptor regulation, and the expression in breast tumors is associated with positive estrogen alpha receptor status (Watson et al. 2003; Wykoff et al. 2001; van't Veer et al. 2002).

Like CA IX, CA XII may also function in metabolons together with ion transport proteins. It has been reported that it regulates the function of the chloride–bicarbonate exchanger (AE2) (Hong et al. 2015; Waheed and Sly 2017). Mutations in the *CA12* gene have been associated with an autosomal recessive form of salt wasting disease that results in hyponatremia in some Bedouin families (Feldshtein et al. 2010; Muhammad et al. 2011). The clinical symptoms of the trait include high sweat chloride concentration, dehydration, and failure to thrive in infancy.

Expression of CA XII has been quite extensively studied in both normal tissues and several types of cancer. It is expressed in the normal kidney (Parkkila et al. 2000), colon (Kivela et al. 2000b), endometrium (Karhumaa et al. 2000), and skin (Syrjanen et al. 2014), and its heterogenous expression pattern in tumors may reduce its potential as a biomarker (Pastorekova et al. 2006). Expression of CA XII transcripts in nonpigmented epithelial cells of retina has also been reported (Liao et al. 2003), and these epithelial cells from glaucoma patients showed increased *CA12* gene expression. From these results, it has been concluded that CA XII is expressed in ciliary cells, and thus, may be involved in aqueous humor production.

One of the first publications on CA XII demonstrated its distribution in colorectal tumors (Kivela et al. 2000b). Most cases of adenomatous polyps were positive for CA XII, and the staining became more diffusely spread within the lesion with a more severe grade of dysplasia. Among 20 malignant colorectal tumors, 19 showed positive reactions that were typically diffuse, being present in both the superficial and deep parts of the mucosa. In contrast, the normal colorectal mucosa shows CA XII-positive signal in the superficial part of the mucosa, whereas staining is usually absent in the deep part of the mucosa. Another early publication described the expression of CA XII in various tumor categories (Ivanov et al. 2001). The highest rates of distinct positive signal were reported in cervical carcinomas and intraepithelial neoplasias, endometrial carcinoma, ovarian carcinomas and cystadenomas, breast ductal and lobular carcinomas, renal cancers excluding Wilms' tumor, colon adenomas, and gliomas.

The original discovery of CA XII was published almost simultaneously by two independent groups (Ivanov et al. 1998; Tureci et al. 1998). The first findings already linked CA XII to kidney function and renal cancer. In the human kidney, CA XII was located to the basolateral plasma membrane of the epithelial cells in the thick ascending limb of Henle, distal convoluted tubules, and collecting ducts (Parkkila et al. 2000). A weak basolateral signal was also detected in the epithelium of the proximal convoluted tubules. In a series of 31 renal tumors, the enzyme showed moderate or strong expression in most oncocytomas and clear cell carcinomas.

CA XII seems to be expressed in the normal stratified squamous epithelium, including the esophagus and skin (Nortunen et al. 2018; Syrjanen et al. 2014). In pathological tumor stage 2–3 of esophageal squamous cell carcinoma, the 3-year survival rate of patients with the high-grade expression of CA XII (29.1%) was significantly lower than that of patients with the low-grade expression of CA XII (70.3%) (Ochi et al. 2015). A multivariate analysis showed that the expression of CA XII was one of the most important independent prognostic factors following radical esophagectomy in tumor stage 3–4 carcinomas.

An alternatively spliced form of CA XII is expressed in brain tumors (Haapasalo et al. 2008). RT-PCR revealed that the enzyme present in diffuse astrocytomas is mainly encoded by a shorter mRNA variant. Anti-CA XII antibody recognized both isoforms in the glioblastoma cell lines. Most diffusely infiltrating astrocytomas (98%) showed positive immunoreactions for CA XII protein. Importantly, the expression correlated with poorer patient prognosis in univariate and multivariate survival analyses. The absence of 11 amino acids in the short variant, which seems to be a common

form in astrocytomas, may affect the normal quaternary structure and biological function of CA XII.

To date, there have been a few studies elucidating the prognostic value of CA XII. Watson et al. examined the CA XII expression in a series of 103 cases of invasive breast cancer and found a positive correlation with a lower relapse rate and a better survival (Watson et al. 2003). Kim et al. analyzed both CA IX and XII expression in cervical cancer and found CA IX and CA XII transcript expression in 62.7 and 88.1% of tumors, respectively (Kim et al. 2006). Multivariate analysis revealed that CA IX expression was the most significant factor associated with lower metastasis-free survival, whereas CA XII expression was linked to a lower risk of metastasis and better survival.

By comparing the current literature on CA IX and XII, it is obvious that CA IX has greater promise as a histological marker protein. Nevertheless, CA XII is physiologically an interesting member of the CA family, and its exact roles still deserve further investigations.

2.6 Carbonic Anhydrases as Therapeutic Targets

CA research has produced large amounts of data on the distribution, functions, and clinical relevance of different isozymes. These enzymes have been considered therapeutic targets for treatments of various diseases, such as glaucoma, mountain sickness, brain edema, cancer, and epilepsy. In most cases, CA II has been considered the main target enzyme, even though several isozymes are typically expressed in target tissues, and inhibitors can inhibit several isozymes with different affinities. Several drugs with CA inhibitory properties are clinically used, and more are under development to treat important diseases. The clinically approved drugs with CA inhibition properties include acetazolamide, methazolamide, ethoxzolamide, dichlorphenamide, dorzolamide, brinzolamide, topiramate, zonisamide, lacosamide, imatinib, and statins (Pastorekova et al. 2004; Temperini et al. 2010; Parkkila et al. 2012, 2009). Because other chapters of this book describe different clinical targets in great detail, only glaucoma and cancer are briefly mentioned here as examples.

Glaucoma has been a major disease target where CA inhibition has been proven a useful therapeutic option. In the 1950s, the effect of acetazolamide on intraocular pressure was first demonstrated (Becker 1955). The first generation CA inhibitors for treatment of glaucoma included systematically acting drugs: acetazolamide, methazolamide, and dichlorphenamide (Scozzafava and Supuran 2013). The second generation CA inhibitors were topically acting sulfonamides, dorzolamide, and brinzolamide, which possess both water solubility and liposolubility to penetrate the cornea, and they can enter the ciliary process where the CAs are present. More recently, the third generation CA sulfonamide inhibitors have been developed based on the novel “tail approach.” These topically administered compounds have shown 2–3 times higher effects in reducing intraocular pressure compared to dorzolamide (Scozzafava and Supuran 2013). Supuran’s group has suggested that dithiocarbamates

could represent the fourth CA inhibitor group for antiglaucoma therapy (Scozzafava and Supuran 2013; Carta et al. 2012). Many dithiocarbamates inhibit CA II in the low nanomolar range, are easy to synthesize, and possess excellent water solubility. Therefore, some dithiocarbamates may arrive in clinical testing soon.

The connections of CAs with various forms of cancer are obvious; therefore, at least CA IX and CA XII are considered potential targets for cancer therapy. Supuran's and DeSimone's groups have recently published an extensive review article covering CA IX as a potential therapeutic target enzyme in primary tumors, metastases, and cancer stem cells (Supuran et al. 2018). Their review describes state-of-the-art of studies on CA IX including structural, functional, and biomedical aspects, as well as the development of molecules with diagnostic and therapeutic potential. Crystal structures of both CA IX and CA XII have been previously described (Alterio et al. 2009; Whittington et al. 2001). The knowledge of the three-dimensional structures of both enzymes has made the design of selective inhibitors more straightforward. There are also several pieces of promising results showing that inactivation of CA IX and/or CA XII indeed inhibits the growth or invasion capacity of cancer cells (Doyen et al. 2013; Lou et al. 2011; Boyd et al. 2017; Pettersen et al. 2015). Combination therapies using CA inhibitors together with other anticancer drugs may represent novel options for improved treatment efficiency, especially in hard-to-treat cancers (Amiri et al. 2016).

2.7 Concluding Remarks

During the last two decades, a great number of publications have suggested CA isozymes as potential biomarkers and therapeutic targets. Most of the studies have illustrated CA expression in various tumors, and many suggested CA isozymes—mainly CA IX and XII—as prognostic factors. In addition, immunological assays have been recently developed in order to monitor CA IX levels in biological samples. The observed association between cancers and different CA isozymes has already stimulated translational CA research, which will hopefully lead to attractive novel discoveries that will provide new hope for cancer patients.

Acknowledgements The studies of the author's group are supported by grants from the Sigrid Juselius Foundation, Academy of Finland and the Jane & Aatos Erkko Foundation.

References

- Alterio V, Hilvo M, Di Fiore A, Supuran CT, Pan P, Parkkila S, Scaloni A, Pastorek J, Pastorekova S, Pedone C, Scozzafava A, Monti SM, De Simone G (2009) Crystal structure of the catalytic domain of the tumor-associated human carbonic anhydrase IX. *Proc Natl Acad Sci USA* 106(38):16233–16238. <https://doi.org/10.1073/pnas.0908301106>

- Amiri A, Le PU, Moquin A, Machkalyan G, Petrecca K, Gillard JW, Yoganathan N, Maysinger D (2016) Inhibition of carbonic anhydrase IX in glioblastoma multiforme. *Eur J Pharm Biopharm* 109:81–92. <https://doi.org/10.1016/j.ejpb.2016.09.018>
- Bartosova M, Parkkila S, Pohlodek K, Karttunen TJ, Galbavy S, Mucha V, Harris AL, Pastorek J, Pastorekova S (2002) Expression of carbonic anhydrase IX in breast is associated with malignant tissues and is related to overexpression of c-erbB2. *J Pathol* 197(3):314–321. <https://doi.org/10.1002/path.1120>
- Beasley NJ, Wykoff CC, Watson PH, Leek R, Turley H, Gatter K, Pastorek J, Cox GJ, Ratcliffe P, Harris AL (2001) Carbonic anhydrase IX, an endogenous hypoxia marker, expression in head and neck squamous cell carcinoma and its relationship to hypoxia, necrosis, and microvessel density. *Cancer Res* 61(13):5262–5267
- Becker B (1955) The mechanism of the fall in intraocular pressure induced by the carbonic anhydrase inhibitor, diamox. *Am J Ophthalmol* 39(2 Pt 2):177–184
- Birner P, Jesch B, Friedrich J, Riegler M, Zacherl J, Hejna M, Wrba F, Schultheis A, Schoppmann SF (2011) Carbonic anhydrase IX overexpression is associated with diminished prognosis in esophageal cancer and correlates with Her-2 expression. *Ann Surg Oncol* 18(12):3330–3337. <https://doi.org/10.1245/s10434-011-1730-3>
- Bleumer I, Oosterwijk E, Oosterwijk-Wakka JC, Voller MC, Melchior S, Warnaar SO, Mala C, Beck J, Mulders PF (2006) A clinical trial with chimeric monoclonal antibody WX-G250 and low dose interleukin-2 pulsing scheme for advanced renal cell carcinoma. *J Urol* 175(1):57–62
- Boyd NH, Walker K, Fried J, Hackney JR, McDonald PC, Benavides GA, Spina R, Audia A, Scott SE, Libby CJ, Tran AN, Bevensee MO, Griguer C, Nozell S, Gillespie GY, Nabors B, Bhat KP, Bar EE, Darley-Usmar V, Xu B, Gordon E, Cooper SJ, Dedhar S, Hjelmeland AB (2017) Addition of carbonic anhydrase 9 inhibitor SLC-0111 to temozolomide treatment delays glioblastoma growth in vivo. *JCI Insight* 2(24). <https://doi.org/10.1172/jci.insight.92928>
- Brennan DJ, Jirstrom K, Kronblad A, Millikan RC, Landberg G, Duffy MJ, Ryden L, Gallagher WM, O'Brien SL (2006) CA IX is an independent prognostic marker in premenopausal breast cancer patients with one to three positive lymph nodes and a putative marker of radiation resistance. *Clin Cancer Res* 12(21):6421–6431
- Bui MH, Seligson D, Han KR, Pantuck AJ, Dorey FJ, Huang Y, Horvath S, Leibovich BC, Chopra S, Liao SY, Stanbridge E, Lerman MI, Palotie A, Figlin RA, Belldegrun AS (2003) Carbonic anhydrase IX is an independent predictor of survival in advanced renal clear cell carcinoma: implications for prognosis and therapy. *Clin Cancer Res* 9(2):802–811
- Carta F, Aggarwal M, Maresca A, Scozzafava A, McKenna R, Masini E, Supuran CT (2012) Dithiocarbamates strongly inhibit carbonic anhydrases and show antiglaucoma action in vivo. *J Med Chem* 55(4):1721–1730. <https://doi.org/10.1021/jm300031j>
- Carvalho S, Troost EG, Bons J, Menheere P, Lambin P, Oberije C (2016) Prognostic value of blood-biomarkers related to hypoxia, inflammation, immune response and tumour load in non-small cell lung cancer—a survival model with external validation. *Radiother Oncol* 119(3):487–494. <https://doi.org/10.1016/j.radonc.2016.04.024>
- Cetin B, Gonul II, Gumusay O, Bilgetekin I, Algin E, Ozet A, Uner A (2018) Carbonic anhydrase IX is a prognostic biomarker in glioblastoma multiforme. *Neuropathology* 38(5):457–462. <https://doi.org/10.1111/neup.12485>
- Chen J, Rocken C, Hoffmann J, Kruger S, Lendeckel U, Rocco A, Pastorekova S, Malferteiner P, Ebert MP (2005) Expression of carbonic anhydrase 9 at the invasion front of gastric cancers. *Gut* 54(7):920–927
- Chia SK, Wykoff CC, Watson PH, Han C, Leek RD, Pastorek J, Gatter KC, Ratcliffe P, Harris AL (2001) Prognostic significance of a novel hypoxia-regulated marker, carbonic anhydrase IX, in invasive breast carcinoma. *J Clin Oncol* 19(16):3660–3668. <https://doi.org/10.1200/JCO.2001.19.16.3660>
- De Schutter H, Landuyt W, Verbeken E, Goethals L, Hermans R, Nuyts S (2005) The prognostic value of the hypoxia markers CA IX and GLUT 1 and the cytokines VEGF and IL 6 in head and neck squamous cell carcinoma treated by radiotherapy +/- chemotherapy. *BMC Cancer* 5(1):42

- Doyen J, Parks SK, Marcie S, Pouyssegur J, Chiche J (2013) Knock-down of hypoxia-induced carbonic anhydrases IX and XII radiosensitizes tumor cells by increasing intracellular acidosis. *Front Oncol* 2:199. <https://doi.org/10.3389/fonc.2012.00199>
- Dungwa JV, Hunt LP, Ramani P (2011) Overexpression of carbonic anhydrase and HIF-1alpha in Wilms tumours. *BMC Cancer* 11:390. <https://doi.org/10.1186/1471-2407-11-390>
- Feldshtein M, Elkrinawi S, Yerushalmi B, Marcus B, Vullo D, Romi H, Ofir R, Landau D, Sivan S, Supuran CT, Birk OS (2010) Hyperchlorhidrosis caused by homozygous mutation in CA12, encoding carbonic anhydrase XII. *Am J Hum Genet* 87(5):713–720. <https://doi.org/10.1016/j.ajhg.2010.10.008>
- Finkelmeier F, Canli O, Peiffer KH, Walter D, Tal A, Koch C, Pession U, Vermehren J, Trojan J, Zeuzem S, Piiper A, Greten FR, Grammatikos G, Waidmann O (2018) Circulating hypoxia marker carbonic anhydrase IX (CA9) in patients with hepatocellular carcinoma and patients with cirrhosis. *PLoS One* 13(7):e0200855. <https://doi.org/10.1371/journal.pone.0200855>
- Genega EM, Ghebremichael M, Najarian R, Fu Y, Wang Y, Argani P, Grisanzio C, Signoretti S (2010) Carbonic anhydrase IX expression in renal neoplasms: correlation with tumor type and grade. *Am J Clin Pathol* 134(6):873–879. <https://doi.org/10.1309/AJCPPPR57HNJMSLZ>
- Giatromanolaki A, Koukourakis MI, Sivridis E, Pastorek J, Wykoff CC, Gatter KC, Harris AL (2001) Expression of hypoxia-inducible carbonic anhydrase-9 relates to angiogenic pathways and independently to poor outcome in non-small cell lung cancer. *Cancer Res* 61(21):7992–7998
- Gigante M, Li G, Ferlay C, Perol D, Blanc E, Paul S, Zhao A, Tostain J, Escudier B, Negrier S, Genin C (2012) Prognostic value of serum CA9 in patients with metastatic clear cell renal cell carcinoma under targeted therapy. *Anticancer Res* 32(12):5447–5451
- Goodison S, Chang M, Dai Y, Urquidí V, Rosser CJ (2012) A multi-analyte assay for the non-invasive detection of bladder cancer. *PLoS One* 7(10):e47469. <https://doi.org/10.1371/journal.pone.0047469>
- Gramlich TL, Hennigar RA, Spicer SS, Schulte BA (1990) Immunohistochemical localization of sodium-potassium-stimulated adenosine triphosphatase and carbonic anhydrase in human colon and colonic neoplasms. *Arch Pathol Lab Med* 114(4):415–419
- Gu M (2015) CA9 overexpression is an independent favorable prognostic marker in intrahepatic cholangiocarcinoma. *Int J Clin Exp Pathol* 8(1):862–866
- Haapasalo JA, Nordfors KM, Hilvo M, Rantala IJ, Soini Y, Parkkila AK, Pastorekova S, Pastorek J, Parkkila SM, Haapasalo HK (2006) Expression of carbonic anhydrase IX in astrocytic tumors predicts poor prognosis. *Clin Cancer Res* 12(2):473–477. <https://doi.org/10.1158/1078-0432.CCR-05-0848>
- Haapasalo J, Nordfors K, Jarvela S, Bragge H, Rantala I, Parkkila AK, Haapasalo H, Parkkila S (2007) Carbonic anhydrase II in the endothelium of glial tumors: a potential target for therapy. *Neuro Oncol* 9(3):308–313. <https://doi.org/10.1215/15228517-2007-001>
- Haapasalo J, Hilvo M, Nordfors K, Haapasalo H, Parkkila S, Hyrskyluoto A, Rantala I, Waheed A, Sly WS, Pastorekova S, Pastorek J, Parkkila AK (2008) Identification of an alternatively spliced isoform of carbonic anhydrase XII in diffusely infiltrating astrocytic gliomas. *Neuro Oncol* 10(2):131–138. <https://doi.org/10.1215/15228517-2007-065>
- Hilvo M, Baranauskienė L, Salzano AM, Scaloni A, Matulis D, Innocenti A, Scozzafava A, Monti SM, Di Fiore A, De Simone G, Lindfors M, Janis J, Valjakka J, Pastorekova S, Pastorek J, Kulomaa MS, Nordlund HR, Supuran CT, Parkkila S (2008) Biochemical characterization of CA IX, one of the most active carbonic anhydrase isozymes. *J Biol Chem* 283(41):27799–27809. <https://doi.org/10.1074/jbc.M800938200>
- Hilvo M, Tolvanen M, Clark A, Shen B, Shah GN, Waheed A, Halmi P, Hanninen M, Hamalainen JM, Vihinen M, Sly WS, Parkkila S (2005) Characterization of CA XV, a new GPI-anchored form of carbonic anhydrase. *Biochem J* 392(Pt 1):83–92. <https://doi.org/10.1042/BJ20051102>
- Hong JH, Muhammad E, Zheng C, Hershkovitz E, Alkrinawi S, Loewenthal N, Parvari R, Muallem S (2015) Essential role of carbonic anhydrase XII in secretory gland fluid and HCO₃⁻ secretion revealed by disease causing human mutation. *J Physiol* 593(24):5299–5312. <https://doi.org/10.1113/JP271378>

- Hoogsteen IJ, Marres HA, Bussink J, van der Kogel AJ, Kaanders JH (2007) Tumor microenvironment in head and neck squamous cell carcinomas: predictive value and clinical relevance of hypoxic markers. *A Review. Head Neck* 29(6):591–604
- Huber AR, Tan D, Sun J, Dean D, Wu T, Zhou Z (2015) High expression of carbonic anhydrase IX is significantly associated with glandular lesions in gastroesophageal junction and with tumorigenesis markers BMI1, MCM4 and MCM7. *BMC Gastroenterol* 15:80. <https://doi.org/10.1186/s12876-015-0310-6>
- Hussain SA, Ganesan R, Reynolds G, Gross L, Stevens A, Pastorek J, Murray PG, Perunovic B, Anwar MS, Billingham L, James ND, Spooner D, Poole CJ, Rea DW, Palmer DH (2007) Hypoxia-regulated carbonic anhydrase IX expression is associated with poor survival in patients with invasive breast cancer. *Br J Cancer* 96(1):104–109
- Hu X, Huang Z, Liao Z, He C, Fang X (2014) Low CA II expression is associated with tumor aggressiveness and poor prognosis in gastric cancer patients. *Int J Clin Exp Pathol* 7(10):6716–6724
- Hynninen P, Vaskivuo L, Saarnio J, Haapasalo H, Kivela J, Pastorekova S, Pastorek J, Waheed A, Sly WS, Puistola U, Parkkila S (2006) Expression of transmembrane carbonic anhydrases IX and XII in ovarian tumours. *Histopathology* 49(6):594–602. <https://doi.org/10.1111/j.1365-2559.2006.02523.x>
- Hynninen P, Parkkila S, Huhtala H, Pastorekova S, Pastorek J, Waheed A, Sly WS, Tomas E (2012) Carbonic anhydrase isozymes II, IX, and XII in uterine tumors. *APMIS* 120(2):117–129. <https://doi.org/10.1111/j.1600-0463.2011.02820.x>
- Hyuga S, Wada H, Eguchi H, Otsuru T, Iwagami Y, Yamada D, Noda T, Asaoka T, Kawamoto K, Gotoh K, Takeda Y, Tanemura M, Umeshita K, Doki Y, Mori M (2017) Expression of carbonic anhydrase IX is associated with poor prognosis through regulation of the epithelial-mesenchymal transition in hepatocellular carcinoma. *Int J Oncol* 51(4):1179–1190. <https://doi.org/10.3892/ijo.2017.4098>
- Ilie M, Mazure NM, Hofman V, Ammadi RE, Ortholan C, Bonnetaud C, Havet K, Venissac N, Mograbi B, Mouroux J, Pousyssegur J, Hofman P (2010) High levels of carbonic anhydrase IX in tumour tissue and plasma are biomarkers of poor prognostic in patients with non-small cell lung cancer. *Br J Cancer* 102(11):1627–1635. <https://doi.org/10.1038/sj.bjc.6605690>
- Ivanov SV, Kuzmin I, Wei MH, Pack S, Geil L, Johnson BE, Stanbridge EJ, Lerman MI (1998) Down-regulation of transmembrane carbonic anhydrases in renal cell carcinoma cell lines by wild-type von Hippel-Lindau transgenes. *Proc Natl Acad Sci USA* 95(21):12596–12601
- Ivanov S, Liao SY, Ivanova A, Danilkovitch-Miagkova A, Tarasova N, Weirich G, Merrill MJ, Proescholdt MA, Oldfield EH, Lee J, Zavada J, Waheed A, Sly W, Lerman MI, Stanbridge EJ (2001) Expression of hypoxia-inducible cell-surface transmembrane carbonic anhydrases in human cancer. *Am J Pathol* 158(3):905–919. [https://doi.org/10.1016/S0002-9440\(10\)64038-2](https://doi.org/10.1016/S0002-9440(10)64038-2)
- Jarvela S, Parkkila S, Bragge H, Kahkonen M, Parkkila AK, Soini Y, Pastorekova S, Pastorek J, Haapasalo H (2008) Carbonic anhydrase IX in oligodendroglial brain tumors. *BMC Cancer* 8:1. <https://doi.org/10.1186/1471-2407-8-1>
- Jarvinen P, Kivela AJ, Nummela P, Lepisto A, Ristimaki A, Parkkila S (2017) Carbonic anhydrase II: a novel biomarker for pseudomyxoma peritonei. *APMIS* 125(3):207–212. <https://doi.org/10.1111/apm.12653>
- Kang HJ, Kim IH, Sung CO, Shim JH, Yu E (2015) Expression of carbonic anhydrase 9 is a novel prognostic marker in resectable hepatocellular carcinoma. *Virchows Arch* 466(4):403–413. <https://doi.org/10.1007/s00428-014-1709-0>
- Karhumaa P, Parkkila S, Tureci O, Waheed A, Grubb JH, Shah G, Parkkila A, Kaunisto K, Tapanainen J, Sly WS, Rajaniemi H (2000) Identification of carbonic anhydrase XII as the membrane isozyme expressed in the normal human endometrial epithelium. *Mol Hum Reprod* 6(1):68–74
- Karhumaa P, Kaunisto K, Parkkila S, Waheed A, Pastorekova S, Pastorek J, Sly WS, Rajaniemi H (2001) Expression of the transmembrane carbonic anhydrases, CA IX and CA XII, in the human male excurrent ducts. *Mol Hum Reprod* 7(7):611–616

- Kaunisto K, Parkkila S, Rajaniemi H, Waheed A, Grubb J, Sly WS (2002) Carbonic anhydrase XIV: luminal expression suggests key role in renal acidification. *Kidney Int* 61(6):2111–2118. <https://doi.org/10.1046/j.1523-1755.2002.00371.x>
- Kim SJ, Rabbani ZN, Vollmer RT, Schreiber EG, Oosterwijk E, Dewhirst MW, Vujaskovic Z, Kelley MJ (2004) Carbonic anhydrase IX in early-stage non-small cell lung cancer. *Clin Cancer Res* 10(23):7925–7933
- Kim SJ, Rabbani ZN, Dewhirst MW, Vujaskovic Z, Vollmer RT, Schreiber EG, Oosterwijk E, Kelley MJ (2005) Expression of HIF-1alpha, CA IX, VEGF, and MMP-9 in surgically resected non-small cell lung cancer. *Lung Cancer* 49(3):325–335
- Kim JY, Shin HJ, Kim TH, Cho KH, Shin KH, Kim BK, Roh JW, Lee S, Park SY, Hwang YJ, Han IO (2006) Tumor-associated carbonic anhydrases are linked to metastases in primary cervical cancer. *J Cancer Res Clin Oncol* 132(5):302–308
- Kindblom LG, Remotti HE, Aldenborg F, Meis-Kindblom JM (1998) Gastrointestinal pacemaker cell tumor (GIPACT): gastrointestinal stromal tumors show phenotypic characteristics of the interstitial cells of Cajal. *Am J Pathol* 152(5):1259–1269
- Kivela AJ, Parkkila S, Saarnio J, Karttunen TJ, Kivela J, Parkkila AK, Pastorekova S, Pastorek J, Waheed A, Sly WS, Rajaniemi H (2000a) Expression of transmembrane carbonic anhydrase isoenzymes IX and XII in normal human pancreas and pancreatic tumours. *Histochem Cell Biol* 114(3):197–204
- Kivela A, Parkkila S, Saarnio J, Karttunen TJ, Kivela J, Parkkila AK, Waheed A, Sly WS, Grubb JH, Shah G, Tureci O, Rajaniemi H (2000b) Expression of a novel transmembrane carbonic anhydrase isozyme XII in normal human gut and colorectal tumors. *Am J Pathol* 156(2):577–584. [https://doi.org/10.1016/S0002-9440\(10\)64762-1](https://doi.org/10.1016/S0002-9440(10)64762-1)
- Kivela AJ, Knuutila A, Rasanen J, Sihvo E, Salmenkivi K, Saarnio J, Pastorekova S, Pastorek J, Waheed A, Sly WS, Salo JA, Parkkila S (2013) Carbonic anhydrase IX in malignant pleural mesotheliomas: a potential target for anti-cancer therapy. *Bioorg Med Chem* 21(6):1483–1488. <https://doi.org/10.1016/j.bmc.2012.09.018>
- Kummola L, Hamalainen JM, Kivela J, Kivela AJ, Saarnio J, Karttunen T, Parkkila S (2005) Expression of a novel carbonic anhydrase, CA XIII, in normal and neoplastic colorectal mucosa. *BMC Cancer* 5(1):41
- Lehtonen J, Shen B, Vihinen M, Casini A, Scozzafava A, Supuran CT, Parkkila AK, Saarnio J, Kivela AJ, Waheed A, Sly WS, Parkkila S (2004) Characterization of CA XIII, a novel member of the carbonic anhydrase isozyme family. *J Biol Chem* 279(4):2719–2727. <https://doi.org/10.1074/jbc.M308984200>
- Leppilampi M, Saarnio J, Karttunen TJ, Kivela J, Pastorekova S, Pastorek J, Waheed A, Sly WS, Parkkila S (2003) Carbonic anhydrase isozymes IX and XII in gastric tumors. *World J Gastroenterol* 9(7):1398–1403
- Leppilampi M, Koistinen P, Savolainen ER, Hannuksela J, Parkkila AK, Niemela O, Pastorekova S, Pastorek J, Waheed A, Sly WS, Parkkila S, Rajaniemi H (2002) The expression of carbonic anhydrase II in hematological malignancies. *Clin Cancer Res* 8(7):2240–2245
- Le QT, Kong C, Lavori PW, O'Byrne K, Erler JT, Huang X, Chen Y, Cao H, Tibshirani R, Denko N, Giaccia AJ, Koong AC (2007) Expression and prognostic significance of a panel of tissue hypoxia markers in head-and-neck squamous cell carcinomas. *Int J Radiat Oncol Biol Phys* 69(1):167–175
- Liao ND, Lee WY (2012) Detection of carbonic anhydrase IX protein in the diagnosis of malignant pleural effusion by enzyme-linked immunosorbent assay and immunocytochemistry. *Cancer Cytopathol* 120(4):269–275. <https://doi.org/10.1002/cncy.21191>
- Liao SY, Brewer C, Zavada J, Pastorek J, Pastorekova S, Manetta A, Berman ML, DiSaia PJ, Stanbridge EJ (1994) Identification of the MN antigen as a diagnostic biomarker of cervical intraepithelial squamous and glandular neoplasia and cervical carcinomas. *Am J Pathol* 145(3):598–609
- Liao SY, Ivanov S, Ivanova A, Ghosh S, Cote MA, Keefe K, Coca-Prados M, Stanbridge EJ, Lerman MI (2003) Expression of cell surface transmembrane carbonic anhydrase genes CA9 and CA12 in the human eye: overexpression of CA12 (CAXII) in glaucoma. *J Med Genet* 40(4):257–261

- Li G, Feng G, Gentil-Perret A, Genin C, Tostain J (2008) Serum carbonic anhydrase 9 level is associated with postoperative recurrence of conventional renal cell cancer. *J Urol* 180(2):510–513; discussion 513–514. <https://doi.org/10.1016/j.juro.2008.04.024>
- Li XJ, Xie HL, Lei SJ, Cao HQ, Meng TY, Hu YL (2012) Reduction of CAII expression in gastric cancer: correlation with invasion and metastasis. *Chin J Cancer Res* 24(3):196–200. <https://doi.org/10.1007/s11670-012-0196-6>
- Loncaster JA, Harris AL, Davidson SE, Logue JP, Hunter RD, Wycoff CC, Pastorek J, Ratcliffe PJ, Stratford IJ, West CM (2001) Carbonic anhydrase (CA IX) expression, a potential new intrinsic marker of hypoxia: correlations with tumor oxygen measurements and prognosis in locally advanced carcinoma of the cervix. *Cancer Res* 61(17):6394–6399
- Lou Y, McDonald PC, Oloumi A, Chia S, Ostlund C, Ahmadi A, Kyle A, Auf dem Keller U, Leung S, Huntsman D, Clarke B, Sutherland BW, Waterhouse D, Bally M, Roskelley C, Overall CM, Minchinton A, Pacchiano F, Carta F, Scozzafava A, Touisni N, Winum JY, Supuran CT, Dedhar S (2011) Targeting tumor hypoxia: suppression of breast tumor growth and metastasis by novel carbonic anhydrase IX inhibitors. *Cancer Res* 71(9):3364–3376. <https://doi.org/10.1158/0008-5472.CAN-10-4261>
- Lucarini L, Magnelli L, Schiavone N, Crisci A, Innocenti A, Puccetti L, Cianchi F, Peri S, Supuran CT, Papucci L, Masini E (2018) Plasmatic carbonic anhydrase IX as a diagnostic marker for clear cell renal cell carcinoma. *J Enzyme Inhib Med Chem* 33(1):234–240. <https://doi.org/10.1080/14756366.2017.1411350>
- Maseide K, Kandel RA, Bell RS, Catton CN, O’Sullivan B, Wunder JS, Pintilie M, Hedley D, Hill RP (2004) Carbonic anhydrase IX as a marker for poor prognosis in soft tissue sarcoma. *Clin Cancer Res* 10(13):4464–4471
- Mayer A, Hockel M, Wree A, Leo C, Horn LC, Vaupel P (2008) Lack of hypoxic response in uterine leiomyomas despite severe tissue hypoxia. *Cancer Res* 68(12):4719–4726. <https://doi.org/10.1158/0008-5472.CAN-07-6339>
- McDonald PC, Swayampakula M, Dedhar S (2018) Coordinated regulation of metabolic transporters and migration/invasion by carbonic anhydrase IX. *Metabolites* 8(1). <https://doi.org/10.3390/metabo8010020>
- McKiernan JM, Buttyan R, Bander NH, Stifelman MD, Katz AE, Chen MW, Olsson CA, Sawczuk IS (1997) Expression of the tumor-associated gene MN: a potential biomarker for human renal cell carcinoma. *Cancer Res* 57(12):2362–2365
- Mehes G, Matolay O, Beke L, Czenke M, Jona A, Miltenyi Z, Illes A, Bedekovics J (2019) Hypoxia related carbonic anhydrase IX expression is associated with unfavourable response to first-line therapy in classical Hodgkin’s lymphoma. *Histopathology*. <https://doi.org/10.1111/his.13808>
- Miettinen M, Lasota J (2006) Gastrointestinal stromal tumors: review on morphology, molecular pathology, prognosis, and differential diagnosis. *Arch Pathol Lab Med* 130(10):1466–1478. [https://doi.org/10.1043/1543-2165\(2006\)130\[1466:GSTROM\]2.0.CO;2](https://doi.org/10.1043/1543-2165(2006)130[1466:GSTROM]2.0.CO;2)
- Mincione F, Scozzafava A, Supuran CT (2007) The development of topically acting carbonic anhydrase inhibitors as anti-glaucoma agents. *Curr Top Med Chem* 7(9):849–854
- Morgan PE, Pastorekova S, Stuart-Tilley AK, Alper SL, Casey JR (2007) Interactions of transmembrane carbonic anhydrase, CAIX, with bicarbonate transporters. *Am J Physiol Cell Physiol* 293(2):C738–748. <https://doi.org/10.1152/ajpcell.00157.2007>
- Muhammad E, Leventhal N, Parvari G, Hanukoglu A, Hanukoglu I, Chalifa-Caspi V, Feinstein Y, Weinbrand J, Jacoby H, Manor E, Nagar T, Beck JC, Sheffield VC, Hershkovitz E, Parvari R (2011) Autosomal recessive hyponatremia due to isolated salt wasting in sweat associated with a mutation in the active site of Carbonic Anhydrase 12. *Hum Genet* 129(4):397–405. <https://doi.org/10.1007/s00439-010-0930-4>
- Nakamura J, Kitajima Y, Kai K, Hashiguchi K, Hiraki M, Noshiro H, Miyazaki K (2011) Expression of hypoxic marker CA IX is regulated by site-specific DNA methylation and is associated with the histology of gastric cancer. *Am J Pathol* 178(2):515–524. <https://doi.org/10.1016/j.ajpath.2010.10.010>

- Niemela AM, Hynninen P, Mecklin JP, Kuopio T, Kokko A, Aaltonen L, Parkkila AK, Pastorekova S, Pastorek J, Waheed A, Sly WS, Orntoft TF, Kruhoffer M, Haapasalo H, Parkkila S, Kivela AJ (2007) Carbonic anhydrase IX is highly expressed in hereditary nonpolyposis colorectal cancer. *Cancer Epidemiol Biomarkers Prev* 16(9):1760–1766. <https://doi.org/10.1158/1055-9965.EPI-07-0080>
- Nordfors K, Haapasalo J, Korja M, Niemela A, Laine J, Parkkila AK, Pastorekova S, Pastorek J, Waheed A, Sly WS, Parkkila S, Haapasalo H (2010) The tumour-associated carbonic anhydrases CA II, CA IX and CA XII in a group of medulloblastomas and supratentorial primitive neuroectodermal tumours: an association of CA IX with poor prognosis. *BMC Cancer* 10:148. <https://doi.org/10.1186/1471-2407-10-148>
- Nortunen M, Huhta H, Helminen O, Parkkila S, Kauppila JH, Karttunen TJ, Saarnio J (2018) Carbonic anhydrases II, IX, and XII in Barrett's esophagus and adenocarcinoma. *Virchows Arch* 473(5):567–575. <https://doi.org/10.1007/s00428-018-2424-z>
- Ochi F, Shiozaki A, Ichikawa D, Fujiwara H, Nakashima S, Takemoto K, Kosuga T, Konishi H, Komatsu S, Okamoto K, Kishimoto M, Marunaka Y, Otsuji E (2015) Carbonic anhydrase XII as an independent prognostic factor in advanced Esophageal squamous cell carcinoma. *J Cancer* 6(10):922–929. <https://doi.org/10.7150/jca.11269>
- Ostheimer C, Bache M, Guttler A, Kotzsch M, Vordermark D (2014) A pilot study on potential plasma hypoxia markers in the radiotherapy of non-small cell lung cancer. Osteopontin, carbonic anhydrase IX and vascular endothelial growth factor. *Strahlenther Onkol* 190(3):276–282. <https://doi.org/10.1007/s00066-013-0484-1>
- Papworth K, Sandlund J, Grankvist K, Ljungberg B, Rasmuson T (2010) Soluble carbonic anhydrase IX is not an independent prognostic factor in human renal cell carcinoma. *Anticancer Res* 30(7):2953–2957
- Parkkila S, Parkkila AK, Saarnio J, Kivela J, Karttunen TJ, Kaunisto K, Waheed A, Sly WS, Tureci O, Virtanen I, Rajaniemi H (2000) Expression of the membrane-associated carbonic anhydrase isozyme XII in the human kidney and renal tumors. *J Histochem Cytochem* 48(12):1601–1608. <https://doi.org/10.1177/002215540004801203>
- Parkkila S, Parkkila AK (1996) Carbonic anhydrase in the alimentary tract. Roles of the different isozymes and salivary factors in the maintenance of optimal conditions in the gastrointestinal canal. *Scand J Gastroenterol* 31(4):305–317
- Parkkila S, Parkkila AK, Juvonen T, Rajaniemi H (1994) Distribution of the carbonic anhydrase isoenzymes I, II, and VI in the human alimentary tract. *Gut* 35(5):646–650
- Parkkila S, Parkkila AK, Juvonen T, Lehto VP, Rajaniemi H (1995a) Immunohistochemical demonstration of the carbonic anhydrase isoenzymes I and II in pancreatic tumours. *Histochem J* 27(2):133–138
- Parkkila AK, Herva R, Parkkila S, Rajaniemi H (1995b) Immunohistochemical demonstration of human carbonic anhydrase isoenzyme II in brain tumours. *Histochem J* 27(12):974–982
- Parkkila S, Innocenti A, Kallio H, Hilvo M, Scozzafava A, Supuran CT (2009) The protein tyrosine kinase inhibitors imatinib and nilotinib strongly inhibit several mammalian alpha-carbonic anhydrase isoforms. *Bioorg Med Chem Lett* 19(15):4102–4106. <https://doi.org/10.1016/j.bmcl.2009.06.002>
- Parkkila S, Lasota J, Fletcher JA, Ou WB, Kivela AJ, Nuorva K, Parkkila AK, Ollikainen J, Sly WS, Waheed A, Pastorekova S, Pastorek J, Isola J, Miettinen M (2010) Carbonic anhydrase II. A novel biomarker for gastrointestinal stromal tumors. *Mod Pathol* 23(5):743–750. <https://doi.org/10.1038/modpathol.2009.189>
- Parkkila S, Vullo D, Maresca A, Carta F, Scozzafava A, Supuran CT (2012) Serendipitous fragment-based drug discovery: ketogenic diet metabolites and statins effectively inhibit several carbonic anhydrases. *Chem Commun (Camb)* 48(29):3551–3553. <https://doi.org/10.1039/c2cc30359k>
- Pastorekova S, Parkkila S, Parkkila AK, Opavsky R, Zelnik V, Saarnio J, Pastorek J (1997) Carbonic anhydrase IX, MN/CA IX: analysis of stomach complementary DNA sequence and expression in human and rat alimentary tracts. *Gastroenterology* 112(2):398–408

- Pastorekova S, Parkkila S, Pastorek J, Supuran CT (2004) Carbonic anhydrases: current state of the art, therapeutic applications and future prospects. *J Enzyme Inhib Med Chem* 19(3):199–229. <https://doi.org/10.1080/14756360410001689540>
- Pastorekova S, Parkkila S, Zavada J (2006) Tumor-associated carbonic anhydrases and their clinical significance. *Adv Clin Chem* 42:167–216
- Pena C, Lathia C, Shan M, Escudier B, Bukowski RM (2010) Biomarkers predicting outcome in patients with advanced renal cell carcinoma: results from sorafenib phase III treatment approaches in renal cancer global evaluation trial. *Clin Cancer Res* 16(19):4853–4863. <https://doi.org/10.1158/1078-0432.CCR-09-3343>
- Pettersen EO, Ebbesen P, Gieling RG, Williams KJ, Dubois L, Lambin P, Ward C, Meehan J, Kunkler IH, Langdon SP, Ree AH, Flatmark K, Lyng H, Calzada MJ, Peso LD, Landazuri MO, Gorchach A, Flamm H, Kieninger J, Urban G, Weltin A, Singleton DC, Haider S, Buffa FM, Harris AL, Scozzafava A, Supuran CT, Moser I, Jobst G, Busk M, Toustrup K, Overgaard J, Alsner J, Pouyssegur J, Chiche J, Mazure N, Marchiq I, Parks S, Ahmed A, Ashcroft M, Pastorekova S, Cao Y, Rouschop KM, Wouters BG, Koritzinsky M, Mujcic H, Cojocari D (2015) Targeting tumour hypoxia to prevent cancer metastasis. From biology, biosensing and technology to drug development: the METOXIA consortium. *J Enzyme Inhib Med Chem* 30(5):689–721. <https://doi.org/10.3109/14756366.2014.966704>
- Pickering LM, Larkin J (2015) Kidney cancer: carbonic anhydrase IX in resected clear cell RCC. *Nat Rev Urol* 12(6):309–310. <https://doi.org/10.1038/nrurol.2015.124>
- Ramsey ML, Yuh BJ, Johnson MT, Yeldandi AV, Zynger DL (2012) Carbonic anhydrase IX is expressed in mesothelioma and metastatic clear cell renal cell carcinoma of the lung. *Virchows Arch* 460(1):89–93. <https://doi.org/10.1007/s00428-011-1178-7>
- Rosenberg V, Pastorekova S, Zatovicova M, Vidlickova I, Jelenka L, Slezak P (2016) High serum carbonic anhydrase IX predicts shorter survival in head and neck cancer. *Bratisl Lek Listy* 117(4):201–204
- Saarnio J, Parkkila S, Parkkila AK, Waheed A, Casey MC, Zhou XY, Pastorekova S, Pastorek J, Karttunen T, Haukipuro K, Kairaluoma MI, Sly WS (1998a) Immunohistochemistry of carbonic anhydrase isozyme IX (MN/CA IX) in human gut reveals polarized expression in the epithelial cells with the highest proliferative capacity. *J Histochem Cytochem* 46(4):497–504. <https://doi.org/10.1177/002215549804600409>
- Saarnio J, Parkkila S, Parkkila AK, Haukipuro K, Pastorekova S, Pastorek J, Kairaluoma MI, Karttunen TJ (1998b) Immunohistochemical study of colorectal tumors for expression of a novel transmembrane carbonic anhydrase, MN/CA IX, with potential value as a marker of cell proliferation. *Am J Pathol* 153(1):279–285. [https://doi.org/10.1016/S0002-9440\(10\)65569-1](https://doi.org/10.1016/S0002-9440(10)65569-1)
- Saarnio J, Parkkila S, Parkkila AK, Pastorekova S, Haukipuro K, Pastorek J, Juvonen T, Karttunen TJ (2001) Transmembrane carbonic anhydrase, MN/CA IX, is a potential biomarker for biliary tumours. *J Hepatol* 35(5):643–649
- Sandlund J, Oosterwijk E, Grankvist K, Oosterwijk-Wakka J, Ljungberg B, Rasmuson T (2007) Prognostic impact of carbonic anhydrase IX expression in human renal cell carcinoma. *BJU Int* 100(3):556–560
- Scozzafava A, Supuran CT (2013) Glaucoma and the applications of carbonic anhydrase inhibitors. *Subcell Biochem* 75:349–359. https://doi.org/10.1007/978-94-007-7359-2_17
- Senol S, Aydin A, Kosemetin D, Ece D, Akalin I, Abuoglu H, Duran EA, Aydin D, Erkol B (2016) Gastric adenocarcinoma biomarker expression profiles and their prognostic value. *J Environ Pathol Toxicol Oncol* 35(3):207–222. <https://doi.org/10.1615/JEnvironPatholToxicolOncol.2016016099>
- Shimizu Y, Furuya H, Bryant Greenwood P, Chan O, Dai Y, Thornquist MD, Goodison S, Rosser CJ (2016) A multiplex immunoassay for the non-invasive detection of bladder cancer. *J Transl Med* 14:31. <https://doi.org/10.1186/s12967-016-0783-2>
- Sly WS, Hu PY (1995) Human carbonic anhydrases and carbonic anhydrase deficiencies. *Annu Rev Biochem* 64:375–401

- Span PN, Bussink J, De Mulder PH, Sweep FC (2007) Carbonic anhydrase IX expression is more predictive than prognostic in breast cancer. *Br J Cancer* 96(8):1309; author reply 1310
- Supuran CT, Scozzafava A (2007) Carbonic anhydrases as targets for medicinal chemistry. *Bioorg Med Chem* 15(13):4336–4350
- Supuran CT, Alterio V, Di Fiore A, DA K, Carta F, Monti SM, De Simone G (2018) Inhibition of carbonic anhydrase IX targets primary tumors, metastases, and cancer stem cells: three for the price of one. *Med Res Rev* 38(6):1799–1836. <https://doi.org/10.1002/med.21497>
- Svastova E, Hulikova A, Rafajova M, Zat'ovicova M, Gibadulinova A, Casini A, Cecchi A, Scozzafava A, Supuran CT, Pastorek J, Pastorekova S (2004) Hypoxia activates the capacity of tumor-associated carbonic anhydrase IX to acidify extracellular pH. *FEBS Lett* 577(3):439–445
- Svastova E, WitarSKI W, Csaderova L, Kosik I, Skvarkova L, Hulikova A, Zatovicova M, Barathova M, Kopacek J, Pastorek J, Pastorekova S (2012) Carbonic anhydrase IX interacts with bicarbonate transporters in lamellipodia and increases cell migration via its catalytic domain. *J Biol Chem* 287(5):3392–3402. <https://doi.org/10.1074/jbc.M111.286062>
- Syrjanen L, Luukkaala T, Leppilampi M, Kallioinen M, Pastorekova S, Pastorek J, Waheed A, Sly WS, Parkkila S, Karttunen T (2014) Expression of cancer-related carbonic anhydrases IX and XII in normal skin and skin neoplasms. *APMIS* 122(9):880–889. <https://doi.org/10.1111/apm.12251>
- Takacova M, Bullova P, Simko V, Skvarkova L, Poturnajova M, Feketeova L, Babal P, Kivela AJ, Kuopio T, Kopacek J, Pastorek J, Parkkila S, Pastorekova S (2014) Expression pattern of carbonic anhydrase IX in medullary thyroid carcinoma supports a role for RET-mediated activation of the HIF pathway. *Am J Pathol* 184(4):953–965. <https://doi.org/10.1016/j.ajpath.2014.01.002>
- Tanaka N, Kato H, Inose T, Kimura H, Faried A, Sohda M, Nakajima M, Fukai Y, Miyazaki T, Masuda N, Fukuchi M, Kuwano H (2008) Expression of carbonic anhydrase 9, a potential intrinsic marker of hypoxia, is associated with poor prognosis in oesophageal squamous cell carcinoma. *Br J Cancer* 99(9):1468–1475. <https://doi.org/10.1038/sj.bjc.6604719>
- Tashian RE, Hewett-Emmett D, Carter N, Bergenheim NC (2000) Carbonic anhydrase (CA)-related proteins (CA-RPs), and transmembrane proteins with CA or CA-RP domains. *Exs* 90:105–120
- Temperini C, Innocenti A, Scozzafava A, Parkkila S, Supuran CT (2010) The coumarin-binding site in carbonic anhydrase accommodates structurally diverse inhibitors: the antiepileptic lacosamide as an example and lead molecule for novel classes of carbonic anhydrase inhibitors. *J Med Chem* 53(2):850–854. <https://doi.org/10.1021/jm901524f>
- Thiry A, Dogne JM, Supuran CT, Masereel B (2007) Carbonic anhydrase inhibitors as anticonvulsant agents. *Curr Top Med Chem* 7(9):855–864
- Tureci O, Sahin U, Vollmar E, Siemer S, Gottert E, Seitz G, Parkkila AK, Shah GN, Grubb JH, Pfreundschuh M, Sly WS (1998) Human carbonic anhydrase XII: cDNA cloning, expression, and chromosomal localization of a carbonic anhydrase gene that is overexpressed in some renal cell cancers. *Proc Natl Acad Sci USA* 95(13):7608–7613
- Turner JR, Odze RD, Crum CP, Resnick MB (1997) MN antigen expression in normal, preneoplastic, and neoplastic esophagus: a clinicopathological study of a new cancer-associated biomarker. *Hum Pathol* 28(6):740–744
- van Kuijk SJ, Yaromina A, Houben R, Niemans R, Lambin P, Dubois LJ (2016) Prognostic significance of carbonic anhydrase IX Expression in cancer patients: a meta-analysis. *Front Oncol* 6:69. <https://doi.org/10.3389/fonc.2016.00069>
- van 't Veer LJ, Dai H, van de Vijver MJ, He YD, Hart AA, Mao M, Peterse HL, van der Kooy K, Marton MJ, Witteveen AT, Schreiber GJ, Kerkhoven RM, Roberts C, Linsley PS, Bernards R, Friend SH (2002) Gene expression profiling predicts clinical outcome of breast cancer. *Nature* 415(6871):530–536. <https://doi.org/10.1038/415530a>
- Viikila P, Kivela AJ, Mustonen H, Koskensalo S, Waheed A, Sly WS, Pastorek J, Pastorekova S, Parkkila S, Haglund C (2016) Carbonic anhydrase enzymes II, VII, IX and XII in colorectal carcinomas. *World J Gastroenterol* 22(36):8168–8177. <https://doi.org/10.3748/wjg.v22.i36.8168>
- Waheed A, Sly WS (2017) Carbonic anhydrase XII functions in health and disease. *Gene* 623:33–40. <https://doi.org/10.1016/j.gene.2017.04.027>

- Watson PH, Chia SK, Wykoff CC, Han C, Leek RD, Sly WS, Gatter KC, Ratcliffe P, Harris AL (2003) Carbonic anhydrase XII is a marker of good prognosis in invasive breast carcinoma. *Br J Cancer* 88(7):1065–1070
- Whittington DA, Waheed A, Ulmasov B, Shah GN, Grubb JH, Sly WS, Christianson DW (2001) Crystal structure of the dimeric extracellular domain of human carbonic anhydrase XII, a bitopic membrane protein overexpressed in certain cancer tumor cells. *Proc Natl Acad Sci USA* 98(17):9545–9550. <https://doi.org/10.1073/pnas.161301298>
- Woelber L, Mueller V, Eulenburg C, Schwarz J, Carney W, Jaenicke F, Milde-Langosch K, Mahner S (2010) Serum carbonic anhydrase IX during first-line therapy of ovarian cancer. *Gynecol Oncol* 117(2):183–188. <https://doi.org/10.1016/j.ygyno.2009.11.029>
- Woelber L, Kress K, Kersten JF, Choschzick M, Kilic E, Herwig U, Lindner C, Schwarz J, Jaenicke F, Mahner S, Milde-Langosch K, Mueller V, Ihnen M (2011) Carbonic anhydrase IX in tumor tissue and sera of patients with primary cervical cancer. *BMC Cancer* 11:12. <https://doi.org/10.1186/1471-2407-11-12>
- Wykoff CC, Beasley N, Watson PH, Campo L, Chia SK, English R, Pastorek J, Sly WS, Ratcliffe P, Harris AL (2001) Expression of the hypoxia-inducible and tumor-associated carbonic anhydrases in ductal carcinoma in situ of the breast. *Am J Pathol* 158(3):1011–1019. [https://doi.org/10.1016/S0002-9440\(10\)64048-5](https://doi.org/10.1016/S0002-9440(10)64048-5)
- Yoshiura K, Nakaoka T, Nishishita T, Sato K, Yamamoto A, Shimada S, Saida T, Kawakami Y, Takahashi TA, Fukuda H, Imajoh-Ohmi S, Oyaizu N, Yamashita N (2005) Carbonic anhydrase II is a tumor vessel endothelium-associated antigen targeted by dendritic cell therapy. *Clin Cancer Res* 11(22):8201–8207
- Zavada J, Zavadova Z, Zat'ovicova M, Hyrsi L, Kawaciuk I (2003) Soluble form of carbonic anhydrase IX (CA IX) in the serum and urine of renal carcinoma patients. *Br J Cancer* 89(6):1067–1071. <https://doi.org/10.1038/sj.bjc.6601264>
- Zhou GX, Ireland J, Rayman P, Finke J, Zhou M (2010) Quantification of carbonic anhydrase IX expression in serum and tissue of renal cell carcinoma patients using enzyme-linked immunosorbent assay: prognostic and diagnostic potentials. *Urology* 75(2):257–261. <https://doi.org/10.1016/j.urology.2009.09.052>

Chapter 3

Targeting Carbonic Anhydrases in Cardiovascular and Pulmonary Disease



Erik R. Swenson, Akshay Kumar, Nimisha Kumar, and Bernardo V. Alvarez

Abstract Carbonic anhydrase (CA) is present within many cells of the heart, lungs, and the vasculature. An understanding of its roles in cardiac muscle and vascular smooth muscle, the vascular endothelium and lungs, was not fully appreciated until the 1980s and even presently more functions are being discovered. Despite its presence and roles in the physiological functioning of the cardiovascular and respiratory systems, its inhibition in some clinical circumstances may be therapeutic. In this chapter, we will review the expression and functions of the enzyme in the heart, lungs, and vasculature as background to a comprehensive discussion of how the enzyme may be targeted and its function altered in various disease afflicting these organs. While activators of CA exist, to date no studies of these compounds have been undertaken beyond a few neurological conditions. Targeting CA has largely involved the use of inhibitors, particularly acetazolamide, the first clinically approved inhibitor and still most widely used in its class. Interestingly, acetazolamide once thought to only bind to CAs at relevant clinical concentrations has many actions independent of CA with relevance to the heart, lungs, and vasculature. These include aquaporin blockade, activation of several membrane ion channels, and oxygen radical scavenging to name a few. Inhibition of carbonic anhydrase and actions of acetazolamide unrelated to enzyme inhibition have possible benefits in heart failure, myocardial infarction, acute lung injury, and systemic and pulmonary hypertension.

Keywords Carbonic anhydrase · Acetazolamide · Inhibitor · Aquaporin · Reactive oxygen species · Potassium channel · Acidosis · Diuretic · Vasodilation ·

E. R. Swenson (✉)

VA Puget Sound Healthcare System, Seattle, WA 98108, USA

e-mail: Erik.Swenson@va.gov

A. Kumar

Department of Cardiothoracic Surgery, University of Pittsburgh, Pittsburgh, PA, USA

N. Kumar

Department of Anesthesiology, University of Texas Health Science Center, Houston, TX, USA

B. V. Alvarez

Department of Biochemistry, University of Alberta, Edmonton, Alberta, Canada

© Springer Nature Switzerland AG 2021

W. R. Chegwidden and N. D. Carter (eds.), *The Carbonic Anhydrases: Current and Emerging Therapeutic Targets*, Progress in Drug Research 75,

https://doi.org/10.1007/978-3-030-79511-5_3

Pulmonary hypertension · Systemic hypertension · Hypoxia ·
Ischemia–reperfusion injury · Heart failure · Cardiac hypertrophy

3.1 Introduction

The discovery of carbonic anhydrase (CA) in red cells in the early 1930s and subsequent determination of its presence in many organs over the next several decades laid the foundation for the application of inhibitors of the enzyme to treat a variety of diseases with the introduction of acetazolamide in the 1950s. Other inhibitors arose out of synthetic efforts to develop even more powerful drugs than acetazolamide, some of which such as furosemide and hydrochlorothiazide interestingly were weaker inhibitors, but more effective diuretics acting on other tubular mechanisms of sodium reabsorption (Maren 1984). Importantly, it was the renal effect of acetazolamide on tubular CA that was quickly exploited in the treatment of edema in heart failure, as the first safe and non-toxic oral and intravenous diuretic agent. Despite the development of other equally or more potent CA inhibitors, acetazolamide remains still the most widely used drug in its class. Perhaps no other enzyme has been targeted in as many disease conditions as CA, owing to the myriad roles it plays in gas exchange, metabolism, membrane ion transport, acid-base regulation, and fluid balance. Given how inextricably linked acetazolamide and carbonic anhydrase are in the minds of most scientists and clinicians, it is ironic that acetazolamide, the prototypical and first clinically available inhibitor, appears also to have several targets and actions independent of CA inhibition that are relevant to cardiopulmonary physiology and disease, and likely in other organ systems as well. The intent of this review is to discuss the functions of CA in pulmonary and cardiovascular medicine, the positive and negative effects of enzyme inhibition in therapy, and in the case of acetazolamide, other actions of the drug that may be therapeutic alone or in combination with CA inhibition.

3.2 Carbonic Anhydrase Isozymes and Activity in the Cardiopulmonary System

Carbonic anhydrase is present in most cells of the vasculature, lungs, heart, and nervous system. The nervous system is included in this survey because of its critical role in regulation of breathing and the circulation. Depending upon the techniques, enzymic activity, histo- and immune-cytochemistry, and mRNA expression, all active isozymes are present. It took over four decades since its discovery for CA activity to be ultimately found in the vasculature, heart, and lungs; in part due to generally lower concentrations below the detection limit of early assay and histochemical methods and roles beyond classic gas exchange, acid-base regulation, and fluid and ion transport.

Heart: The first detection of CA activity in the heart was reported as far back as the 1940s by van Goor (1948), but the amounts were small and residual contamination with red cells could not be fully ruled out. These problems continued to confound efforts to definitively establish CA in the heart. Using an indicator dilution technique in cardiac perfusion studies, Zborowaska-Sluis et al. (1975) could not show an expanded CO₂ space in the myocardium consistent with the absence of CA, although they did so in skeletal muscle. Ellis and Thomas (1970) showed that acetazolamide reduced the rate of intracellular pH (pHi) change to an increase in CO₂ in the myocardium and conducting system. Moynihan (1977) after careful elimination of contaminating red cells was unable to report any activity. De Hemptinne et al. (1986) measured the transients in pHi and surface pH of Purkinje and myocardial fibers and found that acetazolamide altered the kinetics of surface pH changes. Using subcellular fractionation of cardiac myocytes after extensive saline perfusion of the heart to remove red cells, Bruns and Gros (1992) clearly established CA activity, and at roughly at the same time specific radiolabeled acetazolamide binding was demonstrated in the heart by positron emission tomography (Swenson et al. 1992, Swenson 1997).

In the heart, membrane-bound CA IV, CA IX, and CA XIV have been localized to different subcellular compartments of cardiomyocytes (Scheibe et al. 2006), and (CA IV) (Sender et al. 1998) to heart capillaries, and endothelium of coronary cardiac blood vessels. While CA XIV is predominantly localized in the longitudinal sarcoplasmic reticulum (SR), CA IX is mainly expressed in the terminal SR/t-tubular region (Orlowski et al. 2012; Scheibe et al. 2006), with CA IV localization detected in both SR regions. In the sarcolemmal membrane, only CA IV and CA XIV are present (Scheibe et al. 2006; Vargas and Alvarez 2012). In addition to CA IV, CA XIV, and CA IX, CA II has also been found (Brown et al. 2012; Vargas et al. 2013) and in diseased human hearts (Alvarez et al. 2013) hearts; and CA VB expression is reported in heart mitochondria (Fujikawa-Adachi et al. 1999; Vaananen et al. 1991; Vargas et al. 2016). CA III, the isoform with 1–5% of the catalytic activity of the other isozymes and more resistant to inhibition by most CA inhibitors, is also present in the heart (Coats et al., 2018), where it may play a role in anti-oxidant defense or in fatty acid metabolism.

Lung: Like the heart, discovery of CA in the lung was delayed by several decades until the first report in the 1950s by Berfenstam (1952). Relatively, little was further done, until the work of Lonnerholm (1982), Henry et al. (1986), and Nioka et al. (1988) using a variety of histochemical and biochemical techniques. Overall activity is low and only about 1% of that in red cells. CA IV is present in the vascular endothelium and located on the plasma facing aspect of these cells with its activity projected extracellularly (Carter et al. 1990; Fleming et al. 1994) and possibly into the parenchymal interstitial space. While initially not detected on alveolar epithelial cells (Effros et al., 1981a, b), Fleming et al. (1993, 1994) showed its presence in alveolar type II surfactant secreting cells. Chen et al. (2008) found evidence by both immunostaining antibodies and reverse transcriptase polymerase chain reaction (PCR) that CA II is present consistent with the earlier findings in whole lung tissue by Henry et al. (1986) and Lonnerholm (1982). CA II expression and activity is also

present in alveolar type I cells, which constitute most of the alveolar surface area (Chen et al. 2008). CA II, VI, IX, and XII are also present in mucus secreting serous and goblet cells and ciliated epithelium of the airways (Swenson 2000, Leinonen et al. 2004; Sugiura et al. 2009, Park et al. 2019). Lee et al. (2018, 2019) showed that CA IX in lung microvascular endothelial cells is critical to glycolytic metabolism that supports vascular growth particularly under acidotic conditions. Thornell et al. (2018) suggest that any airway epithelial CA activity is not available to the airway lining fluid by measurements in cell culture and in vivo of fluid pH. When CA is added to both models the change in airway pH is very rapid in response to a change in ambient CO₂, but slow and not affected by CA inhibitors under control conditions. Livermore et al. (2015) found CA expressed in airway neuroepithelial bodies, which are a discrete set of cells with both O₂ and CO₂ sensing properties that may contribute to the control of ventilation. The lung also has a rich variety of immune cells residing in the interstitium and alveolar space. CA IV is detectable in alveolar eosinophils (Wen et al. 2014), CA II in alveolar macrophages (Hudalla et al. 2019) and CA I, II, and III in neutrophils (Campbell et al. 1994).

Vasculature: The vasculature of the heart, lungs, brain, and specialized chemoreceptor sites constitutes a smooth muscle layer in vessels regulating vascular tone upstream (arteriolar) and downstream (venular) of the capillaries and a continuous endothelial cell layer from artery to vein. The first histochemical evidence of CA in systemic arterial smooth muscle was CA III (Jeffrey and Carter 1980). Numerous other non-vascular smooth muscle tissues (Berg et al. 2004a, b) have several forms of CA by immunocytochemical staining. In vascular smooth muscle of the bovine aorta stripped of its endothelium, CA activity is present at a very low level of 3.5 units/g tissue. By comparison other tissues with CA have activity in the range of 20–1600 unit/g. CA I is the most abundant isozyme, constituting about 80% of the activity followed by smaller amounts of CA II and only a small fraction attributable to CA III (Berg et al. 2004a, b). The endothelium of blood vessels, which elaborates numerous vasoconstricting and vasodilating substances, expresses several CA cytosolic and membrane-bound isozymes. These in the microcirculation include CA I, II, and III (Mahieu et al. 1995) and several membrane-bound CAs, principally CA IV, but also CA XII and CA XIV (Fleming et al. 1993; Agarwal et al. 2010). In lungs with pulmonary hypertension, local hypoxia is associated with CA IX expression in the medial layer of vascular cells (Howard et al. 2012). Little is known about CA expression in the endothelium of larger resistance vessels, those more importantly involved in blood flow regulation.

3.3 Effects of CA Inhibitors Independent of CA Inhibition

As alluded to above, CA inhibiting sulfonamides including acetazolamide may have effects independent of CA inhibition and considerable evidence is emerging that these actions, either with or without concomitant CA inhibition could be useful in other diseases associated with hypoxia, edema, and ischemia.

Aquaporin (AQP) inhibition. Virtually all cells have specific membrane water channels that contribute to intracellular osmoregulation and extracellular water regulation, and in many organs, they contribute to transepithelial fluid transport. Of the many members of the aquaporin family, AQP-1 and AQP-4 are of special interest with regard to acetazolamide. Both AQP-1 and AQP-4 are expressed in the brain (Benga and Huber 2012), particularly in the choroid plexus and astrocytes, respectively, where they are involved in CSF production (Ameli et al. 2012) and CBF regulation (Nakada 2015), and brain extracellular fluid and water homeostasis (Igarashi et al. 2013). Inhibition of AQP-4 and genetic deletion of AQP-4 are protective against some forms of cerebral edema, and upregulation of these aquaporins causes both cerebral and peripheral nerve edema (Igarashi et al. 2013). AQP-1 is the major isoform in red cells, the kidneys, and peripheral nerves and is intimately involved in whole body osmoregulation.

Acetazolamide and other CA inhibitors may alter aquaporin-mediated water conductance by three possible mechanisms: direct blockade of the water channel of AQP, inhibition of CA that co-localizes with AQP and aids in water formation, and downregulation of AQP gene transcription and translation. With regard to AQP-4 and to some extent AQP-1, acetazolamide in clinically relevant μM concentrations directly blocks water flux across the plasma membrane of oocytes or liposomes *in vitro* (Ameli et al. 2012; Huber et al. 2009; Tanimura et al. 2009), but not all studies confirm these findings in oocytes (Sogaard and Zeuthan 2008; Yamaguchi et al. 2012) or more complex cells (Yang et al. 2008). Somewhat surprisingly, Tanimura et al. (2009) found that methazolamide was inactive in blocking water flux, despite its very close structural similarity to acetazolamide; differing only by a methyl group substitution on the thiadiazole ring. Similarly, *n*-methyl acetazolamide, with a methyl substitution on the sulfonamide binding directly to the active site of CA, does not alter oocyte water fluxes mediated by AQP-1 and 4 (Huber and Swenson, unpublished data). Most recently, it has been shown that AQP-1 covalently binds to CA II and in frog oocytes doubles the rate of water flux. This potentiation requires CA activity because co-expression of a catalytically inactive CA mutant that still binds to AQP-1 does not increase water flux (Vilas et al. 2015). How a tight proximity and co-localization of CA II with AQP-1 enhances water conductance is not clear, but it may involve selective channeling of water molecules concentrated near CA to the H_2O channel of aquaporin.

Acetazolamide also inhibits AQP-1 and AQP-4 gene and protein expression in models of brain and cardiac injury (Ran et al. 2010), as well as possibly accelerating its proteasomal degradation via ubiquitination (Zhang et al. 2012). It has been reported to reduce vasogenic and cytotoxic forms of cerebral edema in animal models (Guo et al. 2012).

Interestingly, aquaporins may also serve as channels for small uncharged gas molecules, such as nitric oxide (NO), NH_3 , O_2 , and CO_2 (Herrera and Garvin 2011). It is not known if acetazolamide and other CA inhibitors block aquaporin-mediated CO_2 diffusion across the cell membrane, but if so, this may represent another mechanism by which acetazolamide would cause intracellular CO_2 retention and acidosis to stimulate ventilation as discussed earlier.

Radical oxygen species modulation: Hypoxic exposure equivalent to typical high altitudes increases ROS formation (Swenson 2016). Acetazolamide, a heterocyclic thiadiazole, might work as an antioxidant given that other numerous compounds containing a 1-3-4 thiadiazole ring are ROS scavengers (Prouillac et al. 2009). Natural defenses against ROS include a number of antioxidant proteins that are upregulated by the gene transcription factor, nuclear related factor-2 (Nrf-2) (Lisk et al. 2013). Recently it has been shown that methazolamide, but surprisingly not acetazolamide, at clinically relevant dosing activates Nrf-2 in the brain and decreases hypoxic-mediated cerebrovascular leakage in a rat model (Lisk et al. 2013). Whether this difference between the drugs just represents the greater lipophilicity of methazolamide over acetazolamide and great BBB penetrance, or some unique attribute of methazolamide will require more extensive pharmacological investigation. Several models of ROS-mediated cellular or organ injury have shown that acetazolamide and methazolamide reduce cerebral damage, apoptosis, neuronal dysfunction and inflammation (Shah et al. 2013; Wang et al. 2009).

Hypoxia-inducible factor (HIF): The master hypoxic transcription factor, HIF-1, is important in surviving hypoxic stress. When normoxic rats were given very large doses of acetazolamide (50–100 mg/kg), HIF-1 alpha was upregulated in brain tissue (Xu et al. 2009). Another study of a similar degree of acidosis (pH ~7.0) in cultured cells found moderate up-regulation of HIF-1 (Willam et al. 2006). Whether the very slightly lower blood pH with acetazolamide compared to those not treated (usually about 0.05 units) causes any differences in HIF-1 activity or its metabolism remains unknown. It will be important to establish whether acetazolamide with more typical administration under the acid–base conditions of high altitude and other diseases alters HIF expression since recent work suggests that the genes for AQP-1 and 4 are HIF responsive and have HIF binding sites (Abreu-Rodriguez et al. 2011).

HCO₃-sensitive soluble adenylyl cyclase: Recently it was reported that acetazolamide at a concentration (500 uM) higher than usually attained with typical clinical administration (100 uM) increased cyclic AMP in ciliary epithelial cells of the eye. The mechanism of action appears to be a stimulation of bicarbonate-sensitive soluble adenylyl cyclase activity (Rahmne et al. 2013), which may be also involved in metabolic communication between astrocytes and neurons (Choi et al. 2012), regulation of mitochondrial oxidative metabolism (De Ramso et al. 2015; Acin-Perez et al. 2009), cholangiocyte secretion (Strazzabosco et al. 2009), and mitochondrial calcium homeostasis (Tanzaarella et al. 2019).

Calcium-activated potassium channel (BKCa): Acetazolamide and some other, but not all, potent CA inhibitors at similarly high concentrations also activate a large capacitance calcium-activated potassium channel in human blood vessels to hyperpolarize vascular smooth muscle and cause vasodilation (Pickkers et al. 2001), protect against hyperkalemia (Tricarico et al. 2013), and treat such disorders as hypokalemic periodic paralysis and myotonic disorders (Tricarico et al. 2006).

3.4 CA Functions in the Normal Heart

3.4.1 *CO₂ Elimination*

A principle role of CA is to increase the rate of transfer of CO₂ from its production in the mitochondria and diffusion through the cytoplasm to the capillaries of the heart. While earlier studies put the total activity of heart CA at very low values, in more recent work, Arias-Hidalgo et al. (2017) have calculated that intracellular CA activity is enough to accelerate CO₂ hydration and HCO₃⁻ decarboxylation rates by 5,000-fold, a value not surprising for an organ with a constant high metabolic rate even at rest. With exercise, CO₂ production and need for rapid extracellular disposal increases 5–10 times, a rate that is facilitated by a very high transmembrane CO₂ permeability of 0.10 cm s⁻¹. To put this newer work in perspective, the value for red cells is on the order of 20,000-fold. The efficient disposal of CO₂ in the heart is the result of both intracellular CA II and membrane-bound forms of CA IV, CA IX, and CA XIV acting to increase CO₂ elimination by ‘facilitated diffusion of CO₂’ (Arias-Hidalgo et al. 2017; Schroeder et al. 2013) within the cytosol by rapid formation of bicarbonate to co-diffuse with CO₂ in the cytosol and then cross the membrane as CO₂ from rapid generation from bicarbonate. This can be considered a microscopic analogy of the same role that red cell CA plays in increasing the efficiency of CO₂ movement from the tissues to the lungs, i.e., by permitting greater flux of CO₂ over smaller PCO₂ gradients through rapid formation and consumption of bicarbonate.

3.4.2 *Cardiac pH Homeostasis*

Another physiological function of CA in the heart appears to be maintenance of both extracellular (pHe) and intracellular pH (pHi) homeostasis. However, CA does not appear to make a significant contribution to the regulation of steady state pHi under normal in vitro perfusion conditions (Vandenburg et al. 1996), but no in vivo data exist. Related to specific CA locations in the heart, an extracellularly active CA (most likely CA XIV and CA IX) increases the availability of the extracellular CO₂/HCO₃⁻ buffer system to affect the surface pH in unstirred layers by accelerating the reversible CO₂ hydration reaction (de Hemptinne et al. 1986). The CA inhibitor acetazolamide (ACTZ) slows the pHi response after CO₂ change in mammalian myocardium and Purkinje fibers (Ellis and Thomas 1976; Lagadic-Gossman et al. 1992) as well as the subsequent pHi recovery (Lagadic-Gossmann et al. 1992).

Intracellular CA facilitates and potentiates the activity of a number of pH regulatory membrane transporters such as Na⁺/H⁺ (NHE) and anion exchangers (Villa-fuerte et al. 2014), as well as effective H⁺ mobility, regulating the spatiotemporal uniformity of pHi (Spitzer et al. 2002; Vaughan-Jones et al. 2002, 2006, 2009). Without CA activity, intracellular HCO₃⁻-dependent buffering, membrane HCO₃⁻ transport, and the CO₂-HCO₃⁻ shuttle are severely hampered (Vaughan-Jones and

Spitzer 2002). There is a functional partnership between CA and HCO_3^- transport, and one physiological role for CA is to act as a pH-coupling protein, linking bulk pH to the allosteric H^+ control sites on sarcolemmal acid/base transporters (Vaughan-Jones and Spitzer 2002). More recently, physical and functional coupling between membrane-associated CA IV, CA IX, and CA XIV and the NBC $\text{Na}^+/\text{HCO}_3^-$ cotransporters and $\text{Cl}^-/\text{HCO}_3^-$ exchangers was demonstrated in isolated cardiomyocytes and ventricular muscle of mammalian hearts (Alvarez et al. 2007; Orłowski et al. 2012; Vargas and Alvarez 2012; Vargas et al. 2013; Morgan et al. 2004), suggesting a pivotal physiological role of CA in myocardial pH regulation. Also intracellular CA II in heart papillary muscles forms a complex with the NHE1 Na^+/H^+ exchanger and contributes to cardiac muscle contractile activity (Krishnan et al. 2015; Vargas et al. 2013).

3.4.3 *Metabolism-Perfusion Matching*

It has been recognized that there are marked spatial heterogeneities in regional blood flow and metabolism even in the healthy heart (Frazen et al. 1988; Gonzalez and Bassingthwaite 1990) and that these vary with time (King and Bassingthwaite 1989). The nature and origin of the fluctuations and spatial differences are not at all clear, but the implication is that there must be local control of regional perfusion in relation to metabolism to prevent metabolism-perfusion mismatch. Local accumulation of metabolites and supply of substrates such as oxygen have long been thought to provide some of the regulatory signals although the mechanisms are still not well understood and other mechanisms are probably operative (Dhainaut et al. 1991).

Carbon dioxide is a metabolite of both aerobic and anaerobic metabolism and contributes to the regulation of local blood flow-metabolism matching. Fiegl and colleagues (Katz and Fiegl 1987; Broten and Fiegl 1992; Broten et al. 1991) have thoroughly investigated the determinants of coronary blood flow in large regions of the heart and have shown that changes in coronary venous PCO_2 , which are an accurate measure of capillary and tissue PCO_2 (Katz and Fiegl 1987), when combined with the accompanying PO_2 change, account for one quarter of the auto regulatory flow response to changes in coronary artery pressure (Broten and Fiegl 1992) and 40% of the blood flow response to induced pacing (Broten et al. 1991). Waxse et al. (1996) found similar results with epinephrine infusion and also demonstrated that these PCO_2 changes in myocardial blood flow are the consequence of the accompanying pH change (Wexels et al. 1986).

These findings suggest a possible rationale for CA activity in the heart as shown for ventilation-perfusion (V_A/Q) matching in the lungs (Swenson et al. 1995, 1993). Myocardial CA activity either in the capillary endothelium and/or the myocardial extracellular space would promote the more rapid attainment of a new pH when myocardial metabolism alters the prevailing PCO_2 . The new pH, in turn, then would increase or decrease blood flow in appropriate direction to establish a better match between local perfusion and metabolism.

3.4.4 *Fatty Acid/Lactate Uptake*

Free fatty acids are the primary cardiac fuel, but the heart also utilizes lactate and pyruvate under normoxic conditions (Goresky et al. 1994; Poole et al. 1989). Lactate, pyruvate, and the free fatty acids are virtually ionized in vivo, since their dissociation constants are several pH until lower than the physiological pH range. In model lipid bilayer systems, the entrance of unionized free fatty acids is several orders of magnitude faster (seconds vs minutes) than that for the charged form (Kamp and Hamilton 1992). In addition to this simple passive mechanism for free unionized acid transfer, there are also specific transport proteins in the membranes of the cardiac capillary endothelium and myocyte that mediate a high extraction (40–50%) of free fatty acids from plasma in association with albumin (Chu and Montrose 1995) and of lactate and pyruvate (Poole et al. 1989). Whether these transporters preferentially utilize the unionized acids is unknown. In some organs, such as the colon (Chu and Montrose 1995; van Englehardt et al. 1993), the rate of uptake of free fatty acids appears to be a function of pH and dependent upon transport mechanisms secreting acid or absorbing base suggesting the quantitative importance of undissociated free fatty acid diffusion. To the extent that free fatty acid uptake (and lactate) in the heart is dependent upon unionized acid movement, there will be a perturbation of the internal and external pH as undissociated acids carry protons across into the cell, as has been shown in the colon (Chu and Montrose 1995; Titus and Ahearn 1992). The resulting intracellular acidification and external alkalization in the vicinity of the membrane will slow the further movement of free fatty acids and lactate. In the presence of other buffers, CA activity will dissipate and blunt development of rate limiting pH gradients. At this time, it is unknown whether cardiac free fatty acid uptake is dependent upon CA and would be reduced by CA inhibition as has been shown in the colon (Hatch 1987).

3.4.5 *Myocardial Contractility and Calcium Mobilization*

Myocardial contractility and relaxation is dependent upon the rapid release and reuptake of calcium during the contractile cycle. The presence of CA IV in the terminal sarcoplasmic reticulum (SR) has a predicted membrane orientation with its catalytically active site facing the interior of the SR. Thus, by accelerating the $\text{CO}_2/\text{HCO}_3^-$ interconversion inside the SR, CA IV can provide buffering of H^+ changes during Ca^{2+} release by $\text{H}^+/\text{Ca}^{++}$ exchange during systolic contraction as well as fast delivery of H^+ for Ca^{2+} reuptake in diastolic relaxation (Scheibe et al. 2006). In isometrically contracting perfused isolated papillary muscles, the two potent CA inhibitors, chlorzalamide (CLZ) or ethoxzolamide (ETZ), caused a reversible decrease in isometric force in muscles maintained in a Krebs–Henseleit bath solution at 20 °C (Geers and Gros 1995). Inhibition of CA with both the potent free membrane-diffusible CA inhibitor ETZ and potent membrane diffusion restricted CA inhibitor 11,366

(benzolamide, BZ), had no effect on baseline pH_i or contractile performance of isolated Langendorff-perfused hearts, under normal perfusion conditions (Vandenberg et al. 1996). Similarly, ETZ did not change the isometric force development of rat papillary muscle after 20 min of incubation in a $\text{CO}_2/\text{HCO}_3^-$ buffered solution at a more physiological (30 °C) temperature (Vargas et al. 2013).

Given the above *in vitro* studies, many of which but not all showing deleterious effects of CA inhibitors on some aspect of myocardial function, it would be predicted that significant CA inhibition in the heart should reduce exercise capacity by limiting myocardial contractility and relaxation. The failure of cardiac output to rise appropriately that might arise due to CO_2 retention, intracellular acidosis and impairment of calcium turnover. Studies in exercising humans and horses, however, surprisingly show little to no reduction in the normal increase in cardiac output with heavy exercise. In humans exercising to maximum levels over 10–15 min 3 mg/kg of acetazolamide does not reduce exercise capacity or cardiac output either in normoxia or while breathing 12.5% oxygen (Jonk et al. 2007) despite the slight systemic metabolic acidosis generated by the drug and resultant increased ventilation. These results at relatively low dosing, were essentially no different in exercising race horses administered 30 mg/kg in showing no impairment in maximal oxygen uptake and cardiac output (Vengust et al. 2006, 2010, 2013). The only suggestion of an impairment of exercise capacity in horses was the finding that time to fatigue with running close to maximal oxygen uptake was shortened with CA inhibition (Rose et al. 1990). This may have been due to the greater acidosis in the drug treated horses and cardiac output was not measured in this study. Thus, it remains something of a mystery that CA inhibition has little impact on cardiac output in normal humans and animals even with the demands of heavy exercise. One explanation, albeit difficult to determine, is whether acetazolamide has enough penetrance into heart muscle to reach critical inhibiting concentrations. However, doses of acetazolamide >20 mg/kg alter function in many other organ systems in which carbonic anhydrase is present and involved. Two other CA inhibitors with greater potency and cellular penetrance, ethoxzolamide, and chlorzolamide have not been studied *in vivo*, but a few studies *in vitro* (see above) do demonstrate some decrease in myocardial contractility. No investigations have been performed in animals with genetic deletion of any isozyme or humans with CA II deficiency. In the case of CA II deficiency the numerous other complications of global deficiency (metabolic acidosis, osteopetrosis, cerebral calcifications, and growth retardation), there might be other reasons that these adults and children would not be able to exercise at high levels.

3.5 CA Functions in the Normal Lung

3.5.1 Alveolar Carbon Dioxide Elimination

Enns and Hill (1983) found that CO₂ diffusion across non-perfused blood-free lung tissue is decreased roughly 40% with CA inhibition, consistent with facilitated diffusion of CO₂ as already described above for the heart. Evidence supporting this role has come from studies of isolated lungs perfused with blood-free solutions alone or those to which sulfonamide-resistant plant CA had been added. Under these circumstances CO₂ excretion can be reduced by 20–75% by lung tissue CA inhibition (Klocke 1978; Hanson et al. 1981; Enns and Hill 1983; Crandall and O’Brasky 1978; Heming et al. 1986, 1994; Schunemann and Klocke 1993). Based upon data with permeant and impermeant inhibitors, CA dependent CO₂ excretion in bloodless lungs depends upon CA IV on the cell membrane of endothelial cells facing the plasma (Heming et al. 1993, 1994). Early results of Heming et al. (1986) with dextran bound sulfonamides suggesting that intracellular CA activity was important has been reinterpreted by this group (Heming et al. 1994) since their extremely large dextran inhibitors did not have access to CA IV in caveolae, small invaginations of the plasma membrane that are still accessible to smaller cytosolic-impermeant compounds but may be beyond the reach of large molecular weight endogenous plasma CA inhibitors.

The situation in vivo greatly reduces the role of either intracellular or membrane bound lung CA in enhancing CO₂ elimination by facilitating CO₂ diffusion or catalyzing plasma HCO₃ dehydration. Firstly, there is no evidence that CO exchange in the lung is predominantly diffusion limited given the thinness of the normal alveolar capillary barrier (Effros et al. 1981a, b). Plewes et al. (1976) found no effect of CA inhibition on transpleural CO₂ excretion in the isolated blood-free perfused lung. Since the gases had to pass the alveolar septa, any effect of facilitated diffusion should have been observed. Secondly, many of the above mentioned lung perfusion studies employed conditions (high PCO₂ gradients, reduced perfusate buffering, no erythrocytes, and no concurrent oxygen exchange) that artificially enhance any contribution of facilitated CO₂ diffusion and plasma HCO₃ dehydration to total CO₂ output (Heming et al. 1994). Thirdly, since red cells have 100 times the enzymic activity of lung tissue and ten times the buffering capacity of plasma it is not surprising that 90% or more of capillary CO₂ traverses the red cells. The confinement of CA within red cells gives it immediate proximity to hemoglobin, the only buffer for the CO₂-HCO₃ reactions of a sufficient amount (in part due to its oxyliable character) to sustain physiological CO₂ output. These conclusions are supported by model simulations of lung gas exchange by Crandall and Bidani (1981) and Mochizuki et al. (1987) which calculate that lung tissue CA can maximally account for no more than 5–10% of normal CO₂ elimination.

In a provocative study, Kawai et al. (2015) proposed that lung CO₂ excretion is dependent upon a blood-flow mediated activation of vascular F1/FO ATPase which generates a H⁺ to combine with plasma bicarbonate to generate CO₂ for diffusion across the alveolar capillary barrier. In this scheme, red cell CA, the majority of

CA within the perfused lung is not necessary for CO₂ exchange. They base their theory on the results of a specific inhibitor of F1/FO ATPase, piceatannol which they show decreases CO₂ excretion in an isolated perfused lung. They find that acetazolamide also decreases CO₂ excretion, since it would be necessary for the generation of carbon dioxide from the reaction of H⁺ and bicarbonate. The problem with this novel mechanism is that piceatannol, a phenolic compound, is likely a CA inhibitor (Swenson et al., unpublished results) as are other compounds with structural similarity to piceatannol (Innocenti et al. 2010) Thus the classical understanding of CO₂ excretion in the lung is not necessarily overturned by this study.

The few relevant in vivo experiments show only a minor small contribution of lung CA to CO₂ elimination. Swenson et al. (1993) found that benzolamide, a highly impermeant CA inhibitor but active against CA IV, reduced CO₂ output by a non-statistically significant 8% in the dog lung in a first pass injection compared to the large decrement with ethoxzolamide. Moreover, there was no further effect of a band 3 inhibitor which was added to force more plasma CO₂-HCO₃ interconversion by limiting red cell Cl-/HCO₃ exchange, as predicted by Bidani (1991). One mg/kg benzolamide did not increase the venous to arterial CO₂ difference in anesthetized dogs (Swenson et al. 1993) although Cardenas et al. (1998) found that 2 mg/kg reduced CO₂ output by about 10%. It is interesting in the context of gas exchange efficiency to note that hypercapnia, a stimulus expected to possibly increase CA IV, does not increase its expression in lung endothelial cells (Rounds et al. 1997) despite an increase in other membrane associated proteins.

Healthy men given a very low dose of acetazolamide (3 mg/kg iv) to avoid significant red cell CA inhibition, but sufficient to inhibit vascular CA IV, showed that only with maximal exercise was there any detectable decrease (5%) in CO₂ excretion (Korotzer et al. 1997). Whether this was due to decreases in oxygen consumption or true CO₂ retention is not clear because there was a non-statistically significant decline in maximal oxygen consumption ($p = 0.06$) and no significant differences in arterial CO₂ and ventilation. The only study to find a large contribution of lung CA to CO₂ elimination in the presence of red cells was that of Klocke (1997) in an isolated blood perfused lung. In a setting of no concurrent oxygen uptake and a non-physiological PCO₂ gradient of almost 40 mmHg, he found that lung CA inhibition alone reduced CO₂ output by 44%. Both of these non-physiological conditions may have served to enhance the contribution of lung CA. Further definitive experiments ideally should use absolutely impermeant CA inhibitors, such as F 3500 (Conroy et al. 1996) under steady-state in vivo conditions.

3.5.2 Lung Fluid Exchange and pH Regulation

The lung parenchyma and airways, especially during their development, actively secrete or reabsorb fluid (Strang 1991; Dorrington and Boyd 1995). The fetal lung secretes an acidic (pH ~6.27, HCO₃ = 2.7 mM) poorly buffered fluid (Adamson et al. 1969) thought necessary for optimal growth and surfactant function at the time

of birth and transition to air breathing (Strang 1991). The mechanism of acidic fluid secretion by the alveolar epithelium appears to be one involving active H^+ secretion via either Na^+/H^+ exchange or H^+/K^+ ATPase (Strang 1991). The capacity for acid secretion is large since fetal lungs of lamb can reduce intra-alveolar HCO_3^- from 60 to 3 mM over 4–5 h (Olver and Strang 1974).

During lung growth in utero, CA II and IV begin to appear in mid-term and reach peak concentrations near birth after which CA II levels decrease while CA IV continues to increase (Carter et al. 1990; Lonnerholm and Wistrand 1982; Fleming et al. 1993). It is interesting to speculate that the rapid postnatal expression of CA IV (Fleming et al. 1993) may be associated with the beginning of air breathing and its appropriate regulation. Acetazolamide reduces fetal lamb lung fluid and H^+ secretion 30–65% (Adamson and Waxman 1976; Davis et al. 1980, 1989). The clinical impact of reduced lung fluid secretion and acidification on survival and growth, however, is unknown, but it possibly may not be crucial since CA II deficient mice appear to have no obvious pulmonary hypoplasia or difficulty at birth in making the transition to air breathing.

Active fluid reabsorption is necessary to counter passive fluid fluxes across the alveolar capillary membrane and to promote efficient gas exchange. Despite the switch from fluid secretion in utero to fluid reabsorption ex utero, the small amount of alveolar lining fluid remains acidic with micropuncture measurements of pH measured between 6.2 and 6.9 (Effros and Chinard 1969; Nielson 1986). The mechanism of acid secretion in the adult lung is uncertain. It may simply be a consequence of greater active sodium uptake relative to chloride (Effros et al. 1989) and a fall in pH on that basis, or to direct H^+ secretion by type II pneumocytes (Lubman et al. 1989) possibly related to the protons secreted into surfactant containing granules (Chander et al. 1986). The purpose of acid secretion may be to enhance the surfactant's surface tension lowering properties (Wildeboer-Venema 1984), to enhance intraacinar collateral ventilation pathways (Traystman et al. 1978; Swenson et al. 1998), or to magnify the pH changes in the parenchymal extracellular space with changes in PCO_2 that may serve as V_A/Q matching signals (see below). It would be predicted given the role of CA in fluid secretion and reabsorption in other epithelia that CA inhibition should decrease alveolar fluid reabsorption, but Chen et al. (2008) found in an isolated rat lung model that acetazolamide and methazolamide did not alter fluid reabsorption during hypercapnia. However, they did not study reabsorption under normal acid–base conditions.

Like many organs the lung is capable of defending its intracellular pH (pHi) against acidic and alkaline stresses (Wood and Schaefer 1978; Lubman and Crandall 1992). pHi control may be important for surfactant synthesis and the rate at which either H^+ or HCO_3^- can be supplied or dissipated by Na^+/H^+ antiport, H^+ ATPase, Cl^-/HCO_3^- exchange and Na^+/HCO_3^- symport (Lubman and Crandall 1992) may be important in a number of metabolic pathways. CA inhibition slows the rate of pHi correction in alveolar epithelial cells (Heming et al. 1991) and the rates at which lung tissue stores or releases CO_2 with a change in alveolar PCO_2 (PIewes et al. 1976).

3.5.3 Ventilation-Perfusion Matching

The efficiency of the lung in gas exchange arises from effective matching of regional alveolar ventilation (V_A) and perfusion (Q). However, even at rest, regional blood flow and ventilation are not constant and may fluctuate 10–20% over intervals as short as one min (Swenson et al. 1998). When blood flow or ventilation change in a region, the alveolar PO_2 and PCO_2 will change accordingly. If these fluctuations in blood flow or ventilation are not quickly matched by corresponding changes in the other flow, V_A/Q mismatch is created. Several mechanisms in the lung evoke rapid responses in one flow to a change in the other including hypoxic pulmonary vasoconstriction (HPV) and pH dependent changes in airway and vascular smooth muscle tone (Swenson et al. 1998). Thus more rapid translation of the pH change arising from a change in local PCO_2 will accelerate pH-mediated compensatory responses. Both HPV (Swenson et al., 1998) and hypocapnic bronchoconstriction and pneumoconstriction (Swenson et al. 1995) are slowed by CA inhibition with the half-time response increasing from roughly 50 to 100 s. When acetazolamide was given to normal dogs or to dogs with an imposed regional perfusion fluctuation, V_A/Q mismatching was greater and arterial oxygenation worse after CA inhibition (Swenson et al. 1993, 1995). The deterioration of V_A/Q matching with acetazolamide cannot be accounted for the associated systemic acid–base effects of CA inhibition.

Airway fluid and bronchial regulation: The presence of CA in the airways has been given relatively little attention. It could possibly subserve fluid secretory or absorptive functions as well as pH regulation. The pH of airway fluid is acidic (pH 6.6–7.0) in many but not all mammalian species (Smith and Welsh 1993; Robinson et al. 1989; Gatto 1981; Jack et al. 1990). Smith and Welsh (1994) and Devor et al. (1999) showed that cultured human lower airway epithelia actively secrete protons or HCO_3^- depending upon the stimulating conditions. Bicarbonate-dependent chloride secretion is also dependent on CA (Cuthbert et al., 2003; Krouse et al. 2004). These regulated functions may provide an optimal lining fluid for mucociliary function and host defense in the upper respiratory tract (Boucher 1994). Cavaliere et al. (1996) found that dichlorophenamide increased the pH of human nasal secretions. Steel et al. (1994) and Devor et al. (1999) showed that 100 μM acetazolamide reduced the short circuit current of both human and sheep airway epithelium. At higher concentrations, acetazolamide (1 mM) combined with bumetanide reduced all anion secretion in serous glands and caused ductal mucus impaction (Inglis et al. 1997). As noted above, by indirect measurements, Thornell et al. (2018) concluded that airway lining liquid has minimal CA activity provided by membrane apical enzyme and propose that this absence helps to maintain a stable pH against the swings in airway PCO_2 during inspiration and expiration. CA XII in the airway epithelium appears to support normal chloride secretion, and its absence leads to symptoms and signs akin to cystic fibrosis (Lee et al. 2016a, b).

Certain diuretics, including furosemide, bumetanide, and chlorothiazide, inhibit non-allergic bronchoconstriction (Elwood et al. 1991). Dose response studies with loop diuretics of differing potency against the $Na^+-K^+-2Cl^-$ cotransporter suggest

that the bronchoprotective action of these drugs is not via Na-Cl-K cotransporter inhibition (O'Connor et al. 1991) nor by Na⁺ channel blockade (O'Connor et al. 1994). Common to all of these diuretics is that they are unsubstituted sulfonamides and as such have CA inhibiting activity. Therefore, inhibition of CA has been proposed to be the relevant property. Indeed, inhaled acetazolamide does block bronchoconstriction in mild asthmatics to cold dry air hyperventilation (O'Donnell et al. 1992), inhaled sodium metabisulfite (O'Connor et al. 1994) and cough induced by hypotonic aerosol inhalation (Foresi et al. 1996). However, the direct bronchodilating action of these drugs in non-constricted airways is not very potent (Barnikol and Diether 1979; O'Connor et al. 1994; O'Donnell et al. 1992).

The locus of action of CA inhibitors and inhaled diuretics on cough and bronchospasm are not known, but are thought to act on airway neural transmission (Elwood et al. 1991) since the enzyme has not been reported in bronchial smooth muscle. Since CA is found in peripheral muscle afferent nerves (Riley et al. 1984; Szabolcs et al. 1989) and acetazolamide reduces contractile neuropeptide release from sensory nerve endings in the airways (Sun et al. 1993), it is proposed that CA inhibition in afferent airway nerves reduces the ability to depolarize and initiate bronchoconstriction in response to an irritant. However, Verlceden et al. (1994) showed that 10⁻⁴M acetazolamide did not alter electric field stimulation-induced cholinergic contraction in human airways. Whether CA is involved in airway neurotransmission is debatable since all the studies cited above except that of Verlceden et al. (1994), the concentrations of acetazolamide generally exceeded 10⁻³¹ M, a concentration at which many non-specific effects of sulfonamides not related to CA inhibition occur (Maren 1977), and in no cases were proper dose response studies performed.

3.5.4 Pleural Fluid Composition and Turnover

Despite lack of biochemical or cytochemical evidence of CA in the pleural epithelium, it appears that the enzyme may be involved in the generation of an alkaline pleural fluid (Rolf and Travis 1971). Zocchi et al. (1991) found that pleural fluid reabsorption was reduced by 30% and had a lower bicarbonate when 100 uM acetazolamide was added to the pleural space. Results with anion and cation transport blockers suggest that CA subserves operation of a Na⁺/H⁺ and Cl⁻/HCO₃ double exchange mechanism on the serosal aspect of the parietal pleura.

3.6 Carbonic Anhydrase Inhibitors and Cardiovascular Disease

3.6.1 Systemic Hypertension

Hypertension is a major factor in coronary heart disease, sudden death, stroke, and congestive heart failure due to the chronic mechanical stress placed on the heart and vasculature (Hollander 1976). Thus, treatment of essential hypertension has become one of the most critical interventions to decrease cardiovascular morbidity and mortality. Treatment of hypertension begins with lifestyle modifications, such as smoking cessation, weight loss, exercise, and cardioprotective diets, but most patients will require pharmacotherapy, using a combination of multiple medications like thiazide-type diuretics, calcium channel blockers, and angiotensin-converting enzyme inhibitors/angiotensin receptor blockers (Ferdinand and Nasser 2017; Taddei 2015).

The use of CA inhibitors in hypertension treatment dates to the release of acetazolamide in treating heart failure. By enhancing the urinary elimination of Na^+ and Cl^- , along with bicarbonate and potassium, sulfonamide CA inhibitors, acetazolamide, ACTZ, and ethoxzolamide, ETZ, reduced elevated blood pressures in patients with congestive heart failure (Relman et al. 1954, Moyer and Ford 1958; Moyer and Hughes 1995; Schwartz et al. 1955) The diuretic effect in these patients results from the inhibition of CA II, IV, XII, and XIV in both the proximal and distal tubule and is likely the most important antihypertensive mechanism. However, with the introduction of furosemide and other more potent loop diuretics, the use of CA inhibitors soon fell out of favor.

Other sites of action of the CA inhibitors on systemic blood pressure include vascular smooth muscle and endothelial cells. When studied in individual organ circulations in vivo and in isolated preparations, much work finds vessel relaxation with CA inhibitors. Likewise, in non-vascular smooth muscle sites, acetazolamide inhibits agonist-mediated ileal and vas deferens constriction (Carmignani et al. 1981), and neural-mediated bronchoconstriction (Elwood et al. 1993). Any consideration of CA inhibition in the vasculature must first recognize that both vascular endothelial cell and the smooth muscle CAs will be inhibited. Lacking studies in isolated cells of either type except in the pulmonary circulation (see below) any change in blood flow or vessel resistance may be the result of CA inhibition in one cell type or both.

The vascular endothelium generates local vasoconstrictors and dilators in response to a variety of stimuli, including shear stress, hypoxia, hypercapnia, and circulating hormones. The transduction and intracellular signalling pathways are complicated and involve numerous ion channels, some of which are pH sensitive (Nilius and Droogmans 2001; Taylor et al. 2006). Endothelial cell generated NO is of considerable interest in this regard. CA IV and other plasma-facing membrane bound isozymes easily accessed by drugs in the blood are associated with caveolae (Ryan et al. 1982); regions of the endothelial cell plasma membrane involved in vasoactive mediator binding and signal transduction, which highly express endothelial nitric

oxide synthase (eNOS). In the retinal circulation, vasodilation with dorzolamide is blocked by inhibiting eNOS-mediated NO production (Kringelholz et al. 2012), but in the cerebral circulation, the vasodilating effect of acetazolamide is independent of NO (Kiss et al. 1999). Thus, not all circulations may share this feature of linkage to NO. One possibility proposed is that the CA can generate NO from nitrite and that this is enhanced by several CA inhibitors (Aamand et al. 2009). Two fundamental problems arising from this study are how CA might have a reductase activity given its active site or how ligating the zinc by these drugs in the active site of the enzyme increases this activity. Several recent studies including *in vitro* and *in vivo* studies have not been able to establish CA-mediated NO generation from nitrite (Andring et al. 2018; Pickerodt et al. 2019; Rosenbaek et al. 2018).

CA inhibition increases cerebral and choroid plexus blood flow (Kiss et al. 1999; Taki et al. 2001; Grossman and Koeberle 2000). Acetazolamide in rats (at 4 mg/kg) increases blood flow in liver, brain, and kidney, but not in the stomach and skeletal muscle (Taki et al. 2001). In the eye, a variety of CA inhibitors (acetazolamide, brinzolamide, and dorzolamide) all induce ciliary and retinal vasorelaxation (Kringelholz et al. 2012; Torring et al. 2009) to improve retinal oxygenation (Pederson et al. 2005). Ethoxzolamide, acetazolamide, and benzolamide, block norepinephrine-mediated mesenteric artery constriction in a dose–response manner and in nM concentrations consistent with their inhibitory potency against CA and diffusibility into tissue (Pickkers et al. 1999). Furthermore, they showed that extracellular acidosis generated by CA inhibitors *in vivo* is not critical in vasorelaxation because the vessels were studied *in vitro* under fixed acid–base conditions. In follow-up human studies, acetazolamide is vasodilating when infused into the forearm (Pickkers et al. 2001). This experimental model has the advantage that within the time frame of the experiment and amount of drug given, there were no systemic effects that might have secondarily altered local vascular tone. However, in these experiments CA inhibitors are only vasodilating at much higher concentrations (μM) and appear to do by inducing membrane hyperpolarization via activation of calcium-activated potassium channels (Pickkers et al. 2001). Whether these drugs bind directly to potassium channels or their activity is altered secondarily by changes in intracellular pH caused by acetazolamide in vascular smooth muscle is not known. In skeletal muscle the evidence suggests they bind directly, and their action is not dependent on CA inhibition since isolated membranes were studied and concentrations needed to alter channel activity were in the μM range (Tricarico et al. 2004). Another potential mechanism of CA inhibitor-induced membrane hyperpolarization is via blockade of membrane voltage gated calcium channels but again at concentrations well above that necessary to inhibit CA (McNaughton et al. 2004). These findings in aggregate suggest a complex picture of both CA-dependent and non-independent effect of these drugs on vascular tone and that any claims made for these drugs relating to CA inhibition must be critically cognizant of the dosing and concentrations employed and whether it is by endothelial or smooth muscle effects.

Any blood pressure changes with CA inhibition will be a summation of changes in extracellular fluid (ECF) volume, cardiac output, neuro-humoral responses, acid–base status, and direct drug-induced vasodilation. Because all CA inhibitors are

diuretics and cause a 5–10% reduction in ECF volume (Brechue et al. 1990), this alone should lead to a reduction in blood pressure. Despite mild volume depletion, many studies in normotensive humans treated with acetazolamide in the usual range of 2–5 mg/kg, sufficient to cause diuresis and a mild metabolic acidosis find no blood pressure reduction at rest or with exercise (Jonk et al. 2007; Swenson and Maren 1978). A few trials of acetazolamide in essential hypertension or renal disease were largely disappointing with only <10% of patients responding with meaningful pressure reduction (Brest et al. 1961; Megibow et al. 1948; Horita et al. 2006). The ineffectiveness of acetazolamide and far greater efficacy and lower side effect profile of the thiazides and other emerging classes of antihypertensive drugs in the 1950s and 1960s, very quickly extinguished any interest in CA inhibitors for hypertension treatment.

The only instances acetazolamide convincingly reduces systemic blood pressure are at high altitude (Parati et al. 2013), in sleep disordered breathing (Eskandari et al. 2018) and in idiopathic intracranial hypertension (Wall et al. 2014). The dosing at high altitude was in the low range (2–4 mg/kg) and this reduced the slight degree of systemic hypertension from hypoxia-mediated sympathetic activation that develops in persons otherwise normotensive at low altitude.

One more possible benefit to acetazolamide at altitude is the better preservation of subendocardial oxygenation (Slavi et al. 2013), which would be of advantage particularly to patients with coronary artery disease who travel to high altitude. In sleep apnea, the improvement in sleep quality and reduction in sympathetic nervous activation like at high altitude best explains the antihypertensive effect. In idiopathic intracranial hypertension, doses used were much higher (20–60 mg/kg) to achieve reductions in cerebrospinal fluid production and it cannot be ruled out that the weight loss and other factors related to widespread CA inhibition at these doses and greater side effects were not also involved.

This disappointing failure of CA inhibition to be more broadly useful in altering blood pressure using acetazolamide and other potent CA inhibitors suggests that any direct vasodilation (as discussed above) to cause blood pressure reduction may be opposed by counter-regulatory responses or consequences of CA inhibition occurring elsewhere in the body. One important response to CA inhibition-induced volume depletion and metabolic acidosis is a compensatory activation of the sympathetic nervous system. Plasma norepinephrine at rest is elevated roughly two-fold in individuals taking acetazolamide suggesting sympathetic activation in response (Goldsmith et al. 1990). The same degree of sympathetic activation was noted with breathing 4% CO₂ which evokes an equal fall in arterial pH (0.08 units) as with acetazolamide. Interestingly at high altitude, the ventilatory response to hypoxia which causes arterial hypocapnia acts to keep blood pH higher than otherwise develops at low altitudes with CA inhibitors and so may explain an effective blood pressure reduction with acetazolamide (Parati et al. 2013). In addition, plasma renin and urinary aldosterone increase with acetazolamide (Favre and Vallotton 1984). Chronic use of acetazolamide and other CA inhibitors causes several mild to distressing side effects in about one third of patients that is not fully explained by the metabolic acidosis caused by renal CA inhibition (Swenson 2014a, b). These likely arise from non-specific effects

of neuronal and GI tract enzyme inhibition. Lastly, because there is no evidence for vasodilation in skeletal muscle (Taki et al. 2001), which constitutes over 60% of total body mass, this may contribute to the lack of in vivo blood pressure reduction. Whether correction of the metabolic acidosis with supplemental bicarbonate or citrate as has been done to reduce other side effects of CA inhibitors would reveal more blood pressure reduction has not been tested.

3.6.2 *Cardiac Hypertrophy and Heart Failure*

Cardiac hypertrophy is a major predictor of developing of heart failure, arrhythmia, and sudden death (de Simone et al. 2008). The heart responds to increased work and/or loss of myocardium with hypertrophic growth of existing cardiomyocytes to enhance pump function and reduce altered ventricular wall tension. This hypertrophic growth is compensatory in the initial stages, but as time progresses it becomes maladaptive and leads to diastolic heart failure (Maillet et al. 2013; van Berlo et al. 2013). Heart failure treatment often requires a combination of beta adrenergic, renin-angiotensin, and aldosterone blockade. Ventricular hypertrophy/failure and the augmented gene and protein expression of the CA isoforms, CA II, IV, and XIV may be induced by the common mechanism of ventricular stretch arising from an increased ventricular workload (Alvarez et al. 2013; Torella et al. 2014). There is also an increase in the hypoxia inducible factor-1 responsive isoform of CA (CA IX) in the pathophysiological response of the failing heart to ischemia (Holotnakova et al. 2008).

Inhibition of these CA isozymes by ETZ and BZ in a rat model of cardiac hypertrophy caused by a chronic coronary artery occlusion leads to decreased pulmonary edema, less LV enlargement and remodeling over a period of several months of treatment (Vargas et al. 2016). The hypertrophic response in ischemic heart disease is in part driven by increased sympathetic nervous activation and catecholamine release within the heart and circulation, dilation and over-stretch of cardiomyocytes, and stimulation of cardiac membrane NHE-1 (sodium-hydrogen exchanger), AE-1 (chloride-bicarbonate exchanger) and NBC (sodium bicarbonate cotransporter). Activation of all these membrane transporters, which non-covalently associate with CA isozymes to form metabolons (a close assembly of various proteins serving a single function), leads to intracellular alkalization, which raises intracellular cytosolic calcium concentration and initiates the generation of a number of hypertrophic signals. By partially blocking the activity of these alkalizing transporters by inhibition of their supporting CAs and causing a slight degree of intracellular CO₂ retention, hypertrophy can be reduced, and cardiac contractile function improved.

In addition to the benefit from CA inhibitors in reducing pathological cardiac hypertrophy, CA inhibitors can contribute to the prevention or reduction of pulmonary and systemic edema in congestive heart failure through their actions in the kidney to block the reabsorption of Na⁺ and causing diuresis and natriuresis. It was this first indication for acetazolamide that markedly improved the treatment of

patients with heart failure in the 1950s (Leaf et al. 1954; Relman et al. 1954; Moyer and Hughes 1995), before the advent of current loop diuretics, such as furosemide. Another more potent CA inhibitor, ETZ) was also clinically used as diuretic agent in patients with heart failure (Moyer and Ford 1958). Two other compounds, chlorothiazide and hydrochlorothiazide, which show CA inhibitory properties and diuretic effects have been used for treatment of patients with congestive heart failure and post-hypertensive cardiac insufficiency. These thiazides, like furosemide and other related loop diuretics are considerably weaker CA inhibitors by several orders of magnitude. In the usual dosing for these transporters, Na–K–2Cl cotransporter in the loop of Henle and the epithelial Na channel in the distal nephron, respectively, they do not achieve concentrations high enough to be effective against renal CAs. The CA inhibitors differ from the loop diuretics and distally acting diuretics in causing bicarbonate loss and metabolic acidosis in contrast to enhanced distal tubular hydrogen ion excretion and metabolic alkalosis.

High-dose loop diuretic therapy is the primary cause of metabolic alkalosis in pediatric and adult patients with heart disease. ACTZ has been safely used in many patients with heart disease to lower serum pH and HCO_3^- , raise Cl^- and correct the metabolic alkalosis of chronic loop diuretic therapy (Moffett et al. 2007; Lopez et al. 2016; Wongboonsin et al. 2019). Acetazolamide can also improve the natriuresis of loop diuretic treatment (Imiela and Budaj 2017; Verbrugge et al. 2019). In June 2018, a multicenter, randomized study, (ADVOR-Acetazolamide in decompensated heart failure with volume overload) was initiated to assess the role of acetazolamide in combination with loop diuretics to limit loop diuretic resistance and metabolic alkalosis to better improve the outcomes of acute heart failure with volume overload (Mullens et al. 2018). Interestingly, the cardiovascular benefits of CA inhibitors may mimic the benefits seen with the introduction of the sodium-glucose cotransport inhibitors on cardiovascular outcomes in patients with diabetes beyond their effects to lower blood glucose by blocking reuptake of glucose in the proximal tubule and promoting natriuresis (Leon-Jimenez et al. 2018).

Another possible benefit of ACTZ in patients with chronic heart failure is reduction of exercise-induced periodic breathing and central sleep apnea which may compromise ventilation and oxygenation (Apostolo et al. 2014; Wongboonsin et al. 2019) in part by caused by loop diuretic induced metabolic alkalosis. Heart failure also leads to myocardial edema. In a mouse study of heart failure, acetazolamide treatment reduced myocardial water content, in part by inhibition and down-regulation of myocardial aquaporin-1 expression (Song et al. 2018).

3.6.3 Coronary Artery Disease and Myocardial Infarction

In experimental animal settings, CA inhibitors benefit the acutely ischemic heart. Benzolamide and ethoxzolamide slow the efflux of H^+ from the isolated buffer-perfused ferret heart and thus recovery of pH_i following a ten minute period of ischemia (Vandenberg et al. 1996). The drugs only very minimally slowed the

recovery of left ventricular developed pressure (LVDP) during reperfusion. In a series of subsequent experiments in the isolated rat heart using longer ischemic times of 60–90 min, benzolamide reduced infarct size by almost 80%, attenuated pathological hypercontracture, and improved post-ischemic recovery of myocardial contractile function (Ciocci-Pardo et al. 2018). The cardioprotective benefits of BZ in terms of reducing infarct size and improving contractility are likely the result of prolongation of the acidic conditions during early reperfusion, since 10 min of initial reperfusion in the same experimental model with a perfusate of 6.4 prevents cardiomyocyte damage occurring during reperfusion. This phenomenon of acidic protection during reperfusion has been termed the pH paradox and has been described in a number of organ ischemia-reperfusion models. In the acidic milieu, the otherwise tissue damaging effects of radical oxygen species and inflammatory cytokines generated when oxygen is returned are blunted and unnecessary apoptosis is limited. The protection afforded by benzolamide is best explained by its inhibition of membrane-bound CAs that enhance the function of membrane acid–base transporting proteins (NHE-1, AE-3, and NBC) to rapidly export the acid accumulated and take up bicarbonate. The protection by benzolamide is dependent upon p38MAP kinase-dependent pathways (Ciocci-Pardo, 2018) and by endothelial nitric oxide synthase upregulated NO production (Gonzalez Arbelaez et al. 2018). These dramatic findings along with those of CA inhibition in chronic heart failure offer a new possible strategy for treating patients with acute and chronic coronary artery disease, if replicated in human studies.

Another potential advantage to acetazolamide administration in acute ST segment myocardial infarction is that it can protect against radiographic contrast induced kidney injury at the time of percutaneous coronary artery stenting, when contrast must be given to visualize the blocked coronary arteries (Assadi 2006; Pakfetrat et al. 2009).

3.7 Carbonic Anhydrase Inhibitors in Pulmonary Disease

3.7.1 *Chronic Obstructive Pulmonary Disease (COPD)*

Within the decade of its introduction, clinicians began to explore whether acetazolamide might be a useful respiratory stimulant for hypoxemic patients with chronic obstructive pulmonary disease (COPD) by the increase in ventilation which occurs with a mild metabolic acidosis generated by renal CA inhibition with the goal of improving arterial oxygenation (McNicol and Pride 1961). Although it was effective in this regard for some patients with mild or moderate lung function impairment, many with moderate or severe disease could not tolerate the worsened dyspnea when forced to breathe more. In some cases, the drug led to hypercapnic respiratory failure (McNicol and Pride 1961; Schwartz et al. 1955). While the increased work of breathing with hyperventilation is trivial in healthy persons, in those with limited lung function and weaker chronically fatigued respiratory muscles the added

effort may not be possible or sustainable. Following a brief period of enthusiasm for use in COPD, this approach with few exceptions has been largely abandoned.

Seven studies in stable patients with hypercapnic COPD have shown that acetazolamide at 250–500 mg dosing increases arterial PO_2 by roughly 4–8 mmHg and decreases pH by 0.04–0.07, $PaCO_2$ by 3–7 mmHg and HCO_3^- by 6–9 mM (reviewed in Adamson and Swenson 2017). Five of these seven were randomized placebo-controlled studies and all gave detailed pulmonary function data as well as exclusion criteria, most notably renal disease and $FEV_1 < 500$ ml. Of critical importance to issues of safety, tolerability and effectiveness, mean FEV_1 across all these studies was 24 to 39% predicted and only a handful of patients had $FEV_1 < 20\%$ predicted. No study was longer than four weeks, and side effects and quality of life were not measured. There were no reductions in exacerbations, hospital admissions, or mortality. In one such study (Skatrud and Dempsey 1983) comparing acetazolamide with medroxyprogesterone, responders to drug therapy were identified as those sustaining a fall in $PaCO_2$ of >5 mmHg during treatment. Responders were also able to lower $PaCO_2$ by 5 mmHg during 30–60 s of voluntary hyperventilation. The non-responders (mean fall in $PaCO_2$ of 1 ± 1 mmHg) were characterized by a lower mean FEV_1 of 24% predicted versus 33% in the responders. This capacity to lower $PaCO_2$ by greater than 5 mmHg by voluntary hyperventilation is largely dependent on the ability to increase tidal volume rather than rate (Skatrud et al. 1980). These studies in stable outpatients demonstrate that acetazolamide can increase ventilation and improve arterial blood gas values in patients with mild to moderate COPD, but it may not be effective in very severe COPD. Recent work by Dominelli et al. (2018) has shown that even in healthy humans, acetazolamide in typical clinical dosing reduces both maximal diaphragmatic strength as well as peripheral skeletal muscle strength, results not found with methazolamide, findings confirming earlier work by Kiwull-Schöne et al. (2001) in the rabbit. Thus the improvements in PO_2 with acetazolamide are no better than either beginning or slightly increasing low flow supplemental oxygen, which has no side effects and does not reduce diaphragmatic muscle strength.

Similar to outpatients, studies in hospitalized patients show that acetazolamide improves arterial oxygenation and lowers HCO_3^- equivalently when given intravenously in doses of 250–500 mg to mechanically ventilated patients with co-existing metabolic alkalosis (Swenson 1998; Adamson and Swenson 2017). In most studies, this also was associated with reductions in $PaCO_2$, but no change in pH as reductions in HCO_3^- were generally matched by decreases in PCO_2 . The intent in most of these studies was to correct or diminish a metabolic alkalosis considered to be hindering liberation from the ventilator, but the degree to which the co-existing metabolic alkalosis, either primary (from diuretics, steroids, gastric suctioning, hypokalemia or hypoproteinemia) or secondary (post-hypercapnic) caused true arterial alkalemia (i.e., $pH > 7.45$) was less than 5%.

Whether acetazolamide enhances weaning or alters other clinically relevant outcomes in COPD exacerbations, the limited literature is informative. In a double blind randomized placebo-controlled study of 70 patients with hypercapnic respiratory failure and coexisting metabolic alkalosis ($PaCO_2 > 53$ mmHg and base excess $>$

8 mM), but not requiring intubation, acetazolamide (250 mg twice daily) or placebo was given for five days (Gulsvik et al. 2013). In comparison to the control arm, PaO₂ improved by 4 mmHg more in the treated group, while PaCO₂, base excess, pH, and potassium fell. Although this study was not powered to study hospital length of stay, it was no different in the two groups. Forty percent of patients given acetazolamide complained of non-specific side effects. Three patients had to be withdrawn because their arterial pH fell below 7.30.

In a retrospective 1:1 pair-wise case–control study of 72 mechanically ventilated patients with COPD and hypercapnic respiratory failure, acetazolamide (250 mg twice daily) did not alter time on the ventilator (Bahloul et al. 2015). Most recently, a randomized, placebo-controlled, double-blind, multicenter study of 380 patients with COPD exacerbations requiring intubation was performed to study the primary outcome of the effect of acetazolamide on the duration of invasive mechanical ventilation (Faisy et al. 2016). Placebo or acetazolamide (500–1000 mg daily) was given for the first two days after intubation. No significant difference was found in the primary outcome, or in weaning duration or ICU length of stay, despite achieving a significant reduction in serum bicarbonate concentration in the treatment group. Again, as in many studies, the degree of metabolic alkalosis (HCO₃ 26 ± 7 mM) was minor; none of the patients had arterial pHs >7.45, renal function was normal and baseline FEV₁ values were greater than one liter.

Thus, while these studies in mechanically ventilated patients demonstrate that acetazolamide can improve oxygenation, it does not reduce the duration of mechanical ventilation. This position is supported by two reviews (Bales and Timpe 2004; Jones and Greenstone 2001) and the US Food and Drug Administration has not approved the use of acetazolamide to hasten liberation of patients with COPD from mechanical ventilation.

3.7.2 *Chronic Cough*

Carbonic anhydrase is expressed in the airway mucosa and nerves (Hanson et al. 1981; Kumpulainen and Korhonen 1982) and in CO₂ sensitive receptors termed neuroepithelial bodies (Livermore et al. 2015; Domnik and Cutz 2011). Sensory nerves in the airways are intimately involved in cough responses (Lee and Yu 2014). Inhibition of airway CA by deposition of several inhaled CA inhibitors given as aerosols and achieving enzyme inhibiting concentrations, including acetazolamide, furosemide and hydrochlorothiazide, all suppress cough reflexes and irritant-mediated cough (Foresi et al. 1996; Elwood et al. 1993; Ventresca et al. 1990; Stone et al. 1993). Chronic cough caused by Pertussis infection in an animal model is reduced with acetazolamide (Scanlon et al. 2014). These findings all suggest a role of inhaled acetazolamide for chronic cough, which the first author has used successfully in several patients after extensive investigation could find no remediable cause of protracted cough.

3.7.3 *Pulmonary Hypertension (PH)*

More recent and on-going studies point to a possible role of CA inhibitors in the treatment of several forms of pulmonary hypertension. The first of these include several diseases with hypoxia as a primary cause—WHO Group III PH. Hypoxia at the alveolar level is a pulmonary vasoconstrictor. Pulmonary artery pressure rises at high altitude or in hypoxic lung diseases due to hypoxic pulmonary vasoconstriction (HPV) which is a normal response of the lung vasculature to low oxygen levels in the alveolar gas that cause the surrounding blood vessels to constrict (Swenson 2013). HPV can cause both an acute problem within days known as high altitude pulmonary edema (HAPE) in which the lungs become congested as a result of the higher pulmonary artery pressure and to a more chronic problem of fixed pulmonary hypertension. In the chronic situation the constant elevation of pulmonary artery pressure ultimately causes the right side of the heart to weaken and fail to pump enough blood to the left side of the heart to maintain an adequate cardiac output.

3.7.3.1 **High Altitude Pulmonary Edema (HAPE)**

HAPE is the sudden development of pulmonary edema in otherwise healthy persons who have ascended within one to five days to high altitude. It is caused by pressures high enough within the microvasculature and capillaries of the lung to overcome the structural integrity of the ultrathin alveolar capillary barrier that maintains a dry fluid-free airspace. This hydrostatic breach of the normal permeability leads to alveolar hemorrhage and fluid accumulation that prevent normal oxygen and carbon dioxide exchange. The edema causes even lower arterial oxygen levels than otherwise at that altitude, cough, breathlessness, fatigue, inability to do minimal exertion, and ultimately death if not treated (Bartsch and Swenson 2013). In some persons HPV is quite excessive and pressures can rise enough to lead to capillary stress failure (Bartsch and Swenson 2013). Drugs which lower pulmonary artery pressure, oxygen, and descent are used for HAPE treatment and certain of the same drugs used to treat HAPE can be used prophylactically to prevent its occurrence. Acetazolamide, in principle, should be beneficial in preventing HAPE since the ventilatory stimulation it induces will raise alveolar PO_2 and thus diminish the principle stimulus for HPV. Furthermore, its diuretic effect might lower the total amount of fluid available to leak into the lung. A third possible benefit is a direct action on the pulmonary vasculature.

On the basis of earlier studies into the role of CA in gas exchange, ventilation–perfusion heterogeneity and control of ventilation, it emerged that acetazolamide and other CA inhibitors might directly inhibit HPV and offer protection against HAPE. The first report of HPV inhibition by acetazolamide was buried in a report on the effects of hypercapnia on the isolated perfused lung (Emery et al. 1977). This novel and unprecedented finding of a CA inhibitor effect on a process not thought to involve acid–base exchange or a pH transduction signal went wholly unrecognized for more than a decade until CA mediation in the peripheral chemoreceptor response

to hypoxia was demonstrated (Iturriaga et al. 1991). To explore the question fully, my colleagues and I conducted work in isolated pulmonary artery smooth muscle cells, isolated perfused lungs and live animals. A comprehensive approach was necessary since CA is ubiquitously expressed throughout the body and consequences of CA inhibition might arise from direct pulmonary effects and/or secondary systemic effects.

The isolated perfused lung permits the study of HPV without the possible confounding effects of systemic hypercapnia and metabolic acidosis following CA inhibition in the whole animal, which in general are known to augment HPV. Acetazolamide (30 μM in the perfusate) reduced HPV by roughly 50% and reduced the rate of rise by 40% (Deem et al. 2000). Without providing any explanation for HPV inhibition, there was no rise in exhaled nitric oxide (NO) as a marker for increased NO production to account for HPV moderation.

Studies in the live animal are important to determine whether findings in the isolated perfused lung are reproducible *in vivo*, in which non-pulmonary effects of CA inhibition; systemic acidosis, effects on peripheral chemoreceptors, and neural transmission might potentiate or oppose HPV at the lung and vascular level. In unanesthetized beagles (Hohne et al., 2004, 2007) with invasive monitoring of pulmonary hemodynamics, ventilation, lung gas exchange, and renal function, acetazolamide (20 mg/kg) to achieve an equivalent concentration in blood to that used in the isolated perfused lung completely inhibited HPV when the dogs breathed 10% oxygen gas ($F_{\text{I}}\text{O}_2$ of 0.10). Lowering the dose of acetazolamide to 5 mg/kg, intravenous or oral (a dosing more relevant to human use) in a series of preliminary experiments also inhibited HPV, but not to the complete extent as 20 mg/kg (Hohne et al. 2007; Pickerodt et al. 2014). Inhibition of HPV could not be correlated with changes in plasma potassium, endothelin 1, or angiotensin II; factors that themselves alter HPV. Furthermore, HPV suppression in the whole animal occurs despite the systemic acidosis with CA inhibition. In several subsequent human studies, HPV is reduced by as much as 50–70% (Teppema et al. 2007; Ke et al. 2013; Boulet et al. 2018).

Altogether the data in the isolated perfused lung and whole animal clearly established that CA could be involved in the full expression of HPV, what process(es) it subserves and what cell type(s) in the lung (alveolar epithelial, vascular endothelial or arterial smooth muscle) are relevant could not be resolved by these experiments. Although HPV is a complex process (Swenson 2013), it is an inherent property of the pulmonary arterial and venous smooth muscle cells. In rat pulmonary artery smooth muscle cells obtained from small to mid-sized resistance vessels, acetazolamide had no effect on intracellular calcium (Ca^{2+}) in normoxia, but the drug markedly slowed and reduced the magnitude of Ca^{2+} uptake upon exposure of these cells to 4% O_2 (Shimoda et al. 2007) with an I_{50} of roughly 50 μM . To explore the mechanism by which acetazolamide inhibits HPV, experiments showed that acetazolamide does not act by inhibiting voltage-gated Ca^{2+} channels, does not alter membrane potential, or cause significant intracellular pH changes.

It is a general rule in pharmacology that one should never base conclusions on a single drug or concentration and CA pharmacology is no exception (Maren 1977).

When two more potent CA inhibitors, benzolamide (a hydrophilic membrane impermeant inhibitor) and ethoxzolamide (a lipophilic cell membrane-permeant inhibitor), were studied in both the isolated smooth muscle cells and the unanesthetized dog, neither of these more powerful CA inhibitors (Shimoda et al. 2007) had any effect on the intracellular rise in Ca^{2+} of hypoxic pulmonary artery smooth muscle cells and were equally ineffective in the conscious dog since neither inhibits HPV (Hohne et al. 2007). Finally, methylation of the sulfonamide nitrogen critical to the binding with zinc at the active site of the enzyme to yield an inactive drug, N-methyl acetazolamide (NMA), surprisingly showed in both the pulmonary artery smooth muscle cells and in the dog, that this drug with otherwise the exact same structure beyond the sulfonamide moiety, pK, water and lipid solubility, and intramolecular electronic charge distribution to acetazolamide, but no CA inhibiting activity was equipotent at inhibiting Ca^{2+} elevation with hypoxia and reducing HPV (Shimoda et al. 2007; Pickerodt et al. 2014). In the cell studies NMA did not lower intracellular pH, and in the dogs, it did not cause a diuresis, change urinary bicarbonate excretion, or stimulate ventilation—all the expected findings of CA inhibition.

It is clear that acetazolamide inhibits HPV at the level of the pulmonary artery smooth muscle. It does so by a mechanism not dependent upon carbonic anhydrase and is not substantially altered by the effects of inhibition of carbonic anhydrase elsewhere in the body. In this case, the response of the pulmonary vasculature interestingly differs from that of the systemic vasculature in which the evidence is more compelling for a CA mediated role in vasomotor regulation. It has been shown that isolated porcine mesenteric arteries pre-constricted with norepinephrine relaxed with acetazolamide but also to methazolamide and ethoxzolamide in a dose response manner consistent with their respective CA inhibitory potencies (Pickkers et al. 1999). Intra-arterial infusions of acetazolamide into the human forearm reduce local vascular resistance and the response can be blocked by an inhibitor of Ca^{2+} activated K^{+} channels (Pickkers et al. 2001). The molecular receptor for acetazolamide involved in HPV remains unknown.

As to whether acetazolamide itself prevents HAPE, it does so in a rat model in which 20 mg/kg prevents the typical alveolar protein, red cell, and lung water accumulation typical of human HAPE when rats are exposed to one-half atmosphere (~18,000 feet) for 24 h (Berg et al. 2004a, b). In humans the only supportive data are anecdotal unpublished reports by physicians in the mountains of Colorado who use acetazolamide to prevent re-entry HAPE in children returning home to high altitude after long holidays at sea level. A placebo controlled randomized study is presently underway to determine if acetazolamide or congeners of acetazolamide are efficacious. Use of a non-CA inhibiting form of acetazolamide if proven effective would be superior to acetazolamide in that the many side effects of CA inhibition could be avoided.

3.7.3.2 High-Altitude Pulmonary Hypertension

There has been very little work done in residents of high altitude who have pulmonary hypertension exploring whether acetazolamide or other CA inhibitors lower pulmonary artery pressures. The best studies have been performed in high altitude natives of the South American Andes, who develop a unique condition called chronic mountain sickness (CMS). CMS is characterized by greater erythrocytosis or polycythemia than that expected for the altitude of residence. By consensus, CMS is a hemoglobin concentration >21 g/dl in men and >18 in women. This degree of polycythemia causes increased blood viscosity, pulmonary hypertension, worse arterial oxygenation, thromboembolism, reduced cardiac output and work capacity along with a relative degree of hypoventilation compared to the higher ventilation of healthy high altitude residents. In both animal studies modeling CMS (Pinchon et al. 2012) and three studies in patients with CMS, acetazolamide lowers pulmonary artery pressure and hemoglobin concentration, increases ventilation and arterial oxygenation, and improves exercise capacity and quality of life (Richalet et al. 2005, 2008; Sharma et al. 2017). These improvements are indicative of a multifactorial effect of acetazolamide acting favourably on erythropoiesis, hemorheology, cardiac output, ventilation and tissue oxygenation. The limitation of the use of acetazolamide for CMS arises from the fact that the areas of the world where CMS is most prevalent do not have extensive health care systems to cover the costs of chronic treatment even with relatively low cost non-patent protected drugs.

Elsewhere in the world, the Himalayan and the Rocky Mountains, high altitude pulmonary hypertension in the absence of excessive erythrocytosis is just beginning to come under study with various drugs used to treat pulmonary hypertension at low altitude. Faoro et al. (2007) studied humans after ten days at 4,700 m and found that oral acetazolamide for one day at 250 mg tid did not reduce pulmonary artery (PA) pressures at rest or during exercise. Similarly, Basnyat et al. (2008) found that acetazolamide also did not reduce PA pressure in trekkers when started many days after reaching a high altitude start site (4,250 m). To date, however, acetazolamide or other CA inhibitors have not been tested except in rat and mice models. In mice and rat hypoxia models, it appears that hypoxia up-regulates the expression of aquaporin-1 (which is blocked by acetazolamide as discussed above) and knockdown of aquaporin-1 by different means limits hypoxic pulmonary hypertension (Schuoler et al. 2017; Yun et al. 2017; Liu et al. 2019). Very recently, acetazolamide in the same mouse model of (Schuoler et al. 2017) was efficacious in reducing aquaporin-1 expression and reducing pulmonary hypertension (Haider et al. 2019 submitted for publication). In an inflammatory/hypoxia pulmonary hypertension created by the combination of a vascular endothelial growth factor inhibitor in combination with ambient hypoxia, acetazolamide was effective in reducing pulmonary artery pressure. It did so by reducing inflammation possibly by inhibition of alveolar macrophage CA II, which is expressed at high concentrations in the hypertensive rats and in patients with pulmonary artery hypertension (Hudalla et al. 2019) or by the metabolic acidosis arising from renal CA inhibition (Christou et al. 2019). The only human studies suggestive of a salutary effect on a form of hypoxic pulmonary hypertension have

been in patients with sleep apnea treated with acetazolamide (Thurnheer et al. 2017; Ulrich et al. 2015). Given the improved ventilation with sleep and the resultant higher mean alveolar PO_2 , a major contributor to lowered pulmonary artery pressure and vascular resistance will be the reduction in sleep disordered breathing, but a direct effect on the pulmonary vasculature remains a compelling possibility. Thus, acetazolamide as a treatment for high altitude pulmonary hypertension is worthy of greater investigation.

3.7.3.3 Non-hypoxic Pulmonary Hypertension

Pulmonary hypertension often develops in patients with congestive heart failure and depressed left ventricular diastolic and systolic function as a result of chronic pulmonary venous hypertension and propagation of the elevated pressure to the pulmonary arteries. The early studies of acetazolamide mentioned above in heart failure included some with cor pulmonale, or right heart failure due to left heart failure. In those studies, cor pulmonale was improved. The improvements were certainly due to diuresis and reduction in peripheral and pulmonary edema, but direct effects on the pulmonary vasculature were never studied in those days due to the lack of now widely available flow directed pulmonary artery catheters and more recently echocardiography. Another possible benefit already shown in the heart of reduced pathological remodeling of the left ventricle (Vargas et al. 2016) could be the same in the right ventricle. Despite mounting evidence in several forms of hypoxic pulmonary hypertension, there have been no studies of the other many causes of pulmonary hypertension in patients with CA inhibitors. Presently there is a large placebo controlled trial of acute and chronic acetazolamide treatment in patients with various forms of non-hypoxic pulmonary hypertension underway in Switzerland (Ulrich and colleagues, personal communication).

3.7.4 Lung Ischemia–Reperfusion Injury

Similar to positive results in moderating ischemia-reperfusion injury in the heart as described above (Ciocci-Pardo et al. 2018; Gonzalez Arbelaez et al. 2018), brain (Di Cesare Mannelli et al. 2016), liver (Bejaoui et al. 2015), and kidney (An et al. 2013), two studies in the lung have shown excellent preservation of structure and function, reduction in inflammation and apoptosis if acetazolamide is given just before the return of perfusion. In the first (Lan et al. 2017), the dosing of acetazolamide in a rat model was very high 100–400 mg/kg, dosing not practical or tolerable in humans. The second studied lower doses (30 mg/kg) of acetazolamide, benzolamide, and n-methyl acetazolamide (an analog of acetazolamide unable to inhibit CA) and found reductions in injury by all three drugs. The findings in this study (Kumar and Swenson unpublished results) suggest that acetazolamide acts both by CA inhibition

and perhaps through its suppression of hypoxic calcium signaling, a non-CA dependent process (Shimoda et al. 2007). The approximate rate of lung ischemia-perfusion injury in human lung transplantation is such that 10–20% of all patients suffer early graft dysfunction requiring longer periods of mechanical ventilation and extended post-operative periods in intensive care.

3.8 Conclusions

Acetazolamide and other CA inhibitors have multiple actions involving both inhibition of CA and of other processes independent of CA that give foundation and promise to a greater role of these drugs in the treatment of many cardiovascular and pulmonary diseases. Under certain circumstances, such as in hypoxic situations and high sympathetic nervous system activation, CA inhibitors act as good antihypertensives in both the systemic and pulmonary circulations. They also appear to alter pathological left ventricular hypertrophic remodeling in ischemic coronary artery disease, and this may equally apply to diseases leading to cor pulmonale involving the right side of the heart. At high altitude, reduction of hypoxic pulmonary vasoconstriction may be useful in preventing high altitude pulmonary edema. Lastly, the protection afforded by acetazolamide and other CA inhibitors in many animal models of acute organ ischemia-reperfusion injury involving the brain, kidney, liver, heart, and lung offers the possibility of using these safe and clinically approved drugs in myocardial infarction and stroke, and in surgical procedures involving long durations of ischemia, such as is necessary in organ transplantation. Work for the future should be aimed at moving appropriately to well-designed clinical trials and in animal studies seeking to better understand the myriad ways, particularly for acetazolamide, of how this class of drugs work in such a variety of conditions.

References

- Aamand R, Dalsgaard T, Jensen FB et al (2009) Generation of nitric oxide from nitrite by carbonic anhydrase: a possible link between metabolic activity and vasodilation. *Am J Physiol* 297:H2068–H2074
- Abreu-Rodriguez I, Silva R, Martins AP et al (2011) Functional and transcriptional induction of aquaporin-1 by hypoxia: Analysis of promoter and role of HIF-1alpha. *PLoSOne* 6:e28385
- Acin-Perez R, Salazar E, Kamenetsky M et al (2009) Cyclic AMP produced inside mitochondria regulates oxidative phosphorylation. *Cell Metab* 9:265–276
- Adamson R, Swenson ER (2017) Acetazolamide use in severe chronic obstructive pulmonary disease. Pros and cons. *Ann Am Thorac Soc* 14:1086–1093
- Adamson T, Waxman B (1976) Carbonate dehydratase (carbonic anhydrase) and the fetal lung. *Lung Liquids*. Ciba Fdn Series 38:221–234
- Adamson T, Boyd R, Platt H, Strang L (1969) Composition of alveolar liquid in the fetal lamb. *J Physiol* 204:159–168

- Agarwal N, Lippman ES, Shusta EV (2010) Identification and expression profiling of blood brain barrier membrane proteins. *J Neurochem* 112:625–635
- Alvarez BV, Johnson DE, Sowah D et al (2007) Carbonic anhydrase inhibition prevents and reverts cardiomyocyte hypertrophy. *J Physiol* 579:127–145
- Alvarez BV, Quon A, Mullen J, Casey JR (2013) Quantification of carbonic anhydrase gene expression in ventricle of hypertrophic and failing human heart. *BMC Cardiovasc Disord* 13:2
- Ameli PA, Madan M, Chigurupati S et al (2012) Effect of acetazolamide on aquaporin-1 and fluid flow in cultured choroid plexus. *Acta Neurochir Suppl* 113:59–64
- An Y, Zhang JZ, Han J et al (2013) Hypoxia-Inducible factor-1A dependent pathways mediate the renoprotective role of acetazolamide against renal ischemia-reperfusion injury. *Cell Physiol Biochem* 32:1151–1166
- Andring JT, Lomelino CL, Tu C et al (2018) Carbonic anhydrase II does not exhibit Nitrite reductase or Nitrous Anhydrase Activity. *Free Radic Biol Med* 117:1–5
- Apostolo A, Agostoni P, Contini M et al (2014) Acetazolamide and inhaled carbon dioxide reduce periodic breathing during exercise in patients with chronic heart failure. *J Card Fail* 20:278–288
- Arias-Hidalgo M, Al-Samir S, Weber N et al (2017) CO₂ permeability and carbonic anhydrase activity of a rat cardiomyocytes. *Acta Physiol* 115–128
- Arias-Hidalgo M, Yuan Q, Carta F et al (2018) CO₂ permeability of rat hepatocytes and relation of CO₂ permeability to CO₂ production. *Cell Physiol Biochem* 46:1198–1208
- Assadi F (2006) Acetazolamide for prevention of contrast-induced nephropathy: a new use for an old drug. *Pediatr Cardiol* 27:238–242
- Bahloul M, Chaari A, Tounsi A et al (2015) Impact of acetazolamide use in severe exacerbation of chronic obstructive pulmonary disease requiring invasive mechanical ventilation. *Int J Crit Illn Inj Sci* 5:3–8
- Bales MJ, Timpe EM (2004) Respiratory stimulant use in chronic obstructive pulmonary disease. *Ann Pharmacother* 38:1722–1725
- Barnikol W, Diether K (1979) Die broncholytische Wirkung von Carboanhydrasehemmern bei Lungengesunden. *Drug Res* 29:1642–1644
- Bärtsch P, Swenson ER (2013) Clinical practice: acute high altitude illnesses. *N Engl J Med* 368:2294–2302
- Basnyat B, Hargrove J, Holck PS et al (2008) Acetazolamide fails to decrease pulmonary artery pressure at high altitude in partially acclimatized humans. *High Alt Med Biol* 9:209–216
- Bejaoui M, Pantazi E, De Luca V et al (2015) Acetazolamide protects steatotic liver grafts against cold ischemia reperfusion injury. *J Pharmacol Exp Ther* 355:191–198
- Benga O, Huber VJ (2012) Brain water channel proteins in health and disease. *Mol Aspects Med* 33:562–578
- Berfenstam R (1952) Carbonic anhydrase activity in fetal organs. *Acta Paediatr* 41:310–315
- Berg JT, Ramanathan S, Gabrielli MG, Swenson ER (2004a) Carbonic anhydrase in mammalian vascular smooth muscle. *J Histochem Cytochem* 52:1101–1106
- Berg JT, Ramanathan S, Swenson ER (2004b) Inhibition of hypoxic pulmonary vasoconstriction prevents high altitude pulmonary edema in rats. *Wild Environ Med* 15:32–37
- Bidani A (1991) Analysis of abnormalities of capillary CO₂ exchange in vivo. *J Appl Physiol* 70:1686–1699
- Boucher R (1994) Human airway ion transport. *Am J Respir Crit Care Med* 150:271–281
- Boulet LM, Teppema LJ, Hackett HK et al (2018) Attenuation of human hypoxic pulmonary vasoconstriction by acetazolamide and methazolamide. *J Appl Physiol* 125:1803–1975
- Brechue WF, Stager JM, Lukaski HC (1990) Body water and electrolyte responses to acetazolamide in humans. *J Appl Physiol* 69:1397–1401
- Brest AN, Onesti G, Sekine G et al (1961) Acetazolamide alone and in combination with reserpine in the treatment of hypertension. *Angiology* 12:589–592
- Broten TP, Feigl EO (1992) Role of myocardial oxygen and carbon dioxide in coronary autoregulation. *Am J Physiol* 262:H1231–H1237

- Broten TP, Romson JP, Fullerton DA et al (1991) Synergistic action of myocardial oxygen and carbon dioxide in controlling coronary blood flow. *Circ Res* 68:531–542
- Brown BF, Quon A, Dyck JR, Casey JR (2012) Carbonic anhydrase II promotes cardiomyocyte hypertrophy. *Can J Physiol Pharmacol* 90:1599–1610
- Bruns W, Gros G (1992) Membrane-bound carbonic anhydrase in the heart. *Am J Physiol* 262:H577–H584
- Campbell AR, Andress DL, Swenson ER (1994) Identification and characterization of human neutrophil carbonic anhydrase. *J Leukoc Biol* 55:343–348
- Cardenas Y, Heming T, Bidani A (1998) Kinetics of CO₂ excretion and Intravascular pH disequilibria during carbonic anhydrase inhibition. *J Appl Physiol* 184:683–689
- Carmignani M, Ranelletti FO, Marchetti P, Ripanti G (1981) Acetazolamide and smooth muscle: possible mechanisms conditioning the contractile responses induced by various experimental procedures in several isolated preparations. *Pharmacol Res Commun* 13:185–194
- Carter ND, Fryer A, Grant AG et al (1990) Membrane specific carbonic anhydrase (CAIV) expression in human tissue. *Biochim Biophys Acta* 1026:113–116
- Cavaliere F, Masieri S, Non S, Magalini S, Allegra S (1996) Carbonic anhydrase in human nasal epithelium. *Am J Rhin* 10:113–117
- Chander A, Johnson RG, Reicherter J, Fisher AB (1986) Lung lamellar bodies maintain an acidic internal pH. *J Biol Chem* 261:6126–6131
- Chen J, Lecuona E, Briva A et al (2008) Carbonic anhydrase II and alveolar fluid reabsorption during hypercapnia. *Am J Respir Cell Mol Biol* 38:32–37
- Choi HB, Gordon GRJ, Zhou N et al (2012) Metabolic communication between astrocytes and neurons via bicarbonate-responsive soluble adenylyl cyclase. *Neuron* 75:1094–1104
- Christou H, Reslan OM, Mam V et al (2019) Improved Pulmonary vascular reactivity and decreased hypertrophic remodeling during nonhypercapnic acidosis in experimental pulmonary hypertension. *Am J Physiol* 302:L875–L890
- Chu S, Montrose MH (1995) Extracellular pH regulation in microdomains of colonic crypts: effects of short-chain fatty acids. *Proc Natl Acad Sci* 92:3303–3307
- Ciocco Pardo A, Diaz RG, Swenson ER et al (2018) Benzolamide perpetuates acidic conditions during reperfusion and reduces myocardial ischemia-reperfusion injury. *J Apple Physiol* 125:340–352
- Coats CJ, Heywood WE, Virasami A et al (2018) Proteomic analysis of the myocardium in hypertrophic obstructive cardiomyopathy. *Circ Genom Precis Med* 11:e001974
- Conroy CW, Wynns GC, Maren TH (1996) Synthesis and properties of two new membrane impermeant high molecular weight carbonic anhydrase inhibitors. *Bioorg Chem* 24:262–272
- Crandall ED, Bidani A (1981) Effects of red blood cell HCO₃/Cl exchange kinetics on lung CO₂ transfer: theory. *J Appl Physiol* 50:265–271
- Crandall E, O’Brasky J (1978) Direct evidence for participation of rat lung carbonic anhydrase in CO₂ reactions. *J Clin Invest* 62:618–622
- Cuthbert AW, Supuran CT, MacVinish LJ (2003) Bicarbonate-dependent chloride secretion in Calu-3 epithelia in response to 7,8-benzoquinoline. *J Physiol* 551:79–92
- Davis T, Gause G, Perks A, Kuck H, Cassin S (1980) The effects of acetazolamide on fetal lung liquid secretion. *FASEB J* A1140
- Davis T, Kucks H, Perks A, Maren T, Cassin S (1989) Measurement of the H⁺ secretion in fetal ovine lung liquid. *Physiologist* 32:202
- De Hemptinne A, Marrannes R, Vanheel B (1986) Surface pH and the control of intracellular pH in cardiac and skeletal muscle. *Can J Physiol Pharmacol* 65:970–977
- De Rasmio D, Signorile A, Santeramo A et al (2015) Intramitochondrial adenylyl cyclase controls the turnover of the nuclear-encoded subunits and activity of mammalian complex respiratory chain. *Biochem Biophys Acta* 1853:183–191
- de Simone G, Gottdiener JS, Chinali M, Maurer MS (2008) Left ventricular mass predicts heart failure not related to previous myocardial infarction: the cardiovascular health study. *Eur Heart J* 29:741–747

- Deem S, Hedges RG, Kerr ME, Swenson ER (2000) Acetazolamide reduces hypoxic pulmonary vasoconstriction in isolated perfused rabbit lung. *Respir Physiol* 123:109–119
- Devor DC, Singh AK, Lambert Let Deluca A, Frizzell RA, Bridges RJ (1999) Bicarbonate and chloride secretion in Calc-3 human airway epithelial cells. *J Gen Physiol* 113:743–760
- Dhainaut JF, Schremmer B, Lanore JJ (1991) The coronary circulation and the myocardial oxygen supply/uptake relationship: a short review. *J Crit Care* 6:52–60
- Di Cesare Mannelli L, Micheli L, Carta F et al (2016) Carbonic Anhydrase inhibition for the management of cerebral ischemia: in vivo evaluation of sulfonamide and coumarin inhibitors. *J Enzyme Inhib Med Chem* 894–899
- Dominelli PB, McNeil CL, Vermeulen TD et al (2018) Effect of acetazolamide and methazolamide on diaphragm and dorsiflexor fatigue: a randomized controlled trial. *J Appl Physiol* 125:770–779
- Domnik NJ, Cutz E (2011) Pulmonary neuroepithelial bodies as airway sensors: putative role in the generation of dyspnea. *Curr Opin Pharmacol* 11:211–217
- Dorrington K, Boyd C (1995) Active transport in the alveolar epithelium of the adult lung: vestigial or vital? *Respir Physiol* 100:177–183
- Effros R, Chinard F (1969) The in vivo pH of extravascular space of the lung. *J Clin Invest* 48:1983–1996
- Effros RM, Mason G, Silverman P (1981a) Asymmetric distribution of carbonic anhydrase in the alveolar-capillary barrier. *J Appl Physiol* 51:190–193
- Effros R, Mason G, Silverman P (1981b) Role of perfusion and diffusion in 14CO_2 exchange in the rabbit lung. *J Appl Physiol* 51:1136–1144
- Effros R, Mason G, Hukkanen J, Silverman P (1989) New evidence for active sodium transport from fluid-filled rat lungs. *J Appl Physiol* 66:906–919
- Ellis D, Thomas RC (1976) Direct measurement of the intracellular pH of mammalian cardiac muscle. *J Physiol* 262:755–771
- Elwood W, Lotvall J, Barnes P, Chung F (1991) Loop diuretics inhibit cholinergic and non-cholinergic nerves in guinea pig airways. *Am Rev Respir Dis* 143:1340–1344
- Elwood W, Barnes PJ, Chung KF (1993) Effect of thiazide diuretics against neurally mediated contraction of guinea pig airways. Contribution of carbonic anhydrase. *Am Rev Respir Dis* 148:902–908
- Emery CJ, Sloan PJ, Mohammed FH, Barer GR (1977) Action of hypercapnia during hypoxia on pulmonary vessels. *Bull Eur Physiopath Respir* 13:763–776
- Enns T, Hill E (1983) CO_2 diffusing capacity in isolated dog lung lobes and the role of carbonic anhydrase. *J App Physiol* 54:483–490
- Eskandari D, Zou D, Grote L et al (2018) Acetazolamide reduces blood pressure and sleep-disordered breathing in patients with hypertension and obstructive sleep apnea: a randomized controlled trial. *J Clin Sleep Med* 14:309–317
- Faisy C, Meziani F, Planquette B et al (2016) Effect of acetazolamide vs placebo on duration of invasive mechanical ventilation among patients with chronic obstructive pulmonary disease: a randomized clinical trial. *J Am Med Assoc* 315:480–488
- Faoro V, Huez S, Giltaire S (2007) Effects of acetazolamide on aerobic exercise capacity and pulmonary hemodynamics at high altitudes. *J Appl Physiol* 103:1161–1165
- Favre L, Vallotton MB (1984) Relationship of renal prostaglandins to three diuretics. *Prostaglandins Leukot Med* 14:313–319
- Ferdinand KC, Nasser S (2017) Management of essential hypertension. *Cardiol Clin* 35:231–246
- Fernley RT, Wright RD, Coghlan JP (1991) Radioimmunoassay of carbonic anhydrase VI in saliva and sheep tissues. *Biochem J* 274:313–316
- Fleming RE, Crouch EC, Ruzicka CA, Sly WS (1993) Pulmonary carbonic anhydrase IV: developmental regulation and cell-specific expression in the capillary endothelium. *Am J Physiol* 265:L627–635
- Fleming RE, Moxley MA, Waheed EC et al (1994) Carbonic anhydrase II expression in rat type II Pneumocytes. *Am J Respir Cell Mol Biol* 10:499–505

- Foresi A, Caviglioli G, Pelucchi A et al (1996) Effect of acetazolamide on cough induced by low-chloride-ion solutions in normal subjects: comparison with furosemide. *J Allergy Clin Immunol* 97:1093–1099
- Franzen D, Conway RS, Zhang H et al (1988) Spatial heterogeneity of local blood flow and metabolite content in dog hearts. *Am J Physiol* 254:H344–H353
- Fujikawa-Adachi K, Nishimori I, Taguchi T, Onishi S (1999) Human mitochondrial carbonic anhydrase VB. cDNA cloning, mRNA expression, subcellular localization, and mapping to chromosome x. *J Biol Chem* 274:21228–21233
- Gatto L (1981) pH of mucus in rat trachea. *J Appl Physiol* 50:1224–1226
- Geers C, Gros G (1995) Contractile function of papillary muscles with carbonic anhydrase inhibitors. *Life Sci* 57:591–597
- Goldsmith SR, Iber C, McArthur CD et al (1990) Influence of acid-base status on plasma catecholamines during exercise in normal humans. *Am J Physiol* 258:R1411–R1416
- Gonzalez Arbelaez LF, Ciocci Pardo A, Swenson ER et al (2018) Cardioprotection of benzolamide in a regional ischemia model: role of eNOS/NO. *Exp Mol Pathol* 105:345–351
- Gonzalez F, Bassingthwaighe JB (1990) Heterogeneities in regional volumes of distribution and flows in rabbit heart. *Am J Physiol* 258:H1012–H1024
- Goresky CA, Stremmel W, Rose CP et al (1994) The capillary transport system for free fatty acids in the heart. *Circ Res* 74:1015–1026
- Grossman WM, Keoberle B (2000) The dose response relationship of acetazolamide on the cerebral blood flow in normal subjects. *Cerebrovasc Dis* 10:65–69
- Gulsvik R, Skjorten I, Undhjem K et al (2013) Acetazolamide improves oxygenation in patients with respiratory failure and metabolic alkalosis. *Clin Respir J* 7:390–396
- Guo F, Hua Y, Wang J et al (2012) Inhibition of carbonic anhydrase reduces brain injury after intracerebral hemorrhage. *Transl Stroke Res* 3:130–137
- Hanson M, Nye P, Torrance R (1981) Studies on the localization of pulmonary carbonic anhydrase in the cat. *J Physiol* 319:93–109
- Hatch M (1987) Short chain fatty acid and its effect on ion transport by rabbit cecum. *Am J Physiol* 253:G171–178
- Heming A, Bidani A (1992) Influence of proton availability on intracapillary CO_2H^+ reactions in 10 isolated rat lungs. *J Appl Physiol* 72:2140–2148
- Heming T, Geers C, Gros G, Bidani A, Crandall E (1986) Effects of dextran-bound inhibitors on carbonic anhydrase activity in isolated rat lungs. *J Appl Physiol* 61:1849–1856
- Heming TA, Brown SES, Bidani A (1991) Role of CA in pH regulation in the lung. In: Symposium on carbonic anhydrase, Hannover, Germany
- Heming T, Vanoye C, Stabenau E, Roush E, Fierke C, Bidani A (1993) Inhibitor sensitivity of pulmonary vascular carbonic anhydrase. *J Appl Physiol* 75:1642–1649
- Heming T SE, Vanoye C, Moghadasi H, Bidani A (1994) Roles of intra- and extra-cellular carbonic anhydrase in alveolar-capillary CO_2 equilibration. *J Appl Physiol* 77:697–705
- Henry RP, Dodgson SJ, Forster RE et al (1986) Rat Lung carbonic anhydrase: activity, localization and isozymes. *J Appl Physiol* 60:638–645
- Herrera M, Garvin JL (2011) Aquaporins as gas channels. *Pflugers Arch* 462:623–630
- Höhne C, Krebs MO, Seiferheld M et al (2004) Acetazolamide prevents hypoxic pulmonary vasoconstriction in conscious dogs. *J Appl Physiol* 97:515–521
- Höhne C, Pickerodt PA, Francis RC, Swenson ER (2007) Pulmonary vasodilation by acetazolamide during hypoxia is unrelated to carbonic anhydrase inhibition. *Am J Physiol* 292:L178–L184
- Hollander W (1976) Role of hypertension in atherosclerosis and cardiovascular disease. *Am J Cardiol* 38:786–800
- Holotnakova T, Ziegelhoffer A, Ohradanova A et al (2008) Induction of carbonic anhydrase IX by hypoxia and chemical disruption of oxygen sensing in rat fibroblasts and cardiomyocytes. *Pflugers Arch* 456:323–337
- Horita Y, Yakabe K, Tadokoro M et al (2006) Renal circulatory effects of acetazolamide in patients with essential hypertension. *Am J Hypertension* 19:282–285

- Howard LS, Crosby A, Vaughan P, Sobolewski A et al (2012) Distinct responses to hypoxia in subpopulations of distal pulmonary artery cells contribute to pulmonary vascular remodeling in emphysema. *Pulm Circ* 2:241–249
- Huber VJ, Tsujita M, Kwee IL et al (2009) Inhibition of aquaporin-4 by antiepileptic drugs. *Bioorg Med Chem* 17:418–424
- Hudalla H, Michael Z, Christodoulou N et al (2019) Carbonic anhydrase inhibition ameliorates inflammation and experimental pulmonary hypertension. *Am J Respir Cell Mol Biol* (in press)
- Igarashi H, Tsujita M, Suzuki Y et al (2013) Inhibition of aquaporin-4 significantly increases regional brain blood flow. *NeuroReport* 24:324–328
- Imiela T, Budaj A (2017) Acetazolamide as add-on diuretic therapy in exacerbations of chronic heart failure: a pilot study. *Clin Drug Investig* 37:1175–1181
- Inglis S, Corboz M, Taylor A, Ballard S (1997) Effect of anion transport inhibition on mucus secretion by airway submucosal glands. *Am J Physiol* 272:L372–L377
- Innocenti A, Gülçin I, Scozzafava A, Supuran CT (2010) Carbonic anhydrase inhibitors. Antioxidant polyphenols effectively inhibit mammalian isoforms I–XV. *Bioorg Med Chem Lett* 20:5050–5053
- Iturriaga R, Lahiri S, Mokashi A (1991) Carbonic anhydrase and chemoreception in the cat carotid body. *Am J Physiol* 261:C565–C573
- Jack C, Tran J, Donnelly R, Hind C, Evans C (1990) Endobronchial pH measurements in anaesthetized subjects. *Thorax* 45:315P
- Jeffrey S, Carter ND (1980) Distribution of carbonic anhydrase III in fetal and adult human tissue. *Biochem Gene* 18:143–147
- Jones PW, Greenstone M (2001) Carbonic anhydrase inhibitors for hypercapnic ventilatory failure in chronic obstructive pulmonary disease. *Cochrane Database Syst Rev* d002881
- Jonk AM, van den Berg IP, Olfert IM et al (2007) Effect of acetazolamide on pulmonary and muscle gas exchange during normoxic and hypoxic exercise. *J Physiol* 579:909–921
- Kamp F, Hamilton JA (1992) pH gradients across phospholipid membranes caused by fast flip-flop of un-ionized fatty acids. *Proc Natl Acad Sci* 89:11367–11370
- Katz SA, Feigl EO (1987) Little carbon dioxide diffusional shunting in coronary circulation. *AM J Physiol* 253:H614–625
- Kawai Y, Ajima K, Kaidoh M et al (2015) In vivo support for the new concept of pulmonary blood flow-mediated CO₂ gas excretion in the lungs. *Am J Physiol* 308:L1224–L1236
- Ke T, Wang J, Swenson ER et al (2013) Effect of acetazolamide and ginkgo biloba on the human pulmonary vascular response to an acute altitude ascent. *High Alt Med Biol* 14:162–167
- King RB, Bassingthwaighe JB (1989) Temporal fluctuations in regional myocardial flows. *Pflugers Arch* 413:336–342
- Kiss B, Dallinger S, Findl O et al (1999) Acetazolamide-induced cerebral and ocular vasodilation in humans is independent of nitric oxide. *Am J Physiol* 276:R1661–R1667
- Kiwull-Schöne HF, Teppema LJ, Kiwull PJ (2001) Low dose acetazolamide does affect respiratory muscle function in spontaneously anesthetized rabbits. *Am J Respir Crit Care Med* 163:478–483
- Klocke R (1978) Catalysis of CO₂ reactions by lung carbonic anhydrase. *J Appl Physiol* 44:882–888
- Klocke RA (1997) Potential role of endothelial carbonic anhydrase in dehydration of plasma bicarbonate. *Trans Am Clin Clim Assoc* 108:44–58
- Korotzer B, Tyler J, Stringer W, Nguyen P, Wasserman K (1997) The effect of acetazolamide on lactate, lactate threshold, and acid-base balance during exercise. *Am J Respir Crit Care Med* 155:A171
- Kringelholz S, Simonsen U, Bek T (2012) Dorzolamide-induced relaxation of intraocular porcine ciliary arteries in vitro depends on nitric oxide and the vascular endothelium. *Curr Eye Res* 37:1107–1113
- Krishnan D, Liu L, Wiebe SA, Casey JR et al (2015) Carbonic anhydrase II binds to and increases the activity of the epithelial sodium proton exchanger, NHE3. *Am J Physiol* 309:F383–392
- Krouse ME, Talbott JF, Lee MM, Joo NS, Wine JJ (2004) Acid and base secretion in the Calu-3 model of human serous cells. *Am J Physiol* 287:L1274–1283

- Kumpulainen T, Korhonen LK (1982) Immunohistochemical localization of carbonic anhydrase isoenzyme C in the central and peripheral nervous system of the mouse. *J Histochem Cytochem* 30:283–292
- Lagadic-Gossmann D, Buckler KJ, Vaughan-Jones RD (1992) Role of bicarbonate in pH recovery from intracellular acidosis in the guinea-pig ventricular myocyte. *J Physiol* 458:361–384
- Lan CC, Peng CK, Tang SE et al (2017) Carbonic Anhydrase inhibitor attenuates ischemia-reperfusion induces acute lung injury. *PLoS One* E0179822
- Leaf A, Schwartz WB, Relman AS (1954) Oral administration of a potent carbonic anhydrase inhibitor (Diamox). Changes in electrolyte and acid-base balance. *N Engl J Med* 250:800–804
- Lee LY, Yu J (2014) Sensory nerves in the lung and airways. *Compr Physiol* 4:287–324
- Lee M, Vecchio-Pagán B, Sharma N, Waheed A et al (2016) Loss of carbonic anhydrase XII function in individuals with elevated sweat chloride concentration and pulmonary airway disease. *Hum Mol Genet* 25:1923–1933
- Lee M, Vecchio-Pagan B, Sharma N et al (2016) Loss of carbonic anhydrase XII function in individuals with elevated sweat chloride concentration and pulmonary airway disease. *Hum Mol Genet*
- Lee JY, Alexeyev M, Kozhukhar N, Pastukh V et al (2018) Carbonic anhydrase IX is a critical determinant of pulmonary microvascular endothelial cell pH regulation and angiogenesis during acidosis. *Am J Physiol* 315:L41–L51
- Lee JY, Onanyan M, Garrison I, White R et al (2019) Extrinsic acidosis suppresses glycolysis and migration while increasing network formation in pulmonary microvascular cells. *Am J Physiol* 317:L188–L201
- Leinonen JS, Saari KA, Seppanen et al (2004) Immunohistochemical demonstration of carbonic anhydrase isoenzyme VI (CA VI) expression in rat lower airways and lung. *J Histochem Cytochem* 52:1107–1112
- Leon Jimenez D, Gomez Huelgas R, Miramontes Gonzalez JP (2018) The mechanism of action of sodium-glucose co-transporter 2 inhibitors is similar to carbonic anhydrase inhibitors. *Eur J Heart Fail* 20:409
- Lisk C, McCord J, Bose S et al (2013) Nrf2 activation: a potential strategy for the prevention of acute mountain sickness. *Free Radic Biol Med* 63:264–273
- Liu M, Liu Q, Pei Y, Gong M et al (2019) Aqp-1 gene knockout attenuates hypoxic pulmonary hypertension of mice. *Atheroscler Thromb Vasc Biol* 39:48–62
- Livermore S, Zhou Y, Pan J, Yeger H et al (2015) Pulmonary neuroepithelial bodies are polymodal airway sensors: evidence for CO₂/H⁺ sensing. *Am J Physiol* 308:L807–L815
- Lonnerholm G (1982) Pulmonary carbonic anhydrase in the human, monkey, and rat. *J Appl Physiol* 52:352–356
- Lonnerholm G, Wistrand P (1982) Carbonic anhydrase in the human fetal lung. *Pediatr Res* 16:407–411
- Lopez C, Alcaraz AJ, Toledo B et al (2016) Acetazolamide therapy for metabolic alkalosis in pediatric intensive care patients. *Pediatr Crit Care Med* 17:e551–e558
- Lubman R, Crandall E (1992) Regulation of intracellular pH in alveolar epithelial cells. *Am J Physiol* 262:L1–L14
- Lubman R, Danto S, Crandall E (1989) Evidence for active H⁺ secretion by rat alveolar epithelial cells. *Am J Physiol* 257:L438–L445
- Mahieu I, Sagar-Malik A, Hollande E et al (1995) Localisation and characterisation of carbonic anhydrase isozymes (CA I, CA II, CA III and CA IV) in an umbilical vein endothelial cell line (EA-hy926). *Biochem Soc Trans* 23:308S
- Maillet M, van Berlo JH, Molkentin JD (2013) Molecular basis of physiological heart growth fundamental concepts and new players. *Nat Rev Mol Cell Biol* 14:38–48
- Maren TH (1977) Use of inhibitors in physiological studies of carbonic anhydrase. *Am J Physiol* 232:F291–F297
- Maren TH (1984) Carbonic anhydrase: the middle years, 1945–1960, and the introduction to pharmacology of sulfonamides. *Ann NY Acad Sci* 429:10–17

- McNaughton NC, Davies CH, Randall A (2004) Inhibition of alpha(1E) Ca(2+) channels by carbonic anhydrase inhibitors. *J Pharmacol Sci* 95:240–247
- McNicol M, Pride NB (1961) Dichlorophenamide in chronic respiratory failure. *Lancet* 1:906–908
- Megibow RS, Pollack H, Stollerman GH et al (1948) The treatment of hypertension by accelerated sodium depletion. *J Mt Sinai Hosp* 15:233
- Mochizuki M, Shibuya I, Uchida K, Kagawa T (1987) A method for estimating contact time of red blood cells through lung capillary from O₂ and CO₂ concentration in rebreathing air in man. *Jpn J Physiol* 37:283–301
- Moffett BS, Moffett TI, Dickerson HA (2007) Acetazolamide therapy for hypochloremic metabolic alkalosis in pediatric patients with heart disease. *Am J Ther* 14:331–335
- Morgan PE, Supuran CT, Casey JR (2004) Carbonic anhydrase inhibitors that directly inhibit anion transport by the human Cl⁻/HCO₃⁻-exchanger, AE1. *Mol Memb Biol* 21:423–433
- Moyer JH, Ford RV (1958) Laboratory and clinical observations on ethoxzolamide (cardrase) as a diuretic agent. *Am J Cardiol* 1:497–504
- Moyer JH, Hughes WM (1995) A comparative study of neohydrin and diamox when used alone and in combination for the treatment of severe congestive heart failure. *J Chronic Dis* 2:678–686
- Moynihan JB (1977) Carbonic anhydrase activity in mammalian skeletal muscle and cardiac muscle. *Biochem J* 168:567–569
- Mullens W, Verbrugge FH, Nijst P et al (2018) Rationale and design of the advor (acetazolamide in decompensated heart failure with volume overload) trial. *Eur J Heart Fail* 20:1591–1600
- Nakada T (2015) The molecular mechanisms of neural flow coupling. A new concept. *J Neuroimaging*. 25:681–685
- Nielson D (1986) Electrolyte composition of pulmonary alveolar subphase in anesthetized rabbits. *J Appl Physiol* 60:972–979
- Nilius B, Droogmans G (2001) Ion channels and their functional role in vascular endothelium. *Physiol Rev* 81:1415–1459
- Nioka S, Henry RP, Forster RE (1988) Total CA activity in isolated perfused guinea pig lung by 180-exchange method. *J Appl Physiol* 65:2236–2244
- O'Connor B, Chung F, Chen-Worsdell M, Fuller R, Barnes P (1991) Effect of inhaled furosemide and bumetanide on adenosine 5'-monophosphate- and sodium metabisulfite-induced bronchoconstriction in asthmatic subject. *Am Rev Respir Dis* 143:1329–1333
- O'Connor B, Yeo C, Chen-Worsdell Y, Barnes P, Chung K (1994) Effect of acetazolamide and amiloride against sodium metabisulphite-induced bronchoconstriction in mild asthma. *Thorax* 49:1096–1098
- O'Donnell W, Rosenberg M, Niven R, Drazen J, Israel E (1992) Acetazolamide and furosemide attenuate asthma induced by hyperventilation of cold, dry air. *Am Rev Respir Dis* 146:1518–1523
- Olver R, Strang L (1974) Ion fluxes across the pulmonary epithelium and the secretion of lung liquid in the fetal lamb. *Am J Physiol* 241:327–357
- Orlowski A, De Giusti VC, Morgan PE et al (2012) Binding of carbonic anhydrase IX to extracellular loop 4 of the NBCe₁ Na⁺/HCO₃⁻- cotransporter enhances NBCe₁-mediated HCO₃⁻- influx in the rat heart. *Am J Physiol* 303:C69–80
- Pakfetrat M, Nikoo MH, Malekmakan L et al (2009) A comparison of sodium bicarbonate infusion versus normal saline infusion and its combination with oral acetazolamide for prevention of contrast-induced nephropathy: a randomized, double-blind trial. *Int Urol Nephrol* 41:629–634
- Parati G, Revera M, Giuliano A et al (2013) Effects of acetazolamide on central blood pressure, peripheral blood pressure, and arterial distensibility at acute high altitude exposure. *Eur Heart J* 34:759–766
- Park EJ, Park YJ, Lee SJ et al (2019) Whole cigarette smoke condensates induce ferroptosis in human bronchial epithelial cells. *Toxicol Lett* 303:55–66
- Pedersen DB, Koch Jensen P et al (2005) Carbonic anhydrase inhibition increases retinal oxygen tension and dilates retinal vessels. *Graefes Arch Clin Exp Ophthalmol* 243:163–168
- Pichon A, Connes P, Quidu P et al (2012) Acetazolamide and chronic hypoxia: effects on hemorheology and pulmonary hemodynamics. *Eur Respir J* 40:1401–1409

- Pickerodt P, Francis R, Hoehne C et al (2014) Pulmonary vasodilation by acetazolamide during hypoxia: impact of methyl-group substitutions and administration route in conscious, spontaneously breathing dogs. *J Appl Physiol* 116:715–723
- Pickerodt PA, Kronfeldt S, Russ M, Swenson ER (2019) Carbonic anhydrase is not a relevant nitrite reductase or nitrous anhydrase in the lung. *J Physiol* 597:1045–1058
- Pickkers P, Garcha RS, Schachter M et al (1999) Inhibition of carbonic anhydrase accounts for the direct vascular effects of hydrochlorothiazide. *Hypertension* 33:1043–1048
- Pickkers P, Hughes AD, Russel FGM et al (2001) In vivo evidence of K_{Ca} channel opening properties of acetazolamide in the human vasculature. *Brit J Pharmacol* 132:443–450
- Plewes J, Olszowka A FL (1976) Amount and rates of CO₂ storage in lung tissue. *Respr Physiol* 28:359–370
- Plewes J, Olszowka A, Farhi L (1976) Transpleural diffusion of carbon dioxide. *Respir Physiol* 44:187–194
- Poole C, Halestrap AP, Price J et al (1989) The kinetics of transport of lactate and pyruvate into isolated myocytes from Guinea pig. *Biochem J* 264:409–418
- Prouillac C, Vicendo P, Garrigues JC et al (2009) Evaluation of new thiazoles and benzothiazoles as potential radioprotectors: free radical scavenging activity in vitro and theoretical studies (QSAR, DFT). *Free Radic Biol Med* 46:1139–1148
- Rahmne N, Buck J, Levin LR (2013) pH sensing via bicarbonate-regulated soluble adenylyl cyclase (sAC). *Front Physiol* 4:343
- Ran X, Wang H, Chen Y et al (2010) Aquaporin-1 expression and angiogenesis in rabbit chronic myocardial ischemia is reduced by acetazolamide. *Heart Vessels* 25:237–247
- Relman AS, Leaf A, Schwartz WB (1954) Oral administration of a potent carbonic anhydrase inhibitor (Diamox). II. Its use as a diuretic in patients with severe congestive heart failure. *N Engl J Med* 250:800–804
- Richalet JP, Riviera M, Bouchet P et al (2005) Acetazolamide: a treatment of chronic mountain sickness. *Am J Respir Crit Care Med* 172:1427–1433
- Richalet JP, Riviera-Ch M, Maignan M et al (2008) Acetazolamide for Monge's disease: efficacy and tolerance of 6-month treatment. *Am J Respir Crit Care Med* 177:1370–1376
- Riley DA, Ellis S, Bain JL (1984) Ultrastructural cytochemical localization of carbonic anhydrase activity in rat peripheral sensory and motor nerves, dorsal root ganglia and dorsal column nuclei. *Neurosci* 13:189–206
- Robinson N, Kyle H, Webber S, Widdicombe J (1989) Electrolyte and other chemical concentrations in tracheal airway surface liquid and mucus. *J App Physiol* 66:2129–2135
- Rolf L, Travis D (1971) Pleural fluid-blood bicarbonate gradient in oxygen toxic and normal rats. *Fed Proc* 12:A127
- Rose RJ, Hodgson DR, Kelso TB et al (1990) Effects of acetazolamide on metabolic and respiratory responses to exercise at maximal O₂ uptake. *J Appl Physiol* 68:617–626
- Rosenbaek JB, Pedersen EB, Bech JN (2018) The effect if sodium nitrite infusion on renal function, brachial and central blood pressure during enzyme or acetazolamide in health subjects: a randomized, double-blind, placebo-controlled, crossover study. *BMC Nephrol* 19:244
- Rounds S, Piggott D, Dawicki DD, Farber HWF (1997) Effect of hypercarbia on surface proteins of cultured bovine endothelial cells. *Am J Physio* 273:L1141–L114
- Ryan US, Whitney PL, Ryan JW (1982) Localization of carbonic anhydrase on pulmonary artery endothelial cells in culture. *J Appl Physiol* 53:914–919
- Scanlon KM, Gau Y, Zhu J et al (2014) Epithelial anion transporter pendrin contributes to inflammatory lung pathology in mouse models of Bordetella pertussis infection. *Infect Immun* 82:4212–4221
- Scheibe RJ, Gros G, Parkkila S et al (2006) Expression of membrane-bound carbonic anhydrases IV, IX, and XIV in the mouse heart. *J Histochem Cytochem* 54:1379–1391
- Schroeder MA, Ali MA, Hulikova A et al (2013) Extramitochondrial domain rich in carbonic anhydrase activity improves myocardial energetics. *Proc Natl Acad Sci* 110:E958-967

- Schunemann H, Klocke R (1993) Influence of carbon dioxide kinetics on pulmonary carbon dioxide exchange. *J Appl Physiol* 74:715–721
- Schuoler C, Haider T, Leuenberger C, Vogel J et al (2017) Aquaporin-1 controls the functional phenotype of pulmonary smooth muscle cells in hypoxia-induced pulmonary hypertension. *Basic Res Cardiol* 112:30
- Schwartz WB, Relman AS, Leaf A (1955) Oral administration of a potent carbonic anhydrase inhibitor (diamox). III. Its use as a diuretic in patients with severe congestive heart failure due to cor pulmonale. *Ann Intern Med* 42:79–89
- Sender S, Decker B, Fenske CD et al (1998) Localization of carbonic anhydrase IV in rat and human heart muscle. *J Histochem Cytochem* 46:855–861
- Shah GN, Morofuji Y, Banks WA, Price TO (2013) High glucose-induced mitochondrial respiration and reactive oxygen species in mouse cerebral pericytes is reversed by pharmacological inhibition of mitochondrial carbonic anhydrases: implications of cerebral microvascular disease in diabetes. *Biochem Biophys Res Comm* 440:354–358
- Sharma S, Gralla J, Ordonez JG et al (2017) Acetylcysteine in the treatment of chronic mountain sickness—Monge’s disease. *Respir Physiol Neurobiol* 246:1–8
- Shimoda LA, Luke T, Sylvester JT, Swenson ER (2007) Inhibition of hypoxia-induced calcium responses in pulmonary arterial smooth muscle by acetazolamide is independent of carbonic anhydrase inhibition. *Am J Physiol* 292:L1002–L1012
- Skatrud JB, Dempsey JA (1983) Relative effectiveness of acetazolamide versus medroxyprogesterone in correction of chronic carbon dioxide retention. *Am Rev Respir Dis* 127:405–412
- Skatrud JB, Dempsey JA, Bhansali P, Irvin C (1980) Determinants of chronic carbon dioxide retention and its correction in humans. *J Clin Invest* 65:813–821
- Slavi P, Revera M, Faini A et al (2013) Changes in subendocardial viability ratio with acute high-altitude exposure and protective role of acetazolamide. *Hypertension* 61:79–799
- Smith J, Welsh M (1993) Fluid and electrolyte transport by cultured human airway epithelia. *J Clin Invest* 91:1590–1597
- Sogaard R, Zeuthen T (2008) Test of blockers of AQP-1 water permeability by a high resolution method: no effects of tetraethylammonium ions or acetazolamide. *Pflugers Arch* 456:285–292
- Song D, Yang Y, He N et al (2018) The involvement of AQP1 in myocardial edema induced by pressure overload in mice. *Eur Rev Med Pharmacol Sci* 22:4969–4974
- Spitzer KW, Skolnick RL, Peercy BE et al (2002) Facilitation of intracellular H(+) ion mobility by CO₂/HCO₃⁻ in rabbit ventricular myocytes is regulated by carbonic anhydrase. *J Physiol* 541:159–167
- Steel D, Graham A, Geddes D, Alton E (1994) Characterization and comparison of ion transport across sheep and human airway epithelium. *Epithel Cell Bio* 3:24–31
- Stone RA, Barnes PJ, Chung KF (1993) Effect of frusemide on cough responses to chloride-deficient solution in normal and mild asthmatic subjects. *Eur Respir J* 6:862–867
- Strang L (1991) Fetal lung liquid secretion and reabsorption. *Physiol Rev* 71:91–109
- Strazzabosco M, Fiorotta R, Melero S et al (2009) Differentially expressed adenylyl cyclase isoforms mediate secretory functions in cholangiocyte subpopulation. *Hepatology* 50:244–252
- Sugiura Y, Oishi M, Amasaki T et al (2009) Immunohistochemical localization and gene expression of carbonic anhydrase isoenzymes CA-II and CA-VI in canine lower airways and lung. *J Vet Med Sci* 71:1525–1528
- Sun J, Elwood W, Barnes PJ et al (1993) Effect of thiazide diuretics against neutrally mediated contraction of guinea pig airways. Contribution of carbonic anhydrase. *Am Rev Respir Dis* 148:902–908
- Swenson ER (1997) Carbonic Anhydrase and the Heart. *Cardiologica* 42:453–462
- Swenson ER (1998) Carbonic anhydrase inhibitors and ventilation: a complex interplay of stimulation and suppression. *Eur Respir J* 12:1242–1247
- Swenson ER (2000) Respiratory and renal roles of carbonic anhydrase. In: Chegwiddden WR, Carter ND, Edwards YN (eds) *The carbonic anhydrases: new horizons*. EXS Birkhauser, Basel, pp 281–341

- Swenson ER (2013a) Hypoxic pulmonary vasoconstriction. *High Alt Med Biol* 14:101–110
- Swenson ER (2014b) Safety of carbonic anhydrase inhibitors. *Expert Opin Drug Saf* 13:459–472
- Swenson ER (2014) Carbonic anhydrase inhibitors and high altitude illnesses. In: Frost SC, McKenna R (eds) *Carbonic anhydrase: mechanism, regulation, links to disease, and industrial applications*. Springer, Heidelberg, pp 361–386
- Swenson ER (2016) Hypoxia and its acid-base consequences: from mountains to malignancy. *Adv Exp Med Biol* 903:301–322
- Swenson ER, Maren TH (1978) A quantitative analysis of CO₂ transport at rest and during maximal exercise. *Respir Physiol* 35:129–159
- Swenson ER, Robertson HT, Hlastala MP (1993) Effects of carbonic anhydrase inhibition on ventilation–perfusion matching in the dog lung. *J Clin Invest* 92:702–709
- Swenson ER, Graham MM, Hlastala MP (1995) Acetazolamide slows ventilation–perfusion matching after changes in regional blood flow. *J Appl Physiol* 78:1312–1318
- Szabolcs MJ, Kopp M, Schaden GE (1989) Carbonic anhydrase activity in the peripheral nervous system of rat the enzyme as a marker for muscle afferents. *Brain Res* 492:129–138
- Taddei S (2015) Combination therapy in hypertension: what are the best options according to clinical pharmacology principles and controlled clinical trial evidence? *Am J Cardiovasc Drugs* 15:185–194
- Taki K, Oogushi K, Hirahara K et al (2001) Preferential acetazolamide-induced vasodilation based upon vessel size and organ. *Angiology* 52:483–488
- Tamimura Y, Hiroaki Y, Fujiyoshi Y (2009) Acetazolamide reversibly inhibits water conduction by aquaporin-4. *J Struct Biol* 166:16–21
- Tanzarella P, Ferretta A, Barile SN et al (2019) Increased levels of cAMP by the calcium-dependent activation of soluble adenylyl cyclase in Parkin-Mutant fibroblasts. *MDPI Cells* (in press)
- Taylor CJ, Nicola PA, Wang S et al (2006) Transporters involved in regulation of intracellular pH in primary cultured brain endothelial cells. *J Physiol* 576:769–785
- Teppema LJ, Balanos GM, Steinbeck CD et al (2007) Effects of acetazolamide on ventilatory, cerebrovascular, and pulmonary vascular responses to hypoxia. *Am J Respir Crit Care Med* 175:277–281
- Thornell IM, Li X, Tang XX et al (2018) Nominal carbonic anhydrase activity minimizes airway-surface liquid pH changes during breathing. *Physiol Rep* 10:14814
- Thurnheer R, Ulrich S, Bloch KE (2017) Precapillary pulmonary hypertension and sleep-disordered breathing: is there a link? *Respiration* 93:65–77
- Titus E, Ahearn GA (1992) Vertebrate gastrointestinal fermentation: transport mechanisms for volatile fatty acids. *Am J Physiol* 262:R547–R553
- Torella D, Ellison GM, Torella M et al (2014) Carbonic anhydrase activation is associated with worsened pathological remodeling in human ischemic diabetic cardiomyopathy. *J Am Heart Assoc* 26:e000434
- Torring MS, Holmgaard K, Hesselund A et al (2009) The vasodilating effect of acetazolamide and dorzolamide involves mechanisms other than carbonic anhydrase inhibition. *Invest Ophthalmol vis Sci* 50(345–51):29
- Traystman RJ, Terry PB, Menkes HA (1978) Carbon dioxide: a major determinant of collateral ventilation. *J Appl Physiol* 45:69–74
- Tricarico D, Barbieri M, Mele A et al (2004) Carbonic anhydrase inhibitors are specific openers of skeletal muscle BK channel of K⁺-deficient rats. *FASEB J* 18:760–761
- Tricarico D, Mele A, Camerino DA (2006) Carbonic anhydrase inhibitors ameliorate the symptoms of hypokalaemic periodic paralysis in rats by opening the muscular Ca²⁺-activated- K⁺ channels. *Neuromuscul Disord* 16:39–45
- Tricarico D, Mele A, Calzolaria S et al (2013) Emerging role of calcium-activated potassium channel in the regulation of cell viability following potassium ions challenge in HEK293 cells and pharmacological modulation. *PLoSOne* 8:E69551

- Ulrich S, Keusch S, Hildenbrand FF et al (2015) Effect of nocturnal oxygen and acetazolamide on exercise performance in patients with pre-capillary pulmonary hypertension and sleep-disturbed breathing: randomized, double-blind, cross-over trial. *Eur Heart J* 36:615–623
- Vaananen HK, Carter ND, Dodgson SJ (1991) Immunocytochemical localization of mitochondrial carbonic anhydrase in rat tissues. *J Histochem Cytochem* 39:451–459
- van Berlo JH, Maillet M, Molkentin JD (2013) Signaling effectors underlying pathologic growth and remodeling of the heart. *J Clin Invest* 123:37–45
- Van Goor H (1948) Carbonic anhydrase. Its properties, distribution and significance for carbon dioxide transport. *Enzymologica* 13:73–164
- Van Engelhardt W, Burmester M, Hansen K et al (1993) Effects of amiloride and ouabain on short-chain fatty acid transport in Guinea pig large intestine. *J Physiol* 460:455–466
- Vargas LA, Alvarez BV (2012) Carbonic anhydrase XIV in the normal and hypertrophic myocardium. *J Mol Cell Cardiol* 52:741–752
- Vargas LA, Díaz RG, Swenson ER et al (2013) Inhibition of carbonic anhydrase prevents the Na(+)/H(+) exchanger 1-dependent slow force response to rat myocardial stretch. *Am J Physiol* 305:H228–H237
- Vargas LA, Pinilla OA, Diaz RG et al (2016) Carbonic anhydrase inhibitors reduce cardiac dysfunction after sustains coronary artery ligation in rats. *Cardiovasc Pathol* 25:468–477
- Vaughan-Jones RD, Spitzer KW (2002) Role of bicarbonate in the regulation of intracellular pH in the mammalian ventricular myocyte. *Biochem Cell Biol* 80:579–596
- Vaughan-Jones RD, Peercy BE, Keener JP, Spitzer KW (2002) Intrinsic H(+) ion mobility in the rabbit ventricular myocyte. *J Physiol* 541:139–158
- Vaughan-Jones RD, Spitzer KW, Swietach P (2006) Spatial aspects of intracellular pH regulation in heart muscle. *Prog Biophys Mol Biol* 90:207–224
- Vaughan-Jones RD, Spitzer KW, Swietach P (2009) Intracellular pH regulation in heart. *J Mol Cell Cardiol* 46:318–331
- Vengust M, Staempfli H, De Moraes AN et al (2010) Effects of chronic acetazolamide administration on gas exchange and acid-base control in pulmonary circulation in exercising horses. *Equine Vet J Suppl* 38:40–50
- Vengust M, Staempfli H, Viel L et al (2013) Acetazolamide attenuates transvascular fluid flux in equine lungs during intense exercise. *J Physiol* 591:4499–4513
- Vengust M, Staempfli H, Heigenhauser G (2006) Effects of chronic acetazolamide administration on fluid flux from the pulmonary vasculature at rest and during exercise in horses. *Equine Vet J Suppl* 36:508–515
- Ventresca PG, Nichel GM, Barnes PJ et al (1990) Inhaled furosemide inhibits cough induced by low chloride content solutions but not by capsaicin. *Am Rev Respir Dis* 142:143–146
- Verbrugge FH, Martens P, Ameloot K et al (2019) Acetazolamide to increase natriuresis on congestive heart failure at high risk for diuretic resistance. *Eur J Heart Fail* 2019(10):1002
- Verlenden G, Pype J, Deneffe G, Demedts M (1994) Effect of loop diuretics on cholinergic neurotransmission in human airways in vitro. *Thorax* 49:657–663
- Vilas G, Krishnan D, Loganatha S et al (2015) Increased water flux induced by an aquaporin-1/carbonic anhydrase II interaction. *Mol Biol Cell* 26:1106–1118
- Villafuerte FC, Swietach P, Youm JB et al (2014) Facilitation by intracellular carbonic anhydrase of Na⁺-HCO₃⁻ co-transport but not Na⁺/H⁺ exchange activity in the mammalian ventricular myocyte. *J Physiol* 592:991–1007
- Wall M, McDermott MP, Kieburz KD et al (2014) Effect of acetazolamide on visual function in patients with idiopathic intracranial hypertension and mild visual loss: the idiopathic intracranial hypertension treatment trial. *J Am Med Assoc* 311:1641–1651
- Wang X, Figueroa BE, Zhang Y et al (2009) Methazolamide and melatonin inhibit mitochondrial cytochrome C release and are neuroprotective in experimental models of ischemic injury. *Stroke* 40:1877–1885
- Wen T, Mingler MK, Wahl B et al (2014) Carbonic anhydrase IV is expressed on IL-5-activated murine eosinophils. *J Immunol* 192:5481–5489

- Wexels JC, Eivind SPM, Mjos OD (1986) Effects of hypo- and hypercapnia on myocardial blood flow and metabolism with epinephrine infusion in dogs. *Can J Physiol Pharmacol* 64:44–49
- Wildboer-Venema F (1984) Influence of nitrogen, air and alveolar gas upon surface tension of lung surfactant. *Respir Physiol* 58:1–14
- Willam C, Warnecke C, Schofeld JC et al (2006) Inconsistent effects of acidosis on HIF-alpha protein and its target genes. *Pfluegers Arch* 451:534–543
- Wongboonsin J, Thongprayoon C, Bathini T et al (2019) Acetazolamide therapy in patients with heart failure: a meta-analysis. *J Clin Med* e349.
- Wood SC, Schaefer KE (1978) Regulation of intracellular pH in lungs and other tissues during hypercapnia. *J Appl Physiol* 45:115–118
- Xu J, Peng Z, Li R et al (2009) Normoxic induction of cerebral HIF-1alpha by acetazolamide in rats. *Neurosci Lett* 451:274–278
- Yamaguchi T, Iwata Y, Miura S, Kawada K (2012) Reinvestigation of drugs and chemicals as aquaporin-1 inhibitors using pressure-induced hemolysis in human erythrocytes. *Biol Pharm Bull* 35:2088–2091
- Yang B, Zhang H, Verkmann AS (2008) Lack of aquaporin-4 water transport inhibition by antiepileptics and arylsulfonamides. *Bioorg Med Chem* 16:7489–7493
- Yun X, Jiang H, Lai L, Want J et al (2017) Aquaporin 1-mediated changes in pulmonary arterial smooth muscle cell migration and proliferation involve beta-catenin. *Am J Physiol* 313:L889–898
- Zborowaska-Sulis DT, L'Abbate A, Mildenburg RR et al (1975) The effect of acetazolamide on myocardial carbon dioxide space. *Respir Physiol* 23:311–316
- Zhang J, An Y, Gao J, et al. (2012) Aquaporin-1 translocation and degradation mediates the water transportation mechanism of acetazolamide. *PLoSOne* 7:e45976
- Zocchi L, Agostoni E, Cremaschi D (1991) Electrolyte transport across the pleura of rabbits. *Respir Physiol* 86:125–131

Chapter 4

Carbonic Anhydrase Inhibitors in Ophthalmology: Glaucoma and Macular Oedema



Marianne Levon Shahsuvaryan

Abstract Carbonic anhydrase inhibitors (CAIs) are commonly used pharmacologic agents. A myriad of CAI classes and inhibition mechanisms has been identified over the past decade. The classical CAI is acetazolamide, which has been used for the systemic treatment of glaucoma since 1953. A topical CAI was introduced more than 40 years after the introduction of this systemic agent. The rationale for the development of topically active CAIs—dorzolamide and brinzolamide—was to eliminate the systemic side effects seen with the oral route, which currently makes them popular therapeutics that are used as ocular hypotensives in medical therapy of ocular hypertension and primary open-angle glaucoma. Carbonic anhydrase is one of the most ubiquitous enzyme systems in the body and also acts as an inflammatory mediator. It is found both in the ciliary body epithelium and in different retinal cells, thus revealing new intraocular targets and new roles for carbonic anhydrase inhibitors. Scientific understanding of glaucoma and of macular oedema accompanying several ocular diseases continues to develop, producing a consequent re-evaluation of the role of carbonic anhydrase in the pathogenesis of these conditions. This underscores the importance of accurate evaluation of the therapeutic potential of carbonic anhydrase inhibitors.

Keywords Carbonic anhydrase inhibitors · Acetazolamide · Dorzolamide · Brinzolamide · Glaucoma · Macular oedema

4.1 Introduction

The therapeutic carbonic anhydrase inhibitors (CAIs) employed hitherto are sulfonamide derivatives. A myriad of CAI classes and inhibition mechanisms has been identified over the past decade, mainly through structure-based drug design approaches (Supuran 2017).

M. L. Shahsuvaryan (✉)
Yerevan State Medical University, Yerevan, Armenia
e-mail: mar_shah@hotmail.com

The main drug from this group is acetazolamide (2-acetylamino-1,3,4-thiadiazole-5-sulfonamide; Diamox), developed by Roblin and Clapp in 1950 (Roblin and Clapp 1950).

Acetazolamide acts as a diuretic by inhibiting carbonic anhydrase. This results in metabolic acidosis due to increased renal elimination of $\text{Na}^+/\text{HCO}_3^-$ and K^+ and decreased plasma bicarbonate respectively (Kaplan 2000).

4.2 Carbonic Anhydrase Inhibitors in Glaucoma

Glaucoma has been considered as a major cause of worldwide irreversible blindness (Nuzzi et al. 2018), affecting about 70 million people worldwide (Quigley and Broman 2006). Glaucoma is currently recognized to be a multifactorial, progressive neurodegenerative disorder. It is characterized by the death of retina ganglion cells and loss of their axons as well as optic nerve atrophy and loss of neurons in the lateral geniculate nucleus and the visual cortex (Kaushik et al. 2003; Nuzzi et al. 2018). The main risk factor for progression is an elevated intraocular pressure (IOP), which can cause damage to the optic nerve head and then to the visual field. Some clinical trials have shown that decreasing the IOP can be useful for slowing down glaucoma progression (Kass et al. 2002; Heijl et al. 2002; Leske et al. 2004), and IOP has been the only recognized modifiable risk factor until now (Jutley et al. 2017). Thus the mainstay of treatment has been aimed at the reduction of IOP with drugs.

4.2.1 Systemic Carbonic Anhydrase Inhibitors

4.2.1.1 Acetazolamide

The first study on the treatment of glaucoma with the CAI acetazolamide was initiated by Breinin and Görtz in 1953 and covered a four-month period of observation. The authors concluded that inhibition of carbonic anhydrase by acetazolamide was a new and useful means of lowering the IOP. Other researchers also observed that systemic inhibition of carbonic anhydrase by the administration of acetazolamide and related compounds results in a partial secretion of aqueous humor. These agents have proved most useful clinically in lowering IOP in glaucomatous eyes (Becker 1954, 1955a, b, Grant 1954, Breinin and Görtz 1954) by the ability to partially suppress the formation of aqueous humor. The physiology of aqueous humor formation with respect to ion transport is discussed by these authors, and it was shown that a key event is the catalytic formation of HCO_3^- from CO_2 and OH^- . The newly formed HCO_3^- is linked to Na^+ and fluid movement to produce aqueous humor. Researchers highlighted that inhibition of HCO_3^- production by sulfonamides reduces aqueous humor formation and lowers pressure both in healthy individuals and in patients with glaucoma.

In the early 1960s a sustained release formulation (Sustet) containing 500 mg of the active drug was marketed (Drance and Carr, 1961; Mestre et al. 1963). Several studies have confirmed the efficacy of regular tablets and a sustained release preparation in lowering IOP (Becker 1955a, b; Kupfer et al. 1955; de Carvalho et al. 1958; Drance and Carr 1961; Mestre et al. 1963; Garner et al. 1963; Garrison et al. 1967). However, with both formulations many side effects were encountered and these were thought to be dose-related (Lichter et al. 1978; Berson and Epstein 1980). In an effort to reduce these effects, smaller doses of acetazolamide were tried over short periods of time (Friedland et al. 1977; Foster et al. 1982). The effect on IOP, over 12- or 24-h dosage intervals, of the same doses of these two formulations (available in the UK) were also compared.

In 1990 Joyce and Mills compared the effects of the same dose of the two formulations on IOP over 12- or 24-h dosage intervals. Twenty patients with primary open-angle glaucoma, uncontrolled on single topical therapy, completed a double-dummy crossover study to compare acetazolamide tablets with a sustained-release formulation (Sustet). The two preparations were equally effective. The authors stated that most patients in this study, who had primary open-angle glaucoma uncontrolled on single topical treatment, were adequately controlled on the addition of 500 mg (2×250 mg) of acetazolamide tablets or one Sustet (500 mg) at night. The severity of side effects was also reduced. Thus an evening dose of acetazolamide in conjunction with topical therapy may well have a beneficial effect on compliance in the treatment of open-angle glaucoma. Lichter et al. (1989) tested the effect on IOP of three commonly used oral CAI preparations in a controlled, randomized, comparative study also on patients with primary open-angle glaucoma. Preparations tested included acetazolamide tablets, acetazolamide Sequels, and methazolamide tablets. The authors concluded that maximal rapid reduction of intraocular pressure was obtained with a 500-mg dosage of acetazolamide.

Since several CA isozymes are widespread throughout the body, systemic CAIs possess undesired side effects such as numbness and tingling of extremities, metallic taste, depression, fatigue, malaise, weight loss, decreased libido, gastrointestinal irritation, metabolic acidosis, renal calculi and transient myopia (Mincione et al. 2007, 2008), Stevens-Johnson syndrome, toxic epidermal necrolysis, fulminant hepatic necrosis, aplastic anemia, drug hypersensitivity, serum sickness, and nephritis.

4.2.2 Topical Carbonic Anhydrase Inhibitors

The general consensus, in order to avoid these undesirable side effects, was to search and develop topically effective CAIs free of such effects (Maren 1987; Mincione et al. 2011; Fabrizi et al. 2012). Four sulfonamides—acetazolamide, methazolamide, ethoxzolamide, and dichlorophenamide—have been used systemically. None of these works topically, since they do not reach the ciliary process in adequate concentrations. Consequently, subsequent research focused on the development of sulfonamides of different properties that cross the cornea in effective concentrations to inhibit

carbonic anhydrase (CA) in the ciliary process. The key to the problems was to search for a balance between water and lipid solubility, maintaining high activity against the enzyme. This has been achieved, and new structures described from different laboratories lower pressure in the rabbit nearly as well as systemic sulfonamides (Sugrue 1996; Pfeiffer 1997; Borrás et al. 1999; Supuran et al. 1999; Menabuoni et al. 1999; Ilies et al. 2000; Renzi et al. 2000; Kobayashi and Naito 2000; Casini et al. 2001; Scozzafava et al. 2002; de Leval et al. 2004; Mincione et al. 2005).

The corneal permeabilities of these test compounds *in vitro* were found to be similar in rabbit and human, but access to the aqueous humor *in vivo* was less in human.

Topical CAIs took many years to develop. A topical version was first introduced more than 40 years after the introduction of the systemic agent. The rationale for the development of a topically active CAI was to eliminate the systemic side effects seen with oral acetazolamide use, such as drowsiness, confusion, allergic reactions, paresthesias, myelosuppression, renal calculi, loss of potassium, or hyperchloremic metabolic acidosis from extended use. Thus this class of drugs became the commonly used pharmacologic agents as ocular hypotensives in medical therapy for glaucoma, as a consequence of their ability to reduce aqueous humour production through decreased bicarbonate formation in ciliary body epithelium. In contrast to acetazolamide, the first topical CAI—dorzolamide—has a lipid-soluble nature and high affinity for carbonic anhydrase, which significantly increases the bioavailability of the drug (Kellner et al. 2004). The effects on intraocular pressure of the novel topical carbonic anhydrase inhibitor MK-927 were investigated for the first time in patients by Bron et al. (1989). Three drops of 2% MK-927 were administered in a two-center, double-masked, randomized, placebo-controlled, two-period crossover study to 25 patients with bilateral primary open-angle glaucoma or ocular hypertension, and it was shown that the peak mean percent change in intraocular pressure in eyes treated with MK-927 was -26.7% at six hours after the dose.

4.2.2.1 Dorzolamide

The multiple-dose, dose–response relationship, and duration of action of the novel, topical carbonic anhydrase inhibitor dorzolamide (previously known as MK-507) were investigated in a double-masked, randomized, placebo-controlled, parallel study in 73 patients with bilateral primary open-angle glaucoma or ocular hypertension (Lippa et al. 1991, 1992). Dorzolamide (0.7, 1.4%, or 2%) or placebo was administered every 12 h for five days and then every eight hours for seven days. Intraocular pressure was investigated with multiple 12-h diurnal curves. All concentrations of dorzolamide demonstrated substantial lowering of IOP throughout the day when given twice daily (9–21%) or three times daily (14–24%). Although a dose-dependent response was observed immediately following the first dose, there were no significant differences between concentrations or dose–response at either the twice or three times daily dosing regimen. Three times daily administration of 2% dorzolamide demonstrated a mean percent decrease in IOP of 18–22% throughout

the day (mean decrease, 4.5–6.1 mm Hg). Consequently the authors concluded that dorzolamide appeared to have substantial potential in the treatment of glaucoma and ocular hypertension.

Wilkerson et al. (1993) conducted a four-week, double-masked, randomized, placebo-controlled, parallel, three-center study, investigating the activity and local and systemic safety of dorzolamide hydrochloride in forty-eight patients with bilateral open-angle glaucoma or ocular hypertension and IOP greater than 22 mm Hg. Dorzolamide showed significant IOP lowering activity over four weeks. It was well tolerated and there were no clinically significant changes in ocular or systemic safety parameters.

Dorzolamide was approved by the FDA in 1994 for the treatment of elevated intraocular pressure in primary open-angle glaucoma and ocular hypertension. Strahlman and associates (1995) reported a 1-year study of the safety profile and efficacy of a topical CAI, dorzolamide hydrochloride (Trusopt), as either primary or supplemental therapy in addition to 0.5% timolol maleate or 0.5% betaxolol hydrochlorid for primary open-angle glaucoma and ocular hypertension. This was the first topical CAI to show sufficient efficacy for clinical use and that appeared to nearly match the pressure-lowering of oral CAIs without having their systemic side effects. Having advanced to Food and Drug Administration phase three trials, it was approved and marketed (Palmberg 1995).

Similar research, to assess the safety and intraocular pressure (IOP)-lowering activity of 2% dorzolamide compared to 0.5% timolol and 0.5% betaxolol eyedrops, was conducted by Simpson et al. (1996) as a parallel, masked, randomized one-year clinical trial evaluating 16 patients with open-angle glaucoma or ocular hypertension. This was a subset of a multicentre study which enrolled 523 subjects. The authors observed that dorzolamide 2% given thrice daily was well tolerated and safe, with a clinically significant effect on IOP comparable to betaxolol 0.5% twice daily, but not as great as timolol 0.5% twice daily. The data of Gillies and Brooks (1996) were in agreement with this. In a comparative study comparing the efficacy of topical dorzolamide with that of systemic acetazolamide in lowering ocular pressure dorzolamide (1% eye drops) proved to be as effective as acetazolamide tablets in reducing the IOP curve (Centofanti et al. 1997).

In the eye, carbonic anhydrase is expressed in the ciliary processes of the ciliary body, in the corneal endothelial cells, and in the pigment epithelium. In the corneal endothelium CAII plays a role in the pumping mechanism, which helps to maintain the relatively dehydrated state of the corneal stroma. Inhibition of this mechanism may lead to the development of corneal decompensation and oedema, with secondary impaired vision.

To check long-term corneal tolerability of dorzolamide hydrochloride (Trusopt, Merck and Co Inc, White-house Station, NJ), timolol maleate, and betaxolol hydrochloride, measuring corneal endothelial cell density and corneal thickness in patients with normal corneas at baseline, Lass et al. (1998) initiated a 1-year multi-center study in 298 patients with ocular hypertension or open-angle glaucoma. At the end of the study it was noted that dorzolamide was equivalent to timolol and betaxolol in terms of the change in central endothelial cell density and thickness after

one year of therapy and exhibited good long-term corneal tolerability. Another study conducted to evaluate the impact of dorzolamide on corneal thickness, endothelial cell count, and corneal sensibility after 90 days use, confirmed that dorzolamide, applied topically three times a day as a monotherapy or in combination with timolol or pilocarpine, was not associated with clinically meaningful changes in the cornea (Kaminski et al. 1998).

In contrast to the presented findings in two published case reports, corneal decompensation has been described in patients with keratopathy after treatment with dorzolamide (Adamson 1999; Konowal et al. 1999).

The latest findings on the matter, presented by Inoue et al. (2003), reconfirm the safety of the topical use of 1% dorzolamide during three months, without negative impact on corneal endothelial morphology.

The most frequently reported adverse side effects of dorzolamide are burning, stinging, discomfort, and bitter taste following administration of the solution (Lippa et al. 1992; Wilkerson et al. 1993; Strahlman et al. 1995). Ocular allergy and superficial punctuate keratitis occur in 10–15% of patients. Other side effects include conjunctivitis, eyelid inflammation, and irritation. Blurred vision, dryness, tearing, and photophobia have been reported in 1–5% of patients.

Balfour and Wilde (1997) evaluated dorzolamide hydrochloride, the first topical, highly water-soluble CAI to become available for clinical use as a 2% eyedrop for the management of glaucoma and ocular hypertension. They reported that, when administered three times daily, it was effective in lowering IOP. The mean IOP was reduced by approximately 4–6 mm Hg at peak (two hours post-dose) and 3–4.5 mm Hg at trough (eight hours post-dose). Dorzolamide has additive ocular hypotensive effects when used in conjunction with topical beta-adrenergic antagonists and was as effective as pilocarpine (2%), administered four times daily, as adjunctive therapy in patients receiving timolol. Dorzolamide does not appear to produce the acid–base or electrolyte disturbances and severe systemic adverse events associated with oral CAIs, and unlike beta-adrenergic antagonists, it is not contraindicated in patients with asthma, reactive airways disease, or heart disease. Furthermore, as CAIs do not cause miosis, they may cause less interference with vision than pilocarpine or epinephrine (adrenaline). The most common adverse effects associated with dorzolamide are bitter taste and transient local burning or stinging. The authors concluded that dorzolamide has potential as an alternative therapy option in patients with glaucoma or ocular hypertension who are intolerant of, or unable to receive, ophthalmic beta-adrenergic antagonists, and as adjunctive therapy in patients already receiving these agents.

However, the need still exists to increase the duration of action of dorzolamide. In an effort to reach this goal Kouchak et al. (2018) prepared a dorzolamide-loaded nanoliposome and tested it in a randomized comparative study with marketed dorzolamide solution in 20 patients with primary open-angle glaucoma or ocular hypertension. A statistically significantly higher hypotensive effect was demonstrated in the dorzolamide-loaded eye drop group. The authors have argued that the long-lasting efficacy of the dorzolamide-loaded nanoliposome eye drops may be attributed to

their highly enhanced permeability through the cornea due to small particle size and similarity between phospholipid bilayer of liposomes and the biological membrane.

4.2.2.2 Brinzolamide

Brinzolamide is a highly specific, non-competitive, reversible, and effective inhibitor of carbonic anhydrase II (CA II) (DeSantis 2000). It was launched more recently and was approved by the FDA in 1998 for the treatment of elevated intraocular pressure in primary open-angle glaucoma and ocular hypertension.

The commercially available preparation of brinzolamide is Azopt® (Alcon Laboratories, Inc, Ft. Worth, Texas, USA) (Cvetkovic and Perry 2003, Iester I2008a, b). To achieve pharmacological effect, the near total inhibition of CA is required (Maren 1967; Kaur et al 2002). Brinzolamide is cleared from the aqueous humor and cornea with half-lives of approximately three and five hours, respectively. Therefore, the cornea acts as a reservoir, providing sustained release of the drug to the ciliary processes of the ciliary body long after topical dosing (Maren 1967; Kaur et al. 2002).

The efficacy of brinzolamide in different concentrations 0.3–3% twice daily has been evaluated in several randomized, double-blind, multicenter, comparative clinical trials (March and Ochsner, 2000; Sall 2000; Shin 2000; Silver 1998, 2000; Michaud and Friren 2001). A dose–response study, comparing brinzolamide in concentrations of 0.3%, 1%, 2%, and 3%, demonstrated mean IOP reductions of 3 mmHg (11.3%), 4.4 mmHg (16.1%), 4.3 mmHg (16.1%), and 4.2 mmHg (15.4%), respectively. When diurnal IOP was measured, 1% or 3% brinzolamide reduced IOP significantly better than 0.3% brinzolamide (Silver 2000). These observations suggested that the optimal therapeutic concentration for IOP reduction was 1%. Its recommended dosing frequency is three times daily in the US and twice daily in the EU and Japan. However, three phase III trials have reported that brinzolamide 1% *b.i.d.* and *t.i.d.* produced statistically significant IOP reductions from baseline and that both treatments were clinically equivalent to one another (Silver 1998; March and Ochsner 2000; Shin 2000).

In a randomized, double-blind clinical trial, 372 glaucomatous and ocular hypertension (OH) patients received brinzolamide 1% or timolol 0.5%. After 18 months of treatment, no significant change was found in corneal thickness and corneal endothelium cell density (March and Ochsner 2000). However, in this study only subjects with healthy corneas were included. Some concerns remained in patients with compromised corneas. Zhau and Chen (2005) have reported two cases of corneal decompensation after 15 months and two years of brinzolamide therapy. Corneal oedema reversed with discontinuation of the treatment; however, the reason was difficult to assess, and neither patient was re-challenged after recovery. No change in central corneal thickness was found (Wang et al. 2004).

Several clinical trials (Zeyen and Caprioli 1993; Silver 1998; Sall 2000; Shin 2000; Wang et al. 2004; Zhao and Chen 2005; Menon and Vernon 2006) have evaluated the safety of brinzolamide 1% ophthalmic suspension. The most common ocular

adverse events were blurred vision (3–8%), ocular discomfort (1.8–5.9%), and eye pain (0.7–4.0%). Other ocular adverse events occurring at an incidence of less than 3% included hyperemia, pruritus, tearing, discharge, blepharitis, keratitis, foreign body sensation, dry eye, conjunctivitis, and lid margin crusting.

The most common systemic adverse event was taste perversion, which occurred in 3.0–7.8% of patients (Silver 1998; Sall 2000; Shin 2000). There were no clinically significant changes from baseline in heart rate and blood pressure, and in laboratory values for hematology, blood chemistry, or urinalysis variables. In addition, mean total carbonic anhydrase activity in red blood cells was reduced by only 51–55%. However, one case of systemic metabolic acidosis has been described by Menon and Vernon (2006).

Detailed pharmacokinetics of topically-administered brinzolamide were evaluated by DeSantis (2000) and March and Ochsner (2000). Systemic absorption of brinzolamide has been demonstrated in the tissues of healthy volunteers (DeSantis 2000). Brinzolamide, administered topically, enters the blood circulation and binds preferentially to CA in the erythrocytes, leaving the concentration of free brinzolamide in plasma below the quantification level. In the red cells, less than 1% of CA-II activity is required to maintain physiological function (March and Ochsner 2000). Thus, in the erythrocytes the concentration of CAIs was insufficient to produce complete saturation of CA. In the kidney, the concentration of free brinzolamide is not sufficient to inhibit in the proximal convoluted tubules and luminal CA. Furthermore, the low affinity of brinzolamide for the other CA isoforms, and the low blood concentration, may explain the low incidence of systemic adverse effects after topical administration (March and Ochsner 2000).

In a meta-analysis of randomized clinical trials, Van der Valk et al. (2005) estimated the IOP reduction achieved by the most frequently prescribed glaucoma drugs and a placebo: they found that the highest reduction of IOP achieved by brinzolamide was 17%.

Wang et al. (2004) conducted a small, prospective, double-masked study, comparing brinzolamide 1% *b.i.d.* with timolol 0.5% *b.i.d.*, in 50 patients with open-angle glaucoma. After six weeks of treatment, IOP dropped 4.8 mm Hg (17%) in brinzolamide-treated eyes and 5.7 mm Hg (19.7%) in timolol-treated eyes.

A multicenter, double-masked, prospective, parallel-group study was conducted to compare brinzolamide (1.0%), administered two and three times a day, dorzolamide (2.0%) three times a day, and timolol (0.5%) twice a day in 572 patients with primary open-angle glaucoma or ocular hypertension (Silver 1998). Brinzolamide (1.0%) produced clinically relevant intraocular pressure reductions in substantial numbers of patients, with efficacy equaling that of dorzolamide (2.0%), and produced less ocular discomfort (burning and stinging) on application.

Clinical studies comparing the two drugs as adjuncts as well as monotherapy have shown them to have comparable efficacy, with brinzolamide having a more favorable adverse event profile (Silver 1998; Silver 2000; Sall 2000; March and Ochsner 2000; Barnebey and Kwok 2000; Michaud and Friren 2001; Stewart et al. 2004; Tsukamoto et al. 2005; Mundorf et al. 2008; Manni et al. 2009; Martínez and Sánchez-Salorio 2009; Rossi et al. 2011).

The latest similar research to assess the safety and intraocular pressure (IOP)-lowering activity of 1% brinzolamide compared to 2% dorzolamide eyedrops was initiated by Yadav et al. (2014). In a prospective, randomized study, 100 eyes (50 subjects) received dorzolamide 2% three times daily or brinzolamide 1% twice daily for three months. The authors observed that both brinzolamide (1.0%) and dorzolamide (2%) produced clinically relevant and statistically significant IOP reductions and were statistically equivalent when compared. They also noted that brinzolamide produced significantly less ocular discomfort (burning and stinging) both immediately on application and on chronic use.

4.2.3 Carbonic Anhydrase Inhibitors in Ocular Perfusion

Although elevated IOP is the principal risk factor, deterioration of ocular perfusion by the vascular system accelerates progression of glaucomatous optic nerve atrophy (Siesky et al. 2009).

CAIs may improve blood perfusion in the human eye. It has been shown that acetazolamide leads to a dilation of retinal vessels and increases blood flow in the optic nerve head (Haustein et al. 2013). Similarly, topical application of dorzolamide leads to a significant increase of flow velocities of the retrobulbar vessels as measured by color Doppler imaging (Huber-van der Velden et al. 2012).

Few studies have reported the effect of brinzolamide on ocular blood flow. Moreover, the results of these studies have been contradictory, possibly due to the different study designs and measurement methodologies employed. Barnes et al. (2000) found that brinzolamide significantly increased optic nerve head blood flow in Dutch rabbits. However, Martinez and Sanchez-Salorio (2009) noted that, after five years of treatment, brinzolamide did not augment retrobulbar blood flow when added to timolol in glaucoma patients.

Dong et al. (2016) demonstrated that dorzolamide directly induced relaxation of isolated rabbit ciliary arteries. In a later study (Dong et al. 2018), compared the effects of brinzolamide, dorzolamide, and acetazolamide *ex vivo* and found that acetazolamide could not induce vasodilation, and dorzolamide-induced vascular relaxation was smaller than that induced by brinzolamide. It has been shown that brinzolamide decreases IOP and increases ocular blood flow. The direct vasodilatory effect of brinzolamide is mediated by suppression of Ca^{2+} release from intracellular calcium stores.

The mechanism by which IOP-lowering medications increase ocular blood flow in glaucoma remains unclear. Currently it is difficult to determine if the CAI-induced increase in ocular perfusion is secondary to IOP reduction or if it is a primary effect on the ocular vasculature.

Future directions

A new generation of multifunctional compounds has been synthesized, and their functional properties were investigated (Zubriené et al. 2017; Taslimi et al. 2018; Türker et al. 2018; Sari et al. 2017; Zakšauskas et al. 2018).

A novel class of fluoro-substituted tris-chalcones derivatives (5a-5i) was synthesized from phloroglucinol and corresponding benzaldehyde (Burmaoglu et al. 2019). The compounds' inhibitory activities were tested against human carbonic anhydrase I and II isoenzymes (hCA I and hCA II), acetylcholinesterase (AChE), butyrylcholinesterase (BChE), and α -glycosidase (α -Gly). These results strongly supported the promising nature of the tris-chalcone scaffold as a selective carbonic anhydrase, acetylcholinesterase, butyrylcholinesterase, and α -glycosidase inhibitor. Overall, due to these derivatives' inhibitory potential on the tested enzymes, as was stated by the authors, "they are promising drug candidates for the treatment of diseases like glaucoma".

In the preclinical study of Chiamonte et al. (2018), two compounds, evaluated in rabbit models of glaucoma, significantly reduced intraocular pressure, making them interesting candidates for further studies.

These data suggest the advisability of focusing future endeavours on increasing drug delivery and bioavailability by the use of novel formulations, bioadhesive polymers, and micro- and nano-systems (Nagai 2016; Andrés-Guerrero et al. 2017).

4.3 Carbonic Anhydrase Inhibitors in Macular Oedema

Macular oedema (MO) is a swelling within or under a specific area of the retina, known as the macula, caused by extravasation of fluid and plasma components from blood vessels and/or derangements in cellular ion flux leading to the accumulation of intracellular and intercellular fluid in the outer plexiform and inner retinal layers (Kleinman et al. 2010).

The pathophysiology of macular oedema encompasses a cascade of inflammatory events in retinal microvessels and the decay of tight junctions in cell walls. Several decades of basic science research have revealed a growing and complex array of cytokine growth factors and proinflammatory mediators that are capable of initiating the cellular changes that result in accumulation of fluid within the retina. MO commonly develops secondary to vascular insufficiency in disease states such as diabetic retinopathy (DR), branch and/or central retinal vein occlusion, ocular ischemic syndrome, radiation retinopathy, pseudophakia, age-related macular degeneration, uveitis, retinitis pigmentosa, ocular trauma or drug toxicity (Kleinman et al. 2010).

Thus, MO may be considered as the final common pathway of many intraocular and systemic insults and the anatomic result of numerous pathologic processes that alter the blood flow, vascular integrity, and fluidic balance in the neurosensory retina (Tranos et al. 2004). It may develop in a diffuse pattern where the macula appears

generally thickened, or it may acquire the characteristic petaloid appearance referred to as cystoid macular oedema (CMO).

CA is one of the most ubiquitous enzyme systems in the body and also acts as an inflammatory mediator. In addition to the ciliary body epithelium, it is also found in the red-green cones, within the Mueller cells of the retina, and in the retinal pigment epithelium (RPE), thus suggesting new intraocular targets. CA inhibitors have been shown to have direct effects both on retinal and RPE cell function by inducing an acidification of the subretinal space, a decrease of the standing potential, and an increase in retinal adhesiveness. It is thought that acidification of the subretinal space is ultimately responsible for the increase of fluid resorption from the retina through the RPE into the choroid (Marmer 1990; Wolfensberger 1999).

CA plays a role in the biochemical reaction cascades in the universal pathomechanisms of CMO, where prostaglandins accelerate vascular permeability causing leakage, and upregulate generation of vascular endothelial growth factor (VEGF) and carbonic anhydrase-1 (CA-1) expression and downregulation of K^+ channels in Müller cells, resulted to increasing the inflow and reducing the outflow of ions and fluid from the inner nuclear layer and Henle fiber layer in the macular region (Bringmann et al. 2004).

The pigment epithelium of the retina withdraws the fluid through a Na^+/K^+ ATPase located in the basolateral membrane, the activity of which is facilitated when the concentration of H_2CO_3 in the sub-retinal space increases. High levels of CO_2 in the sub-retinal space reduce adhesion among the pigment epithelium and the neurosensory retina, and allows for the accumulation of intra-retinal and sub-retinal fluid (Adijanto et al. 2009); this condition is more common when there are high concentrations of CAs, as in the case of diabetes (Gao et al. 2007).

The anti-oedematic effect of CAI is achieved by increasing the fluid hydrodynamics through the RPE and pump function due to acidification of the sub-retinal space, thus controlling and adjusting the extracellular pH gradients produced by the metabolic activity of cells (Cox et al. 1988; Gallemore et al. 1997; Wolfensberger 1999). At the same time suppression of the inflammatory process underlying the vascular and RPE leakage occurs, causing CMO as was demonstrated by Bringmann et al. (2004).

Recently, synergistic effects between CAIs and some non-steroidal anti-inflammatory drugs (NSAIDs) for the management of CMO were highlighted by Supuran (2016a; b), who argued previously reported positive results of CMO resorption, confirmed by fluorescein angiography and optical coherence tomography (OCT), in a case series treated topically by simultaneous use of a CAI, an NSAID and a steroid (Asahi et al. 2015).

Piozzi et al. (2017) hypothesized that “the efficacy of topical NSAIDs and systemic CAI association indicates that the imbalance in the distribution of RPE membrane-bound CA could play a major role in CMO pathogenesis of gyrate atrophy of the choroid and retina”, a rare chorio-retinal dystrophy.

4.3.1 Systemic Carbonic Anhydrase Inhibitors

Systemic CAIs have been used since 1988 to treat the MO caused by several diseases (Cox et al. 1988), although their use was restricted due to associated systemic adverse events.

It has been reported that the response to treatment with CAIs is better in MO caused by pigment epithelium alterations than that presented in vascular diseases, such as diabetic retinopathy (DR) or venous occlusions (Wolfensberger 1999).

Acetazolamide facilitates the transport of water across the RPE from the subretinal space to the choroids (Fung 1995). One case report suggests a direct correlation of resolution of pseudophakic CMO with acetazolamide therapy (Tripathi et al. 1991).

A study conducted by Cox et al. (1988) demonstrated that 16 of 41 patients responded to acetazolamide treatment with partial or complete resolution of oedema and improved vision. These patients had MO secondary to a host of other conditions, including the Irvine-Gass syndrome.

Hayreh (1998) found that sustained release acetazolamide (Diamox Sequels, 500 mg twice daily) was effective in reducing MO and improving visual acuity in some patients with non-ischemic central retinal vein occlusion and MO. If a patient did not respond within two weeks, the therapy was discontinued because there was little chance of further improvement. In contrast to this, a normal clinical starting dose of acetazolamide is 500 mg/day by Wolfensberger (1999), which should be continued for at least one month to see an effect.

Efficacy of acetazolamide in CMO secondary to diabetes was analyzed by Giusti et al. (2001) in a pilot study, limitations of which were the small number of patients and the short follow-up. However, despite these factors the authors stated that acetazolamide could be effective in reducing fluorescein-angiographic findings and improving perimetric data in diabetes patients with MO, though visual acuity (VA) improved only slightly.

To investigate the impact of acetazolamide on the course of central serous retinopathy (CSR), Pikkell et al. (2002) initiated a prospective, nonrandomized, comparative trial including 15 acetazolamide-treated and seven untreated (control) CSR patients with long-term follow-up of at least 24 months. It was shown that acetazolamide treatment for CSR shortened the time for subjective and objective clinical resolution, but had no effect on either final VA or recurrence rate of the disease.

Pomykala et al. (2016) presented a case of recurring CSR associated with retinitis pigmentosa (RP) successfully treated with oral acetazolamide maintained on alternating and then biweekly doses of the drug.

Acetazolamide also reduced central macular thickness and macular cystic cavities in macular teleangiectasia without, however, improvement of visual acuity (VA) (Chen et al. 2014).

Several authors have described a positive effect of acetazolamide on the resolution of MO from various etiologies. These include uveitis and postoperative inflammation after cataract extraction (Farber et al. 1994), RP (Fishman and Gilbert 1989)

and serpiginous choroiditis (Chen et al. 1990), and in conjunction with epiretinal membrane (Marmer Marmor, 1990).

Schilling et al. (2005) assessed the long-term effect (mean follow-up 3.1 years) of acetazolamide treatment on fifty-two eyes of 45 patients with CMO in the course of intermediate or posterior chronic uveitis. Two subgroups were identified: group 1, quiescence of uveitis with acetazolamide as the single therapeutic agent (33 eyes); and group 2, chronically active uveitis requiring additional systemic anti-inflammatory drugs. In both groups, VA improvement was statistically significant. This treatment was more effective in patients with quiescence of uveitis than in those with chronically active uveitis, leading to the conclusion that low-dose acetazolamide can be a useful therapeutic option for chronic CMO in uveitis, but in active swelling it does not improve vision, which is why its use has decreased (Karim et al. 2013; Shoughy and Kozak, 2014).

Earlier randomised prospective studies (Farber et al. 1994) demonstrated that patients aged less than 55-years, with chronic iridocyclitis-related MO, were more like to respond to 500 mg acetazolamide twice daily comparing to older patients.

CMO is a well-confirmed cause of visual loss in patients with RP, with a prevalence ranging from 10 to 50%. (Adackapara et al. 2008; Hajali et al. 2008; Hajali and Fishman, 2009; Testa et al. 2014; Liew et al. 2018). The study of RP patients with CMO revealed a correlation between anti-carbonic anhydrase antibodies and CMO (Wolfensberger et al. 2000), suggesting that the use of CA inhibitors may be effective in treating this condition.

The efficacy of oral acetazolamide versus placebo, evaluated in a prospective, masked, crossover study, documented VA increase of at least one line, in at least one eye in 10 out of 12 patients with RP (Fishman et al. 1989). Three of these patients, initiated on placebo only, demonstrated improvement once switched to acetazolamide. In other prospective crossover studies (Fishman et al. 1994), nine out of 17 patients, using oral methazolamide, demonstrated angiographic improvement of CMO. However, vision improved in at least one eye, by at least two lines in only three patients. Acetazolamide cannot readily enter the neurosensory retina (Goren et al. 1961) thus explaining its low efficacy. Earlier reports showed a recurrence of CMO in patients with RP by oral CAI (Fishman et al. 1993; Apushkin et al. 2007). In retrospective studies initiated by Liew et al. (2015) involving 81 patients (157 eyes) with RP-CMO, objective improvement on OCT was observed in 28% of eyes of patients using oral acetazolamide and in 40% of eyes of patients using topical dorzolamide. VA improved from 6/15 to 6/12 in most patients. It was shown that autosomal recessive RP and greater initial central macular thickness (CMT) predicted better response to treatment.

4.3.2 Topical Carbonic Anhydrase Inhibitors

CAI drops alone have been known to be effective for treatment of MO in several ocular conditions (Wolfensberger 1999). They have been shown to reduce oedema in

patients with choroideremia (Genead et al. 2012) and more recently were included in a treatment regimen for Vogt–Koyanagi–Harada disease (Onishi et al. 2015). They have been recommended for syndromic retinal dystrophies such as Alström syndrome (Larrañaga-Fragoso et al. 2016), and also for CMO after cataract extraction (Asahi et al. 2015).

4.3.2.1 Dorzolamide

Dorzolamide is an effective ocular hypotensive agent (Harris et al. 1996).

The proposed mechanism of action for dorzolamide is the inhibition of CAs of the RPE, which favors the activity of Na/K⁺ ATPase and increases the transport of fluid toward the choroid.

The impact of topical CA inhibition has been analyzed in multiple studies. The efficacy of topical dorzolamide was evaluated in a prospective, nonrandomized clinical trial (Grover et al. 2006) involving 15 patients who received dorzolamide three times daily, for at least four weeks in both eyes. At the end of the study the researchers highlighted the potential efficacy of topical dorzolamide for treating CMO in patients with RP, but at the same time documented that some patients have shown a “rebound phenomenon” with continued use of the medication.

While Fishman and Apushkin (2007) demonstrated a beneficial effect of dorzolamide in patients with RP, their study followed a limited number of patients for a short period of time. Over a more extended period of time, Genead and Fishman (2010) studied the effect of sustained topical therapy with dorzolamide hydrochloride (2%) on visual acuity and cystic macular lesions verified by OCT, in 32 patients with RP and Usher syndrome. The authors observed that treatment of CMO in these patients, with topical dorzolamide, reduced central foveal thickness in a notable percentage of cases with improvement of VA in some. Similar results were obtained by Ikeda et al. (2012, 2013) in more recent studies. The authors concluded that prolonged use (more than one year) of topical dorzolamide was effective in treating CMO in RP patients, and proposed this as first-line treatment.

As was stated by Salvatore et al. (2013) CA inhibitors have proven to be potentially efficacious, although not in all cases.

Bakthavatchalam et al. (2017) systematically reviewed various treatments advocated for RP-related CMO and concluded that oral CAIs (acetazolamide and methazolamide) and topical CAIs (dorzolamide and brinzolamide) are effective first-line treatments. The authors postulated that oral acetazolamide had the strongest clinical basis for treatment and was superior to topical dorzolamide, which should be reserved as an alternative for cases revealing intolerance to the adverse effects of oral acetazolamide.

The latest meta-analysis conducted by Huang et al. (2017) showed that treatment with CA inhibitors of CMO in RP patients significantly reduced central macular thickness, but the effects on visual acuity were contradictory across studies. It was concluded that multicenter prospective randomized controlled trials were required to evaluate a clinical efficacy of CAI in RP patients.

The efficacy of dorzolamide was evaluated in a comparative, prospective, longitudinal, double-blind study in 69 eyes of patients with diabetes and focal MO, who underwent photocoagulation (Gómez et al. 2015). Diabetic MO with focal leakage did not affect the pigment epithelium and the amount of fluid leaking toward the retina exceeded the capacity of the latter to withdraw it (Gómez et al. 2015).

Treated eyes were randomly assigned three weeks after the procedure to receive dorzolamide (group 1) or placebo (group 2), three times daily for three weeks. The researchers highlighted that dorzolamide applied for three weeks was more effective than a placebo in reducing retinal thickness after focal photocoagulation in diabetic MO, and argued that, by closing microaneurysms with photocoagulation, topical CAIs may increase the transport of fluid toward the choroid, which does not occur when they are administered as the sole treatment. After photocoagulation, fluid is also withdrawn through competent adjacent capillaries, the capacity of which increases through vasodilation. The procedure promotes this effect by increasing gene expression of angiotensin II receptor type 2 in the retina (Wilson et al. 2003). CAIs also induce retinal venous vasodilation (Haustein et al. 2013), which is higher with the administration of dorzolamide than with the administration of acetazolamide (Torrington et al. 2009).

The anti-inflammatory effect of dorzolamide in MO resorption, in patients who have undergone vitrectomy combined with phacoemulsification and intraocular lens implantation for epiretinal membrane, was documented by Suzuki et al. (2013). They demonstrated that topical dorzolamide significantly reduced mean central macular thickness at one month, and mean aqueous flare at two weeks, after surgery for epiretinal membranes. It was previously reported that dorzolamide suppresses production of the proinflammatory cytokine interleukin-6, which is a major participant in the inflammatory process (Kawai et al. 2010).

Effect of dorzolamide on CMO in hydroxychloroquine retinopathy was evaluated in two cases by Kim et al. (2018). The authors observed good therapeutic response.

Another case report on the use of dorzolamide in CMO secondary to paclitaxel, a chemotherapeutic drug, was presented by Dwivedi and Tiroumal (2018). The authors proposed topical dorzolamide as an early treatment option, helping to avoid possible irreversible pigmentary change at the macula, and accelerate CMO resorption and vision recovery.

4.3.2.2 Brinzolamide

Alkin et al. (2013) have evaluated the effect of brinzolamide on RP-related CMO in a retrospective study of six patients (eight eyes) with RP. Despite a positive anatomical change manifested by a decrease of central macular thickness, an increase of VA was not achieved.

A synergistic efficacy of brinzolamide in a therapeutic cocktail containing also difluprednate 0.05% and nepafenac 0.1% was shown by Asahi et al. (2015) in three cases of Irvine-Gass syndrome, and single cases of diabetic CMO and branch retinal vein occlusion, respectively.

Zur (June 2018) initiated a Clinical Trial «**Brinzolamide for the Treatment of Chronic Central Serous Chorioretinopathy**» (<https://ichgcp.net/clinical-trials-register/NCT03542006>) to examine the efficacy of topical brinzolamide given twice daily for three months to patients aged 18–60 years with chronic CSR, affecting the fovea, and non-resolving after four months of follow-up. This is an open-label study based in Argentina and Israel.

In summary, currently available findings are insufficient to conclude that CA inhibition alone has the potential to be a big game changer in the management of MO.

References

- Adackapara CA, Sunness JS, Dibernardo CW, Melia BM, Dagnelie G (2008) Prevalence of cystoid macular edema and stability in OCT retinal thickness in eyes with retinitis pigmentosa during a 48-week lutein trial. *Retina (Philadelphia, Pa)* 28:103–110
- Adamson I (1999) Irreversible corneal decompensation in patients treated with topical dorzolamide. *Am J Ophthalmol* 128:774–775
- Adijanto J, Banzon T, Jalickee S, Wang NS, Miller SS (2009) CO₂-induced ion and fluid transport in human retinal pigment epithelium. *J Gen Physiol* 133(6):603–622. <https://doi.org/10.1085/jgp.200810169>
- Alcon (USA) Inc. Azopt® (brinzolamide ophthalmic suspension) 1%. Prescribing information [Internet]. http://ecatalog.alcon.com/pi/Azopt_us_en.pdf
- Alcon Laboratories (UK) Ltd. Azopt (brinzolamide eye drops suspension) 1%. Summary of product characteristics. eMC [Internet]. <http://emc.medicines.org.uk/emc/assets/c/html/displaydoc.asp?documentid=2808>
- Alkin Z, Özkaya A, Karatas G, Yazici AT, Demirok A (2013) Brinzolamide therapy in cystoid macular edema secondary to retinitis pigmentosa. *Ret-Vit* 21:82–86
- Andrés-Guerrero V, Bravo-Osuna I, Pastoriza P, Molina-Martinez IT, Herrero-Vanrell R (2017) Novel technologies for the delivery of ocular therapeutics in glaucoma. *J Drug Deliv Sci Technol* 42:181–192
- Apushkin MA, Fishman GA, Grover S, Janowicz MJ (2007) Rebound of cystoid macular edema with continued use of acetazolamide in patients with retinitis pigmentosa. *Retina* 27:1112–1128
- Asahi MG, Bobarnac Dogaru GL, Onishi SM, Gallemore RP (2015) Strong topical steroid, NSAID, carbonic anhydrase inhibitor cocktail for treatment of cystoid macular edema. *Int Med Case Rep J* 8:305–312. <https://doi.org/10.2147/IMCRJ.S92794>. eCollection 2015
- Bakthavatchalam M, Lai FHP, Rong SS, Ng DS, Brelen ME (2017) Treatment of cystoid macular edema secondary to retinitis pigmentosa: a systematic review. *Surv Ophthalmol* 63(3):329–339. <https://doi.org/10.1016/j.survophthal.2017.09.009>. Epub 5 Oct 2017
- Balfour JA, Wilde MI (1997) Dorzolamide. A review of its pharmacology and therapeutic potential in the management of glaucoma and ocular hypertension. *Drugs Aging* 10(5):384–403. <https://doi.org/10.2165/00002512-199710050-00006>
- Barnebey H, Kwok SY (2000) Patients' acceptance of a switch from dorzolamide to brinzolamide for the treatment of glaucoma in a clinical practice setting. *Clin Ther* 22:1204–1212
- Barnes GE, Li B, Dean T, Chandler ML (2000) Increased optic nerve head blood flow after 1 week of twice daily topical brinzolamide treatment in Dutch-belted rabbits. *Surv Ophthalmol* 44(2):S131–S140
- Becker B (1954) Decrease in intraocular pressure in man by carbonic anhydrase inhibitor. *Diamox* *Am J Ophthalmol* 37:13–15

- Becker B (1955a) The mechanism of the fall in intraocular pressure induced by the carbonic anhydrase inhibitor. *Diamox Am J Ophthalmol* 39:177–183
- Becker B (1955b) Long-term acetazolamide (Diamox) administration in therapy of glaucomas. *Arch Ophthalmol* 54:187–192
- Berson F, Epstein D (1980) Carbonic anhydrase inhibitors: management of side effects. *Perspect Ophthalmol* 4:91–95
- Borras J, Scozzafava A, Menabuoni L, Mincione F, Briganti F, Mincione G, Supuran CT (1999) Carbonic anhydrase inhibitors: synthesis of water-soluble, topically effective intraocular pressure lowering aromatic/heterocyclic sulfonamides containing 8-quinoline-sulfonyl moieties: is the tail more important than the ring? *Bioorg Med Chem* 7(11):2397–2406
- Breinin GM, Görtz H (1954) Carbonic anhydrase inhibitor acetazoleamide (Diamox). A new approach to the therapy of glaucoma. *AMA Arch Ophthalmol* 52(3):333–348. <https://doi.org/10.1001/archophth.1954.009200503335001>
- Bringmann A, Reichenbach A, Wiedemann P (2004) Pathomechanisms of cystoid macular edema. *Ophthalmic Res* 36(5):241–249
- «Brinzolamide for the Treatment of Chronic Central Serous Chorioretinopathy». <https://ichgcp.net/clinical-trials-registry/NCT03542006>
- Bron AM, Lippa EA, Hofmann HM, Feicht BI, Royer JG, Brunner-Ferber FL, Panbianco DL, Von Denffer HA (1989) MK-927: a topically effective carbonic anhydrase inhibitor in patients. *Arch Ophthalmol* 107(8):1143–1146
- Burmaoglu S, Yilmaz AO, Polat MF, Kaya R, Gulcin İ, Algul O (2019) Synthesis and biological evaluation of novel tris-chalcones as potent carbonic anhydrase, acetylcholinesterase, butyrylcholinesterase and α -glycosidase inhibitors. *Bioorg Chem* 85:191–197. <https://doi.org/10.1016/j.bioorg.2018.12.035>. Epub ahead of print
- Casini A, Mincione F, Ilies MA, Menabuoni L, Scozzafava A, Supuran CT (2001) Carbonic anhydrase inhibitors: synthesis and inhibition against isozymes I, II and IV of topically acting antiglaucoma sulfonamides incorporating cis-5-norbornene-endo-3-carboxy-2-carboxamido moieties. *J Enzyme Inhib* 16(2):113–123
- Centofanti M, Manni GL, Napoli D, Bucci MG (1997) Comparative effects of intraocular pressure between systemic and topical carbonic anhydrase inhibitors: a clinical masked, cross-over study. *Pharmacol Res* 35(5):481–485
- Chen JC, Fitzke FW, Bird AC (1990) Long-term effect of acetazolamide in a patient with retinitis pigmentosa. *Invest Ophthalmol vis Sci* 31:1914–1918
- Chen JJ, Sohn EH, Folk JC, Mahajan VB, Kay CN, Boldt HC, Russell SR (2014) Decreased macular thickness in nonproliferative macular telangiectasia type 2 with oral carbonic anhydrase inhibitors. *Retina* 34(7):1400–1406. <https://doi.org/10.1097/IAE.0000000000000093>
- Chiaromonte N, Bua S, Ferraroni M, Nocentini A, Bonardi A, Bartolucci G et al (2018) 2-Benzylpiperazine: a new scaffold for potent human carbonic anhydrase inhibitors. Synthesis, enzyme inhibition, enantioselectivity, computational and crystallographic studies and in vivo activity for a new class of intraocular pressure lowering agents. *Eur J Med Chem* 151(10):363–375
- Cox SN, Hay E, Bird AC (1988) Treatment of chronic macular edema with acetazolamide. *Arch Ophthalmol* 106:1190–1195
- de Carvalho CA, Lawrence C, Stone H (1958) Acetazolamide (Diamox) therapy in chronic glaucoma. *Arch Ophthalmol* 59:840–849
- de Leval X, Ilies M, Casini A, Dogné JM, Scozzafava A, Masini E, Mincione F, Starnotti M, Supuran CT (2004) Carbonic anhydrase inhibitors: synthesis and topical intraocular pressure lowering effects of fluorine-containing inhibitors devoid of enhanced reactivity. *J Med Chem* 47(11):2796–2804
- DeSantis L (2000) Preclinical overview of brinzolamide. *Surv Ophthalmol* 44(Suppl 2):S119–S129
- Cvetkovic RS, Perry CM (1978) Brinzolamide. A review of its use in the management of primary open-angle glaucoma and ocular hypertension. *Drug Aging* 20:919–947

- Dong Y, Sawada Y, Cui J, Hayakawa M, Ogino D, Ishikawa M, Yoshitomi T (2016) Dorzolamide-induced relaxation of isolated rabbit ciliary arteries mediated by inhibition of extracellular calcium influx. *Jpn J Ophthalmol* 60(2):103–110
- Dong Y, Huang S, Cui J, Yoshitomi T (2018) Effects of brinzolamide on rabbit ocular blood flow *in vivo* and *ex vivo*. *Int J Ophthalmol* 11(5):719–725. <https://doi.org/10.18240/ijo.2018.05.03>
- Drance SM, Carr F (1961) Effect of sustained-release Diamox on the 19 intraocular pressure in man. *Br J Ophthalmol* 45:695–698
- Dwivedi R, Tirumala S (2018) Possible efficacy of topical dorzolamide in the treatment of paclitaxel-related cystoid macular edema. *Retin Cases Brief Rep* 12(1):75–79. <https://doi.org/10.1097/ICB.0000000000000433>
- Fabrizi F, Mincione F, Somma T, Scozzafava G, Galassi F, Masini E, Impagnatiello F, Supuran CT (2012) A new approach to antiglaucoma drugs: carbonic anhydrase inhibitors with or without NO donating moieties. Mechanism of action and preliminary pharmacology. *J Enzyme Inhib Med Chem* 27(1):138–147. <https://doi.org/10.3109/14756366.2011.597749>. Epub 4 Aug 2011
- Farber MD, Lam S, Tessler HH, Jennings TJ, Cross A, Rusin MM (1994) Reduction of macular edema by acetazolamide in patients with chronic iridocyclitis: a randomized prospective crossover study. *Br J Ophthalmol* 78:4–7
- Fishman GA, Gilbert LD (1989) Acetazolamide for treatment of chronic macular edema in retinitis pigmentosa. *Arch Ophthalmol* 107:1445–1452
- Fishman GA, Glenn AM, Gilbert LD (1993) Rebound of macular edema with continued use of methazolamide in patients with retinitis pigmentosa. *Arch Ophthalmol* 111:1640–1646
- Fishman GA, Gilbert LD, Anderson RJ et al (1994) Effect of methazolamide on chronic macular edema in patients with retinitis pigmentosa. *Ophthalmology* 101:687–693
- Fishman GA, Apushkin MA (2007) Continued use of dorzolamide for the treatment of cystoid macular edema in patients with retinitis pigmentosa. *Br J Ophthalmol* 91:743–745
- Foster TS, Kieler RA, Dipiro JT (1982) Clinical and bioavailability studies of two formulations of acetazolamide. A scientific exhibit. Lederle Laboratories, Litho, USA
- Friedland B, Mallonee J, Anderson D (1977) Short-term dose response characteristics of acetazolamide in man. *Arch Ophthalmol* 95:1809–1812
- Gallemore RP, Hughes BA, Miller SS (1997) Retinal pigment epithelial transport mechanisms and their contributions to the electroretinogram. *Prog Retin Eye Res* 16:509–566
- Gao BB, Clermont A, Rook S, Fonda SJ, Srinivasan VJ, Wojtkowski M, Fujimoto JG, Avery RL, Arrigg PG, Bursell SE, Aiello LP, Feener EP (2007) Extracellular carbonic anhydrase mediates hemorrhagic retinal and cerebral vascular permeability through prekallikrein activation. *Nat Med* 13(2):181–188
- Garner L, Franklin CE, Ferweda J (1963) Advantages of sustained-release therapy with acetazolamide in glaucoma. *Am J Ophthalmol* 55:323–327
- Garrison L, Roth A, Rundle H, Christensen R (1967) A clinical comparison of three carbonic anhydrase inhibitors. *Trans Pacific Coast Oto-Ophthalmol Soc* 48:137–145
- Genead MA, Fishman GA (2010) Efficacy of sustained topical dorzolamide therapy for cystic macular lesions in patients with retinitis pigmentosa and usher syndrome. *Arch Ophthalmol* 128:1146–1150
- Genead MA, McAnany JJ, Fishman GA (2012) Topical dorzolamide for treatment of cystoid macular edema in patients with choroideremia. *Retina* 32(4):826–833
- Gillies WE, Brooks AM (1996) A clinical trial of MK-507, Trusopt, for raised intraocular pressure—the Australian experience. *Aust N Z J Ophthalmol* 24(2):111–115
- Giusti C, Forte R, Vingolo EM, Gargiulo P (2001) Is acetazolamide effective in the treatment of diabetic macular edema? A pilot study. *Int Ophthalmol* 24(2):79–88
- Goren SB, Newell FW, O'Toole JJ (1961) The localization of diamox-S35 in the rabbit eye. *Am J Ophthalmol* 51:87–93
- Grover S, Apushkin MA, Fishman GA (2006) Topical dorzolamide for the treatment of cystoid macular edema in patients with retinitis pigmentosa. *Am J Ophthalmol* 141(5):850–858 Epub 20 Mar 2006

- Hajali M, Fishman GA, Anderson RJ (2008) The prevalence of cystoid macular oedema in retinitis pigmentosa patients determined by optical coherence tomography. *Br J Ophthalmol* 92(8):1065–1068
- Hajali M, Fishman GA (2009) The prevalence of cystoid macular edema on optical coherence tomography in retinitis pigmentosa patients without cystic changes on fundus examination. *Eye* 23:915–919
- Harris A, Arend O, Arend S, Martin B (1996) Effects of topical dorzolamide on retinal and retrobulbar hemodynamics. *Acta Ophthalmol Scand* 74(6):569–572
- Haustein M, Spoerl E, Boehm AG (2013) The effect of acetazolamide on different ocular vascular beds. *Graefes Arch Clin Exp Ophthalmol* 251(5):1389–1398
- Hayreh SS (1998) Central retinal vein occlusion. *Ophthalmol Clin North Am* 11:559–590
- Heijl A, Leske MC, Bengtsson B et al (2002) Reduction of intraocular pressure and glaucoma progression: results from the Early Manifest Glaucoma Trial. *Arch Ophthalmol* 120:1268–1279
- Huang Q, Chen R, Lin X, Xiang Z (2017) Efficacy of carbonic anhydrase inhibitors in management of cystoid macular edema in retinitis pigmentosa: A meta-analysis. *PLoS ONE* 12(10):e0186180. <https://doi.org/10.1371/journal.pone.0186180>
- Huber-van der Velden KK, Lux A, Severing K, Klamann MK, Winterhalter S, Remky A (2012) Retrobulbar hemodynamics before and after oculopression with and without dorzolamide. *Curr Eye Res* 37(8):719–725
- Iester M (2008a) Brinzolamide ophthalmic suspension: a review of its pharmacology and use in the treatment of open angle glaucoma and ocular hypertension. *Clin Ophthalmol* 2(3):517–523
- Iester M (2008b) Brinzolamide. *Expert Opin Pharmacother* 9:653–662
- Ikeda Y, Hisatomi T, Yoshida N et al (2012) The clinical efficacy of a topical dorzolamide in the management of cystoid macular edema in patients with retinitis pigmentosa. *Graefes Arch Clin Exp Ophthalmol* 250:809–814
- Ikeda Y, Yoshida N, Notomi S, Murakami Y, Hisatomi T, Enaida H, Ishibashi T (2013) Therapeutic effect of prolonged treatment with topical dorzolamide for cystoid macular oedema in patients with retinitis pigmentosa. *Br J Ophthalmol* 97(9):1187–1191. <https://doi.org/10.1136/bjophthalmol-2012-303005> Epub 2013 Jun 19
- Ilies M, Supuran CT, Scozzafava A, Casini A, Mincione F, Menabuoni L, Caproiu MT, Maganu M, Banciu MD (2000) Carbonic anhydrase inhibitors: sulfonamides incorporating furan-, thiophene- and pyrrole-carboxamido groups possess strong topical intraocular pressure lowering properties as aqueous suspensions. *Bioorg Med Chem* 8(8):2145–2155
- Inoue K, Okugawa K, Oshika T, Amano S (2003) Influence of dorzolamide on corneal endothelium. *Jpn J Ophthalmol* 47(2):129–133
- Joyce PW, Mills KB (1990) Comparison of the effect of acetazolamide tablets and sustets on diurnal intraocular pressure in patients with chronic simple glaucoma. *Br J Ophthalmol* 74:413–416
- Jutley G, Luk SM, Dehabadi MH, Cordeiro MF (2017) Management of glaucoma as a neurodegenerative disease. *Neurodegener Dis Manag* 7(2):157–172. <https://doi.org/10.2217/nmt-2017-0004> Epub 2017 May 22
- Kaminski S, Hommer A, Koyuncu D, Biowski R, Barisani T (1998) Baumgartner I influence of dorzolamide on corneal thickness, endothelial cell count and corneal sensibility. *Acta Ophthalmol Scand* 76(1):78–79
- Kaplan NM (2000) Diuretics as a basis of antihypertensive therapy. An overview. *Drugs* 59(Suppl 2):21–25; discussion 39–40
- Karim R, Sykakis E, Lightman S, Fraser-Bell S (2013) Interventions for the treatment of uveitic macular edema: A systematic review and meta-analysis. *Clin Ophthalmol* 7:1109–1144
- Kass MA, Heuer DK, Higginbotham EJ, Johnson CA, Keltner JL, Miller JP, Parrish RK, Wilson MR, Gordon MO (2002) The ocular hypertension treatment study: a randomized trial determines that topical ocular hypotensive medication delays or prevents the onset of primary open-angle glaucoma. *Arch Ophthalmol* 120:701–713
- Kaur IP, Smitha R, Deepika A, Kapil M (2002) Acetazolamide: future perspective in topical glaucoma therapeutics. *Int J Pharm* 248:1–14

- Kaushik S, Pandav SS, Ram J (2003) Neuroprotection in glaucoma. *J Postgrad Med* 49(1):90–95. Review. PMID: 12865582
- Kawai K, Ohashi H, Suzuki T, Kitagaki H, Fujisawa S (2010) Effect of anti-glaucoma drugs on inflammatory cytokine production by human and murine peripheral blood mononuclear cells. *Nippon Ganka Gakkai Zasshi* 114:669–677
- Kellner U, Renner AB, Tillack H (2004) Hereditary retinohoroidal dystrophies. Part 2: differential diagnosis. *Ophthalmologie* 101(4):397–412; quiz 413–414
- Kim DG, Yoon CK, Kim HW, Lee SJ (2018) Effect of topical dorzolamide therapy on cystoid macular edema in hydroxychloroquine retinopathy. *Can J Ophthalmol* 53:e103–e107
- Kleinman ME, Baffi JZ, Ambati J (2010) The multifactorial nature of retinal vascular disease. *ophthalmologica* 224(suppl 1):16–24
- Kobayashi M, Naito K (2000) Pharmacological profiles of the potent carbonic anhydrase inhibitor dorzolamide hydrochloride, a topical antiglaucoma agent. *Nihon Yakurigaku Zasshi* (6):323–328. Review. Japanese
- Konowal A, Morrison JC, Brown SVL et al (1999) Irreversible corneal decompensation in patients treated with topical dorzolamide. *Am J Ophthalmol* 127:403–406
- Kouchak M, Malekhamadi M, Bavarsad N, Malehi AS, Andishmand L (2018) Dorzolamide nanoliposome as a long action ophthalmic delivery system in open angle glaucoma and ocular hypertension patients. *Drug Dev Ind Pharm* 44(8):1239–1242. <https://doi.org/10.1080/03639045.2017.1386196>
- Kupfer K, Lawrence C, Linner E (1955) Longterm administration of acetazolamide (Diamox) in the treatment of glaucoma. *Am J Ophthalmol* 40:673–680
- Larrañaga-Fragoso P, Pastora N, Bravo-Ljubetic L, Peralta J, Abelairas-Gómez J (2016) Topical carbonic anhydrase inhibitors in macular edema associated with Alström syndrome. *Ophthalmic Genet* 19:1–3. Epub ahead of print
- Lass JH, Khosrof SA, Laurence JK, Horwitz B, Ghosh K, Adamsons I (1998) A double-masked, randomized, 1-year study comparing the corneal effects of dorzolamide, timolol, and betaxolol. Dorzolamide Corneal Effects Study Group. *Arch Ophthalmol* 116(8):1003–1010
- Leske MC, Heijl A, Hussein M, Bengtsson B, Komaroff E (2004) Factors for glaucoma progression and the effect of treatment: the early manifest glaucoma. *Curr Opin Ophthalmol* 15(2):102–106
- Lichter PR, Musch DC, Medzihradsky F, Standardi CL (1989) Intraocular pressure effects of carbonic anhydrase inhibitors in primary open-angle glaucoma. *Am J Ophthalmol* 107(1):11–17
- Lichter P, Newman L, Wheeler N, Beall O (2003) Patient tolerance to carbonic anhydrase inhibitors. *Am J Ophthalmol* 85:495–502. *Arch Ophthalmol* 121:48–56
- Liew G, Moore AT, Webster AR, Michaelides M (2015) Efficacy and prognostic factors of response to carbonic anhydrase inhibitors in management of cystoid macular edema in retinitis pigmentosa. *Invest Ophthalmol vis Sci* 56:1531–1536
- Liew G, Strong S, Bradley P, Severn P, Moore AT, Webster AR, Mitchell P, Kifley A, Michaelides M. Prevalence of cystoid macular oedema, epiretinal membrane and cataract in retinitis pigmentosa. *Br J Ophthalmol*. <https://doi.org/10.1136/bjophthalmol-2018-311964>
- Lippa EA, Aasved H, Airaksinen PJ, Alm A, Bertelsen T, Calissendorff B, Dithmer O, Eriksson LO, Gustad L, Høvdning G et al (1991) Multiple-dose, dose-response relationship for the topical carbonic anhydrase inhibitor MK-927. *Arch Ophthalmol* 109(1):46–49
- Lippa EA, Carlson LE, Ehinger B, Eriksson LO, Finnström K, Holmin C, Nilsson SE, Nyman K, Raitta C, Ringvold A et al (1992) Dose response and duration of action of dorzolamide, a topical carbonic anhydrase inhibitor. *Arch Ophthalmol* 110:495–499
- Manni, G, Denis P, Chew P, Sharpe ED, Orengo-Nania S, Coote MA, Laganovska G, Volksone L, Zeyen T, Filatori I, James J, Aung T (2009) The safety and efficacy of brinzolamide 1%/timolol 0.5% fixed combination versus dorzolamide 2%/timolol 0.5% in patients with open-angle glaucoma or ocular hypertension. *J Glaucoma* 18:293–300
- March WF, Ochsner KI (2000) The long-term safety and efficacy of brinzolamide 1.0% (azopt) in patients with primary open-angle glaucoma or ocular hypertension. The Brinzolamide Long-Term Therapy Study Group. *Am J Ophthalmol* 129:136–143

- Maren TH (1967) Carbonic anhydrase: chemistry, physiology, and inhibition. *Physiol Rev* 47:595–781
- Maren TH (1987) Carbonic anhydrase: general perspective and advances in glaucoma research. *Drug Dev Res* 10(4):255–276. <https://doi.org/10.1002/ddr.430100407>
- Marmor MF (1990) Hypothesis concerning carbonic anhydrase treatment of cystoid macular edema: example with epiretinal membrane. *Arch Ophthalmol* 108(11):1524–1525. <https://doi.org/10.1001/archophth.1990.01070130026013>
- Martínez A, Sánchez-Salorio M (2009) A comparison of the long-term effects of dorzolamide 2% and brinzolamide 1%, each added to timolol 0.5%, on retrobulbar hemodynamics and intraocular pressure in open-angle glaucoma patients. *J Ocul Pharmacol Ther* 25:239–248
- Menabuoni L, Scozzafava A, Mincione F, Briganti F, Mincione G, Supuran CT (1999) Carbonic anhydrase inhibitors. Water-soluble, topically effective intraocular pressure lowering agents derived from isonicotinic acid and aromatic/heterocyclic sulfonamides: is the tail more important than the ring? *J Enzyme Inhib* 14(6):457–474
- Menon GJ, Vernon SA (2006) Topical brinzolamide and metabolic acidosis. *Br J Ophthalmol* 90:247–248
- Mestre C, Galin M, McLean J (1963) Evaluation of sustained-release acetazolamide. *Br J Ophthalmol* 47:31–35
- Michaud JE, Friren B (2001) Comparison of topical brinzolamide 1% and dorzolamide 2% eye drops given twice daily in addition to timolol 0.5% in patients with primary open-angle glaucoma or ocular hypertension. *Am J Ophthalmol* 132:235–243
- Mincione F, Starnotti M, Masini E, Bacciottini L, Scrivanti C, Casini A, Vullo D, Scozzafava A, Supuran CT (2005) Carbonic anhydrase inhibitors: design of thioureido sulfonamides with potent isozyme II and XII inhibitory properties and intraocular pressure lowering activity in a rabbit model of glaucoma. *Bioorg Med Chem Lett* 15(17):3821–3827
- Mincione F, Scozzafava A, Supuran CT (2007) The development of topically acting carbonic anhydrase inhibitors as anti-glaucoma agents. *Curr Top Med Chem* 7(9):849–854
- Mincione F, Scozzafava A, Supuran CT (2008) The development of topically acting carbonic anhydrase inhibitors as antiglaucoma agents. *Curr Pharm Des* 14(7):649–654
- Mincione F, Benedini F, Biondi S, Cecchi A, Temperini C, Formicola G, Pacileo I, Scozzafava A, Masini E, Supuran CT (2011) Synthesis and crystallographic analysis of new sulfonamides incorporating NO-donating moieties with potent antiglaucoma action. *Bioorg Med Chem Lett* 21(11):3216–3221. <https://doi.org/10.1016/j.bmcl.2011.04.046> Epub 2011 Apr 20
- Mundorf TK, Rauchman SH, Williams RD, Notivol R (2008) Brinzolamide/Timolol Preference Study Group. A patient preference comparison of Azarga™ (brinzolamide/timolol fixed combination) vs Cosopt® (dorzolamide/timolol fixed combination) in patients with open-angle glaucoma or ocular hypertension. *Clin Ophthalmol* 2:623–628
- Nagai N (2016) Design of novel ophthalmic formulation containing drug nanoparticles and its usefulness as anti-glaucoma drugs. *Yakugaku Zasshi* 136(10):1385–1390
- Nuzzi R, Dallorto L, Rolle T (2018) Changes of visual pathway and brain connectivity in glaucoma: a systematic review. *Front Neurosci* 12:363. <https://doi.org/10.3389/fnins.2018.00363>. eCollection 2018
- Onishi SM, Asahi MG, Chou C, Gallemore RP (2015) Topical difluprednate for the treatment of Harada's disease. *Clin Ophthalmol* 9:157–167
- Palmberg P (1995) A topical carbonic anhydrase inhibitor finally arrives. *Arch Ophthalmol* 113(8):985–986. <https://doi.org/10.1001/archophth.1995.01100080035025>
- Pfeiffer N (1997) Dorzolamide: development and clinical application of a topical carbonic anhydrase inhibitor. *Surv Ophthalmol* 42(2):137
- Pikkel J, Beiran I, Ophir A, Miller B (2002) Acetazolamide for central serous retinopathy. *Ophthalmology* 109(9):1723–1725
- Piozzi E, Alessi S, Santambrogio S, Cillino G, Mazza M, Iggui A, Cillino S (2017) Carbonic anhydrase inhibitor with topical NSAID therapy to manage cystoid macular edema in a case of gyrate atrophy. *Eur J Ophthalmol* 27(6):e179–e183. <https://doi.org/10.5301/ejo.5001010>

- Pomykala M, Rubin P, Rubin JS (2016) Recurrent central serous chorioretinopathy associated with retinitis pigmentosa treated with carbonic anhydrase inhibitors. *Retinal Cases Brief Rep* 10(3):205–207. <https://doi.org/10.1097/ICB.0000000000000225>
- Quigley HA, Broman AT (2006) The number of people with glaucoma worldwide in 2010 and 2020. *Br J Ophthalmol* 90(3):262–267 PMID: 16488940
- Renzi G, Scozzafava A, Supuran CT (2000) Carbonic anhydrase inhibitors: topical sulfonamide antiglaucoma agents incorporating secondary amine moieties. *Bioorg Med Chem Lett* 10(7):673–676
- Robin RO, Clapp JW (1950) The preparation of heterocyclic sulfonamides. *J Am Chem Soc* 72(11):4890–4892. <https://doi.org/10.1021/ja01167a011>
- Rossi GC, Pasinetti GM, Sandolo F, Bordin M, Bianchi PE (2011) From dorzolamide 2%/timolol 0.5% to brinzolamide 1%/timolol 0.5% fixed combination: a 6-month, multicenter, open-label tolerability switch study. *Expert Opin Pharmacother* 12(16):2425–2431. <https://doi.org/10.1517/14656566.2011.589384>. Epub 16 June 2011
- Sall K (2000) The efficacy and safety of brinzolamide 1% ophthalmic suspension (Azopt) as a primary therapy in patients with open-angle glaucoma or ocular hypertension. Brinzolamide Primary Therapy Study Group. *Surv Ophthalmol* 44(Suppl 2):S155–S162
- Salvatore S, Fishman GA, Genead MA (2013) Treatment of cystic macular lesions in hereditary retinal dystrophies. *Surv Ophthalmol* 58(6):560–584. <https://doi.org/10.1016/j.survophthal.2012.11.006>
- Sarı Y, Aktaş A, Taslimi P, Gök Y, Gulçin İ (2018) Novel N-propylphthalimide- and 4-vinylbenzyl-substituted benzimidazole salts: Synthesis, characterization, and determination of their metal chelating effects and inhibition profiles against acetylcholinesterase and carbonic anhydrase enzymes. *J Biochem Mol Toxicol* 32(1). <https://doi.org/10.1002/jbt.22009>. Epub 17 Nov 2017
- Schilling H, Heiligenhaus A, Laube T, Bornfeld N, Jurklics B (2005) Long-term effect of acetazolamide treatment of patients with uveitic chronic cystoid macular edema is limited by persisting inflammation. *Retina* 25(2):182–188
- Scozzafava A, Menabuoni L, Mincione F, Supuran CT (2002) Carbonic anhydrase inhibitors. A general approach for the preparation of water-soluble sulfonamides incorporating polyamino-polycarboxylate tails and of their metal complexes possessing long-lasting, topical intraocular pressure-lowering properties. *J Med Chem* 45(7):1466–1476
- Shin D (2000) Adjunctive therapy with brinzolamide 1% ophthalmic suspension (Azopt) in patients with open-angle glaucoma or ocular hypertension maintained on timolol therapy. *Surv Ophthalmol* 44(Suppl 2):S163–S168
- Shoughy SS, Kozak I (2014) Updates in uveitic macular edema. *World J Ophthalmol* 4(3):56–62
- Siesky B, Harris A, Brizendine E, Marques C, Loh J, Mackey J, Overton J, Netland P (2009) Literature review and meta-analysis of topical carbonic anhydrase inhibitors and ocular blood flow. *Surv Ophthalmol* 54(1):33–46
- Silver LH (1998) Clinical efficacy and safety of brinzolamide (Azopt), a new topical carbonic anhydrase inhibitor for primary open-angle glaucoma and ocular hypertension. Brinzolamide Primary Therapy Study Group. *Am J Ophthalmol* 126:400–408
- Silver LH (2000) Dose-response evaluation of the ocular hypotensive effect of brinzolamide ophthalmic suspension (Azopt) Brinzolamide Dose-Response Study Group. *Surv Ophthalmol* 44(Suppl 2):S147–S153
- Simpson AJ, Gray TB, Ballantyne C (1996) A controlled clinical trial of dorzolamide: a single-centre subset of a multicentre study. *Aust N Z J Ophthalmol* 24(1):39–42
- Stewart WC, Day DG, Stewart JA, Holmes KT, Jenkins JN (2004) Short-term ocular tolerability of dorzolamide 2% and brinzolamide 1% vs placebo in primary open-angle glaucoma and ocular hypertension subjects. *Eye (Lond)* 18:905–910
- Strahlman E, Tipping R, Vogel R (1995) A double-masked, randomized 1-year study comparing dorzolamide (Trusopt), timolol, and betaxolol. *Arch Ophthalmol* 113(8):1009–1016. <https://doi.org/10.1001/archophth.1995.01100080061030>

- Sugrue MF (1996) The preclinical pharmacology of dorzolamide hydrochloride, a topical carbonic anhydrase inhibitor. *J Ocul Pharmacol Ther* 12(3):363–376. Review
- Supuran CT, Scozzafava A, Menabuoni L, Mincione F, Briganti F, Mincione G (1999) Carbonic anhydrase inhibitors. Part 71. Synthesis and ocular pharmacology of a new class of water-soluble, topically effective intraocular pressure lowering sulfonamides incorporating picolinoyl moieties. *Eur J Pharm Sci* 8(4):317–328
- Supuran CT (2016a) Drug interaction considerations in the therapeutic use of carbonic anhydrase inhibitors. *Expert Opin Drug Metab Toxicol* 12(4):423–431. <https://doi.org/10.1517/17425255.2016.1154534>
- Supuran CT (2017) Advances in structure-based drug discovery of carbonic anhydrase inhibitors. *Expert Opin Drug Discov* 12(1):61–88. Epub 9 Nov 2016
- Suzuki T, Hayakawa K, Nakagawa Y, Onouchi H, Ogata M, Kawai K (2013) Topical dorzolamide for macular edema in the early phase after vitrectomy and epiretinal membrane removal. *Clin Ophthalmol* 7:549–553. <https://doi.org/10.2147/OPHT.S42188>
- Taslimi P, Caglayan C, Farzaliyev V, Nabiye O, Sujayev A, Turkan F, Kaya R, Gulçin İ (2018) Synthesis and discovery of potent carbonic anhydrase, acetylcholinesterase, butyrylcholinesterase, and α -glycosidase enzymes inhibitors: The novel N,N'-bis-cyanomethylamine and alkoxymethylamine derivatives. *J Biochem Mol Toxicol* 32(4):e22042. <https://doi.org/10.1002/jbt.22042>. Epub 19 Feb 2018
- Testa F, Rossi S, Colucci R et al (2014) Macular abnormalities in Italian patients with retinitis pigmentosa. *Br J Ophthalmol* 98:946–950
- Torring MS, Holmgaard K, Hesselund A, Aalkjaer C, Bek T (2009) The vasodilating effect of acetazolamide and dorzolamide involves mechanisms other than carbonic anhydrase inhibition. *Invest Ophthalmol vis Sci* 50(1):345–351
- Tranos PG, Wickremasinghe SS, Stangos NT, Topouzis F, Tsinopoulos I, Pavesio CE (2004) Macular edema. *Surv Ophthalmol* 49(5):470–490
- Tripathi RC, Fekrat S, Tripathy BJ, Ernest JT (1991) A direct correlation of the resolution of pseudophakic cystoid macular edema with acetazolamide therapy. *Ann Ophthalmol* 23:127–129
- Tsukamoto H, Noma H, Mukai S, Ikeda H, Mishima HK (2005) The efficacy and ocular discomfort of substituting brinzolamide for dorzolamide in combination therapy with latanoprost, timolol, and dorzolamide. *J Ocul Pharmacol Ther* 21:395–399
- Türker F, Barut Celepci D, Aktaş A, Taslimi P, Gök Y, Aygün M, Gülçin İ (2018) Meta-Cyanobenzyl substituted benzimidazolium salts: Synthesis, characterization, crystal structure and carbonic anhydrase, α -glycosidase, butyrylcholinesterase, and acetylcholinesterase inhibitory properties. *Arch Pharm (Weinheim)*. 351(7):e1800029. <https://doi.org/10.1002/ardp.201800029>. Epub 22 May 2018
- Van der Valk R, Webers CAB, Schouten JSAG et al (2005) Intraocular pressure-lowering effects of all commonly used glaucoma drugs. A meta-analysis of randomized clinical trials. *Ophthalmology* 112:1177–1185
- Wang TH, Huang JY, Hung PT, Shieh JW, Chen YF (2004) Ocular hypotensive effect and safety of brinzolamide ophthalmic solution in open angle glaucoma patients. *J Formos Med Assoc* 103:369–373
- Wilkerson M, Cyrlin M, Lippa EA, Esposito D, Deasy D, Panebianco D, Fazio R, Yablonski M, Shields MB (1993) Four-week safety and efficacy study of dorzolamide, a novel, active topical carbonic anhydrase inhibitor. *Arch Ophthalmol* 111:1343–1350
- Wilson AS, Hobbs BG, Shen WY, Speed TP, Schmidt U, Begley CG, Rakoczy PE (2003) Argon laser photocoagulation-induced modification of gene expression in the retina. *Invest Ophthalmol Vis Sci* 44(4):1426–1434
- Wolfensberger TJ (1999) The role of carbonic anhydrase inhibitors in the management of macular edema. *Doc Ophthalmol* 97:387–397. <https://doi.org/10.1023/A:1002143802926>
- Wolfensberger TJ, Aptsiauri N, Godley B et al (2000) Antiretinale Antikörper assoziiert mit zystoideM Makulaödem. *Klin Monatsbl Augenheilkd* 216:283–285

- Yadav A, Gupta V, Sethi HS, Kumar A, Kumar S (2014) A comparative study of the efficacy and adverse event profile of topical brinzolamide with topical dorzolamide monotherapy in patients of primary open angle glaucoma and ocular hypertension in a North-Indian population. *J Evol Med Dent Sci* 3(38):9806–9819. <https://doi.org/10.14260/jemds/2014/3270>
- Zakšauskas A, Čapkauskaitė E, Jezepčikas L, Linkuvienė V, Kišonaitė M, Smirnov A, Manakova E, Gražulis S, Matulis D (2018) Design of two-tail compounds with rotationally fixed benzenesulfonamide ring as inhibitors of carbonic anhydrases. *Eur J Med Chem* 5(156):61–78. <https://doi.org/10.1016/j.ejmech.2018.06.059> Epub 27 June 2018
- Zeyen TG, Caprioli J (1993) Progression of disc and field damage in early glaucoma. *Arch Ophthalmol* 111:62–65
- Zhao JC, Chen T (2005) Brinzolamide induced reversible corneal decompensation. *Br J Ophthalmol* 89:389–390
- Zubrienė A, Smirnov A, Dudutienė V, Timm DD, Matulienė J, Michailovienė V, Zakšauskas A, Manakova E, Gražulis S, Matulis D (2017) Intrinsic thermodynamics and structures of 2,4- and 3,4-substituted fluorinated benzenesulfonamides binding to carbonic anhydrases. *ChemMedChem* 12(2):161–176. <https://doi.org/10.1002/cmdc.201600509> Epub 21 Dec 2016

Chapter 5

Targeting Carbonic Anhydrase Isozymes in the Treatment of Neurological Disorders



Ashok Aspatwar, Jukka Peltola, and Seppo Parkkila

Abstract Carbonic anhydrases (CAs) are widely expressed in the nervous system where they play important physiological roles. In the brain and other parts of the system, different isozymes show unique distribution patterns, some of them being present in neurons (CA II, V, VII, XIV), capillary endothelium (CA IV), microglia (CA III), choroid plexus (CA II, III, XII, XIV), astrocytes (CA II and V), oligodendrocytes (CA II and XIII), and myelin sheath (CA II). Nervous tissues also express three carbonic anhydrase-related proteins (CARP VIII, X, XI), which may be involved in the brain development processes. Future research is needed to define the exact roles of these highly conserved CA isoforms and to design novel treatment strategies for the diseases caused by defects or abnormal regulation of CARPs. Enzymatically active CA isozymes are known drug targets to treat various neurological disorders including epilepsy, acute mountain sickness, pseudotumor cerebri, and brain edema. In this review article, we describe how the clinically approved CA inhibitors are used for the treatment of these diseases.

Keywords Brain · Carbonic anhydrase · Drug · Expression · Inhibitor · Neurology

5.1 Expression and Function of Enzymatically Active Carbonic Anhydrases in the Nervous System

The presence of carbonic anhydrase (CA) activity in the brain was described for the first time in 1943 (Ashby 1943). In the nervous system, CAs play various important roles, e.g., in fluid and ion compartmentation (Bourke and Kimelberg 1975), the formation of cerebrospinal fluid (CSF) (Maren 1967), neuronal signal transduction

A. Aspatwar · J. Peltola · S. Parkkila (✉)

Faculty of Medicine and Health Technology, Tampere University, Arvo Ylpön katu 34, 33520 Tampere, Finland

e-mail: seppo.parkkila@tuni.fi

J. Peltola · S. Parkkila

Fimlab Ltd. and Department of Neurology, Tampere University Hospital, Tampere, Finland

© Springer Nature Switzerland AG 2021

W. R. Chegwidden and N. D. Carter (eds.), *The Carbonic Anhydrases: Current and Emerging Therapeutic Targets*, Progress in Drug Research 75,

https://doi.org/10.1007/978-3-030-79511-5_5

Table 5.1 Distribution of CA isozymes in different cell types of the central nervous system

Cell type	Isozymes
Oligodendrocytes	II, XIII (Roussel 1979; Ghandour 1980,1979; Langley 1980; Kumpulainen and Korhonen 1982; Kumpulainen 1983; Kida 2006; Lehtonen 2004)
Astrocytes	II, V (Cammer 1991; Kimelberg et al. 1982; Snyder 1983; Ghandour 2000; Cammer and Tansey 1988a,b; Cammer and Zhang 1992; Jeffrey et al. 1991)
Myelin sheath	II (Roussel 1979; Kumpulainen and Korhonen 1982)
Choroid plexus	II, III, XII, XIV (Kumpulainen and Korhonen 1982; Kida 2006; Nogradi et al. 1993; Parkkila 2001; Kallio 2006; Halmi et al. 2006)
Microglial cells	III (Nogradi 1993)
Endothelial cells	IV (Ghandour 1992)
Neurons	II, V, VII, XIV (Ruusuvoori 2004; Kida 2006; Parkkila 2001; Ghandour 2000)

(Ruusuvoori 2004; Makani 2012), seizure activity (Anderson et al. 1984), the respiratory response to carbon dioxide (Ridderstrale and Hanson 1985), and the generation of bicarbonate for biosynthetic reactions (Cammer 1991).

The distribution of various CA isozymes in the brain is summarized in Table 5.1. In an early histochemical study, the highest CA activity was shown in the areas of mouse brains that were rich in myelinated fibers and glial cells (Korhonen et al. 1964). Several early immunohistochemical studies concluded that the mammalian brain contains CA mainly or exclusively in oligodendrocytes (Roussel 1979; Ghandour 1980,1979; Langley 1980; Kumpulainen and Korhonen 1982; Kumpulainen 1983). Myelin sheaths were also found to contain CA II (Roussel 1979; Kumpulainen and Korhonen 1982), which prompted the idea that CA II could be a biomarker for myelin degradation in demyelinating diseases (Kumpulainen 1985; Parkkila 1997).

The expression of CA II in astrocytes has been a controversial matter, and some findings suggested that these cells may contain CA II at relatively low levels (Roussel 1979; Kimelberg et al. 1982; Snyder 1983). The presence of CA II in astrocytes was questioned since *in situ* hybridization showed CA II mRNA expression in oligodendrocytes but not in astrocytes (Ghandour and Skoff 1991). Neurons have generally been considered to lack CA II, but there have been some exceptions to this notion, and obviously some subpopulations of neurons may express it (Kida 2006; Tanimoto et al. 2005).

Nogradi demonstrated CA II and CA III immunoreactivity in active brain macrophages, whereas resting microglial cells expressed only CA III (Nogradi 1993). The changes in CA II expression that occur in microglial cells during development and activation may correlate with the metabolic and immunological states of the cells.

The choroid plexus is one of the main sites of CA expression within the central nervous system, and the significance of CA activity for CSF formation is well documented (Maren 1967; Tschirgi et al. 1954; Brown 2004). CA II and CA III were found in the epithelial cells of the choroid plexus by Kumpulainen and Korhonen

(1982) and Nogradi et al., respectively (1993). In addition to these cytoplasmic forms, the choroid plexus contains at least three membrane-associated isozymes. First, CA XIV was found in a limited population of choroid plexus epithelial cells (Parkkila 2001). Another immunohistochemical study demonstrated strong expression of both CA IX and CA XII in the choroid plexus (Ivanov 2001). Later, the positive signal for CA XII was located to the basolateral membranes of the choroid plexus epithelial cells (Kallio 2006), and a role for CA XII in the recycling of carbon dioxide into the epithelial cells was proposed (Halmi et al. 2006).

The membrane-associated CA IV has been demonstrated on the luminal surface of capillary endothelial cells (Ghandour 1992). The strategic location on the luminal face of the blood-brain barrier suggests that CA IV may participate in the export of carbon dioxide from brain tissues. In 2006, it was shown that CA IV is expressed on the surfaces of astrocytes (Svichar 2006). Using CA IV and XIV double knockout mice, it was observed that both membrane-associated CAs contribute to extracellular buffering in the central nervous system, and CA IV seems to be the more important extracellular CA in the hippocampus (Shah 2005; Svichar 2009). It has been shown that thyroid hormone signaling regulates the expression of CA IV in the brain (Vujovic 2015).

There have been very few studies on the expression and role of mitochondrial CA VA and VB in the nervous system. In the first paper, Ghandour and coworkers demonstrated that the mitochondrial enzyme is present in both astrocytes and neurons (Ghandour 2000). At that moment, it was not known whether the neuronal isozyme was CA VA or CA VB. Western and Northern blot experiments later confirmed that the isozyme was indeed CA VB, which generally shows a wider expression pattern in tissues compared to CA VA (Shah 2000). Several potential functions have been proposed for the mitochondrial enzyme (Ghandour 2000): It could play a role in gluconeogenesis in astrocytes by providing bicarbonate ions for the pyruvate carboxylase, the neuronal CA V could be involved in the regulation of the intramitochondrial calcium levels, and it could also participate in bicarbonate ion-induced GABA responses by regulating the bicarbonate homeostasis in neurons. Kaila's group later reported that it is the other isozyme, CA VII, that is the key molecule in the generation of high-frequency stimulation-induced tonic GABAergic excitation (Ruusuvaori 2004).

Although the expression of CA IX seems quite limited and generally weak in the central nervous system, it may still carry out important functions in the regulation of behavior and maintenance of tissue integrity. Preliminary observations suggested mild behavioral changes and a morphological disruption of brain histology in CA IX-deficient (*Car9* (-/-)) mice. Therefore, a one-year follow-up study was conducted in which both the behavior and brain histology of *Car9* (-/-) and wild-type mice were monitored (Pan 2012). Morphological analysis revealed vacuolar degenerative changes in the brains of *Car9* (-/-) mice. The changes became visible at the age of eight to ten months. Behavioral tests showed that the *Car9* (-/-) mice exhibited abnormal locomotor activity and poor performance in a memory test. To further identify the transcriptomic responses to CA IX deficiency in the brain, genome-wide cDNA microarray analyses were performed. Functional annotation revealed

that the genes with increased expression were involved in several processes, such as RNA metabolism, and the genes with reduced expression were implicated in other important processes, including the regulation of cellular ion homeostasis. Notably, the biological processes “behavior” and “locomotory behavior” were the two prominent terms overrepresented among the downregulated genes.

The distribution and role of CA XIII are poorly known at this moment. The first article on CA XIII showed a positive mRNA signal in the mouse brain and located the enzyme to the oligodendrocytes and nerve fibers (Lehtonen 2004).

5.2 CA Inhibitors in the Treatment of Neurological Diseases

The classical CA inhibitor acetazolamide is clinically used for the treatment of acute high-altitude illness (AHAI), brain edema, pseudotumor cerebri, and epilepsy, in addition to the nonneurological indications. This inhibitor has also been tested for the treatment of hydrocephalus because there are no significant noninvasive treatment alternatives (Groat and Neumiller 2013), and the reduction of CSF production would be of interest as a treatment strategy. Some studies have indeed shown that both acetazolamide and a well-known diuretic, furosemide, could be useful to reduce CSF production by the choroid plexus. As with lumbar puncture, these agents are used in low-birthweight infants who will have a low success rate with shunt placement or endoscopic ventriculostomy. There is no evidence that either of these medications increases survival rates, and a Cochrane review concluded that therapy with acetazolamide or furosemide is neither effective nor safe for treating posthemorrhagic ventricular dilatation in infants (Whitelaw et al. 2001).

5.3 CA Inhibitors in the Treatment of Acute High-Altitude Illness

Acute high-altitude illness (AHAI) is an encompassing term for the range of pathology that the unacclimatized individual may develop when exposed to hypoxia at high altitude (Smedley and Grocott 2013). The term AHAI covers acute mountain sickness (AMS), high-altitude cerebral edema (HACE) and high-altitude pulmonary edema (HAPE). The symptoms of AMS include headache, dizziness, nausea, insomnia, anorexia, and difficulty sleeping. Progression to HACE is characterized by altered mental status, reduced consciousness and ataxia.

Acetazolamide is considered one of the key medications for both AMS prevention and treatment and can also be used as an adjunct to dexamethasone in HACE treatment (Table 5.2) (Luks 2010). The severity of additional diseases of high altitude may also be reduced by acetazolamide, including HAPE and chronic mountain sickness (CMS) (Swenson 2014). It is noteworthy that the beneficial effect of acetazolamide

Table 5.2 Recommended medications used in the prevention and treatment of AMS and HACE (Luks 2010)

Medication	Indication	Route	Dosage in adults
Acetazolamide	AMS, HACE prevention	Oral	125 mg twice per day
	AMS, HACE ^a treatment	Oral	250 mg twice per day
Dexamethasone	AMS, HACE prevention	Oral	2 mg every 6 h or 4 mg every 12 h
	AMS, HACE treatment	Oral, IV, IM	AMS: 4 mg every 6 h HACE: 8 mg once, then 4 mg every 6 h

IV intravenous; *IM* intramuscular; ^aAcetazolamide can be used at this dose as an adjunct to dexamethasone in HACE treatment, but dexamethasone remains the primary treatment for that disorder

in high-altitude illness may not be related to the reduction of CSF production only. It has been shown that acetazolamide also blocks aquaporin-4 (AQP4) water channels (Huber 2007), the main component of the glial-associated lymphatic pathway called the glymphatic system (Plog and Nedergaard 2018). Therefore, it is obvious that acetazolamide can reduce the swelling of the brain tissue in the hypobaric hypoxia condition by modulation of the glymphatic system.

5.4 CA Inhibitors in the Treatment of Pseudotumor Cerebri

Pseudotumor cerebri is a neurological disease where intracranial pressure increases for no obvious reason. Symptoms mimic those of a brain tumor, even though no tumor is present. When no underlying cause of the increased intracranial pressure is discovered, pseudotumor cerebri may also be called idiopathic or benign intracranial hypertension. It is almost exclusively a disease of obese young women (Wall 2014). The increased intracranial pressure associated with pseudotumor cerebri can cause swelling of the optic nerve and result in vision loss. The key factor for the pathogenesis of pseudotumor cerebri is the accumulation of CSF. This may be caused by either increased fluid production or decreased fluid reabsorption. Several CAs are expressed in the choroid plexus (Table 5.1), the site of CSF production. Therefore, it was reasonable to consider CA inhibitors as potential treatments for pseudotumor cerebri. In fact, it was first documented in the 1950s that acetazolamide reduces intracranial pressure (Atkinson and Ward 1958). Since then, it has been widely used in the first-line therapy of pseudotumor cerebri, although solid documentation of the effectiveness was lacking for many years (Thurtell and Wall 2013). A large, multi-center, randomized controlled trial was conducted in 2010–2014, comparing the efficacy of weight loss and placebo with weight loss and acetazolamide as treatments for mild to moderate idiopathic intracranial hypertension (<https://clinicaltrials.gov/ct2/>

[show/NCT01003639](#)). The main result indicated that the use of acetazolamide with a low-sodium weight-reduction diet compared with diet alone resulted in modest improvement in the visual field function of patients with idiopathic intracranial hypertension and mild vision loss (Committee et al. 2014). There is no standardized dosing regimen for acetazolamide as a treatment of pseudotumor cerebri. It has been suggested that a reasonable starting dose could be 500 mg twice daily, gradually increasing to a maximum of 4 g daily in twice-daily doses depending on the treatment outcome and potential side effects of the drug (Thurtell and Wall 2013). Methazolamide, another CA inhibitor, can be tried when the side effects of acetazolamide are intolerable (Thurtell and Wall 2013). In a recent review, Supuran predicted that no major changes would occur in the use of acetazolamide in the treatment of intracranial hypertension within the near future because it is a safe, nontoxic and inexpensive drug that is not protected by any patents (Supuran 2015).

Topiramate, a widely used anticonvulsant, is the third potential CA inhibitor that has been proposed as a treatment of pseudotumor cerebri (Thurtell and Wall 2013). It has a clear anti-obesity effect causing dose-dependent weight loss (Ben-Menachem 2003; Bray 2003), which is considered a desired outcome in the treatment of pseudotumor cerebri. Compared to acetazolamide, topiramate seems to show similar efficacy for improvement of visual field grades (Celebisoy 2007).

5.5 CA Inhibitors in the Treatment of Brain Edema

As discussed above, acetazolamide is clinically used to reduce intracranial pressure due to pseudotumor cerebri. Even though it has been used much less in other forms of neurological/neurosurgical diseases associated with increased intracranial pressure, it has been successfully applied in certain neurosurgical conditions for diagnostic or therapeutic purposes. Acetazolamide is anti-edematous and has neuroprotective properties that have been discussed in the literature (Szczygielski 2019).

Mild traumatic brain injury is a relatively common disease entity experienced in accidents, on the battlefield, and in sports. Astrocyte cellular edema, where AQP4 is involved, is an important factor leading to high morbidity after brain injury. As a blocking agent of AQP4, acetazolamide could represent a potential drug for the treatment of mild traumatic brain injury. Sturdivant and coworkers recently investigated whether acetazolamide could prevent AQP4-driven cell swelling using a 3D astrocyte model of mild traumatic brain injury (Sturdivant 2016). First, they proved that AQP4 expression was significantly increased 24 h after the procedure, mimicking mild traumatic brain injury. The procedure resulted in an increase in cell swelling within 30 min of mild traumatic brain injury, which was significantly reduced in the presence of acetazolamide. Cell death was also significantly reduced when acetazolamide was added shortly before the trauma procedure, supporting the neuroprotective role of the drug. To date, there are no clinical studies addressing the use of acetazolamide in this indication.

5.6 CA Inhibitors in the Treatment of Epilepsy

Epilepsy is a very common neurological disease, and seizures are possible in any individual in response to an appropriate stimulus. Different stimuli include lack of sleep, smoking, and reduced CO₂ levels in the brain (Aggarwal et al. 2013). Since CO₂ is involved, several CA inhibitors have been considered potential candidates for the treatment of seizures, as they could increase the CO₂ levels in the brain. In fact, CA inhibitors have been used as antiepileptic drugs (AEDs) in the 1970s, when acetazolamide and methazolamide were the most promising choices (Supuran 2018). The mechanisms by which CA inhibitors show antiepileptic action are complex. The inhibition of CA activity leads to a diminished formation of bicarbonate and changes the brain pH, thus contributing to an antiepileptic effect by several diverse pathways. However, the clinical significance of the inhibition of CA in the treatment of epilepsy is not well established, except in the case of acetazolamide, mainly because most of the AEDs in clinical usage with CA inhibition properties also have other, most likely more important, mechanisms of action.

Acetazolamide was the first CA inhibitor used as an anticonvulsant. Because of its numerous side effects, including alterations of taste, paresthesia, and tinnitus, acetazolamide is currently rarely used for this indication (Aggarwal et al. 2013). Catamenial epilepsy is a special subtype of epilepsy in which seizures are clustered around specific points of the menstrual cycle, most often around the perimenstrual or periovulatory period. Three types of catamenial seizures have been identified: perimenstrual (C1), periovulatory (C2), and inadequate luteal (C3) (Navis and Harden 2016). Acetazolamide has been used for decades as a treatment option in catamenial epilepsy, but there are no large-scale, randomized studies available on its efficacy (Aggarwal et al. 2013). In a retrospective analysis, 40% of the women patients reported lower seizure frequency, and 30% claimed a decrease in severity with acetazolamide treatment (Lim 2001). Based on previous studies and present treatment options, acetazolamide is still considered part of the algorithm for the treatment of female patients with suspected catamenial seizure patterns (Navis and Harden 2016).

AEDs with CA inhibitory characteristics, which are commonly used in the treatment of epilepsy, include topiramate, zonisamide and lacosamide. In the case of these three AEDs, CA inhibition has not been considered the defining characteristic as a mechanism of action for efficacy in the treatment of various forms of epilepsy, but it has relevance with regard to their side-effect profiles, especially with topiramate and zonisamide.

Topiramate is a sulfamate-substituted monosaccharide that was originally found to exhibit potent anticonvulsant activity similar to phenytoin (Maryanoff et al. 1987). In the first report, topiramate was described as a weak CA inhibitor (micromolar against erythrocyte CAs), but later Supuran and coworkers demonstrated that topiramate is, in fact, a very potent inhibitor of CAs with a K_i value of 5 nM against human CA II (Masereel 2002). Topiramate inhibits all CA isozymes present in the blood and brain, causing CO₂ retention, which is considered important for the anticonvulsant effect (Aggarwal et al. 2013). Other mechanisms may also be involved, such as the

blockade of Na⁺ channels and AMPA/kainate receptors, as well as the enhancement of GABAergic transmission.

Zonisamide is a sulfonamide antiepileptic drug that is a 1,2 benzisoxazole derivative with multiple mechanisms of action resembling topiramate. It was first used in Japan in 1972 to treat psychiatric disorders, and it has been in use to treat epilepsy since at least the 1990s.

Topiramate and zonisamide have a number of similar side effects attributed to CA inhibition. The most common of these are hypohidrosis (Cheshire and Fealey 2008), tubular acidosis and renal stones (Hamed 2017). Hypohidrosis signifies decreased sweating in response to a proportionate thermal or pharmacological stimulus with its complete form termed anhidrosis. Hypohidrosis is potentially hazardous to health since the inability to generate a thermoregulatory sweating response can seriously challenge one's ability to maintain core temperature in conditions of strenuous physical activity or in hot environments (Cheshire and Fealey 2008). CA inhibitors can interfere with sweat production, probably at the level of the secretory coil clear cell or apex of ductal cells. The risk of hypohidrosis in pediatric patients taking zonisamide or topiramate is significantly higher than that of adults (Cheshire and Fealey 2008). Hypohidrosis has been reported mainly during adjunctive topiramate therapy and is rare in patients on monotherapy (Cerminara 2006). When children who are severely disabled (i.e., neurologically impaired, nonambulatory) are treated with topiramate, they have a very high risk of renal stone formation (Ishikawa 2019).

In addition to epilepsy, zonisamide has been tested for the treatment of other symptoms and diseases, such as essential tremor, myoclonus-dystonia, mania, acute psychotic conditions, neuropathic pain, and Parkinson's disease symptoms (Kadian et al. 2019). A Cochrane review on essential tremor identified only one study with 20 eligible subjects (Bruno et al. 2017). The main conclusion was that there is insufficient evidence to assess the efficacy and safety of zonisamide for the treatment of essential tremor. In 2016, Hainque and coworkers investigated the efficacy and safety of zonisamide in a cohort of 24 patients with myoclonus-dystonia (Hainque 2016). Zonisamide significantly improved action myoclonus, myoclonus-related functional disability, and dystonia symptoms compared to the placebo.

Lacosamide, (2*R*)-2-acetylamino-*N*-benzyl-3-methoxypropanamide, is a relatively new antiepileptic drug that was first introduced into clinical practice in 2008. Although it does not have any of the moieties typically found in well-known CA inhibitors, such as sulfonamide, sulfamate, sulfamide or coumarin, lacosamide acts as an effective inhibitor of all mammalian CA isozymes CA I – XV. Based on crystallographic data, it binds to the active site of CA II similar to the hydrolyzed coumarins, not interacting with the metal ion (Temperini 2010). Experimental data have suggested a dual mechanism of action for lacosamide: (a) modulation of the slow inactivation of sodium channels and (b) modulation of collapsin-response mediator protein 2 (CRMP-2)-mediated neurotrophic signals (Kellinghaus 2009). It seems that the inhibition of CA activity may be the third relevant function, which may lead to the antiepileptic effect. In contrast to topiramate or zonisamide, lacosamide does not seem to have hypohidrosis, tubular acidosis or renal stones as part of its side effect profile (Kwok et al. 2017).

5.7 Carbonic Anhydrase-Related Proteins (CARPs)

The carbonic anhydrase-related proteins (CARPs) are CA isoforms that are evolutionarily well conserved but lack the classical CA enzymatic activity (Aspatwar 2014; Aspatwar et al. 2010). The CARPs occur either independently or as domains of other proteins. The catalytic inactivity of CARPs is due to the absence of one or more of the three histidine residues that are required for the coordination of zinc metal ions in the CA active site. There are three classical CARPs named CARP VIII, X and XI in the order of their discovery. In addition, in the family of protein tyrosine phosphatases (PTPs), there are two receptor-type protein tyrosine phosphatases, PTPR zeta (ζ) and PTPR gamma (γ), that contain an N-terminal CA-like domain (Barnea 1993; Levy 1993) known as the CARP XVI domain (Tolvanen 2012; Ortutay et al. 2010). The enzymatic activity of human CARPs can be regained by restoring the histidine residues (Nishimori 2013). Even though we have gradually learned more about the potential biological functions of CARPs and CA domains, the exact physiological roles of these proteins are still poorly understood.

5.8 Localization and Role of CARP VIII

CARP VIII is catalytically inactive due to the substitution of arginine at the first of the three histidine residues required for coordination of the zinc atom in the active site. CARP VIII was the first CARP isoform that was identified and found in the mouse brain by Kato (1990). Subsequent expression studies included detailed analyses during embryonic development and of adult tissues of humans and mice (Aspatwar et al. 2010; Taniuchi 2002a,b; Lakkis 1997). The expression of the *Car8* gene was studied using in situ hybridization, which localized the *Car8* gene to the cerebellar Purkinje cells (Lakkis et al. 1997). Immunohistochemistry showed that CARP VIII is expressed in both adult and fetal human brains, and the cellular distribution of the protein is shown in Table 5.3 (Taniuchi 2002b). The analysis of *CA8* gene expression in a panel of zebrafish tissues showed that it is predominantly expressed in the brain, similar to the expression in mice and humans (Aspatwar et al. 2010; Okamoto 2001; Aspatwar 2013). In the adult zebrafish tissues, immunohistochemistry of the cerebellar region showed an intense signal for CARP VIII in the Purkinje cells, which is analogous to the expression in mice and humans (Aspatwar 2014,2015).

The role of CARP VIII in neural development became obvious from the studies in waddles (*wdl*) mice that are characterized by a lifelong gait disorder (Jiao 2005). Analysis of *wdl* mice showed a 19 bp deletion in the *Car8* gene (autosomal recessive mutation), which is responsible for the *wdl* phenotype, and the mice showed a complete absence of CARP VIII protein (Jiao 2005).

Along with two reports on *CA8* gene mutations in members of Iraqi and Saudi Arabian families, the role of CARP VIII in neural development has gained renewed interest (Turkmen 2009; Kaya 2011). The affected members of an Iraqi family had

Table 5.3 Expression of CARPs in human adult and fetal brains (Aspatwar et al. 2013)

Adult brain					Fetal brain			
		CARP VIII	CARP X	CARP XI	Days of gestation	CARP VIII	CARP X	CARP XI
Brain part	Region	Level of expression				Level of expression		
Cerebrum	Cx	++	+w	+	84	+	+	+
	Medulla	+	++	–	95	+	+	+
	Hippocampus	++	–	+	121	+	+	+
	Basal ganglia	++	–	+w	141	+	+	+
Diencephalon	Thalamus	++	–	–	222	+	+	+
	Substantia nigra	++	–	–				
Cerebellum	Cx, molecular layer	++	–	–				
	Cx, Purkinje cells	++	+w	+w				
	Cx, granular layer	–	–	–				
Pons	Vestibular nuclei	++	–	+				
	Abducens nucleus	++	–	+				
	Pontine nuclei	++		++				
Medulla	Olivary nuclei	++	+w	–				
	Others	++	+w	–				
Choroid PX		++	+w	++				
Pia Arach		++	–	++				

++ strong expression; + moderate expression in most cells; +w weak expression; – no significant expression; *Cx* cortex; *Choroid PX*. choroid plexus; *Pia Arach*. pia arachnoid

mild mental retardation and congenital ataxia that was associated with quadrupedal gait (Fig. 5.1). In another study, the members of a Saudi Arabian family showed a novel homozygous (G162R) substitution in the CARP VIII protein (Kaya 2011). All the affected members of the family showed mental retardation and cerebellar ataxia similar to the affected members of the Iraqi family, but the Saudi Arabian patients did not exhibit quadrupedal gait (Aspatwar et al. 2013). Brain magnetic resonance imaging showed a loss of cerebellar volume and peritrigonal white matter abnormalities (Kaya 2011). Mild cognitive impairment, a variable degree of cerebellar ataxia, an absence of seizures, and a lack of dysmorphism were the common features that were found in both Saudi Arabian and Iraqi subjects. The absence of quadrupedal gait



Figure 5.1 A mutation in the *CA8* gene in members of an Iraqi family leads to mental retardation and quadrupedal gait. This figure is reproduced from Turkmen (2009) under the Creative Commons Attribution (CC BY) license

in the members of the Saudi Arabian family could be due to environmental factors rather than being a genuine phenotypic variation of the disease.

A report on the interaction of CARP VIII with inositol trisphosphate receptor-1 (ITPR1) provides a plausible mechanism for the cerebellar disorders in humans and mice (Hirota 2003; Yan 2007). However, the precise mechanism of how the regulation of ITPR1 leads to the biological effects is still not known. Later studies in mice showed that *Car8* acts as an allosteric inhibitor of ITPR1 that regulates the intracellular calcium release essential for neuronal excitability, neurite outgrowth, neurotransmitter release (Lamont and Weber 2015), and the calcium pathway that is critical for nociception, inflammatory pain, and possibly other neuropathological states (Zhuang 2015).

Changes in the gene expression profile of human neuroblastoma cells expressing a repeat expansion mutant ataxin-3 showed a ninefold increase in *CA8* gene expression in the presence of mutant ataxin-3 compared to the cells expressing normal ataxin-3 (Hsieh 2012). It was shown earlier that defective ataxin-3 disturbs neuronal calcium signaling by binding to ITPR1 (Chen 2008). There are now many lines of evidence suggesting that CARP VIII plays a role in neural development and motor coordination function in the cerebellum (Shimobayashi et al. 2016).

To further elucidate the function of CARP VIII, we recently developed a zebrafish model by knocking down the *CA8* gene using antisense morpholino oligonucleotides (Aspatwar 2013). The amino acid identity between the human and zebrafish CARP VIII protein is 84%. Such a high degree of conservation between CARP VIII sequences of distant vertebrate species speaks for a conserved, essential function

(Aspatwar 2013). The developed zebrafish model will be helpful in investigating the mechanisms of CARP VIII-related ataxia and mental retardation in humans.

5.9 Distribution and Role of CARP X

The presence of CARP X was reported in the brain while screening CCG repeats in the cDNA libraries from the human brain (Okamoto 2001). The deduced CA-like amino acid sequence showed that two of the three amino acid residues required for binding to zinc were absent in CARP X, suggesting the lack of enzymatic activity (Aspatwar et al. 2013). *CA10* mRNA expression was reported in all parts of the central nervous system analyzed (Okamoto 2001). The studies of the cellular distribution of CARP X using antibodies also showed positive signals in many parts of the human brain (Table 5.3) (Taniuchi 2002b; Aspatwar et al. 2013). A developmental expression study in human brain specimens covering days 84–222 of gestation showed CARP X protein throughout the period (Taniuchi 2002b). In our laboratory, we showed the presence of *Car10* mRNA extensively in the mouse brain (Aspatwar et al. 2010), and similarly, *CA10* was predominantly expressed in both the larval and adult zebrafish brains (Aspatwar 2015). Knockdown studies of *CA10a* and *CA10b* genes using morpholinos in zebrafish larvae showed an abnormal movement pattern, which was later confirmed by inactivation of the genes with the CRISPR/Cas9 system, suggesting a role for these CARPs in motor coordination (Aspatwar 2015).

Recent studies have shown that both CARP X and XI are evolutionarily conserved neurexin ligands in mammals (Sterky 2017). Neurexins are presynaptic proteins that regulate neurotransmitter release. Notably, damage to these synapses precedes neuronal cell death in Alzheimer's disease (Hishimoto 2019). The above results have led to several persuasive hypotheses. First, CARP X and CARP XI may act primarily as neurexin chaperones. Second, they may function as adaptors that enable indirect interactions of neurexins with unknown postsynaptic target molecules, thus mediating the formation of novel transsynaptic complexes (Sterky 2017).

The presence of seven CCG repeats in the 5'-untranslated region of the *CA10* gene followed by two CCG repeats located 16 bp downstream may be associated with various neurological disorders (Kleiderlein 1998). The *CA10* gene with the CCG repeats might play a role in the development of neurodegenerative disorders, and therefore, it will be of interest to explore the expansion mutations of the *CA10* gene in patients with neurological symptoms (Aspatwar et al. 2010). It is of interest that there is a report on cerebellar hypoplasia and quadrupedal movement in members of a Turkish family (Turkmen 2006; Humphrey and Mondalas 2018) who showed a quite similar phenotype to the Iraqi and Saudi Arabian patients with mutations of the *CA8* gene (Turkmen 2009; Kaya 2011). However, the genetic defect in the Turkish family was mapped to chromosome 17p (Turkmen 2006; Humphrey and Mondalas 2018). Because the *CA10* gene is located on chromosome 17q, it may not be the affected gene in this phenotypic trait.

5.10 Distribution and Role of CARP XI

A characteristic feature of CARP XI is the absence of all three histidine residues required for the CA catalytic activity (Aspatwar et al. 2010). The cellular and developmental distribution of the human CARP XI protein is shown in Table 5.3. The expression of *Car11* mRNA in mouse tissues showed that the transcript is predominantly present in the central nervous system (Aspatwar et al. 2010).

Expansion mutations of CAG repeats in ataxin-3 are responsible for spinocerebellar ataxia/Machado-Joseph disease (SCA3/MJD), a neurodegenerative disease (Kawaguchi et al. 1994). Studies using neuroblastoma cells expressing mutant ataxin-3 showed an upregulation of *CA11* similar to that of *CA8* (Hsieh 2013). Further studies on the cellular distribution of CARP XI in cultured neuronal cells from the brain tissues of humans and mice with SCA3 showed altered localization of CARP XI compared to normal specimens (Hsieh 2013). These findings suggest that the altered localization of CARP XI in SCA3 may play a role in the progression of the disease and dysfunction of the nervous system.

5.11 Concluding Remarks

CAs are widely expressed in different cell types of the central nervous system. For decades, they have been important drug targets to treat certain neurological disorders, such as epilepsy, acute mountain sickness, pseudotumor cerebri, and brain edema. In several cases, the drug designers were not initially aiming to develop CA inhibitors, and it was only later that some of them were identified as efficient CA inhibitors.

The presence of highly conserved CARPs in the brain of various species suggests important roles for these proteins in brain development and/or neural functions. Although their exact functions in the developing brain remain uncertain, the findings suggest certain roles for CARPs in the early development or differentiation of neuroprogenitor cells. Screening of patients with unknown neurological disorders for variations in CARPs may reveal novel insights into these proteins. Future research on these inactive CA isoforms may provide us with information on how these proteins work, possibly by coordination with other proteins through protein–protein interactions and might also help us to design novel treatment strategies for the diseases caused by defects or abnormal regulation of these proteins.

We still believe in the same view stated by professor Robert E. Forster 30 years ago at the Carbonic Anhydrase Conference in Spoleto, Italy: “With so many questions about its functions, some about new problems and some about old problems freshly seen, research on CA has a bright future.”

Acknowledgements Our original research has been supported by grants from the Academy of Finland, Sigrid Juselius Foundation, Jane & Aatos Erkko Foundation, and Finnish Cultural Foundation.

References

- Aggarwal M, Kondeti B, McKenna R (2013) Anticonvulsant/antiepileptic carbonic anhydrase inhibitors: a patent review. *Expert Opin Ther Pat* 23(6):717–724
- Anderson RE, Engstrom FL, Woodbury DM (1984) Localization of carbonic anhydrase in the cerebrum and cerebellum of normal and audiogenic seizure mice. *Ann N Y Acad Sci* 429:502–504
- Ashby W (1943) Carbonic anhydrase in mammalian tissue. *J Biol Chem* 151:521–527
- Aspatwar A et al (2013) Abnormal cerebellar development and ataxia in CARP VIII morphant zebrafish. *Hum Mol Genet* 22(3):417–432
- Aspatwar A et al (2014) Carbonic anhydrase related proteins: molecular biology and evolution. *Subcell Biochem* 75:135–156
- Aspatwar A et al (2015) Inactivation of ca10a and ca10b genes leads to abnormal embryonic development and alters movement pattern in zebrafish. *PLoS One* 10(7):e0134263
- Aspatwar A, Tolvanen ME, Parkkila S (2010) Phylogeny and expression of carbonic anhydrase-related proteins. *BMC Mol Biol* 11:25
- Aspatwar A, Tolvanen ME, Parkkila S (2013) An update on carbonic anhydrase-related proteins VIII, X and XI. *J Enzyme Inhib Med Chem*
- Atkinson JR, Ward AA Jr (1958) Effect of diamox on intracranial pressure and blood volume. *Neurology* 8(1):45–50
- Barnea G et al (1993) Identification of a carbonic anhydrase-like domain in the extracellular region of RPTP gamma defines a new subfamily of receptor tyrosine phosphatases. *Mol Cell Biol* 13(3):1497–1506
- Ben-Menachem E et al (2003) Predictors of weight loss in adults with topiramate-treated epilepsy. *Obes Res* 11(4):556–562
- Bourke RS, Kimelberg HG (1975) The effect of HCO-3 on the swelling and ion uptake of monkey cerebral cortex under conditions of raised extracellular potassium. *J Neurochem* 25(3):323–328
- Bray GA et al (2003) A 6-month randomized, placebo-controlled, dose-ranging trial of topiramate for weight loss in obesity. *Obes Res* 11(6):722–733
- Brown PD et al (2004) Molecular mechanisms of cerebrospinal fluid production. *Neuroscience* 129(4):957–970
- Bruno E et al (2017) Zonisamide for essential tremor. *Cochrane Database Syst Rev* 8:CD009684
- Cammer W (1991) Immunostaining of carbamoylphosphate synthase II and fatty acid synthase in glial cells in rat, mouse, and hamster brains suggests roles for carbonic anhydrase in biosynthetic processes. *Neurosci Lett* 129(2):247–250
- Cammer W, Tansey FA (1988a) The astrocyte as a locus of carbonic anhydrase in the brains of normal and dysmyelinating mutant mice. *J Comp Neurol* 275(1):65–75
- Cammer W, Tansey FA (1988b) Carbonic anhydrase immunostaining in astrocytes in the rat cerebral cortex. *J Neurochem* 50(1):319–322
- Cammer W, Zhang H (1992) Carbonic anhydrase in distinct precursors of astrocytes and oligodendrocytes in the forebrains of neonatal and young rats. *Brain Res Dev Brain Res* 67(2):257–263
- Celebisoy N et al (2007) Treatment of idiopathic intracranial hypertension: topiramate vs acetazolamide, an open-label study. *Acta Neurol Scand* 116(5):322–327
- Cerminara C et al (2006) Hypohidrosis during topiramate treatment: a rare and reversible side effect. *Pediatr Neurol* 34(5):392–394
- Chen X et al (2008) Deranged calcium signaling and neurodegeneration in spinocerebellar ataxia type 3. *J Neurosci* 28(48):12713–12724
- Cheshire WP, Fealey RD (2008) Drug-induced hyperhidrosis and hypohidrosis: incidence, prevention and management. *Drug Saf* 31(2):109–126
- Ghandour MS et al (1979) Double labeling immunohistochemical technique provides evidence of the specificity of glial cell markers. *J Histochem Cytochem* 27(12):1634–1637
- Ghandour MS et al (1980) Immunohistochemical and immunohistochemical study of carbonic anhydrase II in adult rat cerebellum: a marker for oligodendrocytes. *Neuroscience* 5(3):559–571

- Ghandour MS et al (1992) Carbonic anhydrase IV on brain capillary endothelial cells: a marker associated with the blood-brain barrier. *Proc Natl Acad Sci U S A* 89(15):6823–6827
- Ghandour MS et al (2000) Mitochondrial carbonic anhydrase in the nervous system: expression in neuronal and glial cells. *J Neurochem* 75(5):2212–2220
- Ghandour MS, Skoff RP (1991) Double-labeling in situ hybridization analysis of mRNAs for carbonic anhydrase II and myelin basic protein: expression in developing cultured glial cells. *Glia* 4(1):1–10
- Groat JJ, Neumiller JJ (2013) Review of the treatment and management of hydrocephalus. *US Pharm* 38(3):HS8–HS11
- Hainque E et al (2016) A randomized, controlled, double-blind, crossover trial of zonisamide in myoclonus-dystonia. *Neurology* 86(18):1729–1735
- Halmi P, Parkkila S, Honkaniemi J (2006) Expression of carbonic anhydrases II, IV, VII, VIII and XII in rat brain after kainic acid induced status epilepticus. *Neurochem Int* 48(1):24–30
- Hamed SA (2017) The effect of antiepileptic drugs on the kidney function and structure. *Expert Rev Clin Pharmacol* 10(9):993–1006
- Hirota J et al (2003) Carbonic anhydrase-related protein is a novel binding protein for inositol 1,4,5-trisphosphate receptor type 1. *Biochem J* 372(Pt 2):435–441
- Hishimoto A et al (2019) Neurexin 3 transmembrane and soluble isoform expression and splicing haplotype are associated with neuron inflammasome and Alzheimer's disease. *Alzheimers Res Ther* 11(1):28
- Hsieh M et al (2012) Altered expression of carbonic anhydrase-related protein XI in neuronal cells expressing mutant ataxin-3. *Cerebellum*
- Hsieh M et al (2013) Altered expression of carbonic anhydrase-related protein XI in neuronal cells expressing mutant ataxin-3. *Cerebellum* 12(3):338–349
- Huber VJ et al (2007) Identification of arylsulfonamides as Aquaporin 4 inhibitors. *Bioorg Med Chem Lett* 17(5):1270–1273
- Humphrey NK, Mondalas S (2018) <https://www.youtube.com/watch?v=6GINQzjii1c>
- Ishikawa N et al (2019) High incidence of renal stones in severely disabled children with epilepsy treated with topiramate. *Neuropediatrics* 50(3):160–163
- Ivanov S et al (2001) Expression of hypoxia-inducible cell-surface transmembrane carbonic anhydrases in human cancer. *Am J Pathol* 158(3):905–919
- Jeffrey M, Wells GA, Bridges AW (1991) Carbonic anhydrase II expression in fibrous astrocytes of the sheep. *J Comp Pathol* 104(4):337–343
- Jiao Y et al (2005) Carbonic anhydrase-related protein VIII deficiency is associated with a distinctive lifelong gait disorder in waddles mice. *Genetics* 171(3):1239–1246
- Kadian R, Kumar A (2019) Zonisamide, in StatPearls. Treasure Island (FL)
- Kallio H et al (2006) Expression of carbonic anhydrases IX and XII during mouse embryonic development. *BMC Dev Biol* 6:22
- Kato K (1990) Sequence of a novel carbonic anhydrase-related polypeptide and its exclusive presence in Purkinje cells. *FEBS Lett* 271(1–2):137–140
- Kawaguchi Y et al (1994) CAG expansions in a novel gene for Machado-Joseph disease at chromosome 14q32.1. *Nat Genet* 8(3):221–228
- Kaya N et al (2011) Phenotypical spectrum of cerebellar ataxia associated with a novel mutation in the CA8 gene, encoding carbonic anhydrase (CA) VIII. *Am J Med Genet B Neuropsychiatr Genet* 156(7):826–834
- Kellinghaus C (2009) Lacosamide as treatment for partial epilepsy: mechanisms of action, pharmacology, effects, and safety. *Ther Clin Risk Manag* 5:757–766
- Kida E et al (2006) Carbonic anhydrase II in the developing and adult human brain. *J Neuropathol Exp Neurol* 65(7):664–674
- Kimelberg HK, Stieg PE, Mazurkiewicz JE (1982) Immunocytochemical and biochemical analysis of carbonic anhydrase in primary astrocyte cultures from rat brain. *J Neurochem* 39(3):734–742
- Kleiderlein JJ et al (1998) CCG repeats in cDNAs from human brain. *Hum Genet* 103(6):666–673

- Korhonen LK, Naeaeetaenen E, Hyyppae M (1964) A histochemical study of carbonic anhydrase in some parts of the mouse brain. *Acta Histochem* 18:336–347
- Kumpulainen T et al (1983) Immunolabeling of carbonic anhydrase isoenzyme C and glial fibrillary acidic protein in paraffin-embedded tissue sections of human brain and retina. *J Histochem Cytochem* 31(7):879–886
- Kumpulainen T et al (1985) A single-step solid phase radioimmunoassay for quantifying human carbonic anhydrase I and II in cerebrospinal fluid. *Clin Chim Acta* 150(3):205–212
- Kumpulainen T, Korhonen LK (1982) Immunohistochemical localization of carbonic anhydrase isoenzyme C in the central and peripheral nervous system of the mouse. *J Histochem Cytochem* 30(4):283–292
- Kwok CS, Johnson EL, Krauss GL (2017) Comparing safety and efficacy of “third-generation” antiepileptic drugs: long-term extension and post-marketing treatment. *CNS Drugs* 31(11):959–974
- Lakkis MM et al (1997) Expression of the acatalytic carbonic anhydrase VIII gene, Car8, during mouse embryonic development. *Histochem J* 29(2):135–141
- Lakkis MM, O’Shea KS, Tashian RE (1997) Differential expression of the carbonic anhydrase genes for CA VII (Car7) and CA-RP VIII (Car8) in mouse brain. *J Histochem Cytochem* 45(5):657–662
- Lamont MG, Weber JT (2015) Mice deficient in carbonic anhydrase type 8 exhibit motor dysfunctions and abnormal calcium dynamics in the somatic region of cerebellar granule cells. *Behav Brain Res* 286:11–16
- Langley OK et al (1980) Carbonic anhydrase: an ultrastructural study in rat cerebellum. *Histochem J* 12(4):473–483
- Lehtonen J et al (2004) Characterization of CA XIII, a novel member of the carbonic anhydrase isozyme family. *J Biol Chem* 279(4):2719–2727
- Levy JB et al (1993) The cloning of a receptor-type protein tyrosine phosphatase expressed in the central nervous system. *J Biol Chem* 268(14):10573–10581
- Lim LL et al (2001) Acetazolamide in women with catamenial epilepsy. *Epilepsia* 42(6):746–749
- Luks AM et al (2010) Wilderness Medical Society consensus guidelines for the prevention and treatment of acute altitude illness. *Wilderness Environ Med* 21(2):146–155
- Makani S et al (2012) NMDA receptor-dependent afterdepolarizations are curtailed by carbonic anhydrase 14: regulation of a short-term postsynaptic potentiation. *J Neurosci* 32(47):16754–16762
- Maren TH (1967) Carbonic anhydrase: chemistry, physiology, and inhibition. *Physiol Rev* 47(4):595–781
- Maryanoff BE et al (1987) Anticonvulsant O-alkyl sulfamates. 2,3,4,5-Bis-O-(1-methylethylidene)-beta-D-fructopyranose sulfamate and related compounds. *J Med Chem* 30(5):880–887
- Masereel B et al (2002) Carbonic anhydrase inhibitors: anticonvulsant sulfonamides incorporating valproyl and other lipophilic moieties. *J Med Chem* 45(2):312–320
- Navis A, Harden C (2016) A treatment approach to catamenial epilepsy. *Curr Treat Options Neurol* 18(7):30
- Nishimori I et al (2013) Restoring catalytic activity to the human carbonic anhydrase (CA) related proteins VIII, X and XI affords isoforms with high catalytic efficiency and susceptibility to anion inhibition. *Bioorg Med Chem Lett* 23(1):256–260
- Nogradi A (1993) Differential expression of carbonic anhydrase isozymes in microglial cell types. *Glia* 8(2):133–142
- Nogradi A, Kelly C, Carter ND (1993) Localization of acetazolamide-resistant carbonic anhydrase III in human and rat choroid plexus by immunocytochemistry and in situ hybridisation. *Neurosci Lett* 151(2):162–165
- Okamoto N et al (2001) cDNA sequence of human carbonic anhydrase-related protein, CA-RP X: mRNA expressions of CA-RP X and XI in human brain. *Biochim Biophys Acta* 1518(3):311–316
- Ortutay C et al (eds) (2010) An evolutionary analysis of insect carbonic anhydrases. In: Berhardt LV (ed) *Advances in medicine and biology*, vol 7, Nova Science Publishers Inc., Hauppauge, NY, pp 145–168

- Pan PW et al (2012) Brain phenotype of carbonic anhydrase IX-deficient mice. *Transgenic Res* 21(1):163–176
- Parkkila AK et al (1997) Carbonic anhydrase II in the cerebrospinal fluid: its value as a disease marker. *Eur J Clin Invest* 27(5):392–397
- Parkkila S et al (2001) Expression of membrane-associated carbonic anhydrase XIV on neurons and axons in mouse and human brain. *Proc Natl Acad Sci U S A* 98(4):1918–1923
- Plog BA, Nedergaard M (2018) The glymphatic system in central nervous system health and disease: past, present, and future. *Annu Rev Pathol* 13:379–394
- Ridderstrale Y, Hanson M (1985) Histochemical study of the distribution of carbonic anhydrase in the cat brain. *Acta Physiol Scand* 124(4):557–564
- Roussel G et al (1979) Demonstration of a specific localization of carbonic anhydrase C in the glial cells of rat CNS by an immunohistochemical method. *Brain Res* 160(1):47–55
- Ruusuvuori E et al (2004) Carbonic anhydrase isoform VII acts as a molecular switch in the development of synchronous gamma-frequency firing of hippocampal CA1 pyramidal cells. *J Neurosci* 24(11):2699–2707
- Shah GN et al (2000) Mitochondrial carbonic anhydrase CA VB: differences in tissue distribution and pattern of evolution from those of CA VA suggest distinct physiological roles. *Proc Natl Acad Sci U S A* 97(4):1677–1682
- Shah GN et al (2005) Carbonic anhydrase IV and XIV knockout mice: roles of the respective carbonic anhydrases in buffering the extracellular space in brain. *Proc Natl Acad Sci U S A* 102(46):16771–16776
- Shimobayashi E, Wagner W, Kapfhammer JP (2016) carbonic anhydrase 8 expression in Purkinje cells is controlled by PKC gamma activity and regulates Purkinje cell dendritic growth. *Mol Neurobiol* 53(8):5149–5160
- Smedley T, Grocott MP (2013) Acute high-altitude illness: a clinically orientated review. *Br J Pain* 7(2):85–94
- Snyder DS et al (1983) Carbonic anhydrase, 5'-nucleotidase, and 2',3'-cyclic nucleotide-3'-phosphodiesterase activities in oligodendrocytes, astrocytes, and neurons isolated from the brains of developing rats. *J Neurochem* 40(1):120–127
- Sterky FH et al (2017) Carbonic anhydrase-related protein CA10 is an evolutionarily conserved pan-neurexin ligand. *Proc Natl Acad Sci U S A* 114(7):e1253–e1262
- Sturdivant NM et al (2016) Acetazolamide mitigates astrocyte cellular edema following mild traumatic brain injury. *Sci Rep* 6:33330
- Supuran CT (2015) Acetazolamide for the treatment of idiopathic intracranial hypertension. *Expert Rev Neurother* 15(8):851–856
- Supuran CT (2018) Applications of carbonic anhydrases inhibitors in renal and central nervous system diseases. *Expert Opin Ther Pat* 28(10):713–721
- Svichar N et al (2006) Functional demonstration of surface carbonic anhydrase IV activity on rat astrocytes. *Glia* 53(3):241–247
- Svichar N et al (2009) Carbonic anhydrases CA4 and CA14 both enhance AE3-mediated Cl⁻-HCO₃⁻ exchange in hippocampal neurons. *J Neurosci* 29(10):3252–3258
- Swenson ER (2014) Carbonic anhydrase inhibitors and high altitude illnesses. *Subcell Biochem* 75:361–386
- Szczygielski J et al (2019) Brain edema formation and functional outcome after surgical decompression in murine closed head injury are modulated by acetazolamide administration. *Front Neurol* 10:273
- Tanimoto T et al (2005) Immunohistochemical co-expression of carbonic anhydrase II with Kv1.4 and TRPV1 in rat small-diameter trigeminal ganglion neurons. *Brain Res* 1044(2): 262–265
- Taniuchi K et al (2002a) cDNA cloning and developmental expression of murine carbonic anhydrase-related proteins VIII, X, and XI. *Brain Res Mol Brain Res* 109(1–2):207–215
- Taniuchi K et al (2002b) Developmental expression of carbonic anhydrase-related proteins VIII, X, and XI in the human brain. *Neuroscience* 112(1):93–99

- Temperini C et al (2010) The coumarin-binding site in carbonic anhydrase accommodates structurally diverse inhibitors: the antiepileptic lacosamide as an example and lead molecule for novel classes of carbonic anhydrase inhibitors. *J Med Chem* 53(2):850–854
- Thurtell MJ, Wall M (2013) Idiopathic intracranial hypertension (pseudotumor cerebri): recognition, treatment, and ongoing management. *Curr Treat Options Neurol* 15(1):1–12
- Tolvanen ME et al (2012) Analysis of evolution of carbonic anhydrases IV and XV reveals a rich history of gene duplications and a new group of isozymes. *Bioorg Med Chem*
- Tschirgi RD, Frost RW, Taylor JL (1954) Inhibition of cerebrospinal fluid formation by a carbonic anhydrase inhibitor, 2-acetyl-amino-1,3,4-thiadiazole-5-sulfonamide (diamox). *Proc Soc Exp Biol Med* 87(2):373–376
- Turkmen S et al (2006) Cerebellar hypoplasia and quadrupedal locomotion in humans as a recessive trait mapping to chromosome 17p. *J Med Genet* 43(5):461–464
- Turkmen S et al (2009) CA8 mutations cause a novel syndrome characterized by ataxia and mild mental retardation with predisposition to quadrupedal gait. *PLoS Genet* 5(5):e1000487
- Vujovic M et al (2015) Thyroid hormone drives the expression of mouse carbonic anhydrase Car4 in kidney, lung and brain. *Mol Cell Endocrinol* 416:19–26
- Wall M et al (2014) The idiopathic intracranial hypertension treatment trial: clinical profile at baseline. *JAMA Neurol* 71(6):693–701
- Wall M, McDermott MP, Kiebertz KD, Corbett JJ, Feldon SE, Friedman DI, Committee et al (2014) Effect of acetazolamide on visual function in patients with idiopathic intracranial hypertension and mild visual loss: the idiopathic intracranial hypertension treatment trial. *JAMA* 311(16):1641–1651
- Whitelaw A, Kennedy CR, Brion (2001) Diuretic therapy for newborn infants with posthemorrhagic ventricular dilatation. *Cochrane Database Syst Rev* 2001(2):CD002270
- Yan J et al (2007) Effects of carbonic anhydrase VIII deficiency on cerebellar gene expression profiles in the wdl mouse. *Neurosci Lett* 413(3):196–201
- Zhuang GZ et al (2015) Carbonic anhydrase-8 regulates inflammatory pain by inhibiting the ITPR1-cytosolic free calcium pathway. *PLoS One* 10(3):e0118273

Chapter 6

Potential of Carbonic Anhydrase Inhibitors in the Treatment of Oxidative Stress and Diabetes



Zafer Gurel and Nader Sheibani

Abstract Increased oxidative stress has been recognized as a major contributing factor to various pathological conditions including diabetes and its complications. Although, several mechanisms contribute to increased oxidative stress (OxS) in diabetes, increased levels of glucose and altered metabolic activities are major contributors to production of reactive oxygen species (ROS) and OxS. The identity of the target cells and metabolic pathways involved in ROS production provide a venue for treatment of the underlying causes and mitigation of diabetes complications including diabetic retinopathy. Diabetic retinopathy affects retinal neurovasculature, and loss of retinal vascular pericytes (PC) has been recognized as one of the early targets. We have shown that retinal PC are most sensitive to high glucose conditions in culture compared with retinal vascular endothelial cells (EC) and astrocytes (AC). We have proposed that retinal PC may differ in their metabolism of glucose compared with EC. Pericytes likely prefer oxidative metabolism for energy production, especially under high glucose conditions, generating excess ROS that drives their demise. This is mediated, in part, through activation of hexose biosynthetic pathway, enhanced O-GlcNAc modification and stabilization of P53, and attenuation of the Warburg effect. In support of this hypothesis, we recently showed retinal PC, but not EC, generate more superoxide under high glucose conditions. We also

Z. Gurel · N. Sheibani (✉)

Department of Ophthalmology and Visual Sciences, School of Medicine and Public Health, University of Wisconsin, Madison, WI, USA

e-mail: nsheibanikar@wisc.edu

McPherson Eye Research Institute, School of Medicine and Public Health, University of Wisconsin, Madison, WI, USA

Z. Gurel

e-mail: zgurel@wisc.edu

N. Sheibani

Department of Cell and Regenerative Biology, School of Medicine and Public Health, University of Wisconsin, Madison, WI, USA

Department of Biomedical Engineering, School of Medicine and Public Health, University of Wisconsin, Madison, WI, USA

© Springer Nature Switzerland AG 2021

W. R. Chegwidden and N. D. Carter (eds.), *The Carbonic Anhydrases: Current and Emerging Therapeutic Targets*, Progress in Drug Research 75,

https://doi.org/10.1007/978-3-030-79511-5_6

showed inhibition of carbonic anhydrases (CA) protects PC from adverse effects of high glucose. The inhibition of CA, especially those in the mitochondria (mCA), limits the production of bicarbonate that is essential for the first step of oxidative metabolism in the mitochondria. Thus, targeting of the mCA may provide a unique opportunity for modulation of PC metabolism mitigating the development and progression of diabetic retinopathy and likely other complications of diabetes.

Keywords Mitochondrial carbonic anhydrases · Retinal pericytes · Diabetic retinopathy · Oxidative stress · Oxidative metabolism

Abbreviations

AC	Astrocytes
AGE	Advanced glycation end product
AGER	AGE receptor
CA	Carbonic anhydrases
EC	Endothelial cells
mCA	Mitochondrial CA
OxS	Oxidative stress
PC	Pericytes
RPE	Retinal pigment epithelium
ROS	Reactive oxygen species
SMC	Smooth muscle cells
STZ	Streptozotocin
8OHdG	8-Hydroxy-2'-deoxyguanosine

6.1 Introduction

Diabetes is a chronic disease which affects a large portion of the working age population worldwide. The prevalence of diabetes has significantly increased in the past couple of decades and is continuing to rise at an alarming rate (Antonetti et al. 2012; Duh et al. 2017; Solomon et al. 2017; Shin et al. 2014a). Chronic exposure to high concentrations of glucose has adverse effects on the cellular metabolic activity affecting various vascular and tissue functions (Rask-Madsen and King 2013; Aghdam and Sheibani 2013; Bahtiyar et al. 2016; Campesi et al. 2017; Moran et al. 2013). High glucose levels is a major contributing factor to the development and progression of the disease, and epidemiological studies have demonstrated control of glucose levels is most effective in improvement of diabetes adverse health effects (Agardh et al. 1997; Sun et al. 2011; The Diabetes Control and Complications Trial Research G 1993). Chronic exposure to high glucose is associated with a

variety of pathologies including diabetic retinopathy, diabetic neuropathy, diabetic nephropathy, and cardiovascular and motor neuron dysfunctions. Over the years many studies have focused on delineating the underlying mechanisms that contribute to these pathologies. These studies have identified inflammation and oxidative stress (OxS) as key early mediators of diabetes adverse pathologies (Jha et al. 2018; King 2008; Mohamed et al. 2012; Nguyen et al. 2012; Roy et al. 2013; Scott and King 2004; Su and Xiao 2015; Reyk et al. 2003; Duarte et al. 2013). How diabetes leads to inflammation and OxS in various organs has been extensively studied. We know a great deal about the potential pathways that are impacted by high glucose conditions (Aboualizadeh et al. 2017; Bae et al. 2013; Chen et al. 2007; Cogan et al. 1984; Costa and Soares 2013; Ding et al. 2017; Du et al. 2002, 2013; Dugan et al. 2013; Frey and Antonetti 2011; Ibrahim et al. 2011; Stitt et al. 2005; Tang et al. 2013; Wang et al. 2009). These include the NADPH-oxidase pathway, the hexose-biosynthetic pathway, the pentose phosphate pathway, the polyol pathway, and the advanced-glycation end product pathway, all of which contribute to redox homeostasis. Increased OxS and activation of inflammatory pathways are considered as key contributors to the development and progression of diabetes complications. Thus, identification of the key pathways and major players involved may provide suitable targets for early intervention and attenuation of disease progression. Here we will focus on the impact of diabetes on ocular redox homeostasis and development and progression of diabetic retinopathy. We will also discuss the important role of mitochondrial carbonic anhydrases (mCA) in oxidative metabolism of glucose and their potential contribution to pathogenesis of diabetic retinopathy. We propose that inhibition of mCA may provide a novel intervention mechanism for elevation of OxS in retinal vasculature as a way to protect loss and dysfunction of retinal PC and retinal neurovasculature degeneration during diabetes.

6.2 Oxidative Stress and Diabetes

The majority of cells in various tissues are equipped with different machineries to maintain cellular redox homeostasis. Generally, OxS is caused when the stress levels surpass the capacity of cellular protective mechanisms, which help to overcome this stress. As eluded to earlier, multiple pathways contribute to OxS during diabetes, and various tissues and cells utilize different means to overcome this stress. These differences in the capacity of different cells and/or tissues to overcome OxS, may in part, contribute to their selective sensitivity to adverse effects of hyperglycemia, including retinal neurovasculature and retinal vascular cells (Scott and King 2004; Reyk et al. 2003; Aboualizadeh et al. 2017; Du et al. 2013; Shah et al. 2013a; Hayden et al. 2010; Patrick et al. 2015). Hyperglycemia causes OxS in tissues whose glucose uptake is insulin independent, including the eye and brain microvascular cells (Balasubramanyam et al. 2002). Pericytes, in close contact with EC in the capillary beds of the retina (with the highest PC density of any tissue), are vital to microvessel integrity and are especially susceptible to OxS (Caldwell et al. 2005; Qaum et al.

2001). Pericyte death leads to EC dysfunction and death, thus altering production of factors essential for retinal vascular homeostasis (Aiello et al. 1995; Boeri et al. 2001; Caldwell et al. 2003; Jousseaume et al. 2004; Kowluru and Odenbach 2004a; Chan et al. 2010). Rupture-prone microaneurysms and acellular capillaries (Hammes et al. 2011; Giacco and Brownlee 2010) then arise leading to retinal ischemia, growth of leaky new blood vessels toward the vitreous, and retinal detachment and vision loss.

Diabetes is associated with chronic hyperglycemia and diabetic retinopathy (DR), a leading cause of blindness in the working age population (Bhavsar 2006). The disease affects PC vital for stabilization and function of retinal blood vessels as well as for proliferation and differentiation of the single layer of EC that line the vessels (Cogan et al. 1961; Haefliger et al. 1994; Kuwabara et al. 1961). Pericyte loss, an early event in DR (Kowluru and Abbas 2003; Li et al. 1999; Miller et al. 2006; Mizutani et al. 1996; Podesta et al. 2000; Zhang et al. 2008), leads to inflammation, vascular dysfunction and degeneration, and altered production of regulatory factors essential for retinal vascular homeostasis (Aiello et al. 1995; Boeri et al. 2001; Caldwell et al. 2003; Jousseaume et al. 2004; Chan et al. 2010; Kowluru and Odenbach 2004b). This enables fragile, rupture-prone new capillaries to grow toward the vitreous. Left untreated, the result is retinal detachment and vision loss. The key mechanism for PC glucose sensitivity in early diabetes remains elusive but may be linked to respiration (mitochondrial oxidative metabolism of glucose), their preferential source of energetics and OxS.

The role retinal PC loss has in DR is well documented (Hammes et al. 2011; Miller et al. 2006; Mizutani et al. 1996). Pericytes are sensitive to hyperglycemia-induced OxS, which is likely caused by excess superoxide generated during respiration (Du et al. 2003; Nishikawa et al. 2000; Wallace 1992) (Fig. 6.1). Superoxide is the precursor to all ROS (Turrens 2003). Kowluru et al. (2006) reported that overexpression of mitochondrial superoxide dismutase, an enzyme that neutralizes superoxide, prevents diabetic retinal damage. ROS produced during respiration triggers other pathogenic pathways, such as the polyol pathway (Das Evcimen et al. 2004; Nishimura et al. 1997), advanced glycation end product (AGE) formation (Du et al. 2000; Hammes et al. 1991; Nakamura et al. 1997), protein kinase C activation (Koya and King 1998; Xia et al. 1994) and the hexosamine pathway (Nerlich et al. 1998; Schleicher and Weigert 2000), all of which propagate even more ROS and OxS. Nishikawa et al. (Nishikawa et al. 2000) reported that normalized superoxide blocked these three pathways of hyperglycemic damage. Du et al. (2000) showed that superoxide overproduction activates the hexosamine pathway. We recently demonstrated this pathway is highly activated in PC, but not EC and AC, under high glucose conditions, and promotes *O*-GlcNAc modification, stabilization of P53 protein, and likely the death of retinal PC (Gurel et al. 2013; Gurcel et al. 2008).

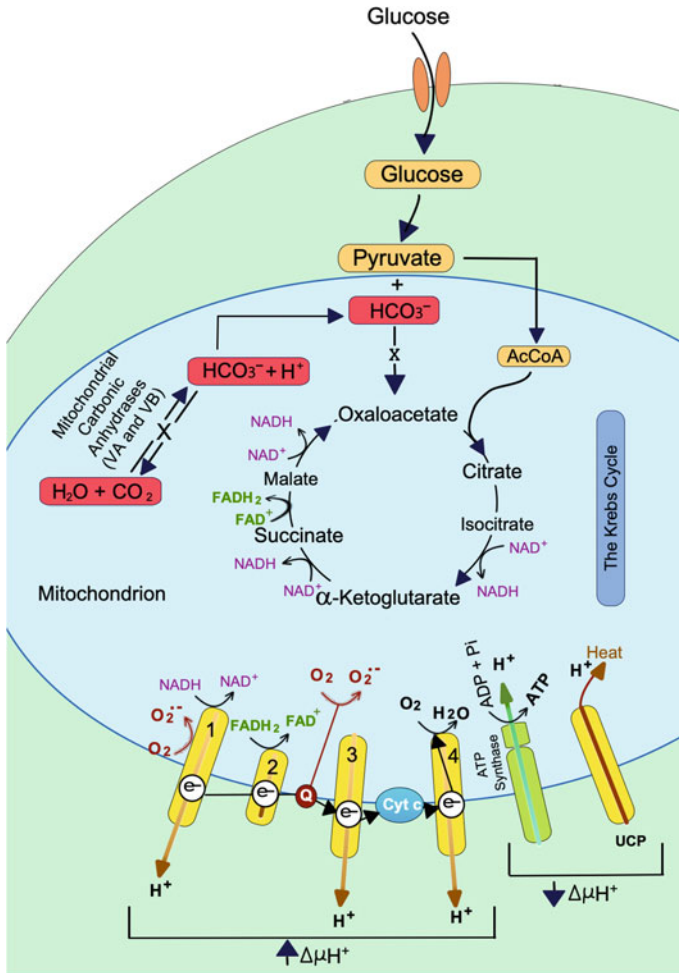


Fig. 6.1 Role of mitochondrial carbonic anhydrases (mCA) in oxidative metabolism of glucose and superoxide ($O_2^{\cdot -}$) production

6.3 Retinal Pericytes and Metabolic Activity

Our lab has developed a novel method for culturing vascular cells, including EC, PC, and AC from mouse retina (Scheef et al. 2005, 2009; Su et al. 2003). Using these cells, we have determined the impact of high glucose on various cellular functions. High glucose stimulated EC migration (Huang and Sheibani 2008), and increased OxS and inflammatory cytokines in AC, impacting their proliferation, adhesion and migration (Shin et al. 2014b). High glucose induced significant apoptosis in PC, but not in EC or AC (Huang and Sheibani 2008; Shin et al. 2014b, c). This finding is supported by the fact that EC have a relatively low mitochondrial content (Groschner

et al. 2012) and rely primarily on glycolysis with in vitro glycolysis rates comparable to or even greater than cancer cells, and exceeding glucose and fatty acid flux by >200-fold (Dagher et al. 2001; Bock et al. 2013; Ghesquiere et al. 2014; Mertens et al. 1990). The advantages of glycolysis to EC include lower oxidative phosphorylation-generated ROS, maximum preservation of oxygen for transfer to perivascular supporting cells (SMC/PC), adaptation of EC to the hypoxic surroundings they will grow into, and production of lactate as a proangiogenic signaling molecule with free radical scavenging and anti-oxidant activity (Groussard et al. 2000). However, whether glycolysis is a predominant bioenergetics pathway for retinal EC needed further confirmation.

The enhanced pro-migratory activity of retinal EC in high glucose (Huang and Sheibani 2008) is consistent with glycolysis as their preferred bioenergetics (Eelen et al. 2013). This is further confirmed by gene expression profile of glucose metabolizing enzymes in these cells under various glucose conditions (our unpublished data). In contrast little is known about the bioenergetics pathway of SMC/PC. However, clear metabolic differences between EC and SMC/PC in the brain have been demonstrated (Spatz et al. 1986). Our preliminary investigations indicate that retinal EC and PC possess a distinct mechanism for controlling glucose uptake and perhaps its metabolism. Thus, elucidating retinal microvascular cell metabolic preferences is not only important for understanding normal vascular function but also for comprehending vascular diseases such as DR.

We have detected that glucose uptake and phosphorylation by PC increases under higher glucose conditions. However, EC, AC and retinal pigment epithelial (RPE) cells had tighter control of glucose uptake and phosphorylation under high glucose conditions. These results are consistent with enhanced glucose transport reported in bovine retinal PC compared with EC (Mandarino et al. 1994), and attenuation of PC migration and increased apoptosis under high glucose conditions (Gurel et al. 2013, 2014). Potential differences in glucose uptake and metabolism have been examined in SMC/PC and EC (Spatz et al. 1986; Betz et al. 1983; Kaiser et al. 1993; Li et al. 1985). These studies have defined “facilitative-diffusion mechanisms” for glucose transport in endothelial and perivascular supporting cells, including retinal EC and PC (Betz et al. 1983; Li et al. 1985). Pericytes and SMC have about a 3- to fivefold greater glucose transport than EC (Kaiser et al. 1993; Li et al. 1985). In addition, EC have more lactate and intracellular glucose (Mandarino et al. 1994; Kaiser et al. 1993). Glucose transport differences were attributed to changes in expression of glucose transporters, mainly Glut 1, in these cells (Mandarino et al. 1994). Our preliminary results are consistent with increased transport of glucose and phosphorylation in PC and different metabolic pathways used by EC compared to PC. However, no significant changes were observed in the expression of various glucose transport proteins in these cells. We propose that preferential glucose transport and respiration is responsible for increased OxS and loss of retinal PC under high glucose conditions. Our recent unpublished observations that EC have higher levels of citrate and succinate compared to PC, which further increases in high glucose conditions, give credence to this hypothesis. The levels of succinate decreased in PC under high glucose conditions.

The increased succinate levels in EC is consistent with increased levels of citrate and its conversion to itaconic acid, a blocker of mitochondrial complex II, resulting in accumulation of succinate and decreased respiration (Sapieha et al. 2008). Succinate acting through its receptor GPR91 enhances Hif-1 α expression promoting PKM2 activity and glycolysis driving angiogenesis (Corcoran and O'Neill 2016). Gene expression analyses with an RT² ProfilerTM PCR Array Mouse Glucose Metabolism, also showed upregulation of genes involved in glycolysis, in retinal EC exposed to high glucose conditions (our unpublished data). For example, the expression of pyruvate dehydrogenase kinase isozyme 4 (Pdk4, a major suppressor of mitochondrial activity) increased by twofold. On the other hand, the expression of genes that promote pyruvate generation and its utilization in TCA cycle were significantly upregulated in PC under high glucose conditions. There was a 21-, 5-, 4-, and 2.5-fold increase in Glucose-6-Phosphatase catalytic subunit (G6pc), Phosphoribosyl pyrophosphate synthetase 1-Like 1 (Prps1i1), Phosphoglycerate kinase 2 (Pgk2), and Phosphorylase b kinase gamma catalytic chain 1 (Phkg1), respectively. Also, a twofold increase was observed both in Fructose-Bisphosphatase 1 (Fbp1) and Hexokinase 3 (Hk3) gene expression.

Hyperglycemia results in higher glucose levels in tissues whose glucose uptake is insulin independent such as the brain, eye, and kidney (Balasubramanyam et al. 2002), which could not down regulate glucose transport into the cells in the face of chronic high glucose in the surrounding medium (Kaiser et al. 1993). Increased respiration has been implicated in hyperglycemia-induced OxS (Brownlee 2001, 2005), mitochondrial dysfunction, and mitophagy (Singh et al. 2017; Devi et al. 2013). However, actual respiration changes were not reported until we showed that PC challenged with high glucose exhibit significant increases in respiration and mitochondrial ROS production (Shah et al. 2013a). We also showed OxS and apoptosis in PC in response to high glucose (Shah et al. 2013b). Thus, it is important to determine how altered respiration rates affect ROS, OxS, mitophagy flux, and apoptosis in retinal vascular cells. Our published results strongly suggest that these approaches will provide a new therapeutic target for tackling the adverse effects of diabetes on retinal vasculature. These studies can lead to projects with drug developers, clinical endocrinologists and ophthalmologists, shifting the paradigm of treating diabetic complications in the retina and possibly in other tissues such as brain and kidney.

6.4 Metabolic Activity, Oxidative Stress, and Diabetic Retinopathy

Although mitochondria play an important role in OxS associated with diabetes the target cells involved remain unknown. Previous studies have shown that OxS, resulting from hyperglycemia, contributes to the early retinal PC dysfunction during diabetes (Hammes et al. 2002; Ejaz et al. 2008) and initiation of neuroinflammation through MCP-1 production (Kowluru et al. 2010). We showed that these adverse

effects of high glucose on PC were attenuated by topiramate treatment, a sulfamate substituted monosaccharide, which inhibits carbonic anhydrases (CA). We proposed that superoxide production is likely impacted by CA expressed in the mitochondria (mCA) (Shah et al. 2000).

Glucose is metabolized to pyruvate by phosphorylation of phosphoenolpyruvate in the last step of glycolysis, which is catalyzed by pyruvate kinase (PK), a multi-subunit enzyme that exists in several isoforms (Mazurek 2011). The PKM2 isoform predominantly expressed in muscle is also expressed in the retina (Morohoshi et al. 2012), and its activity depends on its tetramerization (Lincet and Icard 2015). PK is regulated by phosphofructokinase (PFK) and its phosphorylation status, and was recently shown to be a substrate of protein tyrosine phosphatase 1B (PTP1B) (Bettaieb et al. 2013), consistent with a role of PTP1B in obesity and diabetes (Panzhinskiy et al. 2013). The resulting pyruvate then enters the mitochondria, where it is metabolized to acetyl CoA and oxaloacetate. The carboxylation of pyruvate to oxaloacetate requires bicarbonate (HCO_3^-), which is provided by mCA by catalyzing the reversible hydration of carbon dioxide. HCO_3^- must be produced in mitochondria and cannot be imported from the cytosol, as mitochondrial membranes are impermeant to HCO_3^- . Oxaloacetate condenses with acetyl CoA to yield citrate. Citrate is oxidatively decarboxylated to succinate via α -ketoglutarate. Finally, oxaloacetate is regenerated from succinate to complete the cycle (Fig. 6.1).

The elevated succinate level could promote angiogenesis in hypoxia and ischemia through interaction with its receptor GPR91, expressed on retinal ganglion (Sapieha et al. 2008) and pigment epithelial cells (Favret et al. 2013). In addition, alterations in succinate levels during diabetes may contribute to the development and progression of DR perhaps through its interaction with GPR91 (Li et al. 2014). Thus, a careful temporal evaluation of changes in succinate levels with diabetes, and identification of cellular targets is essential.

The electron donors, NADH and FADH_2 , generated in the Krebs cycle, enter the electron transport chain reaction where ATP is generated, and superoxide is a byproduct. Small fluctuations in the steady state concentration of superoxide may actually play a role in intracellular signaling (Droge 2002). Uncontrolled increases lead to free radical mediated chain reactions, which indiscriminately target proteins (Stadtman and Levine 2000), lipids (Rubbo et al. 1994), polysaccharides (Kaur and Halliwell 1994), and DNA (LeDoux et al. 1999; Richter et al. 1988). In diabetes, excess glucose in tissues whose glucose uptake is insulin independent such as retina (Balasubramanyam et al. 2002) leads to excess superoxide. The ROS triggered by superoxide cause oxidative inactivation of $-\text{SH}$ containing enzymes such as glyceraldehyde 3-phosphate dehydrogenase (GAPDH) and PK, thus compromising glycolysis, a major bioenergetic pathway in the retina (Hegde et al. 2010).

We proposed that mCA inhibition, by virtue of its ability to reduce HCO_3^- , could slow DR onset and progression by three mechanisms: reducing superoxide production, altering Krebs cycle intermediate levels such as succinate with important role in DR, and increasing pyruvate. Pyruvate inhibits oxidative inactivation of GAPDH and PK by scavenging ROS. In addition, pyruvate provides NAD^+ , a cofactor for GAPDH. NAD^+ is produced during reduction of pyruvate to lactate. The published

results showed that inhibiting CA with topiramate prevents OxS build up and PC loss in the diabetic mouse (Price et al. 2012, 2015). Our unpublished studies show that germline deletion of mCA reduces retinal OxS and topiramate prevents acellular capillary formation in diabetic mouse retina. Topiramate is a sulfamate substituted monosaccharide with impressive safety record (Leniger et al. 2004; Nishimori et al. 2005) in clinical use for other diseases (Deutsch et al. 2003; Liang et al. 2005; Roy Chengappa et al. 2001) and can be tested for prevention of DR. This is further encouraged with the low dose of topiramate needed (Price et al. 2015) and lack of potential systemic effect if given topically. No published reports explain how mCA inhibition affects PK isoforms or succinate and pyruvate pathways. Thus, how diabetes and mCA inhibition affect these pathways are of significant importance.

6.5 Carbonic Anhydrases

The carbonic anhydrases (CA) are a family of zinc metalloenzymes that catalyzes the hydration of CO₂ and dehydration of bicarbonate (Sly and Hu 1995) in the following reaction:

$\text{CO}_2 + \text{H}_2\text{O} \rightleftharpoons \text{H}^+ + \text{HCO}_3^-$. Twelve enzymatically active CA isozymes have been identified, including five cytosolic forms (CA I, CA II, CA III, CA VII and CA XIII), five membrane bound isozymes (CA IV, CA IX, CA XII, CA XIV and CA XV), two mitochondrial forms (CA VA and CA VB), and a secreted CA isozyme (CA VI) (Sly and Hu 1995; Hewett-Emmett and Tashian 1996; Carter et al. 1990; Tureci et al. 1998; Mori et al. 1999). These isozymes differ widely in tissue specification, enzymatic kinetics, subcellular localization, participated pathways and in susceptibility to varied inhibitors (Hewett-Emmett and Tashian 1996; Carter et al. 1990; Tureci et al. 1998; Mori et al. 1999; Karler and Woodbury 1960). Three catalytically not active forms are also known, which are denominated CA-related proteins (CARP), CARP VIII, CARP X, and CARP XI (Hewett-Emmett and Tashian 1996). It was reported in the 1960s that mitochondria contain CA activity, which is classified as a separate isozyme, CA V (Karler and Woodbury 1960; Williams 1965; Chappell and Crofts 1965). It was later revealed that mCA are encoded by two separate genes, CA VA and CA VB (Nagao et al. 1993; Fujikawa-Adachi et al. 1999).

The human orthologue for the CA VA has been mapped to chromosome 16q24 (Nagao et al. 1995), while CA VB was mapped to chromosome Xp22.1 (Fujikawa-Adachi et al. 1999). The genes in mice are referred to as Car5A and Car5B and in humans as CA5A and CA5B by The Human Genome Organization Nomenclature Committee. Further studies reported that CA VB are much more highly conserved between mouse and human (95% identity) than the CA domains of mouse and human CA VA (78% identity) (Shah et al. 2000). Western blot analyses indicated that CA VA and CA VB represented in close molecular weights, 29 and 31 kDa, respectively. However, their tissue expressions are different, CA VA is only detectable in liver and skeletal muscle, whereas CA VB expression is detected in a wide range of tissues including heart, liver, lung, kidney, testes, muscle, and in most other tissues (Shah

et al. 2000). These differences in tissue-specific expression suggest that these two isoforms may replace each other's in different tissues. Furthermore, the difference in sequence conservation between CA VB and CA VA may indicate the functional variations in between these two isoforms.

CO_2 and HCO_3^- cycle plays an important role in mitochondrial metabolism and their regulation is crucial for mitochondrial functions (Dodgson et al. 1980). The enzymes of the tricarboxylic acid cycle that produce CO_2 are located within the mitochondrial matrix (Karler and Woodbury 1960), as are those enzymes that fix CO_2 in the pathways of gluconeogenesis and urea production. CO_2 freely penetrates into the mitochondria; however, mCA are required to convert CO_2 to HCO_3^- to support the metabolic needs for essential pathways. The synthesis of carbamoyl phosphate is the first irreversible step of ureagenesis. This reaction is catalyzed by carbamoyl phosphate synthetase-I, and it consumes HCO_3^- rather than CO_2 (Lusty 1978). Furthermore, carbamoyl phosphate is used as a co-substrate by ornithine transcarbamylase in the synthesis of citrulline, which is the first intermediate of the urea cycle (Cohen 1981). The use of CA inhibitors (e.g., acetazolamide) significantly reduced the synthesis of citrulline in isolated mitochondria (Dodgson et al. 1983) and hepatocytes (Dodgson and Forster 1986a). This confirmed that liver mCA plays its physiological role in urea synthesis by supplying the HCO_3^- .

Besides ureagenesis, mCA are involved in gluconeogenesis. The mammalian liver is the primary site of gluconeogenesis, and the carboxylation of pyruvate occurs exclusively in the mitochondria (Winter et al. 1982). Pyruvate carboxylase mediates the first reaction in gluconeogenesis from pyruvate, and HCO_3^- is required for this step (Dodgson and Forster 1986b). The treatment of hepatocytes with a membrane permeant sulfonamide, ethoxzolamide resulted in a reduction in the rate of pyruvate carboxylation in intact mitochondria (Dodgson and Forster 1986b). As such, when there is a requirement for bicarbonate as substrate, mCA are functionally important for gluconeogenesis in the male guinea pig liver (Dodgson and Forster 1986b). The importance of mCA in gluconeogenesis is supported by studies on other mammals, such as mouse (Shah et al. 2013c) and rat tissues (Dodgson and Contino 1988). It has been shown that ethoxzolamide inhibits lipogenesis from pyruvate, similar to gluconeogenesis (Lynch et al. 1995). The effects of sulfonamides on hepatic de novo lipogenesis was initially reported as a result of the regulation of acetyl CoA carboxylase. However, later reported studies suggested that pyruvate carboxylase may be responsible for these effects (Lynch et al. 1995). A recent study indicated that ethoxzolamide and another sulfonamide, trifluoromethanesulfonamide reduced de novo lipogenesis in 3T3-L1 adipocytes (Hazen et al. 1996). Furthermore, citrate concentration was reduced in ethoxzolamide treated adipocytes, which was possibly caused by a decrease in the export of mitochondrial citrate to the cytosol. This reduction of mitochondrial citrate appeared to be enough to cause the decrease in de novo lipogenesis (Hazen et al. 1996). This is consistent with the hypothesis that sulfonamide CA inhibition of de novo lipogenesis is through a decrease in substrate (i.e., bicarbonate) availability to pyruvate carboxylase, rather than acetyl CoA carboxylase inhibition alone causing an increase in citrate levels (Hazen et al. 1996).

Along with studies that used CA inhibitors, Shah and associates performed targeted disruption of the murine CA genes, Car5A and Car5B (Shah et al. 2013c). In this study, Car5A null mice were reported as poor breeders, with smaller litters as compared to wild-type littermates. However, their breeding normalized when their water was supplemented with sodium–potassium citrate. Their blood ammonia concentrations were significantly higher, yet their fasting blood sugars were normal (Shah et al. 2013c). Car5B null mice had normal growth, normal blood ammonia and fasting blood sugars levels. Car5A/B double-knockout (DKO) mice showed more severe growth problems and hyperammonemia than Car5A null mice. Supplementation with sodium–potassium water was not enough to normalize breeding. In addition, DKO mice survival rate and fasting blood glucose levels were markedly lower than wild type mice. This study indicated that both Car5A and Car5B contribute to ureagenesis and gluconeogenesis. Car5A plays a predominant role in ammonia detoxification, and while Car5B plays a role in both ureagenesis and gluconeogenesis, its role became evident only in a Car5A null background (Shah et al. 2013c).

Although CA are traditionally considered to be transport enzymes, especially mCA are involved in several biosynthetic pathways. Studies carried out with CA inhibitors, or with CA mutations, indicate that mCA are important for providing HCO_3^- to the initial steps in urea, fatty acid and glucose synthesis. Thus, modulation of their activity might have various therapeutic potential, such as reduced OxS and obesity.

6.6 Mitochondrial Carbonic Anhydrases and Oxidative Stress

Oxidative stress in diabetes is generated by excess ROS (Nishikawa et al. 2000; Du et al. 2000), which are normal byproducts of electron transport chain (ETC) reactions in the reduction of glucose to H_2O and CO_2 in the production of ATP (Chen et al. 2003; Liu et al. 2002). In diabetes, more glucose floods to the Krebs cycle, especially in insulin-insensitive tissues (Liu et al. 2002), thus increasing the rate of production of electron donors (reduced flavin adenine dinucleotide and reduced nicotinamide adenine dinucleotide). These electron donors create a proton gradient across the inner mitochondrial membrane during ETC reactions. Under higher electrochemical potential difference, the life time of superoxide-generating electron-transport intermediates are prolonged (Brownlee 2001). This causes a marked increase in the production of ROS, superoxide dismutase, and hydroxyl radicals and when it surpasses the threshold value generates OxS in tissues. Hyperglycemia induced OxS and mitochondrial dysfunction are involved in the pathogenesis of various complication of diabetes (Jha et al. 2018; Wu et al. 2018). Higher mitochondrial superoxide level has been detected in human aortic EC under high glucose conditions (Brownlee 2005). Mitochondrial CA regulate the oxidative metabolism of glucose, and thus, play important roles in the generation of ROS and OxS.

Recent studies indicated that using mCA inhibitors may decrease OxS in various tissues. The application of topiramate, a potent mCA inhibitor, prevented the OxS in the brain of diabetic mice (Price et al. 2012). Same study also reported a significant decline in cerebral PC numbers, at 12 weeks of diabetes that was also rescued by topiramate treatment (Price et al. 2012). This study has provided the first evidence that inhibition of CA activity reduces diabetes-induced OxS in the mouse brain and rescues cerebral PC loss. Similar results were obtained in an in vitro study using immortalized cerebral PC cultures (Shah et al. 2013b). This study indicated that both high glucose-induced OxS and apoptosis of PC could be rescued by pharmacological inhibition of CA (Shah et al. 2013b). Furthermore, the overexpression of mCA VA significantly increased intracellular ROS and apoptosis of PC (Patrick et al. 2015). In contrast, the genetic knockdown of mCA VA significantly reduced high glucose-induced ROS and apoptosis in PC (Price and Sheibani 1863).

6.7 Carbonic Anhydrase Inhibitors and Prevention of Diabetic Retinopathy

Currently available CA inhibitors are grouped under two main classes: the metal-chelating anions and the unsubstituted sulfonamides and their bioisosteres. These inhibitors target the Zn^{2+} ion, preventing its interaction with enzymes by substituting or changing its coordination (Boddy et al. 1989). Sulfonamides, which are the most important CA inhibitors, such as the clinically used derivatives acetazolamide, methazolamide, ethoxzolamide, dichlorophenamide, dorzolamide and brinzolamide, bind to Zn^{2+} ion in the deprotonated state and form a slightly distorted tetrahedral adduct (Supuran and Scozzafava 2007). Carbonic anhydrase inhibitors are widely used for different clinical applications. They were first used as diuretics and are currently as anti-epileptic, anti-obesity, anticancer and antiglaucoma agents. The diversity of CA isoforms, their tissue diffusion, and their different biological functions have created some hurdles to overcome in the pursuit of the use of CA inhibitors as therapeutics. Conversely, these specific attributes of the CA isoforms can also provide extensive opportunities to create more specific drug-design approaches.

Several studies have provided evidence that CA inhibitors may be effective against obesity (Picard et al. 2000; Gadde et al. 2003,2011; Allison et al. 2012). Topiramate and zonisamide are potent anticonvulsant agents and are currently in use as antiepileptic drugs (Ben-Menachem 1996; Kellett et al. 1999; Schmidt et al. 1993). Some studies indicate that topiramate and zonisamide also cause loss of body weight in obese animals (Picard et al. 2000) and patients (Supuran 2008; Scozzafava et al. 2013) via the disruption of the de novo lipogenesis. Topiramate inhibits several CA isozymes, such as CA II, VA, VB, VI, VII, XII and XIII. The mechanisms of CA inhibitor-induced weight loss are not well defined. However, the inhibition of CA VA and VB may play an important role due to the involvement of mCA VA and VB in various metabolic pathways, such as lipogenesis and gluconeogenesis (described

above). Indeed, molecular modeling and structural studies have indicated that topiramate and zonisamide have strong affinity for mCA VA and VB (Ki's for mCA VA and VB are of 63 and 30 nM, respectively) (Nishimori et al. 2005; Vitale et al. 2007; Dodgson et al. 2000). Another study suggested that the inhibition of mCA cause weight loss due to a reduction in the rate of pyruvate that passes through the pathway, and disruption in glycolysis, allowing for fatty acid oxidation to become the dominant pathway (Arechederra et al. 2013).

Indeed, mCA regulate the metabolism of pyruvate by accelerating the rate at which pyruvate carboxylase can convert pyruvate and bicarbonate into oxaloacetate (Jitrapakdee et al. 2008). The pyruvate is derived from glucose through glycolysis, and this pathway is in equilibrium with the fatty acid pathway. Therefore, mCA inhibitors may shift the flux of mitochondrial metabolism toward using fatty acids and slow the metabolism of pyruvate (Arechederra et al. 2013).

Recent studies indicate that the inhibition of mCA can be effective against diabetes complications, such as diabetic retinopathy. Initial studies reported that the use of CA inhibitors, such as acetazolamide is effective in treatment of macular edema when administered systemically (Gelissen et al. 1990). During the past two decades, emerging evidence has suggested that CA inhibitors may hold promise in the treatment of diabetic retinopathy (Weiwei and Hu 2009). A series of study by Shah and associates indicated that genetic knockout (Shah et al. 2013c) or pharmacological inhibition (Shah et al. 2013b; Price et al. 2012) of CA were able to reduce respiration, ROS, and PC apoptosis in brain. As one of the most metabolically active tissues in the body, the brain is notably vulnerable to OxS. Therefore, reducing OxS may protect the brain from the damage caused by hyperglycemia. One of the first reports about the effect of CA inhibitors against diabetes was from streptozotocin (STZ)-induced diabetic mouse model (Price et al. 2012). STZ treated mice have progressive hyperglycemia, OxS and decreased PC to EC ratio in the mouse brain, which can lead to deterioration of the blood-brain barrier (BBB). Price et al. reported that the inhibition of CA with topiramate prevented the OxS in the brain and restored normal cerebral PC to EC ratio (Price et al. 2012). Shah and Sheibani (2013) later showed that high glucose-induced intracellular OxS can cause brain PC death by apoptosis, and treatment with pharmacological inhibition of CA significantly reduced PC apoptosis (Shah et al. 2013b).

Increased ROS production is a major cause of OxS in diabetes. Cerebral PC generate ROS by oxidative metabolism of glucose (respiration) under high glucose conditions (Shah et al. 2013a). The rate of respiration and ROS production are reversed upon pharmacological inhibition of CA in high glucose challenged cerebral PC (Shah et al. 2013a). Furthermore, the overexpression of mCA VA significantly increased intracellular ROS and apoptosis of PC. Both ROS and the percent of apoptotic PC were significantly reduced upon inhibition of mCA VA (Patrick et al. 2015). Similarly, the genetic knockdown of mCA VA significantly reduced high glucose-induced ROS and apoptosis in brain PC (Price and Sheibani 1863). Animal studies supported in vitro studies; morphologic and permeability abnormalities detected in BBB of STZ-induced diabetic CD-1 mice. The CA inhibitor topiramate was able to prevent STZ-induced BBB damage in certain regions (Salameh et al. 2016). These

data demonstrated that mCA are important in the regulation of high glucose-induced ROS production and cerebral PC death, with CA inhibitors affording protection of cerebral PC during diabetes.

Besides cerebral PC, retinal PC are also highly sensitive to hyperglycemia, and loss of retinal PC are recognized as one of the earliest signs of DR (Cogan et al. 1961; Hammes et al. 2002). Retinal PC, but not retinal EC or AC, undergo significant apoptosis in response to chronic exposure to high glucose conditions (Gurel et al. 2014). High-glucose induced OxS detected in pig retinal PC by increased 8-OHdG (Kubo et al. 2009) and in bovine retinal PC by advanced glycation end products (AGEs) and receptor of AGE (RAGE) (Yamagishi et al. 1995). Recently, a time-lapse microscopy study by our group demonstrated that the rate of mitochondrial ROS production in mouse retinal PC was significantly higher under high glucose condition, whereas this rate remained unchanged in retinal EC. In this study, we used MitoSOX™ to indicate the production of superoxide in mitochondria. Therefore, this study provided direct evidence on mitochondria-related ROS generation in retinal PC under high glucose conditions (Ghanian et al. 2018). Furthermore, various studies reported that diabetes or high glucose-driven PC loss may be prevented by anti-oxidative agents such as the treatment with nicanartine (Hammes et al. 1997), Trolox (Ansari et al. 1998), pigment epithelium-derived factor (Yamagishi et al. 2002; Sheikpranbabu et al. 2011) and resveratrol (Kim et al. 2012).

Retinal PC have different metabolic dynamics than their companion, retinal EC. Under high glucose conditions, glucose uptake increased significantly in retinal PC, however retinal EC demonstrated better control on glucose flow into the cell (our unpublished data). Thus, elevated glucose uptake and increased oxidative phosphorylation may explain increased ROS production and retinal PC loss during diabetes. Interestingly, mouse retinal PC had higher Car5a expression than other cells, including retinal ChEC, REC, RAC and RPE. For Car5b, both retinal PC and RAC had high expression compared to ChEC, REC, and RPE cells (Fig. 6.2). Currently, there is a lack of studies that indicate a protective effect of CA inhibitors on retinal PC under diabetic conditions. However, we propose that CA inhibitors could reduce OxS in retinal PC as occurs in cerebral PC. Thus, CA inhibitors have great potential for use against DR through anti-obesity and protective effects in cerebral and retinal PC.

6.8 Conclusions

Attenuation of oxidative metabolism by CA inhibitors provide protection in retinal PC under high glucose conditions. Additional studies of current CA inhibitors and discovery of new and more specific mCA inhibitors will be important in prevention and treatment of diabetic retinopathy. Topiramate is one of the most investigated agents among CA inhibitors. Zonisamide has similar effects, and it is a more potent inhibitor of CA VA than CA II (Vitale et al. 2007; Simone et al. 2005). Furthermore, investigators have reported other CA inhibitors that are effective on mCA.

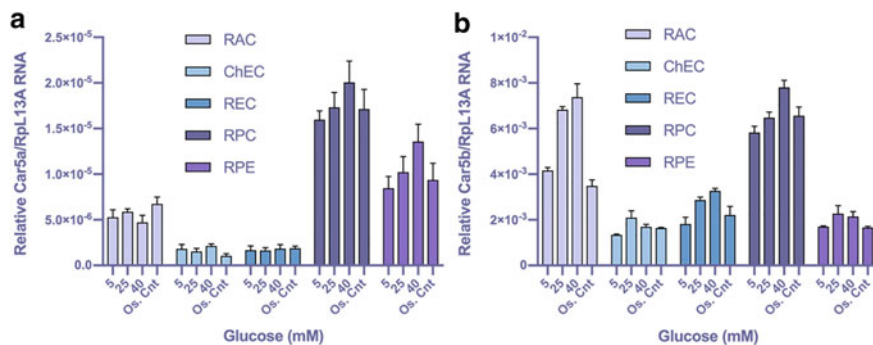


Fig. 6.2 RNA expression of Car5a and Car5b in retinal cells. Car5a (a) and Car5b (b) expression levels were determined by qPCR for each cell type grown under D-glucose (5, 25 or 40 mM) conditions for five days as well as an osmotic control (5 mM D-Glucose plus 35 mM L-Glucose; “Os. Cnt; Osmotic Control”). RNA expression for each gene was normalized to Rpl13A. Cell types assessed included Retinal astrocyte (RAC), Choroidal endothelial cells (ChEC), Retinal endothelial cells (REC), Retinal pericytes (RPC), and Retinal pigment epithelial (RPE) cells. The qPCRs were performed with three biological replicates and in triplicates

Some of the investigated sulfonamides, such as the ureido benzenesulfonamides and the acylated sulfanilamides showed higher affinity for CA V than for the other isozymes, CA II included (Vullo et al. 2004). (*N*-(2-fluoro-4-sulfamoyl-phenyl)-2-(2-thienyl)acetamide (II) and *N*-(2-bromo-4-sulfamoyl-phenyl)-2-phenyl-acetamide (IV)) compounds are reported as highly selective for CA VA and CA VB over CA I and CA II (Guzel et al. 2009). Investigation of 4-(4-phenyltriazole-1-yl)-benzene sulfonamide derivatives (Poulsen et al. 2008), series of aromatic/heterocyclic sulfonamides (Winum et al. 2007) and a small series of 2-substituted-1,3,4-thiadiazole-5-sulfamides (Smaine et al. 2008) indicated that several of them from each group are selectivity effective for mCA VA and VB. Another report indicated that sulpiride and ethoxzolamide were almost two times more effective inhibitors of the mCA VB over the cytosolic isozymes (Nishimori et al. 2005). Moreover, testing a series of (*R*)-/(*S*)-10-camphorsulfonyl-substituted aromatic/heterocyclic sulfonamides demonstrated that all tested compounds are selective for mCA VA and VB over CA I, CA II with the best being thiadiazol sulfonamide X (Maresca and Supuran 2011).

Inhibiting mCA deprives the mitochondria of bicarbonate, thus reducing the respiration rate, OxS, PC loss, and retinal vascular degeneration. A key question that still needs further exploration is whether PC respiration rate is key to retinal microvasculature disruption and dysfunction in early diabetes. These findings would also establish mCA as possible therapeutic targets whose inhibition can delay the onset and/or slow down the progression of DR and neuroinflammation. Topiramate is in clinical use for other diseases, which makes the translational research potential of this work a distinct possibility. In addition, confirmation that topiramate protects the retina would spur novel studies to determine whether it protects from other microvascular complications of diabetes, including neuropathy and nephropathy. Therefore,

the selective inhibition of mCA may lead to the development of novel pharmacological applications for prevention and treatment of diabetes complications with limited potential systemic adverse effects.

Acknowledgements The work in NS lab is supported by an award from RPB to the Department of Ophthalmology and Visual Sciences, Retina Research Foundation, P30 EY016665, P30 CA014520, EPA 83573701, EY022883, and EY026078. NS is a recipient of RPB Stein Innovation Award. The authors wish to thank Dr. Gul Shah, Dr. Mahsa Ranji, and Dr. Christine Sorenson for their collaborations in a number of studies cited here and their long interest in carbonic anhydrases and oxidative stress in neuroinflammatory dysfunctions.

References

- Aboulzadeh E, Ranji M, Sorenson CM, Sepehr R, Sheibani N, Hirschmugl CJ (2017) Retinal oxidative stress at the onset of diabetes determined by synchrotron FTIR widefield imaging: towards diabetes pathogenesis. *Analyst* 142(7):1061–1072. <https://doi.org/10.1039/c6an02603f>
- Agardh CD, Agardh E, Torffvit O (1997) The association between retinopathy, nephropathy, cardiovascular disease and long-term metabolic control in type 1 diabetes mellitus: a 5 year follow-up study of 442 adult patients in routine care. *Diabetes Res Clin Pract* 35(2–3):113
- Aghdam SY, Sheibani N (2013) The ubiquitin-proteasome system and microvascular complications of diabetes. *J Ophthalmic vis Res* 8(3):244–256
- Aiello LP, Pierce EA, Foley ED, Takagi H, Chen H, Riddle L, Ferrara N, King GL, Smith LE (1995) Suppression of retinal neovascularization in vivo by inhibition of vascular endothelial growth factor (VEGF) using soluble VEGF-receptor chimeric proteins. *Proc Natl Acad Sci U S A* 92(23):10457–10461
- Allison DB, Gadde KM, Garvey WT, Peterson CA, Schwiers ML, Najarian T, Tam PY, Troupin B, Day WW (2012) Controlled-release phentermine/topiramate in severely obese adults: a randomized controlled trial (EQUIP). *Obesity (silver Spring)* 20(2):330–342. <https://doi.org/10.1038/oby.2011.330>
- Ansari NH, Zhang W, Fulep E, Mansour A (1998) Prevention of pericyte loss by trolox in diabetic rat retina. *J Toxicol Environ Health A* 54(6):467–475
- Antonetti DA, Klein R, Gardner TW (2012) Diabetic retinopathy. *N Engl J Med* 366(13):1227–1239. <https://doi.org/10.1056/NEJMra1005073>
- Archederra RL, Waheed A, Sly WS, Supuran CT, Minter SD (2013) Effect of sulfonamides as carbonic anhydrase VA and VB inhibitors on mitochondrial metabolic energy conversion. *Bioorg Med Chem* 21(6):1544–1548. <https://doi.org/10.1016/j.bmc.2012.06.053>
- Bae ON, Wang JM, Baek SH, Wang Q, Yuan H, Chen AF (2013) Oxidative stress-mediated thrombospondin-2 upregulation impairs bone marrow-derived angiogenic cell function in diabetes mellitus. *Arterioscler Thromb Vasc Biol* 33(8):1920–1927. <https://doi.org/10.1161/atvbaha.113.301609>
- Bahtiyar G, Gutterman D, Lebovitz H (2016) Heart failure: a major cardiovascular complication of diabetes mellitus. *Curr Diab Rep* 16(11):116. <https://doi.org/10.1007/s11892-016-0809-4>
- Balasubramanyam M, Premanand C, Mohan V (2002) The lymphocyte as a cellular model to study insights into the pathophysiology of diabetes and its complications. *Ann N Y Acad Sci* 958:399–402
- Ben-Menachem E (1996) Expanding antiepileptic drug options: clinical efficacy of new therapeutic agents. *Epilepsia* 37(Suppl 2):S4–S7
- Bettaieb A, Bakke J, Nagata N, Matsuo K, Xi Y, Liu S, AbouBechara D, Melhem R, Stanhope K, Cummings B, Graham J, Bremer A, Zhang S, Lyssiotis CA, Zhang ZY, Cantley LC,

- Havel PJ, Haj FG (2013) Protein tyrosine phosphatase 1B regulates pyruvate kinase M2 tyrosine phosphorylation. *J Biol Chem* 288(24):17360–17371. <https://doi.org/10.1074/jbc.M112.441469>
- Betz AL, Bowman PD, Goldstein GW (1983) Hexose transport in microvascular endothelial cells cultured from bovine retina. *Exp Eye Res* 36(2):269–277
- Bhavsar AR (2006) Diabetic retinopathy: the latest in current management. *Retina* 26(6 Suppl):S71–79. <https://doi.org/10.1097/01.iae.0000236466.23640.c9>
- Boddy A, Edwards P, Rowland M (1989) Binding of sulfonamides to carbonic anhydrase: influence on distribution within blood and on pharmacokinetics. *Pharm Res* 6(3):203–209
- Boeri D, Maiello M, Lorenzi M (2001) Increased prevalence of microthromboses in retinal capillaries of diabetic individuals. *Diabetes* 50(6):1432–1439
- Brownlee M (2001) Biochemistry and molecular cell biology of diabetic complications. *Nature* 414(6865):813–820
- Brownlee M (2005) The pathobiology of diabetic complications: a unifying mechanism. *Diabetes* 54(6):1615–1625
- Caldwell RB, Bartoli M, Behzadian MA, El-Remessy AE, Al-Shabrawey M, Platt DH, Caldwell RW (2003) Vascular endothelial growth factor and diabetic retinopathy: pathophysiological mechanisms and treatment perspectives. *Diabetes Metab Res Rev* 19(6):442–455. <https://doi.org/10.1002/dmrr.415>[doi]
- Caldwell RB, Bartoli M, Behzadian MA, El-Remessy AE, Al-Shabrawey M, Platt DH, Liou GI, Caldwell RW (2005) Vascular endothelial growth factor and diabetic retinopathy: role of oxidative stress. *Curr Drug Targets* 6(4):511–524
- Campesi I, Franconi F, Seghieri G, Meloni M (2017) Sex-gender-related therapeutic approaches for cardiovascular complications associated with diabetes. *Pharmacol Res* 119:195–207. <https://doi.org/10.1016/j.phrs.2017.01.023>
- Carter ND, Dodgson SJ, Quant PA (1990) Expression of hepatic mitochondrial carbonic anhydrase V. *Biochim Biophys Acta* 1036(3):237–241
- Chan PS, Kanwar M, Kowluru RA (2010) Resistance of retinal inflammatory mediators to suppress after reinstatement of good glycemic control: novel mechanism for metabolic memory. *J Diabetes Complications* 24(1):55–63. <https://doi.org/10.1016/j.jdiacomp.2008.10.002>
- Chappell JB, Crofts AR (1965) Calcium ion accumulation and volume changes of isolated liver mitochondria. Calcium Ion-Induced Swelling *Biochem J* 95:378–386. <https://doi.org/10.1042/bj0950378>
- Chen Q, Vazquez EJ, Moghaddas S, Hoppel CL, Lesnfsky EJ (2003) Production of reactive oxygen species by mitochondria: central role of complex III. *J Biol Chem* 278(38):36027–36031. <https://doi.org/10.1074/jbc.M304854200>
- Chen P, Guo AM, Edwards PA, Trick G, Scicli AG (2007) Role of NADPH oxidase and ANG II in diabetes-induced retinal leukostasis. *Am J Physiol Regul Integr Comp Physiol* 293(4):R1619–1629. <https://doi.org/10.1152/ajpregu.00290.2007>
- Cogan DG, Toussaint D, Kuwabara T (1961) Retinal vascular patterns. IV. Diabetic Retinopathy. *Arch Ophthalmol* 66:366–378
- Cogan DG, Kinoshita JH, Kador PF, Robison G, Datilis MB, Cobo LM, Kupfer C (1984) NIH conference. Aldose reductase and complications of diabetes. *Ann Intern Med* 101 (1):82–91
- Cohen PP (1981) The ornithine-urea cycle: biosynthesis and regulation of carbamyl phosphate synthetase I and ornithine transcarbamylase. *Curr Top Cell Regul* 18:1–19
- Corcoran SE, O'Neill LA (2016) HIF1 α and metabolic reprogramming in inflammation. *J Clin Invest* 126(10):3699–3707. <https://doi.org/10.1172/jci84431>
- Costa PZ, Soares R (2013) Neovascularization in diabetes and its complications. Unraveling the Angiogenic Paradox *Life Sci* 92(22):1037–1045. <https://doi.org/10.1016/j.lfs.2013.04.001>
- Dagher Z, Ruderman N, Tornheim K, Ido Y (2001) Acute regulation of fatty acid oxidation and amp-activated protein kinase in human umbilical vein endothelial cells. *Circ Res* 88(12):1276–1282

- Das Evcimen N, Ulusu NN, Karasu C, Dogru B (2004) Adenosine triphosphatase activity of streptozotocin-induced diabetic rat brain microsomes. Effect of vitamin E. *Gen Physiol Biophys* 23(3):347–355
- De Bock K, Georgiadou M, Schoors S, Kuchnio A, Wong BW, Cantelmo AR, Quaegebeur A, Ghesquiere B, Cauwenberghs S, Eelen G, Phng LK, Betz I, Tembuysers B, Brepoels K, Welti J, Geudens I, Segura I, Cruys B, Bifari F, Decimo I, Blanco R, Wyns S, Vangindertael J, Rocha S, Collins RT, Munck S, Daelemans D, Imamura H, Devlieger R, Rider M, Van Veldhoven PP, Schuit F, Bartrons R, Hofkens J, Fraisl P, Telang S, Deberardinis RJ, Schoonjans L, Vinckier S, Chesney J, Gerhardt H, Dewerchin M, Carmeliet P (2013) Role of PFKFB3-driven glycolysis in vessel sprouting. *Cell* 154(3):651–663. <https://doi.org/10.1016/j.cell.2013.06.037>
- De Simone G, Di Fiore A, Menchise V, Pedone C, Antel J, Casini A, Scozzafava A, Wurl M, Supuran CT (2005) Carbonic anhydrase inhibitors. Zonisamide is an effective inhibitor of the cytosolic isozyme II and mitochondrial isozyme V: solution and X-ray crystallographic studies. *Bioorg Med Chem Lett* 15(9):2315–2320. <https://doi.org/10.1016/j.bmcl.2005.03.032>
- Deutsch SI, Schwartz BL, Rosse RB, Mastropaolo J, Marvel CL, Drapalski AL (2003) Adjuvant topiramate administration: a pharmacologic strategy for addressing NMDA receptor hypofunction in schizophrenia. *Clin Neuropharmacol* 26(4):199–206
- Devi TS, Hosoya K, Terasaki T, Singh LP (2013) Critical role of TXNIP in oxidative stress, DNA damage and retinal pericyte apoptosis under high glucose: implications for diabetic retinopathy. *Exp Cell Res* 319(7):1001–1012. <https://doi.org/10.1016/j.yexcr.2013.01.012>
- Ding Y, Sun X, Shan PF (2017) MicroRNAs and cardiovascular disease in diabetes mellitus. *Biomed Res Int* 2017:4080364. <https://doi.org/10.1155/2017/4080364>
- Dodgson SJ, Contino LC (1988) Rat kidney mitochondrial carbonic anhydrase. *Arch Biochem Biophys* 260(1):334–341
- Dodgson SJ, Forster RE (1986) Carbonic anhydrase: inhibition results in decreased urea production by hepatocytes. *J Appl Physiol* (Bethesda, Md: 1985) 60(2):646–652. <https://doi.org/10.1152/jappl.1986.60.2.646>
- Dodgson SJ, Forster RE 2nd (1986b) Inhibition of CA V decreases glucose synthesis from pyruvate. *Arch Biochem Biophys* 251(1):198–204
- Dodgson SJ, Forster RE 2nd, Storey BT, Mela L (1980) Mitochondrial carbonic anhydrase. *Proc Natl Acad Sci U S A* 77(9):5562–5566
- Dodgson SJ, Forster RE 2nd, Schwed DA, Storey BT (1983) Contribution of matrix carbonic anhydrase to citrulline synthesis in isolated guinea pig liver mitochondria. *J Biol Chem* 258(12):7696–7701
- Dodgson SJ, Shank RP, Maryanoff BE (2000) Topiramate as an inhibitor of carbonic anhydrase isoenzymes. *Epilepsia* 41(Suppl 1):S35–39
- Droge W (2002) Free radicals in the physiological control of cell function. *Physiol Rev* 82(1):47–95. <https://doi.org/10.1152/physrev.00018.2001>
- Duarte DA, Silva KC, Rosales MA, Lopes de Faria JB, Lopes de Faria JM (2013) The concomitance of hypertension and diabetes exacerbating retinopathy: the role of inflammation and oxidative stress. *Curr Clin Pharmacol* 8(4):266–277
- Dugan LL, You Y-H, Ali SS, Diamond-Stanic M, Miyamoto S, DeClevés A-E, Andreyev A, Quach T, Ly S, Shekhtman G, Nguyen W, Chepetan A, Le TP, Wang L, Xu M, Paik KP, Fogo A, Viollet B, Murphy A, Brosius F, Naviaux RK, Sharma K (2013) AMPK dysregulation promotes diabetes-related reduction of superoxide and mitochondrial function. *J Clin Invest* 123(11):4888–4899. <https://doi.org/10.1172/JCI66218>
- Duh EJ, Sun JK, Stitt AW (2017) Diabetic retinopathy: current understanding, mechanisms, and treatment strategies. *JCI insight* 2 (14). <https://doi.org/10.1172/jci.insight.93751>
- Du XL, Edelstein D, Rossetti L, Fantus IG, Goldberg H, Ziyadeh F, Wu J, Brownlee M (2000) Hyperglycemia-induced mitochondrial superoxide overproduction activates the hexosamine pathway and induces plasminogen activator inhibitor-1 expression by increasing Sp1 glycosylation. *Proc Natl Acad Sci U S A* 97(22):12222–12226. <https://doi.org/10.1073/pnas.97.22.12222>

- Du Y, Smith MA, Miller CM, Kern TS (2002) Diabetes-induced oxidative stress in the retina, and correction by aminoguanidine. *J Neurochem* 80(5):771–779
- Du Y, Miller CM, Kern TS (2003) Hyperglycemia increases mitochondrial superoxide in retina and retinal cells. *Free Radic Biol Med* 35(11):1491–1499
- Du Y, Veenstra A, Palczewski K, Kern TS (2013) Photoreceptor cells are major contributors to diabetes-induced oxidative stress and local inflammation in the retina. *Proc Natl Acad Sci U S A* 110(41):16586–16591. <https://doi.org/10.1073/pnas.1314575110>
- Eelen G, Cruys B, Welti J, De Bock K, Carmeliet P (2013) Control of vessel sprouting by genetic and metabolic determinants. *Trends Endocrinol Metab* 24(12):589–596. <https://doi.org/10.1016/j.tem.2013.08.006>
- Ejaz S, Chekarova I, Ejaz A, Sohail A, Lim CW (2008) Importance of pericytes and mechanisms of pericyte loss during diabetic retinopathy. *Diabetes Obes Metab* 10(1):53–63. <https://doi.org/10.1111/j.1463-1326.2007.00795.x>
- Favret S, Binet F, Lalpalm E, Leboeuf D, Carbadillo J, Rubic T, Picard E, Mawambo G, Tetreault N, Joyal JS, Chemtob S, Sennlaub F, Sangiovanni JP, Guimond M, Sapiéha P (2013) Deficiency in the metabolite receptor SUCNR1 (GPR91) leads to outer retinal lesions. *Aging (alban NY)* 5(6):427–444
- Frey T, Antonetti DA (2011) Alterations to the blood-retinal barrier in diabetes: cytokines and reactive oxygen species. *Antioxid Redox Signal* 15(5):1271–1284. <https://doi.org/10.1089/ars.2011.3906>
- Fujikawa-Adachi K, Nishimori I, Taguchi T, Onishi S (1999) Human mitochondrial carbonic anhydrase VB. cDNA cloning, mRNA expression, subcellular localization, and mapping to chromosome X. *J Biol Chem* 274(30):21228–21233. <https://doi.org/10.1074/jbc.274.30.21228>
- Gadde KM, Franciscy DM, Wagner HR 2nd, Krishnan KR (2003) Zonisamide for weight loss in obese adults: a randomized controlled trial. *JAMA* 289(14):1820–1825. <https://doi.org/10.1001/jama.289.14.1820>
- Gadde KM, Allison DB, Ryan DH, Peterson CA, Troupin B, Schwiers ML, Day WW (2011) Effects of low-dose, controlled-release, phentermine plus topiramate combination on weight and associated comorbidities in overweight and obese adults (CONQUER): a randomised, placebo-controlled, phase 3 trial. *Lancet* 377(9774):1341–1352. [https://doi.org/10.1016/S0140-6736\(11\)60205-5](https://doi.org/10.1016/S0140-6736(11)60205-5)
- Gelissen O, Gelissen F, Ozcetin H (1990) Treatment of chronic macular oedema with low dosage acetazolamide. *Bull Soc Belge Ophthalmol* 238:153–160
- Ghanian Z, Mehrvar S, Jamali N, Sheibani N, Ranji M (2018) Time-lapse microscopy of oxidative stress demonstrates metabolic sensitivity of retinal pericytes under high glucose condition. *J Biophotonics* 11(9):e201700289. <https://doi.org/10.1002/jbio.201700289>
- Ghesquiere B, Wong BW, Kuchnio A, Carmeliet P (2014) Metabolism of stromal and immune cells in health and disease. *Nature* 511(7508):167–176. <https://doi.org/10.1038/nature13312>
- Giacco F, Brownlee M (2010) Oxidative stress and diabetic complications. *Circ Res* 107(9):1058–1070. <https://doi.org/10.1161/circresaha.110.223545>
- Groschner LN, Waldeck-Weiermair M, Malli R, Graier WF (2012) Endothelial mitochondria-less respiration, more integration. *Pflugers Arch* 464(1):63–76. <https://doi.org/10.1007/s00424-012-1085-z>
- Grossard C, Morel I, Chevanne M, Monnier M, Cillard J, Delamarche A (2000) Free radical scavenging and antioxidant effects of lactate ion: an in vitro study. *Journal of applied physiology* (Bethesda, Md: 1985) 89(1):169–175. <https://doi.org/10.1152/jappl.2000.89.1.169>
- Gurcel C, Vercoutter-Edouart AS, Fonbonne C, Mortuaire M, Salvador A, Michalski JC, Lemoine J (2008) Identification of new O-GlcNAc modified proteins using a click-chemistry-based tagging. *Anal Bioanal Chem* 390(8):2089–2097. <https://doi.org/10.1007/s00216-008-1950-y>
- Gurel Z, Sieg KM, Shallow KD, Sorenson CM, Sheibani N (2013) Retinal O-linked N-acetylglucosamine protein modifications: implications for postnatal retinal vascularization and the pathogenesis of diabetic retinopathy. *Mol vis* 19:1047–1059

- Gurel Z, Zaro BW, Pratt MR, Sheibani N (2014) Identification of O-GlcNAc modification targets in mouse retinal pericytes: implication of p53 in pathogenesis of diabetic retinopathy. *PLoS ONE* 9(5):e95561. <https://doi.org/10.1371/journal.pone.0095561>
- Guzel O, Innocenti A, Scozzafava A, Salman A, Supuran CT (2009) Carbonic anhydrase inhibitors. Aromatic/heterocyclic sulfonamides incorporating phenacetyl, pyridylacetyl and thienylacetyl tails act as potent inhibitors of human mitochondrial isoforms VA and VB. *Bioorg Med Chem* 17(14):4894–4899. <https://doi.org/10.1016/j.bmc.2009.06.006>
- Haefliger IO, Zschauer A, Anderson DR (1994) Relaxation of retinal pericyte contractile tone through the nitric oxide-cyclic guanosine monophosphate pathway. *Invest Ophthalmol vis Sci* 35(3):991–997
- Hammes HP, Martin S, Federlin K, Geisen K, Brownlee M (1991) Aminoguanidine treatment inhibits the development of experimental diabetic retinopathy. *Proc Natl Acad Sci U S A* 88(24):11555–11558
- Hammes HP, Bartmann A, Engel L, Wulfroth P (1997) Antioxidant treatment of experimental diabetic retinopathy in rats with nicanartine. *Diabetologia* 40(6):629–634. <https://doi.org/10.1007/s001250050726>
- Hammes HP, Lin J, Renner O, Shani M, Lundqvist A, Betsholtz C, Brownlee M, Deutsch U (2002) Pericytes and the pathogenesis of diabetic retinopathy. *Diabetes* 51(10):3107–3112
- Hammes HP, Feng Y, Pfister F, Brownlee M (2011) Diabetic retinopathy: targeting vasoregression. *Diabetes* 60(1):9–16. <https://doi.org/10.2337/db10-0454>
- Hayden MR, Yang Y, Habibi J, Bagree SV, Sowers JR (2010) Pericytopathy: Oxidative stress and impaired cellular longevity in the pancreas and skeletal muscle in metabolic syndrome and type 2 diabetes. *Oxid Med Cell Longev* 3(5):290–303
- Hazen SA, Waheed A, Sly WS, LaNoue KF, Lynch CJ (1996) Differentiation-dependent expression of CA V and the role of carbonic anhydrase isozymes in pyruvate carboxylation in adipocytes. *FASEB J* 10(4):481–490
- Hegde KR, Kovtun S, Varma SD (2010) Inhibition of glycolysis in the retina by oxidative stress: prevention by pyruvate. *Mol Cell Biochem* 343(1–2):101–105. <https://doi.org/10.1007/s11010-010-0503-9>
- Hewett-Emmett D, Tashian RE (1996) Functional diversity, conservation, and convergence in the evolution of the alpha-, beta-, and gamma-carbonic anhydrase gene families. *Mol Phylogenet Evol* 5(1):50–77. <https://doi.org/10.1006/mpev.1996.0006>
- Huang Q, Sheibani N (2008) High glucose promotes retinal endothelial cell migration through activation of Src, PI3K/Akt1/eNOS, and ERKs. *Am J Physiol Cell Physiol* 295(6):C1647–1657
- Ibrahim AS, El-Remessy AB, Matragoon S, Zhang W, Patel Y, Khan S, Al-Gayyar MM, El-Shishtawy MM, Liou GI (2011) Retinal microglial activation and inflammation induced by amadori-glycated albumin in a rat model of diabetes. *Diabetes* 60(4):1122–1133. <https://doi.org/10.2337/db10-1160>
- Jha JC, Ho F, Dan C, Jandeleit-Dahm K (2018) A causal link between oxidative stress and inflammation in cardiovascular and renal complications of diabetes. *Clin Sci (lond)* 132(16):1811–1836. <https://doi.org/10.1042/CS20171459>
- Jitrapakdee S, St Maurice M, Rayment I, Cleland WW, Wallace JC, Attwood PV (2008) Structure, mechanism and regulation of pyruvate carboxylase. *Biochem J* 413(3):369–387. <https://doi.org/10.1042/BJ20080709>
- Joussen AM, Poulaki V, Le ML, Koizumi K, Esser C, Janicki H, Schraermeyer U, Kociok N, Fauser S, Kirchhof B, Kern TS, Adamis AP (2004) A central role for inflammation in the pathogenesis of diabetic retinopathy. *FASEB J* 18(12):1450–1452. <https://doi.org/10.1096/fj.03-1476fje>
- Kaiser N, Sasson S, Feener EP, Boukobza-Vardi N, Higashi S, Moller DE, Davidheiser S, Przybylski RJ, King GL (1993) Differential regulation of glucose transport and transporters by glucose in vascular endothelial and smooth muscle cells. *Diabetes* 42(1):80–89
- Karler R, Woodbury DM (1960) Intracellular distribution of carbonic anhydrase. *Biochem J* 75:538–543. <https://doi.org/10.1042/bj0750538>

- Kaur H, Halliwell B (1994) Evidence for nitric oxide-mediated oxidative damage in chronic inflammation. Nitrotyrosine in serum and synovial fluid from rheumatoid patients. *FEBS Lett* 350(1):9–12
- Kellett MW, Smith DF, Stockton PA, Chadwick DW (1999) Topiramate in clinical practice: first year's postlicensing experience in a specialist epilepsy clinic. *J Neurol Neurosurg Psychiatry* 66(6):759–763. <https://doi.org/10.1136/jnnp.66.6.759>
- Kim YH, Kim YS, Roh GS, Choi WS, Cho GJ (2012) Resveratrol blocks diabetes-induced early vascular lesions and vascular endothelial growth factor induction in mouse retinas. *Acta Ophthalmol* 90(1):e31–37. <https://doi.org/10.1111/j.1755-3768.2011.02243.x>
- King GL (2008) The role of inflammatory cytokines in diabetes and its complications. *J Periodontol* 79(8 Suppl):1527–1534. <https://doi.org/10.1902/jop.2008.080246>
- Kowluru RA, Abbas SN (2003) Diabetes-induced mitochondrial dysfunction in the retina. *Invest Ophthalmol vis Sci* 44(12):5327–5334. <https://doi.org/10.1167/iovs.03-0353>
- Kowluru RA, Odenbach S (2004a) Role of interleukin-1beta in the pathogenesis of diabetic retinopathy. *Br J Ophthalmol* 88(10):1343–1347. <https://doi.org/10.1136/bjo.2003.038133>
- Kowluru RA, Odenbach S (2004b) Role of interleukin-1beta in the development of retinopathy in rats: effect of antioxidants. *Invest Ophthalmol vis Sci* 45:4161–4166. <https://doi.org/10.1167/iovs.04-0633>
- Kowluru RA, Atasi L, Ho YS (2006) Role of mitochondrial superoxide dismutase in the development of diabetic retinopathy. *Invest Ophthalmol vis Sci* 47(4):1594–1599. <https://doi.org/10.1167/iovs.05-1276>
- Kowluru RA, Zhong Q, Kanwar M (2010) Metabolic memory and diabetic retinopathy: role of inflammatory mediators in retinal pericytes. *Exp Eye Res* 90(5):617–623. <https://doi.org/10.1016/j.exer.2010.02.006>
- Koya D, King GL (1998) Protein kinase C activation and the development of diabetic complications. *Diabetes* 47(6):859–866
- Kubo E, Singh DP, Fatma N, Akagi Y (2009) TAT-mediated peroxiredoxin 5 and 6 protein transduction protects against high-glucose-induced cytotoxicity in retinal pericytes. *Life Sci* 84(23–24):857–864. <https://doi.org/10.1016/j.lfs.2009.03.019>
- Kuwabara T, Carroll JM, Cogan DG (1961) Retinal vascular patterns. III. Age, hypertension, absolute glaucoma, injury. *Arch Ophthalmol* 65:708–716
- LeDoux SP, Driggers WJ, Hollensworth BS, Wilson GL (1999) Repair of alkylation and oxidative damage in mitochondrial DNA. *Mutat Res* 434(3):149–159
- Leniger T, Thone J, Wiemann M (2004) Topiramate modulates pH of hippocampal CA3 neurons by combined effects on carbonic anhydrase and Cl⁻/HCO₃⁻-exchange. *Br J Pharmacol* 142(5):831–842. <https://doi.org/10.1038/sj.bjp.0705850>
- Liang Y, Chen X, Osborne M, DeCarlo SO, Jetton TL, Demarest K (2005) Topiramate ameliorates hyperglycaemia and improves glucose-stimulated insulin release in ZDF rats and db/db mice. *Diabetes Obes Metab* 7(4):360–369. <https://doi.org/10.1111/j.1463-1326.2004.00403.x>
- Lincet H, Icard P (2015) How do glycolytic enzymes favour cancer cell proliferation by nonmetabolic functions? *Oncogene* 34(29):3751–3759. <https://doi.org/10.1038/onc.2014.320>
- Liu Y, Fiskum G, Schubert D (2002) Generation of reactive oxygen species by the mitochondrial electron transport chain. *J Neurochem* 80(5):780–787
- Li W, Chan LS, Khatami M, Rockey JH (1985) Characterization of glucose transport by bovine retinal capillary pericytes in culture. *Exp Eye Res* 41(2):191–199
- Li W, Yanoff M, Jian B, He Z (1999) Altered mRNA levels of antioxidant enzymes in pre-apoptotic pericytes from human diabetic retinas. *Cell Mol Biol (Noisy-le-grand)* 45(1):59–66
- Li T, Hu J, Du S, Chen Y, Wang S, Wu Q (2014) ERK1/2/COX-2/PGE2 signaling pathway mediates GPR91-dependent VEGF release in streptozotocin-induced diabetes. *Mol vis* 20:1109–1121
- Lusty CJ (1978) Carbamyl phosphate synthetase. Bicarbonate-dependent hydrolysis of ATP and potassium activation. *J Biol Chem* 253(12):4270–4278

- Lynch CJ, Fox H, Hazen SA, Stanley BA, Dodgson S, Lanoue KF (1995) Role of hepatic carbonic anhydrase in de novo lipogenesis. *Biochem J* 310(Pt 1):197–202. <https://doi.org/10.1042/bj3100197>
- Mandarino LJ, Finlayson J, Hassell JR (1994) High glucose downregulates glucose transport activity in retinal capillary pericytes but not endothelial cells. *Invest Ophthalmol vis Sci* 35(3):964–972
- Maresca A, Supuran CT (2011) (R)-/(S)-10-camphorsulfonyl-substituted aromatic/heterocyclic sulfonamides selectively inhibit mitochondrial over cytosolic carbonic anhydrases. *Bioorg Med Chem Lett* 21(5):1334–1337. <https://doi.org/10.1016/j.bmcl.2011.01.050>
- Mazurek S (2011) Pyruvate kinase type M2: a key regulator of the metabolic budget system in tumor cells. *Int J Biochem Cell Biol* 43(7):969–980. <https://doi.org/10.1016/j.biocel.2010.02.005>
- Mertens S, Noll T, Spahr R, Krutzfeldt A, Piper HM (1990) Energetic response of coronary endothelial cells to hypoxia. *Am J Physiol* 258(3 Pt 2):H689–694
- Miller AG, Smith DG, Bhat M, Nagaraj RH (2006) Glyoxalase I is critical for human retinal capillary pericyte survival under hyperglycemic conditions. *J Biol Chem* 281(17):11864–11871. <https://doi.org/10.1074/jbc.M513813200>
- Mizutani M, Kern TS, Lorenzi M (1996) Accelerated death of retinal microvascular cells in human and experimental diabetic retinopathy. *J Clin Invest* 97(12):2883–2890. <https://doi.org/10.1172/jci118746>
- Mohamed IN, Soliman SA, Alhusban A, Matragoon S, Pillai BA, Elmarkaby AA, El-Remessy AB (2012) Diabetes exacerbates retinal oxidative stress, inflammation, and microvascular degeneration in spontaneously hypertensive rats. *Mol vis* 18:1457–1466
- Moran C, Phan TG, Chen J, Blizzard L, Beare R, Venn A, Münch G, Wood AG, Forbes J, Greenaway TM, Pearson S, Srikanth V (2013) Brain atrophy in type 2 diabetes. *Reg Distrib Influence Cognition* 36(12):4036–4042. <https://doi.org/10.2337/dc13-0143>
- Mori K, Ogawa Y, Ebihara K, Tamura N, Tashiro K, Kuwahara T, Mukoyama M, Sugawara A, Ozaki S, Tanaka I, Nakao K (1999) Isolation and characterization of CA XIV, a novel membrane-bound carbonic anhydrase from mouse kidney. *J Biol Chem* 274(22):15701–15705. <https://doi.org/10.1074/jbc.274.22.15701>
- Morohoshi K, Ohbayashi M, Patel N, Chong V, Bird AC, Ono SJ (2012) Identification of anti-retinal antibodies in patients with age-related macular degeneration. *Exp Mol Pathol* 93(2):193–199. <https://doi.org/10.1016/j.yexmp.2012.03.007>
- Nagao Y, Platero JS, Waheed A, Sly WS (1993) Human mitochondrial carbonic anhydrase: cDNA cloning, expression, subcellular localization, and mapping to chromosome 16. *Proc Natl Acad Sci U S A* 90(16):7623–7627. <https://doi.org/10.1073/pnas.90.16.7623>
- Nagao Y, Batanian JR, Clemente MF, Sly WS (1995) Genomic organization of the human gene (CA5) and pseudogene for mitochondrial carbonic anhydrase V and their localization to chromosomes 16q and 16p. *Genomics* 28(3):477–484
- Nakamura S, Makita Z, Ishikawa S, Yasumura K, Fujii W, Yanagisawa K, Kawata T, Koike T (1997) Progression of nephropathy in spontaneous diabetic rats is prevented by OPB-9195, a novel inhibitor of advanced glycation. *Diabetes* 46(5):895–899
- Nerlich AG, Sauer U, Kolm-Litty V, Wagner E, Koch M, Schleicher ED (1998) Expression of glutamine:fructose-6-phosphate amidotransferase in human tissues: evidence for high variability and distinct regulation in diabetes. *Diabetes* 47(2):170–178
- Nguyen DV, Shaw LC, Grant MB (2012) Inflammation in the pathogenesis of microvascular complications in diabetes. *Front Endocrinol (lausanne)* 3:170. <https://doi.org/10.3389/fendo.2012.00170>
- Nishikawa T, Edelstein D, Du XL, Yamagishi S, Matsumura T, Kaneda Y, Yorek MA, Beebe D, Oates PJ, Hammes HP, Giardino I, Brownlee M (2000) Normalizing mitochondrial superoxide production blocks three pathways of hyperglycaemic damage. *Nature* 404(6779):787–790. <https://doi.org/10.1038/35008121>
- Nishimori I, Vullo D, Innocenti A, Scozzafava A, Mastrolorenzo A, Supuran CT (2005) Carbonic anhydrase inhibitors. The mitochondrial isozyme VB as a new target for sulfonamide and sulfamate inhibitors. *J Med Chem* 48(24):7860–7866. doi:<https://doi.org/10.1021/jm050483n>

- Nishimura C, Hotta Y, Gui T, Seko A, Fujimaki T, Ishikawa T, Hayakawa M, Kanai A, Saito T (1997) The level of erythrocyte aldose reductase is associated with the severity of diabetic retinopathy. *Diabetes Res Clin Pract* 37(3):173–177
- Panzhinskiy E, Ren J, Nair S (2013) Pharmacological inhibition of protein tyrosine phosphatase 1B: a promising strategy for the treatment of obesity and type 2 diabetes mellitus. *Curr Med Chem* 20(21):2609–2625
- Patrick P, Price TO, Diogo AL, Sheibani N, Banks WA, Shah GN (2015) Topiramate protects pericytes from glucotoxicity: role for mitochondrial CA VA in cerebrovascular disease in diabetes. *J Endocrinol Diabetes* 2(2)
- Picard F, Deshaies Y, Lalonde J, Samson P, Richard D (2000) Topiramate reduces energy and fat gains in lean (Fa/?) and obese (fa/fa) Zucker rats. *Obes Res* 8(9):656–663. <https://doi.org/10.1038/oby.2000.84>
- Podesta F, Romeo G, Liu WH, Krajewski S, Reed JC, Gerhardinger C, Lorenzi M (2000) Bax is increased in the retina of diabetic subjects and is associated with pericyte apoptosis in vivo and in vitro. *Am J Pathol* 156(3):1025–1032
- Poulsen SA, Wilkinson BL, Innocenti A, Vullo D, Supuran CT (2008) Inhibition of human mitochondrial carbonic anhydrases VA and VB with para-(4-phenyltriazole-1-yl)-benzenesulfonamide derivatives. *Bioorg Med Chem Lett* 18(16):4624–4627. <https://doi.org/10.1016/j.bmcl.2008.07.010>
- Price TO, Sheibani N (1863) Shah GN (2017) Regulation of high glucose-induced apoptosis of brain pericytes by mitochondrial CA VA: A specific target for prevention of diabetic cerebrovascular pathology. *Biochim Biophys Acta Mol Basis Dis* 4:929–935. <https://doi.org/10.1016/j.bbadis.2017.01.025>
- Price TO, Eranki V, Banks WA, Ercal N, Shah GN (2012) Topiramate treatment protects blood-brain barrier pericytes from hyperglycemia-induced oxidative damage in diabetic mice. *Endocrinology* 153(1):362–372. <https://doi.org/10.1210/en.2011-1638>
- Price TO, Farr SA, Niehoff ML, Ercal N, Morley JE, Shah GN (2015) Protective effect of topiramate on hyperglycemia-induced cerebral oxidative stress, pericyte loss and learning behavior in diabetic mice. *Int Lib Diabetes Metab* 1(1):6–12
- Qaum T, Xu Q, Joussen AM, Clemens MW, Qin W, Miyamoto K, Hassessian H, Wiegand SJ, Rudge J, Yancopoulos GD, Adamis AP (2001) VEGF-initiated blood-retinal barrier breakdown in early diabetes. *Invest Ophthalmol vis Sci* 42(10):2408–2413
- Rask-Madsen C, King GL (2013) Vascular complications of diabetes: mechanisms of injury and protective factors. *Cell Metab* 17(1):20–33. <https://doi.org/10.1016/j.cmet.2012.11.012>
- Richter C, Park JW, Ames BN (1988) Normal oxidative damage to mitochondrial and nuclear DNA is extensive. *Proc Natl Acad Sci U S A* 85(17):6465–6467
- Roy Chengappa KN, Levine J, Rathore D, Parepally H, Atzert R (2001) Long-term effects of topiramate on bipolar mood instability, weight change and glycemic control: a case-series. *Eur Psychiatry J Assoc Eur Psychiatrists* 16(3):186–190
- Roy MS, Janal MN, Crosby J, Donnelly R (2013) Inflammatory biomarkers and progression of diabetic retinopathy in African Americans with type 1 diabetes. *Invest Ophthalmol vis Sci* 54(8):5471–5480. <https://doi.org/10.1167/iovs.13-12212>
- Rubbo H, Radi R, Trujillo M, Telleri R, Kalyanaraman B, Barnes S, Kirk M, Freeman BA (1994) Nitric oxide regulation of superoxide and peroxynitrite-dependent lipid peroxidation. Formation of novel nitrogen-containing oxidized lipid derivatives. *J Biol Chem* 269(42):26066–26075
- Salameh TS, Shah GN, Price TO, Hayden MR, Banks WA (2016) Blood-brain barrier disruption and neurovascular unit dysfunction in diabetic mice: protection with the mitochondrial carbonic anhydrase inhibitor topiramate. *J Pharmacol Exp Ther* 359(3):452–459. <https://doi.org/10.1124/jpet.116.237057>
- Sapieha P, Sirinyan M, Hamel D, Zaniolo K, Joyal JS, Cho JH, Honore JC, Kermorvant-Duchemin E, Varma DR, Tremblay S, Leduc M, Rihakova L, Hardy P, Klein WH, Mu X, Mamer O, Lachapelle P, Di Polo A, Beausejour C, Andelfinger G, Mitchell G, Senmlauf F, Chemtob S (2008) The succinate

- receptor GPR91 in neurons has a major role in retinal angiogenesis. *Nat Med* 14(10):1067–1076. <https://doi.org/10.1038/nm.1873>
- Scheef E, Wang S, Sorenson CM, Sheibani N (2005) Isolation and characterization of murine retinal astrocytes. *Mol vis* 11:613–624
- Scheef EA, Sorenson CM, Sheibani N (2009) Attenuation of proliferation and migration of retinal pericytes in the absence of thrombospondin-1. *Am J Physiol Cell Physiol* 296(4):C724–734. <https://doi.org/10.1152/ajpcell.00409.2008>
- Schleicher ED, Weigert C (2000) Role of the hexosamine biosynthetic pathway in diabetic nephropathy. *Kidney Int Suppl* 77:S13–18
- Schmidt D, Jacob R, Loiseau P, Deisenhammer E, Klinger D, Despland A, Egli M, Bauer G, Stenzel E, Blankenhorn V (1993) Zonisamide for add-on treatment of refractory partial epilepsy: a European double-blind trial. *Epilepsy Res* 15(1):67–73
- Scott JA, King GL (2004) Oxidative stress and antioxidant treatment in diabetes. *Ann N Y Acad Sci* 1031:204–213. <https://doi.org/10.1196/annals.1331.020>
- Scozzafava A, Supuran CT, Carta F (2013) Antiobesity carbonic anhydrase inhibitors: a literature and patent review. *Expert Opin Ther Pat* 23(6):725–735. <https://doi.org/10.1517/13543776.2013.790957>
- Shah GN, Hewett-Emmett D, Grubb JH, Migas MC, Fleming RE, Waheed A, Sly WS (2000) Mitochondrial carbonic anhydrase CA VB: differences in tissue distribution and pattern of evolution from those of CA VA suggest distinct physiological roles. *Proc Natl Acad Sci U S A* 97(4):1677–1682
- Shah GN, Morofuji Y, Banks WA, Price TO (2013a) High glucose-induced mitochondrial respiration and reactive oxygen species in mouse cerebral pericytes is reversed by pharmacological inhibition of mitochondrial carbonic anhydrases: Implications for cerebral microvascular disease in diabetes. *Biochem Biophys Res Commun* 440(2):354–358. <https://doi.org/10.1016/j.bbrc.2013.09.086>
- Shah GN, Price TO, Banks WA, Morofuji Y, Kovac A, Ercal N, Sorenson CM, Shin ES, Sheibani N (2013b) Pharmacological inhibition of mitochondrial carbonic anhydrases protects mouse cerebral pericytes from high glucose-induced oxidative stress and apoptosis. *J Pharmacol Exp Ther* 344(3):637–645. <https://doi.org/10.1124/jpet.112.201400>
- Shah GN, Rubbelke TS, Hendin J, Nguyen H, Waheed A, Shoemaker JD, Sly WS (2013c) Targeted mutagenesis of mitochondrial carbonic anhydrases VA and VB implicates both enzymes in ammonia detoxification and glucose metabolism. *Proc Natl Acad Sci U S A* 110(18):7423–7428. <https://doi.org/10.1073/pnas.1305805110>
- Sheikpranbabu S, Haribalaganesh R, Gurunathan S (2011) Pigment epithelium-derived factor inhibits advanced glycation end-products-induced cytotoxicity in retinal pericytes. *Diabetes Metab* 37(6):505–511. <https://doi.org/10.1016/j.diabet.2011.03.006>
- Shin ES, Sorenson CM, Sheibani N (2014a) Diabetes and retinal vascular dysfunction. *J Ophthalmic vis Res* 9(3):362–373. <https://doi.org/10.4103/2008-322x.143378>
- Shin ES, Huang Q, Gurel Z, Sorenson CM, Sheibani N (2014b) High glucose alters retinal astrocytes phenotype through increased production of inflammatory cytokines and oxidative stress. *PLoS ONE* 9(7):e103148. <https://doi.org/10.1371/journal.pone.0103148>
- Shin ES, Huang Q, Gurel Z, Palenski TL, Zaitoun I, Sorenson CM, Sheibani N (2014c) STAT1-mediated Bim expression promotes the apoptosis of retinal pericytes under high glucose conditions. *Cell Death Dis* 5:e986. <https://doi.org/10.1038/cddis.2013.517>
- Singh LP, Devi TS, Yumnamcha T, Devi TS, Somayajulu M, Kowluru RA, Singh LP (2017) The role of Txnip in Mitophagy dysregulation and inflammasome activation in diabetic retinopathy: a new perspective TXNIP regulates mitophagy in retinal Muller cells under high-glucose conditions: implications for diabetic retinopathy. *JOJ Ophthalmology* 4(4):e2777. <https://doi.org/10.19080/jojo.2017.04.555643>
- Sly WS, Hu PY (1995) Human carbonic anhydrases and carbonic anhydrase deficiencies. *Annu Rev Biochem* 64:375–401. <https://doi.org/10.1146/annurev.bi.64.070195.002111>
- Smaine FZ, Pacchiano F, Rami M, Barragan-Montero V, Vullo D, Scozzafava A, Winum JY, Supuran CT (2008) Carbonic anhydrase inhibitors: 2-substituted-1,3,4-thiadiazole-5-sulfamides act as

- powerful and selective inhibitors of the mitochondrial isozymes VA and VB over the cytosolic and membrane-associated carbonic anhydrases I, II and IV. *Bioorg Med Chem Lett* 18(24):6332–6335. <https://doi.org/10.1016/j.bmcl.2008.10.093>
- Solomon SD, Chew E, Duh EJ, Sobrin L, Sun JK, VanderBeek BL, Wykoff CC, Gardner TW (2017) Diabetic retinopathy: a position statement by the American diabetes association. *Diabetes Care* 40(3):412–418. <https://doi.org/10.2337/dc16-2641>
- Spatz M, Mrsulja BB, Wroblewska B, Merkel N, Bembry J (1986) Modulation of glycogen metabolism in cerebromicrovascular smooth muscle and endothelial cultures. *Biochem Biophys Res Commun* 134(2):484–491
- Stadtman ER, Levine RL (2000) Protein oxidation. *Ann N Y Acad Sci* 899:191–208
- Stitt AW, McGoldrick C, Rice-McCaldin A, McCance DR, Glenn JV, Hsu DK, Liu FT, Thorpe SR, Gardiner TA (2005) Impaired retinal angiogenesis in diabetes: role of advanced glycation end products and galectin-3. *Diabetes* 54(3):785–794
- Sun JK, Keenan HA, Cavallerano JD, Asztalos BF, Schaefer EJ, Sell DR, Strauch CM, Monnier VM, Doria A, Aiello LP, King GL (2011) Protection from retinopathy and other complications in patients with type 1 diabetes of extreme duration: the joslin 50-year medalist study. *Diabetes Care* 34(4):968–974. <https://doi.org/10.2337/dc10-1675>
- Supuran CT (2008) Carbonic anhydrases: novel therapeutic applications for inhibitors and activators. *Nat Rev Drug Discov* 7(2):168–181. <https://doi.org/10.1038/nrd2467>
- Supuran CT, Scozzafava A (2007) Carbonic anhydrases as targets for medicinal chemistry. *Bioorg Med Chem* 15(13):4336–4350. <https://doi.org/10.1016/j.bmc.2007.04.020>
- Su L, Xiao H (2015) Inflammation in diabetes and cardiovascular disease: a new perspective on vitamin D. *Cardiovasc Endocrinol* 4(4):127–131. <https://doi.org/10.1097/xce.0000000000000062>
- Su X, Sorenson CM, Sheibani N (2003) Isolation and characterization of murine retinal endothelial cells. *Mol vis* 9:171–178
- Tang J, Du Y, Petrash JM, Sheibani N, Kern TS (2013) Deletion of aldose reductase from mice inhibits diabetes-induced retinal capillary degeneration and superoxide generation. *PLoS ONE* 8(4):e62081. <https://doi.org/10.1371/journal.pone.0062081>
- The Diabetes Control and Complications Trial Research G (1993) The effect of intensive treatment of diabetes on the development and progression of long-term complications in insulin-dependent diabetes mellitus. *N Engl J Med* 329(14):977–986. <https://doi.org/10.1056/nejm199309303291401>
- Tureci O, Sahin U, Vollmar E, Siemer S, Gottert E, Seitz G, Parkkila AK, Shah GN, Grubb JH, Pfreundschuh M, Sly WS (1998) Human carbonic anhydrase XII: cDNA cloning, expression, and chromosomal localization of a carbonic anhydrase gene that is overexpressed in some renal cell cancers. *Proc Natl Acad Sci U S A* 95(13):7608–7613
- Turrens JF (2003) Mitochondrial formation of reactive oxygen species. *J Physiol* 552(Pt 2):335–344. <https://doi.org/10.1113/jphysiol.2003.049478>
- van Reyk DM, Gillies MC, Davies MJ (2003) The retina: oxidative stress and diabetes. *Redox Rep* 8(4):187–192
- Vitale RM, Pedone C, Amodeo P, Antel J, Wurl M, Scozzafava A, Supuran CT, De Simone G (2007) Molecular modeling study for the binding of zonisamide and topiramate to the human mitochondrial carbonic anhydrase isoform VA. *Bioorg Med Chem* 15(12):4152–4158. <https://doi.org/10.1016/j.bmc.2007.03.070>
- Vullo D, Franchi M, Gallori E, Antel J, Scozzafava A, Supuran CT (2004) Carbonic anhydrase inhibitors. Inhibition of mitochondrial isozyme V with aromatic and heterocyclic sulfonamides. *J Med Chem* 47(5):1272–1279. <https://doi.org/10.1021/jm031057>
- Wallace DC (1992) Diseases of the mitochondrial DNA. *Annu Rev Biochem* 61:1175–1212. <https://doi.org/10.1146/annurev.bi.61.070192.005523>
- Wang S, Gottlieb JL, Sorenson CM, Sheibani N (2009) Modulation of thrombospondin 1 and pigment epithelium-derived factor levels in vitreous fluid of patients with diabetes. *Arch Ophthalmol* 127(4):507–513

- Weiwei Z, Hu R (2009) Targeting carbonic anhydrase to treat diabetic retinopathy: emerging evidences and encouraging results. *Biochem Biophys Res Commun* 390(3):368–371. <https://doi.org/10.1016/j.bbrc.2009.10.031>
- Williams GR (1965) Dynamic aspects of the tricarboxylic acid cycle in isolated mitochondria. *Can J Biochem* 43:603–615
- Winter K, Foster JG, Edwards GE, Holtum JA (1982) Intracellular localization of enzymes of carbon metabolism in mesembryanthemum crystallinum exhibiting C(3) photosynthetic characteristics or performing crassulacean acid metabolism. *Plant Physiol* 69(2):300–307
- Winum JY, Thiry A, Cheikh KE, Dogne JM, Montero JL, Vullo D, Scozzafava A, Masereel B, Supuran CT (2007) Carbonic anhydrase inhibitors. Inhibition of isoforms I, II, IV, VA, VII, IX, and XIV with sulfonamides incorporating fructopyranose-thioureido tails. *Bioorg Med Chem Lett* 17(10):2685–2691. <https://doi.org/10.1016/j.bmcl.2007.03.008>
- Wu MY, Yiang GT, Lai TT, Li CJ (2018) The oxidative stress and mitochondrial dysfunction during the pathogenesis of diabetic retinopathy. *Oxid Med Cell Longev* 2018:3420187. <https://doi.org/10.1155/2018/3420187>
- Xia P, Inoguchi T, Kern TS, Engerman RL, Oates PJ, King GL (1994) Characterization of the mechanism for the chronic activation of diacylglycerol-protein kinase C pathway in diabetes and hypergalactosemia. *Diabetes* 43(9):1122–1129
- Yamagishi S, Hsu CC, Taniguchi M, Harada S, Yamamoto Y, Ohsawa K, Kobayashi K, Yamamoto H (1995) Receptor-mediated toxicity to pericytes of advanced glycosylation end products: a possible mechanism of pericyte loss in diabetic microangiopathy. *Biochem Biophys Res Commun* 213(2):681–687
- Yamagishi S, Inagaki Y, Amano S, Okamoto T, Takeuchi M, Makita Z (2002) Pigment epithelium-derived factor protects cultured retinal pericytes from advanced glycation end product-induced injury through its antioxidative properties. *Biochem Biophys Res Commun* 296(4):877–882
- Zhang SX, Wang JJ, Dashti A, Wilson K, Zou MH, Szveda L, Ma JX, Lyons TJ (2008) Pigment epithelium-derived factor mitigates inflammation and oxidative stress in retinal pericytes exposed to oxidized low-density lipoprotein. *J Mol Endocrinol* 41(3):135–143

Chapter 7

An Overview of Carbonic Anhydrase-Related Neoplasms



Martina Takacova and Silvia Pastorekova

Abstract Aberrant control of acid–base homeostasis is an emerging cancer hallmark that results from adaptation to oncogenic metabolism and tumor microenvironment. It has dramatic consequences, contributing to acquisition of aggressive tumor phenotype and disease progression. Regulation of pH is executed by transporters, exchangers, and pumps mediating ion fluxes in rates dictated by actual physiological needs of tumor cells. However, full performance of the pH-regulation machinery requires carbonic anhydrases (CAs) catalyzing a reaction key to acid–base balance: reversible conversion of carbon dioxide to bicarbonate ion and proton. Here, we provide an overview of known and predicted links of the human CA isoforms to various types of neoplasms and summarize the mechanisms, through which they functionally contribute to cancer. We use the approach, in which data from published papers are complemented by publicly available metadata processed by the GEPIA2 instrument. This allows not only for aligning bioinformatics to experimental evidence (supporting a prominent position of CA IX), but also for prediction of novel correlations that remain to be experimentally proven (such as for CA XIV). With a continuous accumulation of the knowledge, it is now becoming clear that CAs are broadly expressed in tumors and actively participate in cancer development and/or progression.

Keywords Carbonic anhydrase · pH regulation · Cancer · Prognosis · GEPIA2

Abbreviations

BRAF	B-Raf oncoprotein
CA	carbonic anhydrase
HIF	hypoxia-inducible factor

M. Takacova · S. Pastorekova (✉)

Department of Tumor Biology, Institute of Virology, Biomedical Research Center, Slovak Academy of Sciences, Dubravska cesta 9, 845 05 Bratislava, Slovakia
e-mail: silvia.pastorekova@savba.sk

© Springer Nature Switzerland AG 2021

W. R. Chegwidden and N. D. Carter (eds.), *The Carbonic Anhydrases: Current and Emerging Therapeutic Targets*, Progress in Drug Research 75,
https://doi.org/10.1007/978-3-030-79511-5_7

147

IDH	isocitrate dehydrogenase
IHC	immunohistochemistry
MCT	monocarboxylate transporter
MET	hepatocyte growth factor receptor
NF1	neurofibromatosis 1
NHE	sodium-proton exchanger
NSCLC	non-small cell lung carcinoma
PG	proteoglycan
RTK	receptor tyrosine kinase
RAS	c-Ras oncoprotein
TPM	transcripts per million
VHL	von Hippel Lindau

7.1 Introduction

Vital functions of cells, tissues, and organs in the human body crucially depend, among other factors, on proper pH regulation, especially in situations of high metabolic performance, gas exchange, and/or fluid production. Such processes occur under physiological conditions in virtually all organs and are particularly intense in stomach, intestine, liver, pancreas, kidney, lung, and brain. However, many pathological conditions including cancer are characterized by aberrant control of acid–base homeostasis as a result of perturbed ion transport and abnormal metabolism. Especially in cancer cells, this has very dramatic consequences, supporting acquisition of an aggressive tumor phenotype and contributing to disease progression (Corbet and Feron 2017).

Regulation of pH is executed by a number of ion transporters, exchangers, and pumps that carry out ion extrusion and/or ion import in a rate dictated by actual physiological needs of the cell and by status of its intracellular and extracellular microenvironment. Among these, lactate and proton exporters, and bicarbonate importers play a major role as pH-modulating mediators of ion fluxes across the plasma membrane, while proton pumps also control pH of certain intracellular organelles (endosomes, lysosomes). However, in addition to these “ion transport managers,” full performance of the pH regulation machinery requires enzymes of the carbonic anhydrase family catalyzing the reaction that is fundamental for acid-base balance, namely, the reversible conversion of carbon dioxide to carbonic acid that spontaneously dissociates to bicarbonate ion and proton (Supuran 2016). The human body contains 15 carbonic anhydrase (CA) isoforms of the α -CA family, namely CA I-IV, CA VA and CA VB, CA VI-XIV. Twelve isoforms are active enzymes, with catalytic activity ranging from low to very high (CA II and CA IX belonging to the most active enzymes in the nature), while three isoforms are inactive (CA VIII, X, and XI). CAs also differ by subcellular localization: CA I-III, VII, VIII, X, XI, XIII are cytoplasmic, CA VA

and VB are mitochondrial, CA IV, IX, XII, XIV are membrane-associated, and CA VI is secreted (Pastorekova et al. 2004; Mboge et al. 2018). The diversity of the human CAs is further widened by their variable expression levels and heterogeneous expression pattern in organs and tissues ranging from almost ubiquitous (e.g., CA II and CA XIII), to limited to certain tissue (e.g., CA VA and CA VI). This makes their complex understanding very difficult and development of general statements very challenging.

It has been long believed that the nature “invented” these enzymes primarily to drive pH-related physiological processes in normal tissues, since the initial efforts to link CAs to cancer did not bring any clear-cut data. However, everything changed in the early 90 's of the twentieth century, with the discovery of two, at that time novel, CA isoforms. First it was CA IX, which showed strong association with a broad range of tumors contrasting to limited expression in normal tissues (Pastorek et al. 1994) followed by CA XII, which was detected in many normal tissues, but showed overexpression in certain tumors (Tureci et al. 1998). Later on, thorough examination of some of the “old” isoforms (CA I, II, IV) revealed that their expression patterns exhibit either positive or negative correlations with cancer within specific contexts. Moreover, inactive isoforms CA X and CA XI, have also been implicated in tumor phenotype. In fact, with continuous accumulation of data, it is now becoming clearly apparent that CAs can actively participate in cancer development and/or progression.

Here we present an overview of known and predicted links of CA isoforms to various types of neoplasms and summarize the mechanisms through which they functionally contribute to cancer. In this overview, data from published papers are complemented by publicly available RNA-seq metadata from TCGA and GTEx databases processed by the GEPIA2 instrument, which uses Transcripts Per Million (TPM) values of transcription levels normalized to transcript's length and divided by the scaling factor to allow for comparison of gene expression levels among different types (Tang et al. 2019). This combined approach allows not only for aligning bioinformatics to experimental evidence, but also for prediction of some correlations that still remain to be experimentally proven. In this way, it is also possible to demonstrate that the cancer-related expression pattern, in some cases, does not necessarily translate to clinically relevant information, suggesting that the experimental evidence including functional studies is an imperative prerequisite for understanding the roles of genes/proteins including carbonic anhydrases in cancer biology and of their potential usefulness for clinical applications. Note that CA genes are written in italic style with Arabic numbers, while CA proteins are written in normal style with Roman numbers, in line with the official nomenclature, and that abbreviations used to designate different cancer types were used according to GEPIA2 (Table 7.1).

7.2 Expression of Cytoplasmic CA Isoforms in Neoplasms

Metadata analysis revealed that all of the five genes encoding the cytoplasmic CAs are primarily expressed in normal tissues, with CA2 exhibiting the highest transcription levels followed by CA1, CA3, CA7, and CA13 (Fig. 7.1). Notably, CA II protein

Table 7.1 An overview of TCGA/GTEX data available within GEPIA2 that were used for the expression and survival analysis of carbonic anhydrase genes

TCGA	Detail	Tumor	Normal	GTEX	Num
ACC	Adrenocortical carcinoma	77	-	Adrenal Gland	128
BLCA	Bladder Urothelial Carcinoma	404	19	Bladder	9
BRCA	Breast invasive carcinoma	1085	112	Breast	179
CESC	Cervical squamous cell carcinoma and endocervical adenocarcinoma	306	3	Cervix Uteri	10
CHOL	Cholangio carcinoma	36	9	-	-
COAD	Colon adenocarcinoma	275	41	Colon	308
DLBC	Lymphoid Neoplasm Diffuse Large B-cell Lymphoma	47	-	Blood	337
ESCA	Esophageal carcinoma	182	13	Esophagus	273
GBM	Glioblastoma multiforme	163	-	Brain	207
HNSC	Head and Neck squamous cell carcinoma	519	44	-	-
KICH	Kidney Chromophobe	66	25	Kidney	28
KIRC	Kidney renal clear cell carcinoma	523	72	Kidney	28
KIRP	Kidney renal papillary cell carcinoma	286	32	Kidney	28
LAML	Acute Myeloid Leukemia	173	-	Bone Marrow	70
LGG	Brain Lower Grade Glioma	518	-	Brain	207
LIHC	Liver hepatocellular carcinoma	369	50	Liver	110
LUAD	Lung adenocarcinoma	483	59	Lung	288
LUSC	Lung squamous cell carcinoma	486	50	Lung	288
MESO	Mesothelioma	87	-	-	-
OV	Ovarian serous cystadenocarcinoma	426	-	Ovary	88
PAAD	Pancreatic adenocarcinoma	179	4	Pancreas	167
PCPG	Pheochromocytoma and Paraganglioma	182	3	-	-
PRAD	Prostate adenocarcinoma	492	52	Prostate	100
READ	Rectum adenocarcinoma	92	10	Colon	308
SARC	Sarcoma	262	2	-	-
SKCM	Skin Cutaneous Melanoma	461	1	Skin	557
STAD	Stomach adenocarcinoma	408	36	Stomach	175
TGCT	Testicular Germ Cell Tumors	137	-	Testis	165
THCA	Thyroid carcinoma	512	59	Thyroid	278

(continued)

Table 7.1 (continued)

TCGA	Detail	Tumor	Normal	GTEx	Num
THYM	Thymoma	118	2	Blood	337
UCEC	Uterine Corpus Endometrial Carcinoma	174	13	Uterus	78
UCS	Uterine Carcinosarcoma	57	-	Uterus	78
UVM	Uveal Melanoma	79	-	-	-

displays also the highest catalytic activity, while the activity of CA III is the lowest among all active CA isoforms (Mboge et al. 2018). In line with these facts, most of the research related to cytoplasmic CAs in cancer has been focused on CA II as described in more detail further below.

As shown in Figs. 7.1 and 7.5, *CAI* gene transcription is relatively low, reaching TPM values of around 30 in normal colon, B-cells, and T-cells, and is not expressed in their neoplastic counterparts. However, *CAI* expression is increased in acute myeloid leukemia (LAML, TPM 40.57) compared to normal myeloid cells (TPM 7). In spite of this differential expression, GEPIA2-performed Mantel-Cox Log-rank test of meta-data from LAML failed to show a significantly better overall survival in the high *CAI* expression cohort, irrespective of whether cutoff was set to median (50%) or whether cutoff-high was set to 75% and cutoff-low to 25% (Fig. 7.6). Nevertheless, the literature contains dozens of papers dealing with the relationship of *CAI* to cancer. CA I protein expression was demonstrated by immunohistochemistry (IHC) in both normal and malignant endocrine tissue of pancreas, with intense positive staining observed particularly in the cells expressing glucagon (Parkkila et al. 1995b). IHC comparison of CA I distribution in normal large intestine versus colorectal tumors showed high CA I expression in normal colon, decreased intensity in benign lesions, and very weak staining in malignant tumors (Kivela et al. 2001). This finding was confirmed by an independent proteomic study suggesting that downregulation of CA I is an early event in colorectal carcinogenesis (Wang et al. 2012). In contrary, no *CAI* expression-based difference in overall survival was predicted by log-rank test of COAD cohorts from TCGA database. CA I protein was also detected by proteomic methods in sera of patients with non-small cell lung carcinoma (Wang et al. 2016). Noteworthy, sera of patients suffering from both acute myeloid leukemia and chronic lymphocytic leukemia were found to contain CA I (and CA II) autoantibodies (Mentese et al. 2017, 2018). Lakota and colleagues observed elevated CA I autoantibodies in sera of patients with spontaneous regression of tumors developing an aplastic anemia-type syndrome after a high-dose therapy with autologous stem cell transplantation (Skultety et al. 2010; Jankovicova et al. 2013). Silencing of CA I in prostatic (PC3) tumor cells was shown to change the composition of exosomes secreted by these cells indicating their enhanced malignant potential (Banova Vulic et al. 2019). However, due to many open questions and generally inconsistent data, it is currently impossible to make any conclusion on the relationship of CA I to cancer.

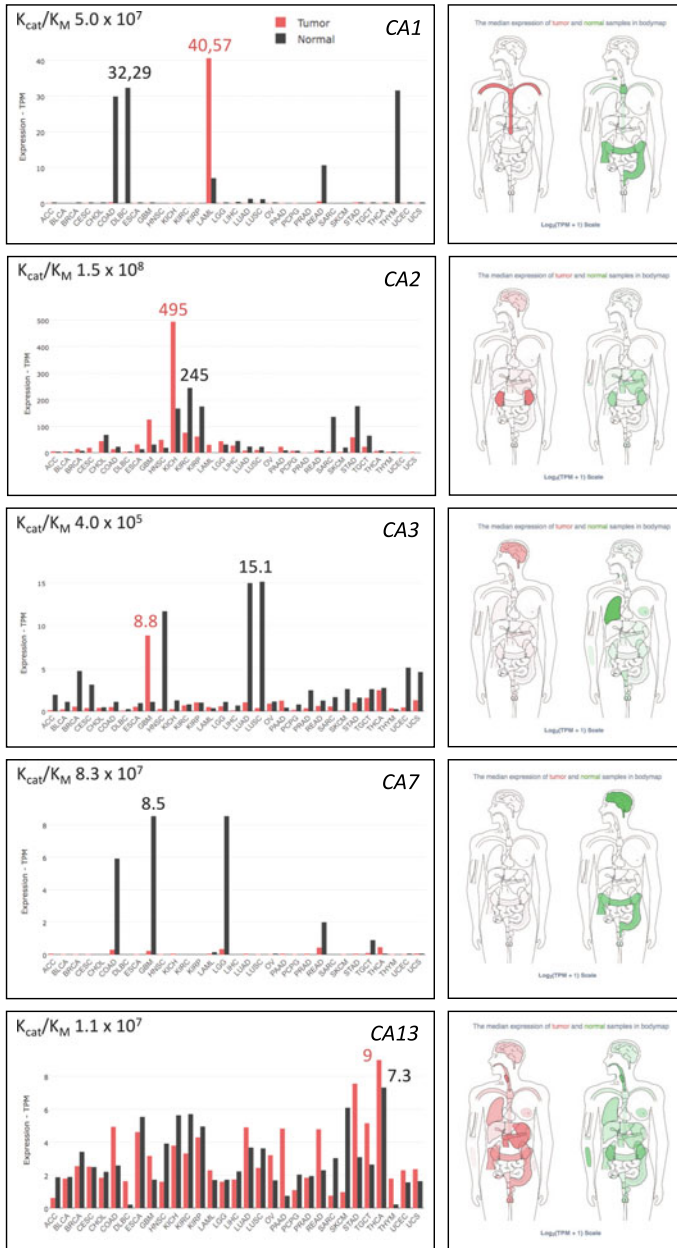


Fig. 7.1 Expression of genes coding for the cytoplasmic carbonic anhydrases in tumors and normal samples. Data extracted from TCGA/GTEX databases were analyzed and converted to graphics using GEPIA2 instrument (Tang et al. 2019). Data in the graphs relate to TPM units and intensities of colors in the bodymaps correspond to Log/TPM+1 Scores in particular tissues. Numbers above the columns highlight the highest TPMs for each CA isoform. K_{cat}/K_M values in the upper left corners inform about the catalytic efficiency of CA isoforms {adopted from (Mboge et al. 2018)}

The *CA3* gene is mostly transcribed in several normal tissues (mainly breast, lung, and uterus), with a TPM value up-to 15 (Fig. 7.1). It is generally not expressed in tumors, except relatively low expression in glioblastoma (GBM, TPM 8.8), which is about 8-times higher than in normal brain (Fig. 7.5). However, this does not translate into the correlation to overall survival of GBM patients, but such correlation exists in LAML (Fig. 7.6). Interestingly, there are only two published studies dealing with CA III expression or function in cancer. Despite metadata showing only very low expression of CA III in liver and liver-derived neoplasms (1 TPM vs 0.1 TPM), an immunohistochemical analysis suggests that CA III is expressed in normal hepatocytes and that it is reduced in hepatocellular carcinoma (Kuo et al. 2003). The second study explored the effects of manipulated CA III expression on invasiveness of HCC (in TCGA abbreviation LIHC) cell line SK-Hep1 (Dai et al. 2008). The authors found that CA III suppression decreases, while CA III overexpression increases cell invasiveness possibly via activation of FAK signaling and extracellular acidification. Taking into account that there is no extension/confirmation of this observation and that CA III activity is very low, biological relevance of that observation remains elusive.

CA7 transcription is detectable only in normal tissues (namely intestine, brain, and testes, TPM up to 8.5) but not in neoplasms (Figs. 7.1 and 7.5). Albeit absent or low, *CA7* levels in tumors derived from these tissues (COAD, READ, GBM, LGG) do not correlate with overall survival in any group of patients. In the published study of Yang and colleagues (Yang et al. 2015), reduced *CA7* mRNA and protein expression in colorectal carcinoma was significantly correlated with poor differentiation, positive lymph node metastasis, advanced TNM stage, and unfavorable clinical outcome. However, no such correlation was confirmed by immunostaining of colorectal carcinoma specimens from an independent cohort of patients, when both extent and intensity of staining were taken into account (Viikila et al. 2016). Thus, further studies are needed to resolve these conflicting results.

CA13 gene transcription is detected both in normal tissues and in tumors, although it appears to be increased in some normal tissues and decreased in other ones when compared to tumors (Figs. 7.1 and 7.5). The significance of this differential expression remains unknown, but taking into account the fact that the levels of *CA13* transcription are rather low (up to 9 TPM), differences are too minor to have a biological relevance. There is only a single paper using immunohistochemistry to detect CA XIII protein expression in colorectal carcinoma (Kummola et al. 2005). The study results suggest that the expression of CA XIII is downregulated in tumor cells compared to the normal tissue, which is actually opposite to RNA-seq data acquired from TCGA database where significant correlation to overall survival was found in KIRC, LAML, LGG, and SKCM.

Lastly, the apparently most important cytoplasmic isoform is encoded by the *CA2* gene. The catalytic activity of CA II is among the highest not only within the CA family but also generally among all known enzymes. Its expression assessed by immunodetection was found to correlate with intracellular CA activity measured in a range of intact human cancer- and fibroblast-derived cells and in their membrane-free lysates. Moreover, genetic knockdown of CA II in HCT116 colon carcinoma

cells demonstrated that majority of intracellular CA activity was attributable to CA II. These data support the view that CA II is a crucial intracellular CA isoenzyme (Hulikova et al. 2014). Studies based on manipulated CA II expression and on use of small molecule inhibitors suggested that CA II activity participates in intracellular pH regulation (irrespective of normal or tumor cell phenotype) through cooperation with ion transporters, namely, by facilitating proton or bicarbonate transport across membranes, or mediating proton diffusion in cytoplasm. Initially, it was proposed that CA II forms a transport metabolon with chloride/bicarbonate exchangers that exploit the CA catalytic activity (Sterling et al. 2001). Later on, this concept was extended to the sodium/proton exchanger NHE1 (Li et al. 2002) and to the sodium/bicarbonate co-transporter (Villafuerte et al. 2014). CA II was also shown to cooperate in a non-catalytic manner with the monocarboxylate transporter MCT1, acting as an antenna collecting and transferring protons to MCT1 in order to facilitate its transport activity (Becker et al. 2005; Noor et al. 2018).

However, these scenarios are partly questioned by the finding of Swietach and colleagues who demonstrated that intracellular CA activity in cancer cell lines does not correlate with resting intracellular pH (pHi), NHE1 flux, or bicarbonate transporter flux measured in these cells, and that proton and bicarbonate fluxes produced by cells over the physiological pHi range are not of sufficient magnitude to require intracellular CA catalysis, with the exception of acid loading by bicarbonate export at high pHi (over 7.4) that is not typical for cancer cells (Hulikova et al. 2014). This study also suggests that high intracellular CA activity (mostly attributable to CA II) is associated with faster and larger pHi oscillations, larger pH-dependent intracellular calcium ion oscillations, and stronger inhibition of mTORC1 pathway in response to extracellular $p\text{CO}_2$ fluctuations (Hulikova et al. 2014). In contrast, pHi of cells exhibiting low intracellular CA activity is less responsive to $p\text{CO}_2$ fluctuations, which might be of key importance for cells' survival especially in tumor tissues with dynamic temporal and/or regional changes of blood flow, delivery of oxygen and nutrients as well as removal of metabolic waste due to aberrant tumor vasculature (Gillies et al. 2018).

Actually, the above-described view can explain why expression of the CA2 gene (as well as the levels of other genes encoding the cytoplasmic CAs with lesser contribution to overall intracellular CA activity) is primarily detected in non-cancerous tissues (with TPM values up to 245) and downregulated in related tumors. In line with this, TCGA/GTEX databases processed by GEPIA2 show that CA II levels are decreased in KIRC, KIRP, SARC, STAD, and TGCT when compared to their normal counterparts. In contrary, CA2 expression is increased in GBM and KICH (with TPM of 126 and 495, see Figs. 7.1 and 7.5). While this increased tumor expression does not predict overall survival of cancer patients in case of GBM and KICH, reduced CA2 transcription is significantly associated with reduced overall survival in patients with KIRC and SARC (Figs. 7.6 and 7.7), but not KIRP, STAD, and TGCT. Interestingly, significantly worse overall survival predicted by GEPIA2 is also linked with decreased CA II levels in COAD (with cutoff-high 75% and cutoff-low 25%) that is principally in line with IHC and proteomic studies of independent patients' cohorts showing that loss of expression of CA II (and CA I) accompanies progression to

malignant phenotype (Kivela et al. 2001; Wang et al. 2012). Moreover, CA II is the most widely distributed isoform in the central nervous system, and its expression was also detected by IHC in different brain tumors (Parkkila et al. 1995a), medulloblastomas and neuroectodermal tumors (Nordfors et al. 2010), hematological malignancies (Leppilampi et al. 2002), esophageal carcinoma (Nortunen et al. 2018), pancreatic tumors (Parkkila et al. 1995b), gastrointestinal stromal tumors (Parkkila et al. 2010; Liu et al. 2013), hepatocellular carcinomas (Kuo et al. 2003), uterine tumors (Hynninen et al. 2012), and urinary bladder cancers (Tachibana et al. 2017). In meningiomas, CA II was found in endothelial cells in association with increasing malignancy grade and tumor proliferation rates (Korhonen et al. 2009). CA II expression also was observed in tumor vessel endothelia of melanoma and esophageal, renal, and lung cancers (Yoshiura et al. 2005).

There are also several papers describing the functional aspects of CA II. It was shown that forced CA II expression in colorectal cancer cells remarkably suppresses tumor cell growth both in vitro and in vivo (Zhou et al. 2013). Similarly, CA II overexpression inhibits cell migration and invasion by reversing EMT in hepatocellular carcinoma cells, while its downregulation promoted invasiveness and metastasis (Zhang et al. 2018). Thus, the link of CA II to neoplastic phenotype is tumor tissue- and cell type-dependent and may also reflect the physiology of tumor microenvironment.

7.3 Expression of Mitochondrial CA Isoforms in Cancer

Mitochondrial CA isoforms are encoded by two phylogenetically-related genes *CA5A* and *CA5B*. Since mitochondria are impermeable to bicarbonate ions, activity of CA VA and CA VB enzymes is required for production of bicarbonate that is utilized by mitochondrial enzymes for metabolic processes, namely, by pyruvate carboxylase for gluconeogenesis and carbamoyl phosphate synthase I for ureagenesis. Targeted disruption of the murine *Car5A* and *Car5B* genes and their double knock-out implicated both enzymes in ammonia detoxication and glucose metabolism (Shah et al. 2013). Despite glucose metabolism being of high importance for tumor biology, so far there are no thorough studies linking *CA5A* and/or *CA5B* to cancers, except a single paper identifying the *CA5A* gene within a signature of genes predicting decreased overall survival in patients with head and neck carcinoma (Bornstein et al. 2016).

Thus, publicly available RNA-seq metadata can provide at least basic insight into possible relationships of *CA5A* and *CA5B* expression to human tumors. GEPIA2 testing showed that *CA5A* gene is transcribed in normal liver (in accord with expectation) at the TPM level of 23.2 and was slightly decreased in liver neoplasms (TPM 16.3). In addition, *CA5A* expression was detected in bile ducts, but not in cholangiocarcinoma (Figs. 7.2 and 7.5). In contrary, *CA5B* is transcribed in many normal tissues (namely in the breast, ovaria, uterus, cervix, testes, TPM up to 9.9) and at lower levels also in the corresponding cancers. The highest *CA5B* expression is

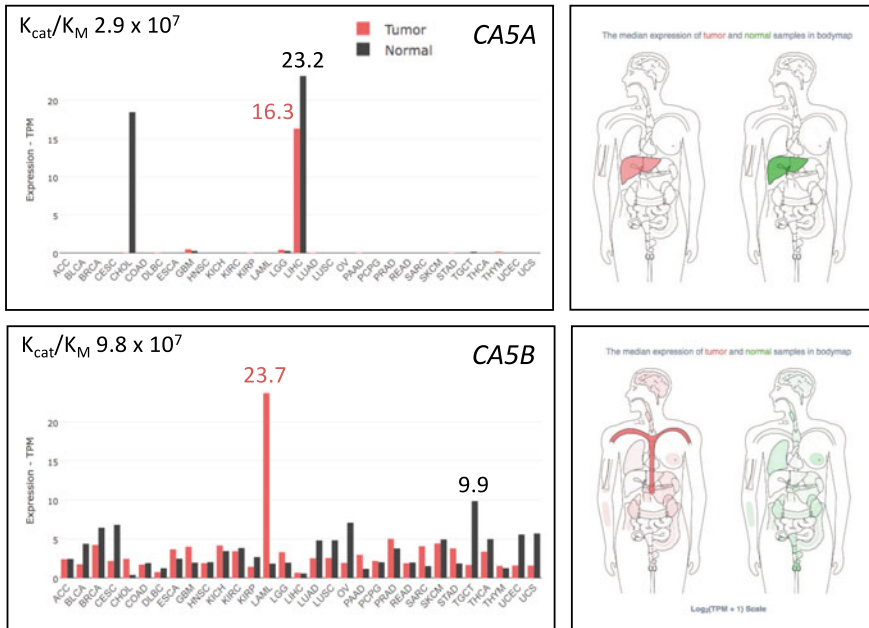


Fig. 7.2 Expression of genes coding for the mitochondrial carbonic anhydrases in tumors and normal samples. Data extracted from TCGA/GTEX databases were analyzed and converted to graphics using GEPIA2 instrument (Tang et al. 2019). Data in the graphs relate to TPM units and intensities of colors in the bodymaps correspond to $\text{Log}/\text{TPM}+1$ Scores in particular tissues. Numbers above the columns highlight the highest TPMs for each CA isoform. $K_{\text{cat}}/K_{\text{M}}$ values in the upper left corners inform about the catalytic efficiency of CA isoforms {adopted from (Mboge et al. 2018)}

present in acute myeloid leukemia (Fig. 7.2), but it has no impact on overall survival (Fig. 7.6). However, these data do not take into consideration the potential role of CA VA/CA VB catalytic activities, which might be involved in adaptation to metabolic demands of tumor cells. Clearly, additional studies are warranted to resolve whether mitochondrial CAs are involved in tumor biology.

7.4 Expression of Membrane-Bound and Secreted CA Isoforms in Cancer

Four membrane-bound isoforms (CA IV, IX, XII, and XIV) and one secreted isoform (CA VI) are active enzymes with the catalytic sites facing the extracellular space. Their catalytic performance is relatively high, with CA IX exhibiting the highest activity (similar to CA II), then followed by CA VI, CA IV, CA XIV, and CA XII, activity of which is approximately 4-times lower than that of CA IX. All these

enzymes appear to support extracellular CO₂ diffusion, and the membrane-bound isoforms also participate in bicarbonate import and proton extrusion.

While CA IV is bound to the plasma membrane by the GPI anchor, three other exofacial CAs are type I membrane proteins, with the N-terminal side at the cell surface and C-terminal side in the cytoplasm (Pastorekova et al. 2004). In addition, CA IX has an extra N-terminal proteoglycan-like domain (PG) linked by the hinge region to the CA domain (Opavsky et al. 1996). This PG domain contains a repetitive stretch of proline-perturbed basic amino acids, and has an intrinsically disordered structure with conformational flexibility that is implicated in non-catalytic functions of CA IX relevant for tumor biology (Zavada et al. 2000; Langella et al. 2018). CA IX isoform was shown to cooperate with extracellular structures of bicarbonate transporters and sodium/proton exchangers facilitating ion transport via its catalytic activity (Morgan et al. 2007; Orłowski et al. 2012; Svastova et al. 2012), and with monocarboxylate transporters MCT1 and MCT4 via a non-catalytic mechanism, in which the PG domain serves as a proton-conducting antenna interacting with MCT4 chaperone CD147 (Jamali et al. 2015; Ames et al. 2018, 2019). Similar model was demonstrated for CA IV, which facilitates lactate export via interaction with chaperons of MCTs (Klier et al. 2014; Forero-Quintero et al. 2019).

TCGA/GTEX metadata-derived expression patterns of the membrane-bound and secreted CAs provided by GEPIA2 instrument are very distinct and remarkable (Figs. 7.3 and 7.5), and generally have a lot of support in the published papers, albeit some previously unknown and potentially interesting connections have also been disclosed as described below.

Noteworthy, the *CA4* gene is mostly expressed in normal tissues, and only occasionally and at a low level in some tumors (Figs. 7.3 and 7.5). The highest TPM values of *CA4* transcription (up to 81.7) are exhibited by normal counterparts of LUAD, LUSC, THCA, BRCA, SARC, DLBC, KIRP, KIRC, KICH, and THYM. However, only KIRC and LUAD show a highly significant correlation between high expression of *CA4* and better overall survival, with hazard risk reduced up to 3-times compared to tumors with low *CA4* (Figs. 7.6 and 7.7). Interestingly, these significant correlations exist independently of whether the analysis includes all *CA4* transcript variants together, or only individual protein-coding transcript variants identified by GEPIA2, namely, *CA4-001*, *CA4-005* (both in KIRC and LUAD), and *CA4-006* (only in KIRC). In addition, both median and quartile cutoffs produced similar probability values.

Experimental data are in agreement with predictions based on bioinformatics. In patients with renal clear cell carcinoma, decreased expression of *CA4* mRNA in tumors was associated with poor survival (Takenawa et al. 1998). Loss of *CA4* was also proposed as a biomarker distinguishing follicular thyroid carcinomas from follicular adenomas (Davidov et al. 2014). *CA4* expression determined by Q PCR was also found to be significantly downregulated in non-small cell lung carcinomas (NSCLC) as well as in six NSCLC-derived cell lines, and lower *CA4* levels were correlated with lymph node metastasis and shorter overall survival (Chen et al. 2017). Importantly, *CA4* was proposed to be a novel tumor suppressor in colorectal cancer (CRC). This proposal was based on the observation that *CA4* gene is silenced in

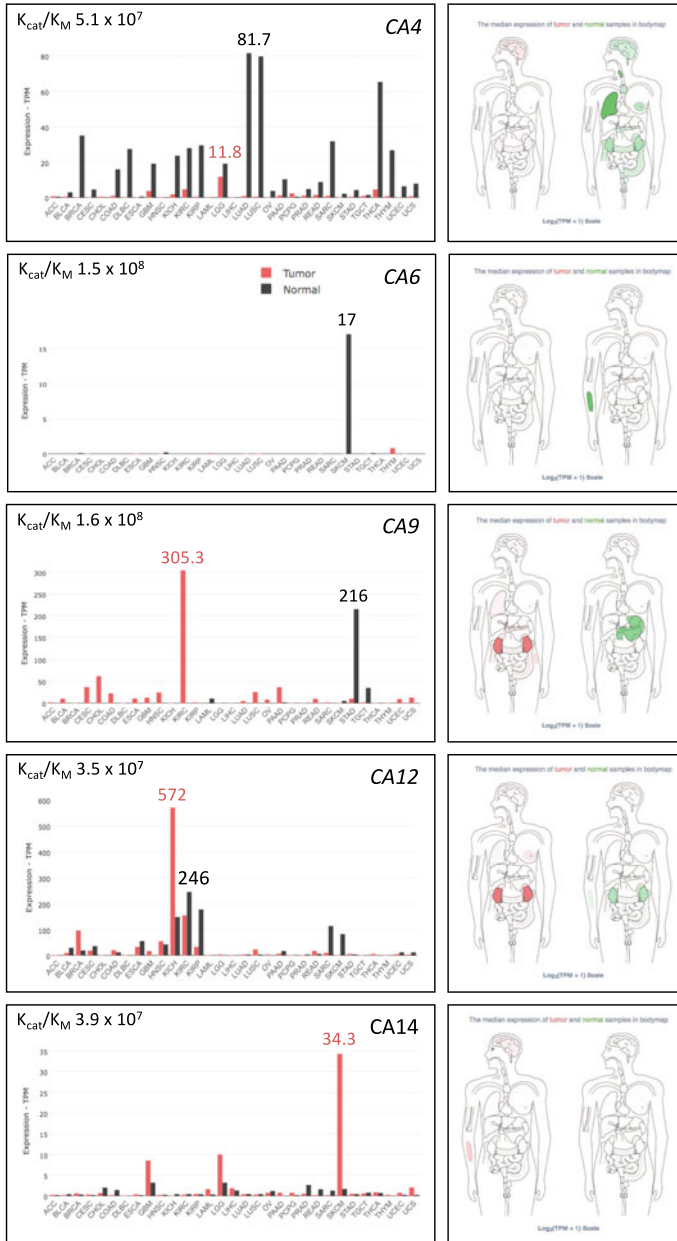


Fig. 7.3 Expression of genes coding for the membrane-bound and secreted carbonic anhydrases in tumors and normal samples. Data extracted from TCGA/GTEX databases were analyzed and converted to graphics using GEPIA2 instrument (Tang et al. 2019). Data in the graphs relate to TPM units and intensities of colors in the bodymaps correspond to Log/TPM+1 Scores in particular tissues. Numbers above the columns highlight the highest TPMs for each CA isoform. K_{cat}/K_M values in the upper left corners inform about the catalytic efficiency of CA isoforms {adopted from (Mboge et al. 2018)}

more than 90% of CRC tumors primarily by the promoter hypermethylation (Zhang et al. 2016). In support of the tumor suppressor concept, re-expression of *CA4* in CRC cells inhibits cell proliferation and induces apoptosis via downregulation of the WNT pathway and degradation of β -catenin (Zhang et al. 2016).

Based on GEPIA2 analysis, *CA6* expression is confined to normal skin (TPM 17, Figs. 7.3 and 7.5), and its reduced level in SKCM predicts worse overall survival (Figs. 7.6 and 7.7). In the published literature, CA VI isoform is primarily known as a component of saliva expressed in serous acinar cells of human salivary glands. Immunostaining revealed its potential diagnostic utility for discrimination of acinic cell carcinoma from mammary analogue secretory carcinoma of the salivary gland (Hsieh et al. 2016). No further information on the relationship of CA VI to cancer is available to date.

In contrast to the other CA genes, *CA9* is predominantly expressed in tumor tissues (CESC, CHOL, COAD, ESCA, GBM, HNSC, KIRC, LUSC, OV, PAAD, READ, UCEC, UCS, TPM up to 305.3) and virtually not in their normal counterparts (Figs. 7.3 and 7.5). According to RNA-seq data from TCGA/GTEX databases, the only normal tissues that exhibit *CA9* transcription levels higher than tumors are stomach (TPM 216) and testes (TPM 35.7), albeit published IHC studies detected CA IX protein also in the epithelia of pancreas, gallbladder, intestinal crypts, and basal skin cells (Pastorekova et al. 1997; Kivela et al. 2001).

In tumors, expression of *CA9* is directed primarily by a HIF-1 transcription factor composed of an oxygen-regulated α subunit and a constitutive β subunit. The α subunit is degraded in proteasome following hydroxylation of its critical prolyl residues and recognition by pVHL tumor suppressor protein acting as E3 ubiquitin ligase, in conditions of normal oxygen delivery (Kaelin and Ratcliffe 2008). When metabolic and proliferative demands of tumor cells exceed the availability of oxygen, which is reduced due to aberrant tumor vasculature, resulting hypoxia inhibits prolyl hydroxylases (including the asparaginyl hydroxylase that hampers HIF- α transcriptional activity) and leads to escape of an α subunit from pVHL recognition and degradation. As a consequence, HIF- α is stabilized and activated, accumulates in the cytoplasm, enters the nucleus, dimerizes with HIF- β , and forms a competent transcription factor that induces expression of hundreds of genes coding for proteins involved in adaptation of tumor cells to hypoxia (Ratcliffe 2013; Semenza 2012). *CA9* is one of the key targets of HIF-1 that drives its transcription in hypoxic tumor cells to a very high magnitude through binding closely to the transcription initiation site of the *CA9* gene (Wykoff et al. 2000). Thus, expression of *CA9* in the majority of tumor types is heterogeneous and regionally distributed in hypoxic or post-hypoxic areas. However, in some cancer entities, *CA9* expression is induced due to activation of pathways driven by oncogenes (such as SRC or RET, Takacova et al. 2010, 2014).

The situation is rather different in KIRC, which express the highest levels of *CA9* transcript as well as CA IX protein (this can be observed both in metadata and IHC studies). These renal clear cell carcinomas are characterized by inactivating mutations of VHL tumor suppressor gene, resulting in constitutive stabilization of HIF- α subunit and sustained activation of the HIF-governed hypoxia-related pathways even in the absence of physiological hypoxia (Wiesener et al. 2001). Since *CA9* is one of the

most highly HIF-1-induced genes, it is expressed in a very high percentage of VHL-defective renal cancer clear cells (Ivanov et al. 1998; Bui et al. 2003; Stillebroer et al. 2010).

When including all four *CA9* alternative transcripts (two protein-coding and two non-translated) into GEPIA2 survival analysis, *CA9* expression shows significant associations with overall survival of patients with several types of cancers, namely, GBM, LUAD, PAAD, and SKCM (Fig. 7.6). However, when solely the full-length transcript *CA9-001* is taken into account, the spectrum of tumor types is extended to KIRC and SARC (Fig. 7.7). *CA9-001* is the only full-length transcript, which is induced by hypoxia and translated to a functional and active CA IX protein (Barathova et al. 2008).

In all mentioned tumor types except KIRC, higher *CA9* expression is related to significantly poorer prognosis (Figs. 7.6 and 7.7). In the case of KIRC, higher *CA9-001* levels (but not total *CA9* levels) show correlation with significantly better overall survival (Figs. 7.6 and 7.7). This appears to be a consequence of a shift from HIF-1 that principally governs the *CA9* transcription in early stages of this disease, towards HIF-2, which drives a kidney cancer progression and determines malignant tumor phenotype in renal clear cell carcinoma, but induces *CA9* to much lower degree (Raval et al. 2005).

Numerous immunohistochemical studies of various tumor tissue specimens suggest significant relationships to clinical variables in a broad spectrum of tumors other than those revealed by GEPIA2 analysis, including BRCA, ESCA, COAD, MESO, OV, READ, STAD, UCEC, etc. {reviewed in (Pastorek and Pastorekova 2015; Pastorekova and Gillies 2019)}. Thorough meta-analysis of the results of 147 publicly available clinical studies (excluding KIRC) reveals a strong significant association between CA IX expression and all survival endpoints: overall, disease-free, loco-regional, disease-specific, metastasis-free, and progression-free survival (van Kuijk et al. 2016). Absence of correlations of TGCT/GTEx *CA9* data to survival in these additional cancer types can be explained by a regionally and temporally heterogeneous, hypoxia-induced *CA9* gene expression pattern, as well as by relatively short half-time of the *CA9* transcripts contrasting with very long half-time of the CA IX protein (Rafajova et al. 2004). Moreover, the CA IX ectodomain can be cleaved by metalloproteinases and released to extracellular space and body fluid, which can affect the CA IX protein expression in tumors (Zatovicova et al. 2005).

In addition to the value of *CA9* gene and/or CA IX protein expression as a surrogate marker of tumor hypoxia {which is the topic of extensive translational research, e.g., for bioimaging (Tafreshi et al. 2012)}, a lot of attention has been paid to the role of CA IX protein in tumor biology. Numerous studies employing genetic manipulation or pharmacologic inhibition of CA IX show that it is a key component of the pH-regulating machinery that enables tumor cells to survive hostile hypoxic and acidotic conditions in the tumor microenvironment and to gain invasiveness and metastatic propensity (Svastova et al. 2004, 2012; Swietach et al. 2009; Chiche et al. 2009; Radvak et al. 2013; Csaderova et al. 2013; Chafe et al. 2015; Swayampakula et al. 2017; Lee et al. 2018; Debreova et al. 2019). In addition, CA IX was found to contribute to stemness and chemoresistance (Ledaki et al. 2015; Vidlickova

et al. 2016; Gibadulinova et al. 2020). Interestingly, CA IX has been associated with invasive phenotype pioneering in a novel and sometimes hostile environment (Lloyd et al. 2016). Moreover, CA IX interacts or communicates with a number of regulatory proteins (besides ion transporters mentioned above), which are involved in important cellular processes, such as β -catenin, $\alpha 2\beta 1$ integrin, CD98hc, MMP14, and other actin-regulatory proteins, hERG1 potassium channel, NCX1 sodium/calcium exchanger, PKA, PI3 kinase, etc. (Svastova et al. 2003; Swayampakula et al. 2017; Debreova et al. 2019; Lastraioli et al. 2019; Liskova et al. 2019; Ditte et al. 2011; Dorai et al. 2005). These interactions can have profound effects on enzymatic and signaling functions of CA IX and also on its accessibility to antibodies and small molecules.

The expression pattern in a broad range of tumors as well as functional involvement of CA IX in tumor biology have raised enormous interest in the development of CA IX-targeting drugs, including inhibitors and specific monoclonal antibodies for immunotherapeutic applications {reviewed in (Neri and Supuran 2011; Oosterwijk-Wakka et al. 2013; Pastorek and Pastorekova 2015; Singh et al. 2018; Pastorekova and Gillies 2019)}. These efforts are continuously ongoing and novel combination strategies are being investigated (McIntyre et al. 2012; Dubois et al. 2013; Boyd et al. 2017; Chafe et al. 2019).

CA12 expression evaluated by GEPIA2 is present in several tumor types including KICH, KIRC, BRCA, and HNSC, but also in the normal counterparts of KIRC, KIRP, KICH, SARC, and SKCM (Figs. 7.3 and 7.5). The highest level is detected in KICH (TPM 572), but the relationship of a high *CA12* level to better overall survival is significant only in SKCM (both for sum of all three protein-coding transcripts and solely for *CA12-001* transcript) (Fig. 7.6). In KIRC, only the *CA12-002* transcript relates to better overall survival while the other transcript variants do not show any significant correlations. Based on the available experimental data, *CA12* expression is regulated by hypoxia, albeit to a lower magnitude than *CA9*, and a direct role of the HIF transcription factor in its regulation has not been clearly defined (Wykoff et al. 2000). However, *CA12* expression appears to be driven by differentiation factors at least in some tumor types (Barnett et al. 2008; Waheed and Sly 2017; Franke et al. 2019). In invasive BRCA, CA XII protein expression assessed by IHC is associated with a lower grade, a lower relapse rate, and a better overall survival (Wykoff et al. 2001; Watson et al. 2003; Li et al. 2019). The link between CA XII expression and better prognosis was demonstrated also in cervical cancer {in association with superior disease-free survival, (Yoo et al. 2010) and resectable NSCLC (Ilie et al. 2011)}. In contrast, IHC staining for CA XII increases with increasing grade of colorectal tumors (Kivela et al. 2000), high CA XII expression is linked to lower survival rate of patients with esophageal squamous cell carcinoma (Ochi et al. 2015). Interestingly, a shorter, alternatively spliced *CA12* transcript has been associated with poor prognosis of patients with diffusely infiltrating astrocytic gliomas (Haapasalo et al. 2008). In cell culture models with genetically manipulated expression, CA XII was shown to participate in pH regulation, tumor growth, and chemoresistance (Chiche et al. 2009; Kopecka et al. 2015). Based on these relationships, also CA XII

is investigated as therapy target for CA inhibitors and monoclonal antibodies (Gondi et al. 2013; Kopecka et al. 2015; Boyd et al. 2017).

Expression of *CA14* has not been experimentally linked to cancer so far, but GEPIA2 analysis disclosed its increased levels in GBM, LGG, and SKCM (TPM up to 34.3), Figs. 7.3 and 7.5. Even more interestingly, higher *CA14* expression (for all transcript variants together and also separately for *CA14-001* and *CA14-005*) shows a significant correlation to worse overall survival of patients with LGG and SKCM, but to better prognosis in case of GBM (Figs. 7.6 and 7.7). This is an unexpected finding that does not have any supporting clinical data in the published literature. Additional links of CA XIV to cancer coming from other publicly available databases are described by Mboge and colleagues (Mboge et al. 2018), but those data also require experimental/clinical validation.

7.5 Expression of Inactive CA Isoforms in Cancer

Three genes coding for inactive CA isoforms, namely, *CA8*, *CA10*, and *CA11* contain mutations affecting the critical residues involved in the coordination of a zinc ion, which is crucial for the CA catalytic activity. This precludes participation of these isoforms in the canonic pH regulation-related metabolons involving bicarbonate transporters and sodium/proton exchangers. However, the non-catalytic cooperation with MCTs can still be feasible and was recently demonstrated for all three proteins CA VIII, CA X, and CA XI (Aspatwar et al. 2019). The authors suggest that the inactive CAs may function as a proton antenna for MCT1, to drive proton-coupled lactate transport across cell membranes.

GEPIA2 shows that the *CA8* gene is differentially transcribed particularly in LAML and TGCT (TPM up to 30.3) where it is strongly decreased in comparison to normal counterparts, but does not show any relationship to overall survival (Figs. 7.4, 7.5, 7.6). On the other hand, *CA8* transcription is elevated in tumor versus normal tissues in UCEC, THYM, OV, PAAD, and PCPG (TPM up to 9.4). Out of these tumor types, only in SKCM higher *CA8* relates to poor prognosis, whereas in UCEC and PAAD (with quartile cutoffs), higher *CA8* expression is linked to better overall survival (Fig. 7.6). This is corresponding to the observation that CA VIII immunopositivity in 13% of astrocytomas and 9% of oligodendrogliomas is associated with more benign behavior (Karjalainen et al. 2018). However, the opposite relationship was found in colorectal and lung carcinomas (Miyaji et al. 2003; Akisawa et al. 2003), and experiments using cell models suggest that CA VIII promotes progression and invasiveness of lung cancer cells (Lu et al. 2004; Ishihara et al. 2006) and growth of colon cancer cells (Nishikata et al. 2007).

CA10 gene expression is increased in PCPG (TPM 19.7) and decreased in GBM, LGG, TGCT, KIRC, KIRP, SARC, and KICH, with no association to overall survival, except a significant correlation of high *CA10* transcription with a better overall survival in LGG patients (Figs. 7.4–7.7). The *CA11* gene expression pattern (tumor vs normal) is similar to *CA10* and includes increased levels in PCPG (TPM 83) and

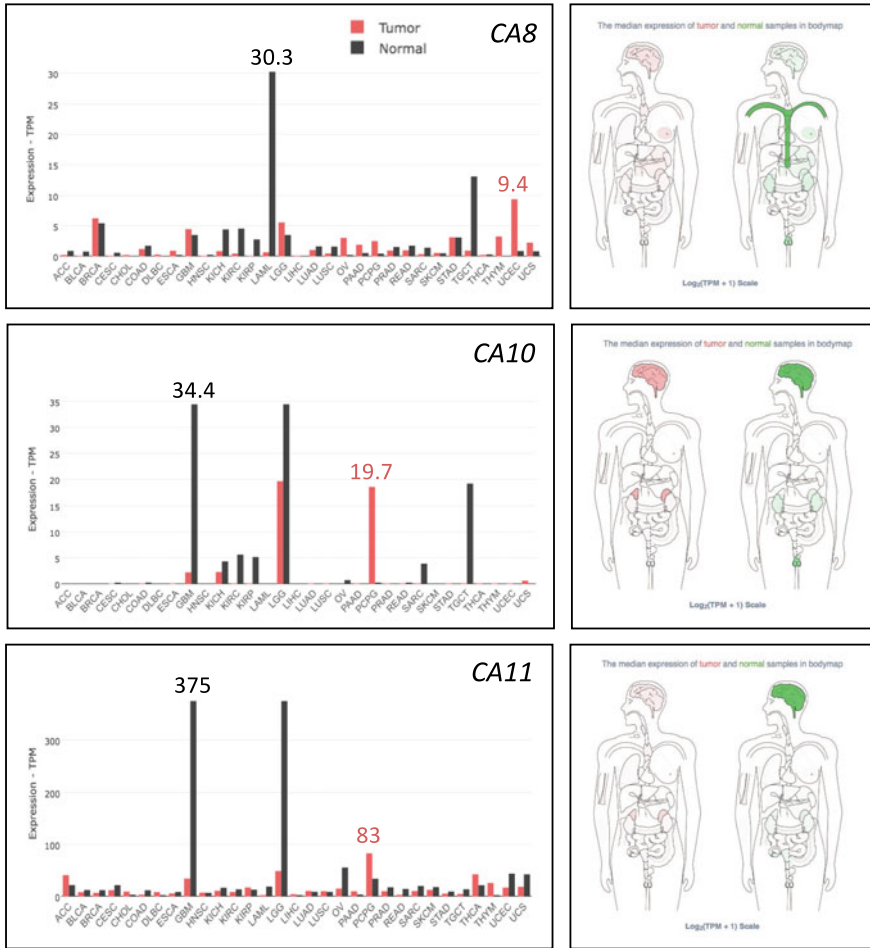


Fig. 7.4 Expression of genes coding for the inactive carbonic anhydrases in tumors and normal samples. Data extracted from TCGA/GTEX databases were analyzed and converted to graphics using GEPIA2 instrument (Tang et al. 2019). Data in the graphs relate to TPM units and intensities of colors in the bodymaps correspond to Log/TPM + 1 Scores in particular tissues. Numbers above the columns highlight the highest TPMs for each CA isoform

decreased levels in GBM, LGG, OV, UCEC, and UCS (Figs. 7.4,7.5). A significant relationship between high *CA11* level and better overall survival was observed only in LGG (Fig. 7.6). In line with this, levels of CA X and CA XI isoforms (that are secreted synaptic proteins inhibiting the growth of glioma cell lines) were reduced in clinical glioma samples and negatively associated with high histological grade (Tao et al. 2019). In preclinical experiments of the same study, *CA11* knockdown promoted cell growth, clone formation and migration, and increased tumor size in xenografted mice. In contrast, CA XI immunostaining was observed in the small

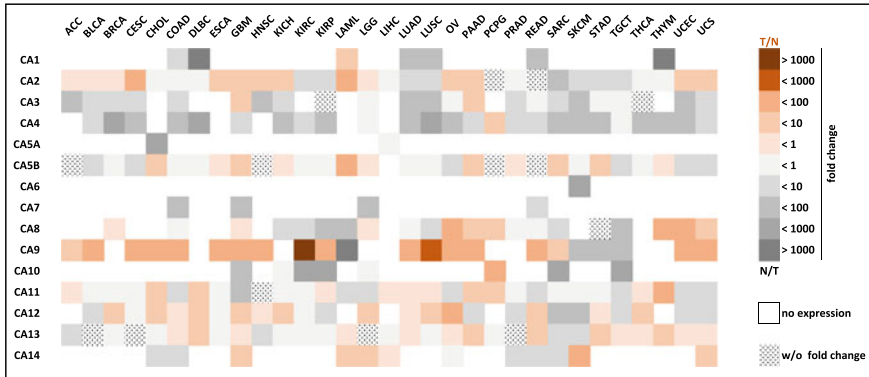


Fig. 7.5 Heatmap visualizing differential expression of the genes coding for CA isoforms in all GEPIA2-analyzed tumors compared to normal samples. Tumor/normal ratio is expressed in color scale shown on the right side, with tumor-related expression illustrated in red shades and normal sample-related expression in grey shades. Lack of expression in both tumor and normal samples is represented by white color and similar expression level in tumor versus normal samples is represented by dotted pattern. The differential expression does not automatically translate to prognostic value as specified in the body text for each CA isoform

fraction of the astrocytic and oligodendroglial tumor specimens, but not in the most benign pilocytic astrocytomas (Karjalainen et al. 2018). These scarce data indicate that our knowledge related to expression and functions of inactive CA isoforms is still limited.

7.6 Carbonic Anhydrase-Related Neoplasms

Taking together all the information extracted from the TCGA/GTEX datasets by the GEPIA2 tool, we can identify few tumor entities that are characterized by expression of carbonic anhydrases, which also show relationship to overall survival (Figs. 7.6 and 7.7).

GBM (Glioblastoma multiforme) is a malignant brain tumor that accounts for about 15% of all brain tumors in adults. GBM patients have a poor prognosis and survive less than 15 months following diagnosis (information extracted from The Cancer Genome Atlas (TCGA), National Cancer Institute at the National Institutes of Health, USA). Recent integrated analysis of genetic alterations in main signaling pathways in tumors suggests that the most frequent alterations in GBM affect the pathways of RTK/Ras, cell cycle, PI3K, and p53 which control cell proliferation and survival and affect diverse aspect of tumor phenotype including metabolism and adaptation to stresses (Sanchez-Vega et al. 2018; Vander Heiden et al. 2009). Moreover, GBM tumors are characterized by hypoxia and acidosis, and thus, it is not surprising that these tumors express several carbonic anhydrases (Figs. 7.5 and 7.6),

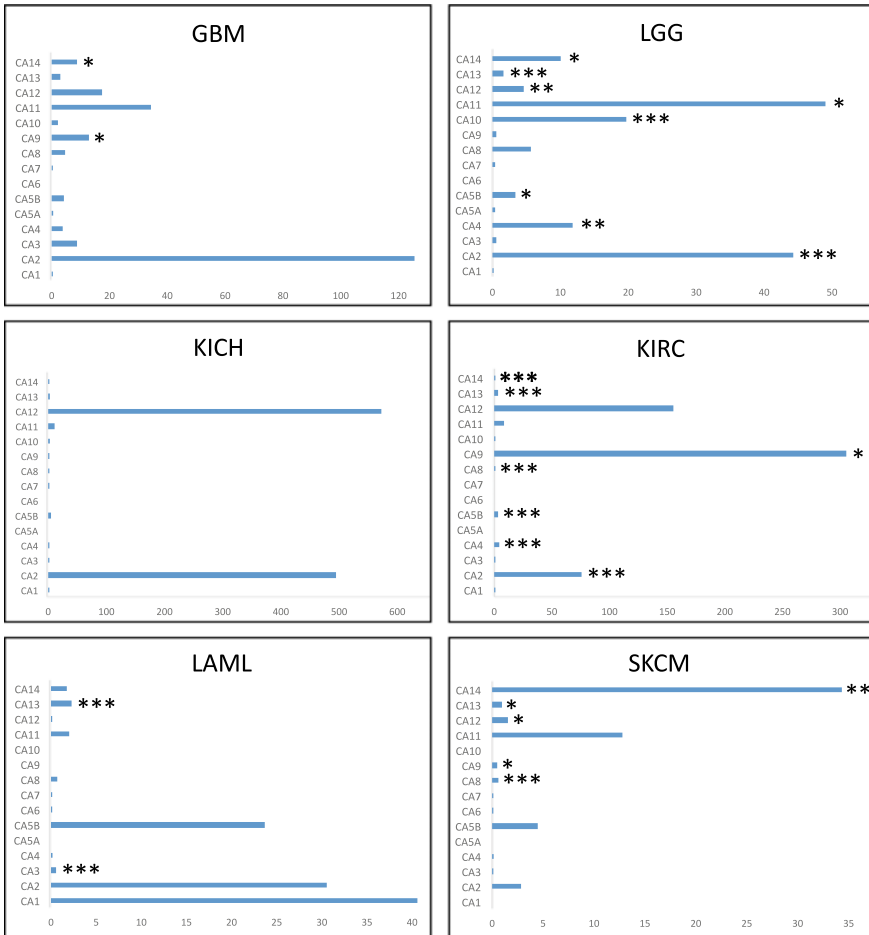


Fig. 7.6 Selection of carbonic anhydrase-related neoplasms with depicted expression levels of CA isoforms (expressed as TPM in the particular cancer type. Graphs do not show expression of the genes in the corresponding normal samples. Data extracted from TCGA/GTEX databases were analyzed using GEPIA2 instrument (Tang et al. 2019). Stars indicate significant relationship to overall survival (* p < 0.05, **p < 0.01, ***p < 0.001) without discriminating positive and negative correlations

of which increased expression of *CA14* is linked to better prognosis, and increased expression of *CA9* is linked to poor prognosis, while the other isoforms' genes (including the highly expressed *CA2*) do not show any significant relationship to overall survival (Fig. 7.6).

LGG (Low grade glioma). Glioma develops in the brain's glial cells, which support the brain's nerve cells and keep them healthy. Tumors are classified into grades I, II, III, or IV based on standards set by the World Health Organization. Lower grade glioma consists of grades II and III. Regardless of grade, growing glioma tumor

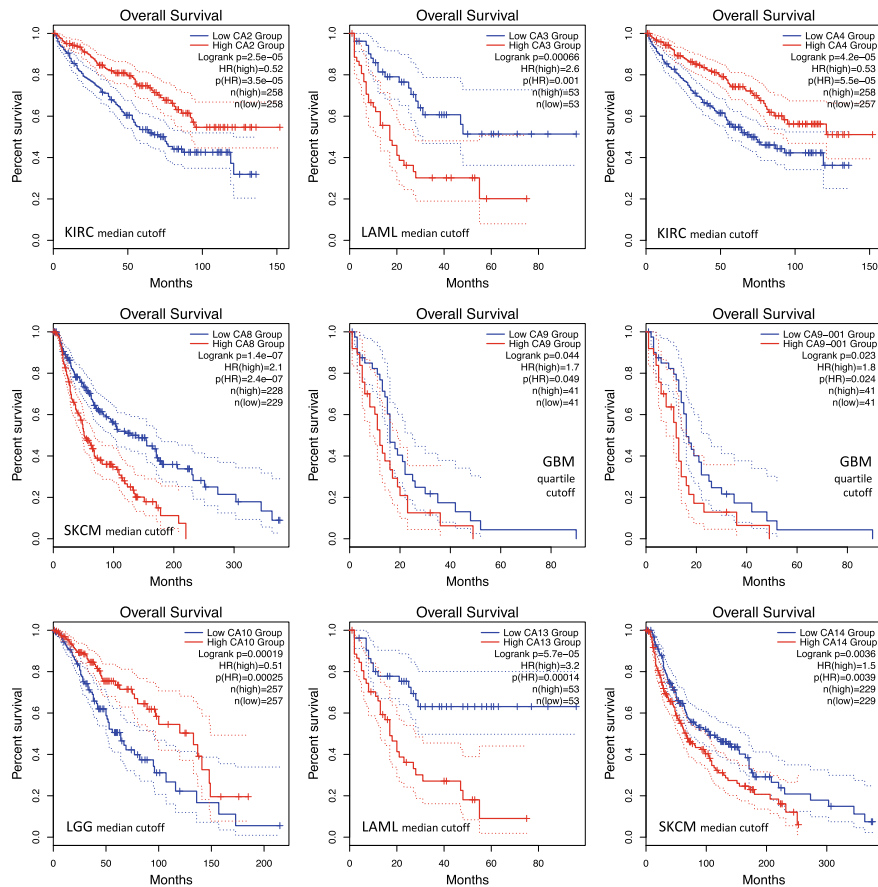


Fig. 7.7 Selected examples of Kaplan-Meier survival plots generated by the analysis of overall survival performed by GEPIA2 instrument (Tang et al. 2019) based on expression of CA genes. GEPIA2 uses Long-rank test (Mantel-Cox test) for hypothesis test. The Cox proportional hazard ratio (HR) and the 95% confidence interval are included in the survival plot

compresses the normal brain tissue, frequently leading to disabling or fatal effects (The Cancer Genome Atlas, NIH, USA). There are three molecular subtypes of LGG with distinct clinical outcomes depending on presence of mutations in *IDH1/IDH2* genes and a co-deletion of a short arm of chromosome 1 and longer arm of chromosome 19. The subtype with the poorest outcomes contains wild-type *IDH* and appears to be a precursor of the more aggressive GBM. *IDH* (isocitrate dehydrogenase) is an $NADP^+$ -dependent enzyme that catalyzes a conversion of isocitrate to α -ketoglutarate and CO_2 . It is a tumor suppressor protein that functions at a crossroad of cellular metabolism in lipid synthesis, cellular defense against oxidative stress, oxidative respiration, and oxygen-sensing signal transduction (Reitman and Yan 2010). *IDH* mutations cause stabilization of HIF transcription factor and hypoxic reprogramming.

Glioma development in IDH-mutant and IDH wild-type tumors is driven by different oncogenic pathways that include mainly RTK/RAS pathway (IDHwt), p53 and Hippo pathways (IDHmut), and Wnt, TGF β , and Hippo (IDHmut-codel), as illustrated in integrative analysis performed by Sanchez-Vega and colleagues (Sanchez-Vega et al. 2018). Interestingly, compared to IDHwt gliomas, IDHmut gliomas have distinct metabolic and microenvironmental characteristics correlated with tumor acidity and hypoxia (Yao et al. 2019). This might be one of the reasons, why LGG display variable expression of CA genes, including *CA2*, *CA4*, *CA5B*, *CA8*, *CA10*, *CA11*, *CA12*, *CA13*, and *CA14* (Fig. 7.5) and all of them, except *CA8*, are significantly associated with prognosis (Fig. 7.6). Tumor-related increases of *CA4*, *CA10*, and *CA11* correlate with better overall survival, increases of *CA2*, *CA5B*, *CA12*, *CA13*, and *CA14* correlate with worse prognosis. Because LGGs are strongly related with carbonic anhydrases, these neoplasms might be a suitable target for anticancer strategies exploiting CA inhibitors.

KICH (Chromophobe renal cell carcinoma) is a rare type cancer that originates in the distal regions of kidney and forms in the cells lining the small tubules, which help filter waste from the blood, making urine. It accounts for 5% of all kidney cancer cases and can have either hereditary or sporadic basis (The Cancer Genome Atlas, NIH, USA). Pathways altered in KICH relate to cell cycle, PI3K, and p53 and often translate to oncogenic metabolism and adaptation to hypoxia and acidosis (Sanchez-Vega et al. 2018; Linehan and Ricketts 2013). Only two CA isoforms show high expression in KICH and decreased expression in the corresponding normal tissues: *CA2* and *CA12*, but none of them is significantly associated with overall survival.

KIRC (Renal cell carcinoma) is the most common type of kidney cancer that forms in the cells lining the small proximal tubules in the kidney, which filter waste from the blood and make urine. When detected early, most cases of KIRC can be treated effectively, but survival rates are low when the cancer has spread from the kidney to other parts of the body. About 92% of KIRC are clear cell carcinoma (The Cancer Genome Atlas, NIH, USA). According to analysis of Sanchez-Vega and colleagues (Sanchez-Vega et al. 2018), altered pathways include RTK/RAS, cell cycle, and PI3K, but the primary genetic event is an inactivating mutation in *VHL* gene, which affects cellular oxygen sensing and leads to constitutive activation of the HIF pathway even in the absence of physiologic hypoxia (Kaelin and Ratcliffe 2008; Wiesener et al. 2001). This also includes metabolic changes associated with poor outcomes. Since *CA9* and *CA12* are upregulated by hypoxia, it is not surprising that these are the main isoforms present in this type of tumor, accompanied by *CA2*. As explained above, due to a HIF-1 to HIF-2 shift in the course of cancer progression, a higher level of HIF-1-regulated *CA9* is associated with a better prognosis, albeit its expression in later stages still remains relatively high and suitable for immunotherapeutic targeting (Bui et al. 2003). *CA12* exhibits a similar relationship, but only when *CA12-002* splicing isoform is tested, otherwise there is no clear relationship to overall survival. Similarly, increased *CA2* expression is associated with a better prognosis, while *CA4* shows a highly significant association with longer overall survival when absent or low (Figs. 7.6 and 7.7).

LAML (Acute myeloid leukemia) is a cancer of the blood and bone marrow, which can quickly worsen and result in death within months, when untreated. Survival decreases with older age because standard treatments are less tolerated (The Cancer Genome Atlas, NIH, USA). LAML cancers carry relatively few mutations compared to other frequently occurring solid tumors. About a half of AMLs include activation of the RTK/RAS pathway, and about one-sixth is affected in the cell cycle and Notch pathways (Sanchez-Vega et al. 2018). *CA1*, *CA2*, and *CA5B* are the most highly expressed CA genes in LAML, but they do not display any link to prognosis in contrast to less expressed *CA3* as well as *CA13*, both being positively associated with poor prognosis (Figs. 7.6 and 7.7).

SKCM (Skin cutaneous melanoma) is a cancer of melanocytes, skin cells that produce melanin. Melanoma is most often discovered because it has metastasized, or spread, to another organ, such as the lymph nodes. There are four major subtypes of cutaneous melanoma: BRAF mutant (most common), RAS mutant, NF1 mutant, and Triple Wild-Type. Mutations in each of the identified driver genes, *BRAF*, *RAS*, and *NF1* lead to uncontrolled cell growth (The Cancer Genome Atlas, NIH, USA). According to integrated analysis of genetic alterations in cancer, RTK/RAS and cell cycle oncogenic pathways predominate in SKCM (Sanchez-Vega et al. 2018). Based on experimental data, hypoxia and acidosis appear to be important components of melanoma progression (Moellering et al. 2008; Marino et al. 2012). Out of CA isoforms, only *CA14* exhibits a tumor-related expression linked to worse prognosis in SKCM (Figs. 7.6 and 7.7). The other CAs (*CA2*, *CA3*, *CA4*, *CA6*, *CA9*, *CA11*, *CA12*, and *CA13*) are expressed at higher levels in normal tissues compared to tumors. In a survival analysis, higher levels of *CA8* and *CA9* predict worse overall survival, while *CA12* and *CA13* show opposite relationships (Fig. 7.6).

Additional CA-related tumor types can be recognized on the basis of immunohistochemical staining of human tumor tissues that were published in hundreds of studies. These include, for example, breast carcinomas that express CA IX as a poor prognostic factor and CA XII as a good prognostic factor; colorectal carcinomas that express CA I, CA II, CA VII, CA XIII (all decreasing as cancer progresses), CA VIII, CA IX, CA XII (increasing with cancer progression); lung carcinomas (mainly NSCLC) expressing CA I and CA IV as good prognostic factors, CA VIII and CA IX as poor prognostic factors, and CA XII as a good prognostic factor (see the references related to the particular CA isoforms).

7.7 Conclusions

Both genomic metadata and immunohistochemical studies discussed here and described elsewhere in the literature indicate that there is virtually no cancer devoid of carbonic anhydrase, apparently because CA-facilitated pH regulation, ion transport, and/or CO₂ diffusion are really fundamental for cell survival, proliferation, and metabolic processes in tumor tissues {see also (Mboge et al. 2018)}. Naturally, histological and mutational diversity combined with all abnormalities characteristic

for malignant cancer, including oncogenic metabolism, aberrant proliferation, deregulated signaling, and adaptations to stresses in tumor microenvironment cause that the expression patterns of diverse CA isoforms in tumor tissues differ from those in normal tissues and are generally very complicated and context-dependent. This complexity of CA isoforms is further elaborated by the differences in the expression dynamics and stability of their transcripts compared to proteins, by the existence of alternative splicing variants of CA transcripts (with only some variants coding for functional proteins), by the posttranslational modifications of CA proteins affecting their functions, subcellular localizations, and regional tissue distribution, etc. Another level of complexity is added by a diversity of CA activities and interactomes. These numerous factors are behind the lack of full agreement between the data from RNA-seq, IHC/proteomic analyses, and clinical parameters. Despite this intricate picture, there are few clearly evident and undisputable relationships between certain CA isoforms and particular tumor types. Out of them, the most prominent position belongs to CA IX, which indicates an aggressive phenotype, poor prognosis, and poor response to therapy in a broad range of tumors (except renal clear cell carcinomas, as explained above), followed by CA XII (in a majority of cases indicating good prognosis), and CA IV that was proposed to be a tumor suppressor. Since these relationships are not new, the bioinformatic data included here can serve to support the existing studies.

In contrast, data mining and their integrated analysis using GEPIA2 instrument brought up very interesting and novel relationships, such as for CA XIV, which has not been previously linked to cancer through other than bioinformatic approaches (Mboge et al. 2018). In this case, but also regarding other *in silico* identified relationships of CAs to cancer, it is clearly evident that the RNA-seq data have to be supplemented and supported by the experimental evidence in order to obtain reliable and clinically useful information. To fulfill such requirement, the field of carbonic anhydrases requires further exploration followed by translation of knowledge to meaningful anticancer strategies.

Acknowledgements The authors would like to thank Prof. Jaromir Pastorek (Biomedical Research Center of the Slovak Academy of Sciences and MABRO, a.s. Bratislava, Slovakia) for the critical reading of the manuscript. The authors would like to thank the TCGA Research Network (<https://www.cancer.gov/tcga>) for providing useful information. The authors' research is supported by grants from: Slovak Research and Development Agency (APVV-19-0098), Slovak Scientific Grant Agency (VEGA 2/0076/20), European Regional Development Fund (University Science Park for Biomedicine in Bratislava, ITMS26240220087), and The George Schwab and Leona Lauder Foundation.

References

- Akisawa Y, Nishimori I, Taniuchi K, Okamoto N, Takeuchi T, Sonobe H, Ohtsuki Y, Onishi S (2003) Expression of carbonic anhydrase-related protein CA-RP VIII in non-small cell lung cancer. *Virchows Arch: Int J Pathol* 442(1):66–70. <https://doi.org/10.1007/s00428-002-0721-y>

- Ames S, Pastorekova S, Becker HM (2018) The proteoglycan-like domain of carbonic anhydrase IX mediates non-catalytic facilitation of lactate transport in cancer cells. *Oncotarget* 9(46):27940–27957. <https://doi.org/10.18632/oncotarget.25371>
- Ames S, Andring JT, McKenna R, Becker HM (2019) CAIX forms a transport metabolon with monocarboxylate transporters in human breast cancer cells. *Oncogene*. <https://doi.org/10.1038/s41388-019-1098-6>
- Aspatwar A, Tolvanen MEE, Schneider HP, Becker HM, Narkilahti S, Parkkila S, Deitmer JW (2019) Catalytically inactive carbonic anhydrase-related proteins enhance transport of lactate by MCT1. *FEBS Open Bio* 9(7):1204–1211. <https://doi.org/10.1002/2211-5463.12647>
- Banova Vulic R, Zduriencikova M, Tyciakova S, Benada O, Dubrovackova M, Lakota J, Skultety L (2019) Silencing of carbonic anhydrase I enhances the malignant potential of exosomes secreted by prostatic tumour cells. *J Cell Mol Med* 23(5):3641–3655. <https://doi.org/10.1111/jcmm.14265>
- Barathova M, Takacova M, Holotnakova T, Gibadulinova A, Ohradanova A, Zatovicova M, Hulikova A, Kopacek J, Parkkila S, Supuran CT, Pastorekova S, Pastorek J (2008) Alternative splicing variant of the hypoxia marker carbonic anhydrase IX expressed independently of hypoxia and tumour phenotype. *Br J Cancer* 98(1):129–136. <https://doi.org/10.1038/sj.bjc.6604111>
- Barnett DH, Sheng S, Charn TH, Waheed A, Sly WS, Lin CY, Liu ET, Katzenellenbogen BS (2008) Estrogen receptor regulation of carbonic anhydrase XII through a distal enhancer in breast cancer. *Can Res* 68(9):3505–3515. <https://doi.org/10.1158/0008-5472.CAN-07-6151>
- Becker HM, Hirnet D, Fecher-Trost C, Sultemeyer D, Deitmer JW (2005) Transport activity of MCT1 expressed in *Xenopus* oocytes is increased by interaction with carbonic anhydrase. *J Biol Chem* 280(48):39882–39889. <https://doi.org/10.1074/jbc.M503081200>
- Bornstein S, Schmidt M, Choonoo G, Levin T, Gray J, Thomas CR Jr, Wong M, McWeeney S (2016) IL-10 and integrin signaling pathways are associated with head and neck cancer progression. *BMC Genomics* 17:38. <https://doi.org/10.1186/s12864-015-2359-6>
- Boyd NH, Walker K, Fried J, Hackney JR, McDonald PC, Benavides GA, Spina R, Audia A, Scott SE, Libby CJ, Tran AN, Bevensee MO, Griguer C, Nozell S, Gillespie GY, Nabors B, Bhat KP, Bar EE, Darley-Usmar V, Xu B, Gordon E, Cooper SJ, Dedhar S, Hjelmeland AB (2017) Addition of carbonic anhydrase 9 inhibitor SLC-0111 to temozolomide treatment delays glioblastoma growth in vivo. *JCI insight* 2(24). <https://doi.org/10.1172/jci.insight.92928>
- Bui MH, Seligson D, Han KR, Pantuck AJ, Dorey FJ, Huang Y, Horvath S, Leibovich BC, Chopra S, Liao SY, Stanbridge E, Lerman MI, Palotie A, Figlin RA, Belldegrun AS (2003) Carbonic anhydrase IX is an independent predictor of survival in advanced renal clear cell carcinoma: implications for prognosis and therapy. *Clin Cancer Res: off J Am Assoc Cancer Res* 9(2):802–811
- Chafe SC, Lou Y, Sceneay J, Vallejo M, Hamilton MJ, McDonald PC, Bennewith KL, Moller A, Dedhar S (2015) Carbonic anhydrase IX promotes myeloid-derived suppressor cell mobilization and establishment of a metastatic niche by stimulating G-CSF production. *Can Res* 75(6):996–1008. <https://doi.org/10.1158/0008-5472.CAN-14-3000>
- Chafe SC, McDonald PC, Saberi S, Nemirovsky O, Venkateswaran G, Burugu S, Gao D, Delaidelli A, Kyle AH, Baker JHE, Gillespie JA, Bashashati A, Minchinton AI, Zhou Y, Shah SP, Dedhar S (2019) Targeting hypoxia-induced carbonic anhydrase IX enhances immune-checkpoint blockade locally and systemically. *Cancer Immunol Res* 7(7):1064–1078. <https://doi.org/10.1158/2326-6066.CIR-18-0657>
- Chen J, Hu L, Zhang F, Wang J, Chen J, Wang Y (2017) Downregulation of carbonic anhydrase IV contributes to promotion of cell proliferation and is associated with poor prognosis in non-small cell lung cancer. *Oncol Lett* 14(4):5046–5050. <https://doi.org/10.3892/ol.2017.6740>
- Chiche J, Ilc K, Laferriere J, Trottier E, Dayan F, Mazure NM, Brahimi-Horn MC, Pouyssegur J (2009) Hypoxia-inducible carbonic anhydrase IX and XII promote tumor cell growth by counteracting acidosis through the regulation of the intracellular pH. *Can Res* 69(1):358–368. <https://doi.org/10.1158/0008-5472.CAN-08-2470>
- Corbet C, Feron O (2017) Tumour acidosis: from the passenger to the driver's seat. *Nat Rev Cancer* 17(10):577–593. <https://doi.org/10.1038/nrc.2017.77>

- Csaderova L, Debreova M, Radvak P, Stano M, Vrestiakova M, Kopacek J, Pastorekova S, Svastova E (2013) The effect of carbonic anhydrase IX on focal contacts during cell spreading and migration. *Front Physiol* 4:271. <https://doi.org/10.3389/fphys.2013.00271>
- Dai HY, Hong CC, Liang SC, Yan MD, Lai GM, Cheng AL, Chuang SE (2008) Carbonic anhydrase III promotes transformation and invasion capability in hepatoma cells through FAK signaling pathway. *Mol Carcinog* 47(12):956–963. <https://doi.org/10.1002/mc.20448>
- Davidov T, Nagar M, Kierson M, Chekmareva M, Chen C, Lu SE, Lin Y, Chernyavsky V, Potdevin L, Arumugam D, Barnard N, Trooskin S (2014) Carbonic anhydrase 4 and crystallin alpha-B immunoreactivity may distinguish benign from malignant thyroid nodules in patients with indeterminate thyroid cytology. *J Surg Res* 190(2):565–574. <https://doi.org/10.1016/j.jss.2014.03.042>
- Debreova M, Csaderova L, Burikova M, Lukacikova L, Kajanova I, Sedlakova O, Kery M, Kopacek J, Zatovicova M, Bizik J, Pastorekova S, Svastova E (2019) CAIX regulates invadopodia formation through both a pH-dependent mechanism and interplay with actin regulatory proteins. *Int J Mol Sci* 20(11). <https://doi.org/10.3390/ijms20112745>
- Ditte P, Dequiedt F, Svastova E, Hulikova A, Ohradanova-Repic A, Zatovicova M, Csaderova L, Kopacek J, Supuran CT, Pastorekova S, Pastorek J (2011) Phosphorylation of carbonic anhydrase IX controls its ability to mediate extracellular acidification in hypoxic tumors. *Can Res* 71(24):7558–7567. <https://doi.org/10.1158/0008-5472.CAN-11-2520>
- Dorai T, Sawczuk IS, Pastorek J, Wiernik PH, Dutcher JP (2005) The role of carbonic anhydrase IX overexpression in kidney cancer. *Eur J Cancer* 41(18):2935–2947. <https://doi.org/10.1016/j.ejca.2005.09.011>
- Dubois L, Peeters SG, van Kuijk SJ, Yaromina A, Lieuwes NG, Saraya R, Biemans R, Rami M, Parvathaneni NK, Vullo D, Vooijs M, Supuran CT, Winum JY, Lambin P (2013) Targeting carbonic anhydrase IX by nitroimidazole based sulfamides enhances the therapeutic effect of tumor irradiation: a new concept of dual targeting drugs. *Radiother Oncol: J Eur Soc Ther Radiol Oncol* 108(3):523–528. <https://doi.org/10.1016/j.radonc.2013.06.018>
- Forero-Quintero LS, Ames S, Schneider HP, Thyssen A, Boone CD, Andring JT, McKenna R, Casey JR, Deitmer JW, Becker HM (2019) Membrane-anchored carbonic anhydrase IV interacts with monocarboxylate transporters via their chaperones CD147 and GP70. *J Biol Chem* 294(2):593–607. <https://doi.org/10.1074/jbc.RA118.005536>
- Frankie CM, Gu VW, Grimm BG, Cassady VC, White JR, Weigel RJ, Kulak MV (2019) TFAP2C regulates carbonic anhydrase XII in human breast cancer. *Oncogene*. <https://doi.org/10.1038/s41388-019-1062-5>
- Gibadulinova A, Bullova P, Strnad H, Pohlodek K, Jurkovicova D, Takacova M, Pastorekova S, Svastova E (2020) CAIX-mediated control of LIN28/let-7 axis contributes to metabolic adaptation of breast cancer cells to hypoxia. *Int J Mol Sci* 21(12):4299. <https://doi.org/10.3390/ijms21124299>
- Gillies RJ, Brown JS, Anderson ARA, Gatenby RA (2018) Eco-evolutionary causes and consequences of temporal changes in intratumoural blood flow. *Nat Rev Cancer* 18(9):576–585. <https://doi.org/10.1038/s41568-018-0030-7>
- Gondi G, Mysliwicz J, Hulikova A, Jen JP, Swietach P, Kremmer E, Zeidler R (2013) Antitumor efficacy of a monoclonal antibody that inhibits the activity of cancer-associated carbonic anhydrase XII. *Can Res* 73(21):6494–6503. <https://doi.org/10.1158/0008-5472.CAN-13-1110>
- Haapasalo J, Hilvo M, Nordfors K, Haapasalo H, Parkkila S, Hyrskyluoto A, Rantala I, Waheed A, Sly WS, Pastorekova S, Pastorek J, Parkkila AK (2008) Identification of an alternatively spliced isoform of carbonic anhydrase XII in diffusely infiltrating astrocytic gliomas. *Neuro Oncol* 10(2):131–138. <https://doi.org/10.1215/15228517-2007-065>
- Hsieh MS, Jeng YM, Jhuang YL, Chou YH, Lin CY (2016) Carbonic anhydrase VI: a novel marker for salivary serous acinar differentiation and its application to discriminate acinic cell carcinoma from mammary analogue secretory carcinoma of the salivary gland. *Histopathology* 68(5):641–647. <https://doi.org/10.1111/his.12792>

- Hulikova A, Aveyard N, Harris AL, Vaughan-Jones RD, Swietach P (2014) Intracellular carbonic anhydrase activity sensitizes cancer cell pH signaling to dynamic changes in CO² partial pressure. *J Biol Chem* 289(37):25418–25430. <https://doi.org/10.1074/jbc.M114.547844>
- Hynninen P, Parkkila S, Huhtala H, Pastorekova S, Pastorek J, Waheed A, Sly WS, Tomas E (2012) Carbonic anhydrase isozymes II, IX, and XII in uterine tumors. *APMIS: Acta Pathol, Microbiol, Et Immunol Scand* 120(2):117–129. <https://doi.org/10.1111/j.1600-0463.2011.02820.x>
- Ilie MI, Hofman V, Ortholan C, Ammadi RE, Bonnetaud C, Havet K, Venissac N, Mouroux J, Mazure NM, Pouyssegur J, Hofman P (2011) Overexpression of carbonic anhydrase XII in tissues from resectable non-small cell lung cancers is a biomarker of good prognosis. *Int J Cancer* 128(7):1614–1623. <https://doi.org/10.1002/ijc.25491>
- Ishihara T, Takeuchi T, Nishimori I, Adachi Y, Minakuchi T, Fujita J, Sonobe H, Ohtsuki Y, Onishi S (2006) Carbonic anhydrase-related protein VIII increases invasiveness of non-small cell lung adenocarcinoma. *Virchows Arch: Int J Pathol* 448(6):830–837. <https://doi.org/10.1007/s00428-006-0199-0>
- Ivanov SV, Kuzmin I, Wei MH, Pack S, Geil L, Johnson BE, Stanbridge EJ, Lerman MI (1998) Down-regulation of transmembrane carbonic anhydrases in renal cell carcinoma cell lines by wild-type von Hippel-Lindau transgenes. *Proc Natl Acad Sci USA* 95(21):12596–12601. <https://doi.org/10.1073/pnas.95.21.12596>
- Jamali S, Klier M, Ames S, Barros LF, McKenna R, Deitmer JW, Becker HM (2015) Hypoxia-induced carbonic anhydrase IX facilitates lactate flux in human breast cancer cells by non-catalytic function. *Sci Rep* 5:13605. <https://doi.org/10.1038/srep13605>
- Jankovicova B, Skultety L, Dubrovcakova M, Stern M, Bilkova Z, Lakota J (2013) Overlap of epitopes recognized by anti-carbonic anhydrase I IgG in patients with malignancy-related aplastic anemia-like syndrome and in patients with aplastic anemia. *Immunol Lett* 153(1–2):47–49. <https://doi.org/10.1016/j.imlet.2013.07.006>
- Kaelin WG Jr, Ratcliffe PJ (2008) Oxygen sensing by metazoans: the central role of the HIF hydroxylase pathway. *Mol Cell* 30(4):393–402. <https://doi.org/10.1016/j.molcel.2008.04.009>
- Karjalainen SL, Haapasalo HK, Aspatwar A, Barker H, Parkkila S, Haapasalo JA (2018) Carbonic anhydrase related protein expression in astrocytomas and oligodendroglial tumors. *BMC Cancer* 18(1):584. <https://doi.org/10.1186/s12885-018-4493-4>
- Kivela A, Parkkila S, Saarnio J, Karttunen TJ, Kivela J, Parkkila AK, Waheed A, Sly WS, Grubb JH, Shah G, Tureci O, Rajaniemi H (2000) Expression of a novel transmembrane carbonic anhydrase isozyme XII in normal human gut and colorectal tumors. *Am J Pathol* 156(2):577–584. [https://doi.org/10.1016/S0002-9440\(10\)64762-1](https://doi.org/10.1016/S0002-9440(10)64762-1)
- Kivela AJ, Saarnio J, Karttunen TJ, Kivela J, Parkkila AK, Pastorekova S, Pastorek J, Waheed A, Sly WS, Parkkila TS, Rajaniemi H (2001) Differential expression of cytoplasmic carbonic anhydrases, CA I and II, and membrane-associated isozymes, CA IX and XII, in normal mucosa of large intestine and in colorectal tumors. *Dig Dis Sci* 46(10):2179–2186. <https://doi.org/10.1023/a:1011910931210>
- Klier M, Andes FT, Deitmer JW, Becker HM (2014) Intracellular and extracellular carbonic anhydrases cooperate non-enzymatically to enhance activity of monocarboxylate transporters. *J Biol Chem* 289(5):2765–2775. <https://doi.org/10.1074/jbc.M113.537043>
- Kopecka J, Campia I, Jacobs A, Frei AP, Ghigo D, Wollscheid B, Riganti C (2015) Carbonic anhydrase XII is a new therapeutic target to overcome chemoresistance in cancer cells. *Oncotarget* 6(9):6776–6793. <https://doi.org/10.18632/oncotarget.2882>
- Korhonen K, Parkkila AK, Helen P, Valimaki R, Pastorekova S, Pastorek J, Parkkila S, Haapasalo H (2009) Carbonic anhydrases in meningiomas: association of endothelial carbonic anhydrase II with aggressive tumor features. *J Neurosurg* 111(3):472–477. <https://doi.org/10.3171/2008.10.17672>
- Kummola L, Hamalainen JM, Kivela J, Kivela AJ, Saarnio J, Karttunen T, Parkkila S (2005) Expression of a novel carbonic anhydrase, CA XIII, in normal and neoplastic colorectal mucosa. *BMC Cancer* 5:41. <https://doi.org/10.1186/1471-2407-5-41>

- Kuo WH, Chiang WL, Yang SF, Yeh KT, Yeh CM, Hsieh YS, Chu SC (2003) The differential expression of cytosolic carbonic anhydrase in human hepatocellular carcinoma. *Life Sci* 73(17):2211–2223. [https://doi.org/10.1016/s0024-3205\(03\)00597-6](https://doi.org/10.1016/s0024-3205(03)00597-6)
- Langella E, Buonanno M, Vullo D, Dathan N, Leone M, Supuran CT, De Simone G, Monti SM (2018) Biochemical, biophysical and molecular dynamics studies on the proteoglycan-like domain of carbonic anhydrase IX. *Cell Mol Life Sci: CMLS* 75(17):3283–3296. <https://doi.org/10.1007/s00018-018-2798-8>
- Lastraioli E, Pillozzi S, Mari A, Tellini R, Duranti C, Baldazzi V, Venturini S, Minervini A, Lapini A, Nesi G, Carini M, Arcangeli A (2019) hERG1 and CA IX expression are associated with disease recurrence in surgically resected clear cell renal carcinoma. *Eur J Surg Oncol*. <https://doi.org/10.1016/j.ejso.2019.10.031>
- Ledaki I, McIntyre A, Wigfield S, Buffa F, McGowan S, Baban D, Li JL, Harris AL (2015) Carbonic anhydrase IX induction defines a heterogeneous cancer cell response to hypoxia and mediates stem cell-like properties and sensitivity to HDAC inhibition. *Oncotarget* 6(23):19413–19427. <https://doi.org/10.18632/oncotarget.4989>
- Lee SH, McIntyre D, Honess D, Hulikova A, Pacheco-Torres J, Cerdan S, Swietach P, Harris AL, Griffiths JR (2018) Carbonic anhydrase IX is a pH-stat that sets an acidic tumour extracellular pH in vivo. *Br J Cancer* 119(5):622–630. <https://doi.org/10.1038/s41416-018-0216-5>
- Leppilampi M, Koistinen P, Savolainen ER, Hannuksela J, Parkkila AK, Niemela O, Pastorekova S, Pastorek J, Waheed A, Sly WS, Parkkila S, Rajaniemi H (2002) The expression of carbonic anhydrase II in hematological malignancies. *Clin Cancer Res: off J Am Assoc Cancer Res* 8(7):2240–2245
- Li X, Alvarez B, Casey JR, Reithmeier RA, Fliegel L (2002) Carbonic anhydrase II binds to and enhances activity of the Na⁺/H⁺ exchanger. *J Biol Chem* 277(39):36085–36091. <https://doi.org/10.1074/jbc.M111952200>
- Linehan WM, Ricketts CJ (2013) The metabolic basis of kidney cancer. *Semin Cancer Biol* 23(1):46–55. <https://doi.org/10.1016/j.semcancer.2012.06.002>
- Liskova V, Hudecova S, Lencesova L, Iuliano F, Sirova M, Ondrias K, Pastorekova S, Krizanova O (2019) Type 1 sodium calcium exchanger forms a complex with carbonic anhydrase IX and via reverse mode activity contributes to pH control in hypoxic tumors. *Cancers* 11(8). <https://doi.org/10.3390/cancers11081139>
- Liu LC, Xu WT, Wu X, Zhao P, Lv YL, Chen L (2013) Overexpression of carbonic anhydrase II and Ki-67 proteins in prognosis of gastrointestinal stromal tumors. *World J Gastroenterol* 19(16):2473–2480. <https://doi.org/10.3748/wjg.v19.i16.2473>
- Li Y, Lei B, Zou J, Wang W, Chen A, Zhang J, Fu Y, Li Z (2019) High expression of carbonic anhydrase 12 (CA12) is associated with good prognosis in breast cancer. *Neoplasma* 66(3):420–426. https://doi.org/10.4149/neo_2018_180819N624
- Lloyd MC, Cunningham JJ, Bui MM, Gillies RJ, Brown JS, Gatenby RA (2016) Darwinian dynamics of intratumoral heterogeneity: not solely random mutations but also variable environmental selection forces. *Can Res* 76(11):3136–3144. <https://doi.org/10.1158/0008-5472.CAN-15-2962>
- Lu SH, Takeuchi T, Fujita J, Ishida T, Akisawa Y, Nishimori I, Kohsaki T, Onishi S, Sonobe H, Ohtsuki Y (2004) Effect of carbonic anhydrase-related protein VIII expression on lung adenocarcinoma cell growth. *Lung Cancer* 44(3):273–280. <https://doi.org/10.1016/j.lungcan.2003.12.011>
- Marino ML, Pellegrini P, Di Lernia G, Djavaheri-Mergny M, Brnjic S, Zhang X, Hagg M, Linder S, Fais S, Codogno P, De Milito A (2012) Autophagy is a protective mechanism for human melanoma cells under acidic stress. *J Biol Chem* 287(36):30664–30676. <https://doi.org/10.1074/jbc.M112.339127>
- Mboge MY, Mahon BP, McKenna R, Frost SC (2018) Carbonic anhydrases: role in pH control and cancer. *Metabolites* 8(1). <https://doi.org/10.3390/metabo8010019>
- McIntyre A, Patiar S, Wigfield S, Li JL, Ledaki I, Turley H, Leek R, Snell C, Gatter K, Sly WS, Vaughan-Jones RD, Swietach P, Harris AL (2012) Carbonic anhydrase IX promotes tumor growth

- and necrosis in vivo and inhibition enhances anti-VEGF therapy. *Clin Cancer Res: off J Am Assoc Cancer Res* 18(11):3100–3111. <https://doi.org/10.1158/1078-0432.CCR-11-1877>
- Mentese A, Fidan E, Alver A, Demir S, Yaman SO, Sumer A, Fidan S, Kavgaci H, Turan I (2017) Detection of autoantibodies against carbonic anhydrase I and II in the plasma of patients with gastric cancer. *Cent-Eur J Immunol* 42(1):73–77. <https://doi.org/10.5114/ceji.2017.67320>
- Mentese A, Erkut N, Demir S, Yaman SO, Sumer A, Erdem M, Alver A, Sonmez MG (2018) Serum carbonic anhydrase I and II autoantibodies in patients with chronic lymphocytic leukaemia. *Cent-Eur J Immunol* 43(3):276–280. <https://doi.org/10.5114/ceji.2018.80046>
- Miyaji E, Nishimori I, Taniuchi K, Takeuchi T, Ohtsuki Y, Onishi S (2003) Overexpression of carbonic anhydrase-related protein VIII in human colorectal cancer. *J Pathol* 201(1):37–45. <https://doi.org/10.1002/path.1404>
- Moellering RE, Black KC, Krishnamurty C, Baggett BK, Stafford P, Rain M, Gatenby RA, Gillies RJ (2008) Acid treatment of melanoma cells selects for invasive phenotypes. *Clin Exp Metas* 25(4):411–425. <https://doi.org/10.1007/s10585-008-9145-7>
- Morgan PE, Pastorekova S, Stuart-Tilley AK, Alper SL, Casey JR (2007) Interactions of transmembrane carbonic anhydrase, CAIX, with bicarbonate transporters. *Am J Physiol Cell Physiol* 293(2):C738–748. <https://doi.org/10.1152/ajpcell.00157.2007>
- Neri D, Supuran CT (2011) Interfering with pH regulation in tumours as a therapeutic strategy. *Nat Rev Drug Discov* 10(10):767–777. <https://doi.org/10.1038/nrd3554>
- Nishikata M, Nishimori I, Taniuchi K, Takeuchi T, Minakuchi T, Kohsaki T, Adachi Y, Ohtsuki Y, Onishi S (2007) Carbonic anhydrase-related protein VIII promotes colon cancer cell growth. *Mol Carcinog* 46(3):208–214. <https://doi.org/10.1002/mc.20264>
- Noor SI, Jamali S, Ames S, Langer S, Deitmer JW, Becker HM (2018) A surface proton antenna in carbonic anhydrase II supports lactate transport in cancer cells. *eLife* 7. <https://doi.org/10.7554/eLife.35176>
- Nordfors K, Haapasalo J, Korja M, Niemela A, Laine J, Parkkila AK, Pastorekova S, Pastorek J, Waheed A, Sly WS, Parkkila S, Haapasalo H (2010) The tumour-associated carbonic anhydrases CA II, CA IX and CA XII in a group of medulloblastomas and supratentorial primitive neuroectodermal tumours: an association of CA IX with poor prognosis. *BMC Cancer* 10:148. <https://doi.org/10.1186/1471-2407-10-148>
- Nortunen M, Huhta H, Helminen O, Parkkila S, Kauppila JH, Karttunen TJ, Saarnio J (2018) Carbonic anhydrases II, IX, and XII in Barrett's esophagus and adenocarcinoma. *Virchows Arch: Int J Pathol* 473(5):567–575. <https://doi.org/10.1007/s00428-018-2424-z>
- Ochi F, Shiozaki A, Ichikawa D, Fujiwara H, Nakashima S, Takemoto K, Kosuga T, Konishi H, Komatsu S, Okamoto K, Kishimoto M, Marunaka Y, Otsuji E (2015) Carbonic anhydrase XII as an independent prognostic factor in advanced esophageal squamous cell carcinoma. *J Cancer* 6(10):922–929. <https://doi.org/10.7150/jca.11269>
- Oosterwijk-Wakka JC, Boerman OC, Mulders PF, Oosterwijk E (2013) Application of monoclonal antibody G250 recognizing carbonic anhydrase IX in renal cell carcinoma. *Int J Mol Sci* 14(6):11402–11423. <https://doi.org/10.3390/ijms140611402>
- Opavsky R, Pastorekova S, Zelnik V, Gibadulinova A, Stanbridge EJ, Zavada J, Kettmann R, Pastorek J (1996) Human MN/CA9 gene, a novel member of the carbonic anhydrase family: structure and exon to protein domain relationships. *Genomics* 33(3):480–487. <https://doi.org/10.1006/geno.1996.0223>
- Orlowski A, De Giusti VC, Morgan PE, Aiello EA, Alvarez BV (2012) Binding of carbonic anhydrase IX to extracellular loop 4 of the NBCe1 Na⁺/HCO³⁻ cotransporter enhances NBCe1-mediated HCO³⁻ influx in the rat heart. *Am J Physiol Cell Physiol* 303(1):C69–80. <https://doi.org/10.1152/ajpcell.00431.2011>
- Parkkila AK, Herva R, Parkkila S, Rajaniemi H (1995a) Immunohistochemical demonstration of human carbonic anhydrase isoenzyme II in brain tumours. *Histochem J* 27(12):974–982
- Parkkila S, Parkkila AK, Juvonen T, Lehto VP, Rajaniemi H (1995b) Immunohistochemical demonstration of the carbonic anhydrase isoenzymes I and II in pancreatic tumours. *Histochem J* 27(2):133–138. <https://doi.org/10.1007/bf00243908>

- Parkkila S, Lasota J, Fletcher JA, Ou WB, Kivela AJ, Nuorva K, Parkkila AK, Ollikainen J, Sly WS, Waheed A, Pastorekova S, Pastorek J, Isola J, Miettinen M (2010) Carbonic anhydrase II: a novel biomarker for gastrointestinal stromal tumors. *Mod Pathol: Off J U S Can Acad Pathol, Inc* 23(5):743–750. <https://doi.org/10.1038/modpathol.2009.189>
- Pastorekova S, Gillies RJ (2019) The role of carbonic anhydrase IX in cancer development: links to hypoxia, acidosis, and beyond. *Cancer Metastasis Rev* 38(1–2):65–77. <https://doi.org/10.1007/s10555-019-09799-0>
- Pastorekova S, Parkkila S, Parkkila AK, Opavsky R, Zelnik V, Saarnio J, Pastorek J (1997) Carbonic anhydrase IX, MN/CA IX: analysis of stomach complementary DNA sequence and expression in human and rat alimentary tracts. *Gastroenterology* 112(2):398–408. <https://doi.org/10.1053/gast.1997.v112.pm9024293>
- Pastorekova S, Parkkila S, Pastorek J, Supuran CT (2004) Carbonic anhydrases: current state of the art, therapeutic applications and future prospects. *J Enzyme Inhib Med Chem* 19(3):199–229. <https://doi.org/10.1080/14756360410001689540>
- Pastorek J, Pastorekova S (2015) Hypoxia-induced carbonic anhydrase IX as a target for cancer therapy: from biology to clinical use. *Semin Cancer Biol* 31:52–64. <https://doi.org/10.1016/j.semcancer.2014.08.002>
- Pastorek J, Pastorekova S, Callebaut I, Mornon JP, Zelnik V, Opavsky R, Zat'ovicova M, Liao S, Portetelle D, Stanbridge EJ et al (1994) Cloning and characterization of MN, a human tumor-associated protein with a domain homologous to carbonic anhydrase and a putative helix-loop-helix DNA binding segment. *Oncogene* 9(10):2877–2888
- Radvak P, Repic M, Svastova E, Takacova M, Csaderova L, Strnad H, Pastorek J, Pastorekova S, Kopacek J (2013) Suppression of carbonic anhydrase IX leads to aberrant focal adhesion and decreased invasion of tumor cells. *Oncol Rep* 29(3):1147–1153. <https://doi.org/10.3892/or.2013.2226>
- Rafajova M, Zatovicova M, Kettmann R, Pastorek J, Pastorekova S (2004) Induction by hypoxia combined with low glucose or low bicarbonate and high posttranslational stability upon reoxygenation contribute to carbonic anhydrase IX expression in cancer cells. *Int J Oncol* 24(4):995–1004
- Ratcliffe PJ (2013) Oxygen sensing and hypoxia signalling pathways in animals: the implications of physiology for cancer. *J Physiol* 591(8):2027–2042. <https://doi.org/10.1113/jphysiol.2013.251470>
- Raval RR, Lau KW, Tran MG, Sowter HM, Mandriota SJ, Li JL, Pugh CW, Maxwell PH, Harris AL, Ratcliffe PJ (2005) Contrasting properties of hypoxia-inducible factor 1 (HIF-1) and HIF-2 in von Hippel-Lindau-associated renal cell carcinoma. *Mol Cell Biol* 25(13):5675–5686. <https://doi.org/10.1128/MCB.25.13.5675-5686.2005>
- Reitman ZJ, Yan H (2010) Isocitrate dehydrogenase 1 and 2 mutations in cancer: alterations at a crossroads of cellular metabolism. *J Natl Cancer Inst* 102(13):932–941. <https://doi.org/10.1093/jnci/djq187>
- Sanchez-Vega F, Mina M, Armenia J, Chatila WK, Luna A, La KC, Dimitriadoy S, Liu DL, Kantheti HS, Saghafinia S, Chakravarty D, Daiyan F, Gao Q, Bailey MH, Liang WW, Foltz SM, Shmulevich I, Ding L, Heins Z, Ochoa A, Gross B, Gao J, Zhang H, Kundra R, Kandoth C, Bahceci I, Dervishi L, Dogrusoz U, Zhou W, Shen H, Shen H, Laird PW, Way GP, Greene CS, Liang H, Xiao Y, Wang C, Iavarone A, Berger AH, Bivona TG, Lazar AJ, Hammer GD, Giordano T, Kwong LN, McArthur G, Huang C, Tward AD, Frederick MJ, McCormick F, Meyerson M, Cancer Genome Atlas Research N, Van Allen EM, Cherniack AD, Ciriello G, Sander C, Schultz N (2018) Oncogenic signaling pathways in the cancer genome atlas. *Cell* 173(2):321–337 e310. <https://doi.org/10.1016/j.cell.2018.03.035>
- Semenza GL (2012) Hypoxia-inducible factors: mediators of cancer progression and targets for cancer therapy. *Trends Pharmacol Sci* 33(4):207–214. <https://doi.org/10.1016/j.tips.2012.01.005>
- Shah GN, Rubbelke TS, Hendin J, Nguyen H, Waheed A, Shoemaker JD, Sly WS (2013) Targeted mutagenesis of mitochondrial carbonic anhydrases VA and VB implicates both enzymes in

- ammonia detoxification and glucose metabolism. *Proc Natl Acad Sci USA* 110(18):7423–7428. <https://doi.org/10.1073/pnas.1305805110>
- Singh S, Lomelino CL, Mboge MY, Frost SC, McKenna R (2018) Cancer drug development of carbonic anhydrase inhibitors beyond the active site. *Molecules* 23(5). <https://doi.org/10.3390/molecules23051045>
- Skultety L, Jankovicova B, Svobodova Z, Mader P, Rezacova P, Dubrovackova M, Lakota J, Bilkova Z (2010) Identification of carbonic anhydrase I immunodominant epitopes recognized by specific autoantibodies which indicate an improved prognosis in patients with malignancy after autologous stem cell transplantation. *J Proteome Res* 9(10):5171–5179. <https://doi.org/10.1021/pr1004778>
- Sterling D, Reithmeier RA, Casey JR (2001) A transport metabolon: functional interaction of carbonic anhydrase II and chloride/bicarbonate exchangers. *J Biol Chem* 276 (51):47886–47894. <https://doi.org/10.1074/jbc.M105959200>
- Stillebroer AB, Mulders PF, Boerman OC, Oyen WJ, Oosterwijk E (2010) Carbonic anhydrase IX in renal cell carcinoma: implications for prognosis, diagnosis, and therapy. *Eur Urol* 58(1):75–83. <https://doi.org/10.1016/j.eururo.2010.03.015>
- Supuran CT (2016) Structure and function of carbonic anhydrases. *Biochem J* 473(14):2023–2032. <https://doi.org/10.1042/BCJ20160115>
- Svastova E, Zilka N, Zat'ovicova M, Gibadulinova A, Ciampor F, Pastorek J, Pastorekova S (2003) Carbonic anhydrase IX reduces E-cadherin-mediated adhesion of MDCK cells via interaction with beta-catenin. *Exp Cell Res* 290(2):332–345. [https://doi.org/10.1016/s0014-4827\(03\)00351-3](https://doi.org/10.1016/s0014-4827(03)00351-3)
- Svastova E, Hulikova A, Rafajova M, Zat'ovicova M, Gibadulinova A, Casini A, Cecchi A, Scoz-zafava A, Supuran CT, Pastorek J, Pastorekova S (2004) Hypoxia activates the capacity of tumor-associated carbonic anhydrase IX to acidify extracellular pH. *FEBS Lett* 577(3):439–445. <https://doi.org/10.1016/j.febslet.2004.10.043>
- Svastova E, Witariski W, Csaderova L, Kosik I, Skvarkova L, Hulikova A, Zatovicova M, Barathova M, Kopacek J, Pastorek J, Pastorekova S (2012) Carbonic anhydrase IX interacts with bicarbonate transporters in lamellipodia and increases cell migration via its catalytic domain. *J Biol Chem* 287(5):3392–3402. <https://doi.org/10.1074/jbc.M111.286062>
- Swayampakula M, McDonald PC, Vallejo M, Coyaud E, Chafe SC, Westerback A, Venkateswaran G, Shankar J, Gao G, Laurent EMN, Lou Y, Bennewith KL, Supuran CT, Nabi IR, Raught B, Dedhar S (2017) The interactome of metabolic enzyme carbonic anhydrase IX reveals novel roles in tumor cell migration and invadopodia/MMP14-mediated invasion. *Oncogene* 36(45):6244–6261. <https://doi.org/10.1038/onc.2017.219>
- Swietach P, Patiar S, Supuran CT, Harris AL, Vaughan-Jones RD (2009) The role of carbonic anhydrase 9 in regulating extracellular and intracellular pH in three-dimensional tumor cell growths. *J Biol Chem* 284(30):20299–20310. <https://doi.org/10.1074/jbc.M109.006478>
- Tachibana H, Gi M, Kato M, Yamano S, Fujioka M, Kakehashi A, Hirayama Y, Koyama Y, Tamada S, Nakatani T, Wanibuchi H (2017) Carbonic anhydrase 2 is a novel invasion-associated factor in urinary bladder cancers. *Cancer Sci* 108(3):331–337. <https://doi.org/10.1111/cas.13143>
- Tafreshi NK, Bui MM, Bishop K, Lloyd MC, Enkemann SA, Lopez AS, Abrahams D, Carter BW, Vagner J, Grobmyer SR, Gillies RJ, Morse DL (2012) Noninvasive detection of breast cancer lymph node metastasis using carbonic anhydrases IX and XII targeted imaging probes. *Clin Cancer Res*: off J Am Assoc Cancer Res 18(1):207–219. <https://doi.org/10.1158/1078-0432.CCR-11-0238>
- Takacova M, Holotnakova T, Barathova M, Pastorekova S, Kopacek J, Pastorek J (2010) Src induces expression of carbonic anhydrase IX via hypoxia-inducible factor 1. *Oncol Rep* 23(3):869–874
- Takacova M, Bullova P, Simko V, Skvarkova L, Poturnajova M, Feketeova L, Babal P, Kivela AJ, Kuopio T, Kopacek J, Pastorek J, Parkkila S, Pastorekova S (2014) Expression pattern of carbonic anhydrase IX in Medullary thyroid carcinoma supports a role for RET-mediated activation of the HIF pathway. *Am J Pathol* 184(4):953–965. <https://doi.org/10.1016/j.ajpath.2014.01.002>
- Takenawa J, Kaneko Y, Kishishita M, Higashitsuji H, Nishiyama H, Terachi T, Arai Y, Yoshida O, Fukumoto M, Fujita J (1998) Transcript levels of aquaporin 1 and carbonic anhydrase IV as predictive indicators for prognosis of renal cell carcinoma patients after nephrectomy. *Int J*

- Cancer 79(1):1–7. [https://doi.org/10.1002/\(sici\)1097-0215\(19980220\)79:1%3c1::aid-ijc1%3e3.0.co;2-5](https://doi.org/10.1002/(sici)1097-0215(19980220)79:1%3c1::aid-ijc1%3e3.0.co;2-5)
- Tang Z, Kang B, Li C, Chen T, Zhang Z (2019) GEPIA2: an enhanced web server for large-scale expression profiling and interactive analysis. *Nucleic Acids Res* 47(W1):W556–W560. <https://doi.org/10.1093/nar/gkz430>
- Tao B, Ling Y, Zhang Y, Li S, Zhou P, Wang X, Li B, Jun Z, Zhang W, Xu C, Shi J, Wang L, Zhang W, Li S (2019) CA10 and CA11 negatively regulate neuronal activity-dependent growth of gliomas. *Mol Oncol* 13(5):1018–1032. <https://doi.org/10.1002/1878-0261.12445>
- Tureci O, Sahin U, Vollmar E, Siemer S, Gottert E, Seitz G, Parkkila AK, Shah GN, Grubb JH, Pfreundschuh M, Sly WS (1998) Human carbonic anhydrase XII: cDNA cloning, expression, and chromosomal localization of a carbonic anhydrase gene that is overexpressed in some renal cell cancers. *Proc Natl Acad Sci USA* 95(13):7608–7613. <https://doi.org/10.1073/pnas.95.13.7608>
- Vander Heiden MG, Cantley LC, Thompson CB (2009) Understanding the Warburg effect: the metabolic requirements of cell proliferation. *Science* 324(5930):1029–1033. <https://doi.org/10.1126/science.1160809>
- van Kuijk SJ, Yaromina A, Houben R, Niemans R, Lambin P, Dubois LJ (2016) Prognostic Significance of Carbonic Anhydrase IX Expression in Cancer Patients: A Meta-Analysis. *Front Oncol* 6:69. <https://doi.org/10.3389/fonc.2016.00069>
- Vidlickova I, Dequiedt F, Jelenska L, Sedlakova O, Pastorek M, Stuchlik S, Pastorek J, Zatovicova M, Pastorekova S (2016) Apoptosis-induced ectodomain shedding of hypoxia-regulated carbonic anhydrase IX from tumor cells: a double-edged response to chemotherapy. *BMC Cancer* 16:239. <https://doi.org/10.1186/s12885-016-2267-4>
- Viikila P, Kivela AJ, Mustonen H, Koskensalo S, Waheed A, Sly WS, Pastorek J, Pastorekova S, Parkkila S, Haglund C (2016) Carbonic anhydrase enzymes II, VII, IX and XII in colorectal carcinomas. *World J Gastroenterol* 22(36):8168–8177. <https://doi.org/10.3748/wjg.v22.i36.8168>
- Villafuerte FC, Swietach P, Youm JB, Ford K, Cardenas R, Supuran CT, Cobden PM, Rohling M, Vaughan-Jones RD (2014) Facilitation by intracellular carbonic anhydrase of Na^+ - HCO_3^- -co-transport but not Na^+/H^+ exchange activity in the mammalian ventricular myocyte. *J Physiol* 592(5):991–1007. <https://doi.org/10.1113/jphysiol.2013.265439>
- Waheed A, Sly WS (2017) Carbonic anhydrase XII functions in health and disease. *Gene* 623:33–40. <https://doi.org/10.1016/j.gene.2017.04.027>
- Wang N, Chen Y, Han Y, Zhao Y, Liu Y, Guo K, Jiang Y (2012) Proteomic analysis shows down-regulations of cytoplasmic carbonic anhydrases, CAI and CAII, are early events of colorectal carcinogenesis but are not correlated with lymph node metastasis. *Tumori* 98(6):783–791. <https://doi.org/10.1700/1217.13504>
- Wang DB, Lu XK, Zhang X, Li ZG, Li CX (2016) Carbonic anhydrase 1 is a promising biomarker for early detection of non-small cell lung cancer. *Tumour Biol: J Int Soc Oncodevelopmental Biol Med* 37(1):553–559. <https://doi.org/10.1007/s13277-015-3834-z>
- Watson PH, Chia SK, Wykoff CC, Han C, Leek RD, Sly WS, Gatter KC, Ratcliffe P, Harris AL (2003) Carbonic anhydrase XII is a marker of good prognosis in invasive breast carcinoma. *Br J Cancer* 88(7):1065–1070. <https://doi.org/10.1038/sj.bjc.6600796>
- Wiesener MS, Munchenhagen PM, Berger I, Morgan NV, Roigas J, Schwiertz A, Jurgensen JS, Gruber G, Maxwell PH, Loning SA, Frei U, Maher ER, Groner HJ, Eckardt KU (2001) Constitutive activation of hypoxia-inducible genes related to overexpression of hypoxia-inducible factor-1alpha in clear cell renal carcinomas. *Can Res* 61(13):5215–5222
- Wykoff CC, Beasley N, Watson PH, Campo L, Chia SK, English R, Pastorek J, Sly WS, Ratcliffe P, Harris AL (2001) Expression of the hypoxia-inducible and tumor-associated carbonic anhydrases in ductal carcinoma in situ of the breast. *Am J Pathol* 158(3):1011–1019. [https://doi.org/10.1016/S0002-9440\(10\)64048-5](https://doi.org/10.1016/S0002-9440(10)64048-5)
- Wykoff CC, Beasley NJ, Watson PH, Turner KJ, Pastorek J, Sibtain A, Wilson GD, Turley H, Talks KL, Maxwell PH, Pugh CW, Ratcliffe PJ, Harris AL (2000) Hypoxia-inducible expression of tumor-associated carbonic anhydrases. *Can Res* 60(24):7075–7083

- Yang GZ, Hu L, Cai J, Chen HY, Zhang Y, Feng D, Qi CY, Zhai YX, Gong H, Fu H, Cai QP, Gao CF (2015) Prognostic value of carbonic anhydrase VII expression in colorectal carcinoma. *BMC Cancer* 15:209. <https://doi.org/10.1186/s12885-015-1216-y>
- Yao J, Chakhoyan A, Nathanson DA, Yong WH, Salamon N, Raymond C, Mareninov S, Lai A, Nghiemphu PL, Prins RM, Pope WB, Everson RG, Liau LM, Cloughesy TF, Ellingson BM (2019) Metabolic characterization of human IDH mutant and wild type gliomas using simultaneous pH- and oxygen-sensitive molecular MRI. *Neuro Oncol.* <https://doi.org/10.1093/neuonc/noz078>
- Yoo CW, Nam BH, Kim JY, Shin HJ, Lim H, Lee S, Lee SK, Lim MC, Song YJ (2010) Carbonic anhydrase XII expression is associated with histologic grade of cervical cancer and superior radiotherapy outcome. *Radiat Oncol* 5:101. <https://doi.org/10.1186/1748-717X-5-101>
- Yoshiura K, Nakaoka T, Nishishita T, Sato K, Yamamoto A, Shimada S, Saida T, Kawakami Y, Takahashi TA, Fukuda H, Imajoh-Ohmi S, Oyaizu N, Yamashita N (2005) Carbonic anhydrase II is a tumor vessel endothelium-associated antigen targeted by dendritic cell therapy. *Clin Cancer Res: off J Am Assoc Cancer Res* 11(22):8201–8207. <https://doi.org/10.1158/1078-0432.CCR-05-0816>
- Zatovicova M, Sedlakova O, Svastova E, Ohradanova A, Ciampor F, Arribas J, Pastorek J, Pastorekova S (2005) Ectodomain shedding of the hypoxia-induced carbonic anhydrase IX is a metalloprotease-dependent process regulated by TACE/ADAM17. *Br J Cancer* 93(11):1267–1276. <https://doi.org/10.1038/sj.bjc.6602861>
- Zavada J, Zavadova Z, Pastorek J, Biesova Z, Jezek J, Velek J (2000) Human tumour-associated protein MN/CA IX: identification of M75 epitope and of the region mediating cell adhesion. *Br J Cancer* 82(11):1808–1813. <https://doi.org/10.1054/bjoc.2000.1111>
- Zhang J, Tsoi H, Li X, Wang H, Gao J, Wang K, Go MY, Ng SC, Chan FK, Sung JJ, Yu J (2016) Carbonic anhydrase IV inhibits colon cancer development by inhibiting the Wnt signalling pathway through targeting the WTAP-WT1-TBL1 axis. *Gut* 65(9):1482–1493. <https://doi.org/10.1136/gutjnl-2014-308614>
- Zhang C, Wang H, Chen Z, Zhuang L, Xu L, Ning Z, Zhu Z, Wang P, Meng Z (2018) Carbonic anhydrase 2 inhibits epithelial-mesenchymal transition and metastasis in hepatocellular carcinoma. *Carcinogenesis* 39(4):562–570. <https://doi.org/10.1093/carcin/bgx148>
- Zhou R, Huang W, Yao Y, Wang Y, Li Z, Shao B, Zhong J, Tang M, Liang S, Zhao X, Tong A, Yang J (2013) CA II, a potential biomarker by proteomic analysis, exerts significant inhibitory effect on the growth of colorectal cancer cells. *Int J Oncol* 43(2):611–621. <https://doi.org/10.3892/ijo.2013.1972>

Chapter 8

Carbonic Anhydrase IX Interactome and the Regulation of Cancer Progression



Mridula Swayampakula, Geetha Venkateswaran, Paul C. McDonald, and Shoukat Dedhar

Abstract Solid tumours are characterized by poor vasculature, which presents a hypoxic and nutrient-deprived environment for cancer cells. To adapt and survive in these conditions, cancer cells undergo metabolic rewiring to actively acquire and utilize nutrients. Efficient pH regulatory mechanisms establish an alkaline intracellular and acidic extracellular pH that is favourable for tumour progression. A major player in this pH regulatory mechanism is carbonic anhydrase IX (CAIX), a metalloenzyme that mediates the reversible hydration of carbon dioxide. CAIX is expressed in several solid tumours and is a marker of poor prognosis and response to therapy. Multiple pre-clinical studies have elucidated the role of CAIX in promoting various stages of tumour progression. We recently performed an unbiased proteomic screen to identify the interactome of CAIX using proximity-dependent biotin identification (BioID) technique. In this chapter, we illustrate a comprehensive analysis of the CAIX interactome by classifying the interactors based on cellular functions. Furthermore, we discuss the role of some of these interactions that are involved in the metastatic cascade and metabolic adaptation of cancer cells.

Keywords Carbonic anhydrase IX · Hypoxia · Interactome · pH regulation · Metastatic cascade · Cell migration · Cell–cell adhesion · Cell invasion · Combination therapy · MMP14 · Integrins · Amino acid transporters

M. Swayampakula · G. Venkateswaran · P. C. McDonald · S. Dedhar (✉)
Department of Integrative Oncology, BC Cancer Research Centre, Vancouver, BC V5Z 1L3,
Canada
e-mail: sdedhar@bccrc.ca

S. Dedhar
Department of Biochemistry and Molecular Biology, University of British Columbia, Vancouver,
BC V6T 1Z3, Canada

G. Venkateswaran · S. Dedhar
Department of Interdisciplinary Oncology, University of British Columbia, Vancouver, BC V6T
1Z3, Canada

8.1 Tumour Microenvironment and Hypoxia

With over 250 different types of clinical forms, cancer is one of the leading causes of mortality in the world (Hassanpour and Dehghani 2017). In tumours, the stroma (supportive tissue) surrounding cancer cells is made up of a complex network of non-malignant cells such as fibroblasts, endothelial and immune cells in an environment with fluctuating levels of oxygen and nutrients. The complex nature of the interplay between the stromal cells and the cancer cells results in the release of myriad of secreted factors such as cytokines, chemokines, extracellular matrix (ECM) components and matrix modulating proteins. The generation of tumour promoting and tumour suppressing signals by various components of the stroma and cancer cells define the nature of the tumour microenvironment and consequently, decide the fate of tumour progression.

One of the features of a solid tumour microenvironment is the presence of an irregular, leaky network of tumour vasculature with poor coverage that creates regions of hypoxia and nutrient deficiency within the proliferating tumour core. These hypoxic tumour cells adapt by turning on the hypoxia-induced transcription factor Hif1, the master regulator of the hypoxic tumour response (Lendahl et al. 2009). Hif1 contains an oxygen-sensitive α subunit and a constitutively expressed β subunit. Whereas in normoxia, the Hif1 α subunit is marked for degradation by pVHL (the Von Hippel-Lindau factor) tumour suppressor protein, in hypoxia the Hif1 α remains stable and translocates to the nucleus to form a heterodimer with Hif1 β (otherwise known as ARNT) to form a transcriptionally active Hif1 (Haase 2006). In hypoxia, Hif1 modulates energy metabolism, ion-transport, cellular pH maintenance, angiogenesis, epithelial-mesenchymal-transition (EMT), cell migration and invasion.

Hypoxic tumour cells undergo a metabolic shift (Warburg effect) to utilize glycolysis instead of oxidative phosphorylation as their primary source of energy. Hif-induced upregulation of metabolic proteins such as Glucose transporter 1 (GLUT1), Lactate dehydrogenase A (LDHA) and Pyruvate dehydrogenase kinase 1 (PDK1) not only enhances the entry of glucose into the glycolytic pathway but also suppresses the entry of acetyl-CoA into the TCA cycle (Kim et al. 2006) (Fig. 8.1A). This increase in glycolysis leads to the production of large amounts of acidic metabolic by-products such as carbon dioxide (CO_2), lactate and proton (H^+) that must be eliminated from the cells to prevent the development of fatal, acidic intracellular pH (pH_i). While the excess lactate and H^+ are extruded out of the cells by the monocarboxylate transporter, MCT4 and the Na^+ - H^+ exchanger (NHE1), respectively, leading to the generation of acidic extracellular pH (pH_e), Hif1-regulated carbonic anhydrase IX (CAIX) catalyses the hydration of membrane-permeant CO_2 to bicarbonate (HCO_3^-) and H^+ . This activity of CAIX enables the maintenance of a steep efflux gradient causing the continual elimination of the intracellular CO_2 . Furthermore, the H^+ production lowers the pH_e , while bicarbonate transporters such as the Cl^- - HCO_3^- anion exchanger (AE2) and the Na^+ - HCO_3^- co-transporter (NBC) recaptures the HCO_3^- into the cell to maintain a slightly alkaline pH_i (Fig. 8.1A). Consequently, the hypoxic tumour pH_i is maintained at ~ 7.3 – 7.6 while the pH_e is

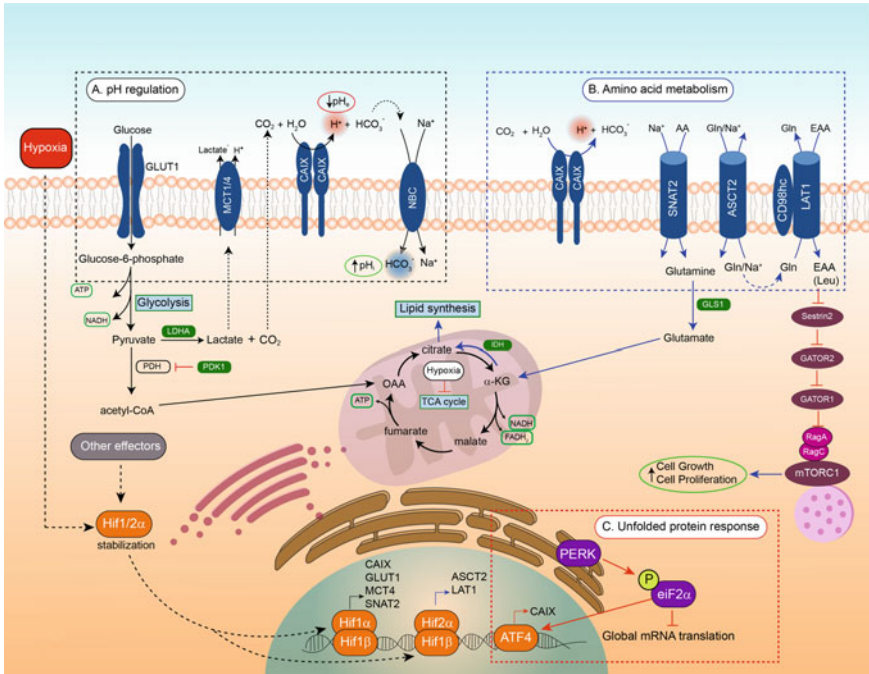


Fig. 8.1 Adaptive cellular responses to hypoxia via (A) pH regulation: Hypoxia induces Hif1 stabilization (<2% O₂) resulting in the transcriptional activation of several genes such as GLUT1, MCT1/4, NBC, LDHA and PDK1. As a consequence, cells undergo a metabolic shift to engage glycolysis and repress TCA cycle, increasing the production of lactate, H⁺ and CO₂. MCT1/4 eliminates the H⁺ from the intracellular space while CAIX vitally contributes to the elimination of CO₂ by hydrating it to HCO₃⁻ and H⁺. While the H⁺ continually acidifies the extracellular space, the HCO₃⁻ is transported into the cells through bicarbonate transporters such as NBCs to maintain slightly alkaline pH_i. The acidic pH_e promotes tumour invasion and therapy resistance while the alkaline pH_i promotes tumour cell survival. **(B) Amino acid metabolism:** Hypoxic cells also undergo metabolic reprogramming to favour amino acid metabolism such as glutamine. Under low amino acid conditions and hypoxia, cells recruit transporters such as SNAT2 and ASCT2 to acquire glutamine. The glutamine is metabolized to α-KG, which undergoes reductive carboxylation to produce citrate. Citrate is utilized for fatty acid synthesis and support cell proliferation. Alternatively, hypoxic cells can utilize the intracellular glutamine for importing EAA such as leucine, by coupling the transport activity of ASCT2 with LAT1. The imported leucine binds to a leucine sensor, Sestrin2, removing its inhibitory effect on the RagA/B and activates mTORC1. The activated mTORC1 mediates downstream effects such as promoting protein translation and cell proliferation. **(C) Unfolded protein response:** Extreme hypoxia or anoxia (<0.2% O₂) causes endoplasmic reticulum stress. A response to such an extreme stress activates the unfolded protein response (UPR), an evolutionarily conserved pathway. One of the arms of the UPR signal pathway consists of the ER stress sensor protein—PERK (EIF2AK3). PERK phosphorylates the Ser51 residue of the eIF2α, which, in turn, inhibits global translation. Additionally, eIF2α preferentially activates the translation of a subset of transcripts such as the ATF4 which has been shown to regulate CAIX expression during UPR

at ~6.8–7.0 (White et al. 2017). The alkaline pH_i promotes tumour cell survival, proliferation, cell migration, actin remodelling and promotes cell invasion, whereas the acidic pH_e promotes the development of chemo- and radio-resistance in tumour cells and enhances the enzymatic activity of the MMPs promoting tumour invasion (White et al. 2017).

8.2 CAIX—regulation, Protein and Function

Hif1-induced Carbonic Anhydrase IX (CAIX) is considered one of the primary pH regulators of the hypoxic tumour microenvironment. In hypoxia and in high-density cell cultures (with pericellular hypoxia), the CA9 promoter is activated through the joint cooperation of sub-hypoxic levels of Hif1 and the specificity protein-1 (SP-1) transcription factor mediated via PI3K (Kaluzova et al. 2001) and MAPK (Kopacek et al. 2005) pathway. In normoxia, CAIX is expressed due to Hif1 α stabilization by Src (Takacova et al. 2010) and lactate-induced reactive oxygen species (ROS) (Panisova et al. 2017). In conditions of extreme hypoxia/anoxia (<0.2% O_2), however, the CA9 promoter is activated by direct binding of the Activating Transcription Factor 4 (ATF4) which is an integral part of the unfolded protein response (UPR) pathway (van den Beucken et al. 2009) (Fig. 8.1).

CAIX is a homodimeric, transmembrane enzyme with its catalytic domain in the extracellular portion of the protein and a small intracellular tail peptide (Opavsky et al. 1996). CAIX has a unique proteoglycan domain in its extracellular domain that has been shown to enhance the catalytic activity of CAIX (Hilvo et al. 2008) and implicated in cell adhesion (Zavada et al. 2000). The intracellular tail peptide has been found to be essential for membrane localization, catalytic activity (Hulikova et al. 2009) and contains three putative phosphorylation sites (T443, S448 and Y449). The phosphorylation of the Y449 site is implicated in EGF-induced Akt signalling pathway (Dorai et al. 2005), Thr443 has been found to be phosphorylated by protein kinase A *in vivo* and the phosphorylation of Ser448 diminishes CAIX activity (Ditte et al. 2011).

CAIX has now been shown to be a prominent prognostic marker of patient prognosis and treatment resistance in many types of solid cancers including bladder, breast, cervix, gliomas, kidney, pancreas, and uterine (McDonald et al. 2012). CAIX is a membrane protein that is predominantly upregulated in tumour tissue and absent from most of the normal tissues except the gastro-intestinal (GI) tract, and makes an ideal tumour biomarker and pharmacological target for anti-cancer therapy. Multiple studies have shown an important role of CAIX in tumour cell survival, proliferation (Lou et al. 2011), pH homeostasis (Chiche et al. 2009; Pastorekova et al. 2008), maintenance of cancer stem cell function (Lock et al. 2013), cell–cell de-adhesion (Svastova et al. 2003), focal contact formation (Shin et al. 2011), migration (Shin et al. 2011) and invadopodia-mediated invasion (Swayampakula et al. 2017). However, little is known about the different molecular partners of CAIX that facilitate its participation in the above listed biological processes.

An interactome is defined as the comprehensive set of binding partners of a macromolecule. The study of CAIX interactome would substantially enhance our understanding of its functional and structural role in cellular processes and provide valuable information about its cellular neighbourhood. In this chapter, we have taken up the task of assimilating information on all the validated and predicted molecular interactors of CAIX to create a comprehensive map of the CAIX interactome. We then focus our discussions on identifying important functional clusters within the interactome, and discuss the functional implications of the interactions between select proteins and CAIX in the context of cancer metastasis, unfolded protein response and amino acid transport.

8.3 Overview of the CAIX Interactome

Over the past two decades, a few individual publications have identified, validated and characterized some of the molecular binding partners of CAIX. We recently conducted a comprehensive, unbiased study to identify the protein interactome of CAIX (Swayampakula et al. 2017) in the MDA-MB-231 triple-negative breast cancer cell line using the proximity-dependent biotinylation labelling technique (Roux et al. 2012) called the BioID method. This study identified over 140 high confidence significant protein interactors of CAIX, specifically to its intracellular tail domain (Swayampakula et al. 2017). Figure 8.2 shows a map of the protein interactome of CAIX deduced by amalgamating these studies and identifying and displaying the important functional clusters.

An analysis of the cellular localization of the proteins in the CAIX interactome map showed that there are over 100 membrane proteins localized to the plasma membrane, endoplasmic reticulum (ER) and exosomes. Interestingly, classification by protein class showed that the interactome is largely comprised of transporters, transferases, enzyme modulators, calcium binding proteins, cell adhesion/migration related molecules and enzyme modulators. Functional clustering analysis of the genes based on Gene Ontology (GO) revealed that the biggest clusters of genes belonged to the biological processes of ion transmembrane transport, lipid metabolism, biological adhesion/migration organization and endoplasmic reticulum stress (Fig. 8.2). The ion transporter cluster contains proteins that can transport monovalent cations, divalent cations, bicarbonate ions, H^+ , ATP as well as amino acids. The biological adhesion cluster contains integrins, cell adhesion molecules (CAMs) and proteases. We will now specifically explore some of the proteins in the interactome that are known to influence molecular processes involving metastasis, unfolded protein response and amino acid transport. We will also discuss potential protein interactions involving CAIX that should be the focus of future explorations and studies.

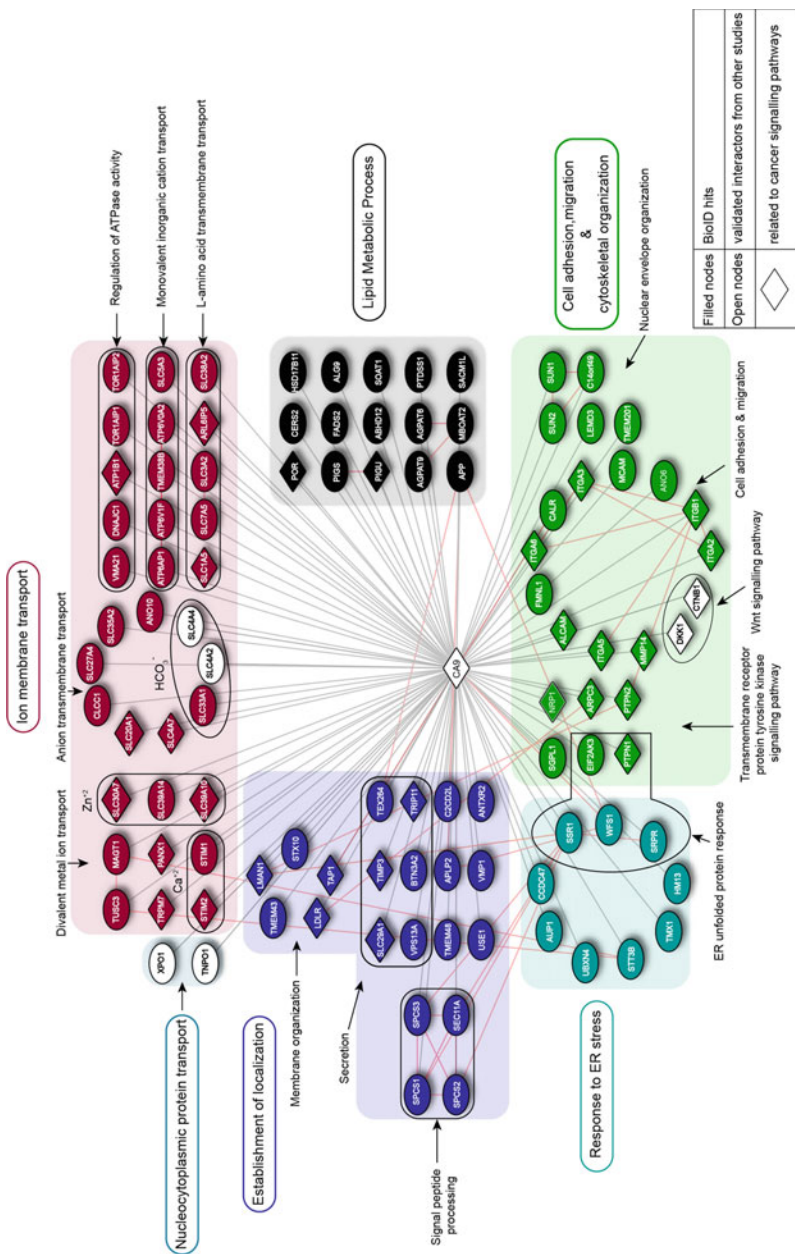


Fig. 8.2 Map of the CAIX interactome. A representative protein interactome map of CAIX by combining data from the BioID study (filled nodes) and other individual studies from the literature (open nodes). Nodes represent proteins, and edges represent physical interaction between two proteins. The grey edges indicate experimentally obtained interactions with CAIX, and red edges indicate protein–protein interactions obtained from the STRING database. The genes are functionally clustered according to their Gene Ontology (GO)–Biological processes and each group is labelled using a suitably representative term. The visualization software used to create this figure is cytoscape (Shannon et al. 2003)

8.4 CAIX in Metastasis

One of the first steps in the metastatic cascade involves the cells undergoing morphological changes from a polarized epithelial phenotype to a migratory phenotype through the epithelial and mesenchymal transition (EMT). In this section, we will examine interactions of CAIX and some of its protein partners (Fig. 8.2) in the context of three critical stages of the metastatic cascade: cell–cell de-adhesion, cell migration and cell invasion.

8.4.1 CAIX and Cell–cell De-Adhesion

8.4.1.1 β -catenin and CAIX

Adherens junctions are multi-protein complexes that are important sites for intercellular adhesion and communication between adjacent cells. E-cadherin, a member of the cadherin family of cell adhesion molecules, is an important part of the adherens junctions. It provides a structural foundation that links adhesion complex proteins to the actin cytoskeleton and other signalling molecules in a calcium-dependent manner (Perez-Moreno et al. 2003). The cytoplasmic tail of E-cadherin binds to the catenins—p120 and β -catenin (Fig. 8.3A.1) (Gavard and Mege 2005). β -catenin, in turn, binds to monomeric α -catenin that then dissociates from the complex, dimerizes and regulates the actin filament assembly at cell–cell adhesion sites mediated by E-cadherin. Dimeric α -catenin works by concomitantly maintaining parallel F-actin bundles and suppressing membrane protrusions caused by the actin branching molecule, Arp2/3 complex (Drees et al. 2005) (Fig. 8.3A.1). As seen in many epithelial derived tumours, loss of E-cadherin is one of the primary markers of epithelial-mesenchymal transition (EMT), and indicates disruption of cell–cell adhesion, leading to tumour dissemination and metastasis. Destabilization of cell–cell adhesions also occurs by disrupting the link between E-cadherin and actin cytoskeleton through the catenins.

Several studies have shown that CAIX overexpression disrupts cell–cell adhesion in cancer cells (Svastova et al. 2003; Shin et al. 2011; Radvak et al. 2013). CAIX was shown to co-localize with E-cadherin in MDCK cells, and through co-immunoprecipitation studies, it was postulated that CAIX disrupts the association between E-cadherin and the actin cytoskeleton through its direct binding with β -catenin (Svastova et al. 2003). However, an in-depth characterization of the interaction of CAIX with the β - α -catenin complex in cancer cells is required to determine the scope of its role in adherens junctions.

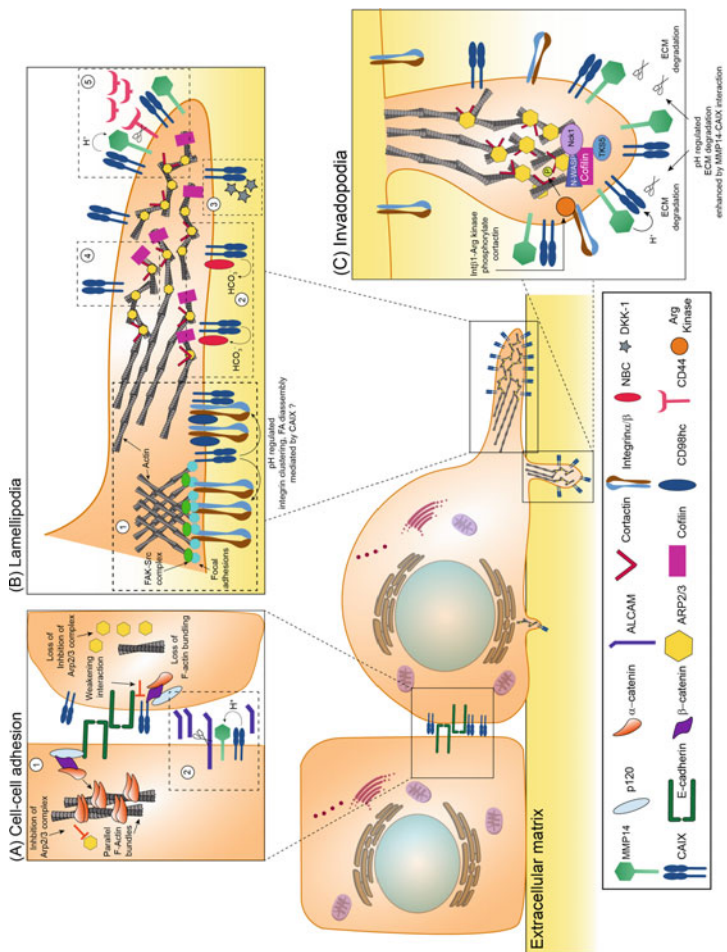


Fig. 8.3 A graphical representation of direct and indirect protein interactions of CAIX in a cancer cell at (A) Adherens junctions where CAIX potentially interacts with (A.1) β -catenin to disrupt its binding to E-cadherin (A.2) MMP14 (enhances its proteolytic activity through proton donation) and indirectly increases the shedding of ALCAM (B) Leading edge of a lamellipodia where CAIX interacts with (B.1) Integrins— α 2, α 3, α 5, α 6, β 1 and regulate their clustering and FA assembly/disassembly and CD98hc (B.2) bicarbonate transporters such as NBCn1 to maintain an optimum pH gradient from the leading edge to trailing edge (B.3) DKK-1 causing FA turnover (B.4) Arp3 of the Arp2/3 complex (B.5) MMP14 and indirectly increases CD44 shedding (C) Invadopodia of an invasive cell where CAIX interacts with MMP14 and increases ECM degradation

8.4.1.2 ALCAM, MMP14 and CAIX

Activated Leukocyte Cell Adhesion Molecule (ALCAM), a member of the immunoglobulin superfamily (IgSF) family of cell adhesion molecules is present in the CAIX interactome. ALCAM mediates calcium-independent cell–cell adhesions through homo- and hetero-typic interactions that contribute to refining and potentiating adhesion sites during tissue formation and maintenance (von Lersner et al. 2019). The expression of ALCAM has been shown to decrease in solid tumour malignancies and is increasingly being used as a prognostic marker for many solid tumours (von Lersner et al. 2019).

The adhesive abilities of ALCAM, a membrane protein, are regulated by its surface distribution and exposure of ectodomain. Studies have now linked higher levels of ALCAM shedding to poor patient outcomes (Hansen et al. 2014; Hebron et al. 2018; Rosso et al. 2007). Full-length ALCAM has two isoforms, iso1 and iso2 (slightly truncated), that differ in their proteolytic susceptibilities. Studies have found that the ALCAM iso2 is cleaved by the protease, matrix metalloproteinase-14 (MMP14, also known as MT1-MMP) and has a tenfold higher shedding rate compared to the canonical isoform ALCAM-iso1. Furthermore, the shed ectodomain, in turn, binds to cell surface ALCAM, further disrupting cell–cell adhesions, thereby showing that MMP14 induces high rates of ALCAM shedding and destabilizes cell–cell adhesion sites leading to tumour cell dissemination (Hebron et al. 2018) (Fig. 8.3A.2).

MMP14 is a member of the matrix metalloproteinase (MMP) family and is well known for its role in tumour cell invasion. It has been shown that decreased pH_e in cancer cells enhances the proteolytic activity of all the MMPs (Brown and Murray 2015; Yamamoto et al. 2015). The expression of MMP14 is directly linked to metastasis and poor overall survival (Jacob and Prekeris 2015). In addition to its matrix degrading activities, MMP14 also serves as a shedding protease and activates other MMPs such as MMP2 and MMP9 (Li et al. 2017). A recent study from our lab showed that CAIX directly binds to MMP14 in migrating cells and increases invasion through enhancing the catalytic activity of MMP14 in invasive structures by donating protons (Swayampakula et al. 2017).

As ALCAM is one of the proteins in the CAIX interactome map, it could potentially indicate a direct interaction between CAIX and ALCAM. Alternatively, a more plausible hypothesis, that needs validation, is that CAIX enhances the catalytic activity of MMP14 and indirectly causes an increase in ALCAM shedding leading to faster destabilization of cell–cell adhesion sites in hypoxia (Fig. 8.3A.2).

8.4.2 CAIX and Cell Migration

8.4.2.1 Integrins, CD98hc and CAIX

The different stages of cell migration on a two-dimensional substrate involve the formation of a lamellipodia, cell adhesion site assembly, leading edge stabilization,

cell body movement, adhesion site disassembly and detachment of the cell's dorsal end from the ECM (Huttenlocher and Horwitz 2011). A lamellipodium is a dynamic wave-like cellular extension that is devoid of organelles and contains the leading edge of a cell with densely packed branched actin filaments. As the lamellipodia form, the leading edge continually undergoes cycles of protrusion and retraction. During the protrusion stage, integrins cluster at the leading edge and form adhesion sites called focal adhesions (FA) that anchor the actin filaments to the underlying ECM stabilizing the lamellipodium. These FA function as major hubs for integrin receptor signaling, and comprise integrin clusters in association with a network of signaling molecules and structural proteins linked to the actin cytoskeleton (Huttenlocher and Horwitz 2011). The disassembly/turnover of focal adhesion sites is heavily regulated by the focal adhesion kinase (FAK) and Src tyrosine kinases. Phosphorylation of FAK and c-Src activate numerous pathways that controls cell migration, invasion, survival, proliferation and metastasis (Fig. 8.3B.1).

NHE1 is one of the most important pH regulators that co-localizes with the integrins at the leading edge of lamellipodia (Grinstein et al. 1993). NHE1 also strongly modulates $\alpha 2/\beta 1$ integrin-dependent adhesion and migration in melanoma cells (Stock et al. 2005) (Fig. 8.3B.1). Additionally, NHE1 enhances cell spreading through regulating integrin clustering, FAK phosphorylation and assembly of FA proteins (Tominaga and Barber 1998), suggesting that pH regulation plays a very important role in regulating cell adhesion to the matrix, cell spreading and migration.

CAIX is a very important pH regulator of hypoxic cancer cells, and the BioID study showed that CAIX associates with collagen and laminin-binding integrins— $\alpha 2/\beta 1$, $\alpha 3/\beta 1$, $\alpha 5/\beta 1$, and $\alpha 6/\beta 1$ (Swayampakula et al. 2017). Experimentally, CAIX was also found to co-localize with integrin $\beta 1$ and $\alpha 2$ in the lamellipodia of migrating cells and was distinctly absent from mature FAs, which is in agreement with a previous study that showed CAIX was localized only in nascent, dynamic FAs of migrating cells but not mature FAs (Csaderova et al. 2013). CAIX knockdown cells show reduced adhesion, spreading and migration in agreement with the gene expression profiling data that showed that the loss of CAIX, induced downregulation of FA and actin cytoskeleton regulation genes (Radvak et al. 2013). We know from previous studies that CAIX overexpression increases cell–substrate adhesion and cell spreading in a PG domain-dependent manner, and that CAIX overexpressing cells form prominent, mature focal adhesion sites compared to the CAIX-negative cells (Csaderova et al. 2013). Paradoxically, CAIX overexpression also increases migration rates in multiple cell lines in a catalytic domain-dependent manner (Swayampakula et al. 2017; Csaderova et al. 2013; Svastova et al. 2012).

A hypothesis that might explain these contradicting observations is that through its pH regulation activity, CAIX similar to NHE1, impacts integrin clustering, FA assembly/disassembly, FA turnover rates and consequently, cell migration. There is a wide scope for future explorations into the functional significance of integrins in hypoxic cells and the role of CAIX in regulating integrin signalling to affect cell migration.

SLC3A2 (otherwise known as, CD98) is a heterodimeric protein comprising a single-pass transmembrane heavy chain called CD98hc that crosslinks with either

the amino acid transporter, LAT1, or integrin $\beta 1$ (Feral et al. 2005). Studies have found that the cross-linking of CD98hc increases cell surface exposure of integrin $\beta 1$ and promotes integrin clustering and mediates integrin downstream signalling via FAK/PI3K pathway (Kim and Hahn 2008) (Fig. 8.3B.1). Overexpression of CD98hc increases cell proliferation, whereas genetic depletion studies showed that CD98hc regulates cell spreading, cell migration and protection from apoptosis in an integrin $\beta 1$ -dependent manner (Feral et al. 2005). CAIX binds to CD98hc, integrin $\beta 1$ (Swayampakula et al. 2017) as well as LAT1 (unpublished). We propose that CAIX binds to CD98hc and in turn, effects integrin $\beta 1$ -mediated signalling and/or LAT1-mediated amino acid transport capabilities (Sect. 5). It would also be a matter for future investigations to determine if CAIX, in fact, causes CD98hc to switch its binding between integrin $\beta 1$ and LAT1.

8.4.2.2 Transport Metabolon and CAIX

Multiple studies have shown that a constitutive increase in pH_i along with a concomitant decrease in pH_e leads to increased migration in cancer cells, and dysregulation of pH inhibits cell migration (White et al. 2017; Cong et al. 2014; Parks and Pouyssegur 2015). Optimal pH_i has also been shown to influence directed cell migration through remodelling of the actin cytoskeleton (Frantz et al. 2008). Alkaline pH_i also decreases focal adhesion stability (Srivastava et al. 2008) and increases the rates of migration (Choi et al. 2013).

Central to CAIX-mediated pH regulation pathway is the formation of a transport metabolon with bicarbonate transporters to coordinate the transport of the bicarbonate ions generated by CAIX into the tumour cells to regulate their pH_i . Interestingly, findings indicate that the formation of the transport metabolon intensifies the pH regulatory activity at the leading edge of a migrating cell and induces the formation of a pH_i gradient with an alkaline leading edge and an acidic trailing edge (Fig. 8.3B.2). Studies have shown that catalytically active CAIX co-localizes with sodium-bicarbonate transporter SLC4A4 (NBCe1) and chloride-bicarbonate transporter SLC4A2 (or AE2) at the leading edge of migrating cells (Svastova et al. 2012).

The sodium-bicarbonate transporter, SLC4A7 (also known as NBCn1), is a bicarbonate transporter that emerged in the CAIX-BioID study. Genome-wide association studies have shown that NBCn1 is a causative gene in breast cancer (Ahmed et al. 2009). NBCn1 is an important acid extruder that creates a favourable pH gradient in tumours (Boedtker et al. 2013; Lee et al. 2016). Furthermore, genetic depletion studies have elucidated its role in tumour growth (Lee et al. 2016) and cell cycle progression (Flinck et al. 2018). It is a highly likely possibility that NBCn1 is part of the bicarbonate transport metabolon with CAIX, and interacts with it at the leading edge of migrating cells. However, evidence of their direct interaction remains to be acquired.

8.4.2.3 Dickkopf-1 and CAIX

Overexpression of CAIX has been associated with inactivation of the Rho/ROCK pathway leading to paxillin-induced FA turnover (Shin et al. 2011). CAIX overexpression has also been shown to stimulate the PI3K/Akt/mTOR pathway via the upregulation of FAK/Src axis (Kim et al. 2012) leading to epithelial-mesenchymal-transition (EMT) and the acquisition of metastatic properties such as cytoskeletal remodelling, weak cell–cell adhesion and higher cell migration/invasion (Shin et al. 2011). The Dickkopf-1 (DKK-1), a negative regulator of Wnt signalling pathway, has been implicated in regulating this function of CAIX. DKK-1, present upstream of the Rho/ROCK pathway, was found to inhibit the CAIX-induced activation of the Akt/mTOR pathway making it an inhibitor of tumour progression. DKK-1 and CAIX co-localize on cellular plasma membrane (Kim et al. 2012), and a yeast two-hybrid screen determined CAIX directly binds to Dickkopf-1 (DKK-1) through its PG domain (Shin et al. 2011) (Fig. 8.3B.3).

8.4.2.4 Actin-Cytoskeletal Proteins and CAIX: Arp3 and Cofilin

An interesting finding in the CAIX interactome map was the presence of the cytoskeletal organization protein Arp3 which is an integral part of the Arp2/3 complex, an evolutionarily conserved major actin nucleating complex (Molinie and Gautreau 2018). The actin-related protein Arp2/3 complex is considered a major architect of the leading edge of the lamellipodia. Overactivation of the Arp2/3 complex has been shown to promote cancer progression. The Arp2/3 complex works in close conjunction with the actin depolymerization factor, Cofilin, in the formation and maturation of lamellipodia. Upon activation by nucleation promoting factors (NPFs), such as WAVE1, Arp2/3 complex contributes actin branching junctions that can crosslink the network of actin filaments required for membrane protrusions, migration and trafficking of vesicles (Innocenti 2018). Cofilin then supports the Arp2/3 complex and creates new actin filaments, dissociates branches produced on older actin filaments and maintains monomeric G-actin pool enabling lamellipodia elongation and promoting cell migration (Bravo-Cordero et al. 2013) (Fig. 8.3B.4).

Many studies have shown that pH_i regulation influences directed cell migration through remodelling of the actin cytoskeleton (Srivastava et al. 2008). Cofilin, in particular, has a pH sensitive domain that is activated at higher pH_i and enhances actin polymerization and membrane protrusions leading to cell migration (Frantz et al. 2008). While the validation of the interaction between CAIX and Arp3 is pending, data from our lab has already shown that CAIX co-localizes to the leading edge of migrating cells specifically to regions of active actin remodelling and positive cofilin staining (Swayampakula et al. 2017). Studies have already shown that NHE1 is the most critical pH regulator necessary for cofilin-dependent actin assembly at leading edges. However, analysis of TCGA data specifically in triple-negative breast cancers, showed lower levels of NHE1 in hypoxia indicating that CAIX could potentially be the primary driver of pH regulation and migration in such a case (Amith

et al. 2017). Regardless, a case can be made for CAIX to be contributing to actin cytoskeletal remodelling through pH modulation at leading edges of hypoxic cells, and the emergence of Arp3 in the BioID is most likely an indication of its cellular neighbourhood in regions of dynamic actin remodelling (Fig. 8.3B.4).

8.4.2.5 Matrix Metalloproteinase-14 and CAIX

Several studies have shown that MMP14 localizes to the lamellipodia of migrating cells where it binds to the CD44 receptor through its hemopexin domain causing its enzymatic shedding (Mori et al. 2002). CD44 is a hyaluron receptor expressed on many migratory cells and is known to assimilate adhesive and signalling activities through actin cytoskeletal remodelling leading to stimulation of cell migration. High CD44 expression is correlated with EMT, cancer stem cells, and is a marker of metastasis, invasion, resistance and disease recurrence in multiple types of cancers (Xu et al. 2015). The shedding of CD44 is observed in multiple tumours in vivo (Okamoto et al. 2002), and high serum levels of soluble CD44 is correlated with tumour burden and metastatic potential in gastric and colon cancer (Nagano and Saya 2004). The migration of highly aggressive melanoma cells on hyaluronan is associated with increased shedding and turnover of CD44 (Goebeler et al. 1996). Post-shedding, the intracellular domain of CD44 is translocated to the nucleus to trigger signalling pathways and regulate CD44-mediated functions and provide positive-feedback regulation for CD44 expression (Nagano and Saya 2004).

Although many MMPs possess CD44 shedding activity, it is only MMP14 that has been implicated in promoting migration (Kajita et al. 2001). CAIX has already been shown to localize to the migrating lamellipodia and directly bind to MMP14 through its intracellular tail to enhance its catalytic activity (Swayampakula et al. 2017). Even though the precise mechanism of CAIX-stimulated migration has not been studied, it is a plausible hypothesis that CAIX enhances migratory potential of cells by increasing MMP14-mediated shedding of CD44 (Fig. 8.3B.5). This hypothesis, however, needs to be validated.

8.4.2.6 TRPM7 and CAIX

Transient Receptor Potential Cation Channel Subfamily M Membrane (TRPM7) is a unique divalent cation (Ca^{+2} and Mg^{+2}) transporter that has an α -kinase domain fused to it. TRPM7 is known for regulation of actomyosin contractility, cell adhesion, migration, FA turnover, polarized cell movement, EMT and localized Ca^{+2} signalling. TRPM7 plays a mechanosensory role in metastasis, and senses both physical and chemical stimuli, such as mechanical stretch, changes in cell volume, oxidative stress and alteration in extracellular or cytosolic pH (Li et al. 2006). The overexpression of TRPM7 is an independent predictor of poor outcome in breast, neuroblastoma, pancreatic, nasopharyngeal and prostate cancer (Kuipers et al. 2018).

Interestingly, one of the most important functions of TRPM7 during cell migration is the regulation of FA assembly/ disassembly through its interactions with Calpain-2, a critical Ca^{+2} -dependent regulator of FA disassembly. TRPM7 is recruited to focal adhesion sites where it enhances local Ca^{+2} ion concentration and induces FA disassembly by stimulating Calpain-2. Concomitantly, it is thought that the kinase domain of TRPM7 also plays a key role in regulating the cleavage of pH sensitive Talin from the cytoskeleton for FA remodelling (Srivastava et al. 2008; Su et al. 2006). The overexpression of TRPM7 increases cell rounding and loss of cell adhesions, and indicates impaired FA dynamics, whereas silencing TRPM7 increases cell adhesions. TRPM7 activity is regulated by levels of intracellular c-AMP, pH_i and pH_e , and the activity of the ion transporter significantly increases in acidic pH_e (Li et al. 2006).

The BioID data shows that TRPM7 is a potential direct interactor of CAIX. The localization of the catalytic domain of CAIX and the pH sensitive domain of TRPM7 in the extracellular space is ideal for a CAIX-induced activation of TRPM7 ion transporter activity. Future investigations should attempt to determine if indeed one of the mechanisms of CAIX-induced FA turnover is through activation of the TRPM7-calpain-2 axis of FA disassembly.

8.4.3 *Invadopodia-Mediated Cell Invasion*

Invadopodia are matrix-degrading pseudopods with a rich F-actin core and long protrusions found both *in vitro* and *in vivo* (Eddy et al. 2017). Recent findings have shown that invadopodia can sense and integrate signals obtained from the tumour microenvironment, and are involved in chemotaxis and locomotion (Gould and Courtneidge 2014). The tumour cell invadopodia are initiated by growth factor/ECM mediated Src and can last for hours. Hif1 α is a major regulator of invadopodia formation in hypoxia. Studies in head, neck, lung and pancreatic cancer have shown an increase in invadopodia through Hif1 α induction (Diaz et al. 2013). The Hif1 α -induced EMT transcription factor, Twist-1, also stimulates invadopodia formation, and Hif1 α regulated Caveolin1, a major component of lipid rafts, has been found to be important for invadopodia formation and recruitment of MMP14 (Gould and Courtneidge 2014). Integrin-mediated ECM binding is essential for invadopodium formation and maturation. The integrins $\beta 1$, $\alpha 2$, $\alpha 3$, $\alpha 5$, and $\alpha 6$ but not $\beta 3$ are localized to the invadopodia (Eddy et al. 2017).

The invadopodium initiation starts with the formation of an unstable complex via the recruitment of N-WASp, Arp2/3 complex and cofilin to an actin–cortactin complex (Fig. 8.3BC) (Millard et al. 2004). Through a cascade of molecular events beyond the scope of this review, Tks5 stabilizes this complex by anchoring it to the plasma membrane. The maturation phase starts with integrin $\beta 1$ /Arg Kinase-mediated phosphorylation of cortactin at Y421 leading to the recruitment of Nck1 to the N-WASp-Arp2/3-cofilin complex that enhances Arp2/3 complex-mediated actin polymerization. Phosphorylated cortactin also recruits moesin-NHE1 complex to increase the local pH, which in turn activates and causes the disengagement of

cofilin from cortactin (Bailly et al. 2001). The dissociated cofilin severs the actin filaments to generate free barbed ends, which function as nucleation sites for the activated Arp2/3 complex to create branched actin filament network to elongate the invadopodium. This is followed by the recruitment of proteases such as matrix metalloproteinases (MMPs), serine proteases and cathepsins to the invadopodia and ECM degradation (Eddy et al. 2017).

The CAIX interactome has integrins $\beta 1$, $\alpha 2$, $\alpha 3$, $\alpha 5$, and $\alpha 6$ as well as Arp3 and MMP14 that contribute to the formation and/or function of the invadopodia. pH affects invadopodia formation and function in two ways—first, by affecting cofilin-based actin cytoskeletal dynamics within the invadopodia, and second, by controlling the proteolytic activity of proteases recruited to the invadopodia. We have previously shown that CAIX co-localizes with cortactin, Tks5 and MMP14 in mature invadopodia (Swayampakula et al. 2017). We have also unambiguously shown that CAIX stimulates MMP14-mediated ECM degradation and consequently, cell invasion through direct binding with MMP14 and increasing its proteolytic activity through reducing pH_e (Swayampakula et al. 2017). Hence, it is already known that CAIX effects invadopodia function by regulating the proteolytic activity. It remains to be determined if CAIX affects the cytoskeletal dynamics within the invadopodia.

In order to determine the role of CAIX in formation of invadopodia and its cytoskeletal remodelling, future studies must be designed to first determine the recruitment of CAIX to the invadopodia, at what stage of the invadopodia formation does CAIX get recruited to it and is the structure of invadopodia different in the presence or absence of CAIX?

8.4.3.1 PTPN1 and CAIX

Protein tyrosine phosphatase non-receptor type 1 (PTPN1, more commonly known as PTP1B) is a tyrosine phosphatase that has been implicated in the regulation of multiple cellular processes such as signaling, proliferation, intracellular transport, cell adhesion, migration and apoptosis (Arregui et al. 2013). PTP1B expression is associated with less aggressive tumours with higher survival rates in breast cancer (Soysal et al. 2013). PTP1B is crucial for the maintenance of E-cadherin- β -catenin complex in the organization of adherens junctions (Sheth et al. 2007). PTP1B also promotes Src activation resulting in signaling through Rac1 and RhoA pathways (Arregui et al. 2013).

PTP1B is sensitive to calpain-2-dependent cleavage. The resulting truncated, soluble form of PTP1B has enhanced activity compared to the membrane-bound form and plays role in Src-dependent formation and maturation of invadopodia. PTP1B-deficient cell lines show reduction in invadopodia formation, and treatment with PTP1B inhibitors impairs invadopodia formation and invasion (Cortesio et al. 2008). Studies have now shown that in invadopodia, PTP1B suppresses cortactin phosphorylation which is an essential step in invadopodia-maturation (Weidmann

et al. 2016), clearly evidenced in the study where PTP1B null mice show a five-fold increase in cortactin phosphorylation.

PTP1B is predominantly located in the endoplasmic reticulum (ER) with its catalytic domain facing the cytosol. Most of the substrates of PTP1B such as Src, paxillin and catenins are commonly present at cell periphery in FA sites near the leading edges in lamellipodia of migrating cells. In order to facilitate the dephosphorylation activity of PTP1B, microtubules pull the ER network to place them over FA sites allowing access to its substrates (Arregui et al. 2013).

The BioID dataset shows PTP1B is one of the potential interactors with CAIX. We know that the catalytic domain of PTP1B is in the cytosol, whereas the catalytic domain of CAIX is present in the extracellular domain. Therefore, it is unlikely, that PTP1B is affected by the pH regulating activity of CAIX. Hence, a likely reason for the emergence of PTP1B in the BioID screen is that CAIX and PTP1B are part of the same cellular neighbourhood such as the integrin-FAK-Src adhesion sites or the cadherin adhesion sites or even the invadopodia sites that are rich in CAIX. However, as previously mentioned, CAIX has three phosphorylation sites in its intracellular domain. Hence, there is also a possibility that PTP1B directly interacts with CAIX and regulates its phosphorylation status.

8.5 Amino Acid Transporters and CAIX

Hypoxic zones in tumours are characterized by poor perfusion and are therefore, prone to nutrient deficiency. It is well established that hypoxic tumour cells are glycolytic, however, in the past decade, studies have unraveled the ability of tumour cells to adapt and favour metabolism of other nutrients like amino acids and fatty acids to promote cancer progression (Samanta and Semenza 2018). Specific to amino acid metabolism, cancer cells heavily rely on glutamine for biosynthesis and energy production. In hypoxic tumour cells, the α -ketoglutarate (α -KG) produced in the first step of glutaminolysis (glutamine catabolism) is converted to citrate by isocitrate dehydrogenase1 (IDH1). Citrate is subsequently utilized for lipid biosynthesis to support cell proliferation (Metallo et al. 2011) (Fig. 8.3B). Furthermore, a recent study also showed how the carbon and nitrogen in glutamine are efficiently utilized to support lipid biosynthesis under hypoxia (Wang et al. 2019). In this section, we will discuss three AATs that were identified as potential interactors of CAIX from the BioID screen.

SLC38A2 (or SNAT2) belongs to the SLC38 family of AAT, is ubiquitously expressed across various tissues and transports an array of aliphatic amino acids, including glutamine in a sodium-dependent manner (Mackenzie and Erickson 2004). SLC1A5 (or ASCT2) belongs to the Alanyl Serine Cysteine preferring family of transporters (ASCT). Despite what the name suggests, ASCT2 also transports glutamine with the same affinity as the other amino acids (Garaeva et al. 2018). Although SNAT2 and ASCT2 import other amino acids, in cancer cells, they play an important role in importing glutamine. SLC7A5, also known as LAT1, is a member

of the heteromeric amino acid transporters that are composed of two subunits: the light subunit, LAT1, and the heavy subunit, CD98. The binding of CD98 to LAT1 has been found to be essential for transporter activity of LAT1 (Yan et al. 2019). LAT1 transports large neutral amino acids including essential amino acids (EAA) such as Leucine. While HIF1 α induces SNAT2 expression in hypoxia (Morotti et al. 2018), HIF2 α regulates the expression of ASCT2 (Corbet et al. 2014) and LAT1 (Elorza et al. 2012) in chronic acidosis and hypoxia, respectively. The expression of both ASCT2 and LAT1 in cancer is independently associated with poor prognosis (Kandasamy et al. 2018).

SNAT2 is a rescue transporter that is upregulated under amino acid deprivation (Broer et al. 2016) and to compensate for the loss of function of ASCT2 (Broer et al. 2019). On the other hand, both ASCT2 and LAT1 are obligatory transporters with the influx through one transporter coupled to efflux through the second transporter (Nicklin et al. 2009). ASCT2 inhibition has shown effective reduction in tumour growth in multiple cancers (Marshall et al. 2017; van Geldermalsen et al. 2016; Ye et al. 2018) by decreasing glutamine metabolism (van Geldermalsen et al. 2016; Hassanein et al. 2013) and mTOR signaling pathway (Wang et al. 2014,2015). Genetic depletion of LAT1 is shown to reduce tumour growth by decreasing mTOR pathway, particularly under low amino acid conditions (Cormerais et al. 2016).

In addition to being utilized for lipid biosynthesis, glutamine can be utilized to activate mTOR signaling and enhance cell proliferation (Fig. 8.1B). LAT1 can exchange the intracellular glutamine to import essential amino acids (EAA) such as leucine, an important amino acid for the activation of mTOR signaling (Wolfson et al. 2016). Considering the importance of glutamine metabolism in hypoxic tumour cells, it is possible that the transporters such as SNAT2, ASCT2 and LAT1 play an important role in enhancing the glutamine and EAA flux into cells. BioID data indicates potential interactions of these transporters with CAIX. We hypothesize that CAIX plays an important role in switching to and/or enhancing the metabolic shift from glucose to glutamine by co-regulating the transport activity of these transporters. However, the mechanism of co-regulation of CAIX with the AATs remains a topic for future investigation.

8.6 CAIX and Unfolded Protein Response

While Hif1 is stabilized in moderate hypoxia (<2% O₂), it is only in extreme hypoxia or anoxia (<0.2% O₂) that tumour cells initiate a survival mechanism called the unfolded protein response (UPR) (Koumenis and Wouters 2006). eIF2aK3 otherwise known as protein kinase-like endoplasmic reticulum kinase PERK is an endoplasmic reticulum (ER) stress sensor that drives one of the three signalling pathways in UPR (Ron and Walter 2007). Under anoxic conditions, PERK activation leads to phosphorylation of the α subunit of the eukaryotic translation initiation factor 2 (eIF2 α) resulting in an immediate repression of global protein translation. Additionally, phosphorylated eIF2 α initiates a response to restore cellular homeostasis

by preferentially promoting the translation of selective mRNA such as the activating transcription factor 4 (ATF4). In fact, in severe hypoxic conditions, the Hif1 pathway and UPR cooperate to upregulate Hif1-induced genes. ATF4 has now been shown to bind to the CA9 promoter and mediate its transcriptional activation (Fig. 8.1C). Cells with impaired PERK/eIF2 α signaling have shown significantly reduced CAIX *in vitro* and *in vivo*, in spite of the presence of activated Hif1 (van den Beucken et al. 2009; Ivanova et al. 2018). PERK (EIF2aK3) is one of the proteins identified in the BioID screen (Fig. 8.1C). It would be a matter for future investigations to validate the presence of a direct interaction between PERK and CAIX in anoxic cells, the cellular location of their interaction and to determine if the interaction is due to a positive-feedback mechanism to regulate the transcriptional activation of CAIX in anoxia to promote cell survival at low pH.

8.7 Summary and Therapeutic Implications

The function of CAIX in pH homeostasis via the transport metabolon is well accepted. The involvement of CAIX in cell-cell de-adhesion/migration via its involvement with β -catenin and DKK-1 (FAK/Akt/mTOR), respectively, has also been established. The unbiased study of the CAIX interactome conducted in our lab not only corroborated some roles of CAIX in these cellular processes but also revealed the presence of novel protein interactions (direct and indirect) that could potentially enhance tumour cell dissemination and metastasis in a CAIX-dependent manner. Additionally, an in-depth analysis of the interactome map revealed that CAIX may participate in other cellular processes, such as ion-membrane transport, ER stress-response and lipid metabolism. In particular, the presence of amino acid transporters in the interactome map indicated the potential involvement of CAIX in a metabolic switch from glucose to an amino acid (Gln/Leu)-dependent mechanism to enable cell growth and proliferation in a hypoxic and nutrient-deficient microenvironment. Also interesting was the presence of PERK, indicating the involvement of CAIX in the regulation of the UPR response.

The analysis of CAIX interactome using BioID study (Swayampakula et al. 2017) underlines the potential implications of dual inhibition of CAIX-MMP14 and CAIX-Integrins to target cellular processes, such as the tumour cell adhesion, migration and invasion. We also show other avenues for designing combination therapy by targeting CAIX-bicarbonate transporters and CAIX-amino acid transporters to inhibit pH regulation and alternate metabolic adaptations by hypoxic cells, respectively. Several studies have now showed that combination treatment of standard of care chemotherapy with the CAIX inhibitor, SLC-0111, show better tumour growth inhibition in mouse models of multiple cancers (Lou et al. 2011; Lock et al. 2013; McDonald et al. 2019; Boyd et al. 2017; Chafe et al. 2019). Newly published papers from our lab show that treatment with SLC-0111 reduces intracellular pH and glycolysis in cells, and makes combination treatment with gemcitabine in K-Ras-activated PDAC (McDonald et al. 2019) and check point inhibitor in melanoma and TNBCs (Chafe et al. 2019) more effective. Currently, SLC-0111 has progressed to a multi-centre Phase Ib clinical trial (NCT03450018) with CAIX positive, metastatic pancreatic cancer. The validation of many of the interactors identified using the CAIX interactome would further our understanding of the involvement of CAIX in cancer progression and contribute to designing novel, more effective combination treatments with reduced toxicity and to tackling chemo- and radio-resistance in multiple cancers.

References

- Ahmed S, Thomas G, Ghousaini M, Healey CS, Humphreys MK, Platte R, et al (2009) Newly discovered breast cancer susceptibility loci on 3p24 and 17q23.2. *Nat Genet* 41(5):585–590. PubMed PMID: 19330027. Pubmed Central PMCID: PMC2748125. Epub 2009/03/31. eng
- Amith SR, Vincent KM, Wilkinson JM, Postovit LM, Fliegel L (2017) Defining the Na(+)/H(+) exchanger NHE1 interactome in triple-negative breast cancer cells. *Cell Signal* 29:69–77. PubMed PMID: 27751915. Epub 2016/11/05. eng
- Arregui CO, González Á, Burdisso JE, González Wusener AE (2013) Protein tyrosine phosphatase PTP1B in cell adhesion and migration. *Cell Adhes Migrat* 7(5):418–423. PubMed PMID: 24104540. Epub 09/12. eng
- Bailly M, Ichetovkin I, Grant W, Zebda N, Machesky LM, Segall JE, et al (2001) The F-actin side binding activity of the Arp2/3 complex is essential for actin nucleation and lamellipod extension. *Curr Biol* CB 11(8):620–625. PubMed PMID: 11369208. Epub 2001/05/23. eng
- Boedtker E, Moreira JM, Mele M, Vahl P, Wielenga VT, Christiansen PM, et al (2013) Contribution of Na⁺,HCO₃⁻-cotransport to cellular pH control in human breast cancer: a role for the breast cancer susceptibility locus NBCn1 (SLC4A7). *International journal of cancer*. 2013 Mar 15;132(6):1288–1299. PubMed PMID: 22907202. Epub 2012/08/22. eng
- Boyd NH, Walker K, Fried J, Hackney JR, McDonald PC, Benavides GA, et al (2017) Addition of carbonic anhydrase 9 inhibitor SLC-0111 to temozolomide treatment delays glioblastoma growth in vivo. *JCI Insight* 2(24). PubMed PMID: 29263302. Pubmed Central PMCID: PMC5752277. Epub 2017/12/22. eng
- Bravo-Cordero JJ, Magalhaes MA, Eddy RJ, Hodgson L, Condeelis J (2013) Functions of cofilin in cell locomotion and invasion. *Nat Rev Mol Cell Biol* 14(7):405–415. PubMed PMID: 23778968. Pubmed Central PMCID: PMC3878614. Epub 2013/06/20. eng

- Broer A, Rahimi F, Broer S (2016) Deletion of amino acid transporter ASCT2 (SLC1A5) reveals an essential role for transporters SNAT1 (SLC38A1) and SNAT2 (SLC38A2) to sustain glutaminolysis in cancer cells. *J Biol Chem* 291(25):13194–13205. PubMed PMID: 27129276. Pubmed Central PMCID: PMC4933233. Epub 2016/04/30. eng
- Broer A, Gauthier-Coles G, Rahimi F, van Geldermalsen M, Dorsch D, Wegener A, et al (2019) Ablation of the ASCT2 (SLC1A5) gene encoding a neutral amino acid transporter reveals transporter plasticity and redundancy in cancer cells. *J Biol Chem* PubMed PMID: 30635397. Epub 2019/01/13. eng
- Brown GT, Murray GI (2015) Current mechanistic insights into the roles of matrix metalloproteinases in tumour invasion and metastasis. *J Pathol* 237(3):273–281
- Chafe SC, McDonald PC, Saberi S, Nemirovsky O, Venkateswaran G, Burugu S, et al Targeting hypoxia-induced carbonic anhydrase IX enhances immune checkpoint blockade locally and systemically. *Cancer Immunol Res* 2019:canimm.0657.2018. PubMed PMID: 31088846
- Chiche J, Ilc K, Laferrriere J, Trottier E, Dayan F, Mazure NM, et al (2009) Hypoxia-inducible carbonic anhydrase IX and XII promote tumor cell growth by counteracting acidosis through the regulation of the intracellular pH. *Cancer research*. 69(1):358–368. PubMed PMID: 19118021. Epub 2009/01/02. eng
- Choi C-H, Webb BA, Chimenti MS, Jacobson MP, Barber DL (2013) pH sensing by FAK-His58 regulates focal adhesion remodeling. *J Cell Biol* 202(6):849–859
- Cong D, Zhu W, Shi Y, Pointer KB, Clark PA, Shen H et al (2014) Upregulation of NHE1 protein expression enables glioblastoma cells to escape TMZ-mediated toxicity via increased H⁺ extrusion, cell migration and survival. *Carcinogenesis* 35(9):2014–2024
- Corbet C, Draoui N, Polet F, Pinto A, Drozak X, Riant O, et al (2014) The SIRT1/HIF2alpha axis drives reductive glutamine metabolism under chronic acidosis and alters tumor response to therapy. *Cancer Res* 74(19):5507–5519. PubMed PMID: 25085245. Epub 2014/08/03. eng
- Cormerais Y, Giuliano S, LeFloch R, Front B, Durivault J, Tambutte E, et al (2016) Genetic disruption of the multifunctional CD98/LAT1 complex demonstrates the key role of essential amino acid transport in the control of mTORC1 and tumor growth. *Cancer Res* 76(15):4481–4492. PubMed PMID: 27302165. Epub 2016/06/16. eng
- Cortesio CL, Chan KT, Perrin BJ, Burton NO, Zhang S, Zhang ZY, et al (2008) Calpain 2 and PTP1B function in a novel pathway with Src to regulate invadopodia dynamics and breast cancer cell invasion. *J Cell Biol* 180(5):957–971. PubMed PMID: 18332219. Pubmed Central PMCID: PMC2265405. Epub 2008/03/12. eng
- Csaderova L, Debreova M, Radvak P, Stano M, Vrestiakova M, Kopacek J, et al (2013) The effect of carbonic anhydrase IX on focal contacts during cell spreading and migration. *Front Physiol* 4(271)
- Diaz B, Yuen A, Iizuka S, Higashiyama S, Courtneidge SA (2013) Notch increases the shedding of HB-EGF by ADAM12 to potentiate invadopodia formation in hypoxia. *J Cell Biol* 201(2):279–292. PubMed PMID: 23589494. Pubmed Central PMCID: PMC3628517. Epub 2013/04/17. eng
- Ditte P, Dequiedt F, Svastova E, Hulikova A, Ohradanova-Repic A, Zatovicova M, et al (2011) Phosphorylation of carbonic anhydrase IX controls its ability to mediate extracellular acidification in hypoxic tumors. *Cancer Res* 71(24):7558–7567. PubMed PMID: 22037869. Epub 2011/11/01. eng
- Dorai T, Sawczuk IS, Pastorek J, Wiernik PH, Dutcher JP. (2005) The role of carbonic anhydrase IX overexpression in kidney cancer. *Eur J Cancer* 41(18):2935–2947. PubMed PMID: 16310354. Epub 2005/11/29. eng
- Drees F, Pokutta S, Yamada S, Nelson WJ, Weis WI (2005) Alpha-catenin is a molecular switch that binds E-cadherin-beta-catenin and regulates actin-filament assembly. *Cell* 123(5):903–915. PubMed PMID: 16325583. Pubmed Central PMCID: PMC3369825. Epub 2005/12/06. eng
- Eddy RJ, Weidmann MD, Sharma VP, Condeelis JS (2017) Tumor cell invadopodia: invasive protrusions that orchestrate metastasis. *Trends Cell Biol*. 27(8):595–607. PubMed PMID: 28412099. Pubmed Central PMCID: PMC5524604. Epub 2017/04/17. eng

- Elorza A, Soro-Arnaiz I, Melendez-Rodriguez F, Rodriguez-Vaello V, Marsboom G, de Carcer G, et al (2012) HIF2alpha acts as an mTORC1 activator through the amino acid carrier SLC7A5. *Mol Cell* 48(5):681–691. PubMed PMID: 23103253. Epub 2012/10/30. eng
- Feral CC, Nishiya N, Fenczik CA, Stuhlmann H, Slepak M, Ginsberg MH (2005) CD98hc (SLC3A2) mediates integrin signaling. *Proc Natl Acad Sci USA* 102(2):355–360. PubMed PMID: 15625115. Pubmed Central PMCID: PMC544283. Epub 2004/12/31. eng
- Flinck M, Kramer SH, Schnipper J, Andersen AP, Pedersen SF (2018) The acid-base transport proteins NHE1 and NBCn1 regulate cell cycle progression in human breast cancer cells. *Cell Cycle* 17(9):1056–1067. PubMed PMID: 29895196. Pubmed Central PMCID: PMC6110587. Epub 2018/06/14. eng
- Frantz C, Barreiro G, Dominguez L, Chen X, Eddy R, Condeelis J, et al (2008) Cofilin is a pH sensor for actin free barbed end formation: role of phosphoinositide binding. *J Cell Biol* Dec 1;183(5):865–879. PubMed PMID: 19029335. Pubmed Central PMCID: PMC2592832. Epub 2008/11/26. eng
- Garaeva AA, Oostergetel GT, Gati C, Guskov A, Paulino C, Slotboom DJ (2018) Cryo-EM structure of the human neutral amino acid transporter ASCT2. *Nat Struct Mol Biol* 25(6):515–521. PubMed PMID: 29872227. Epub 2018/06/07. eng
- Gavard J, Mege RM (2005) Once upon a time there was beta-catenin in cadherin-mediated signalling. *Biol Cell* 97(12):921–926. PubMed PMID: 16293110. Epub 2005/11/19. eng
- Goebeler M, Kaufmann D, Brocker EB, Klein CE (1996) Migration of highly aggressive melanoma cells on hyaluronic acid is associated with functional changes, increased turnover and shedding of CD44 receptors. *J Cell Sci* 109 (Pt 7):1957–1964. PubMed PMID: 8832418. Epub 1996/07/01. eng
- Gould CM, Courtneidge SA (2014) Regulation of invadopodia by the tumor microenvironment. *Cell Adhes Migrat* 8(3):226–235. PubMed PMID: 24714597. Pubmed Central PMCID: PMC4198346. Epub 2014/04/10. eng
- Grinstein S, Woodside M, Waddell TK, Downey GP, Orłowski J, Pouyssegur J, et al (1993) Focal localization of the NHE-1 isoform of the Na⁺/H⁺ antiport: assessment of effects on intracellular pH. *EMBO J* 12(13):5209–5218. PubMed PMID: 8262063. Pubmed Central PMCID: PMC413785. Epub 1993/12/15. eng
- Haase VH (2006) The VHL/HIF oxygen-sensing pathway and its relevance to kidney disease. *Kid Int* 69(8):1302–1307. PubMed PMID: 16531988. Epub 2006/03/15. eng
- Hansen AG, Arnold SA, Jiang M, Palmer TD, Ketova T, Merkel A, et al (2014) ALCAM/CD166 is a TGF-beta-responsive marker and functional regulator of prostate cancer metastasis to bone. *Cancer research*. 74(5):1404–1415. PubMed PMID: 24385212. Pubmed Central PMCID: PMC4149913. Epub 2014/01/05. eng
- Hassanein M, Hoeksema MD, Shiota M, Qian J, Harris BK, Chen H, et al (2013) SLC1A5 mediates glutamine transport required for lung cancer cell growth and survival. *Clin Cancer Res Off J Am Assoc Cancer Res* 19(3):560–570. PubMed PMID: 23213057. Pubmed Central PMCID: PMC3697078. Epub 2012/12/06. eng
- Hassanpour SH, Dehghani M (2017) Review of cancer from perspective of molecular. *J Cancer Res Pract* 4(4):127–129
- Hebron KE, Li EY, Arnold Egloff SA, von Lersner AK, Taylor C, Houkes J, et al (2018) Alternative splicing of ALCAM enables tunable regulation of cell-cell adhesion through differential proteolysis. *Scientific Reports*. 8(1):3208
- Hilvo M, Baranauskienė L, Salzano AM, Scaloni A, Matulis D, Innocenti A, et al (2008) Biochemical characterization of CA IX, one of the most active carbonic anhydrase isozymes. *J Biol Chem* 283(41):27799–27809. PubMed PMID: 18703501. Epub 2008/08/16. eng
- Hulikova A, Zatovicova M, Svastova E, Ditte P, Brasseur R, Kettmann R, et al (2009) Intact intracellular tail is critical for proper functioning of the tumor-associated, hypoxia-regulated carbonic anhydrase IX. *FEBS Lett* 583(22):3563–3568. PubMed PMID: 19861127. Epub 2009/10/29. eng

- Huttenlocher A, Horwitz AR (2011) Integrins in cell migration. *Cold Spring Harb Perspect Biol* 3(9):a005074. PubMed PMID: 21885598. Pubmed Central PMCID: PMC3181029. Epub 2011/09/03. eng
- Innocenti M (2018) New insights into the formation and the function of lamellipodia and ruffles in mesenchymal cell migration. *Cell Adhes Migrat* 12(5):401–416. PubMed PMID: 29513145. Pubmed Central PMCID: PMC6363039. Epub 2018/03/08. eng
- Ivanova IG, Park CV, Yemm AI, Kenneth NS (2018) PERK/eIF2alpha signaling inhibits HIF-induced gene expression during the unfolded protein response via YB1-dependent regulation of HIF1alpha translation. *Nucleic Acids Res* 46(8):3878–3890. PubMed PMID: 29529249. Pubmed Central PMCID: PMC5934640. Epub 2018/03/13. eng
- Jacob A, Prekeris R (2015) The regulation of MMP targeting to invadopodia during cancer metastasis. *Front Cell Dev Biol* 3:4. PubMed PMID: 25699257. Pubmed Central PMCID: PMC4313772. Epub 2015/02/24. eng
- Kajita M, Itoh Y, Chiba T, Mori H, Okada A, Kinoh H, et al (2001) Membrane-type 1 matrix metalloproteinase cleaves CD44 and promotes cell migration. *J Cell Biol* 153(5):893–904. PubMed PMID: 11381077. Pubmed Central PMCID: PMC2174329. Epub 2001/05/31. eng
- Kaluzova M, Pastorekova S, Svastova E, Pastorek J, Stanbridge EJ, Kaluz S (2001) Characterization of the MN/CA 9 promoter proximal region: a role for specificity protein (SP) and activator protein 1 (AP1) factors. *Biochem J* 359(Pt 3):669–677. PubMed PMID: 11672442. Pubmed Central PMCID: PMC1222189. Epub 2001/10/24. eng
- Kandasamy P, Gyimesi G, Kanai Y, Hediger MA (2018) Amino acid transporters revisited: New views in health and disease. *Trends Biochem Sci* 43(10):752–789
- Kim SM, Hahn JH (2008) CD98 activation increases surface expression and clustering of beta1 integrins in MCF-7 cells through FAK/Src- and cytoskeleton-independent mechanisms. *Exp Mol Med* 40(3):261–270. PubMed PMID: 18587263. Pubmed Central PMCID: PMC2679289. Epub 2008/07/01. eng
- Kim JW, Tchernyshyov I, Semenza GL, Dang CV (2006) HIF-1-mediated expression of pyruvate dehydrogenase kinase: a metabolic switch required for cellular adaptation to hypoxia. *Cell Metab* 3(3):177–185. PubMed PMID: 16517405. Epub 2006/03/07. eng
- Kim BR, Shin HJ, Kim JY, Byun HJ, Lee JH, Sung YK, et al (2012) Dickkopf-1 (DKK-1) interrupts FAK/PI3K/mTOR pathway by interaction of carbonic anhydrase IX (CA9) in tumorigenesis. *Cell Signal* 24(7):1406–1413. PubMed PMID: 22430125. Epub 2012/03/21. eng
- Kopacek J, Barathova M, Dequiedt F, Sepelakova J, Kettmann R, Pastorek J, et al (2005) MAPK pathway contributes to density- and hypoxia-induced expression of the tumor-associated carbonic anhydrase IX. *Biochim Biophys Acta* 1729(1):41–49. PubMed PMID: 15833446. Epub 2005/04/19. eng
- Koumenis C, Wouters BG (2006) “Translating” tumor hypoxia: Unfolded protein response (UPR)-dependent and UPR-independent pathways. *Mol Cancer Res* 4(7):423–436
- Kuipers AJ, Middelbeek J, Vrenken K, Perez-Gonzalez C, Poelmans G, Klarenbeek J, et al (2018) TRPM7 controls mesenchymal features of breast cancer cells by tensional regulation of SOX4. *Biochimica et biophysica acta Molecular basis of disease*. 1864(7):2409–2419. PubMed PMID: 29684587. Epub 2018/04/24. eng
- Lee S, Axelsen TV, Andersen AP, Vahl P, Pedersen SF, Boedtkjer E (2016) Disrupting Na(+), HCO(3)(-)-cotransporter NBCn1 (Slc4a7) delays murine breast cancer development. *Oncogene*. 2016 Apr 21;35(16):2112–2122. PubMed PMID: 26212013. Epub 2015/07/28. eng
- Lendahl U, Lee KL, Yang H, Poellinger L (2009) Generating specificity and diversity in the transcriptional response to hypoxia. *Nat Rev Genet* 10(12):821–832. PubMed PMID: 19884889. Epub 2009/11/04. eng
- Li M, Jiang J, Yue L (2006) Functional characterization of homo- and heteromeric channel kinases TRPM6 and TRPM7. *J Gen Physiol* 127(5):525–537. PubMed PMID: 16636202. Pubmed Central PMCID: PMC2151519. Epub 2006/04/26. eng

- Li Z, Takino T, Endo Y, Sato H (2017) Activation of MMP-9 by membrane type-1 MMP/MMP-2 axis stimulates tumor metastasis. *Cancer Sci.* 108(3):347–353. PubMed PMID: 27987367. Pubmed Central PMCID: PMC5378257. Epub 2016/12/18. eng
- Lock FE, McDonald PC, Lou Y, Serrano I, Chafe SC, Ostlund C, et al (2013) Targeting carbonic anhydrase IX depletes breast cancer stem cells within the hypoxic niche. *Oncogene.* 32(44):5210–5219. PubMed PMID: 23208505. Epub 2012/12/05. eng
- Lou Y, McDonald PC, Oloumi A, Chia S, Ostlund C, Ahmadi A, et al (2011) Targeting tumor hypoxia: suppression of breast tumor growth and metastasis by novel carbonic anhydrase IX inhibitors. *Cancer Res* 71(9):3364–3376. PubMed PMID: 21415165. Epub 2011/03/19. eng
- Mackenzie B, Erickson JD (2004) Sodium-coupled neutral amino acid (System N/A) transporters of the SLC38 gene family. *Pflugers Archiv Eur J Physiol* 447(5):784–795. PubMed PMID: 12845534. Epub 2003/07/08. eng
- Marshall AD, van Geldermalsen M, Otte NJ, Lum T, Vellozzi M, Thoeng A, et al (2017) ASCT2 regulates glutamine uptake and cell growth in endometrial carcinoma. *Oncogenesis* 6(7):e367. PubMed PMID: 28759021. Pubmed Central PMCID: PMC5541720. Epub 2017/08/02. eng
- McDonald PC, Winum JY, Supuran CT, Dedhar S (2012) Recent developments in targeting carbonic anhydrase IX for cancer therapeutics. *Oncotarget* 3(1):84–97. PubMed PMID: 22289741. Pubmed Central PMCID: PMC3292895. Epub 2012/02/01. eng
- McDonald PC, Chafe SC, Brown WS, Saberi S, Swayampakula M, Venkateswaran G, et al (2019) Regulation of pH by carbonic anhydrase 9 mediates survival of pancreatic cancer cells with activated KRAS in response to hypoxia. *Gastroenterology* PubMed PMID: 31078621. Epub 2019/05/13. eng
- Metallo CM, Gameiro PA, Bell EL, Mattaini KR, Yang J, Hiller K, et al (2011) Reductive glutamine metabolism by IDH1 mediates lipogenesis under hypoxia. *Nature* 481(7381):380–384. PubMed PMID: 22101433. Pubmed Central PMCID: PMC3710581. Epub 2011/11/22. eng
- Millard TH, Sharp SJ, Machesky LM (2004) Signalling to actin assembly via the WASP (Wiskott-Aldrich syndrome protein)-family proteins and the Arp2/3 complex. *Biochem J* 380(Pt 1):1–17. PubMed PMID: 15040784. Pubmed Central PMCID: PMC1224166. Epub 2004/03/26. eng
- Molinie N, Gautreau A (2008) The Arp2/3 regulatory system and its deregulation in cancer. *Physiol Rev* 98(1):215–238. PubMed PMID: 29212790. Epub 2017/12/08. eng
- Mori H, Tomari T, Koshikawa N, Kajita M, Itoh Y, Sato H, et al (2002) CD44 directs membrane-type 1 matrix metalloproteinase to lamellipodia by associating with its hemopexin-like domain. *EMBO J* 21(15):3949–59. PubMed PMID: 12145196. Pubmed Central PMCID: PMC126155. Epub 2002/07/30. eng
- Morotti M, Bridges E, Valli A, Choudhry H, Sheldon H, Wigfield S, et al (2018) Hypoxia-induced switch in SNAT2/SLC38A2 regulation generates endocrine-resistance in breast cancer. *Proc Natl Acad Sci U S A* 116(25):12452–12461. PubMed PMID: 31152137
- Nagano O, Saya H (2004) Mechanism and biological significance of CD44 cleavage. *Cancer Sci* 95(12):930–935. PubMed PMID: 15596040. Epub 2004/12/15. eng
- Nicklin P, Bergman P, Zhang B, Triantafellow E, Wang H, Nyfeler B, et al (2009) Bidirectional transport of amino acids regulates mTOR and autophagy. *Cell* 136(3):521–534. PubMed PMID: 19203585. Pubmed Central PMCID: PMC3733119. Epub 2009/02/11. eng
- Okamoto I, Tsuiji H, Kenyon LC, Godwin AK, Emler DR, Holgado-Madruga M, et al (2002) Proteolytic Cleavage of the CD44 Adhesion Molecule in Multiple Human Tumors. *Am J Pathol* 160(2):441–447
- Opavsky R, Pastorekova S, Zelnik V, Gibadulinova A, Stanbridge EJ, Zavada J, et al (1996) Human MN/CA9 gene, a novel member of the carbonic anhydrase family: structure and exon to protein domain relationships. *Genomics* 33(3):480–487. PubMed PMID: 8661007. Epub 1996/05/01. eng
- Panisova E, Kery M, Sedlakova O, Brisson L, Debreova M, Sboarina M, et al. (2017) Lactate stimulates CA IX expression in normoxic cancer cells. *Oncotarget* 8(44):77819–77835. PubMed PMID: 29100428. Pubmed Central PMCID: PMC5652817. Epub 2017/11/05. eng

- Parks SK, Pouyssegur J (2015) The Na⁺/HCO₃⁻ Co-transporter SLC4A4 plays a role in growth and migration of colon and breast cancer cells. *J Cell Physiol* 230(8):1954–1963
- Pastorekova S, Ratcliffe PJ, Pastorek J (2008) Molecular mechanisms of carbonic anhydrase IX-mediated pH regulation under hypoxia. *BJU international*. 101 (Suppl 4):8–15. PubMed PMID: 18430116. Epub 2008/04/24. eng
- Perez-Moreno M, Jamora C, Fuchs E (2003) Sticky business: orchestrating cellular signals at adherens junctions. *Cell* 112(4):535–548. PubMed PMID: 12600316. Epub 2003/02/26. eng
- Radvak P, Repic M, Svastova E, Takacova M, Csaderova L, Strnad H, et al (2013) Suppression of carbonic anhydrase IX leads to aberrant focal adhesion and decreased invasion of tumor cells. *Oncol Rep* 29(3):1147–1153. PubMed PMID: 23291973. Epub 2013/01/08. eng
- Ron D, Walter P (2007) Signal integration in the endoplasmic reticulum unfolded protein response. *Nat Rev Mol Cell Biol* 8(7):519–529. PubMed PMID: 17565364. Epub 2007/06/15. eng
- Rosso O, Piazza T, Bongarzone I, Rossello A, Mezzanzanica D, Canevari S, et al. (2007) The ALCAM shedding by the metalloprotease ADAM17/TACE is involved in motility of ovarian carcinoma cells. *Mol Cancer Res* 5(12):1246–1253. PubMed PMID: 18171982. Epub 2008/01/04. eng
- Roux KJ, Kim DI, Raida M, Burke B (2012) A promiscuous biotin ligase fusion protein identifies proximal and interacting proteins in mammalian cells. *J Cell Biol* 196(6):801–810. PubMed PMID: 22412018. Pubmed Central PMCID: PMC3308701. Epub 2012/03/14. eng
- Samanta D, Semenza GL (2018) Metabolic adaptation of cancer and immune cells mediated by hypoxia-inducible factors. *Biochim Biophys Acta Rev Cancer* 870(1):15–22
- Shannon P, Markiel A, Ozier O, Baliga NS, Wang JT, Ramage D, et al (2003) Cytoscape: a software environment for integrated models of biomolecular interaction networks. *Genome Res*. 13(11):2498–2504. PubMed PMID: 14597658. Pubmed Central PMCID: PMC403769. Epub 2003/11/05. eng
- Sheth P, Seth A, Atkinson KJ, Gheyi T, Kale G, Giorgianni F, et al (2007) Acetaldehyde dissociates the PTP1B-E-cadherin-beta-catenin complex in Caco-2 cell monolayers by a phosphorylation-dependent mechanism. *Biochem J* 402(2):291–300. PubMed PMID: 17087658. Epub 02/12. eng
- Shin HJ, Rho SB, Jung DC, Han IO, Oh ES, Kim JY (2011) Carbonic anhydrase IX (CA9) modulates tumor-associated cell migration and invasion. *J Cell Sci* 124(Pt 7):1077–1087. PubMed PMID: 21363891. Epub 2011/03/03. eng
- Soysal S, Obermann EC, Gao F, Oertli D, Gillanders WE, Viehl CT, et al (2013) PTP1B expression is an independent positive prognostic factor in human breast cancer. *Breast Cancer Res Treatment* 137(2):637–644. PubMed PMID: 23242616. Epub 12/16. eng
- Srivastava J, Barreiro G, Groscurth S, Gingras AR, Goult BT, Critchley DR et al (2008) Structural model and functional significance of pH-dependent talin–actin binding for focal adhesion remodeling. *Proc Natl Acad Sci* 105(38):14436–14441
- Stock C, Gassner B, Hauck CR, Arnold H, Mally S, Eble JA, et al (2005) Migration of human melanoma cells depends on extracellular pH and Na⁺/H⁺ exchange. *J Physiol* 567(Pt 1):225–238. PubMed PMID: 15946960. Pubmed Central PMCID: PMC1474168. Epub 2005/06/11. eng
- Su LT, Agapito MA, Li M, Simonson WT, Huttenlocher A, Habas R, et al (2006) TRPM7 regulates cell adhesion by controlling the calcium-dependent protease calpain. *J Biol Chem* 281(16):11260–11270. PubMed PMID: 16436382. Pubmed Central PMCID: PMC3225339. Epub 2006/01/27. eng
- Svastova E, Zilka N, Zat'ovicova M, Gibadulinova A, Ciampor F, Pastorek J, et al (2003) Carbonic anhydrase IX reduces E-cadherin-mediated adhesion of MDCK cells via interaction with beta-catenin. *Experimental cell research*. 290(2):332–345. PubMed PMID: 14567991. Epub 2003/10/22. eng
- Svastova E, Witarski W, Csaderova L, Kosik I, Skvarkova L, Hulikova A, et al (2012) Carbonic anhydrase IX interacts with bicarbonate transporters in lamellipodia and increases cell migration via its catalytic domain. *J Biol Chem* 287(5):3392–3402. PubMed PMID: 22170054. Pubmed Central PMCID: PMC3270993. Epub 2011/12/16. eng

- Swayampakula M, McDonald PC, Vallejo M, Coyaud E, Chafe SC, Westerback A, et al (2017) The interactome of metabolic enzyme carbonic anhydrase IX reveals novel roles in tumor cell migration and invadopodia/MMP14-mediated invasion. *Oncogene* 36(45):6244–6261. PubMed PMID: 28692057. Pubmed Central PMCID: PMC5684442. Epub 2017/07/12. eng
- Takacova M, Holotnakova T, Barathova M, Pastorekova S, Kopacek J, Pastorek J (2010) Src induces expression of carbonic anhydrase IX via hypoxia-inducible factor 1. *Oncology reports*. Mar;23(3):869–874. PubMed PMID: 20127031. Epub 2010/02/04. eng.
- Tominaga T, Barber DL (1998) Na-H exchange acts downstream of RhoA to regulate integrin-induced cell adhesion and spreading. *Mol Biol Cell* 9(8):2287–2303. PubMed PMID: 9693382. Pubmed Central PMCID: PMC25483. Epub 1998/08/07. eng
- van den Beucken T, Koritzinsky M, Niessen H, Dubois L, Savelkoul K, Mujcic H, et al (2009) Hypoxia-induced expression of carbonic anhydrase 9 is dependent on the unfolded protein response. *J Biol Chem* 284(36):24204–24212. PubMed PMID: 19564335. Pubmed Central PMCID: PMC2782014. Epub 2009/07/01. eng
- van Geldermalsen M, Wang Q, Nagarajah R, Marshall AD, Thoeng A, Gao D, et al (2016) ASCT2/SLC1A5 controls glutamine uptake and tumour growth in triple-negative basal-like breast cancer. *Oncogene* 35(24):3201–3208. PubMed PMID: 26455325. Pubmed Central PMCID: PMC4914826. Epub 2015/10/13. eng
- von Lersner A, Drosen L, Zijlstra A (2019) Modulation of cell adhesion and migration through regulation of the immunoglobulin superfamily member ALCAM/CD166. *Clin Exp Metast* 36(2):87–95. PubMed PMID: 30778704. Epub 2019/02/20. eng
- Wang Q, Beaumont KA, Otte NJ, Font J, Bailey CG, van Geldermalsen M, et al (2014) Targeting glutamine transport to suppress melanoma cell growth. *Int J Cancer* 135(5):1060–1071. PubMed PMID: 24531984. Epub 2014/02/18. eng
- Wang Q, Hardie RA, Hoy AJ, van Geldermalsen M, Gao D, Fazli L, et al (2015) Targeting ASCT2-mediated glutamine uptake blocks prostate cancer growth and tumour development. *J Pathol* 236(3):278–289. PubMed PMID: 25693838. Pubmed Central PMCID: PMC4973854. Epub 2015/02/20. eng
- Wang Y, Bai C, Ruan Y, Liu M, Chu Q, Qiu L, et al (2019) Coordinative metabolism of glutamine carbon and nitrogen in proliferating cancer cells under hypoxia. *Nat Commun* 10(1):201. PubMed PMID: 30643150. Pubmed Central PMCID: PMC6331631. Epub 2019/01/16. eng
- Weidmann MD, Surve CR, Eddy RJ, Chen X, Gertler FB, Sharma VP, et al (2016) MenaINV dysregulates cortactin phosphorylation to promote invadopodium maturation. *Sci Rep* 6:36142
- White KA, Grillo-Hill BK, Barber DL (2017) Cancer cell behaviors mediated by dysregulated pH dynamics at a glance. *J Cell Sci* 130(4):663–669. PubMed PMID: 28202602. Pubmed Central PMCID: 5339414
- Wolfson RL, Chantranupong L, Saxton RA, Shen K, Scaria SM, Cantor JR, et al (2016) Sestrin2 is a leucine sensor for the mTORC1 pathway. *Science* 351(6268):43–48. PubMed PMID: 26449471. Pubmed Central PMCID: PMC4698017. Epub 2015/10/10. eng
- Xu H, Tian Y, Yuan X, Wu H, Liu Q, Pestell RG, et al (2015) The role of CD44 in epithelial-mesenchymal transition and cancer development. *Oncotargets Ther* 8:3783–3892. PubMed PMID: 26719706. eng
- Yamamoto K, Murphy G, Troeberg L (2015) Extracellular regulation of metalloproteinases. *Matrix Biol* 44–46:255–63
- Yan R, Zhao X, Lei J, Zhou Q (2019) Structure of the human LAT1–4F2hc heteromeric amino acid transporter complex. *Nature* 568(7750):127–130. PubMed PMID: 30867591. Epub 2019/03/15. eng
- Ye J, Huang Q, Xu J, Huang J, Wang J, Zhong W, et al. (2018) Targeting of glutamine transporter ASCT2 and glutamine synthetase suppresses gastric cancer cell growth. *J Cancer Res Clin Oncol* 144(5):821–833. PubMed PMID: 29435734. Pubmed Central PMCID: PMC5916984. Epub 2018/02/13. eng

Zavada J, Zavadova Z, Pastorek J, Biesova Z, Jezek J, Velek J (2000) Human tumour-associated cell adhesion protein MN/CA IX: identification of M75 epitope and of the region mediating cell adhesion. *British journal of cancer*. 82(11):1808–1813. PubMed PMID: 10839295. Pubmed Central PMCID: PMC2363230. Epub 2000/06/06. eng

Chapter 9

Carbonic Anhydrase IX: Current and Emerging Therapies



R. I. J. Merkx, P. F. A. Mulders, and E. Oosterwijk

Abstract Carbonic anhydrase IX (CAIX) is a transmembranous enzyme that is present in multiple carcinomas, including clear cell renal cell carcinoma (ccRCC). CAIX is a validated cell marker for hypoxia, an important asset in the prediction of radiotherapeutic efficacy. CAIX expression in ccRCC is high and homogenous, the consequence of mutations in the von Hippel Lindau gene, leading to a pseudohypoxic phenotype. CAIX is recognized, amongst others, by the monoclonal antibody G250. The high expression of CAIX in the most common malignant renal cancer in combination with very limited expression in normal tissue endorses CAIX as a promising candidate for multiple antibody-based applications in this disease. This chapter explores potential clinical applications, including the guidance of clinical decision making in case of diagnostic dilemmas concerning ccRCC suspicion, the use of real-time monitoring of surgical margins during renal surgery, the development of novel therapeutic options in patients with advanced ccRCC, and the use of CAIX imaging in hypoxic tumors.

Keywords G250 · Girentuximab · CAIX imaging · Hypoxia · Renal Cancer

9.1 Introduction

Carbonic anhydrases (CA) form a family of zinc metalloenzymes that catalyze the reversible hydration of carbon dioxide, producing bicarbonate and a proton (Hilvo et al. 2008).

CAIX was initially named MN protein after being identified as a cell surface protein in a human cervical carcinoma cell line (HeLa) (Pastorek et al. 1994; Zavada et al. 1993; Pastorekova et al. 1992). When it became clear that this protein belonged to the family of Cas, it was adequately denominated as the ninth member of the CA family: CAIX. CAIX is a suitable pHi regulator in conditions of environmental acidosis (Innocenti et al. 2009). In normal tissue, CAIX expression is limited to the

R. I. J. Merkx · P. F. A. Mulders · E. Oosterwijk (✉)
Department of Urology, Radboud University Medical Center, Nijmegen, The Netherlands
e-mail: Egbert.Oosterwijk@radboudumc.nl

© Springer Nature Switzerland AG 2021

W. R. Chegwidden and N. D. Carter (eds.), *The Carbonic Anhydrases: Current and Emerging Therapeutic Targets*, Progress in Drug Research 75,
https://doi.org/10.1007/978-3-030-79511-5_9

205

gastrointestinal tract, mainly the gastric mucosa and the bile ducts, where it plays a role in maintaining the acid–base balance.

Prominent expression of CAIX has been observed in multiple carcinomas, including lung, kidney, brain, colon, pancreas, liver, breast, endometrium, esophagus, ovary, and skin (Ivanov et al. 2001). The most homogeneous expression has been observed in clear cell Renal Cell Carcinoma (ccRCC). Elegant studies have demonstrated that regulation of CAIX expression is mainly dependent on transcription factor hypoxia inducible factor 1 (HIF-1 α) (Wykoff et al. 2000). In normoxic conditions, HIF-1 α is hydroxylated by prolyl hydroxylase domain proteins (PHDs) and bound by pVHL, inciting the polyubiquitylation of prolyl hydroxylated HIF-1 α for subsequent degradation via the 26S proteasome (Aprelikova et al. 2004). Under hypoxic conditions, hydroxylation does not occur, leading to HIF accumulation since pVHL binding is inhibited and HIF degradation prevented (Mucaj et al. 2012). This leads to nuclear translocation, and after heterodimerization with HIF-1 β , the transcription factor binds to hypoxic responsive elements in gene promotor regions leading to expression of multiple genes, amongst others CAIX (Benej et al. 2014).

The main driver event in the development of ccRCC is a mutation of VHL. This also leads to expression of hypoxia responsive genes, as the mutated pVHL cannot bind HIF-1 α , leading to HIF1 α accumulation and nuclear translocation, a so-called pseudohypoxic response. The almost ubiquitous mutation of VHL in ccRCC also explains the homogeneous expression of CAIX in these tumors (Fig. 9.1).

CAIX is recognized by, amongst others, the monoclonal antibody (mAbG250). This antibody was discovered in 1986 (Oosterwijk et al. 1986). Initial studies with G250 indicated specific expression in renal cell carcinoma (RCC), while expression in normal renal tissue was absent. Other normal tissue sites with CAIX expression included bile-duct epithelium and mucous cells in the stomach. Interestingly, G250 antigen expression was also found in other tumor types, albeit less homogenous and at a lower rate. Molecular identification of the recognized antigen lasted until 2000, and it became clear that it was identical to the tumor-associated antigen MN/CAIX (Grabmaier et al. 2000).

This high expression of CAIX in the most common malignant renal cancer in combination with very limited expression in normal tissue endorsed CAIX as a

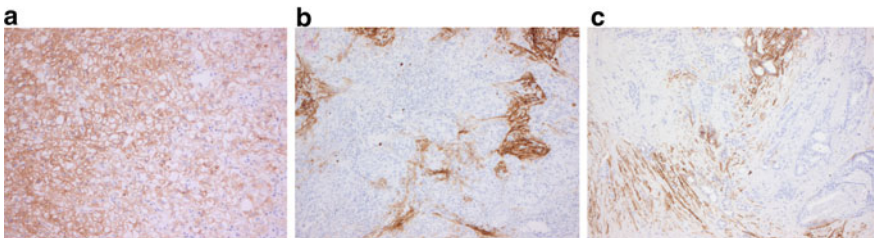


Fig. 9.1 Immunohistochemical staining of CAIX in various carcinomas. A: Renal cell carcinoma B: Lung carcinoma. C: Breast carcinoma

promising candidate for diagnostic and therapeutic modalities in this disease. While current research has mostly focused on ccRCC, the potential of CAIX-targeting extends to other CAIX-expressing malignancies, albeit that the less homogeneous expression may hamper success.

9.2 Carbonic Anhydrase IX Imaging

9.2.1 CAIX Imaging in RCC

CAIX imaging in RCC has been extensively investigated over the last decades. Renal tumors are divergent and their behavior is highly dependent on the pathophysiological subtype. This ranges from benign (20%, including oncocytoma and angiomyolipoma) to indolent (papillary and chromophobe carcinoma) with limited metastatic potential to the more aggressive metastatic clear cell renal cell carcinoma (ccRCC) (Leibovich et al. 2010). Due to more frequent radiological evaluation of the abdomen, the incidence of RCC has increased (Capitanio et al. 2019). Identification of the tumor phenotype is paramount to improve clinical decision making and enable individualized treatment planning. Importantly, approximately 20–30% of kidney lesions are non-malignant and watchful waiting may be possible. Currently, the differential diagnosis is achieved through renal tumor biopsies. This is an invasive procedure with a poor predictive value. Conventional imaging methods (i.e., computed tomography (CT) and ultrasound) cannot reliably distinguish between the indolent and aggressive malignancies (Kutikov et al. 2006). Positron emission tomography (PET) and single photon emission computed tomography (SPECT) are nuclear imaging modalities that offer the ability to non-invasively visualize pathophysiological characteristics of tumors. For this purpose, noninvasive imaging of CAIX using radiolabeled G250 has been developed.

Multiple preclinical studies in various mouse models using different radionuclides have shown excellent selective uptake of mAbG250 in CAIX-expressing xenografts (Brouwers et al. 2004a; Steffens et al. 1998,1999a; Dijk et al. 1991; Kranenborg et al. 1997). The very limited expression of CAIX in normal tissue combined with the homogenous CAIX expression in ccRCC led to the initiation of multiple clinical studies.

In 1993, the first clinical study was published, documenting the imaging and biodistribution characteristics of ^{131}I -mAbG250 in patients suspected for RCC. The explicit visualization of primary and metastatic RCC lesions combined with remarkable uptake of antibody in CAIX-positive tumor tissue demonstrated its diagnostic potential. However, development of human-anti-mouse-antibodies (HAMA) prevented repeated administration (Oosterwijk et al. 1993).

The potential of CAIX imaging in RCC was supported after the chimeric version of the mAbG250 (cG250/girentuximab) was successfully used in a similar study. The characteristics and performance of cG250 were similar to the murine antibody in

terms of optimal protein dose, tumor-specific uptake, and visual assessment (Steffens et al. 1997). More importantly, the chimerization greatly reduced the immunogenicity of the antibody, and development of human anti-chimeric antibody (HACA) was rare. Thus, multiple administrations became feasible.

At the same time, with a gradually increasing availability of various radionuclides, careful selection of the radionuclide based on physical half-life and other characteristics for specific indications became possible. Subsequently, the most promising radionuclides (^{131}I ($t_{1/2} = 8.0$ days), ^{125}I ($t_{1/2} = 59.4$ days), ^{124}I ($t_{1/2} = 4.2$ days), ^{111}In ($t_{1/2} = 2.8$ days), and ^{89}Zr ($t_{1/2} = 3.3$ days)) were used in combination with cG250 in phase I/II studies.

Although the tumor uptake of the radiolabeled cG250 was high, intratumoral uptake was surprisingly heterogeneous and could not be explained by antigen expression alone. As intratumoral necrosis and tumor vasculature did not seem to consistently associate with the heterogeneity, the impact of multiple administrations on tumor uptake of the antibody was studied. Patients with primary kidney tumors received two presurgical administrations, separated by four days, of ^{125}I - and ^{131}I -cG250, respectively. Analysis of the surgically removed specimen showed an identical uptake pattern of both radiolabeled cG250, indicating that two consecutive administrations did not significantly alter the heterogeneous pattern (Steffens et al. 1999b).

In order to compare the CAIX targeting ^{131}I -cG250 with the clinically available PET-tracer ^{18}F -FDG, an inpatient comparison study in patients with advanced RCC was initiated. Remarkably, the PET-tracer ^{18}F -FDG proved to be superior in comparison to ^{131}I -cG250 for detection of RCC metastases (Brouwers et al. 2002). Since ^{131}I is physiologically excreted from the cell after intracellular proteolytic digestion of labeled antibody, the intracellular retainment of the radionuclide could play an important role in achieving improved tumor to background ratios. This intracellular retainment of a radioisotope after internalization is called residualization. Radiometals, such as ^{64}Cu , ^{111}In , and ^{89}Zr are not excreted, and are also suited for diagnostic and therapeutic purposes when bound to (internalizing) antibodies.

In view of the former, an inpatient comparison study was initiated using the residualizing ^{111}In and the non-residualizing ^{131}I as radiolabels. ^{111}In -cG250 showed superior tumor to background ratios compared to ^{131}I -cG250 (Brouwers et al. 2003a). Moreover, the diagnostic accuracy of ^{111}In -cG250 in detecting ccRCC lesions in both primary as well as metastasized disease was excellent, providing evidence that antibody internalization does play a role for cG250 imaging (Muselaers et al. 2013).

Although ^{111}In -cG250 showed promising diagnostic ability, the more favorable characteristics of PET compared to SPECT, such as higher spatial resolution and superior quantitative analysis of images, incited the development of immuno-PET tracers. To match the relatively slow pharmacokinetics of intravenously administered mAb ($\sim t_{1/2} = 70$ h), the radioisotopes ^{89}Zr and ^{124}I were deemed good candidates for this modality.

The first clinical study using CAIX-directed immuno-PET was performed with ^{124}I -cG250 in 26 patients with suspected renal lesions. The aim of the study was to unequivocally distinguish ccRCC from non-ccRCC. Sensitivity and specificity of

^{124}I -cG250 PET/CT to detect ccRCC were 94% and 100%, respectively. The negative and predictive values were 90% and 100%, respectively (Divgi et al. 2007). In a large follow-up multicenter comparison study, 226 patients, who were scheduled for surgery of a renal mass were evaluated. ^{124}I -cG250 PET imaging outperformed conventional imaging in the form of contrast-enhanced CT (CECT). In 195 patients, comparative data was available, and showed superior sensitivity and specificity of ^{124}I -cG250 compared to CECT (86.2 versus 75.5% and 85.9 versus 46.8%, respectively) (Divgi et al. 2013). However, the non-residualizing characteristics of ^{124}I combined with a scarce availability of this radioisotope were hampering clinical implementation.

With the residualizing radioisotope ^{89}Zr becoming more widely available, which was a limiting factor for clinical development, animal experiments with ^{89}Zr -cG250 were performed to investigate its value as imaging agent. Comparison of ^{89}Zr -cG250 with ^{124}I -cG250 demonstrated superiority in terms of tumor to background ratio (Stillebroer et al. 2013a). This led to a phase I/II clinical trial to evaluate the value of ^{89}Zr -cG250 in aiding clinicians when facing diagnostic dilemmas in RCC. A total of 30 patients were enrolled, in 16 patients immuno-PET imaging was used in the decision to perform either surgery or active surveillance. In 70% of patients, the clinical management was changed based on ^{89}Zr -cG250 PET imaging. Nine patients showed no tumor uptake of ^{89}Zr -cG250, suggesting non-malignancy progression of lesions during follow-up (mean 13.0 ± 4.9 mo) was absent. In seven patients, tumor uptake of ^{89}Zr -cG250 was observed which led to surgical intervention in five cases: in all five cases, ccRCC was histologically proven after surgery. In 5/14 patients suspected of recurrent or metastatic ccRCC, use of ^{89}Zr -cG250 PET/CT imaging led to a major change in clinical management. Additionally, in three patients, repeated biopsies were avoided. Therefore, the authors concluded that ^{89}Zr -cG250 PET/CT is of diagnostic value, and it may guide clinical decision making when a diagnostic dilemma concerning ccRCC suspicion presents (Hekman et al. 2018).

More recently, a phase I safety and dosimetry study using ^{89}Zr -cG250 was performed [NCT03556046]. The primary aim of this study was safety assessment, while secondary outcomes included radiation dosimetry, tumor dosimetry, and diagnostic efficacy (Merkx et al. 2021).

Furthermore, a prospective, multi-center phase III study to evaluate sensitivity and specificity of ^{89}Zr -cG250 PET/CT-imaging to detect ccRCC in patients with suspected primary renal mass for which surgery is scheduled is currently recruiting [NCT03849118].

As described, the tumor-targeting properties of the intact antibodies cG250 and mG250 have been extensively studied. However, these macromolecular radiotracers are known for their slow blood-clearing (~ 70 h). To optimize imaging properties, radioisotopes with matching half-life are required. As a result, the radiation burden to the patient are relatively high. Use of CAIX-targeting, rapid clearing small-molecules could decrease this radiation burden. However, the development of these fast-clearing tracers has been limited to preclinical work so far. One of these newly developing small molecules is a acetazolamide derivative, a carbonic anhydrase ligand with high affinity for CAIX that is able to transport cytotoxic drugs. The $^{99\text{m}}\text{Tc}$ -labeled

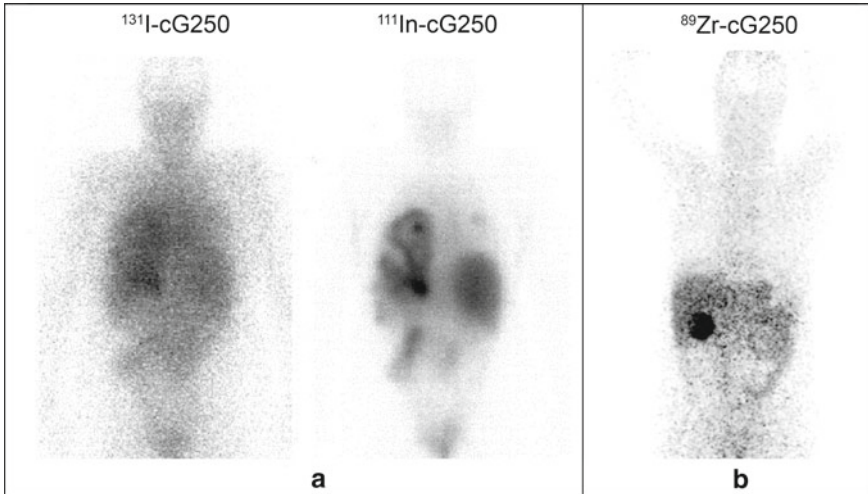


Fig. 9.2 Visualization of clear cell renal cell cancer metastases in different regions using ^{131}I -cG250, ^{111}In -cG250, and ^{89}Zr -cG250. A) An inpatient comparison in which the ^{131}I -cG250 image shows faint accumulation in the chest region, whereas the ^{111}In -cG250 image convincingly demonstrates lung and pleural metastases. B) PET image of ^{89}Zr -cG250 accumulation in a tumor in the right kidney

acetazolamide conjugate showed high tumor uptake and decent tumor-to-organ ratios at 3 h p.i. in a mice model using SK-RC-52 xenografts (Krall et al. 2016). Similarly, a range of affibodies radiolabeled with $^{99\text{m}}\text{Tc}$ and ^{125}I showed specific targeting of CAIX-expressing xenografts at 4 h p.i. Even though the development of these rapid-clearing CAIX-targeting tracers looks promising, clinical studies are required to fully assess their potential (Honarvar et al. 2015; Garousi et al. 2016).

In conclusion, clinical trials have convincingly shown that CAIX-directed antibody imaging is capable of detecting ccRCC lesion in primary as well as metastatic settings. Furthermore, the ongoing development leads to improved tumor to background ratios, thus, enhancing diagnostic accuracy (Fig. 9.2).

However, implementation in regular clinical practice still has to be achieved. A currently recruited phase III trial might lead to clinical implementation of CAIX-targeting antibody imaging.

9.2.2 CAIX Imaging in Non-RCC

While current clinical studies with CAIX-targeting antibodies have been limited to RCC, another area of interest for CAIX imaging is the hypoxic tumor. Tumor hypoxia is associated with a poor prognosis, related to an increased resistance to conventional treatment modalities such as radiotherapy and chemotherapy (Bussink

et al. 2003; Hockel and Vaupel 2001). As mentioned earlier, hypoxia can increase the levels of HIF-1 α and as a result lead to CAIX expression. In non-RCC tumors, CAIX expression is mostly detected in perinecrotic areas and regions that are distanced from perfused vasculature. As a result, you see a much more variable and heterogenous expression in non-RCC tumors compared to ccRCC. Despite the heterogenous CAIX expression in hypoxic tumors, it has been validated as an intrinsic hypoxia-related cell marker and is particularly attractive for in vivo assessment of hypoxia (Wykoff et al. 2000; Pastorekova et al. 2006). However, the half-life of HIF-1 α (5–8 min) is significantly lower than that of CAIX (38 h) (Rafajova et al. 2004; Moroz et al. 2009). In the context of transient and fluctuating hypoxia, the evaluation of CAIX expression could lead to an overestimation of actual hypoxic regions. This potential discrepancy requires awareness when considering CAIX quantification as an indicator of hypoxia.

The leaky vasculature of solid tumors is known to increase permeability of macromolecules. As the diffusion of an antibody within a tumor is dependent on the size, it was initially thought that intact IgG might not be suitable for imaging purposes in these tumors. Antibody fragments (F(ab')₂) are smaller than intact IgG (~100 and ~150 kDa, respectively) and have shown higher tumor penetration (Schmidt and Wittrup 2009). Additionally, the F(ab')₂ fragments are more rapidly cleared in comparison to intact IgG. A fast-clearing tracer allows for imaging at early time-points, this is of particular interest in the setting of the intratumoral hypoxic region, which are susceptible to fluctuation. To evaluate the potential of these antibody fragments in detecting and quantifying hypoxic areas, several preclinical studies have been performed (Hoeben et al. 2010; Huizing et al. 2017, 2019).

The feasibility of noninvasive hypoxia imaging with ⁸⁹Zr-cG250-F(ab')₂ in head and neck carcinomas has been studied, and demonstrated that the maximum tumor uptake of ⁸⁹Zr-cG250-F(ab')₂ was reached at day 1 post injection (p.i.), while specific accumulation was seen at 4 h p.i. In comparison, the maximum tumor uptake and earliest specific accumulation for ⁸⁹Zr-cG250 were 3 days and 1 day, respectively. A significant spatial correlation between the binding of the radiolabeled fragment and CAIX at the microscopic level was established, indicating that sufficient tumor penetration is achieved and accurate microscopic hypoxia localization is possible (Hoeben et al. 2010). Additionally, it was shown that CAIX expression was quantifiable in two different head and neck carcinoma xenograft models (Huizing et al. 2019). Similar results were found in a preclinical study that was designed to compare molecular targeting properties of ¹¹¹In-Fab-cG250, ¹¹¹In-F(ab')₂-cG250, and ¹¹¹In-cG250 in a colorectal xenograft model (Carlin et al. 2010). It was demonstrated that the antibody fragments are capable of targeting CAIX in hypoxic regions at shorter time periods p.i, compared to intact IgG. However, this comes at the cost of reduced absolute uptake and severely reduced tumor-to-muscle ratio. Therefore, the authors concluded that noninvasive imaging with the intact IgG was favored.

Besides the intact cG250 and fragments thereof (Fab), numerous CAIX-targeted imaging agents have been studied in preclinical setting. While none of these surpass the radiolabeled cG250 in terms of tumor uptake, they might prove to be of added values in specific niches, such as visualizing intratumoral hypoxia.

A quantitative biodistribution study of the radiolabeled CAIX ligand VM4-037 in an HT-29 model (human colorectal tumor model) showed no tumor-specific uptake (Peeters et al. 2015). Comparable results were observed with ^{99m}Tc -labeled derivatives of phenylsulfonamide in mice bearing HT-29 xenografts (Akurathi et al. 2014). More success was achieved with ^{68}Ga -labeled sulfonamide inhibitors. In a preclinical study using HT-29 xenografted mice, the biodistribution of three tracers (^{68}Ga -DOTA-AEBSA, ^{68}Ga -DOTA-(AEBSA)₂, and ^{68}Ga -DOTA-(AEBSA)₃) was assessed. While tumor-to-muscle ratios were decent (3.18–9.55), the absolute tumor uptake remained low (Lau et al. 2016).

While CAIX imaging of hypoxic regions has been validated as a prognostic marker in several tumor types, a more interesting application might be predicting therapy resistance and expected efficacy. The visualization and quantification of intratumor hypoxic regions could be used to individualize treatment modalities (i.e., radiotherapeutic “dose painting”). Whether an intact antibody, antibody fragment(s), or other small molecules are best fit for this purpose is yet to be determined.

9.3 Intraoperative Imaging

Intraoperative (fluorescence) imaging is a valuable asset in cancer surgery. It improves tumor visualization in challenging situations such as multifocal disease or organ-sparing surgery by enabling differentiation of tumor and normal tissue. In fluorescence imaging, a fluorophore is excited by light of a distinct wavelength, resulting in emission of a photon. These emitted photons are detected by a fluorescence camera and converted into an image. In a first-in-man trial, fluorescent CAIX imaging was combined with radiodetection to intraoperatively detect ccRCC with cG250. The aim of the dual-label modality technique is to enable real-time monitoring of the surgical margins, ensuring radical surgery. This combination has the advantage that the emitted gamma radiation with its high penetration depth can be used to guide the surgeon to the place of interest, whereas the fluorescent label with the limited penetration depth can be used for live visualization, for instance, to detect positive surgical margins. Complete intraoperative assessment of CAIX-expressing tumors was achieved (Hekman et al. 2016), showing that this can aid the surgeon in achieving complete tumor resection, while sparing normal tissue (Hekman et al. 2018). Further research is needed to advance the use of cG250 for this detection method to show whether this novel technique reduces positive surgical margins and recurrence of tumor. Particularly, the technical hardware needs to be improved.

9.4 CAIX-Directed Radioimmunotherapy

Over the last decades, the armamentarium of therapies against cancer has rapidly expanded with antibody therapies becoming more prominent. One of the most promising application is combining the monoclonal antibody with radiation therapy

(radioimmunotherapy). Initial studies were mainly limited to hematologic malignancies, which are perceived as the most radiosensitive tumors. For radioimmunotherapy (RIT) to be successful, several variables are imperative. Most obviously, the best cell surface target antigen and corresponding targeting antibody need to be selected and developed. To elaborate, the ideal target antigen should preferably be highly and homogeneously expressed on the surface of all tumor cells with minimal expression on normal tissues. Additionally, the antibody should be internalized after binding, be able to rapidly achieve tumor penetration, and effectively bind the antigen without interacting with non-malignant tissues. Lastly, the antibody should be rapidly cleared from the body after reaching maximum tumor binding. The antibody–antigen pair that meet all these criteria has yet to be discovered. Nonetheless, cG250 in combination with CAIX seems to be a promising pair. Since the high and homogeneous expression of CAIX has been observed in ccRCC, the potential of RIT in this disease has been extensively studied.

The choice of therapeutic radionuclide has been a point of discussion since the RIT was studied. In theory, several radionuclides are more favorable than others, but historically it has been shown that availability plays an important role in the development of RIT.

The first RIT studies in ccRCC were performed in 1998 and used the murine version of the G250 antibody radiolabeled with ^{131}I , a β -emitter. ^{131}I had shown its therapeutic efficacy in thyroid-related diseases and was readily available. Additionally, radiolabeling of the antibody with ^{131}I was technically straightforward. Initial results with a single injection of ^{131}I -mG250 showed stabilization of disease in half of the patients. Despite the lack of major responses, the overall survival of patients treated with ^{131}I -mG250 when compared to historic control patients suggested clinical benefit (Divgi et al. 1998). As mentioned earlier, the development of human anti-mouse monoclonal antibody (HAMA), prevented retreatment. For this purpose, cG250/girentuximab was developed. In the subsequent study, patients with RCC metastases received a single therapeutic-dose ^{131}I -cG250 injection preceded by an imaging dose of the tracer to ensure the presence of CAIX-positive metastases. Due to extended serum half-life of the chimeric version, maximum tolerable dose (MTD) of ^{131}I -cG250 was significantly lower than ^{131}I -mG250, and hematological toxicity remained the dose limiting factor (Steffens et al. 1999c). Development of human-anti-chimeric-antibodies (HACA) was limited to a single patient, who received multiple cG250 injection in a previous study. Unfortunately, the therapeutic efficacy of a single dose ^{131}I -cG250 was lacking. In an attempt to increase the RIT efficacy, a study in which patients received fractionated doses of ^{131}I -cG250 was designed. The fractionated approach is associated with lower toxicity profile, possibly due to hematopoietic recovery in between the administrations. Moreover, multiple administration potentially increases the therapeutic efficacy by achieving higher absorbed tumor dose. However, this could not be confirmed in the study as fractionated radionuclide therapy with ^{131}I -cG250 in metastatic ccRCC did not show major clinical responses in two separate studies (Divgi et al. 2004; Brouwers et al. 2005). The hematological toxicity remained an issue, and due to the limited efficacy of ^{131}I -cG250, the search for more suitable radionuclides was initiated.

As more radionuclides became available for use in pre- and clinical studies, new studies were initiated. In a preclinical study, the therapeutic efficacy of lutetium-177 (^{177}Lu)-, yttrium-90 (^{90}Y)-and rhenium-186 (^{186}Re) labeled to girentuximab were compared to ^{131}I -cG250. The tumor growth in mice with subcutaneous xenografts was delayed most effectively by ^{177}Lu -cG250 (Brouwers et al. 2004b; Muselaers et al. 2014). This led to the initiation of a clinical study to investigate the therapeutic efficacy and maximum tolerable dose (MTD) of ^{177}Lu -cG250 in patients with advanced RCC. ^{177}Lu -cG250 RIT was well tolerated and resulted in disease stabilization in the majority of patients (Stillebroer et al. 2013b). The ensuing study used the observed MTD of 2405 MBq/m² in a similar patient population. In absence of persistent toxicity and progressive disease after initial treatment, patients were eligible for retreatment of ^{177}Lu -cG250 after 3 months with 75% of the initial activity dose. Similar to the phase I study, ^{177}Lu -cG250 RIT led to stabilized disease in the majority of patients. After the first cycle of ^{177}Lu -cG250 RIT, grade 3–4 thrombocytopenia and grade 3–4 leukocytopenia were observed in all but one patient (Muselaers et al. 2016). This is caused by the relatively long circulation combined with the range of the beta-emitting radionuclide. No clinical studies with cG250 RIT have been performed since then. To prevent irreversible myelotoxicity, treatment regimen need to be adjusted properly. Preclinical studies suggest that this might be achieved by combining RIT in a lower dose with VEGFR-TKIs or immune-checkpoint inhibitors (Stewart et al. 2014). Alternatively, modifying monoclonal antibodies to decrease the circulation time may provide a solution.

A promising alternative might be the use of cG250 labeled with α -emitting radionuclides such as ^{225}Ac and ^{227}Th . Alpha-emitting radionuclides provide a higher linear energy transfer (LET) and have a lower range, avoiding damage to unrelated nearby tissues. The higher LET causes irreversible double-strand DNA breaks, resulting in a higher relative biological effectiveness (RBE) compared to beta radiation. Targeted α therapy (TAT) has shown impressive anti-tumor effects in multiple clinical studies (Kratochwil et al. 2016). However, TAT with monoclonal antibodies is challenging: whenever an α -emitting radionuclide decays, the daughter nuclide is released from the chelater. This so-called recoil effect leads to excretion of unbound radionuclides in the bloodstream. If these accumulate, other organs will be at risk. Moreover, the availability of α -emitting radionuclides is limited, inhibiting their use in clinical studies. Nevertheless, based on the results with cG250 in RIT, the potential of TAT in CAIX-targeted therapy needs to be further explored. Considering that the hypoxic regions within a tumor are resistant to conventional radiotherapy, CAIX-targeted RIT might be an effective alternative.

9.5 Carbonic Anhydrase IX Immunotherapy

Monoclonal antibodies have been approved for cancer treatment in multiple oncological entities. The therapeutic effect of antibodies may depend on the capacity to lyse cells by complement activation or by antibody-dependent cellular toxicity

(ADCC). In vitro studies showed that cG250 initiates cell lysis through ADCC of CAIX-positive cells. Additionally, preclinical mouse studies showed significant tumor growth reduction after treatment with unmodified G250. These findings led to the first clinical study using unmodified cG250 in RCC patients in which optimal dosing and safety were assessed. Weekly infusions with unmodified cG250 were deemed safe and well tolerated (Davis et al. 2007a). The subsequent study in 36 patients with advanced RCC suggested clinical benefit after one treatment cycle of 50mg cG250 in 28% of progressive patients. During the follow-up, one minor partial response (<50% decrease) and one complete response (CR) were observed (Bleumer et al. 2004). The complete response was observed in patient who underwent a nephrectomy before starting treatment, therefore, it was unclear whether the CR was part of the natural disease course or an antibody-induced response. At the same time, the Adjuvant Rencarex® Immunotherapy (ARISER) study was initiated to study if cG250 was able to reduce the recurrence of disease in high risk patients who underwent nephrectomy for non-metastasized RCC. There was no improvement in median disease free survival (DFS) for patients that received adjuvant cG250 compared to placebo which was the primary objective of this study, and therefore, the study was pre-emptively terminated (Chamie et al. 2017). A retrospective subanalysis showed that adjuvant cG250 therapy did increase the DFS in patients with high expressing CAIX tumors, emphasizing that high CAIX expression is a prerequisite to achieve this benefit.

To enhance the therapeutic potential of cG250 mAb in RCC therapy, combination therapy with immune agents such as interleukin-2 and interferon- α have been used (Davis et al. 2007b; Bleumer et al. 2006). Interleukin-2 (IL-2) has the ability to enhance ADCC of monoclonal antibodies including cG250 (Brouwers et al. 2003b). Admission of cG250 combined with IL-2 was well tolerated with little toxicity, but the value of adding IL-2 in this therapeutic setting was unclear. Currently, the role of CAIX targeting with cG250 in the immunotherapy is not well defined, particularly because the patient numbers in these phase I trials were small, and randomization and comparison with control groups were not performed. Larger controlled trials are needed to define the role of cG250 (or derivatives thereof) as a therapy modality.

9.6 Conclusion and Future Perspectives

The landscape of cancer treatment is constantly changing, and CAIX-targeted therapy has the potential to become an important asset in the growing armamentarium against cancer. CAIX represents an ideal target for treatment of clear cell renal cell carcinoma and hypoxic tumors. The rare expression in normal tissues enables the exploration of tumor-specific therapies such as RIT. RIT is considered to have a high anti-tumor effect, but a balance between therapeutic efficacy and toxicity is challenging. The search for the most suitable radionuclide is ongoing, and the increased availability of α -emitters has opened up a new path.

With immunotherapy finding its way into clinical practice, combination of RIT and immunotherapy are of future interest.

Beyond the clear therapeutic potential, CAIX has shown to be an excellent target for accurate diagnosis of clear cell renal cell carcinoma. This aids clinical decision making and enables individualized treatment plans. Other modalities that are being explored are intraoperative use of CAIX-targeting in patients planned for partial or total nephrectomy for RCC.

References

- Akurathi V, Dubois L, Celen S, Lieuwes NG, Chitneni SK, Cleynhens BJ et al (2014) Development and biological evaluation of (9)(9m)Tc-sulfonamide derivatives for in vivo visualization of CA IX as surrogate tumor hypoxia markers. *Eur J Med Chem* 71:374–384
- Aprelikova O, Chandramouli GV, Wood M, Vasselli JR, Riss J, Maranchie JK et al (2004) Regulation of HIF prolyl hydroxylases by hypoxia-inducible factors. *J Cell Biochem* 92(3):491–501
- Benej M, Pastorekova S, Pastorek J (2014) Carbonic anhydrase IX: regulation and role in cancer. *Subcell Biochem* 75:199–219
- Bleumer I, Knuth A, Oosterwijk E, Hofmann R, Varga Z, Lamers C et al (2004) A phase II trial of chimeric monoclonal antibody G250 for advanced renal cell carcinoma patients. *Br J Cancer* 90(5):985–990
- Bleumer I, Oosterwijk E, Oosterwijk-Wakka JC, Voller MC, Melchior S, Warnaar SO et al (2006) A clinical trial with chimeric monoclonal antibody WX-G250 and low dose interleukin-2 pulsing scheme for advanced renal cell carcinoma. *J Urol* 175(1):57–62
- Brouwers AH, Buijs WC, Oosterwijk E, Boerman OC, Mala C, De Mulder PH et al (2003a) Targeting of metastatic renal cell carcinoma with the chimeric monoclonal antibody G250 labeled with (131)I or (111)In: an inpatient comparison. *Clin. Cancer Res.* 9(10 Pt 2):3953s–s3960
- Brouwers AH, Dorr U, Lang O, Boerman OC, Oyen WJ, Steffens MG et al (2002) 131 I-cG250 monoclonal antibody immunoscintigraphy versus [18 F]FDG-PET imaging in patients with metastatic renal cell carcinoma: a comparative study. *Nucl Med Commun* 23(3):229–236
- Brouwers AH, Frielink C, Oosterwijk E, Oyen WJ, Corstens FH, Boerman OC (2003b) Interferons can upregulate the expression of the tumor associated antigen G250-MN/CA IX, a potential target for (radio)immunotherapy of renal cell carcinoma. *Cancer Biother Radiopharm* 18(4):539–547
- Brouwers A, Verel I, Van Eerd J, Visser G, Steffens M, Oosterwijk E et al (2004a) PET radioimmunoscintigraphy of renal cell cancer using 89Zr-labeled cG250 monoclonal antibody in nude rats. *Cancer Biother Radiopharm* 19(2):155–163
- Brouwers AH, van Eerd JE, Frielink C, Oosterwijk E, Oyen WJ, Corstens FH et al (2004b) Optimization of radioimmunotherapy of renal cell carcinoma: labeling of monoclonal antibody cG250 with 131I, 90Y, 177Lu, or 186Re. *J Nucl Med Offi Publ Soc Nucl Med* 45(2):327–337
- Brouwers AH, Mulders PF, de Mulder PH, van den Broek WJ, Buijs WC, Mala C et al (2005) Lack of efficacy of two consecutive treatments of radioimmunotherapy with 131I-cG250 in patients with metastasized clear cell renal cell carcinoma. *J Clin Oncol Offi J Am Soc Clin Oncol* 23(27):6540–6548
- Bussink J, Kaanders JH, van der Kogel AJ (2003) Tumor hypoxia at the micro-regional level: clinical relevance and predictive value of exogenous and endogenous hypoxic cell markers. *Radiother Oncol J Eur Soc Ther Radiol Oncol* 67(1):3–15
- Capitanio U, Bensalah K, Bex A, Boorjian SA, Bray F, Coleman J et al (2019) Epidemiology of renal cell carcinoma. *Eur Urol* 75(1):74–84

- Carlin S, Khan N, Ku T, Longo VA, Larson SM, Smith-Jones PM (2010) Molecular targeting of carbonic anhydrase IX in mice with hypoxic HT29 colorectal tumor xenografts. *PLoS One* 5(5):e10857
- Chamie K, Donin NM, Klopfer P, Bevan P, Fall B, Wilhelm O et al (2017) Adjuvant weekly girentuximab following nephrectomy for high-risk renal cell carcinoma: the ARISER randomized clinical trial. *JAMA Oncol* 3(7):913–920
- Davis ID, Wiseman GA, Lee FT, Gansen DN, Hopkins W, Papenfuss AT et al (2007a) A phase I multiple dose, dose escalation study of cG250 monoclonal antibody in patients with advanced renal cell carcinoma. *Cancer Immun* 7:13
- Davis ID, Liu Z, Saunders W, Lee FT, Spirkoska V, Hopkins W et al (2007b) A pilot study of monoclonal antibody cG250 and low dose subcutaneous IL-2 in patients with advanced renal cell carcinoma. *Cancer Immun* 7:14
- Divgi CR, Bander NH, Scott AM, O'Donoghue JA, Sgouros G, Welt S et al (1998) Phase I/II radioimmunotherapy trial with iodine-131-labeled monoclonal antibody G250 in metastatic renal cell carcinoma. *Clin Cancer Res Off J Am Assoc Cancer Res* 4(11):2729–2739
- Divgi CR, O'Donoghue JA, Welt S, O'Neil J, Finn R, Motzer RJ et al (2004) Phase I clinical trial with fractionated radioimmunotherapy using 131I-labeled chimeric G250 in metastatic renal cancer. *J Nucl Med Off Publ Soc Nucl Med* 45(8):1412–1421
- Divgi CR, Pandit-Taskar N, Jungbluth AA, Reuter VE, Gonen M, Ruan S et al (2007) Preoperative characterisation of clear-cell renal carcinoma using iodine-124-labelled antibody chimeric G250 (124I-cG250) and PET in patients with renal masses: a phase I trial. *Lancet Oncol* 8(4):304–310
- Divgi CR, Uzzo RG, Gatsonis C, Bartz R, Treutner S, Yu JQ et al (2013) Positron emission tomography/computed tomography identification of clear cell renal cell carcinoma: results from the REDECT trial. *J Clin Oncol* 31(2):187–194
- Garousi J, Honarvar H, Andersson KG, Mitran B, Orlova A, Buijs J et al (2016) Comparative evaluation of affibody molecules for radionuclide imaging of in vivo expression of carbonic anhydrase IX. *Mol Pharm* 13(11):3676–3687
- Grabmaier K, Vissers JL, De Weijert MC, Oosterwijk-Wakka JC, Van Bokhoven A, Brakenhoff RH et al (2000) Molecular cloning and immunogenicity of renal cell carcinoma-associated antigen G250. *Int J Cancer* 85(6):865–870
- Hekman MC, Boerman OC, de Weijert M, Bos DL, Oosterwijk E, Langenhuijsen JF et al (2016) Targeted dual-modality imaging in renal cell carcinoma: an ex vivo kidney perfusion study. *Clin Cancer Res Off J Am Assoc Cancer Res* 22(18):4634–4642
- Hekman MCH, Rijpkema M, Aarntzen EH, Mulder SF, Langenhuijsen JF, Oosterwijk E et al (2018) Positron emission tomography/computed tomography with (89)Zr-girentuximab can aid in diagnostic dilemmas of clear cell renal cell carcinoma suspicion. *Eur Urol* 74(3):257–260
- Hekman MC, Rijpkema M, Muselaers CH, Oosterwijk E, Hulsbergen-Van de Kaa CA, Boerman OC, et al (2018) Tumor-targeted dual-modality imaging to improve intraoperative visualization of clear cell renal cell carcinoma: a first in man study. *Theranostics* 8(8):2161–70.
- Hilvo M, Baranauksiene L, Salzano AM, Scaloni A, Matulis D, Innocenti A et al (2008) Biochemical characterization of CA IX, one of the most active carbonic anhydrase isozymes. *J Biol Chem* 283(41):27799–27809
- Hockel M, Vaupel P (2001) Tumor hypoxia: definitions and current clinical, biologic, and molecular aspects. *J Natl Cancer Inst* 93(4):266–276
- Hoeben BA, Kaanders JH, Franssen GM, Troost EG, Rijken PF, Oosterwijk E et al (2010) PET of hypoxia with 89Zr-labeled cG250-F(ab')₂ in head and neck tumors. *J Nucl Med Off Publ Soc Nucl Med* 51(7):1076–1083
- Honarvar H, Garousi J, Gunneriusson E, Hoiden-Guthenberg I, Altai M, Widstrom C et al (2015) Imaging of CAIX-expressing xenografts in vivo using 99mTc-HEHEHE-ZCAIX:1 affibody molecule. *Int J Oncol* 46(2):513–520
- Huizing FJ, Hoeben BAW, Franssen G, Lok J, Heskamp S, Oosterwijk E et al (2017) Preclinical validation of (111)In-girentuximab-F(ab')₂ as a tracer to image hypoxia related marker CAIX

- expression in head and neck cancer xenografts. *Radiother Oncol J Eur Soc Ther Radiol Oncol* 124(3):521–525
- Huizing FJ, Hoeben BAW, Franssen GM, Boerman OC, Heskamp S, Bussink J (2019) Quantitative imaging of the hypoxia-related marker CAIX in head and neck squamous cell carcinoma xenograft models. *Mol Pharm* 16(2):701–708
- Innocenti A, Pastorekova S, Pastorek J, Scozzafava A, De Simone G, Supuran CT (2009) The proteoglycan region of the tumor-associated carbonic anhydrase isoform IX acts as an intrinsic buffer optimizing CO₂ hydration at acidic pH values characteristic of solid tumors. *Bioorg Med Chem Lett* 19(20):5825–5828
- Ivanov S, Liao SY, Ivanova A, Danilkovitch-Miagkova A, Tarasova N, Weirich G et al (2001) Expression of hypoxia-inducible cell-surface transmembrane carbonic anhydrases in human cancer. *Am J Pathol* 158(3):905–919
- Krall N, Pretto F, Mattarella M, Muller C, Neri D (2016) A ^{99m}Tc-labeled ligand of carbonic anhydrase IX selectively targets renal cell carcinoma in vivo. *J Nucl Med* 57(6):943–949
- Kranenborg MH, Boerman OC, de Weijert MC, Oosterwijk-Wakka JC, Corstens FH, Oosterwijk E (1997) The effect of antibody protein dose of anti-renal cell carcinoma monoclonal antibodies in nude mice with renal cell carcinoma xenografts. *Cancer* 80(12 Suppl):2390–2397
- Kratochwil C, Bruchertseifer F, Giesel FL, Weis M, Verburg FA, Mottaghy F et al (2016) ²²⁵Ac-PSMA-617 for PSMA-targeted alpha-radiation therapy of metastatic castration-resistant prostate cancer. *J Nucl Med Off Publ Soc Nucl Med* 57(12):1941–1944
- Kutikov A, Fossett LK, Ramchandani P, Tomaszewski JE, Siegelman ES, Banner MP et al (2006) Incidence of benign pathologic findings at partial nephrectomy for solitary renal mass presumed to be renal cell carcinoma on preoperative imaging. *Urology* 68(4):737–740
- Lau J, Zhang Z, Jenni S, Kuo HT, Liu Z, Vullo D et al (2016) PET imaging of carbonic anhydrase IX expression of HT-29 tumor xenograft mice with (68)Ga-labeled Benzenesulfonamides. *Mol Pharm* 13(3):1137–1146
- Leibovich BC, Lohse CM, Crispen PL, Bootjian SA, Thompson RH, Blute ML et al (2010) Histological subtype is an independent predictor of outcome for patients with renal cell carcinoma. *J Urol* 183(4):1309–1315
- Merkx et al (2021) <https://pubmed.ncbi.nlm.nih.gov/33651116/>
- Moroz E, Carlin S, Dyomina K, Burke S, Thaler HT, Blasberg R, et al (2009) Real-time imaging of HIF-1 α stabilization and degradation. *PLoS One* 4(4):e5077
- Mucav J, Shay JES, Simon MC (2012) Effects of hypoxia and HIFs on cancer metabolism. *Int J Hematol* 95(5):464–470
- Muselaers CH, Boerman OC, Oosterwijk E, Langenhuijsen JF, Oyen WJ, Mulders PF (2013) Indium-111-labeled girentuximab immunoSPECT as a diagnostic tool in clear cell renal cell carcinoma. *Eur Urol* 63(6):1101–1106
- Muselaers CH, Oosterwijk E, Bos DL, Oyen WJ, Mulders PF, Boerman OC (2014) Optimizing lutetium 177-anti-carbonic anhydrase IX radioimmunotherapy in an intraperitoneal clear cell renal cell carcinoma xenograft model. *Mol Imaging* 13:1–7
- Muselaers CH, Boers-Sonderen MJ, van Oostenbrugge TJ, Boerman OC, Desar IM, Stillebroer AB et al (2016) Phase 2 study of lutetium 177-labeled anti-carbonic anhydrase IX monoclonal antibody girentuximab in patients with advanced renal cell carcinoma. *Eur Urol* 69(5):767–770
- Oosterwijk E, Ruiters DJ, Hoedemaeker PJ, Pauwels EK, Jonas U, Zwartendijk J et al (1986) Monoclonal antibody G 250 recognizes a determinant present in renal-cell carcinoma and absent from normal kidney. *Int J Cancer* 38(4):489–494
- Oosterwijk E, Bander NH, Divgi CR, Welt S, Wakka JC, Finn RD et al (1993) Antibody localization in human renal cell carcinoma: a phase I study of monoclonal antibody G250. *J Clin Oncol* 11(4):738–750
- Pastorekova S, Zavadova Z, Kostal M, Babusikova O, Zavada J (1992) A novel quasi-viral agent, MaTu, is a two-component system. *Virology* 187(2):620–626
- Pastorekova S, Parkkila S, Zavada J (2006) Tumor-associated carbonic anhydrases and their clinical significance. *Adv Clin Chem* 42:167–216

- Pastorek J, Pastorekova S, Callebaut I, Mormon JP, Zelnik V, Opavsky R et al (1994) Cloning and characterization of MN, a human tumor-associated protein with a domain homologous to carbonic anhydrase and a putative helix-loop-helix DNA binding segment. *Oncogene* 9(10):2877–2888
- Peeters SG, Dubois L, Lieuwes NG, Laan D, Mooijer M, Schuit RC et al (2015) [(18)F]VM4-037 MicroPET imaging and biodistribution of two in vivo CAIX-expressing tumor models. *Mol Imaging Biol MIB Offi Publ Acad Mol Imaging* 17(5):615–619
- Rafajova M, Zatovicova M, Kettmann R, Pastorek J, Pastorekova S (2004) Induction by hypoxia combined with low glucose or low bicarbonate and high posttranslational stability upon reoxygenation contribute to carbonic anhydrase IX expression in cancer cells. *Int J Oncol* 24(4):995–1004
- Schmidt MM, Wittrup KD (2009) A modeling analysis of the effects of molecular size and binding affinity on tumor targeting. *Mol Cancer Ther* 8(10):2861–2871
- Steffens MG, Boerman OC, Oosterwijk-Wakka JC, Oosterhof GO, Witjes JA, Koenders EB et al (1997) Targeting of renal cell carcinoma with iodine-131-labeled chimeric monoclonal antibody G250. *J Clin Oncol* 15(4):1529–1537
- Steffens MG, Kranenborg MH, Boerman OC, Zegwaart-Hagemeier NE, Debruyne FM, Corstens FH et al (1998) Tumor retention of 186Re-MAG3, 111In-DTPA and 125I labeled monoclonal antibody G250 in nude mice with renal cell carcinoma xenografts. *Cancer Biother Radiopharm* 13(2):133–139
- Steffens MG, Oosterwijk E, Kranenborg MH, Manders JM, Debruyne FM, Corstens FH et al (1999a) In vivo and in vitro characterizations of three 99mTc-labeled monoclonal antibody G250 preparations. *J Nuclear Med* 40(5):829–836
- Steffens MG, Boerman OC, Oyen WJ, Kniest PH, Witjes JA, Oosterhof GO et al (1999b) Intratumoral distribution of two consecutive injections of chimeric antibody G250 in primary renal cell carcinoma: implications for fractionated dose radioimmunotherapy. *Can Res* 59(7):1615–1619
- Steffens MG, Boerman OC, de Mulder PH, Oyen WJ, Buijs WC, Witjes JA et al (1999c) Phase I radioimmunotherapy of metastatic renal cell carcinoma with 131I-labeled chimeric monoclonal antibody G250. *Clin Cancer Res Offi J Am Assoc Cancer Res* 5(10 Suppl):3268s-s3274
- Stewart GD, O'Mahony FC, Laird A, Rashid S, Martin SA, Eory L et al (2014) Carbonic anhydrase 9 expression increases with vascular endothelial growth factor-targeted therapy and is predictive of outcome in metastatic clear cell renal cancer. *Eur Urol* 66(5):956–963
- Stillebroer AB, Franssen GM, Mulders PF, Oyen WJ, van Dongen GA, Laverman P et al (2013a) ImmunoPET imaging of renal cell carcinoma with (124)I- and (89)Zr-labeled anti-CAIX monoclonal antibody cG250 in mice. *Cancer Biother Radiopharm* 28(7):510–515
- Stillebroer AB, Boerman OC, Desar IM, Boers-Sonderen MJ, van Herpen CM, Langenhuijzen JF et al (2013b) Phase I radioimmunotherapy study with lutetium 177-labeled anti-carbonic anhydrase IX monoclonal antibody girentuximab in patients with advanced renal cell carcinoma. *Eur Urol* 64(3):478–485
- van Dijk J, Zegveld ST, Fleuren GJ, Warnaar SO (1991) Localization of monoclonal antibody G250 and bispecific monoclonal antibody CD3/G250 in human renal-cell carcinoma xenografts: relative effects of size and affinity. *Int J Cancer* 48(5):738–743
- Wykoff CC, Beasley NJ, Watson PH, Turner KJ, Pastorek J, Sibtain A et al (2000) Hypoxia-inducible expression of tumor-associated carbonic anhydrases. *Can Res* 60(24):7075–7083
- Zavada J, Zavadova Z, Pastorekova S, Ciampor F, Pastorek J, Zelnik V (1993) Expression of MaTu-MN protein in human tumor cultures and in clinical specimens. *Int J Cancer* 54(2):268–274

Chapter 10

Carbonic Anhydrase Inhibitors: Designing Isozyme-Specific Inhibitors as Therapeutic Agents



Claudiu T. Supuran

Abstract Inhibition of human (h) CAs has pharmacologic applications in the many medical fields. New classes of CA inhibitors (CAIs) were described in the last decade with enzyme inhibition mechanisms differing considerably from the classical inhibitors of the sulfonamide or anion type. Five different CA inhibition mechanisms are known: (i) the zinc binders coordinate to the catalytically crucial Zn(II) ion from the enzyme active site. Sulfonamides and their isosters, anions, dithiocarbamates and their isosters, carboxylates, and hydroxamates bind in this way; (ii) inhibitors that anchor to the zinc-coordinated water molecule/hydroxide ion (phenols, carboxylates, polyamines, 2-thioxocoumarins, sulfocoumarins); (iii) inhibitors which occlude the entrance to the active site cavity (coumarins and their isosters), this binding site coinciding with that where CA activators bind; (iv) compounds which bind out of the active site cavity; and (v) compounds for which the inhibition mechanism is not known, among which are the secondary/tertiary sulfonamides as well some protein kinase inhibitors. CAIs are used clinically in many pathologies, with a sulfonamide inhibitor (SLC-0111) in Phase II clinical trials for the management of metastatic solid tumors. Considerable efforts were made to obtain isoform-selective compounds targeting the 12 catalytically active human isoforms for obtaining pharmacological agents with less side effects compared to the first and second generation inhibitors.

Keywords Carbonic anhydrase · Inhibitors · Inhibition mechanism · Zinc binder · Anchoring to zinc-coordinated water · Occlusion of the active site entrance · Out of the active site binding

C. T. Supuran (✉)

Neurofarba Department, Sezione Di Chimica Farmaceutica E Nutraceutica, Università Degli Studi Di Firenze, Via U.Schiff6, 50019 Sesto Fiorentino, Florence, Italy
e-mail: claudiu.supuran@unifi.it

© Springer Nature Switzerland AG 2021

W. R. Chegwidden and N. D. Carter (eds.), *The Carbonic Anhydrases: Current and Emerging Therapeutic Targets*, Progress in Drug Research 75,
https://doi.org/10.1007/978-3-030-79511-5_10

221

10.1 Introduction: Classical CA Inhibitors (CAIs)

The CAIs have clinical applications for decades, and such drugs belonging to the sulfonamide class are used for various pathologies (Nocentini and Supuran 2019; Supuran 2008, 2016a, 2016b; Neri and Supuran 2011; Alterio et al. 2012), as antiglaucoma drugs (Alterio et al. 2012), diuretics (Supuran 2016a), antiobesity agents (Supuran 2016b), for some neurologic pathologies (Supuran 2018a), and more recently as antitumor agents (Supuran 2018b, 2017a; Supuran et al. 2018). The first and second generation drugs, belonging to the sulfonamide/sulfamate classes, have a range of side effects due to the indiscriminate inhibition of most human CA isoforms (15 CAs are presently known in our species, 12 of which are catalytically active) (Nocentini and Supuran 2019; Supuran 2016a, 2017b). Sulfonamides are the most important class of CAIs (Nocentini and Supuran 2019; Supuran 2008; Neri and Supuran 2011), with at least 20 such compounds in clinical use for decades or clinical development in the last period, Fig. 10.1 (Nocentini and Supuran 2019; Supuran 2008, 2016a, 2016b; Neri and Supuran 2011; Alterio et al. 2012). They include acetazolamide **1**, methazolamide **2**, ethoxzolamide **3**, sulthiame **4**, dichlorophenamide **5**, dorzolamide **6**, brinzolamide **7**, sulpiride **8**, zonisamide **9**, topiramate **10**, saccharin **11**, celecoxib **12**, chlorothiazide/high ceiling diuretics of types **13–19**, including the widely prescribed hydrochlorothiazide **13a**, furosemide **18**, bumethanide **19**, compounds in clinical use for many years, as diuretics, antiglaucoma agents, antiepileptics (Nocentini and Supuran 2019; Supuran 2008, 2016a, 2016b, 2018a, 2018b; Neri and Supuran 2011; Alterio et al. 2012; Supuran et al. 2018). Compound **20**, SLC-0111, is in Phase II clinical trials as an antitumor/antimetastatic agent, and was discovered in the author's laboratory (Supuran 2018b) (Fig. 10.1). Most of the sulfonamides **1–19** act as potent CAIs and are in clinical use for decades, but their main problem is related to the fact that by inhibiting most of the catalytically active CA isoforms found in vertebrates, they show a wide range of side effects (Nocentini and Supuran 2019; Supuran 2008; Neri and Supuran 2011). The inhibition data against all hCAs with compounds 1–20 are provided in refs. (Nocentini and Supuran 2019; Supuran 2008; Neri and Supuran 2011).

10.2 CA Inhibition Mechanisms and the Drug Design

For a long period, the only CA inhibition mechanisms known was the binding of inhibitors to the metal ion from the Ca active site, either in tetrahedral geometry of the metal ion (as the sulfonamides), shown in Fig. 10.2a, or by adding to the metal coordination sphere and generating trigonal bipyramidal geometries (Nocentini and Supuran 2019; Supuran 2008; Neri and Supuran 2011). However, this situation changed dramatically in the last decade, with a large number of novel CA inhibition mechanisms reported (Fig. 10.2) and new classes of CA inhibitors (CAIs) discovered

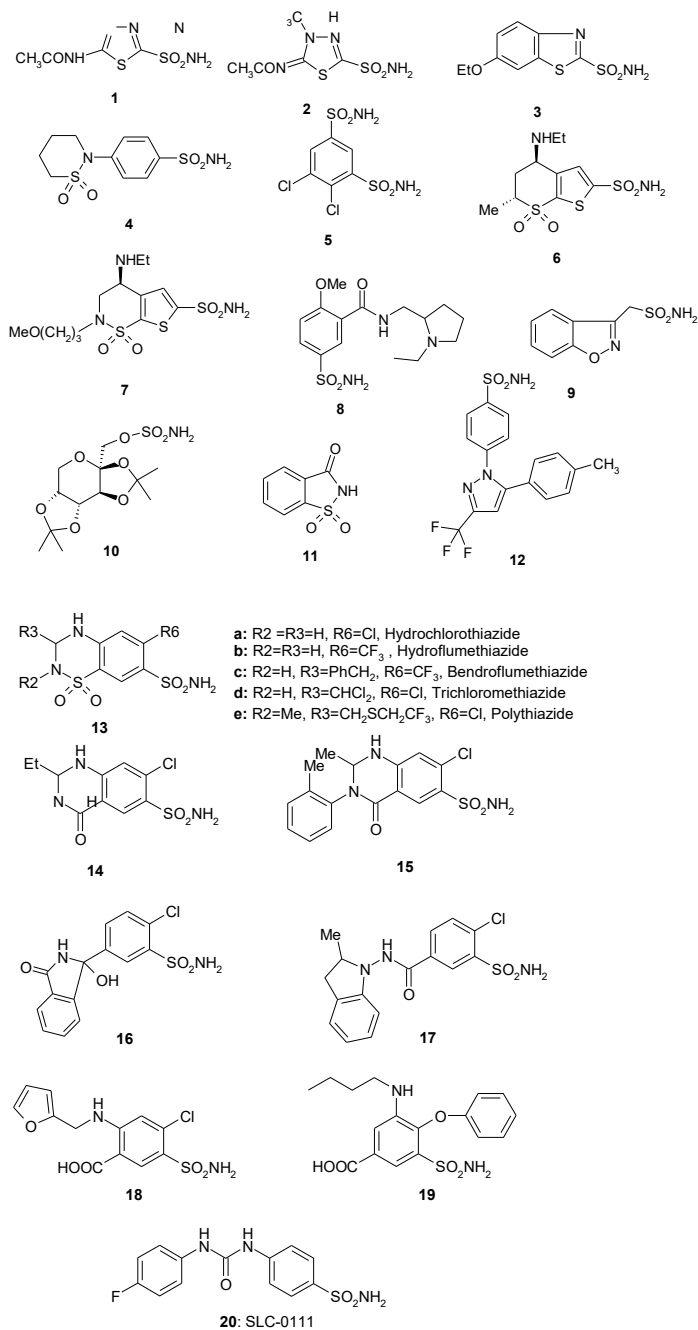


Fig. 10.1 Chemical structures of sulfonamide/sulfamate CAIs **1–20** in clinical use or clinical development (Supuran 2016b)

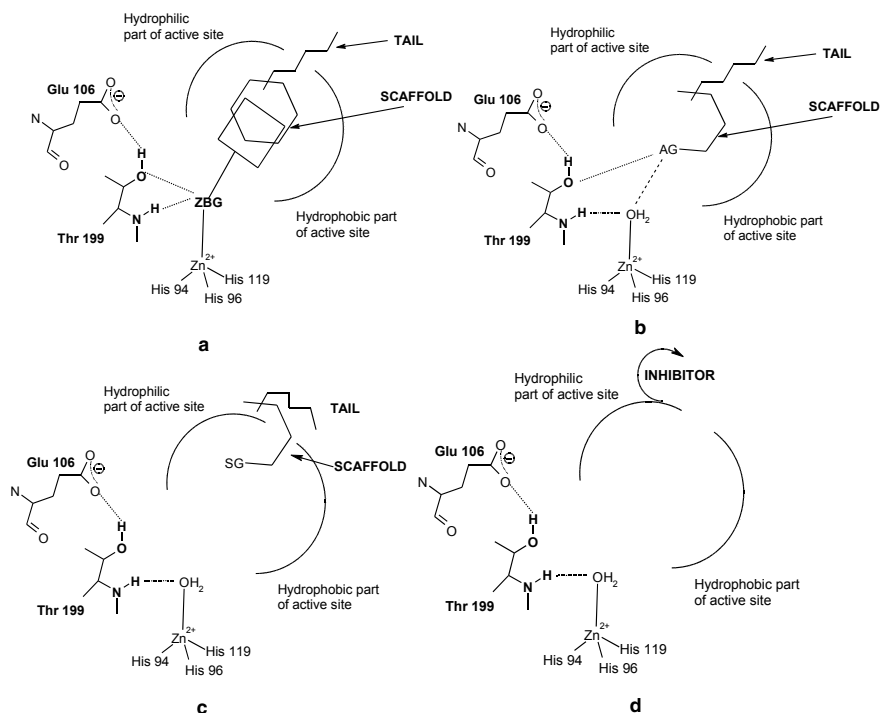


Fig. 10.2 CA inhibition mechanisms: A. Zinc-binding; B. Anchoring to the metal ion coordinated water; C. Occlusion of the active site entrance; and D. Out of the active site binding (Nocentini and Supuran 2019; Supuran 2008, 2016b; Neri and Supuran 2011)

apart the zinc binders shown in Fig. 10.4 (Nocentini and Supuran 2019; Supuran 2008; Neri and Supuran 2011).

Many classes of CAIs act as zinc binders (Fig. 10.1A). The classical ones are the sulfonamide and their isosteres (sulfamates, sulfamides) (Nocentini and Supuran 2019; Supuran 2008; Neri and Supuran 2011), in which the zinc-binding group (ZBG) is a SO_2NH - moiety. Such compounds also incorporate a scaffold which may interact with either the hydrophobic, the hydrophilic (or both) halves of the active site, as well as tails which bind towards the exit of the active site cavity which is the most variable region of the various CA isoforms (Nocentini and Supuran 2019; Supuran 2008, 2012, 2010, 2018c; Neri and Supuran 2011; Simone and Supuran 2012). Other classes of inhibitors which bind to the metal ion include carboxylates (Mori et al. 2015), hydroxamates (Fiore et al. 2012; Supuran and Gupta 2013), dithiocarbamates and isosteres (Carta et al. 2012a, 2012b), and the benzoxaborroles (Alterio et al. 2016; Nocentini et al. 2018)).

A second CA inhibition mechanism, anchoring to the metal ion coordinated water molecule/hydroxide ion is shown in Fig. 10.2B. These inhibitors incorporate an

anchoring group (AG) which is hydrogen bonded to the metal ion coordinated nucleophile, eventually making additional hydrogen bonds with neighboring residues such as the gate keeping ones (Thr199, Glu106) in the α -class enzymes. Phenol was the first inhibitor for which this mechanism was documented by X-ray crystallography (Nair et al. 1994), followed thereafter by polyamines (Carta et al. 2010), esters (Lopez et al. 2011), and sulfocoumarins (Tars et al. 2013). As the zinc binders, the scaffold of this type of inhibitors may interact with one or both halves of the active site, and a tail may also be present for enhancing the isoform selectivity profile of the inhibitors (Simone et al. 2013).

Situated even further away from the metal ion, at the entrance of the active site cavity are the inhibitors which occlude the active site entrance, shown in Fig. 10.2C. Such compounds incorporate a sticky group (SG) which may be of the OH, amino, COOH, and other types, as well as the scaffold/tail, as the previous classes of inhibitors discussed above. This mechanism has been discovered for coumarins (Maresca et al. 2009, 2010a) being later shown that many other classes of structurally similar compounds bind in this manner to the enzyme (Touisoni et al. 2011; Bonneau et al. 2013). More recently, a fourth CA inhibition mechanism (Fig. 10.4D) was also documented by X-ray crystallography (D'Ambrosio et al. 2015). A benzoic acid derivative was observed bound outside the active site cavity, in a hydrophobic pocket adjacent to the entrance within the active site. The inhibition is achieved by blocking the proton shuttle residue (His64) in its out conformation, which leads to the collapse of the entire catalytic cycle (D'Ambrosio et al. 2015).

A fifth inhibition mechanism probably exists, but no X-ray crystallographic data are available for such derivatives. Some secondary/tertiary sulfonamides (Monte et al. 2014) as well as some protein tyrosine kinase inhibitors (e.g., imatinib, nilotinib) (Parkkila et al. 2009) belong to this class of inhibitors with an unknown inhibition mechanism (Nocentini and Supuran 2019; Supuran 2008; Neri and Supuran 2011).

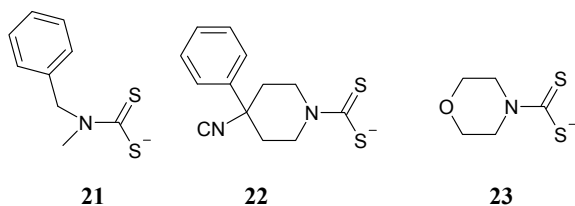
10.3 Strategies for Obtaining Isoform-Selective CAIs

The main scope of the drug design campaigns in the last years was to obtain isoform-selective CAIs for the various isoforms involved specifically in different pathologies, as noted above (Nocentini and Supuran 2019; Supuran 2008, 2016a, 2016b, 2018a, 2018b, 2017a, 2017b; Neri and Supuran 2011; Alterio et al. 2012; Supuran et al. 2018). This is, however, not an easy task, since the 12 catalytically active isoforms present in primates all possess a similar active site architecture (Nocentini and Supuran 2019; Supuran 2008; Neri and Supuran 2011). In fact, all human isoforms have the three conserved His residues (His94, 96, and 119) acting as zinc ligands, as well as half the active site mainly lined with hydrophobic residues and the opposite one with hydrophilic residues (Nocentini and Supuran 2019; Supuran 2008; Neri and Supuran 2011). However, there are also important differences in amino acid residues mainly in the middle and towards the exit of the active site cavity (Scozzafava et al. 2019b). Most of the inhibitors mentioned above, of types 1–9, do not make extensive

contacts with them as their scaffolds are rather compact, and these sulfonamides bind deep within the active site cavity which is rather similar in all mammalian isoforms (Nocentini and Supuran 2019; Supuran 2008, 2016a, 2016b; Neri and Supuran 2011; Alterio et al. 2012; Scozzafava et al. 2019b). Thus, it appeared of considerable interest to devise alternative approaches for obtaining isoform-selective CAIs. One of the most successful one was termed “the tail approach” (Borras et al. 1999; Supuran et al. 1999; Scozzafava et al. 1999a). It consists in appending “tails” to the scaffolds of aromatic/heterocyclic sulfonamides possessing derivatizable moieties of the amino, imino, or hydroxy type, in such a way that an elongated molecule is obtained with its tail being able to interact with amino acid residues from the middle and edge of the active site cavity, as shown in Fig. 10.2 for a general zinc-binder CAI (Borras et al. 1999; Supuran et al. 1999; Scozzafava et al. 1999a). By choosing tails with a diverse chemical nature, it was also possible to modulate the physico-chemical properties of such CAIs, which are crucial for their biological activity (Menabuoni et al. 1999; Simone et al. 2014). For example, antiglaucoma agents should possess an appropriate hydrophilicity and water solubility in order to be formulated as eye drops, but also a balanced lipophilicity for being able to penetrate through the plasma membranes and arrive at the ciliary processes where the enzymes responsible for aqueous humor secretion are found (i.e., CA II, IV, and XII) (Borras et al. 1999; Supuran et al. 1999; Scozzafava et al. 1999a). This approach was subsequently expanded to all classes of CAIs, such as among others to the dithiocarbamates (DTCs) **21–23**, Fig. 10.3 (Carta et al. 2012a, b), xanthates (Carta et al. 2013), carboxylates (Langella et al. 2016), phosphonates (Temperini et al. 2007), and hydroxamates (Fiore et al. 2012; Supuran and Gupta 2013). X-ray crystal structures are available for adducts of various isoforms (mainly hCA I and II) with all these classes of CAIs except the xanthates for which computational methods were used to assess their inhibition mechanism (Fiore et al. 2012; Supuran and Gupta 2013; Menabuoni et al. 1999; Simone et al. 2014; Carta et al. 2013; Langella et al. 2016; Temperini et al. 2007).

Among the sulfonamides obtained by the tail approach should be mentioned SLC-0111 (compound **20**) and many of its congeners, which are among the most isoforms-selective inhibitors in this class of derivatives (Pacchiano et al. 2011). Their selectivity was explained when the X-ray crystal structures of five of them were reported in complex with CA II (Pacchiano et al. 2010) and IX (Mboge et al. 2017). It was observed that the ureido linker present in these compounds allows the orientation of the inhibitor scaffold towards various regions of the active site cavity in the different

Fig. 10.3. DTCs designed by using the tail approach (Carta et al. 2012a, b)



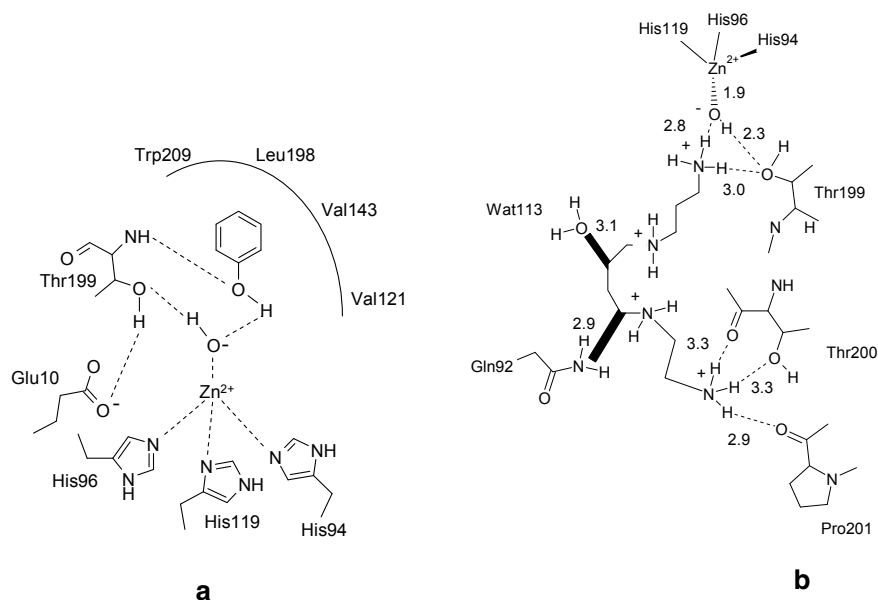


Fig. 10.4 Schematic representation of inhibitors that bind CAs by anchoring to the zinc-coordinated water molecule: A. Phenol **24** (Nair et al. 1994). B. Spermine **25** (Carta et al. 2010)

isoforms, and the possibility to interact with specific amino acid residues which are isoform-specific (Pacchiano et al. 2010; Mboge et al. 2017).

The second approach for enhancing the isoform selectivity of CAIs was that of considering the alternative inhibition mechanisms to the zinc binders discussed above.

As shown in Fig. 10.4, phenol **24** (as well as many of its congeners (Innocenti et al. 2008)) inhibit CAs by anchoring to the zinc-coordinated water molecule/hydroxide ion (Nair et al. 1994). The same inhibition mechanism was thereafter discovered for polyamines, such as spermine **25** (Carta et al. 2010). However, as the scaffold of spermine is much longer compared to phenol, the polyamine is one of the first examples of highly CA IV-selective inhibitor (Carta et al. 2010). The highest level of selectivity was, however, achieved for other compounds acting by this inhibition mechanism, the sulfocoumarins (Grandane et al. 2015) and homosulfocoumarins (Pustenko et al. 2017). Such CAIs were in fact discovered by considering coumarins as lead molecules. Coumarins such as **26** and **27** were among the first such derivatives investigated in detail (Maresca et al. 2009, 2010a). The first compound with this interesting CA inhibition mechanism was the natural product coumarin **27**, isolated from the Australian plant *Leionema ellipticum* (Maresca et al. 2009). When this natural product, 6-(1*S*-hydroxy-3-methylbutyl)-7-methoxy-2*H*-chromen-2-one **27** as well as the simple, unsubstituted coumarin **26** were co-crystallized with hCA II, the electron density data showed the presence of the hydrolyzed derivatives **29** and **28**,

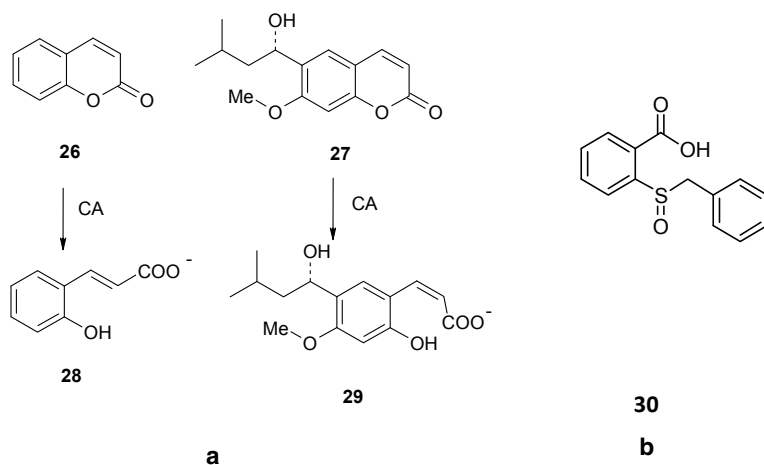


Fig. 10.5 A. Coumarins **26** and **27** and their hydrolysis products **28** and **29** acting as CAIs which occlude the entrance of the active site cavity (Maresca et al. 2009, 2010a). B. Benzoic acid derivative **30** binding out of the active site cavity (D’Ambrosio et al. 2015)

respectively, bound within the CA active site (Fig. 10.5A). The formation of the 2-hydroxy-cinnamic acids **29** and **28**, which represent the de facto enzyme inhibitors, is due to the esterase activity of the CAs, which leads to the hydrolysis of the lactone ring of coumarins (or thiocoumarins, as these last compounds were also shown to act as CAIs (Maresca et al. 2010a)). However, the rather bulky nature of the obtained hydrolysis products interferes with their binding in the neighborhood of the metal ion. Thus, the obtained 2-hydroxy-cinnamic acids may bind as *cis* isomers (as for **29** (Maresca et al. 2009)) or as *trans* isomers (as for **28** (Maresca et al. 2010a)) within the enzyme active site. But the most notable aspect of this inhibition mechanism is the fact that the inhibitors bind in an active site region which is the most variable between the various isoforms, i.e., the entrance to the cavity (Nocentini and Supuran 2019; Supuran 2008, 2016a, 2016b, 2018a, 2018b; Neri and Supuran 2011; Alterio et al. 2012). This has important consequences for the drug design of CAIs, since compounds binding in that region interact differently with the various CAs, and thus show high levels of isoform-selective inhibitory profiles. In fact, this was indeed the case when a larger series of diversely substituted coumarin/thiocoumarin derivatives were investigated (Maresca et al. 2010a), which showed a high level of isoform-selective behavior against many isoforms such as CA IX, XII, XIII, XIV, etc. (Maresca et al. 2010a). Subsequent work from our group showed this situation to be the case for many classes of coumarins/thiocoumarins as well as many structurally related derivatives which were investigated as CAIs against a large number of human isoforms (Sharma et al. 2014; Maresca and Supuran 2010; Maresca et al. 2010b; Bozdag et al. 2019).

The CA inhibition mechanism shown in Fig. 10.2D is the last one to be discovered (D’Ambrosio et al. 2015). When the 2-(benzylsulfonyl)-benzoic acid **30** (Fig. 10.5B)

was co-crystallized with hCA II, the electronic density of the inhibitor was not observed within the active site but in an adjacent binding pocket to the active site, where other inhibitors were never observed earlier. Thus, this compound binds quite far away, outside the active site of the enzyme (Fig. 10.2B). But how does it inhibit the CA activity when the binding is in an outside region of the active site pocket? The same crystallographic study (D'Ambrosio et al. 2015) showed that **30** blocks the proton shuttle of the enzyme, His64, in its *out* conformation, interfering thus with the rate determining step of the entire catalytic cycle, which is indeed the transfer of a proton from the zinc-coordinated water molecule to the environment, with generation of the zinc hydroxide species of the enzyme (Nocentini and Supuran 2019; Supuran 2008, 2016a; Neri and Supuran 2011; Alterio et al. 2012). This amino acid residue (His64) has a high flexibility with two main conformations, the *in* one (closer to the metal ion) and the *out* one, towards the exit of the active site cavity. By accepting a proton from the zinc-coordinated water, the imidazole moiety of this residue becomes protonated (in its *in* conformation), whereas when it is in the *out* one, the same proton may be transferred to the environment. Interfering with this process may block the entire catalytic cycle, and this is exactly how compound **30** inhibits the enzyme, blocking the proton shuttle through a network of hydrogen bonds (D'Ambrosio et al. 2015). This compound also shows an interesting degree of isoform selectivity (D'Ambrosio et al. 2015).

In the last period, relevant evidence accumulated on other classes of compounds, which show various levels of selective CA inhibitory properties, but for which the precise mechanism of action is not known due to the fact that they were not yet crystallized in adducts with the enzyme (Monte et al. 2014; Alp et al. 2012; Compain et al. 2013; Métayer et al. 2013).

The secondary sulfonamide moiety is present in a large variety of clinically used drugs, among which the sulfa drugs are the best-known examples. Alp et al. (Alp et al. 2012) investigated a panel of such derivatives, of type **31–39** (Fig. 10.6), for their interaction with the physiologically dominant isoforms hCA I and II, proving that many of them show sub-micromolar affinity for both enzymes. The investigated derivatives incorporated both secondary sulfonamide as well as tertiary sulfonamide functionalities in their molecules, as well as quite bulky substituents at the sulfonamide group, and clearly are unable to bind to the metal ion from the CA active site due to steric hindrance. In fact, the available space in the active site funnel, at its bottom, is rather restricted to allow such sterically impaired compounds (Nocentini and Supuran 2019; Supuran 2008, 2016a; Neri and Supuran 2011; Alterio et al. 2012). It has been hypothesized that similar to lacosamide (Temperini et al. 2010) and the hydrolyzed coumarins (Maresca et al. 2009, 2010a), these CAIs may bind at the entrance of the active site, in the coumarin-binding site, but this hypothesis has not yet been confirmed by X-ray crystallography. However, many other such secondary/tertiary sulfonamides were thereafter investigated as CAIs (Compain et al. 2013; Métayer et al. 2013; Temperini et al. 2010; D'Ascenzio et al. 2014; Carradori et al. 2015), some of which are shown in Fig. 10.6. By using superacid chemistry, Thibaudeau's group reported a wide range of halogenated secondary/tertiary derivatives (e.g., **39–41**), some of which showed selective inhibitory action against the

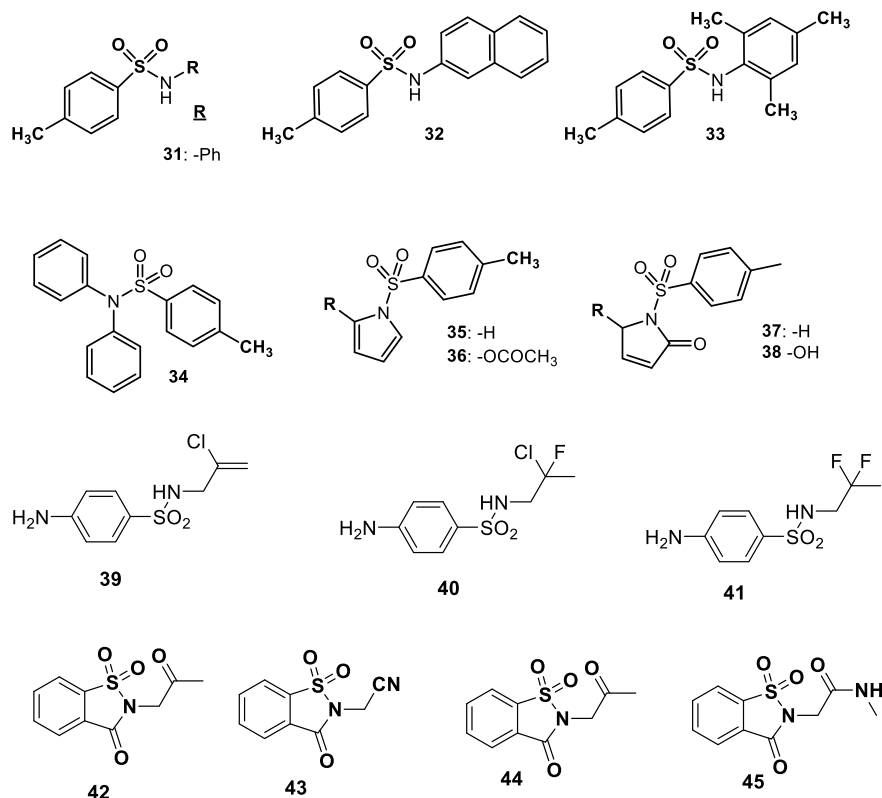


Fig. 10.6 Secondary and tertiary sulfonamides **31–45** acting as CAIs by an unknown inhibition mechanism (Monte et al. 2014; Alp et al. 2012; Compain et al. 2013; Métayer et al. 2013)

tumor-associated isoforms hCA IX/XII, without significant inhibition of hCA I and II (Compain et al. 2013; Métayer et al. 2013). By using saccharin **11** as lead (Mboge et al. 2017), Carradori's group reported a range of N-substituted saccharins, among which **42–45** (and some of their congeners) showed CA XII selective inhibitory action (D'Ascenzio et al. 2014). Again, notable CA selective inhibitory activity has been observed for many such tertiary sulfonamide derivatives, although their inhibition mechanism is unclear at this moment.

10.4 Conclusions

By catalyzing the simple but highly important hydration of carbon dioxide to bicarbonate and protons, CAs are involved in critical steps of the life cycle of many organisms, including eukaryotes, *Bacteria*, and *Archaea*. In fact, a large number of new such enzymes are constantly being cloned, purified, and characterized in detail from

many pathogenic as well as non-pathogenic organisms. Modulation of the activity of these enzymes, mainly by using selective inhibitors, has been used pharmacologically for decades for various applications (diuretics, antiglaucoma agents, antiepileptics, antiobesity drugs, and more recently antitumor therapies/diagnostic agents as well as novel anti-infectives (Supuran 2016c)). One of the main problems with the CAIs was however the lack of selectivity of the sulfonamides for the inhibition of the many mammalian (human) CAs, which led to a range of side effects for the first and second generation inhibitors of types **1–19** (Nocentini and Supuran 2019; Supuran 2008, 2016a, 2016b, 2018a, 2018b, 2017a; Neri and Supuran 2011; Alterio et al. 2012; Supuran et al. 2018). However, this situation changed substantially in the last decade, when a large number of isoform-selective primary sulfonamides (Pacchiano et al. 2011) were reported by using the tail approach (Borras et al. 1999; Supuran et al. 1999; Scozzafava et al. 1999a) and with the discovery of new classes of CAIs, such as the coumarins and their isomers, the polyamines, dithiocarbamates, xanthates, etc., as shown in detail in this review. However, the breakthrough in the field of highly isoform-selective CAIs was represented by the discovery of coumarins as a totally new chemotype with a particular inhibition mechanism (Maresca et al. 2009, 2010a). As shown here, coumarins were also used as lead compounds, leading to the discovery of a large number of structurally related chemotypes possessing prodrug-like CA inhibitory properties, among which are the thiocoumarins, thioxocoumarins, coumarin oximes, 5-/6-membered ring lactones and thiolactones, sulfocoumarins, etc. (Nocentini and Supuran 2019; Supuran 2008, 2016a; Neri and Supuran 2011; Alterio et al. 2012). Polyamines were then discovered as CAIs in 2010 (Carta et al. 2010), followed shortly thereafter by dithiocarbamates and xanthates (Carta et al. 2012a, 2012b, 2013). Finally, the out of the active site CA inhibition mechanism was reported in 2015 (D'Ambrosio et al. 2015). A particular feature of the new classes of CAIs discovered in the last years is that they show a much higher isoform selectivity profile compared to most sulfonamides and sulfamates (of which **1–19** are the typical representatives, see Fig. 10.1). Thus, there is enthusiasm and optimism that the new generations of CAIs will show less side effects and more efficacy for the treatment of the classical pathologies associated with these enzymes, but also to newer ones such as neuropathic pain (Supuran 2016c), cerebral ischemia (Cesare et al. 2016), arthritis (Bua et al. 2017), and obviously tumors (with SLC-0111 **20** in Phase II clinical trials, as mentioned above (Supuran 2018b; Supuran et al. 2018; Supuran 2017a)).

Overall, nowadays, there is a huge choice for isoform-selective CAIs targeting all mammalian isoforms, but there are still no inhibitors selective for other classes of CAs, such as the β -, γ -, or η -CAs present in various pathogenic organisms (Capasso and Supuran 2013, 2015; Supuran and Capasso 2015; Nocentini et al. 2021). Thus, the next challenges in the drug design of CAIs will be that of finding class-selective inhibitors. However, very recently, acetazolamide-based CAIs were validated as anti-infectives targeting the enzymes from pathogenic bacteria which showed impressive levels of drug resistance to other antibiotics (Kaur et al. 2020; Supuran and Capasso 2020; Hewitt et al. 2021 Mar 25).

References

- Alp C, Ozsoy S, Alp NA et al (2012) Sulfapyridine-like benzenesulfonamide derivatives as inhibitors of carbonic anhydrase isoenzymes I, II and VI. *J Enzyme Inhib Med Chem* 27:818–824
- Alterio V, Di Fiore A, D' Ambrosio K et al (2012) Multiple binding modes of inhibitors to carbonic anhydrases: how to design specific drugs targeting 15 different isoforms? *Chem Rev* 112:4421–4468
- Alterio V, Cadoni R, Esposito D, Vullo D, Fiore AD, Monti SM, Caporale A, Ruvo M, Sechi M, Dumy P, Supuran CT, De Simone G, Winum JY (2016) Benzoxaborole as a new chemotype for carbonic anhydrase inhibition. *Chem Commun* 52:11983–11986
- Bonneau A, Maresca A, Winum JY, Supuran CT (2013) Metronidazole-coumarin conjugates and 3-cyano-7-hydroxy-coumarin act as isoform-selective carbonic anhydrase inhibitors. *J Enzyme Inhib Med Chem*. 28:397–401.32.
- Borras J, Scozzafava A, Menabuoni L, et al (1999) Carbonic anhydrase inhibitors. Part 73. Synthesis of water-soluble, topically effective intraocular pressure lowering aromatic/ heterocyclic sulfonamides containing 8-quinoline-sulfonyl moieties: is the tail more important than the ring? *Bioorg Med Chem* 7:2397–406.
- Bozdog M, Ferraroni M, Ward C, Carta F, Bua S, Angeli A, Langdon SP, Kunkler IH, Al-Tamimi AS, Supuran CT (2019) Carbonic anhydrase inhibitors based on sorafenib scaffold: design, synthesis, crystallographic investigation and effects on primary breast cancer cells. *Eur J Med Chem*. 182:111600
- Bua S, Di Cesare ML, Vullo D et al (2017) Design and synthesis of novel nonsteroidal anti-inflammatory drugs and carbonic anhydrase inhibitors hybrids (NSAIDs-CAIs) for the treatment of rheumatoid arthritis. *J Med Chem* 60:1159–1170
- Capasso C, Supuran CT (2013) Anti-infective carbonic anhydrase inhibitors: a patent and literature review. *Expert Opin Ther Pat* 23:693–704
- Capasso C, Supuran CT (2015) An overview of the alpha-, beta- and gamma-carbonic anhydrases from bacteria: can bacterial carbonic anhydrases shed new light on evolution of bacteria? *J Enzyme Inhib Med Chem* 30:325–332
- Carradori S, Mollica A, Ceruso M et al (2015) New amide derivatives of probenecid as selective inhibitors of carbonic anhydrase IX and XII: biological evaluation and molecular modelling studies. *Bioorg Med Chem* 23:2975–2981
- Carta F, Aggarwal M, Maresca A et al (2012a) Dithiocarbamates strongly inhibit carbonic anhydrases and show antiglaucoma action in vivo. *J Med Chem* 55:1721–1730
- Carta F, Aggarwal M, Maresca A et al (2012b) Dithiocarbamates: a new class of carbonic anhydrase inhibitors Crystallographic and Kinetic Investigations. *Chem Commun* 48:1868–1870
- Carta F, Temperini C, Innocenti A, et al (2010) Polyamines inhibit carbonic anhydrases by anchoring to the zinc-coordinated water molecule. *J Med Chem*. 53:5511–22.
- Carta F, Akdemir A, Scozzafava A et al (2013) Xanthates and trithiocarbonates strongly inhibit carbonic anhydrases and show antiglaucoma effects in vivo. *J Med Chem* 56:4691–4700
- Compain G, Martin-Mingot A, Maresca A et al (2013) Superacid synthesis of halogen containing N-substituted-4-aminobenzene sulfonamides : new selective tumor-associated carbonic anhydrase inhibitors. *Bioorg Med Chem* 21:1555–1563
- D' Ambrosio K, Carradori S, Monti SM et al (2015) Out of the active site binding pocket for carbonic anhydrase inhibitors. *Chem Commun* 51:302–305
- D'Ascenzio M, Carradori S, De Monte C et al (2014) Design, synthesis and evaluation of N-substituted saccharin derivatives as selective inhibitors of tumor-associated carbonic anhydrase XII. *Bioorg Med Chem* 22:1821–1831
- De Monte C, Carradori S, Secci D et al (2014) Cyclic tertiary sulfamates: selective inhibition of the tumor-associated carbonic anhydrases IX and XII by N- and O-substituted acesulfame derivatives. *Eur J Med Chem* 84:240–246
- De Simone G, Supuran CT (2012) (In)organic anions as carbonic anhydrase inhibitors. *J Inorg Biochem* 111:117–129

- De Simone G, Alterio V, Supuran CT (2013) Exploiting the hydrophobic and hydrophilic binding sites for designing carbonic anhydrase inhibitors. *Expert Opin Drug Discov* 8:793–810
- De Simone G, Pizika G, Monti SM, et al (2014) Hydrophobic substituents of the phenylmethylsulfamide moiety can be used for the development of new selective carbonic anhydrase inhibitors. *Biomed Res Int* 2014:523210.
- Di Cesare ML, Micheli L, Carta F et al (2016) Carbonic anhydrase inhibition for the management of cerebral ischemia: in vivo evaluation of sulfonamide and coumarin inhibitors. *Enzyme Inhib Med Chem* 31:894–899
- Di Fiore A, Maresca A, Supuran CT, De Simone G (2012) Hydroxamate represents a versatile zinc binding group for the development of new carbonic anhydrase inhibitors. *Chem Commun* 48:8838–8840
- Grandane A, Tanc M, Di Cesare ML et al (2015) 6-Substituted sulfocoumarins are selective carbonic anhydrase IX and XII inhibitors with significant cytotoxicity against colorectal cancer cells. *J Med Chem* 58:3975–3983
- Hewitt CS, Abutaleb NS, Elhassanny AEM, Nocentini A, Cao X, Amos DP, Youse MS, Holly KJ, Marapaka AK, An W, Kaur J, Krabill AD, Elkashif A, Elgammal Y, Graboski AL, Supuran CT, Seleem MN, Flaherty DP (2021) Structure-activity relationship studies of acetazolamide-based carbonic anhydrase inhibitors with activity against *Neisseria gonorrhoeae*. *ACS Infect Dis*. <https://doi.org/10.1021/acsinfectdis.1c00055>
- Innocenti A, Vullo D, Scozzafava A, Supuran CT (2008) Carbonic anhydrase inhibitors. Inhibition of mammalian isoforms I—XIV with a series of substituted phenols including paracetamol and salicylic acid. *Bioorg Med Chem* 16:7424–7428
- Kaur J, Cao X, Abutaleb NS, Elkashif A, Graboski AL, Krabill AD, AbdelKhalek AH, An W, Bhardwaj A, Seleem MN, Flaherty DP (2020) Optimization of acetazolamide-based scaffold as potent inhibitors of vancomycin-resistant enterococcus. *J Med Chem* 63:9540–9562
- Langella E, D'Ambrosio K, D'Ascenzio M et al (2016) A combined crystallographic and theoretical study explains the capability of carboxylic acids to adopt multiple binding modes in the active site of carbonic anhydrases. *Chemistry* 22:97–100
- Lopez M, Vu H, Wang CK, Wolf MG, Groenhof G, Innocenti A, Supuran CT, Poulsen SA. (2011) Promiscuity of carbonic anhydrase II. Unexpected ester hydrolysis of carbohydrate-based sulfamate inhibitors. *J Am Chem Soc* 133:18452–18462.
- Maresca A, Supuran CT (2010) Coumarins incorporating hydroxy- and chloro- moieties selectively inhibit the transmembrane, tumor-associated carbonic anhydrase isoforms IX and XII over the cytosolic ones I and II. *Bioorg Med Chem Lett* 20:4511–4514
- Maresca A, Temperini C, Vu H et al (2009) Non-zinc mediated inhibition of carbonic anhydrases: coumarins are a new class of suicide inhibitors. *J Am Chem Soc* 131:3057–3062
- Maresca A, Temperini C, Pochet L et al (2010a) Deciphering the mechanism of carbonic anhydrase inhibition with coumarins and thiocoumarins. *J Med Chem* 53:335–344
- Maresca A, Scozzafava A, Supuran CT (2010b) 7,8-Disubstituted- but not 6,7-disubstituted coumarins selectively inhibit the transmembrane, tumor-associated carbonic anhydrase isoforms IX and XII over the cytosolic ones I and II in the low nanomolar/subnanomolar range. *Bioorg Med Chem Lett* 20:7255–7258
- Mboge MY, Mahon BP, Lamas N et al (2017) Structure activity study of carbonic anhydrase IX: selective inhibition with ureido-substituted benzenesulfonamides. *Eur J Med Chem* 132:184–191
- Menabuoni L, Scozzafava A, Mincione F, et al (1999) Carbonic anhydrase inhibitors. Water-soluble, topically effective intraocular pressure lowering agents derived from isonicotinic acid and aromatic/heterocyclic sulfonamides: is the tail more important than the ring? *J Enzyme Inhib* 14:457–474.
- Métayer B, Mingot A, Vullo D et al (2013) New superacid synthesized (fluorinated) tertiary benzenesulfonamides acting as selective hCA IX inhibitors: toward a new mode of carbonic anhydrases inhibition by sulfonamides. *Chem Commun* 49:6015–6017
- Mori M, Cau Y, Vignaroli G et al (2015) Hit recycling: discovery of a potent carbonic anhydrase inhibitor by in silico target fishing. *ACS Chem Biol* 10:1964–1969

- Nair SK, Ludwig PA, Christianson DW (1994) Two-site binding of phenol in the active site of human carbonic anhydrase II: structural implications for substrate association. *J Am Chem Soc* 116:3659–3660
- Neri D, Supuran CT (2011) Interfering with pH regulation in tumours as a therapeutic strategy. *Nature Rev Drug Discov* 10:767–777
- Nocentini A, Supuran CT (2019) Advances in the structural annotation of human carbonic anhydrases and impact on future drug discovery. *Expert Opin Drug Discov* 14:1175–1197
- Nocentini A, Supuran CT, Winum JY (2018) Benzoxaborole compounds for therapeutic uses: a patent review (2010–2018). *Expert Opin Ther Pat* 28:493–504
- Nocentini A, Angeli A, Carta F, Winum JY, Zalubovskis R, Carradori S, Capasso C, Donald WA, Supuran CT (2021) Reconsidering anion inhibitors in the general context of drug design studies of modulators of activity of the classical enzyme carbonic anhydrase. *J Enzyme Inhib Med Chem* 36:561–580
- Pacchiano F, Aggarwal M, Avvaru BS et al (2010) Selective hydrophobic pocket binding observed within the carbonic anhydrase II active site accommodate different 4-substituted-ureido-benzenesulfonamides and correlate to inhibitor potency. *Chem Commun* 46:8371–8373
- Pacchiano F, Carta F, McDonald PC et al (2011) Ureido-substituted benzenesulfonamides potently inhibit carbonic anhydrase IX and show antimetastatic activity in a model of breast cancer metastasis. *J Med Chem* 54:1896–1902
- Parkkila S, Innocenti A, Kallio H et al (2009) The protein tyrosine kinase inhibitors imatinib and nilotinib strongly inhibit several mammalian α -carbonic anhydrase isoforms. *Bioorg Med Chem Lett* 19:4102–4106
- Pustenko A, Stepanovs D, Žalubovskis R, Vullo D, Kazaks A, Leitans J, Tars K, Supuran CT (2017) 3H-1,2-benzoxathiepine 2,2-dioxides: a new class of isoform-selective carbonic anhydrase inhibitors. *J Enzyme Inhib Med Chem* 32:767–775
- Scozzafava A, Briganti F, Mincione G et al (1999a) Carbonic anhydrase inhibitors: synthesis of water-soluble, aminoacyl/dipeptidyl sulfonamides possessing long-lasting intraocular pressure-lowering properties via the topical route. *J Med Chem* 42:3690–3700
- Scozzafava A, Menabuoni L, Mincione F, et al (1999b). Carbonic anhydrase inhibitors. Part 74. Synthesis of water-soluble, topically effective, intraocular pressure-lowering aromatic/heterocyclic sulfonamides containing cationic or anionic moieties: is the tail more important than the ring? *J Med Chem*. 42:2641–50.
- Sharma A, Tiwari M, Supuran CT (2014) Novel coumarins and benzocoumarins acting as isoform-selective inhibitors against the tumor-associated carbonic anhydrase IX. *J Enzyme Inhib Med Chem* 2:292–296
- Supuran CT (2008) Carbonic anhydrases: novel therapeutic applications for inhibitors and activators. *Nature Rev Drug Discov* 7:168–181
- Supuran CT (2010) Carbonic anhydrase inhibitors. *Bioorg Med Chem Lett* 20:3467–3474
- Supuran CT (2012) Structure-based drug discovery of carbonic anhydrase inhibitors. *J Enzyme Inhib Med Chem* 27:759–772
- Supuran CT (2013) Hydroxamates as Carbonic anhydrase inhibitors. In: Gupta SP (ed) *Hydroxamic acids: a unique family of chemicals with multiple biological activities*. Springer Verlag, Heidelberg, pp 55–69
- Supuran CT (2016b) How many carbonic anhydrase inhibition mechanisms exist? *J Enzyme Inhib Med Chem* 31:345–360
- Supuran CT (2016c) Carbonic anhydrase inhibition and the management of neuropathic pain. *Expert Rev Neurother* 16:961–968
- Supuran CT (2016a) Structure and function of carbonic anhydrases. *Biochem J* 473:2023–2032
- Supuran CT (2017a) Carbonic anhydrase Inhibition and the management of hypoxic tumors. *Metabolites* 7:E48
- Supuran CT (2017b) Advances in structure-based drug discovery of carbonic anhydrase inhibitors. *Expert Opin Drug Discov* 12:61–88

- Supuran CT (2018a) Applications of carbonic anhydrases inhibitors in renal and central nervous system diseases. *Expert Opin Ther Pat* 28:713–721
- Supuran CT (2018b) Carbonic anhydrase inhibitors as emerging agents for the treatment and imaging of hypoxic tumors. *Expert Opin Investig Drugs* 27:963–970
- Supuran CT (2018c) Carbon- versus sulphur-based zinc binding groups for carbonic anhydrase inhibitors? *J Enzyme Inhib Med Chem* 33:485–495
- Supuran CT, Capasso C (2015) The eta-class carbonic anhydrases as drug targets for antimalarial agents. *Expert Opin Ther Targets* 19:551–563
- Supuran CT, Capasso C (2020) Antibacterial carbonic anhydrase inhibitors: an update on the recent literature. *Expert Opin Ther Pat* 30:963–982
- Supuran CT, Scozzafava A, Menabuoni L, et al (1999) Carbonic anhydrase inhibitors. Part 71. Synthesis and ocular pharmacology of a new class of water-soluble, topically effective intraocular pressure lowering sulfonamides incorporating picolinoyl moieties. *Eur J Pharm Sci* 8:317–328.
- Supuran CT, Alterio V, Di Fiore A et al (2018) Inhibition of carbonic anhydrase IX targets primary tumors, metastases, and cancer stem cells: three for the price of one. *Med Res Rev* 38:1799–1836
- Tars K, Vullo D, Kazaks A et al (2013) Sulfocoumarins (1,2-benzoxathiine-2,2-dioxides): a class of potent and isoform-selective inhibitors of tumor-associated carbonic anhydrases. *J Med Chem* 56:293–300
- Temperini C, Innocenti A, Guerri A et al (2007) Phosph(on)ate as a zinc-binding group in metalloenzyme inhibitors: X-ray crystal structure of the antiviral drug foscarnet complexed to human carbonic anhydrase I. *Bioorg Med Chem Lett* 17:2210–2215
- Temperini C, Innocenti A, Scozzafava A, et al (2010) The coumarin-binding site in carbonic anhydrase accommodates structurally diverse inhibitors: the antiepileptic lacosamide as an example. *J Med Chem* 53: 850–4.30
- Touisni N, Maresca A, McDonald PC et al (2011) Glycosylcoumarin carbonic anhydrase IX and XII inhibitors strongly attenuate the growth of primary breast tumors. *J Med Chem* 54:8271–8277

Chapter 11

Carbonic Anhydrase Inhibitors: Identifying Therapeutic Cancer Agents Through Virtual Screening



Giulio Poli, Claudiu T. Supuran, and Tiziano Tuccinardi

Abstract Computer-aided drug design includes an ensemble of different *in silico* strategies that represent valuable tools for facilitating the discovery and optimization of novel hit compounds endowed with biological activity toward the desired target proteins. Due to the various pathological implications of carbonic anhydrases (CAs), especially in the development and progression of cancer, molecular modeling techniques have been widely applied for the identification of new CA inhibitors. In this chapter, after providing the reader with a brief introduction to computational methods in drug design, we summarize the results of the main virtual screening (VS) studies that led to the discovery of novel ligands of different CA isoforms, describing the various receptor-based and ligand-based approaches employed. Moreover, we report the results of retrospective analyses in which CAs and their known ligands have been used to validate the performance of various VS methods in hit identification. The present chapter should provide the reader with a panoramic view of the most used and reliable *in silico* techniques to be applied in the search for novel CA inhibitors.

Keywords Carbonic anhydrase · Virtual screening · Docking · Pharmacophore model · Fingerprint

11.1 Virtual Screening in Drug Discovery

Computer-aided drug design (CADD) strategies are nowadays widely employed in different areas of medicinal chemistry along the different steps of the drug development process, from hit identification to lead optimization campaigns. The expensive and time consuming trial-and-error approach can be often replaced by a rational drug design approach, which can benefit the guide and support of molecular modeling

G. Poli · T. Tuccinardi (✉)

Department of Pharmacy, University of Pisa, Via Bonanno 6, 56126 Pisa, Italy
e-mail: tiziano.tuccinardi@unipi.it

C. T. Supuran

Neurofarba Department, Università degli Studi di Firenze, Florence, Italy
e-mail: claudiu.supuran@unifi.it

© Springer Nature Switzerland AG 2021

W. R. Chegwidden and N. D. Carter (eds.), *The Carbonic Anhydrases: Current and Emerging Therapeutic Targets*, Progress in Drug Research 75,
https://doi.org/10.1007/978-3-030-79511-5_11

and computational studies. Hit identification is undoubtedly the drug design stage to which *in silico* techniques can offer the most valuable help, thanks to the application of virtual screening (VS) protocols enabling the discovery of novel and structurally diverse active ligands from libraries of commercially available compounds.

VS strategies can be divided into receptor-based and ligand-based approaches. Receptor-based VS methods are the most used and profitable strategies for *in silico* hit identification, since they exploit structural knowledge about the target protein (Ripphausen et al. 2012). The availability of at least an X-ray crystallographic or NMR structure of the target receptor is thus an essential prerequisite for the development of receptor-based VS protocols, although homology modeling can sometimes supply with reliable receptor models when no structural information about the target of interest is available (Thiry et al. 2009). When possible, chemical knowledge of one or more reference ligands with experimentally confirmed activity towards the target of interest can also be employed in receptor-based approaches. In the ideal situation, a ligand–protein co-crystal structure providing both types of information and displaying the bioactive conformation of the ligand bound to the target receptor can be used as a reference for receptor-based methods, as in the case of receptor-based pharmacophore modeling. By following this approach, the fundamental ligand–protein interactions observed in the X-ray complex, known to be mainly responsible for the activity of bound ligand and related compounds, can be used to generate one or multiple pharmacophore models to be employed in pharmacophore-based VS studies. In these studies, libraries of up to millions of commercial compounds can be filtered with the aim of identifying molecules that can reproduce the pattern of fundamental interactions represented by the pharmacophore model and are thus supposed to show affinity for the target receptor (Vuorinen and Schuster 2015). In the recent years, receptor-based pharmacophore screenings have been widely applied and proved to be efficient hit finding strategies for several different target receptors including *h*CAs (Tanrikulu et al. 2009; Pala et al. 2011; Luca et al. 2014; Wang et al. 2015; Tuccinardi et al. 2016; Poli et al. 2016, 2018a; Chiarelli et al. 2018).

The principal and most popular computational approach belonging to receptor-based strategies is however represented by docking, which constitutes the gold standard technique for predicting the potential binding mode of small-molecule ligands within a target receptor. Docking studies are thus widely used in medicinal chemistry for evaluating the most energetically favored disposition of experimentally active compounds within their protein targets (Luger et al. 2015) and for rationalizing structure–activity relationships (SAR) among series of related compounds (Aghazadeh Tabrizi et al. 2016). Nevertheless, docking approaches proved to be a very profitable computational tool also in VS campaigns, allowing the discovery of novel compounds active towards many different types of protein targets and expanding the chemical space of their known ligands (Irwin and Shoichet 2016). However, docking reliability often raised some criticism (Chen 2015). In fact, the performance of docking procedures should be generally tested through self-docking (at least) or possibly with cross-docking studies before applying them for VS workflows, while the use of special parametrizations, force-fields, or post-docking procedures seem to

be valuable strategies for improving docking accuracy when dealing with metalloenzymes such as *h*CAs (Bai et al. 2015; Poli et al. 2018b; Pecina et al. 2018). Anyway, classic high-throughput molecular docking demonstrated to be a useful VS strategy for identifying novel *h*CAs inhibitors even when used alone, without employing other structure-based or ligand-based approaches (Wang et al. 2013; Gidaro et al. 2015; Salmas et al. 2016).

Molecular dynamics (MD) simulations constitute another receptor-based technique that can be employed in VS workflows. For instance, MD simulations can be performed to refine the target protein structures to be used for docking and other receptor-based methods, relaxing the side chains of the protein residues and eliminating possible steric clashes (Salmas et al. 2016). However, MD studies can be employed within VS workflows to perform a thorough evaluation of single ligand binding modes predicted by docking for few top-scored hit compounds selected through the previous VS steps. The behavior of the corresponding ligand–protein complexes is studied by creating a solvated system with explicit water molecules where both the receptor and the bound ligand are provided with sufficient energy to move freely as in a cellular environment. Through such analysis, it is possible to evaluate the stability of the ligand disposition and the ligand–protein interactions predicted by docking for the selected compounds and to assess the reliability of their binding mode. MD simulations studies can thus be employed as a qualitative post-docking filter in the final step of VS workflows to discard those hit compounds whose key interactions with the protein are not properly conserved during the simulations (Poli et al. 2015; Liu and Kokubo 2017; Zhang et al. 2017).

Ligand-based similarity strategies, uniquely based on the molecular structure and properties of known reference compounds experimentally confirmed as active ligands towards the target of interest, are typically the only possible option when no structural information about the target receptor is available. Ligand-based, and in particular 2D similarity methods, such as topological and fingerprint searches, showed to be useful approaches for identifying *h*CAs inhibitors (McGaughey et al. 2007; Sastry et al. 2010), probably because they are constituted by three main functional moieties: (a) a zinc-binding group (ZBG, often represented by a sulfonamide group) coordinating the prosthetic zinc ion of the enzyme, (b) a central core (often an aromatic ring), and (c) a terminal tail that can show either lipophilic or hydrophilic character. Ligand-based techniques are often used in combination with structure-based approaches, especially in the initial steps of the VS workflow, since they are generally less time consuming, and can be employed to rapidly filter large compound databases with the aim of discarding those ligands that are too structurally different with respect to the reference active ligands, and thus less likely to show affinity for the target receptor (Poli et al. 2013; Broccatelli and Brown 2014). Interestingly, ligand-based pharmacophores and substructure searches proved not only to be valuable for selecting potential *h*CA ligands endowed with known ZBGs, but also to identify novel inhibitors with atypical zinc-chelating moieties (Thiry et al. 2009; Pala et al. 2011).

11.2 Virtual Screening Studies Identifying Novel Carbonic Anhydrase Inhibitors

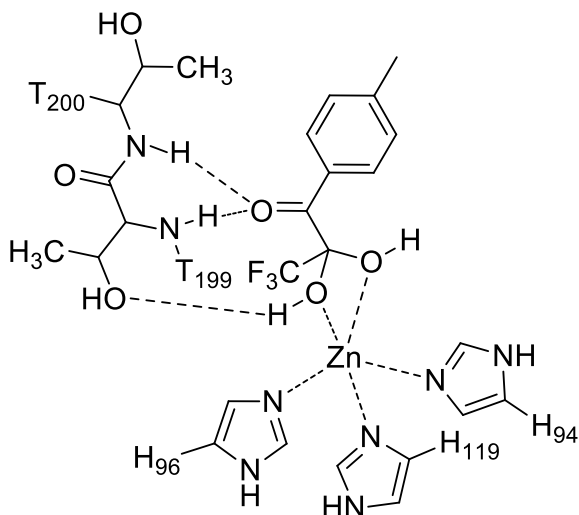
A remarkable example of how ligand-based and receptor-based strategies can be successfully combined into a hierarchic VS workflow that led to the discovery of new *hCA* ligands was reported by Klebe and collaborators in 2002 (Grüneberg et al. 2002). The study was aimed at assessing the general potential of VS for lead discovery, and *hCA* II was selected as a suitable target for this purpose. As a first step of the VS protocol, a dataset of about 99'000 drug-like compounds belonging to Maybridge and LeadQuest databases and respecting the Lipinski rules was created, and subjected to a substructure filter, in order to retain only compounds bearing a series of functional moieties already described as ZBGs in other zinc proteases, including sulfonamide, amide, hydroxamic, and carboxylic groups. In this way, only about 5900 potential zinc chelators were retained from the initial dataset. After this preliminary filter, the selected compounds were subjected to a receptor-based pharmacophore screening. The pharmacophore model was generated through an analysis of the *hCA* II binding site regions in which a potential ligand could form energetically favorable interactions. The mapping of the binding hot spots into *hCA* II catalytic site was performed using four different and complementary methods (i.e., LUDI, GRID, SuperStar, and DrugScore), which essentially searched for favorable H-bond acceptor, H-bond donor, and hydrophobic interactions and used 13 different ligand–protein X-ray reference structures. By considering the hot spots and contour maps obtained using the different computational methods, as well as the experimental disposition of the 13 sulfonamide ligands co-crystallized with *hCA* II, a receptor-based pharmacophore model including five features was eventually generated using UNITY software. The model included an H-bond donor and an H-bond acceptor feature representing the interactions of the ligand sulfonamide group with the key anchoring residue T199, a couple of hydrophobic features representing the central core of the ligands, and a further H-bond acceptor group representing a possible interaction with the side chain of Q92. By considering this latter feature and one of the hydrophobic features as optional, the pharmacophore model successfully retrieved 35 known *hCA* II ligands (the 13 crystallographic compounds and other 22 *hCA* II inhibitors selected from literature) that were used to enrich the subset of about 5900 potential zinc binders. However, more than a half of these compounds (about 3300) passed the pharmacophore-based filter, and the retrieved ligands were thus subjected to a further ligand-based filter through the flexible superposition with FlexS software on two reference co-crystallized inhibitors selected for having a small and a big molecular shape. Out of the 2237 compounds for which a superposition could be computed by the software, the 100 top-scored ligands were then docked into the *hCA* II binding site with FlexX. A final set of 13 compounds was eventually selected after visual inspection of the docking poses, based on the pharmacophore features matched, the key ligand–protein interactions maintained, and docking score calculated by both FlexX and DrugScore scoring functions. The final compounds were purchased and subjected to enzymatic assays, together with the reference inhibitor

acetazolamide, and the results revealed an inhibitory activity for 11 out of the 13 tested compounds. In fact, only two hydroxamic acid derivatives showed no *hCA* II inhibition, while all other sulfonamide ligands presented an inhibitory potency ranging from low micromolar to subnanomolar values (pIC_{50} values between 5.26 and 9.21). Two of the active compounds, including the most potent one, were then co-crystallized with *hCA* II, and the two X-ray structures (PDB codes 1KQW and 1KQR) further demonstrated the reliability of the VS workflow, since the two ligands respected the pharmacophore model in their experimental binding modes, which differed of less than 1.5 Å in terms of root mean squared deviation (RMSD) from the best docking poses selected by DrugScore.

Another example of receptor-based pharmacophore screening that focused on *hCA* II was reported in 2011 by Supuran, Sechi, and co-workers, which identified a novel low micromolar inhibitor incorporating an unusual ZBG (Pala et al. 2011). In this work, high-resolution X-ray structures of *hCA* II in complex with sulfonamide inhibitors were aligned and used as input ligand–protein complexes for generating a receptor-based pharmacophore model using MOE software. The model obtained included four different features: a metal ligator feature and two H-bond acceptor features, representing the sulfonamide group of the reference experimental ligands, and a big hydrophobic/aromatic feature representing both their central aromatic scaffold and the terminal moieties constituting the ligands' tails. Moreover, excluded volume constraints were generated using the binding site of *hCA* II in the X-ray structure in complex with 3-[4-(aminosulfonyl)phenyl]propanoic acid (PDB code 2NNO). The pharmacophore model was used to screen the ZINC lead-like database (Irwin and Shoichet 2005), collecting about 970'000 drug-like compounds, from which about 37'400 ligands were retained as hits. The subset of selected compounds was then further filtered by excluding all molecules bearing sulfur atoms, with the aim of excluding from the following VS step all sulfonamide ligands and compounds bearing sulfonamide-like groups, so that to retain only potential *hCA* II with different ZBGs. The about 4600 retained compounds were then docked into the structure of *hCA* II using FlexX and only the best 29 compounds were subjected to a further docking evaluation using Autodock4. Among these final compounds, a small molecule with a unique original structure was selected to be purchased and subjected to enzymatic assays. The results showed that the compound was able to inhibit *hCA* II with low micromolar potency ($K_i = 9.0 \mu\text{M}$) and demonstrated selectivity over *hCA* I ($K_i = 410.0 \mu\text{M}$). Despite the activity of the identified ligand not being high, the compound was characterized by an unusual ZBG, represented by a gem-dihydroxyl-keto moiety that was supposed to coordinate the zinc ion and to form H-bonds with the key anchoring residues T199 and T200 of *hCA* II (Figure X). The presence of a trifluoromethyl group connected to the germinal diol was also supposed to enhance the polarization of the two hydroxyl groups, thus favoring metal chelation (Fig. 11.1).

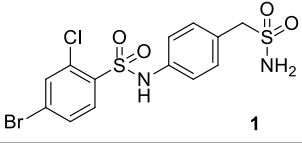
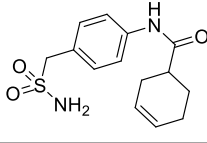
Receptor-based pharmacophore modeling and screening were also successfully applied for the identification of novel *hCA* VII inhibitors by De Luca and co-workers, which discovered two novel nanomolar sulfonamide inhibitors (De Luca et al. 2014). The pharmacophore model was generated based on the X-ray structures of *hCA* VII in complex with the well-known inhibitors acetazolamide (PDB code 3ML5)

Fig. 11.1 Schematized binding mode of the VS hit identified by Supuran and Sechi



and ethoxzolamide (PDB code 3MDZ). The two aligned co-crystal structures were used as input structures for LigandScout software to generate two corresponding receptor-based pharmacophore models, which were then merged into a single final model including six total features: three H-bond acceptor, one H-bond donor, and two hydrophobic features. The H-bond donor and a closely placed H-bond acceptor represented the sulfonamide groups of the co-crystallized ligands, a second H-bond acceptor represented the interaction with the side chain of T200 shared by both inhibitors through their endocyclic nitrogen, while the other three features corresponded to moieties present in either one or the other inhibitor. The merged model was validated using a set of 22 *hCA* inhibitors reported in literature and used to filter a focused library of about 6300 compounds bearing sulfonamide moieties retrieved from the ZINC database. The screening was performed with the software Catalyst, which assigned a fit score valued to reference and database compounds based on the geometric matching between their structures and the pharmacophore features of the model. Since 13 out of the 22 reference actives showed a fit score value higher than 3, this threshold was employed to filter the database compounds, thus obtaining 299 best fitting compounds. After a visual inspection of the pharmacophore hits, 34 ligands selected based on their structural diversity were then docked into the X-ray structure of *hCA* VII in complex with acetazolamide (PDB code 3ML5) using GOLD software. Considering the fitness score calculated by GoldScore scoring function for the docked compounds, the ligand–protein interactions predicted in their docking poses, and the commercial availability of the molecules, two final compounds were purchased and subjected to enzymatic assays. The ligands showed inhibitory activities against *hCA* VII in the nanomolar range (K_i values of 62.9 and 39.4 nM, see Table 11.1), thus demonstrating the reliability of the VS workflow. Nevertheless, the ligands also showed comparable or even higher potency against other *hCA* isoforms,

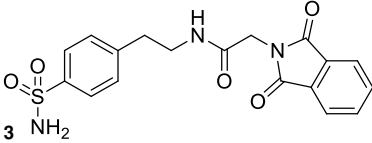
Table 11.1 K_i values against *h*CAs showed by compounds **1** and **2**

					
	K_i (nM)				
	<i>h</i> CA I	<i>h</i> CA II	<i>h</i> CA VII	<i>h</i> CA IX	<i>h</i> CA XIV
1	8.6	6.3	62.9	66.0	19.4
2	8.9	73.2	39.4	53.2	7.6

particularly *h*CA I (K_i values of 8.9 and 8.6 μ M), as the ligands potency for this isoform was higher than that reported for the reference inhibitors.

A ligand-based pharmacophore screening, in combination with other techniques, was instead used in a VS study reported in 2009 by Thiry and co-workers, aimed at identifying new *h*CA IX sulfonamide inhibitors (Thiry et al. 2009). The model was generated using the MOE software, on the basis of the structures of ten known inhibitors reported in literature, with strong activity against *h*CA IX and selectivity over *h*CA II. Although being structurally different, the ten active ligands all shared a sulfonamide moiety as ZBG; therefore, the compounds were flexibly aligned with one another so that the coordinates of their sulfonamide groups were properly superimposed. Based on the aligned reference ligands, a ligand-based pharmacophore model including six different features was obtained: the sulfonamide fragment was represented by a metal ligator and two H-bond acceptor features, while the central aromatic core and the terminal tails of the active ligands were represented, respectively, by an aromatic feature and two mixed features (hydrophobic/H-bond donor and H-bond donor/acceptor). Once generated the model, a dataset of about 1200 compounds was obtained by applying molecular properties and substructure filters to about 4.6 million commercial compounds belonging to the ZINC database. The compounds retained in the dataset were characterized by the presence of a sulfonamide ZBG group and satisfied the following molecular properties: $-2 < \log P < +4$; rotatable bonds < 12 ; H-bond donor < 5 , H-bond acceptor < 10 ; polar surface area < 140 . The selected compounds were then screened using the pharmacophore model, and only the 500 hits respecting all pharmacophore features were subjected to molecular docking using the software GOLD. In this case, the 500 compounds were docked into an *h*CA IX homology model previously developed by the same research group (Thiry et al. 2006). After visual inspection of the top-score 100 compounds, six potential new inhibitors were eventually selected for enzymatic assays, and all ligands showed *h*CA IX inhibitory activities, with K_i values between 2.75 and 0.29 μ M. Furthermore, the compounds demonstrated selectivity over *h*CA I (being 3- to 28-fold less active against this *h*CA isoform) but showed comparable or higher activities against *h*CA II. For instance, the most interesting compound (compound **3** of Table 11.2), with the highest activity for *h*CA IX and selectivity over *h*CA I was also found to be 60-fold

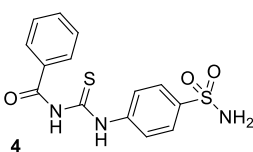
Table 11.2 K_i values against *h*CAs showed by compounds **3**

			
K_i (nM)			
	<i>h</i> CA I	<i>h</i> CA II	<i>h</i> CA VII
3	8350	5	300

more potent against *h*CA II, with a K_i value of 5 nM. These results demonstrated the reliability of the VS workflow in the discovery of new *h*CA IX ligands but confirmed that the identification of *h*CA ligands also endowed with a good selectivity profile represents a more challenging task.

A further VS campaign focused on *h*CA IX allowed the identification of 13 novel sulfonamide inhibitors with nanomolar potency (Wang et al. 2013). In this study, a pure docking-based approach was followed: the whole SPECS database, collecting about 280'000 commercial compounds, was docked into the X-ray structure of *h*CA IX in complex with acetazolamide (PDB code 3IAI) by using Glide software with the standard-precision method (SP). Subsequently, the top-scored 10'000 compounds were subjected to an additional docking evaluation into the same receptor performed with the extra-precision method (XP). The 500 compounds showing the highest score values after this second docking step were visually inspected, and 49 structurally different ligands were eventually selected to be purchased and tested to evaluate their inhibitory activity. Although the final set of selected compounds included molecules bearing different types of ZBGs, only sulfonamide ligands showed activity against *h*CA IX. However, most of the 13 hit compounds showed single- to double-digit nanomolar potency and considerable selectivity over *h*CA II and/or *h*CA I. For instance, compound **4** of Table 11.3 was probably the most interesting, with an IC_{50} value for *h*CA I inhibition of 2.86 nM, a 21-fold selectivity over *h*CA II, and 69-fold

Table 11.3 IC_{50} values against *h*CAs showed by compounds **4** and **5**

			
IC_{50} (nM)			
	<i>h</i> CA I	<i>h</i> CA II	<i>h</i> CA VII
4	197.64	60.93	2.86
5	231.41	3873	28.35

selectivity over *hCA* I, whereas compound **5** (IC_{50} for *hCA* I = 28.35) showed the highest selectivity over *hCA* II (about 137-fold).

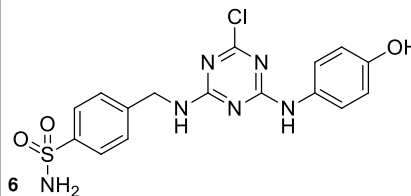
A similar example of *hCA* IX-targeted VS study entirely relying on high-throughput docking was recently reported by Durdagi and collaborators in 2016 (Salmas et al. 2016). In this work, the X-ray co-crystal structure of *hCA* IX in complex with acetazolamide (PDB code 3IAI) was used. Prior to docking studies, the reference ligand–protein complex was subjected to a 10 ns molecular dynamics (MD) simulation performed with NAMD in an explicit water environment, in order to relax the system and the protein side chains. The average protein structure derived from the MD simulation was used for the docking evaluation of 7 million drug-like commercial compounds from ZINC database, performed with the high-throughput virtual screening (HTVS) method of Glide software. Out of the whole database of docked compounds, only the top-scored 70 molecules were selected and subjected to a more thorough docking calculation employing Glide XP method. Out of the 19 compounds showing a docking score better than -8 kcal/mol and forming H-bond interactions with key anchoring residues of *hCA* IX binding site, such as T199 and T200, three compounds were chosen, purchased, and tested for their *hCA* IX inhibitory activity. Surprisingly, none of the top-scored compounds presented a sulfonamide moiety as ZBG. The three tested compounds, all characterized by a central α -hydroxylactam core, showed *hCA* IX inhibitory activity in the low micromolar to submicromolar range, with K_i values between 1.58 and 0.85 μ M. Interestingly, none of them was predicted to directly interact with the zinc ion in their proposed binding mode.

Pure molecular docking screens were also successfully employed for the identification of novel *hCAs* inhibitors from virtual focused libraries of natural compounds or structurally related derivatives designed through combinatorial chemistry. Alcaro and collaborators performed a docking-based virtual screening on a pool of natural compounds belonging from both the volatile and non-volatile fractions of the typical Calabrian products Bergamot and Tropea red onion (Gidaro et al. 2015). Considering different possible tautomeric and protomeric forms of the specific natural compounds, a library of 280 molecules was generated, and the standard-precision method of Glide was used to dock the compounds into the X-ray structures of five different CA isoforms, i.e., *hCAs* I, II, IX, and XII (PDB codes 1AZM, 4CQ0, 3IAI, and 4HT2, respectively), as well as *mCA* VA (PDB code 1DMY). Self-docking studies of the ligands co-crystallized with the different CA isoforms in the selected X-ray structures were used to assess the reliability of the docking protocol; moreover, the estimated binding energies associates to the docking results of acetazolamide into the different X-ray structures were used as reference values for selecting potential *hCA* ligands to be tested for inhibitory activity. Precisely, the ten flavonoid ligands that showed a docking score value better than that obtained for acetazolamide in at least one of the five CA isoforms were selected and subjected to enzymatic assays. The experimental results demonstrated that all tested compounds were endowed with inhibitory activity against all human isoforms of the five CAs with low micromolar to nanomolar potencies (K_i values ranging from 4.24 to 0.11 μ M). Two of the identified hits, namely, eritrocitin and apigenin, showed very interesting activities against *hCA* VA, since they were found to be more potent *hCA* VA inhibitors (K_i for *hCA* VA

of 0.15 and 0.30 μM , respectively) than the reference ligand acetazolamide (K_i for *hCA* VA of 0.38 μM).

Finally, in 2018, Supuran and collaborators reported on the identification of novel nanomolar inhibitors of *hCA* I, II, and IX through a VS study performed on a focused library of sulfonamide compounds with a 1,3,5-triazine core (Havránková et al. 2018), as a continuation of previous works in which they discovered that sulfonamides bound to a triazine skeleton had high potency and usually also specificity for *hCA* IX over *hCA* I or II (Garaj et al. 2004; Carta et al. 2011). The software CombiGlide from Schrodinger suite was used to create a combinatorial library comprising 2200 unique compounds (9766 molecules considering multiple possible isomers and ionization states for each ligand) by combining three different arylsulfonamide moieties and a set of 21 fragments (including aminoalcohols, aryltriazoles, and others) with cyanuric chloride (2,4,6-trichloro-1,3,5-triazine). The library was built by considering the generations of the possible triazine-containing products obtained by substituting cyanuric chloride with an arylsulfonamide group and at least one among the other 21 fragments. The whole set of molecules was docked into the X-ray structure of *hCA* IX (PDB code 3IAI) using Glide HTVS method; the top-scored 2000 compounds were then docked into the same protein structure using the SP method, and the best 400 ligands according to this second step were subjected to further docking calculation using the XP method. Finally, the 80 top-scored molecules based on the XP score (corresponding to 66 unique ligands) were analyzed through an additional docking evaluation using the quantum-polarized ligand docking (QPLD) protocol, which computes ligands partial charges with the semiempirical RM6 method. The same method was used to dock the 66 ligands into the X-ray structure of *hCA* II (PDB code 3MMF) in order to evaluate their potential selectivity over this *hCA* isoform. Among the 20 top-scored molecules resulting from QPLD calculations, 11 compounds and their synthetic intermediates (for a total of 24 ligands) were selected to be synthesized and tested for *hCA* I, II, and IX inhibitory activity. A final set of newly synthesized compounds was thus subjected to enzymatic assays, revealing nanomolar *hCA* IX inhibitory activity for all compounds, among which 14 ligands showed a high potency ($K_i < 50$ nM). All tested compounds were generally selective for *hCA* IX over *hCA* I, but most of them showed either comparable or higher potency against *hCA* II. The best selectivity over *hCA* II was shown by compound **6** of Table 11.4, which represented the most promising compound of the series, presenting subnanomolar activity against *hCA* IX ($K_i = 0.4$ nM) and being 18.5-fold and about 42-fold less active against *hCA* II and I, respectively.

Table 11.4 K_i values against *h*CA s showed by compounds **6**

			
	K_i (nM)	<i>h</i> CA I	<i>h</i> CA II
6	16.7	7.4	0.4

11.3 Retrospective Virtual Screening Studies Using Carbonyl Anhydrases as Target Receptors

Due to the number of known inhibitors and ligand–protein X-ray structures reported in literature, some well-studied *h*CA isoforms such as *h*CA I and *h*CA II have been used as reference target proteins for retrospective analyses aimed at assessing the hit identification performance of several different VS approaches, including docking, 2D fingerprint screenings, 3D shape-based ligand similarity, and machine learning techniques.

In an interesting work reported in 2005, Shoichet and collaborators evaluated the performance of their molecular docking software Dock in identifying potential ligands of metalloenzymes using a standard noncovalent scoring function, i.e., employing molecular mechanics parameters for treating the prosthetic metal ion but without considering the covalent-like interaction between metal and ligands (Irwin et al. 2005). The analysis was performed using a dataset of about 95'000 compounds belonging from the MDL Drug Data Report (MDDR) version 2000.2, a licensable database of biologically relevant compounds from patent literature. The study considered reference metalloenzymes with a minimum of 20 known ligands included in the database and for which various ligand–protein co-crystal structures were available, i.e., xanthine oxidase (XO), neutral endopeptidase (NEP), peptide deformylase (PDF), matrix metalloproteinase 3 (MMP-3), and *h*CA II. In particular, the retrospective analysis focused on *h*CA II was carried out using the X-ray structure of *h*CA II bound to dorzolamide (PDB code 1CIL) and considering the 241 *h*CA II ligands included in the MDDR database as reference actives. The zinc ion was parametrized with van der Waals radius of 1.09 Å and a well-depth minimum of 0.25 kcal/mol (Stote and Karplus 1995) as well as a net charge of + 1.4 (considering a net charge transfer of + 0.2 to each of the three coordinating histidine residues). The enrichment plot analysis performed on the docking results showed that, using these parameters, a satisfying screening performance could be obtained. In fact, the enrichment factor (EF) calculated for the top-scoring 0.1% of the ranked database (EF_{1%}) was 82-fold better than random selection, and 25% of known actives were identified within the

top 1.6% of the ranked database. Moreover, 95% of the reference *hCA* II ligands showed docking poses resembling the experimental disposition of dorzolamide.

McGaughey and co-workers performed an extensive analysis in which they assessed the VS performance of three different docking software (Flog, Fred, and Glide) in comparison with both 2D ligand-based (Daylight, Toposim) and 3D shape-based (SQW, Rocs) similarity strategies (McGaughey et al. 2007). The seven total VS approaches were tested using a set of 11 different target enzymes that also included *hCA* I. In this study, the X-ray structure of the enzyme in complex with acetazolamide (PDB code 1AZM) was used for docking studies, and the co-crystallized ligand was employed as the query structure for ligand-based methods. Two screening databases were used: a dataset of about 24'500 compounds obtained by clustering the MDDR database and a dataset of less than 10'000 elements including compounds randomly selected from Merck's corporate database (MCIDB) and a set of reference active compounds carefully selected for each target. In both datasets, compounds with more than 80 heavy atoms were discarded. For *hCA* I, 80 and 241 reference actives were present in the final MDDR and MCIDB datasets, respectively. This analysis revealed that, on average, the ligand-based VS approaches outperformed the docking methods, as demonstrated by comparing the EF values calculated for the top 1% of both ranked databases. This was particularly true for *hCA* I, which resulted to be one of the most challenging targets for docking-based VS among the 11 enzymes tested in the study, showing EF_{1%} values between 0 and 2.5, compared to mean values ranging from 4.0 to 13.4 (calculated considering all target enzymes). The fact that no special parametrization for the zinc ion was used in docking calculations may have contributed to the low enrichments obtained for *hCA* I, although similar results were showed by other targets with no metal prosthetic groups within the ligand binding site (namely HIV-rt and COX2). Conversely, the 2D ligand similarity methods performed the best on *hCA* I, showing the highest EF values among those obtained for all targets. Particularly, EF_{1%} values of 50.2–56.4 were obtained for MDDR dataset and 17.6–25.5 for MCIDB dataset compared to mean values of 24.5–29.0 and 7.4–10.6, respectively. These results can be however rationalized considering that most of the *hCA* inhibitors present a sulfonamide moiety acting as ZBG, which can facilitate the retrieval of active compounds using VS approaches based on the structural similarity of the ligands. In fact, pure shape-based methods such as Rocs showed a lower performance compared to 2D similarity, but when an atom type-based similarity component was included in the screening (as in Rocs-color), about threefold improvement in the EF values were obtained for *hCA* I.

An in-depth analysis focused on 2D fingerprint methods was reported by Sherman et al. in 2010 (Sastry et al. 2010). In this work, the VS performance of eight different fingerprint types available in the software Canvas (linear, dendritic, radial, pairwise, triplet, torsion, Molprint2D, and MACCS fingerprints) was evaluated using a dataset of about 24'500 MDDR compounds obtained as described by McGaughey and co-workers (McGaughey et al. 2007) and considering the same group of 11 target enzymes, including *hCA* I. The same reference ligand–protein co-crystal structures were also employed for each target. Therefore, acetazolamide was used as the query

structure for the fingerprint similarity analyses aimed at retrieving the 80 reference actives of *hCA I* out of the MDDR compounds dataset. Since for each fingerprint type, the performance evaluation was carried out using different atom typing schemes, bit scaling rules, and similarity/distance metrics, a total number of almost 160'000 different parameter combinations were evaluated based on the $EF_{1\%}$. The analysis demonstrated the robustness of Molprint2D method, which showed the best overall performance across all 11 target enzymes considering both default settings and the best combination of parameters tested. Again, *hCA I* was found to be the target protein for which the best enrichments were obtained, on average. In particular, considering the best settings for each fingerprint type, Molprint2D and radial fingerprints achieved an $EF_{1\%}$ value of 80.0, and even MACCS fingerprints, which produced the worst overall results, showed an $EF_{1\%}$ of 50.0 for *hCA I*. These results are in agreement with the above reported considerations about the structural similarity of *hCAI*s; in fact, although the average tanimoto similarity of the 80 reference *hCA I* ligands was considerably low (around 0.1), the authors themselves pointed out that all ligands presented a sulfonamide group in a similar environment, and this may have contributed to the generally high performance of the fingerprint methods. Notably, atom typing schemes such as Mol2 and Daylight performed better than less specific atom typing (less likely to discriminate specific structural moieties).

The same author reported a further analysis concerning ligand-based techniques performed using the same set of target enzymes, reference actives, query structures, and approximately the same dataset of MDDR compounds. This study was focused on shape-based flexible ligand superposition methods, as the Phase Shape tool implemented in Schrödinger suite was tested for its VS performance, analyzing the impact of multiple parameters such as conformer generation method and atom/feature typing method (Sastry et al. 2011). The results shown in this study were consistent with those reported by McGaughey et al., which were also used to compare the performance of Phase Shape with Rocs-color and SQW. Overall, the $EF_{1\%}$ obtained with *hCA I* were above the average values calculated across all 11 target enzymes, but not the highest as observed for the 2D similarity methods, and the use of MacroModel atom types or better Phase pharmacophore feature types performed substantially better than more generic atom typing-based and shape-only scoring. However, the 3D alignments obtained with shape-only scoring method demonstrated to perform qualitatively well for *hCA I* target. Surprisingly, the use of a low-energy conformer of acetazolamide generated with the conformer generator implemented in Phase Shape as the query structure produced better results than those obtained using the experimental disposition of the ligand.

In summary, the results of these analyses highlighted that a proper parametrization of the prosthetic zinc ion in docking studies focused on *hCA*s can improve the quality and accuracy of the docking results and that ligand-based techniques, particularly 2D similarity approaches, can show superior performance in identifying new potential *hCA* inhibitors, provided that either no or minimal structural diversity at the level of the ZBG is required or expected.

References

- Aghazadeh Tabrizi M, Baraldi PG, Ruggiero E, Saponaro G, Baraldi S, Poli G, Tuccinardi T, Ravani A, Vincenzi F, Borea PA, Varani K (2016) Synthesis and structure activity relationship investigation of Triazolo[1,5-a]Pyrimidines as CB2 cannabinoid receptor inverse agonists. *Eur J Med Chem* 113:11–27
- Bai F, Liao S, Gu J, Jiang H, Wang X, Li H (2015) An accurate metalloprotein-specific scoring function and molecular docking program devised by a dynamic sampling and iteration optimization strategy. *J Chem Inf Model* 55(4):833–847
- Broccatelli F, Brown N (2014) Best of both worlds: on the complementarity of ligand-based and structure-based virtual screening. *J Chem Inf Model* 54(6):1634–1641
- Carta F, Garaj V, Maresca A, Wagner J, Avvaru BS, Robbins AH, Scozzafava A, McKenna R, Supuran CT (2011) Sulfonamides incorporating 1,3,5-triazine moieties selectively and potently inhibit carbonic anhydrase transmembrane isoforms IX, XII and XIV over cytosolic isoforms I and II: solution and X-Ray crystallographic studies. *Bioorg Med Chem* 19(10):3105–3119
- Chen Y-C (2015) Beware of docking! *Trends Pharmacol Sci* 36(2):78–95
- Chiarelli LR, Mori M, Barlocco D, Beretta G, Gelain A, Pini E, Porcino M, Mori G, Stelitano G, Costantino L, Lapillo M, Bonanni D, Poli G, Tuccinardi T, Villa S, Meneghetti F (2018) Discovery and development of novel salicylate synthase (MbtI) furanic inhibitors as antitubercular agents. *Eur J Med Chem* 155:754–763
- De Luca L, Ferro S, Damiano FM, Supuran CT, Vullo D, Chimirri A, Gitto R (2014) Structure-based screening for the discovery of new carbonic anhydrase VII inhibitors. *Eur J Med Chem* 71:105–111
- Garaj V, Puccetti L, Fasolis G, Winum J-Y, Montero J-L, Scozzafava A, Vullo D, Innocenti A, Supuran CT (2004) Carbonic anhydrase inhibitors: synthesis and inhibition of cytosolic/tumor-associated carbonic anhydrase isozymes I, II, and IX with sulfonamides incorporating 1,2,4-triazine moieties. *Bioorg Med Chem Lett* 14(21):5427–5433
- Gitardo M, Alcaro F, Carradori S, Costa G, Vullo D, Supuran C, Alcaro S (2015) Eriocitrin and apigenin as new carbonic anhydrase VA inhibitors from a virtual screening of calabrian natural products. *Planta Med* 81(06):533–540
- Grüneberg S, Stubbs MT, Klebe G (2002) Successful virtual screening for novel inhibitors of human carbonic anhydrase: strategy and experimental confirmation. *J Med Chem* 45(17):3588–3602
- Havránková E, Csöllei J, Vullo D, Garaj V, Pazdera P, Supuran CT (2018) Novel sulfonamide incorporating piperazine, aminoalcohol and 1,3,5-triazine structural motifs with carbonic anhydrase I, II and IX inhibitory action. *Bioorg Chem* 77:25–37
- Irwin JJ, Shoichet BK (2005) ZINC—a free database of commercially available compounds for virtual screening. *J Chem Inf Model*
- Irwin JJ, Raushel FM, Shoichet BK (2005) Virtual screening against metalloenzymes for inhibitors and substrates †. *Biochemistry* 44(37):12316–12328
- Irwin JJ, Shoichet BK (2016) Docking screens for novel ligands conferring new biology. *J Med Chem* 59(9):4103–4120
- Liu K, Kokubo H (2017) Exploring the stability of ligand binding modes to proteins by molecular dynamics simulations: a cross-docking study. *J Chem Inf Model* 57(10):2514–2522
- Luger D, Poli G, Wieder M, Stadler M, Ke S, Ernst M, Hohaus A, Linder T, Seidel T, Langer T, Khom S, Hering S (2015) Identification of the putative binding pocket of valeric acid on GABAA receptors using docking studies and site-directed mutagenesis. *Br J Pharmacol*
- McGaughey GB, Sheridan RP, Bayly CI, Culbertson JC, Kreatsoulas C, Lindsley S, Maiorov V, Truchon J-F, Cornell WD (2007) Comparison of topological, shape, and docking methods in virtual screening. *J Chem Inf Model* 47(4):1504–1519
- Pala N, Dallochio R, Dessì A, Brancale A, Carta F, Ihm S, Maresca A, Sechi M, Supuran CT (2011) Virtual screening-driven identification of human carbonic anhydrase inhibitors incorporating an original new pharmacophore. *Bioorg Med Chem Lett* 21(8):2515–2520

- Pecina A, Brynda J, Vrzal L, Gnanasekaran R, Hořejší M, Eyrilmez SM, Řezáč J, Lepšík M, Řezáčová P, Hobza P, Majer P, Veverka V, Fanfrlík J (2018) Ranking power of the SQM/COSMO scoring function on carbonic anhydrase II-inhibitor complexes. *ChemPhysChem* 19(7):873–879
- Poli G, Jha V, Martinelli A, Supuran C, Tuccinardi T (2018b) Development of a fingerprint-based scoring function for the prediction of the binding mode of carbonic anhydrase II inhibitors. *Int J Mol Sci* 19(7):E1851
- Poli G, Tuccinardi T, Rizzolio F, Caligiuri I, Botta L, Granchi C, Ortore G, Minutolo F, Schenone S, Martinelli A (2013) Identification of new fyn kinase inhibitors using a FLAP-based approach. *J Chem Inf Model* 53(10):2538–2547
- Poli G, Giuntini N, Martinelli A, Tuccinardi T (2015) Application of a FLAP-consensus docking mixed strategy for the identification of new fatty acid amide hydrolase inhibitors. *J Chem Inf Model* 55(3):667–675
- Poli G, Gelain A, Porta F, Asai A, Martinelli A, Tuccinardi T (2016) Identification of a New STAT3 dimerization inhibitor through a pharmacophore-based virtual screening approach. *J Enzyme Inhib Med Chem* 31(6):1011–1017
- Poli G, Scarpino A, Aissaoui M, Granchi C, Minutolo F, Martinelli A, Tuccinardi T (2018a) Identification of lactate dehydrogenase 5 inhibitors using pharmacophore-driven consensus docking. *Curr Bioact Compd* 14(2):197–204
- Ripphausen P, Stumpfe D, Bajorath J (2012) Analysis of structure-based virtual screening studies and characterization of identified active compounds. *Future Med Chem* 4(5):603–613
- Salmas RE, Senturk M, Yurtsever M, Durdagi S (2016) Discovering novel carbonic anhydrase type IX (CA IX) inhibitors from seven million compounds using virtual screening and in vitro analysis. *J Enzyme Inhib Med Chem* 31(3):425–433
- Sastry M, Lowrie JF, Dixon SL, Sherman W (2010) Large-scale systematic analysis of 2D fingerprint methods and parameters to improve virtual screening enrichments. *J Chem Inf Model* 50(5):771–784
- Sastry GM, Dixon SL, Sherman W (2011) Rapid shape-based ligand alignment and virtual screening method based on atom/feature-pair similarities and volume overlap scoring. *J Chem Inf Model* 51(10):2455–2466
- Stote RH, Karplus M (1995) Zinc binding in proteins and solution: a simple but accurate nonbonded representation. *Proteins Struct Funct Genet* 23(1):12–31
- Tanrikulu Y, Rau O, Schwarz O, Proschak E, Siems K, Müller-Kuhrt L, Schubert-Zsilavec M, Schneider G (2009) Structure-based pharmacophore screening for natural-product-derived PPAR γ agonists. *ChemBioChem* 10(1):75–78
- Thiry A, Ledecq M, Cecchi A, Dogné J-M, Wouters J, Supuran CT, Masereel B (2006) Indanesulfonamides as carbonic anhydrase inhibitors: toward structure-based design of selective inhibitors of the tumor-associated isozyme CA IX. *J Med Chem* 49(9), 2743–2749
- Thiry A, Ledecq M, Cecchi A, Frederick R, Dogné J-M, Supuran CT, Wouters J, Masereel B (2009) Ligand-based and structure-based virtual screening to identify carbonic anhydrase IX inhibitors. *Bioorg Med Chem* 17(2):553–557
- Tuccinardi T, Poli G, Corchia I, Granchi C, Lapillo M, Macchia M, Minutolo F, Ortore G, Martinelli A (2016) A virtual screening study for lactate dehydrogenase 5 inhibitors by using a pharmacophore-based approach. *Mol. Inform.* 35(8–9):434–439
- Vuorinen A, Schuster D (2015) Methods for generating and applying pharmacophore models as virtual screening filters and for bioactivity profiling. *Methods* 71:113–134
- Wang L, Yang C, Lu W, Liu L, Gao R, Liao S, Zhao Z, Zhu L, Xu Y, Li H, Huang J, Zhu W (2013) Discovery of new potent inhibitors for carbonic anhydrase IX by structure-based virtual screening. *Bioorg Med Chem Lett* 23(12):3496–3499
- Wang Y, Zhao Y, Sun R, Kong W, Wang B, Yang G, Li Y (2015) Discovery of novel antagonists of glycoprotein IIb/IIIa-mediated platelet aggregation through virtual screening. *Bioorg Med Chem Lett* 25(6):1249–1253

Zhang C, Feng L-J, Huang Y, Wu D, Li Z, Zhou Q, Wu Y, Luo H-B (2017) Discovery of novel phosphodiesterase-2A inhibitors by structure-based virtual screening, structural optimization, and bioassay. *J Chem Inf Model* 57(2):355–364

Chapter 12

Targeting Carbonic Anhydrase IX in Tumor Imaging and Theranostic Cancer Therapy



Joseph Lau, Kuo-Shyan Lin, and François Bénard

Abstract Carbonic anhydrase IX (CA-IX) is an endogenous marker for hypoxia and is regulated by the von Hippel-Lindau/hypoxia-inducible factor (VHL/HIF) oxygen-sensing pathway. CA-IX is overexpressed in many solid malignancies where aberrant vasculature and limited perfusion create low oxygen niches within the tumor microenvironment. Dysregulation of the VHL/HIF signaling pathway can lead to constitutive expression of CA-IX—a phenotype associated with clear cell renal cell carcinomas (ccRCCs). As a cell-surface metalloenzyme, CA-IX works in tandem with other proteins to regulate intracellular pH in response to hypoxia-induced metabolism. In recent years, there has been evidence implicating CA-IX in potentiating cancer invasion and metastasis. Accordingly, the inhibition of CA-IX catalytic activity represents an attractive option for the management of ccRCC and other solid tumors. In this chapter, we discuss the development of CA-IX radiopharmaceuticals and their roles in delineating tumoral CA-IX expression through imaging in preclinical and clinical settings. We will also review agents that have been repositioned as endoradiotherapeutic agents for theranostic application.

Keywords Carbonic anhydrase IX · Hypoxia · Microenvironment · Imaging · Therapy · ccRCC

J. Lau · K.-S. Lin · F. Bénard (✉)

Department of Molecular Oncology, BC Cancer Agency, Vancouver, BC V5Z 1L3, Canada
e-mail: fbenard@bccrc.ca

J. Lau
e-mail: jlau@bccrc.ca

K.-S. Lin
e-mail: klin@bccrc.ca

© Springer Nature Switzerland AG 2021

W. R. Chegwidden and N. D. Carter (eds.), *The Carbonic Anhydrases: Current and Emerging Therapeutic Targets*, Progress in Drug Research 75,
https://doi.org/10.1007/978-3-030-79511-5_12

253

12.1 Introduction

Tumor hypoxia, a salient feature of solid tumors, is a negative prognostic marker for many cancers (Harris 2002; Walsh et al. 2014). Low oxygen availability depresses the efficacy of conventional radiation therapy and chemotherapy (Harris 2002; Walsh et al. 2014). Moreover, a hypoxic tumor microenvironment exerts selection pressure for resistant and aggressive clonal populations, increasing the predisposition for metastasis (Wilson and Hay 2011). Hypoxia-activated prodrugs, tumor vasculature remodeling agents, and modulators of hypoxia-induced metabolism are attractive anti-cancer agents (Wilson and Hay 2011). Carbonic anhydrase IX (CA-IX) is a biomarker for tumor hypoxia and a promising target for treating solid malignancies (Supuran 2008; McDonald et al. 2012). CA-IX regulates intracellular pH and mediates survival under hypoxic conditions. CA-IX acidifies the tumor microenvironment and primes it for invasion and distant metastasis (McDonald et al. 2012). The pharmaceutical inhibition of CA-IX activity by small molecule pharmaceuticals is being investigated in clinical trials (Supuran 2017). The success of these agents will depend on appropriate patient stratification.

Single photon emission computed tomography (SPECT) and positron emission tomography (PET) represent nuclear imaging modalities that can quantify drug-target expression in primary and metastatic lesions to predict drug sensitivity to hypoxia-based treatments (Weissleder and Mahmood 2001; Jadvar et al. 2018). In addition to identifying potential responders, SPECT and PET can be used to assess pharmacokinetic parameters and drug-target engagement, and to monitor treatment responses in a non-invasive manner (Weissleder and Mahmood 2001; Jadvar et al. 2018). Some imaging radiopharmaceuticals used to target CA-IX have been converted to endoradiotherapeutic agents. In this chapter, we will discuss the suitability of CA-IX as a druggable biomarker underpinning tumor hypoxia. We will review the development of CA-IX radiopharmaceutical agents (antibodies, peptides, and small molecules) in clinical and preclinical settings. Finally, we offer our perspectives for the translation and integration of these radiopharmaceuticals in nuclear medicine.

12.2 Targeting CA-IX as a Biomarker of Tumor Hypoxia

Cancer cells in solid tumors are constantly exposed to fluctuating oxygen levels within the tumor microenvironment. The process of developing hypoxia is independent of a tumor's size, stage, grade, or histology (Bennewith and Dedhar 2011). When oxygen tension is low (pO_2 value < 10 mmHg), most cancer cells undergo metabolic reprogramming regulated by the von Hippel-Lindau/hypoxia-inducible factor (VHL/HIF) oxygen-sensing pathway (Bennewith and Dedhar 2011; Parks et al. 2011). HIF-activated cancer cells reduce their reliance on oxidative phosphorylation, and instead shift to glycolysis to produce adenosine triphosphate (ATP) (Parks et al. 2011). Glycolysis provides the requisite ATP and biosynthetic building

blocks for survival, but concurrently lowers intracellular pH (pH_i) (Parks et al. 2011). In response to this new stressor, cancer cells overexpress CA-IX to modulate pH_i . CA-IX is a member of the carbonic anhydrase α -family (Alterio et al. 2012; Wykoff et al. 2000). As a zinc metalloenzyme, CA-IX catalyzes the interconversion of water and carbon dioxide to bicarbonate and hydrogen ions ($\text{H}_2\text{O} + \text{CO}_2 \leftrightarrow \text{HCO}_3^- + \text{H}^+$) (Hilvo et al. 2008). The HCO_3^- ions enter the cell through transporter systems to re-establish an alkaline pH_i . The H^+ ions from the reaction go on to acidify the tumor microenvironment, promoting invasion and metastasis. Researchers often measure pH change in culture medium as a means to assay CA-IX catalytic activity in cancer cell lines (Lou et al. 2011).

CA-IX is the most upregulated protein in response to HIF-1 α activation; thus, it is a well-regarded endogenous marker of cellular hypoxia (Wykoff et al. 2000). While most biomarkers in oncology are specific to cancer subtypes, CA-IX overexpression is broadly observed in solid malignancies including but not limited to head and neck, breast, lung, ovarian, and renal cancers (McDonald et al. 2012). In normal tissues, CA-IX expression is restricted to the small intestine, pancreas, and male efferent epithelial ducts (McDonald et al. 2012). The differential expression of CA-IX in cancer and normal tissues allows for adequate signal-to-noise ratios and therapeutic indices for imaging and treatment, respectively. The stability of CA-IX, its accessibility as a cell-surface protein, and the plethora of potent binders are additional merits that support CA-IX targeting strategies.

It is imperative for researchers to understand that there are situations where CA-IX expression does not correlate with the oxygen level within a tumor. Discordant CA-IX and HIF-1 α expression levels have previously been reported in vivo (Li et al. 2015). In transient hypoxia, leveraging CA-IX expression to interpolate tumor hypoxia may lead to overestimation of the hypoxic subvolume. This observation was attributed to the disparate biological half-lives in re-oxygenated cells (hours for CA-IX and minutes for HIF-1 α) (Rafajová et al. 2004; Moroz et al. 2009). As communicated by Kulaz et al., the expression of CA-IX correlates better with the transcriptional activity of HIF-1 α rather than HIF-1 α expression (Kaluz et al. 2009). At the other extreme, there are instances where CA-IX expression is conspicuously absent in hypoxic conditions. Loss-of-function mutations in HIF-1 α have been observed in cell lines (Morris et al. 2009), and there are cancers that preferentially express HIF-2 α and HIF-2 α -regulated genes in response to hypoxia (Li et al. 2009; Holmquist-Mengelbier et al. 2006).

12.3 Methods for Detecting Tumor Hypoxia

The polarographic electrode is the current gold standard for determining oxygenation levels in live tissues (Walsh et al. 2014). The methodology requires the insertion of electrodes in superficial/accessible tumors. It is limited by sampling bias and an inability to differentiate between hypoxia and necrosis. Given the extensive role of PET imaging in diagnosis, staging, and disease monitoring, an area of active research

has been the development of hypoxia imaging agents (Lopci et al. 2014; Fleming et al. 2015). FMISO, FAZA, EF5, and HX4 are examples of radio-fluorinated nitroimidazole derivatives being evaluated in the clinic. Following passive diffusion into cells, these agents are reduced by one-electron-transfer reactions to form reactive intermediates. In a normoxic cell, the nitro-radical anions undergo oxidation to reform the parent compounds, which then permeate out of the cell. In a hypoxic cell, the nitro-radical anions undergo additional reduction and bind to macromolecules. The binding to proteins or nucleic acids ‘traps’ the radioactivity inside hypoxic cells. FMISO is the most heavily investigated nitroimidazole in the clinic (Rajendran and Krohn 2015). However, the routine clinical use of FMISO and other derivatives is hampered by their slow clearance from normal tissues. Because of pharmacokinetics and mechanism of uptake, image acquisition is performed several hours post-injection (p.i.) and typically results in low-contrasted images. The hypoxia cut-off value for FMISO is institution- and scanner-dependent. For instance, Rajendran and colleagues set a tumor-to-background ratio of ≥ 1.2 at 2 h p.i. to delineate hypoxic tumors for sarcoma patients (Rajendran et al. 2003). The need to identify radiopharmaceuticals with higher sensitivity and faster pharmacokinetic has put a focus on targets like CA-IX.

12.4 CA-IX Expression in Clear Cell Renal Cell Carcinoma

The development of CA-IX radiopharmaceuticals is also prompted by the pathophysiology of clear cell renal cell carcinomas (ccRCCs), a subtype that comprises approximately 75% of all renal cell carcinomas (Hsieh et al. 2017). It is estimated that up to 92% of ccRCCs harbor genetic or epigenetic abnormalities that lead to the inactivation of the von Hippel-Lindau (VHL) tumor suppressor gene (Clark 2009; Zhang and Zhang 2018). VHL is a negative regulator and a binding partner of HIF-1 α . Under normoxic conditions, VHL binds to HIF-1 α to form a complex that is poly-ubiquitinated and targeted for proteasomal degradation (Pastorekova et al. 2008). This process inhibits HIF-1 α activation and CA-IX transcription (Pastorekova et al. 2008). The dysregulation of VHL/HIF-1 α pathway induces the constitutive expression of CA-IX, making it a rational target for ccRCC (Fig. 12.1).

When ccRCC is localized and treatable with surgery, the five-year survival rate for ccRCC is favorable at 91.7% (Ridge et al. 2014). However, diagnosis for ccRCC is not trivial with most cases being discovered as incidental findings (Gorin et al. 2015). Most anatomical imaging modalities are unable to differentiate between malignant and benign lesions as well as histological subtypes (Gorin et al. 2015). PET imaging with ^{18}F -FDG is better-suited for metastatic disease than primary lesion detection due to the renal excretion of imaging agent (Gorin et al. 2015; Escudier et al. 2016). A substantial portion of patients with benign masses, approximately 20%, receive surgical intervention when active monitoring would suffice (Gorin et al. 2015). CA-IX imaging enables radiologists and oncologists to accurately diagnose ccRCC and provide standard of care. Patients with late stage metastatic disease have

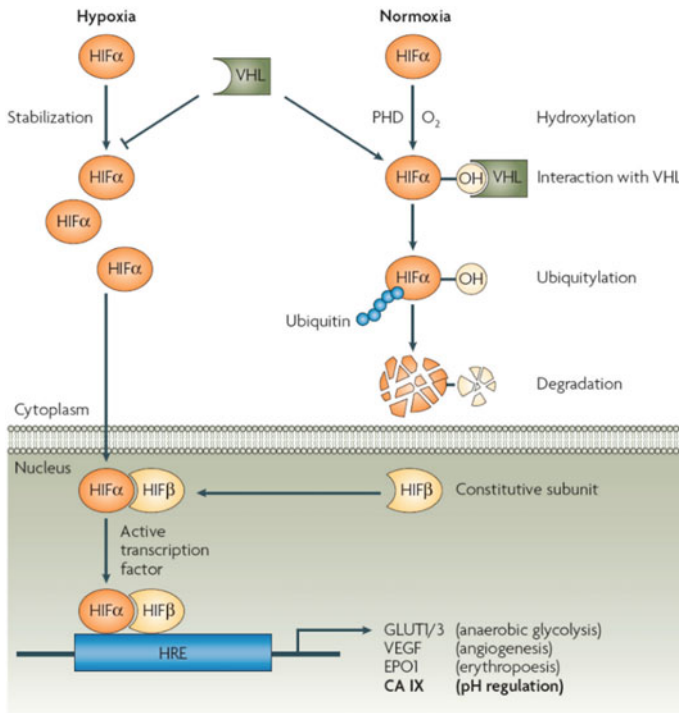


Fig. 12.1 Functional activity of HIF-1 α and its regulation by oxygen. In normoxia, HIF-1 α is post-translationally modified by proline hydroxylases (PHDs). These enzymes use oxygen as a substrate and Fe(II) and 2-oxoglutarate (2-OG) as cofactors. When HIF-1 α is hydroxylated by PHDs, it binds with the VHL tumor suppressor protein. The VHL/HIF-1 α complex becomes rapidly ubiquitinated and degraded. In hypoxia, HIF-1 α escapes hydroxylation and VHL binding, accumulates in cytoplasm, translocates to the nucleus, and dimerizes with HIF-1 β . HIF-1 α / β binds to hypoxia-response elements (HREs) in the promoter region of the target genes like CA-IX, recruits transcriptional co-activators to initiate transcription. Figure adapted with permission from Supuran (2012) in accordance with the Creative Commons Attribution (CC BY-NC 4.0) license

few available treatments. Currently, first-line therapy for metastatic ccRCC consists of targeted therapies against rapamycin and the vascular epidermal growth factor receptor (Hsieh et al. 2017). Unfortunately, the five-year survival rate for ccRCC patients with distant metastasis is dismal at 12.3% (Ridge et al. 2014). The poor prognosis for metastatic ccRCC is the major impetus for developing CA-IX-targeted treatments like radioimmunotherapy (RIT).

12.5 Monoclonal Antibodies

Monoclonal antibodies (mAbs) are a class of biologics that are used in targeted therapies. Known for their stability, binding affinity, and target selectivity, mAbs can abrogate cell-signaling, inhibit angiogenesis, regulate osteoclast function, or modulate immune response (Chiavenna et al. 2017). mAbs can also recruit immune cells to activate antibody-dependent cell-mediated cytotoxicity, complement-dependent cytotoxicity, or antibody-dependent cell phagocytosis (Scott et al. 2012). Finally, they can be modified to selectively deliver cytotoxic drugs or ionizing radiation (Sharkey and Goldenberg 2009).

Many mAbs have been developed for CA-IX targeting (Chrastina et al. 2003; Čepa et al. 2018; Ahlskog et al. 2009), but girentuximab (cG250) remains the most clinically investigated agent (Oosterwijk-Wakka et al. 2013). The first generation of cG250 was isolated as murine G250 by Oosterwijk et al. by hybridoma screening after immunizing mouse splenocytes with renal cancer homogenates (Oosterwdk et al. 1986). The proteoglycan (PG)-like domain of CA-IX is the epitope site for cG250. This domain is exclusive to CA-IX compared to other members of the CA family (McDonald et al. 2012). cG250 can induce antibody-dependent cellular cytotoxicity (Oosterwijk-Wakka et al. 2013). In a phase III study, cG250 was evaluated as an adjuvant monotherapy in patients with localized high-risk ccRCC after nephrectomy (Chamie et al. 2017). Patients treated with cG250 did not show improvement for disease-free survival (DFS) and overall survival (OS). Patients whose tumors showed higher DFS, but this was not statistically significant compared to placebo. Histology scoring was obtained by multiplying intensity of staining (1–3) by percent of positive cells (0–100) to yield a range of 0 to 300. In the subsequent section, we will review radiolabeled derivatives of cG250 for theranostic applications (Table 12.1).

12.5.1 Imaging with G250/cG250

The first clinical study with radiolabeled G250 (^{131}I -mAbG250) was conducted by Oosterwijk et al. at the Ludwig Institute for Cancer Research (Oosterwijk et al. 1993). The primary objective of this phase I study was to assess safety and biodistribution of ^{131}I -mAbG250. Sixteen patients suspected of having RCC received ^{131}I -mAbG250 intravenously 7 or 8 d before scheduled nephrectomy. Twelve patients had positive scans from whole-body planar imaging at 3 d p.i. Histology of the biopsied tissues showed that 11 patients had ccRCC and 1 patient had RCC of the granular subtype. CA-IX expression in the scan-positive lesions ranged from <5% to 100% based on immunohistochemistry. For the 4 negative scans, 3 patients had RCC of the granular or spindle subtype and 1 patient had a benign mass. ^{131}I -mAbG250 was well-tolerated in patients and accumulated specifically in CA-IX expressing lesions.

^{131}I -cG250 was used as part of RIT protocols to identify responders and monitor treatment response; however, the high energy gamma emissions of ^{131}I and reliance

Table 12.1 Clinical studies with radiolabeled G250/cG250 for imaging or therapy. Adapted from Lau et al. (2017) in accordance with the Creative Commons Attribution (CC BY-NC 4.0) license

Imaging						
Agent	# Patients enrolled ^a	Indication	Detection	Sensitivity and selectivity	Clinical stage	Refs.
¹³¹ I-mAbG250	16	Primary RCC	11/11 ccRCC pts	NR	Phase I dose escalation	Oosterwijk et al. (1993)
¹²⁴ I-cG250	26(25)	Primary RCC	15/16 ccRCC pts	94 and 100%	Phase I single dose	Divgi et al. (2007)
¹²⁴ I-cG250	226(195)	Primary RCC	124/143 ccRCC pts	86 and 76%	Phase III	Divgi et al. (2013)
¹¹¹ In-cG250 ¹³¹ I-cG250	5	Metastatic ccRCC	47 lesions 30 lesions	NR	Phase I/II inpatient comparison	Brouwers et al. (2003)
¹¹¹ In-cG250	29(22)	Metastatic ccRCC	15/15 ccRCC pts	NR	Partly retrospective	Muselaers et al. (2013)
⁸⁹ Zr-cG250	30(29)	RCC/ ccRCC	18/19 ccRCC pts	NR	Phase I/II	Hekman et al. (2018a)
Therapy						
Agent	# Patients enrolled ^a	Indication	Response	Duration of response	Clinical stage	Refs.
¹³¹ I-mAbG250	33	Metastatic ccRCC	17 SD 16 PD	2–3 mo	Phase I/II dose escalation	Divgi et al. (1998)
¹³¹ I-cG250	12(8)	Metastatic ccRCC	1 PR 1 SD 6 PD	9 + mo 3–6 mo	Phase I dose escalation	Steffens et al. (1999)
¹³¹ I-cG250	15(14)	Metastatic ccRCC	7 SD 7 PD	4–13 mo	Phase I dose fractionation	Divgi et al. (2004)
¹³¹ I-cG250	29(15)	Metastatic ccRCC	5 SD 10 PD	3–12 mo	Phase I/II two doses	Brouwers et al. (2005)
¹⁷⁷ Lu-cG250	23	Metastatic ccRCC	1 PR 12 SD 10 PD	9 + mo 3 + mo	Phase I dose escalation	Stillebroer et al. (2013)
¹⁷⁷ Lu-cG250	16(14)	Metastatic ccRCC	1 PR 7 SD; 6 PD	NR 3 + mo	Phase II	Muselaers et al. (2016)

^aNumber in bracket represents the number of patients that satisfied evaluation criteria G250: murine monoclonal G250 antibody; cG250: chimeric monoclonal G250 antibody; ccRCC: clear cell renal cell carcinoma; RCC: renal cell carcinoma; SD: stable disease; PD: progressive disease; PR: partial response; pts: patients; NR: not reported

on collimators for detection are not ideal for image quantification (Rault et al. 2007). Subsequently, another iodine isotope ^{124}I was used to radiolabel cG250 (Divgi et al. 2007). ^{124}I -cG250 uses PET imaging, a modality that uses coincidence detection for enhanced sensitivity and resolution. Divgi et al. evaluated ^{124}I -cG250 in a phase I study for preoperative characterization of RCC with indeterminate masses (Divgi et al. 2007). Twenty-six patients received an imaging dose of 185 MBq/10 mg 1 wk prior to surgery. PET/CT imaging was performed within 3 h prior to surgery. When the tumor-to-kidney (T:K) ratio was >3 , the scan was designated as positive. Sixteen cases of ccRCC were confirmed by histology and 15 of those had positive PET scans. Patients ($n = 9$) who had a negative PET scan did not have ccRCC. One patient was excluded from analysis because of an immunologically inactive infusion of ^{124}I -cG250. Overall, the sensitivity and specificity of ^{124}I -cG250 were 94% and 100%.

^{124}I -cG250 advanced to a phase III study, where its average sensitivity and selectivity for ccRCC was compared with contrast-enhanced CT (CECT) (Divgi et al. 2013). In total, 226 patients were enrolled, and 195 patients were assessable. Patients received 185 MBq/13.7 mg ^{124}I -cG250, and PET/CT acquisitions were performed 2–6 d following administration. CECTs were performed within 48 h of the PET/CT session. ^{124}I -cG250 showed better average sensitivity (86% vs. 76%) and selectivity (76% vs. 47%) than CECT for differentiating ccRCC from non-ccRCC. Positive predictive value (PPV), negative predictive value (NPV), and accuracy were calculated as secondary efficacy variables. ^{124}I -cG250 had an accuracy value of 86%, a PPV of 94%, and an NPV 69%. The results suggest that ^{124}I -cG250 PET can guide management and surgical decisions for patients with indiscriminate renal lesions. A secondary phase III study was recommended by the Food and Drug Administration, but commercial development appears stalled. Potential limitations for the clinical adoption of ^{124}I -cG250 include high cost of ^{124}I production, and in vivo dehalogenation.

One of the first radiolabels used for SPECT imaging with cG250 was indium-111 (^{111}In). cG250 was conjugated with the bifunctional chelators 1,4,7,10-tetraazacyclododecane-1,4,7,10-tetraacetic acid (DOTA) or diethylenetriaminepentaacetic acid (DTPA) for ^{111}In -labeling. ^{111}In -DOTA-cG250 was used as a companion imaging agent for ^{177}Lu -DOTA-cG250 RIT studies. Five ccRCC patients that were part of a phase I/II RIT study with ^{131}I -cG250 were recruited for an intrapatient comparison of ^{111}In -DTPA-cG250 versus ^{131}I -cG250 scintigraphy (Brouwers et al. 2003). ^{111}In -DTPA-cG250 enabled the visualization of more metastatic lesions than ^{131}I -cG250 at 4 d p.i. ($n = 47$ vs. $n = 30$). Radioactivity accumulation in 25 lesions were quantified; ^{111}In -DTPA-cG250 had higher uptake in 20 lesions and yielded better tumor-to-blood ratios. In a subsequent study, ^{111}In -DTPA-cG250 was evaluated in a cohort of 29 patients, of which 22 presented with a renal mass (Muselaers et al. 2013). Some of the patients were part of a secondary imaging study in which the effect of sorafenib on ^{111}In -DTPA-cG250 was studied. ^{111}In -DTPA-cG250 showed uptake in 16 patients, with 15 cases confirmed to be ccRCC by histopathology. The remaining patient had a type 2 papillary RCC that was also CA-IX positive.

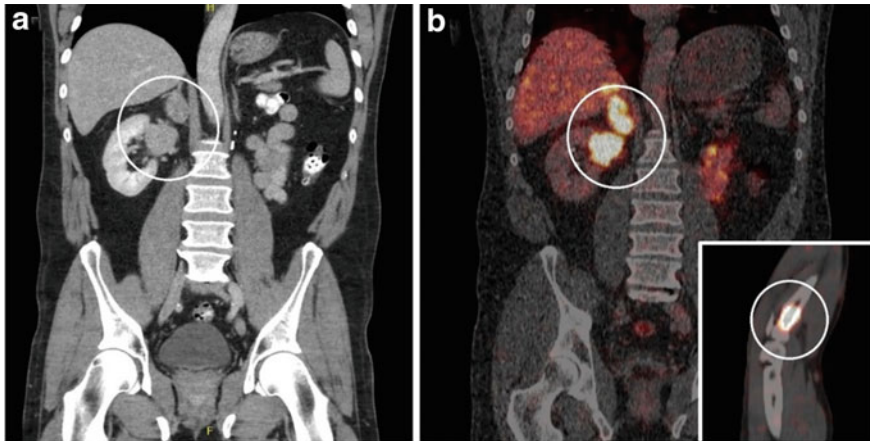


Fig. 12.2 ^{89}Zr -cG250 imaging in a patient who previously underwent a radical nephrectomy but presented with (a) a new renal tumor and a solitary adrenal metastasis on CT. (b) Uptake of ^{89}Zr -cG250 was observed in the primary renal mass, the adrenal lesion, and a previously unidentified lesion in the proximal radius. Patient had surgery and also radiotherapy for the bone lesion. Of note, the proximal radius was not in the field of view of the initial conventional imaging (CT-thorax/abdomen). Figure adapted with permission from Hekman et al. (2018a)

Recently, Hekman et al. reported the evaluation of ^{89}Zr -cG250 in a phase I/II study (Fig. 12.2) (Hekman et al. 2018a). Thirty patients suspected with ccRCC were recruited for the study and divided into two groups. The first group consisted of 16 patients with an indistinct renal mass, while the second group consisted of 14 patients with suspected recurrent/metastatic ccRCC. For the first group, six patients had a positive PET scan. Five of the 6 underwent surgery confirming ccRCC, and the patient with VHL syndrome had additional positive lesions and underwent cyroablation for debulking. One patient had two lesions, one positive and one negative on PET, but was not treated due to complex surgical history. Nine patients with negative PET scans were followed by active surveillance; none progressed within the follow-up period (13 ± 4.9 mo). In the second group, ^{89}Zr -cG250 was used to determine treatment intent. A change in clinical management occurred for 5 patients, with 3 patients avoiding biopsies due to positive PET scans. The decisions to change management was not solely dependent on ^{89}Zr -cG250-PET but included consideration of other clinical parameters.

As demonstrated through these studies, mAbs are powerful targeting vectors for imaging applications. The prolonged residence time of mAbs in blood allows for increased exposure to the target of interest, facilitating more binding events and increasing tumor uptake. However, the slow pharmacokinetics of mAbs often necessitates a clearance period of several days before optimal imaging contrast can be achieved. Antibody fragments generated from enzymatic cleavage by papain or pepsin maintain affinity for their target of interest but are structurally smaller (~55 and 110 kDa for Fab and F(ab')₂) (Sharkey and Goldenberg 2009; Freise and Wu

2015). The removal of the fragment crystallizable region reduces the likelihood of immunogenicity. Using these fragments as imaging agents would reduce radiation exposure and enable same-day imaging, providing logistical and clinical advantages. Predictably, cG250 antibody fragments, cG250-Fab, and cG250-F(ab')₂, have been investigated as imaging agents.

Carlin et al. compared the uptake of ¹¹¹In-DOTA-cG250, ¹¹¹In-DOTA-F(ab')₂-cG250, and ¹¹¹In-DOTA-Fab-cG250 in athymic mice bearing HT-29 human colorectal cancer xenografts (Carlin et al. 2010). This tumor model is considered a hypoxic cancer model. Biodistribution studies were performed at 2, 4, and 7 d p.i. for ¹¹¹In-DOTA-cG250, and at 6 and 24 h p.i. for ¹¹¹In-DOTA-F(ab')₂-cG250 and ¹¹¹In-DOTA-Fab-cG250. The harvested tumors were fluorescently stained for CA-IX, hypoxia (pimonidazole), and blood perfusion (Hoechst). The tumor uptake of ¹¹¹In-DOTA-cG250 at 7 d p.i. was $26.4 \pm 5.7\%$ ID/g, which corresponded to tumor-to-blood (T:B) and tumor-to-muscle (T:M) ratios of 6.6 and 69. ¹¹¹In-DOTA-F(ab')₂-cG250 and ¹¹¹In-DOTA-Fab-cG250 showed focal but lower uptake ($9.3 \pm 2.1\%$ ID/g and $3.5 \pm 1.7\%$ ID/g at 24 h p.i.), and lower T:B (4.6 and 16.6) and T:M ratios (8.9 and 6.7). ¹¹¹In-DOTA-F(ab')₂-cG250 and ¹¹¹In-DOTA-Fab-cG250 are capable of targeting CA-IX in hypoxic niches with a shorter distribution phase, but this comes at the expense of absolute uptake and contrast ratios.

Hoeben et al. used ⁸⁹Zr-cG250-F(ab')₂ for imaging hypoxia-mediated CA-IX expression in the SCCNij3 human head and neck squamous cell carcinoma model (Hoeben et al. 2010). ⁸⁹Zr-cG250-F(ab')₂ was administered intravenously into tumor bearing mice. The tumor xenografts were clearly visible in PET images acquired at 4 and 24 h p.i. Based on biodistribution studies, the tumor uptake of ⁸⁹Zr-cG250-F(ab')₂ was $3.71 \pm 0.97\%$ ID/g and $1.66 \pm 0.48\%$ ID/g at 4 h and 24 h p.i. The T:B and T:M ratios were 8.7 and 7.4 at 24 h p.i., respectively. The uptake in tumor correlated to pimonidazole staining ($r = 0.46\text{--}0.68$) and CA-IX expression ($r = 0.57\text{--}0.74$). Recently, Huizing *et al.* evaluated ¹¹¹In-DTPA-cG250-F(ab')₂ in two other head and neck squamous cell carcinoma models: SCCNij153 and SCCNij202 (Huizing et al. 2019). There was good concordance between SPECT image, autoradiography, and immunofluorescence. The uptake of ¹¹¹In-DTPA-cG250-F(ab')₂ in SCCNij153 tumors was $3.0 \pm 1.5\%$ ID/g and $3.0 \pm 1.8\%$ ID/g at 4 h and 24 h p.i., respectively. At 24 h p.i., T:B and T:M ratios were 19 ± 15 and 8.7 ± 1.9 .

12.5.2 Radioimmunotherapy with G250/cG250

Divgi *et al.* conducted a phase I/II RIT dose escalation study with ¹³¹I-mAbG250 (Divgi et al. 1998). Thirty-three patients with metastatic ccRCC were intravenously administered ¹³¹I-mAbG250 (1110, 1665, 2220, 2775, or 3330 MBq/m²; 10 mg) as a single dose. At doses above 1665 MBq/m², transient elevation of hepatic enzymes indicating impaired liver function was observed but not considered dose-limiting. The maximum tolerated dose (MTD) was determined to be 3330 MBq/m², based on hematological toxicity. Disease stabilization lasting more than 2 mo was observed

in 17 patients; patients were subsequently transferred to other therapies precluding follow-up. The development of human anti-mouse antibody (HAMA) response at 4 wk post-infusion in patients prevented retreatment.

G250 was chimerized to yield cG250, enabling a phase I study of ^{131}I -cG250 in patients with metastatic RCC (Steffens et al. 1999). Twelve patients were enrolled in the study, with each patient receiving a diagnostic dose (222 MBq; 0.5 mg). ^{131}I -cG250 showed similar biodistribution to ^{131}I -mAbG250, but less hepatic uptake was observed. Eight patients who had a positive scan received a therapeutic dose ranging from 1665 to 2775 MBq/m² (0.5 mg). The MTD was determined to be 2200 MBq/m², with dose-limiting hematological toxicity. One patient had stable disease for 3–6 mo, while another had partial response (50% reduction in lesion sizes) that lasted for at least 9 mo. The remaining 6 patients exhibited progressive disease. Of note, 1 patient who received two prior doses of 5 mg cG250 as part of an earlier clinical trial developed human anti-chimeric antibodies (HACA) in this study.

Divgi et al. explored the use of a dose fractionation approach for administration of ^{131}I -cG250 to prevent myeloablation and to improve response (Divgi et al. 2004). In this phase I trial, 15 metastatic RCC patients were enrolled and divided into groups of three. The first group was prescribed an average whole-body absorbed dose of 0.50 Gy, with succeeding groups receiving increased doses of 0.25 Gy increments. The first fraction of ^{131}I -cG250 was administered at 1110 MBq/5 mg, with subsequent fractions given at 2–3 d intervals. Imaging was used for dosimetry analysis. Patients who had no disease progression and demonstrated recovery from treatment toxicity were eligible for additional cycles; 5 patients qualified. Following treatment, 7 patients had stable disease, and 7 had disease progression. One patient developed sepsis during the study and was unable to continue treatment. HACA reactivity was observed in 2 patients. The fractionated approach did not significantly improve hematological toxicity or clinical outcomes.

Twenty-nine patients with metastatic RCC were recruited for a phase I study, in which participants received two sequential high doses of ^{131}I -cG250 (Brouwers et al. 2005). Baseline imaging identified 27 patients with adequate antibody accumulation in tumors for treatment. These patients were given a therapeutic dose of 2220 MBq/m², which was previously determined as the MTD. Patients were eligible for further treatment if they did not have grade 4 hematological toxicity or HACA response. Nineteen patients received another cycle of low dose diagnostic infusion and high dose therapeutic infusion of ^{131}I -cG250 (1110 MBq/m² to 1665 MBq/m²). Fifteen patients completed treatments and were deemed assessable; 10 patients had progressive disease while 5 had stable disease ranging from 3–12 mo. Consistent with previous studies, the therapeutic efficacy of ^{131}I -cG250 was limited. The authors postulated that RIT with cG250 using metal radionuclides would improve tumor accumulation and retention.

Given the lack of clinical efficacy for ^{131}I -cG250, preclinical research on cG250 quickly shifted to other beta emitters ^{90}Y , ^{177}Lu , and ^{186}Re (Brouwers et al. 2004). ^{90}Y and ^{177}Lu are residualizing radionuclides and will remain inside the cell if internalized. Biodistribution and RIT studies were performed in mice bearing SK-RC-52 human ccRCC xenografts. $^{88}\text{Y}/^{125}\text{I}$ and $^{90}\text{Y}/^{131}\text{I}$ isotopes were used for

biodistribution and RIT studies, respectively. Depending on the chelator used, the cG250 conjugates radiolabeled with ^{88}Y and ^{177}Lu had approximately 8–10 times higher tumor accumulation than those labeled with ^{125}I or ^{186}Re . Tumor uptake for ^{177}Lu -SCN-Bz-DTPA-cG250, ^{177}Lu -DOTA-cG250, ^{88}Y -SCN-Bz-DTPA-cG250, ^{88}Y -DOTA-cG250, ^{125}I -cG250, and ^{186}Re -MAG₃-cG250 (MAG₃: mercaptoacetyl-triglycine) were 87.3 ± 14.0 , 74.5 ± 10.5 , 70.9 ± 8.4 , 55.3 ± 10.7 , 9.1 ± 2.0 , and $7.9 \pm 2.0\%$ ID/g, respectively. At their respective MTDs, the calculated absorbed tumor dose for ^{177}Lu -SCN-Bz-DTPA-cG250 was 807 Gy, while other radioimmunoconjugates delivered between 76 and 104 Gy. ^{177}Lu -SCN-Bz-DTPA-cG250 delayed tumor growth by 186.4 ± 34.7 d compared to 26.6 ± 10.2 d for ^{131}I -cG250. The respective median survivals for the two groups were 294 d and 164 d, respectively.

^{177}Lu -DOTA-cG250 (^{177}Lu -cG250) was subsequently evaluated in a phase I trial by Stillebroer et al. (Fig. 12.3) (Stillebroer et al. 2013). DOTA was selected as it formed a more stable ^{177}Lu -chelator complex than DTPA according to the preclinical study. Twenty-three patients with progressive metastatic RCC were recruited for the study and divided into groups of three or more. The first dose level was 1110 MBq/m²,

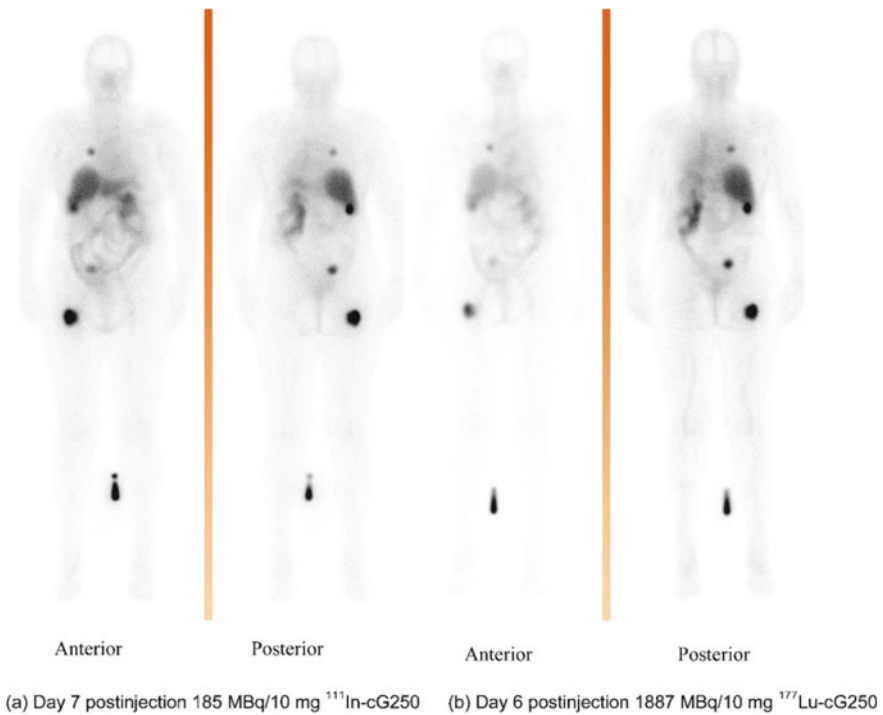


Fig. 12.3 Visualization of ccRCC metastases in lung, abdomen, and pelvis in a patient by immunoscintigraphy. **a** ^{111}In -DOTA-cG250 immunoscintigram of a patient with metastatic ccRCC acquired 7 d after injection of 185 MBq. **b** ^{177}Lu -cG250 immunoscintigram of the same patient acquired 6 d after injection of 1887 MBq. Figure adapted with permissions from Stillebroer et al. (2013)

and successive groups received increased dose increments of 370 MBq/m². MTD based on hematological toxicity was 2405 MBq/m². Similar to previous trials, patients were retreated if no disease progression was observed and recovery from hematological toxicity was demonstrated. Subsequent dose(s) was given at 75% of the previous dose level. Nine patients received 2 cycles and 4 patients received 3 cycles of ¹⁷⁷Lu-cG250. Three months after the first cycle, 17 patients had stable disease, but several patients progressed after receiving a second or third cycle. One patient showed partial response lasting 9 mo after two cycles of ¹⁷⁷Lu-cG250.

The latest evaluation of ¹⁷⁷Lu-cG250 was a phase II study by Muselaers et al. (2016). Fourteen patients received an infusion of 2405 MBq/m² ¹⁷⁷Lu-cG250. Similar to the phase I study, patients received additional cycles of RIT at 75% of the previous dose if they have no progressive disease and show recovery from toxicity. Only 6 patients received two cycles of RIT and none received a third cycle due to prolonged thrombocytopenia and/or neutropenia. After the first cycle, 8 patients had stable disease and 1 had partial response. Although ¹⁷⁷Lu-cG250 was able to stabilize disease progression, further reduction of treatment-associated toxicity is needed before it can be integrated into clinical practice.

12.5.3 Dual Modality Imaging with cG250

Muselaers et al. reported the synthesis and evaluation of ¹¹¹In-DTPA-cG250-IRDye800CW, a cG250 derivative that can be used for dual SPECT and near infrared fluorescence (NIRF) imaging (Muselaers et al. 2015). The radioactivity allows for preoperative localization of disease by SPECT imaging and for intraoperative detection of residual disease after resection by hand-held gamma probes. NIRF imaging helps surgeons to delineate surgical margins, supplementing the auditory cues from gamma detection. ¹¹¹In-DTPA-cG250-IRDye800CW was intravenously injected into nude mice bearing intraperitoneal SK-RC-52 ccRCC xenografts. Image acquisition was performed 48 h after tracer administration. Peak uptake in tumor, 58.5 ± 18.7%ID/g, was observed in those established 1 wk post-administration. The good concordance between SPECT and fluorescence images supports the utility of this dual-modality agent.

In a phase I study, Hekman et al. evaluated the safety and feasibility of ¹¹¹In-DOTA-G250-IRDye800CW for intraoperative dual-modality imaging (Fig. 12.4) (Hekman et al. 2018b). This cG250 derivative differs from the one studied by Muselaers et al. as it employs DOTA as the chelator instead of DTPA. Fifteen patients were included in this study, and different dose levels (5, 10, 30, or 50 mg, $n \geq 3$) of ¹¹¹In-DOTA-G250-IRDye800CW were administered intravenously. SPECT/CT imaging was performed 4 days p.i., and surgery was performed 6–7 d p.i. with the assistance of a gamma probe and a NIRF camera. No severe study-related adverse events were observed indicating safety of this agent. All cases of ccRCC were visible on SPECT/CT and localizable by gamma probe (T:K ratio of 2.5 ± 0.8). In contrast,

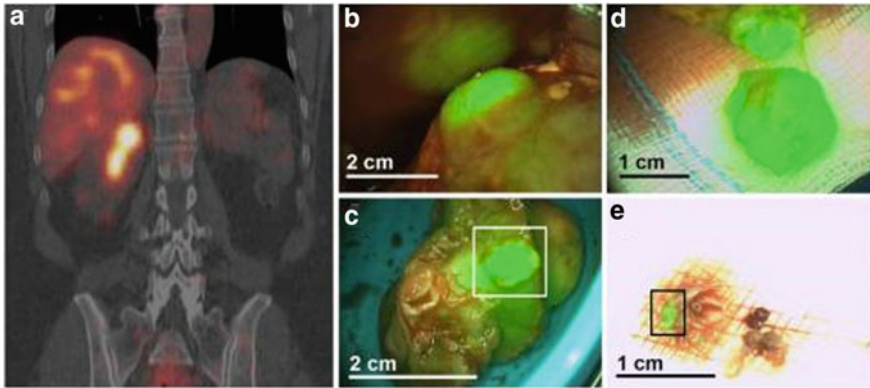


Fig. 12.4 Dual modality imaging after injection of ^{111}In -DOTA-cG250-IRDye800CW. **a** Preoperative SPECT/CT confirming presence of a CA-IX expressing ccRCC. **b** Intraoperative NIRF showed hyperfluorescence of tumor. **c** Assessment of the resected tumor specimen with NIRF suggested tumor within the surgical margin (square), which was subsequently confirmed by histopathology. **d** NIRF demonstrated that further resection contained vital tumor, again confirmed by histopathology. **e** NIRF was used to assess presence of tumor (square) in additional resected tissues. Histology confirmed that the fragment consisted mostly of fibrotic tissue, but also a 2 mm tumor. Scale bars are approximations. Figure adapted with permissions from Hekman et al. (2018b) in accordance with the Creative Commons Attribution (CC BY-NC 4.0) license

the T:K ratio for CA-IX non-expressing tumors was 1.0 ± 0.1 . NIRF greatly aided in tumor delineation and assessing residual disease in surgical cavity.

12.6 Peptides and Affibodies

Peptides are commonly used in nuclear medicine as delivery vectors to target receptors overexpressed in various cancer subtypes (Fani and Maecke 2012). Peptides can bind rapidly to tumor and clear from non-target tissues. The pharmacokinetics, stability, and targeting of peptides can be optimized by using different combinations of radionuclides, linkers, amino acids, and structural configurations. Phage display peptide libraries were used to identify CA-IX binders. Askoxylakis et al. identified a dodecapeptide, YNTNHVPLSPKY (CaIX-P1), that binds to the extracellular domain of CA-IX (Askoxylakis et al. 2010). The *N*-terminal tyrosine was used for $^{125}\text{I}/^{131}\text{I}$ radiolabeling. ^{131}I -CaIX-P1 was evaluated in ccRCC SK-RC-52 xenograft mice. From biodistribution study, tumor uptake at 1 h p.i. was $\sim 2.5\% \text{ID/g}$ and decreasing thereafter. The highest contrast for ^{131}I -CaIX-P1 was at 1 h p.i., when T:B and T:M ratios were 0.65 ± 0.24 and 4.11 ± 2.44 , respectively. The peptide was unstable in plasma, and had a half-life of 25 min.

To optimize stability and targeting properties of CaIX-P1, Rana et al. performed alanine panning and peptide truncation studies (Rana et al. 2012). They identified

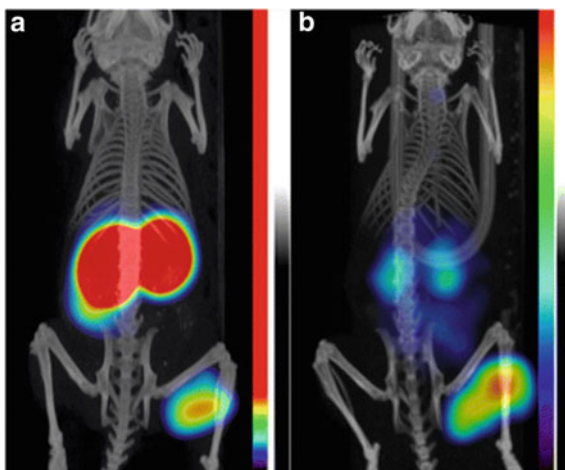
NHVPLSPy (CaIX-P1-4-10) as the minimal sequence necessary for CA-IX binding. A D-tyrosine residue was added at the C-terminus for radiolabeling purposes. In vitro, CaIX-P1-4-10 showed serum stability of 90 min, and 5.8 times higher uptake in cells compared to CaIX-P1. However, this peptide was unable to delineate SK-RC-52 xenografts from background tissues despite showing good uptake ($\sim 2.5\%$ ID/g at 1 h p.i.). The IC_{50} value for CaIX-P1-4-10 against CA-IX was later determined to be in the micromolar range. Recently, Jia et al. synthesized an ^{18}F -fluorine derivative of CaIX-P1 and evaluated its uptake properties in the hypoxia HT-29 tumor model (Jia et al. 2019). An ^{18}F -labeled azide prosthetic group was used for click chemistry with the terminal alkyne group for radiolabeling (^{18}F -CA-IX-P1-4-10). PET imaging studies were conducted, but minimal uptake was observed in tumor.

The Heidelberg group which isolated CaIX-P1 performed a secondary phage display to isolate another dodecapeptide NMPKDVTTTRMSS (PGLR-P1) (Rana et al. 2013). To improve isoform selectivity, the PG-like domain of CA-IX was used as the bait in this set up. Once again, a D-tyrosine residue was added to the C-terminus for radiolabeling with $^{125}\text{I}/^{131}\text{I}$. In vitro studies indicated that binding affinity for CA-IX was in the micromolar range. SK-RC-52 tumor xenografts showed low uptake ($0.48 \pm 0.20\%$ ID/g at 1 h p.i.), and no contrast was observed. While these short peptides have limited application for CA-IX targeting, another class of peptide-based probes (affibodies) have been far more successful.

Affibodies are protein scaffolds developed from the immunoglobulin G binding domain of staphylococcal protein A (Feldwisch and Tolmachev 2012). An affibody molecule is $\sim 6\text{--}7$ kDa in molecular weight depending on the composition. Each affibody contains 58 amino acids, of which 13 are responsible for mediating nano or picomolar binding to a target of interest. Affibodies are less sensitive to temperature and pH and have faster pharmacokinetics than mAbs. Honarvar et al. used an affibody library to identify a CA-IX targeting affibody (ZCAIX:1) for imaging ccRCC (Honarvar et al. 2015). ZCAIX:1 was radiolabeled with $^{99\text{m}}\text{Tc}$ and ^{125}I for comparison. SPECT imaging and biodistribution studies were performed in mice bearing SK-RC-52 xenografts. The binding affinity of $^{99\text{m}}\text{Tc}$ -(HE) $_3$ -ZCAIX:1 for SK-RC-52 cells was determined to be 1.3 nM. Following intravenous injection, $^{99\text{m}}\text{Tc}$ -(HE) $_3$ -ZCAIX:1 showed high and rapid uptake in tumor ($22.3 \pm 3.2\%$ ID/g at 1 h p.i.). The uptake in tumor dropped to $9.7 \pm 0.7\%$ ID/g and $7.3 \pm 3.0\%$ ID/g at 4 h and 8 h p.i., respectively. The highest T:B and T:M ratios were 53 ± 10 and 104 ± 52 observed at 4 h p.i. Kidney uptake was $>100\%$ ID/g at all timepoints. With a non-residualizing radionuclide, renal uptake of ^{125}I -(HE) $_3$ -ZCAIX:1 was significantly lower ($2.7 \pm 1.4\%$ ID/g at 6 h p.i.); however, this was accompanied by a decrease in tumor uptake ($2.2 \pm 1.4\%$ ID/g at 6 h p.i.). The data suggests that $^{99\text{m}}\text{Tc}$ -(HE) $_3$ -ZCAIX:1 has the potential for imaging extrarenal lesions that express CA-IX.

Garousi et al. performed a comparison study with ZCAIX:1 and three novel affibody variants (ZCAIX:2, ZCAIX:3, and ZCAIX:4) for CA-IX imaging (Fig. 12.5) (Garousi et al. 2016). The new variants showed nanomolar binding affinity (K_D : 1.2–7.3 nM) for SK-RC-52 cells. The affibodies were radiolabeled with $^{99\text{m}}\text{Tc}$ and ^{125}I . The uptake in SK-RC-52 tumors ranged from $4.3 \pm 0.7\%$ ID/g to $16.3 \pm 0.9\%$ ID/g at 4 h p.i. for the $^{99\text{m}}\text{Tc}$ -labeled derivatives. At this time point, $^{99\text{m}}\text{Tc}$ -(HE) $_3$ -ZCAIX:2

Fig. 12.5 Maximum intensity projections of microSPECT/CT using CA-IX targeting affibodies at 4 h p.i. **a** Imaging using $^{99m}\text{Tc}-(\text{HE})_3\text{-ZCAIX:2}$. The linear color scale was adjusted to provide clear visualization of a tumor. **b** Imaging using $^{125}\text{I}-(\text{HE})_3\text{-ZCAIX:4}$. Full linear color scale was applied. Figure adapted with permission from Garousi et al. (2016). Copyright 2016 American Chemistry Society



showed the highest contrast ratios (T:B of 44 ± 7 and T:M of 109 ± 11). Consistent with previous study, high renal retention ($>100\% \text{ID/g}$) was observed for all time points. On the other hand, the ^{125}I -labeled derivatives showed 5–50 times less uptake ($4\text{--}22\% \text{ID/g}$ at 4 h p.i.) in kidneys. ^{125}I -ZCAIX:2 had the highest tumor uptake ($19 \pm 2\% \text{ID/g}$) at 4 h p.i., which corresponded to T:B and T:M ratios of 21 ± 5 and 129 ± 42 , respectively. The authors concluded that the pairing of a non-residualizing radionuclide with an affibody may be useful for imaging primary ccRCC.

12.7 Small Molecule Inhibitors

Small molecule inhibitors are the most diverse group of antigen recognition molecules for CA-IX targeting. Most small molecule inhibitors that have been explored for imaging/therapy are sulfonamide derivatives. Sulfonamides inhibit CA-IX by forming coordination with the zinc ion and displacing water in the catalytic domain (Supuran et al. 2001). The major challenge for developing small molecule-based theranostic agents for CA-IX is selectivity since the catalytic domain is relatively conserved between isoforms (Alterio et al. 2012). There are three extracellular CA isoenzymes: CA-IX, CA-XII, and CA-XIV. To confer CA-IX selectivity, successful radiopharmaceuticals generally have features that render them cell impermeable (Alterio et al. 2012). Even when selectivity is achieved, some tracers have been hampered by low uptake or instability (Lau et al. 2014).

12.7.1 Net Charge

^{18}F -VM4-037 is an ethoxzolamide derivative developed for CA-IX PET imaging and remains the only small molecule inhibitor to advance to clinical studies (Doss et al. 2014). ^{18}F -VM4-037 has a free carboxylate group that is deprotonated at physiological pH. When this occurs, the negative charge restricts entry of the molecule into the cell conferring selectivity for CA-IX. Doss et al. reported the biodistribution and dosimetry of ^{18}F -VM4-037 in healthy volunteers in a phase I study (Doss et al. 2014). From PET images, ^{18}F -VM4-037 was immediately taken up by the liver and kidneys with minimal clearance (4% through kidneys) during the 133 min study period. Almost 50% of the dose were sequestered by these two organs. Based on a 370 MBq dose, the predicted effective dose for a patient was 10 ± 0.5 mSv. The kidneys would receive 101 ± 11 mGy, while the liver would receive 89 ± 25 mGy.

Turkbey et al. evaluated ^{18}F -VM4-037 in a phase II study with 11 RCC patients (Turkbey et al. 2016). Ten patients had histology-confirmed ccRCC, and 2 patients had metastatic lesions. Primary lesion detection of ^{18}F -VM4-037 (tumor SUV_{mean} : 3.04) was obscured by high uptake in normal renal parenchyma (kidney SUV_{mean} : 35.4). While primary lesions were difficult to ascertain without CT, extrarenal lesions in patients with metastasis were readily identified (SUV_{max} : 5.92). Since preclinical data for ^{18}F -VM4-037 was previously unpublished, Peeters et al. synthesized ^{18}F -VM4-037 and evaluated its ability to image CA-IX expression in the U373 human glioma and HT-29 human colorectal xenograft models (Peeters et al. 2015). Consistent with the clinical studies, ^{18}F -VM4-037 showed high accumulation in the liver and kidneys. However, no uptake was observed in either tumor model raising questions about the sensitivity of ^{18}F -VM4-037 for targeting CA-IX in vivo. In this study, the K_i of ^{18}F -VM4-037 for CA-IX was found to be $0.12 \mu\text{M}$.

Our research group reported the synthesis and evaluation of an ^{18}F -labeled cationic sulfonamide derivative (Zhang et al. 2017). The cationic quaternary ammonium group maintains a net positive charge, conferring selectivity for CA-IX. Biodistribution and PET imaging studies were performed in HT-29 tumor xenograft mice. Tumor uptake was $0.41 \pm 0.06\% \text{ID/g}$ at 1 h p.i., and corresponded to T:B and T:M ratios of <2 . HT-29 tumors were visible in PET images despite the low absolute uptake. Although contrast was less than that of the other sulfonamides, results were encouraging considering the modest affinity for CA-IX. The compound had a K_i value of $0.22 \mu\text{M}$ for CA-IX.

12.7.2 Multivalence and Size

In addition to incorporating net charge, our group successfully leveraged a multivalent approach to confer in vivo selectivity for CA-IX (Lau et al. 2015). We hypothesized that a trimeric sulfonamide inhibitor would have sufficient bulk (>1 kDa)

to restrict intracellular entry. To achieve this, we first prepared azide derivatives of two CA inhibitors, 4-(2-aminoethyl)benzenesulfonamide (AEBS) and 4-aminobenzenesulfonamide (ABS). These inhibitors were subsequently conjugated to a radio-prosthetic group containing three alkyne groups and an ammoniomethyltrifluoroborate (AmBF_3) moiety to form $^{18}\text{F}\text{-AmBF}_3\text{-(AEBS)}_3$ and $^{18}\text{F}\text{-AmBF}_3\text{-(ABS)}_3$. Biodistribution and PET imaging studies were performed in HT-29 tumor-bearing mice. For the two compounds, tumor uptake was $0.30\text{--}0.33\%\text{ID/g}$ at 1 h p.i., which was 5 times higher than the activity in blood ($0.07\text{--}0.09\%\text{ID/g}$). CA-I and CA-II are off-target isoenzymes that are expressed in the cytosol of red blood cells. Tumors were clearly visible in PET images, and the T:B (3.93 ± 1.26) and T:M (9.55 ± 2.96) ratios were the highest reported small molecule-based imaging of CA-IX at the time of publication. $^{18}\text{F}\text{-AmBF}_3\text{-(AEBS)}_3$ and $^{18}\text{F}\text{-AmBF}_3\text{-(ABS)}_3$ had K_i values of 35.7 nM and 8.5 nM, respectively.

12.7.3 Radiometal Chelator Complex

Rami et al. demonstrated that sulfonamides conjugated to polyaminocarboxylate chelators (e.g., DTPA and DOTA) are unable to penetrate red blood cells (Rami et al. 2008). This observation spurred our group to synthesize three ^{68}Ga -labeled sulfonamide derivatives with different chelators (Fig. 12.6) (Lau et al. 2016). Monomeric (Ga-DOTA-AEBSA), dimeric (Ga-DOTA-(AEBSA)_2), and trimeric ($\text{Ga-NOTGA-(AEBSA)}_3$; NOTGA: 1,4,7-triazacyclononane-1,4,7-tris-(glutaric acid)) derivatives were prepared. Biodistribution and PET imaging studies were performed in HT-29 tumor xenograft mice. Tumor uptake ranged from 0.81 to 2.30%ID/g at 1 h p.i. and positively correlated to the number of targeting moieties and molecular weight. The monomer cleared predominantly through the kidneys, while the dimer and trimer were cleared by the renal and hepatobiliary pathways. $^{68}\text{Ga-DOTA-AEBSA}$ exhibited the lowest tumor uptake but had the highest contrast (T:M ratio: 5.02 ± 0.22) due its favorable pharmacokinetics. Good-contrast PET images were generated by all three derivatives. $^{68}\text{Ga-DOTA-AEBSA}$ showed heterogeneous distribution in tumors and areas of focal uptake. The K_i values of the three compounds ranged from 7.7 nM to 25.4 nM.

Following a similar strategy, Sneddon et al. synthesized a monomeric $^{68}\text{Ga-DOTA-sulfonamide}$ derivative (Sneddon et al. 2016). Instead of directly conjugating the sulfonamide group to one of the carboxylic groups in DOTA, the authors inserted a polyethylene glycol linker as a pharmacokinetic modifier. In vivo evaluations were conducted in mice bearing HCT116 human colorectal cancer xenografts. Tumors were visible in PET images at 1 h p.i.; however, the uptake was not retained and there was washout of signal by 2 h p.i. Absolute uptake values were not reported, but the T:B ratio was reportedly 2.36 ± 0.42 at 1 h p.i. Compared to $^{68}\text{Ga-DOTA-AEBSA}$, the K_i value of this monomeric compound was higher at 63.1 nM.

Krall et al. reported the synthesis and evaluation of a $^{99\text{m}}\text{Tc}$ -labeled acetazolamide derivative (Krall et al. 2016). The tracer contained an acetazolamide derivative, a

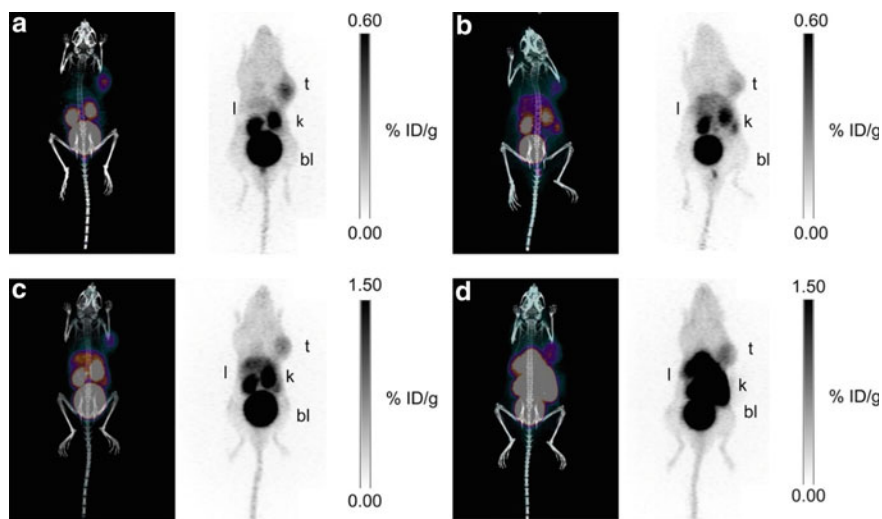


Fig. 12.6 Maximal intensity projection images of PET/CT and PET with ^{68}Ga tracers at 1 h p.i. **a** ^{68}Ga -DOTA-AEBSA; **b** ^{68}Ga -DOTA-AEBSA preblocked with 10 mg/kg of acetazolamide; **c** ^{68}Ga -DOTA-(AEBSA)₂; **d** ^{68}Ga -NOTGA-(AEBSA)₃. Tumor uptake was observed for all three compounds with ^{68}Ga -DOTA-AEBSA displaying highest contrast. *t* = tumor; *l* = liver; *k* = kidney; *bl* = bladder. Figure adapted with permissions from Lau et al. (2016). Copyright 2016 American Chemistry Society

triazine-based linker, and a Lys-Asp-Cys motif for $^{99\text{m}}\text{Tc}$ -labeling. In vivo evaluations were performed in the SK-RC-52 ccRCC model that overexpresses CA-IX. Based on biodistribution studies, tumor uptake peaked at 3 h p.i. at $22.1 \pm 0.16\% \text{ID/g}$ with a T:B ratio of 69.9 ± 0.21 . Unlike other small molecules that washout from tumor, uptake was well retained by 6 h p.i. ($19.8 \pm 0.13\% \text{ID/g}$; T:B ratio of 100 ± 0.94). SPECT images showed clear delineation of tumors from background tissues. While not directly measured, it was assumed that the compound had nanomolar binding affinity to CA-IX since acetazolamide was used as the targeting pharmacophore.

Wichert et al. identified a novel dual motif CA-IX inhibitor from a DNA encoded chemical library (Wichert et al. 2015). This inhibitor consists of an acetazolamide and a 4,4-bis(4-hydroxyphenyl)valeric acid; the binding site of the latter remains unknown. The Pomper group radiolabeled this inhibitor by adding either an ^{111}In -DOTA or ^{64}Cu -NOTA (NOTA: 1,4,7-triazacyclononane-1,4,7-triacetic acid) complex for ccRCC imaging (Yang et al. 2015; Minn et al. 2016). Biodistribution and imaging studies were performed in mice bearing SK-RC-52 xenografts. For ^{111}In -XYIMSR-01, maximal tumor uptake was observed at 8 h p.i. ($34.0 \pm 15.2\% \text{ID/g}$) with corresponding T:B and T:M ratios of 77.0 ± 32.5 and 34.2 ± 16.0 . Tumor uptake of ^{111}In -XYIMSR-01 decreased slightly to $25.6 \pm 17.7\% \text{ID/g}$ at 24 p.i., while T:B and T:M ratios improved to 178.1 ± 145.4 and 68.4 ± 29.0 . For ^{64}Cu -XYIMSR-06, maximal tumor uptake was observed at 4 h p.i. ($19.3 \pm 4.51\% \text{ID/g}$) with corresponding T:B and T:M ratios of 57.7 ± 9.3 , and 29.4 ± 9.9 . Similarly, tumor uptake

decreased to $6.23 \pm 1.41\%ID/g$ by 24 h p.i., but T:B and T:M ratios improved to 142.6 ± 115.8 and 261.3 ± 47.3 . Based on imaging modality and faster pharmacokinetics, ^{64}Cu -XYIMSR-06 is likely more favorable for translation despite the lower absolute tumor uptake.

More recently, Yang et al. synthesized ^{64}Cu -XYIMSR-06 and evaluated its ability to image the orthotopic U87 MG glioblastoma model (Fig. 12.7) (Yang et al. 2019). Due to lower expression of CA-IX in this hypoxia model, maximal tumor uptake was $3.13 \pm 0.26\%ID/g$ with T:B and T:M ratios of 7.67 ± 1.08 and 3.01 ± 0.68 . The tumor-to-brain ratio was 4.46 ± 0.86 . From PET images, orthotopic xenografts were readily visualized at 2 h and 8 h p.i. While initial results look promising, the ability of ^{64}Cu -XYIMSR-06 to effectively cross the blood–brain-barrier (BBB) needs to be further assessed. The BBB is generally disrupted during the establishment of glioma models. The binding affinity of ^{64}Cu -XYIMSR-06 for the U87 MG cell line was determined to be 4.22 nM.

Iikuni et al. developed three ureidosulfonamide-based inhibitors for SPECT imaging and radioligand therapy (Iikuni et al. 2018). Ureidosulfonamides have better binding affinity for CAs compared to unsubstituted sulfonamides. The authors synthesized a monovalent inhibitor conjugated to a DOTA chelator for ^{111}In -labeling (^{111}In -US1), and a bivalent inhibitor conjugated to DOTA for $^{111}In/^{90}Y$ -labeling ($^{111}In/^{90}Y$ -US2). Biodistribution studies were performed in mice bearing both HT-29 colorectal cancer (high CA-IX expression) and MDA-MB-231 (low CA-IX expression) breast cancer xenografts. ^{111}In -US2 showed higher uptake in both models compared to ^{111}In -US1. HT-29 tumor uptake of ^{111}In -US2 peaked at 1 h p.i. at $4.57 \pm 0.21\%ID/g$ (T:B and T:M ratios of 1.11 ± 0.16 and 2.86 ± 0.43) and decreased gradually over the course of the study. The uptake in MDA-MB-231 tumor was lower than HT-29 tumor at all time points. Radioligand therapy with ^{90}Y -US2 (1.85, 3.7 and 7.4 MBq) was performed in mice bearing only HT-29 tumors. The administration of ^{90}Y -US2 led to inhibition of HT-29 tumor growth, in a dose-dependent manner. This is one of the first endoradiotherapy studies targeting CA-IX using a small molecule inhibitor.

12.8 Perspectives and Conclusion

CA-IX represents as a theranostic target for all solid tumors, especially for ccRCCs where CA-IX expression is mainly driven by genetic aberrations in lieu of oxygen availability. According to the 2018 GLOBOCAN report, there were over 400,000 new incidences of ccRCC worldwide with over 175,000 associated mortalities (Bray et al. 2018). cG250 and its derivatives are promising for targeting ccRCCs because they clear through the hepatobiliary system. This reduces background when attempting to image primary or recurrent lesions. A multi-center phase III study to investigate the sensitivity and specificity of ^{89}Zr -cG250 for ccRCC has begun recruitment (ClinicalTrials.gov Identifier: NCT03849118). It is anticipated that this compound will displace ^{124}I -cG250 as the imaging agent of choice. In terms of RIT with cG250,

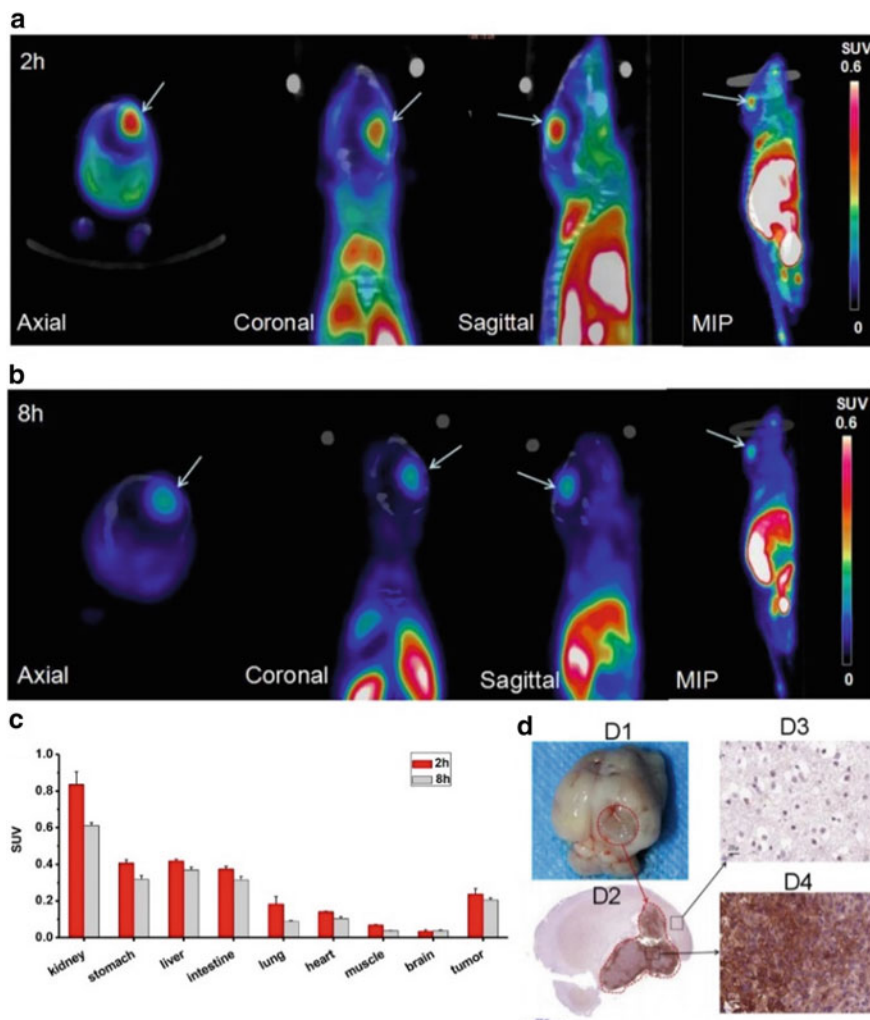


Fig. 12.7 PET images of orthotopic U87 MG xenografts after injection of ^{64}Cu -XYIMSR-06. **a**, **b** Detection of the intracranial tumor at 2 and 8 h after injection. Arrows indicate the tumor. **c** SUV values for selected organs based on drawn ROIs. **d** Orthotopic glioma and immunohistochemistry. (**D1**) Tumor in the right cerebral hemisphere in red circle. (**D2**) CA-IX immunohistochemical staining. (**D3**) CA-IX expression is absent in normal brain tissue. (**D4**) CA-IX expression tumor tissue (40 \times magnification of original micrographs). Figure adapted with permissions from Yang et al. (2019). Copyright 2016 American Chemistry Society

myelotoxicity must be safely mitigated or controlled. Since ^{177}Lu has imageable photons, personalized dosing based on imaging dosimetric analyses is one way to reduce toxicity. Merckx et al. recently disclosed the development of ^{225}Ac -cG250 at a conference proceeding (Merckx et al. 2019). ^{225}Ac is an alpha particle emitter and is able to induce more dsDNA breakages in cancer cells than ^{177}Lu , which is a beta particle emitter (Kozempel et al. 2018). At the same time, the particle range of ^{225}Ac is limited which helps to reduce off-target toxicity.

While the other classes of CA-IX radiopharmaceuticals can also be used for ccRCC, they are more ideal for targeting hypoxic niches. The barriers for small molecule inhibitors have been low uptake and subsequent retention in tumors. However, recent work by Krall et al. and Yang et al. demonstrate that these challenges can be met by structure–activity relationship optimization. As more potent and selective inhibitors are discovered (Dudutiene et al. 2014), we anticipate that there will be continued interest in advancing small molecule-based agents for CA-IX. Hypoxic tumors are difficult to treat with monotherapy; therefore, combinatorial treatments are necessary especially for disseminated disease. Small molecule inhibitors can be used to target CA-IX in combination with other agents like tyrosine kinase inhibitors (Oosterwijk-Wakka et al. 2011) or immune checkpoint inhibitors (Chafe et al. 2019). Radiotherapeutic agents derived from small molecules are likely to be less toxic because they have faster clearance and are non-immunogenic, compared to RIT. In summary, given the multifaceted role CA-IX has in cancer biology, CA-IX theranostic agents have the potential to ameliorate cancer management and patient outcomes.

References

- Ahlskog JKJ, Schliemann C, Mårilind J, Qureshi U, Ammar A, Pedley RB, Neri D (2009) Human monoclonal antibodies targeting carbonic anhydrase IX for the molecular imaging of hypoxic regions in solid tumours. *Br J Cancer* 101:645–657
- Alterio V, Di Fiore A, D’Ambrosio K, Supuran CT, De Simone G (2012) Multiple binding modes of inhibitors to carbonic anhydrases: how to design specific drugs targeting 15 different isoforms? *Chem Rev* 112:4421–4468
- Askoxylakis V, Garcia-Boy R, Rana S, Krämer S, Hebling U, Mier W, Altmann A, Markert A, Debus J, Haberkorn U (2010) A new peptide ligand for targeting human carbonic anhydrase IX, identified through the phage display technology. *PLoS One* 5:e15962
- Bennewith KL, Dedhar S (2011) Targeting hypoxic tumour cells to overcome metastasis. *BMC Cancer* 11:504
- Bray F, Ferlay J, Soerjomataram I, Siegel RL, Torre LA, Jemal A (2018) Global cancer statistics 2018: GLOBOCAN estimates of incidence and mortality worldwide for 36 cancers in 185 countries. *CA Cancer J Clin* 68:394–424
- Brouwers AH, Buijs WCAM, Oosterwijk E, Boerman OC, Mala C, De Mulder PHM, Corstens FHM, Mulders PFA, Oyen WJG (2003) Targeting of metastatic renal cell carcinoma with the chimeric monoclonal antibody G250 labeled with ^{131}I or ^{111}In : an inpatient comparison. *Clin Cancer Res* 9:3953S–3960

- Brouwers AH, van Eerd JEM, Frielink C, Oosterwijk E, Oyen WJG, Corstens FHM, Boerman OC (2004) Optimization of radioimmunotherapy of renal cell carcinoma: labeling of monoclonal antibody cG250 with ^{131}I , ^{90}Y , ^{177}Lu , or ^{186}Re . *J Nucl Med* 45:327–337
- Brouwers AH, Mulders PFA, De Mulder PHM, Van Den Broek WJM, Buijs WCAM, Mala C, Joosten FBM, Oosterwijk E, Boerman OC, Corstens FHM, Oyen WJG (2005) Lack of efficacy of two consecutive treatments of radioimmunotherapy with ^{131}I -cG250 in patients with metastasized clear cell renal cell carcinoma. *J Clin Oncol* 23:6540–6548
- Carlin S, Khan N, Ku T, Longo VA, Larson SM, Smith-Jones PM (2010) Molecular targeting of carbonic anhydrase ix in mice with hypoxic HT29 colorectal tumor xenografts. *PLoS One* 5:e10857
- Čepa A, Ráliš J, Král V, Paurová M, Kučka J, Humajová J, Lázníček M, Lebeda O (2018) In vitro evaluation of the monoclonal antibody ^{64}Cu -IgG M75 against human carbonic anhydrase IX and its in vivo imaging. *Appl Radiat Isot* 133:9–13
- Chafe SC, McDonald PC, Saberi S, Nemirovsky O, Venkateswaran G, Burugu S, Gao D, Delaidelli A, Kyle AH, Baker JHE, Gillespie JA, Bashashati A, Minchinton AI, Zhou Y, Shah SP, Dedhar S (2019) Targeting hypoxia-induced carbonic anhydrase IX enhances immune checkpoint blockade locally and systemically. *Cancer Immunol Res* canimm.0657.2018
- Chamie K, Donin NM, Klöpfer P, Bevan P, Fall B, Wilhelm O, Störkel S, Said J, Gambla M, Hawkins RE, Jankilevich G, Kapoor A, Kopyltsov E, Staehler M, Taari K, Wainstein AJA, Pantuck AJ, Belldegrun AS (2017) Adjuvant weekly girentuximab following nephrectomy for high-risk renal cell carcinoma: the ARISER randomized clinical trial. *JAMA Oncol* 3:913–920
- Chiavenna SM, Jaworski JP, Vendrell A (2017) State of the art in anti-cancer mAbs. *J Biomed Sci* 24:15
- Chrastina A, Závada J, Parkkila S, Kaluz Š, Kaluzová M, Rajčáni J, Pastorek J, Pastoreková S (2003) Biodistribution and pharmacokinetics of ^{125}I -labeled monoclonal antibody M75 specific for carbonic anhydrase IX, an intrinsic marker of hypoxia, in nude mice xenografted with human colorectal carcinoma. *Int J Cancer* 105:873–881
- Clark PE (2009) The role of VHL in clear-cell renal cell carcinoma and its relation to targeted therapy. *Kidney Int* 76:939–945
- Divgi CR, Bander NH, Scott AM, O'Donoghue JA, Sgouros G, Welt S, Finn RD, Morrissey F, Capitelli P, Williams JM, Deland D, Nakhre A, Oosterwijk E, Gulec S, Graham MC, Larson SM, Old LJ (1998) Phase I/II radioimmunotherapy trial with iodine- ^{131}I -labeled monoclonal antibody G250 in metastatic renal cell carcinoma. *Clin Cancer Res* 4:2729–2739
- Divgi CR, O'Donoghue JA, Welt S, O'Neel J, Finn R, Motzer RJ, Jungbluth A, Hoffman E, Ritter G, Larson SM, Old LJ (2004) Phase I clinical trial with fractionated radioimmunotherapy using ^{131}I -labeled chimeric G250 in metastatic renal cancer. *J Nucl Med* 45:1412–1421
- Divgi CR, Pandit-Taskar N, Jungbluth AA, Reuter VE, Gönen M, Ruan S, Pierre C, Nagel A, Pryma DA, Humm J, Larson SM, Old LJ, Russo P (2007) Preoperative characterisation of clear-cell renal carcinoma using iodine- ^{124}I -labelled antibody chimeric G250 (^{124}I -cG250) and PET in patients with renal masses: a phase I trial. *Lancet Oncol* 8:304–310
- Divgi CR, Uzzo RG, Gatsonis C, Bartz R, Treutner S, Yu JQ, Chen D, Carrasquillo JA, Larson S, Bevan P, Russo P (2013) Positron emission tomography/computed tomography identification of clear cell renal cell carcinoma: results from the REDECT trial. *J Clin Oncol* 31:187–194
- Doss M, Kolb HC, Walsh JC, Mocharla VP, Zhu Z, Haka M, Alpaugh RK, Chen DYT, Yu JQ (2014) Biodistribution and radiation dosimetry of the carbonic anhydrase IX imaging agent ^{18}F VM4-037 determined from PET/CT scans in healthy volunteers. *Mol Imaging Biol* 16:739–746
- Dudutiene V, Matuliene J, Smirnov A, Timm DD, Zubriene A, Baranauskiene L, Morkunaite V, Smirnoviene J, Michailoviene V, Juozapaitiene V, Mickevičiute A, Kazokaite J, Bakšyte S, Kasiliauskaite A, Jachno J, Revuckiene J, Kišonaite M, Pilipuityte V, Ivanauskaite E, Mili- navičiute G, Smirnovas V, Petrikaite V, Kairys V, Petrauskas V, Norvaišas P, Linge D, Gibieža P, Čapkauskaite E, Zakšauskas A, Kazlauskas E, Manakova E, Gražulis S, Ladbury JE, Matulis D (2014) Discovery and characterization of novel selective inhibitors of carbonic anhydrase IX. *J Med Chem* 57:9435–9446

- Escudier B, Porta C, Schmidinger M, Rioux-Leclercq N, Bex A, Khoo V, Gruenvald V, Horwich A (2016) Renal cell carcinoma: ESMO clinical practice guidelines for diagnosis, treatment and follow-up†. *Ann Oncol* 27:v58–v68
- Fani M, Maecke HR (2012) Radiopharmaceutical development of radiolabelled peptides. *Eur J Nucl Med Mol Imaging* 39:11–30
- Feldwisch J, Tolmachev V (2012) Engineering of affibody molecules for therapy and diagnostics. *Methods Mol Biol* 899:103–126
- Fleming IN, Manavaki R, Blower PJ, West C, Williams KJ, Harris AL, Domarkas J, Lord S, Baldry C, Gilbert FJ (2015) Imaging tumour hypoxia with positron emission tomography. *Br J Cancer* 112:238–250
- Freise AC, Wu AM (2015) In vivo imaging with antibodies and engineered fragments. *Mol Immunol* 67:142–152
- Garousi J, Honarvar H, Andersson KG, Mitran B, Orlova A, Buijs J, Löfblom J, Frejd FY, Tolmachev V (2016) Comparative evaluation of affibody molecules for radionuclide imaging of in vivo expression of carbonic anhydrase IX. *Mol Pharm* 13:3676–3687
- Gorin MA, Rowe SP, Allaf ME (2015) Nuclear imaging of renal tumours: a step towards improved risk stratification. *Nat Rev Urol* 12:445–450
- Harris AL (2002) Hypoxia—a key regulatory factor in tumour growth. *Nat Rev Cancer* 2:38–47
- Hekman MCH, Rijpkema M, Aarntzen EH, Mulder SF, Langenhuijsen JF, Oosterwijk E, Boerman OC, Oyen WJG, Mulders PFA (2018a) Positron emission tomography/computed tomography with 89zr-girentuximab can aid in diagnostic dilemmas of clear cell renal cell carcinoma suspicion. *Eur Urol* 74:257–260
- Hekman MC, Rijpkema M, Muselaers CH, Oosterwijk E, Hulsbergen-Van de Kaa CA, Boerman OC, Oyen WJ, Langenhuijsen JF, Mulders PF (2018b) Tumor-targeted dual-modality imaging to improve intraoperative visualization of clear cell renal cell carcinoma: a first in man study. *Theranostics* 8:2161–2170. <https://doi.org/10.7150/thno.23335>
- Hilvo M, Baranauskienė L, Salzano AM, Scaloni A, Matulis D, Innocenti A, Scozzafava A, Monti SM, Di Fiore A, De Simone G, Lindfors M, Jänis J, Valjakka J, Pastoreková S, Pastorek J, Kulomaa MS, Nordlund HR, Supuran CT, Parkkila S (2008) Biochemical characterization of CA IX, one of the most active carbonic anhydrase isozymes. *J Biol Chem* 283:27799–27809
- Hoeben BAW, Kaanders JHAM, Franssen GM, Troost EGC, Rijken PFJW, Oosterwijk E, Dongen GAMS, Oyen WJG, Boerman OC, Bussink J (2010) PET of hypoxia with 89Zr-labeled cG250-F(ab')₂ in head and neck tumors. *J Nucl Med* 51:1076–1083
- Holmquist-Mengelbier L, Fredlund E, Löfstedt T, Noguera R, Navarro S, Nilsson H, Pietras A, Vallon-Christersson J, Borg Å, Gradin K, Poellinger L, Pålman S (2006) Recruitment of HIF-1 α and HIF-2 α to common target genes is differentially regulated in neuroblastoma: HIF-2 α promotes an aggressive phenotype. *Cancer Cell* 10:413–423
- Honarvar H, Garousi J, Gunneriusson E, Höidén-Guthenberg I, Altai M, Widström C, Tolmachev V, Frejd FY (2015) Imaging of CAIX-expressing xenografts in vivo using 99mTc-HEHEHE-ZCAIX:1 Affibody molecule. *Int J Oncol* 46:513–520
- Hsieh JJ, Purdue MP, Signoretti S, Swanton C, Albiges L, Schmidinger M, Heng DY, Larkin J, Ficarra V (2017) Renal cell carcinoma. *Nat Rev Dis Prim* 3:17009
- Huizing FJ, Hoeben BAW, Franssen GM, Boerman OC, Heskamp S, Bussink J (2019) Quantitative imaging of the hypoxia-related marker CAIX in head and neck squamous cell carcinoma xenograft models. *Mol Pharm* 16:701–708
- Iikuni S, Ono M, Watanabe H, Shimizu Y, Sano K, Saji H (2018) Cancer radiotheranostics targeting carbonic anhydrase-IX with 111In- and 90Y-labeled ureidosulfonamide scaffold for SPECT imaging and radionuclide-based therapy. *Theranostics* 8:2992–3006
- Jadvar H, Chen X, Cai W, Mahmood U (2018) Radiotheranostics in cancer diagnosis and management. *Radiology* 286:388–400
- Jia L, Li X, Cheng D, Zhang L (2019) Fluorine-18 click radiosynthesis and microPET/CT evaluation of a small peptide—a potential PET probe for carbonic anhydrase IX. *Bioorg Med Chem* 27:785–789

- Kaluz S, Kaluzová M, Liao SY, Lerman M, Stanbridge EJ (2009) Transcriptional control of the tumor- and hypoxia-marker carbonic anhydrase 9: a one transcription factor (HIF-1) show? *Biochim Biophys Acta Rev Cancer* 1795:162–172
- Kozempel J, Mokhodoeva O, Vlk M (2018) Progress in targeted alpha-particle therapy. What we learned about recoils release from in vivo generators. *Molecules* 23
- Krall N, Pretto F, Mattarella M, Muller C, Neri D (2016) A ^{99m}Tc -labeled ligand of carbonic anhydrase IX selectively targets renal cell carcinoma in vivo. *J Nucl Med* 57:943–949
- Lau J, Pan J, Zhang Z, Hundal-Jabal N, Liu Z, Bénard F, Lin KS (2014) Synthesis and evaluation of 18 F-labeled tertiary benzenesulfonamides for imaging carbonic anhydrase IX expression in tumours with positron emission tomography. *Bioorganic Med Chem Lett* 24:3064–3068
- Lau J, Liu Z, Lin K-S, Pan J, Zhang Z, Vullo D, Supuran CT, Perrin DM, Bénard F (2015) Trimeric radiofluorinated sulfonamide derivatives to achieve in vivo selectivity for carbonic anhydrase IX-targeted PET imaging. *J Nucl Med* 56:1434–1440
- Lau J, Zhang Z, Jenni S, Kuo HT, Liu Z, Vullo D, Supuran CT, Lin KS, Bénard F (2016) PET imaging of carbonic anhydrase IX expression of HT-29 tumor xenograft mice with ^{68}Ga -labeled benzenesulfonamides. *Mol Pharm* 13:1137–1146
- Lau J, Lin KS, Bénard F (2017) Past, present, and future: development of theranostic agents targeting carbonic anhydrase IX. *Theranostics* 7:4322–4339
- Li Z, Bao S, Wu Q, Wang H, Eyler C, Sathornsumetee S, Shi Q, Cao Y, Lathia J, McLendon RE, Hjelmeland AB, Rich JN (2009) Hypoxia-inducible factors regulate tumorigenic capacity of glioma stem cells. *Cancer Cell* 15:501–513
- Li J, Zhang G, Wang X, Li X-F (2015) Is carbonic anhydrase IX a validated target for molecular imaging of cancer and hypoxia? *Futur Oncol* 11:1531–1541
- Lopci E, Grassi I, Chiti A, Nanni C, Cicoria G, Toschi L, Fonti C, Lodi F, Mattioli S, Fanti S (2014) PET radiopharmaceuticals for imaging of tumor hypoxia: a review of the evidence. *Am J Nucl Med Mol Imaging* 4:365–384
- Lou Y, McDonald PC, Oloumi A, Chia S, Ostlund C, Ahmadi A, Kyle A, Auf Dem Keller U, Leung S, Huntsman D, Clarke B, Sutherland BW, Waterhouse D, Bally M, Roskelley C, Overall CM, Minchinton A, Pacchiano F, Carta F, Scozzafava A, Touisni N, Winum JY, Supuran CT, Dedhar S (2011) Targeting tumor hypoxia: suppression of breast tumor growth and metastasis by novel carbonic anhydrase IX inhibitors. *Cancer Res* 71:3364–3376
- McDonald PC, Winum J-Y, Supuran CT, Dedhar S, McDonald PC, Winum J-Y, Supuran CT, Dedhar S (2012) Recent developments in targeting carbonic anhydrase IX for cancer therapeutics. *Oncotarget* 3:84–97
- Merkx R, Heskamp S, Mulders P, Rijpkema M, Oosterwijk E, Wheatcroft M, Kip A, Morgenstern A, Bruchertseifer F (2019) ^{225}Ac -labeled girentuximab for targeted alpha therapy of CAIX-expressing renal cell cancer xenografts. *J Med Imaging Radiat Sci* 50:S25
- Minn I, Koo SM, Lee HS, Brummet M, Rowe SP, Gorin MA, Sysa-Shah P, Lewis WD, Ahn H-H, Wang Y, Banerjee SR, Mease RC, Nimmagadda S, Allaf ME, Pomper MG, Yang X (2016) [^{64}Cu]XYIMSR-06: A dual-motif CAIX ligand for PET imaging of clear cell renal cell carcinoma. *Oncotarget* 7:56471–56479
- Moroz E, Carlin S, Dyomina K, Burke S, Thaler HT, Blasberg R, Serganova I (2009) Real-time imaging of HIF-1 α stabilization and degradation. *PLoS One* 4:e5077
- Morris MR, Hughes DJ, Tian YM, Ricketts CJ, Lau KW, Gentle D, Shuib S, Serrano-Fernandez P, Lubinski J, Wiesener MS, Pugh CW, Latif F, Ratcliffe PJ, Maher ER (2009) Mutation analysis of hypoxia-inducible factors HIF1A and HIF2A in renal cell carcinoma. *Anticancer Res* 29:4337–4343
- Muselaers CHJ, Boerman OC, Oosterwijk E, Langenhuijsen JF, Oyen WJG, Mulders PFA (2013) Iodine-111-labeled girentuximab immunoSPECT as a diagnostic tool in clear cell renal cell carcinoma. *Eur Urol* 63:1101–1106
- Muselaers CHJ, Rijpkema M, Bos DL, Langenhuijsen JF, Oyen WJG, Mulders PFA, Oosterwijk E, Boerman OC (2015) Radionuclide and fluorescence imaging of clear cell renal cell carcinoma using dual labeled anti-carbonic anhydrase IX antibody G250. *J Urol* 194:532–538

- Muselaers CHJ, Boers-Sonderen MJ, Van Oostenbrugge TJ, Boerman OC, Desar IME, Stillebroer AB, Mulder SF, Van Herpen CML, Langenhuijsen JF, Oosterwijk E, Oyen WJG, Mulders PFA (2016) Phase 2 study of lutetium 177-labeled anti-carbonic anhydrase IX monoclonal antibody girentuximab in patients with advanced renal cell carcinoma. *Eur Urol* 69:767–770
- Oosterwijk E, Ruiter DJ, Hoedemaeker PJ, Pauwels EKJ, Jonas U, Zwartendijk I, Warnaar SO (1986) Monoclonal antibody G 250 recognizes a determinant present in renal-cell carcinoma and absent from normal kidney. *Int J Cancer* 38:489–494
- Oosterwijk-Wakka JC, Kats-Ugurlu G, Leenders WPJ, Kiemeny LALM, Old LJ, Mulders PFA, Oosterwijk E (2011) Effect of tyrosine kinase inhibitor treatment of renal cell carcinoma on the accumulation of carbonic anhydrase IX-specific chimeric monoclonal antibody cG250. *BJU Int* 107:118–125
- Oosterwijk-Wakka JC, Boerman OC, Mulders PFA, Oosterwijk E (2013) Application of monoclonal antibody G250 recognizing carbonic anhydrase IX in renal cell carcinoma. *Int J Mol Sci* 14:11402–11423
- Oosterwijk E, Bander NH, Divgi CR, Welt S, Wakka JC, Finn RD, Carswell EA, Larson SM, Warnaar SO, Fleuren GJ, Oettgen HF, Old LJ (1993) Antibody localization in human renal cell carcinoma: a phase I study of monoclonal antibody G250. *J Clin Oncol* 11:738–750
- Parks SK, Chiche J, Pouyssegur J (2011) pH control mechanisms of tumor survival and growth. *J Cell Physiol* 226:299–308
- Pastorekova S, Ratcliffe PJ, Pastorek J (2008) Molecular mechanisms of carbonic anhydrase IX-mediated pH regulation under hypoxia. *BJU Int* 101:8–15
- Peeters SGJA, Dubois L, Lieuwes NG, Laan D, Mooijer M, Schuit RC, Vullo D, Supuran CT, Eriksson J, Windhorst AD, Lambin P (2015) [18F]VM4-037 MicroPET imaging and biodistribution of two in vivo CAIX-expressing tumor models. *Mol Imaging Biol* 17:615–619
- Rafajová M, Zatovicová M, Kettmann R, Pastorek J, Pastoreková S (2004) Induction by hypoxia combined with low glucose or low bicarbonate and high posttranslational stability upon reoxygenation contribute to carbonic anhydrase IX expression in cancer cells. *Int J Oncol* 24:995–1004
- Rajendran JG, Krohn KA (2015) F-18 fluoromisonidazole for imaging tumor hypoxia: imaging the microenvironment for personalized cancer therapy. *Semin Nucl Med* 45:151–162
- Rajendran JG, Wilson DC, Conrad EU, Peterson LM, Bruckner JD, Rasey JS, Chin LK, Hofstrand PD, Grierson JR, Eary JF, Krohn KA (2003) [18F]FMISO and [18F]FDG PET imaging in soft tissue sarcomas: Correlation of hypoxia, metabolism and VEGF expression. *Eur J Nucl Med Mol Imaging* 30:695–704
- Rami M, Cecchi A, Montero JL, Innocenti A, Vullo D, Scozzafava A, Winum JY, Supuran CT (2008) Carbonic anhydrase inhibitors: design of membrane-impermeant copper(II) complexes of DTPA-, DOTA-, and TETA-tailed sulfonamides targeting the tumor-associated transmembrane isoform IX. *ChemMedChem* 3:1780–1788
- Rana S, Nissen F, Marr A, Markert A, Altmann A, Mier W, Debus J, Haberkorn U, Askoxylakis V (2012) Optimization of a novel peptide ligand targeting human carbonic anhydrase IX. *PLoS One* 7:e38279
- Rana S, Nissen F, Lindner T, Altmann A, Mier W, Debus J, Haberkorn U (2013) Askoxylakis V (2013) Screening of a novel peptide targeting the proteoglycan-Like region of human carbonic anhydrase 9. *Mol Imaging* 12(7290):00066
- Rault E, Vandenberghe S, Van Holen R, De Beenhouwer J, Staelens S, Lemahieu I (2007) Comparison of image quality of different iodine isotopes (I-123, I-124, and I-131). *Cancer Biother Radiopharm* 22:423–430
- Ridge CA, Pua BB, Madoff DC (2014) Epidemiology and staging of renal cell carcinoma. *Semin Intervent Radiol* 31:3–8
- Scott AM, Wolchok JD, Old LJ (2012) Antibody therapy of cancer. *Nat Rev Cancer* 12:278–287
- Sharkey RM, Goldenberg DM (2009) Targeted therapy of cancer: new prospects for antibodies and immunoconjugates. *CA Cancer J Clin* 56:226–243

- Sneddon D, Niemans R, Bauwens M, Yaromina A, Van Kuijk SJA, Lieuwes NG, Biemans R, Pooters I, Pellegrini PA, Lengkeek NA, Greguric I, Tonissen KF, Supuran CT, Lambin P, Dubois L, Poulsen SA (2016) Synthesis and in vivo biological evaluation of ^{68}Ga -labeled carbonic anhydrase IX targeting small molecules for positron emission tomography. *J Med Chem* 59:6431–6443
- Steffens MG, Boerman OC, de Mulder PH, Oyen WJ, Buijs WC, Witjes JA, van den Broek WJ, Oosterwijk-Wakka JC, Debruyne FM, Corstens FH, Oosterwijk E (1999) Phase I radioimmunotherapy of metastatic renal cell carcinoma with ^{131}I -labeled chimeric monoclonal antibody G250. *Clin Cancer Res* 5:3268s–3274s
- Stillebroer AB, Boerman OC, Desar IME, Boers-Sonderen MJ, Van Herpen CML, Langenhuijsen JF, Smith-Jones PM, Oosterwijk E, Oyen WJG, Mulders PFA (2013) Phase I radioimmunotherapy study with lutetium 177-labeled anti-carbonic anhydrase ix monoclonal antibody girentuximab in patients with advanced renal cell carcinoma. *Eur Urol* 64:478–485
- Supuran CT (2008) Carbonic anhydrases: novel therapeutic applications for inhibitors and activators. *Nat Rev Drug Discov* 7:168–181
- Supuran CT (2017) Carbonic anhydrase inhibition and the management of hypoxic tumors. *Metabolites* 7:48
- Supuran CT, Briganti F, Tilli S, Chegwiddden WR, Scozzafava A (2001) Carbonic anhydrase inhibitors: sulfonamides as antitumor agents? *Bioorganic Med Chem* 9:703–714
- Turkbey B, Lindenberg ML, Adler S, Kurdziel KA, McKinney YL, Weaver J, Vocke CD, Anver M, Bratslavsky G, Eclarinal P, Kwarteng G, Lin FI, Yaqub-Ogun N, Merino MJ, Marston Linehan W, Choyke PL, Metwalli AR (2016) PET/CT imaging of renal cell carcinoma with ^{18}F -VM4-037: a phase II pilot study. *Abdom Radiol* 41:109–118
- Walsh JC, Lebedev A, Aten E, Madsen K, Marciano L, Kolb HC (2014) The clinical importance of assessing tumor hypoxia: relationship of tumor hypoxia to prognosis and therapeutic opportunities. *Antioxid Redox Signal* 21:1516–1554
- Weissleder R, Mahmood U (2001) Molecular imaging. *Radiology* 219:316–333
- Wichert M, Krall N, Decurtins W, Franzini RM, Pretto F, Schneider P, Neri D, Scheuermann J (2015) Dual-display of small molecules enables the discovery of ligand pairs and facilitates affinity maturation. *Nat Chem* 7:241–249
- Wilson WR, Hay MP (2011) Targeting hypoxia in cancer therapy. *Nat Rev Cancer* 11:393–410
- Wykoff CC, Beasley NJP, Watson PH, Turner KJ, Pastorek J, Sibtain A, Wilson GD, Turley H, Talks KL, Maxwell PH, Pugh CW, Ratcliffe PJ, Harris AL (2000) Hypoxia-inducible expression of tumor-associated carbonic anhydrases. *Cancer Res* 60:7075–7083
- Yang X, Minn I, Rowe SP, Banerjee SR, Gorin MA, Brummet M, Lee HS, Koo SM, Sysa-Shah P, Mease RC, Nimmagadda S, Allaf ME, Pomper MG (2015) Imaging of carbonic anhydrase IX with an ^{111}In -labeled dual-motif inhibitor. *Oncotarget* 6:33733–33742
- Yang X, Zhu H, Yang X, Li N, Huang H, Liu T, Guo X, Xu X, Xia L, Deng C, Tian X, Yang Z (2019) Targeting CAIX with ^{64}Cu XYIMSR-06 small molecular radiotracer enables noninvasive PET imaging of malignant glioma in U87 MG tumor cell xenograft mice. *Mol Pharm* 16:1532–1540
- Zhang J, Zhang Q (2018) VHL and hypoxia signaling: beyond HIF in cancer. *Biomedicines* 6:35
- Zhang Z, Lau J, Zhang C, Colpo N, Nocentini A, Supuran CT, Bénard F, Lin KS (2017) Design, synthesis and evaluation of ^{18}F -labeled cationic carbonic anhydrase IX inhibitors for PET imaging. *J Enzyme Inhib Med Chem* 32:722–730

Index

A

Acellular capillaries, 124, 129
Acetazolamide, 1, 3, 5, 37–43, 46, 48–65, 106–109, 270, 271
Acetazolamide in glaucoma, 79, 80
Acetazolamide in macular oedema, 90
Acid-base balance, 147, 148
Acid/Base Regulation, 4, 38
Acidification, 45, 49
Acidosis, 41, 42, 46, 53, 61
Acid secretion, 49
Activated Leukocyte Cell Adhesion Molecule (ALCAM), 186, 187
Acute high-altitude illness, 106
Acute mountain sickness, 1, 3, 6, 106, 107, 115
Acute myeloid leukemia, 16, 150, 151, 156, 168
Adenocarcinoma, 15, 18–20
Adenoma, 15, 25
Advanced-glycation end products, 123
Aerosol, 51, 59
Affibody, 266–268
Airway nerves, 51
Airways, 40, 48, 50, 51, 59
Alanine Serine Cysteine Transporter (ASCT), 194
Alkalinization, 55
Alveolar, 39, 40, 47, 49, 50, 60–64
Alveolar epithelium, 49
Alveolar fluid reabsorption, 49
Alveolar fluid secretion, 49
Alzheimer disease, 5, 6
Amino acid transporter, 189, 194–197
Ammonia, 131, 155

Anchoring to the metal ion coordinated water, 224
Antibody, 161, 162
Anticonvulsant, 108, 109
Antiepileptic drug, 109, 110
Anti-oxidant, 39
Apoptosis, 19, 20, 42, 57, 64
Aquaporin, 37, 41, 56, 63
Aqueous humour production, 4
Arp3, 186, 190, 191, 193
Arterial oxygenation, 50, 57, 58, 63
Asthma, 51
Astrocytes, 41, 42, 104, 105, 108, 121
Astrocytom, 19, 25, 26
Ataxia, 106, 112, 114
Ataxin-3, 113, 115
Azopt, 5

B

Barrett's, 15, 18
Benzolamide, 46, 48, 53, 56, 57, 62, 64
Benzoxaborroles, 224
Bicarbonate, 1, 2, 4, 42, 43, 47, 48, 50–52, 55–57, 59, 62, 104, 105, 109, 122, 128–130, 133, 135, 180, 181, 183, 186, 189, 197
Bicarbonate ion, 147, 148, 155
Bicarbonate transporters, 154, 157, 162
Bile production, 4
Biliary, 17, 18
Bioimaging, 160
Bioinformatics, 147, 149, 157, 169
Biomarker, 13, 15–17, 19, 20, 23–25, 27
Biotin Identification (BioID), 179, 183, 184, 188, 191, 192, 194–197

- Bipolar disorder, 3, 6
 Birth, 49
 Blast, 16
 Blood, 39, 40, 42, 44, 47, 48, 50, 52–56, 58, 60, 61, 63
 Blood-brain barrier, 105
 Bone development, 4
 Bone resorption, 14
 Brain, 17, 19, 25, 26, 103–109, 111, 112, 114, 115
 Brain cancer, 7
 Brain edema, 106, 108, 115
 Brain neoplasms, 167
 Breast, 20, 21, 24–26
 Brinzolamide, 5
 Brinzolamide in glaucoma, 79
 Brinzolamide in macular oedema, 79
 Bronchoconstriction, 50–52
 Bumetanide, 50
- C**
- CA I / Carbonic anhydrase I, 2–4, 6, 40, 151, 168
 CA II / Carbonic anhydrase II, 2–6, 39–41, 43, 44, 49, 52, 55, 63, 148, 149, 151, 153–156, 168
 CA II deficiency, 46
 CA III / Carbonic anhydrase III, 2, 3, 5, 6, 39, 40, 151, 153
 CA IV / Carbonic anhydrase IV, 2–6, 39, 40, 43–45, 47–49, 52, 149, 156, 157, 168, 169
 CA V, 4, 105, 129, 135
 CA VI / Carbonic anhydrase VI, 2–4, 6, 148, 149, 156, 159
 CA VII / Carbonic anhydrase VII, 2, 3, 6, 168
 CA VIII / Carbonic anhydrase VIII, 148, 162, 168
 CA IX / Carbonic anhydrase IX, 1–3, 5–7, 39, 40, 43, 44, 55, 147–149, 156, 157, 159–161, 168, 169
 CA IX biomarker, 17–22, 24
 CA IX expression, 7
 CA IX targeting, 161, 255, 258, 267, 268
 CA X / Carbonic anhydrase X, 149, 162, 163
 CA XI / Carbonic anhydrase XI, 149, 162, 163
 CA XII / Carbonic anhydrase XII, 2–4, 6, 40, 50, 149, 156, 161, 168, 169
 CA XIII / Carbonic anhydrase XIII, 2, 3, 5, 149, 153, 168
 CA XIV / Carbonic anhydrase XIV, 2, 3, 6, 39, 40, 43, 44, 147, 156, 162, 169
 CA XV, 2
 CA activity, 153, 154, 169
 CA1 gene, 151
 CA2 gene, 153, 154
 CA3 gene, 153
 CA4 gene, 157
 CA5A gene, 155
 CA6 gene, 159, 168
 CA7 gene, 149, 153
 CA8 gene, 162, 167, 168
 CA9 gene, 159–161, 165, 167, 168
 CA10 gene, 162
 CA11 gene, 162
 CA12 gene, 161, 167, 168
 CA13 gene, 149, 153, 167, 168
 CA14 gene, 162, 165, 167, 168
 CA5B gene, 155, 167, 168
 CACA, 228
 CA inhibitor (CAI), 221–231
 CA isoforms, 147, 149, 151, 152, 155, 156, 158, 162–165, 167–169
 Cajal cell, 16
 Calcium, 42, 45, 46, 52, 53, 55, 61, 65
 Calcium activated potassium channel, 42, 53
 Cancer, 1, 3, 6, 7, 13, 15–22, 24–27, 147–149, 151, 153–157, 159–162, 164, 166–169, 179, 180, 182, 183, 185–195, 197
 Capillaries, 39, 40, 43, 60
 Carbon dioxide CO₂, 1, 44, 47, 48, 60, 104, 105, 147, 148, 179–181
 Carbon dioxide production, 43
 Carbonic Anhydrase IX (CAIX), 1, 2, 5–7, 13, 14, 23, 26, 37, 38, 46, 52, 57, 59, 62, 103, 115, 147, 148, 150, 152, 156, 158, 163–165, 167–169, 179–197, 182, 183, 253–258, 260, 262, 266–274
 Carbonic anhydrase inhibitors, 130–134
 Carbonic anhydrase inhibitors in eye diseases, 79–82, 87, 88, 90, 91
 Carbonic anhydrase in the eye, 83
 Carbonic anhydrase-related protein, 14, 111–115
 Carbonic anhydrases, 122, 128, 129, 136
 Carboxylates, 221, 224, 226
 Carcinoma, 15, 16, 18–20, 22, 25, 150, 151, 153, 155, 157, 159–162, 167–169
 Cardiac hypertrophy, 55
 Cardiac output, 46, 53, 60, 63
 Cardiovascular, 37, 38, 52, 56, 65

CA-related proteins, 1, 2
 Cariogenesis, 6
 CARP VIII, 2
 CARP X, 2
 CARP XI, 2
 Catalytic activity, 148, 151, 153, 154, 156, 157, 162, 182, 187, 191
 Catamenial epilepsy, 109
 Cataract surgery, 5
 CA VA / Carbonic anhydrase VA, 2, 3, 6, 148, 149, 155, 156
 CA VB / Carbonic anhydrase VB, 2, 3, 6, 148, 155, 156
 Caveolae, 47, 52
 CcRCC metastases, 264
 CD98hc, 186–189
 Cell adhesion, 182, 183, 185, 187, 188, 191–193, 197
 Cell death, 108, 114
 Cell proliferation, 19, 159, 164, 181, 189, 194, 195
 Choroid plexus, 4, 17, 41, 53, 103–106, 112
 Chronic obstructive lung disease, 57
 Combinatorial therapy, 274
 Cell invasiveness, 153
 Cell migration, 155
 Cerebellar ataxia, 112, 115
 Cerebellum, 112, 113
 Cerebral amyloidosis, 6
 Cerebral edema, 6, 41
 Cerebrospinal fluid, 54, 103
 Cervical cancer, 20, 24, 26
 Chemoresistance, 160, 161
 Chloride, 49, 50, 55
 Chlorzalamide, 45, 46
 Cholangiocarcinoma, 18
 Choroidal endothelial cells, 134, 135
 Choroid plexus, 104–107, 112
 Chromophobe renal cell carcinoma, 167
 Chronic central serous retinopathy (CSCR), 5
 Chronic mountain sickness, 63
 Chronic obstructive pulmonary disease, 3
 Citrate, 126–128, 130, 131
 Cl/HCO₃ exchanger, 44
 Clear cell carcinoma, 19, 21, 25
 Clear cell renal cell carcinoma (ccRCC), 21, 22, 205–213, 215, 216, 253, 256–269, 271, 272, 274
 Clinical, 13, 15, 19–21, 24, 26, 27
 Clinical trial, 197
 Cofilin, 190, 192, 193
 CO₂-hydration activity, 3

Colon, 17, 25, 150, 151, 153, 162
 Colorectal, 15, 16, 18, 25
 Colorectal carcinoma, 153, 168
 Computer-aided drug design, 237
 Computerized Tomography (CT), 260, 261, 265, 266, 268, 269, 271
 Conducting system, 39
 Congestive heart failure, 1, 5
 Contrast Enhanced CT (CECT), 260
 Contrast induced kidney injury, 57
 COPD, 3, 6
 Coronary artery disease, 54, 56, 57, 65
 Cough, 51, 59, 60
 Coumarins, 221, 225, 227–229, 231
 CSF production, 4, 5
 Cystadenocarcinoma, 20
 Cystadenoma, 20, 25
 Cytokine, 57
 Cytoplasmic, 14
 Cytoskeleton, 185, 188–190, 192

D

Dextran bound sulfonamide, 47
 Diabetes, 121–124, 127–129, 131–135
 Diabetes complications, 121, 123, 133, 136
 Diabetic brain injury, 5
 Diabetic retinopathy, 121–124, 127, 132–134
 Diagnosis, 164
 Diagnostics, 13, 15, 16, 19, 20, 23, 27
 Diamox, 5
 Diaphragm, 58
 Dichlorphenamide, 50
 Differentiation, 17, 115
 Diffusion, 41, 43, 45, 47
 Disease, 13, 15, 16, 18, 20, 22, 24, 26, 104, 106–110, 113–115
 Distribution, 13, 14, 19, 24–26, 104, 106, 111, 114, 115
 Dithiocarbamates, 26, 27, 221, 224, 226, 231
 Diuretic, 38, 50–52, 54, 56, 58, 60
 Dorzolamide, 5, 53
 Dorzolamide in glaucoma, 83
 Dorzolamide in macular oedema, 93
 Drug, 15, 20, 26, 27, 108, 115
 Drug delivery, 1, 7
 Duodenum, 17

E

Edema, 6
 Electron transport chain, 128, 131
 ELISA, 23, 24

Endometrium, 25
 Endothelial NO synthase, 53, 57
 Endothelium, 37, 39, 40, 44, 45, 52
 Enzyme, 148, 149, 153, 155–157, 166
 Eosinophil, 40
 Epidermal growth factor receptor, 19
 Epilepsy, 3, 5, 6, 15, 26
 Esophageal, 15, 17–19, 25
 Esters, 225
 Ethoxzolamide, 45, 46, 48, 52, 53, 56, 62, 269
 Exercise, 43, 46, 48, 52, 54, 56, 63
 Expression, 149–169
 Extracellular, 41, 43, 44, 49, 53
 Extracellular acidification, 153
 Extracellular fluid volume, 53
 Extracellular matrix, 180
 Extracellular pH, 179, 180

F

Fatigue, 46, 60
 Fatty acid, 39, 45
 Fatty acid metabolism, 39
 Fatty acid oxidation, 133
 Fatty acid synthesis, 4
 Fluid exchange, 48
 Focal adhesion, 188, 189, 192
 Function, 14, 24–26, 148, 153, 157, 161, 162, 164, 166, 169
 Functions of CA isozymes, 2
 Furosemide, 38, 50, 52, 56, 59

G

G250 (cG250 & mG250), 205–215
 GABA, 105
 GABAergic, 105, 110
 Gas exchange, 38, 47–50, 60, 61
 Gastric, 15–19
 Gastric acid production, 4
 Gastric ulcer, 3
 Gastrointestinal, 16, 17
 Gastrointestinal stromal tumors, 13, 16, 155
 Genetic deletion, 41, 46
 GEPIA2 instrument, 147, 149, 152, 156–158, 163, 165, 166, 169
 G.I. protection, 4
 Girentuximab (cG250), 207, 213, 214, 258–266, 272, 274
 Glaucoma, 1, 3, 5, 6, 15, 25, 26
 Glioblastoma, 150, 153, 164
 Glioma, 19, 25
 Gluconeogenesis, 4, 14, 105, 130, 131

Glucose transporter, 180
 Glucose uptake, 123, 126–128, 134
 Glutamine, 181, 194, 195
 Glycolysis, 126–128, 133, 180, 181, 197
 GPR91, 127, 128
 Growth retardation, 46
 GTEx database, 149, 152, 154, 156, 158, 159, 163, 165
 Gustation, 4

H

H⁺ ATPase, 49
 HCO₃ sensitive adenylyl cyclase, 42
 Head and neck cancer, 7
 Head and neck carcinoma, 155
 Head and neck squamous cell carcinoma, 21
 Heart, 37–40, 43–47, 52, 55–57, 60, 64, 65
 Heart failure, 37, 38, 52, 55–57, 64
 Hematological, 16
 Hemoglobin, 47, 63
 Hemorrhagic brain injury, 6
 Hemorrhagic stroke, 3
 Hepatocellular, 18, 19
 Hepatocellular cancer, 7
 Hepatocellular carcinoma, 150, 153, 155
 Hereditary retinoschisis, 5
 Hexose biosynthetic pathway, 121
 HIF-1, 7
 Hif-1 α , 127, 206
 High altitude, 42, 54, 60, 62–65
 High-altitude cerebral edema, 106, 107
 High altitude pulmonary edema, 60, 65, 106
 Histological, 26
 Histology scoring, 258
 Histopathological, 13, 15
 H/K ATPase, 49
 Hodgkin's lymphoma, 22
 Homeostasis, 14
 Horse, 46
 Human, 39, 42, 46, 50, 51, 53, 54, 57, 58, 61–65
 Human Anti-Chimeric Antibodies (HACA), 263
 Hydrochlorothiazide, 56
 Hydrocephalus, 106
 Hydrogen ion, 56
 Hydroxamates, 221, 224, 226
 Hypercapnia, 48, 49, 52, 60, 61
 Hyperglycemia, 123, 124, 127, 131, 133, 134
 Hyperkalemia, 42
 Hyperventilation, 51, 57, 58
 Hypocapnia, 54

Hypohidrosis, 110
Hypokalemic periodic paralysis, 42
Hypoxia, 13, 19, 20, 40, 42, 52, 54, 60–63, 159–161, 164, 167, 168
Hypoxia imaging, 256
Hypoxia-inducible factor, 55, 159, 161, 166, 167
Hypoxia inducible factor 1 alpha (HIF-1 α), 180, 192, 195, 255–257
Hypoxia-inducible factor-2 α (HIF-2 α), 255
Hypoxia-response elements (HREs), 257
Hypoxic pulmonary vasoconstriction, 50, 60, 65

I

Idiopathic intracranial hypertension, 54
Ileum, 17
Imatinib, 26
Immunoassay, 22, 23
Immunohistochemical, 13, 19, 20, 22
Immunohistochemistry, 15, 111, 148, 151, 153–155, 159, 161, 169
Immuno-liposomes, 7
Infantile nystagmus syndrome (INS), 5
Infarct, 57
Inflammation, 42, 63, 64
Inflammatory cytokines, 125
Inhibition, 20, 26
Inhibition mechanism, 221, 222, 224–228, 230, 231
Inhibitors, 15, 26, 27, 37–43, 45–48, 51–57, 59, 60, 62–65, 106–110, 113, 115, 190, 193, 197, 221, 222, 224–229, 231
Inositol trisphosphate receptor-1, 113
In silico techniques, 237, 238
Insulin secretion, 4
Integrin, 183, 186–189, 192–194, 197
Interactome, 179, 183, 184, 187, 190, 193, 196, 197
Interstitial, 40
Intestine, 148, 151, 153
Intracellular, 41, 43–47, 52, 55, 61, 62
Intracellular pH, 39, 43, 49, 53, 61, 62, 154, 180, 197
Invadopodia, 182, 186, 192–194
Invasion, 16, 17, 19, 27, 180, 182, 185, 187, 188, 190–193, 197
Ion, 103, 105, 106, 110, 111
Ion transport, 14, 17, 24, 148, 157, 168
Ischemia, 124, 128
Ischemia-reperfusion injury, 64

Ischemic brain injury, 6
Isozyme, 13–18, 20, 26, 27

J

Jejunum, 17

K

Kidney, 2, 4, 6, 21, 22, 25, 41, 53, 55, 57, 64, 65, 148, 150, 160, 167
Krebs cycle, 128, 131

L

Lacosamide, 109, 110
Lactate, 45, 126, 128, 148, 157, 162
Lamellipodia, 186–188, 190, 191, 194
LAT1, 181, 189, 194, 195
Leaky blood vessels, 124
Leiomyoma, 20
Ligand-protein interactions, 238–240, 242
Lipogenesis, 130, 132
Liver, 18
Localization, 14, 148, 169
Loop diuretic, 50, 52, 56
Low grade glioma, 165
Lung, 17, 19, 20, 24, 37–40, 43, 44, 47–50, 57, 60–62, 64, 65
Lung cancer (NSCLC), 7
Lung transplantation, 65
Lutetium-177 (¹⁷⁷Lu), 214
Lymphatic, 16
Lymphoblastic leukemia, 16

M

Macular edema, 3, 5
Malignancy, 15, 16, 19
Marker, 13, 18, 21, 22, 24, 26
Matrix metalloproteinase -14 (MMP14, also known as MT1-MMP), 187
MCP-1, 127
Medulloblastoma, 19, 155
Melanoma, 17, 151, 155, 168
Membrane-associated, 14
Membrane ion transport, 38
Meningioma, 155
Mental retardation, 112–114
Mesothelioma, 19, 20
Mesothelium, 17
Metabolic acidosis, 46, 54–57, 61, 63
Metabolic activity, 121, 122, 125, 127
Metabolic alkalosis, 56, 58, 59

- Metabolism, 38, 40, 42, 44, 148, 155, 164, 166, 169, 180, 181, 183, 194–196
- Metabolism-perfusion matching, 44
- Metabolon, 24, 55, 189, 196
- Metadata, 147, 149, 151, 153, 155, 157, 159, 168
- Metaplasia, 18
- Metastasis, 15, 16, 19, 26, 153, 155, 157, 160, 183, 185, 187, 188, 191, 196
- Metastasis-free survival, 26
- Metastatic renal cell carcinoma (RCC), 263, 264
- Methazolamide, 41, 42, 49, 58, 62
- Microaneurysms, 124
- Microenvironment, 148
- Migraine, 3, 5
- Migration, 180, 182, 183, 185, 187–193, 196, 197
- Mitochondria, 39, 43, 155
- Mitochondrial, 14, 105
- Mitochondrial carbonic anhydrase, 6, 123, 125, 131
- Mitophagy, 127
- MN protein, 7
- Molecular dynamics, 239, 245
- Molecule, 13, 27
- Mono-Carboxylate Transporter (MCT), 148, 154, 157, 180, 181
- Monoclonal antibodies (mAbs), 258, 261, 267
- Monoclonal G250 antibody, 259
- Morpholino, 113, 114
- Motor coordination, 113, 114
- Mountain sickness, 106
- Muscle function, 5
- Myasthenia gravis, 6
- Myelin, 104
- Myeloid, 16
- Myelomonocytic leukemia, 16
- Myocardial, 37, 39, 44–46, 56, 57, 65
- Myocardial blood flow, 44
- Myocardium, 39, 43, 55
- N**
- Na-Cl-K co-transporter, 154
- Na/HCO₃ symport, 49
- Na/H exchange, 49
- Nanoparticles, 7
- Natriuresis, 55, 56
- Near infrared fluorescence (NIRF) imaging, 265
- Necrosis, 21
- Necrotic area, 19
- Neoplasia, 15, 16, 25
- Neoplasms, 147, 149, 150, 153, 155, 164, 165
- Neovessel, 17
- Nephrectomy, 258, 261
- Nervous system, 38, 54, 65, 103–105, 114, 115
- Neural development, 111, 113
- Neural transmission, 51, 61
- Neurexin, 114
- Neuroectodermal, 19
- Neuroepithelial body, 40, 59
- Neuroinflammation, 127, 135
- Neurology, 106–110, 114, 115
- Neuron, 104, 105
- Nitric oxide, 41, 53, 57, 61
- N-methyl acetazolamide, 41, 62, 64
- Non-catalytic mechanism, 157
- Norepinephrine, 53, 54, 62
- Nuclear related factor 2, 42
- O**
- Obesity, 3, 6, 128, 131, 132
- Occlusion of the active site entrance, 224
- O-GlcNAc modification, 121, 124
- Olfaction, 4
- Oligodendrocyte, 104, 106
- Oligodendroglial, 19
- Oncogenesis, 5
- Oncogenic, 16
- Oncogenic metabolism, 147, 167
- 1,3,5-Triazine, 246
- Osmoregulation, 41
- Osteopetrosis, 46
- Out of the active site binding, 224
- Ovarian cancer, 7
- Ovarian carcinoma, 25
- Oxaloacetate, 128, 133
- Oxidative metabolism, 121–125, 131, 133, 134
- Oxidative phosphorylation, 180
- Oxidative stress, 6, 121, 123, 127, 131, 136
- Oxygen, 37, 42, 44, 46–48, 57, 58, 60, 61
- Oxygen uptake, 46, 48
- Oxylabile, 47
- P**
- P53, 19
- Pancreas, 148, 150, 151, 159
- Pancreatic, 15, 17
- Pancreatic cancer, 7

Pancreatic juice production, 5
Papillary carcinoma, 22
Pathology, 13, 24
Pentose phosphate pathway, 123
Periodic breathing, 56
Peripheral chemoreceptor, 60, 61
PET/CT, 209
PET imaging, 255, 256, 260, 267, 269, 270
PET scan, 260, 261
PH, 14, 39, 40, 42–45, 48–50, 52, 54, 56–60, 109
Pharmacophore, 238–243, 249
Phenols, 221, 225, 227
PH regulation, 148, 161, 168, 181, 188–190, 197
Physiological functions of CA, 2
Piceatannol, 48
PKM2, 127, 128
Plasma, 39, 41, 45, 47, 48, 52, 54, 61
Pleural fluid, 51
Pneumoconstriction, 50
Pneumocyte, 49
Polyamines, 221, 225, 227, 231
Polycythemia, 63
Polyol pathway, 123, 124
Positive emission tomography (PET), 254, 260–262, 269–273
Potassium channel, 53
Prickly nanoparticles, 7
Prognosis, 13, 15, 16, 18–22, 24, 25, 160–162, 164, 165, 167–169
Proliferation, 17–19
Protein kinase C, 124
Protein tyrosine phosphatases, 111
Proteoglycan-like, 24
Proton, 147, 148, 154, 157, 162
Proton antenna, 162
Proton (H), 180, 186, 187
Pseudomyxoma peritonei, 16
Pseudotumor cerebri, 5, 6, 106–108, 115
Pulmonary edema, 55, 64
Pulmonary hypertension, 6, 37, 40, 60, 63, 64
Purkinje cells, 111, 112
Purkinje fiber, 43
Pyrimidine synthesis, 4
Pyruvate, 45, 127–130, 133
Pyruvate carboxylase, 130, 133

Q
Quadrupedal gait, 112, 113

R
Rabbit, 58
Radioimmunotherapy (RIT), 213, 257, 258, 260, 262–265, 272, 274
Radioligand therapy, 272
Radiometal chelator complex, 270
Rat, 42, 46, 49, 53, 55, 57, 61–64
Reactive oxygen species (ROS), 5, 6
Receptor, 148
Red cells, 38, 39, 41, 43, 47, 48, 62
Redox homeostasis, 123
Regulation, 147, 148, 154, 161
Renal, 17, 19, 21, 22, 25
Renal cancer, 7
Renal Cell Carcinoma (RCC), 206–211, 213–216
Reperfusion, 57, 64, 65
Reproductive system, 5
Respiration, 4, 14, 124, 126, 127, 133, 135
Respiratory, 37, 50, 57–59
Retina, 53, 123, 125, 127–129, 135, 136
Retinal detachment, 124
Retinal endothelial cells, 134, 135
Retinal pericytes, 125
Retina pigment epithelium, 89
Retinitis pigmentosa, 5, 6
Retinopathy, 6
RNA, 149, 153, 159, 169
RT-PCR, 25

S
Saliva, 159
Saliva production, 4
Sarcolemma, 39, 44
Sarcoma, 20
Sarcoplasmic reticulum, 39, 45
Secreted, 14
Side effects, 54, 55, 58, 59, 62, 108–110
Single photon emission tomography (SPECT), 254, 262, 265, 266, 268, 271
Skeletal muscle, 39, 53, 55, 58
Skin, 21, 25
Skin cutaneous melanoma, 150, 168
SLC-0111, 7
Sleep apnea, 3, 6
Sleep disordered breathing, 54, 64
Small molecular drug conjugated (SMDCs), 7
Small molecule inhibitors, 268, 269, 272, 274
Smooth muscle, 37, 40, 42, 50–53, 61, 62

Sodium-bicarbonate transporter, 189
 Sodium glucose co-transporter, 56
 Sodium reabsorption, 38
 SPECT imaging, 260, 265, 267, 272
 Squamous cell carcinoma, 19–21, 25
 Stomach, 53
 Stroke, 6
 Structure, 157
 Subcellular, 14
 Succinate, 126–129
 Sulfamate, 222–224, 231
 Sulfamide, 224
 Sulfooumarins, 221, 225, 227, 231
 Sulfonamide, 26, 221–226, 229–231, 239–246, 248, 249, 268–270, 272
 Superoxide, 121, 124, 125, 128, 131, 134
 Surfactant, 39, 48, 49
 Survival, 15, 16, 18–22, 25, 26, 150, 151, 153–157, 159–168
 Systemic hypertension, 52, 54

T

Tail approach, 226, 231
 Target, 13, 21, 26, 27
 TCGA database, 151, 153
 Theranostic agent, 268, 274
 Theranostic targeting, 272
 Therapeutic, 13, 15, 21, 26, 27
 Therapeutic target, 167, 196
 Therapy, 13, 20, 21, 24, 27
 Topiramate, 108–110, 128, 129, 132–135
 Transcription, 149, 151, 153, 154, 157, 159–162, 166
 Transpleural, 47
 Transporter, 180, 181, 183, 189, 191, 192, 194, 195
 Transport metabolon, 154
 Treatment, 106–110, 115, 168
 Trusopt, 5
 Tubule, 52, 56
 Tumor, 13, 15–22, 24–27, 107, 147–165, 167–169
 Tumor acidosis, 167
 Tumor growth, 161
 Tumorigenesis, 18

Tumor microenvironment, 147, 155, 160, 169
 Tumor stage, 21, 25
 Tumor suppressor, 157, 159, 166, 169
 Tumor xenografts, 7
 Tumour hypoxia, 254, 255
 Tumour imaging, 253
 Tumour microenvironment, 180, 182, 192, 253–255

U

Unfolded protein response, 181–183, 195
 Ureagenesis, 14
 Ureogenesis, 4
 Uterine tumors, 155

V

Vascular endothelial growth factor (VEGF), 89
 Vascular F1/FO ATPase, 47
 Vasculature, 37, 38, 40, 52, 60, 62, 64
 Vasodilation, 42, 53–55
 VEGF receptor, 257
 Ventilation, 40, 41, 44, 46, 48–50, 56–65
 Ventilation-perfusion matching, 50
 VHL/HIF-1 α pathway, 256
 VHL syndrome, 261
 Virtual screening, 237, 238, 240, 245, 247
 Vision loss, 124
 Vitreoretinal surgery, 5
 Von Hippel-Lindau, 21
 Von Hippel-Lindau (VHL) tumour suppressor gene, 256

W

Waddles, 111

Z

Zebrafish, 111, 114
 Zinc-binding inhibitor, 224
 Zirconium-89 (^{89}Zr), 208–211
 Zonisamide, 109, 110